The use of near infrared spectroscopy (NIRS) to measure vascular haemodynamics in human bone tissue *in vivo.*

Submitted by Robert Meertens to the University of Exeter as a thesis for the degree of Doctor of Philosophy in Medicine in April 2020.

Signature: 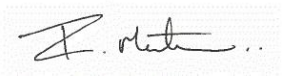

Acknowledgements

There are a number of people I would like to acknowledge, as their contributions towards my development during this PhD project have been invaluable.

I would like to thank the College of Radiographers for their endorsement of this project via the College of Radiographers Doctoral Fellowship Grant. The purpose of this grant is to provide both financial and professional support to a radiographer developing their research career. I am extremely grateful to have received this support as an inaugural awardee of the grant.

I would like to thank my PhD supervisors Karen Knapp, David Strain, Francesco Casanova, and Sue Ball for their continued role in my academic development and for their continued encouragement with this project. Likewise, thanks goes to Dave Richards for his pastoral support. Thanks also to the extended staff of the Medical Imaging programme for their continued support and encouragement.

I wish to thank all the staff at the Exeter Clinical Research Facility for their invaluable assistance with the development and execution of the research presented in this thesis. Of course this includes those volunteer participants who gave up their time to assist with my research.

Finally I would like to thank my wife Alison and my family for their support, encouragement, patience, and tolerance during the years of my PhD study.

Abstract

Rationale: Poor cardiovascular health is associated with reduced bone strength and increased risk of fragility fracture. However, direct measurement of intraosseous vascular health is difficult due to the density and mineral content of bone. The aim of this PhD project was to investigate the feasibility of near infrared spectroscopy (NIRS) for the investigation of vascular haemodynamics in human bone *in vivo*. NIRS provides inexpensive, non-invasive, safe, and real time data on changes in oxygenated and deoxygenated haemoglobin concentration at superficial anatomical sites. NIRS utilises a source optode of near infrared (NIR) light and detector optode that obtains representative data of the interactions of NIR photons with tissue.

Method: A systematic review was performed identifying the current existing applications of NIRS (and similar technologies) for measuring human bone tissue *in vivo*. This review informed the development of an arterial occlusion protocol for obtaining haemodynamic measurements of the proximal tibia and lateral calf, including assessment of the protocol's reliability. For thirty-six participants, NIRS results were also compared to alternative tests of bone haemodynamics involving dynamic contrast enhanced MRI (DCE-MRI), and measures of general bone health based on dual x-ray absorptiometry testing and blood markers of bone metabolism.

Results: This thesis presents novel data demonstrating NIRS can obtain acceptably reliable markers of haemodynamics at the proximal tibia *in vivo*, comparable with reliability assessments of alternative modalities measuring intraosseous haemodynamics, and the use of NIRS for measuring muscle. Novel associations have been demonstrated between haemodynamic markers measured with NIRS and DCE-MRI, giving confidence NIRS truly represents bone haemodynamics. Increased NIRS markers of oxygen extraction during occlusion, and greater post-ischaemic vascular response to occlusion, were both associated with greater bone mineral density.

Conclusion: As a feasibility study, this PhD project has demonstrated the potential for NIRS to contribute to research around the potential pathophysiological role of vascular dysfunction within bone tissue, but also the limitations and need for further development of NIRS technology.

List of Contents

List of Figures

List of Tables

List of Equations

List of Publications and Presentations

Meertens RM, Strain WD, Knapp KM. A review of the mechanisms, diagnosis and preventative treatment options of osteoporotic fragility fractures in patients with type 2 diabetes mellitus, *Journal of Endocrinology and Metabolism;* 2015;5(1-2):157-162.

Meertens RM, Knapp KM, Casanova F, Strain WD. The use of near infrared spectroscopy (NIRS) as a diagnostic tool to measure microvascular haemodynamics in bone tissue. *Osteoporosis International*, 2016; Vol27(Sup2), S636-S637.

Meertens RM, Knapp KM, Casanova F, Strain WD. The effects of lumbar sympathectomy on bone and soft tissue haemodynamics of the leg recorded using near infrared spectroscopy: A case report. *Journal of Biomedical Engineering and Informatics*. 2016;3(1):28.

Meertens RM, Casanova F, Knapp KM, Thorn C, Strain WD. Use of Near-Infrared Systems for Investigations of Haemodynamics in Human in Vivo Bone Tissue: a Systematic Review. *International Society of Oxygen Transport in Tissue 2017*, Halle, Germany, 19-23rd August 2017.

Meertens RM, Casanova F, Knapp KM, Thorn C, Strain WD. Use of Near-Infrared Systems for Investigations of Haemodynamics in Human in Vivo Bone Tissue: a Systematic Review. *Journal of Orthopaedic Research*; 2018;36(10):2595-603.

Meertens RM, Knapp KM, Casanova F, Ball, S, Strain WD. Exploring the potential relationships between microvascular haemodynamics and density in bone: A feasibility study utilising near infrared spectroscopy. *United Kingdom Imaging and Oncology Congress 2019*, Liverpool, June 10-12th 2019.

Meertens RM, Strain WD, Casanova F, Ball S, Knapp KM. The reproducibility of near infrared spectroscopy markers of microvascular haemodynamics at the proximal tibia and gastrocnemius. *United Kingdom Imaging and Oncology Congress 2019*, Liverpool, June 10-12th 2019.

Meertens RM, Knapp KM, Casanova F, Ball S, Fulford J, Merson S, Strain WD. Vascular measurements of the proximal tibia and their associations with bone mineral density. *European Congress of Radiology 2020*, Vienna, Austria, July 15-19th July 2020.

Meertens RM, Knapp KM, Casanova F, Ball S, Fulford J, Merson S, Strain WD. Sex-based differences in vascular haemodynamics at the proximal tibia. *European Congress of Radiology 2020*, Vienna, Austria, July 15-19th July 2020.

Meertens RM, Strain WD, Casanova F, Ball S, Knapp KM. Near infrared spectroscopy for the investigation of vascular haemodynamics in human bone in vivo. Bone Research Society Annual Meeting 2020, Manchester, July 6-8th 2020.

Key Abbreviations

AO	Arterial occlusion
ACR	Albumin to creatinine ratio
ATP	Adenosine triphosphate
BMD	Bone mineral density
CCO	Cytochrome c-oxidase
cHb	Total haemoglobin concentration
CI	Confidence interval
CRF	Clinical research facility
CTX	C-terminal telopeptide of type I collagen
CW-NIRS	Continuous wave-near infrared spectroscopy
DCE-MRI	Dynamic contrast enhanced-magnetic resonance imaging
DCS	Diffusion correlation spectroscopy
DO	During occlusion
DVRC	Diabetes and Vascular Research Centre
DXA	Dual absorption x-ray absorptiometry
EXTEND	Exeter Ten Thousand Research Register
FD-NIRS	Frequency domain-near infrared spectroscopy
FRAX	Fracture risk assessment tool
Hb	Haemoglobin
HHb	Deoxygenated haemoglobin
ICC	Intra class correlation
ICG	Indocyanine green
IQR	Interquartile range
LDF	Laser Doppler flowmetry
MBL	Modified Beer Lambert
MCID	Minimal clinically important difference
MM	Medial malleolus
MRS	Magnetic resonance spectroscopy
NIR	Near infrared
NIRS	Near infrared spectroscopy
NO	Nitric oxide
NOF	Neck of femur
nTHI	Normalised total haemoglobin index

O2C	Oxygen To See (optical device)
O_2Hb	Oxygenated haemoglobin
P1NP	N-terminal propeptide of type 1 procollagen
PO	Post occlusion
PPG	Photoplethysmography
pQCT	Peripheral quantitative computed tomography
PRESS	Point resolved spectroscopy sequence
PRISMA	Preferred Reporting Items for Systematic Reviews and Meta-analyses
PROSPERO	International Prospective Register of Systematic Reviews
RBC	Red Blood Cell
RC	Repeatability coefficient
RMSCV	Root mean square coefficient of variation
RMSSD	Root mean square standard deviation
RVO	Repeat vascular occlusion
SD	Standard deviation
SRS	Spatially resolved spectroscopy
T2DM	Type 2 diabetes mellitus
TBS	Trabecular bone scoring
TD	Tibial diaphysis
TOI	Tissue oxygenation index
TP	Proximal tibia
TRS	Time resolved spectroscopy

Key Definitions

Absorption coefficient: A constant value for a tissue type representing the sum of absorption contributed by all chromophores within the tissue at a specific wavelength. As such this incorporates both the concentration and absorptive properties of each chromophore [(1)].

Chromophore: Any compound of interest that attenuates (i.e. absorbs and scatters) different near infrared wavelengths of light in a predictable manner [(2)].

Differential pathlength factor: A factor applied to modified Beer Lambert Law calculations to allow for the extra distance travelled by near infrared photons through tissue due to elastic scattering events [(2)].

Normalised Total Haemoglobin Index (nTHI): The relative change in total haemoglobin concentration within the measured volume from the initial haemoglobin concentration at the commencement of measurements [(2)].

Reduced scattering coefficient: A constant value for a tissue type representing the sum of scattering losses contributed by all chromophores within the tissue at a specific wavelength. As such this incorporates both the concentration and the scattering properties of each chromophore, as well as adjusting for the anisotropy of scattering [(1)].

Reliability: The ability of a test to produce similar results when measuring the same thing [(3)].

Reproducibility: The variability of repeated measurements taken during different testing sessions [(3)].

Repeatability: The variability of repeated measurements taken during the same testing session [(3)].

Specific extinction coefficient: A constant value representing how efficient a chromophore is at attenuating NIR light of a specific wavelength [(2)].

Tissue Oxygenation Index (TOI): The ratio of oxygenated haemoglobin to total haemoglobin, presented as a percentage. This is analogous to oxygen saturation (sO_2) measurements [(2)].

Validity: The ability of a test to produce results representative of the true value of the measurement in question [(4)].

Chapter 1: Introduction

1.1: Introduction to the PhD project

Haemodynamic measurements of the vascular blood supply within any organ or tissue can provide invaluable diagnostic information on disease processes with a vascular component. Laroche 2002 contends that blood supply to bone is just as pivotal to homeostasis in bone as blood perfusion is to the brain or myocardium [5]. The latter are often imaged routinely in clinical practice, however measuring the contribution and extent of blood supply within bone is difficult with existing methods [6].

Typical haemodynamic measurements can include oxygen saturation in tissue (an indicator of general tissue health), blood perfusion rates to tissue (an indicator of metabolism and/or vascular function) and blood volume measurements (an indicator of blood demand to tissue and tissue vascularity). It is important to establish a context for these measures. For example, blood may be perfusing well but could be low in oxygenation, or blood may be well oxygenated but tissue is receiving an inadequate blood volume [7].

Bone is a dynamic and vascular tissue type that is constantly self-regulating, with around 5% of the body's blood volume supplying the skeleton [8]. However because of its density and high mineral content, its vascular supply is notoriously difficult to image using existing modalities [6]. Imaging protocols for measuring bone haemodynamics involve nuclear medicine scans, positron emission tomography (PET) or magnetic resonance imaging (MRI) (discussed further in Chapter 2). These tests are expensive, have limited clinical access, have logistical considerations (radiation burden for nuclear medicine and PET; magnetic safety for MRI), involve invasive injections, and therefore don't allow easily repeated measurements over time [6, 9]. In addition, oxygen saturations in bone tissue cannot be measured with these techniques and therefore neither can markers of oxygen consumption metabolism [10]. These modalities measure markers of gross perfusion and blood volume to tissue based on quantitative descriptors of radiopharmaceutical or gadolinium contrast uptake [11]. The gold standard to measure bone oxygenation at a specific anatomical site is bone biopsy, which is invasive and painful for the participant [12].

Near infrared spectroscopy (NIRS) is a potential technological solution. NIRS is non-invasive, non-destructive and non-ionising. As a diagnostic tool it is relatively inexpensive and convenient for repeat measurements or for continual monitoring of

tissue in real time [13]. It can measure oxygen saturation as well as markers of gross blood perfusion and vascular health in tissue [14]. NIRS utilises similar technology to a pulse oximeter, involving transmitting and receiving designated optical wavelengths using non-invasive probes at a specific anatomical sight [2]. NIRS takes advantage of the difference in attenuation characteristics of oxygenated and deoxygenated haemoglobin to record markers of bone haemodynamics in real time [15]. Therefore NIRS can also measure changes in haemoglobin concentration over time in response to different stimuli (such as a medical drug, simulated ischaemic occlusion, or exercise) or positional changes from the participant [14]. Although near infrared (NIR) light (700-1000nm) is not very penetrating in human tissue, NIRS has been shown to be able to record data through bone to depths of up to three centimetres [16].

1.2: Aims and objectives

The primary aim of this PhD project was to explore the potential feasibility of NIRS as a research tool in the measurement of *in vivo* vascular haemodynamics in human bone tissue, including markers indicative of bone tissue oxygenation and vascular function.

Objectives of the PhD project were:

- To gauge the existing knowledge base on the use of NIRS (and similar NIR based technologies) for measuring markers of vascular blood supply within bone *in vivo.*

- To determine if NIRS measurements of vascular blood supply can be:

    - representative of bone tissue;

    - reliable across different operators;

    - reliable across different participants; and,

    - tolerable for participants.

- To investigate the performance of NIRS against a test that also measures markers of vascular haemodynamics within bone: dynamic contrast enhanced magnetic resonance imaging (DCE-MRI; discussed in Section 2.3.1).

- To observe any potential relationships between NIRS bone haemodynamic results and other bone health markers, such as bone mineral density (BMD), trabecular bone scoring (TBS) and blood markers of bone metabolism (discussed in Section 2.4).

- To observe any difference in bone haemodynamics between sexes and between matched participants with and without type 2 diabetes mellitus (T2DM), which may indicate whether NIRS could be useful for investigating bone pathogenesis.

1.3: Chapter summary

With the above primary aim and objectives in mind, this chapter will first present a background on the anatomy and physiology of bone, with particular focus on intraosseous vascular supply (Section 1.4). This will then lead to background information on the role of vascular haemodynamics in normal and altered states of bone homeostasis (Section 1.5). Section 1.6 will discuss the tibia as an illustrative example, and as the primary bone of investigation in this thesis. Section 1.7 will present a detailed rationale for the methodological approaches adopted in this PhD project. Section 1.8 outlines the structure of the thesis.

1.4: The anatomy and physiology of bone tissue

Bone tissue is a heterogeneous form of connective tissue made of specialised cells surrounded by an extracellular organic collagenous matrix with associated inorganic mineralization (primarily hydroxyapatite) [17]. Bone plays a protective and supportive role, as well as facilitating movement as an anchoring point for muscle and ligamentous attachments. It also facilitates much of the body's haematopoiesis [18]. It is constantly being remodelled with an estimated 10% of bony adult skeleton turned over each year, with blood borne hormones and proteins often providing the triggers for these homeostatic processes [19].

1.4.1: Macrostructure features of bone

Figure 1.1 demonstrates the general macro structure of a typical long bone. Cortical bone (or compact bone) forms the outer dense shell of human bones and is pivotal in providing strength with its dense and highly mineralised structure [17]. The periosteum is a fibrocollagenous layer on the external surface of cortical bone [17]. Collagen from the periosteum is extrinsically cross linked by thick collagenous fibres (called Sharpey's fibres) with cortical bone securing the periosteum against cortical bone [19]. Likewise, the endosteum is a membrane which covers all internal surfaces of bone, including inside Haversian canals and trabeculae [17].

Trabecular bone (also known as cancellous or spongy bone) is characterised by a honeycomb structure of lattice-like bony plates and bar structures (trabeculae) with

cavitating spaces occupied by bone marrow [17]. Trabeculae can have wide variations in orientation, thickness and spacing within different bones in the same individual, but are typically 50-200µm in diameter with bone marrow filling spaces with distances in the region of 200-1000µm between adjacent trabeculae [20]. Trabeculae are lined with endosteal tissue and consist of lamellae of bone formed as described below in Section 1.4.2. Trabecular bone is found internally within bone at the articulating ends of long bones, within vertebrae, and within flat bones such as the patella and skull plates. It provides extra strength to the external cortical bone and often supports red marrow [17, 19].

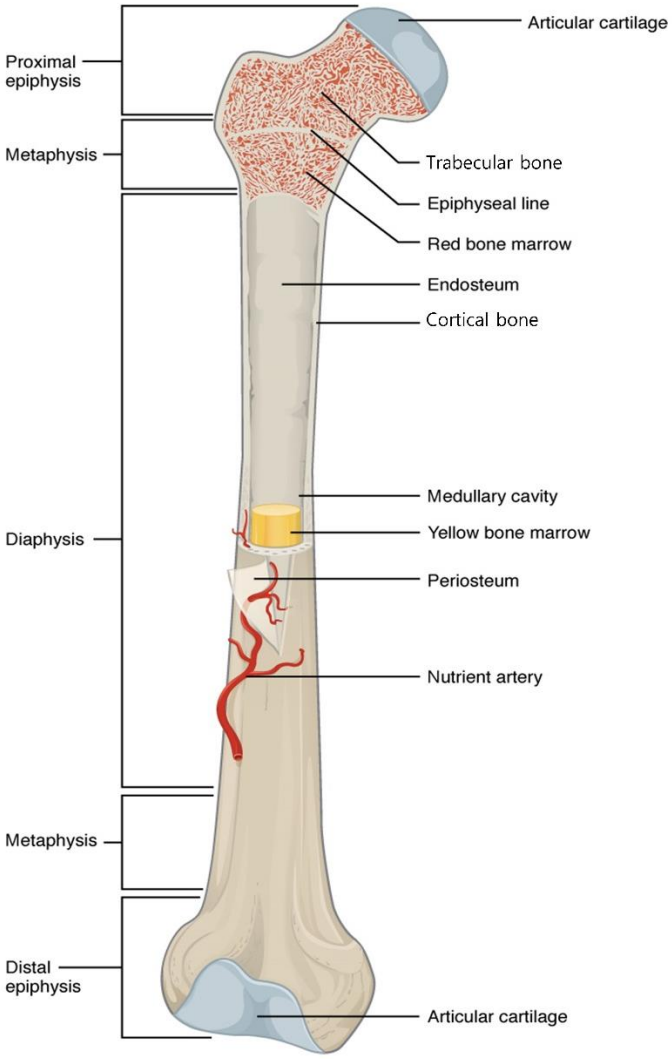

Figure 1.1: Typical long bone macro structure. Reprinted with permissions from Betts et al 2013 [21].

The medullary cavity is that space within bone containing bone marrow. Typically, in long bones the diaphysis is the central shaft section of the medullary cavity devoid of trabecular bone. The diaphysis is surrounded by the cortical bone of the shaft and extensive areas of trabecular bone within the articulating ends of the long bone. These

end sections of long bones containing trabeculae are termed the epiphyses, with the metaphysis defined as the region of bone where the diaphysis and epiphysis have fused during development [21]. As the endosteum surrounds all cortical and trabecular bone it effectively forms a barrier between marrow (and therefore the medullary cavity) and cortical bone [17, 19].

Bone marrow is a heterogeneous tissue type found within bone. It can be broadly characterised into two types: red (haematopoietic) or yellow (fatty) marrow. Red marrow is typically 40-60% lipids and has the higher concentration of erythrocytes. It is also haematopoietic, producing red and white blood cells, as well as platelets [18]. In humans, all marrow is haematopoietic at infancy, but in adults red marrow is typically found within the axial skeleton including vertebrae, skull and pelvic bones, as well as potentially in the epiphyseal ends of long bones where trabecular bone is also found [22]. With age, red marrow is replaced by yellow marrow, especially in peripheral long bones, and as such blood cell production decreases. Yellow marrow is constituted of approximately 80% lipids. Although it is vascular tissue it is not haematopoietic, but still plays a role in the genesis of osteoblasts and osteoclasts. It is typically found in the diaphysis of adult long bones [22]. McCarthy 2006 [23] reports a wide variation in estimated mean blood flow rates between cancellous bone containing red marrow (20mL/min/100g), cortical bone (5mL/min/100g) and yellow marrow (1mL/min/100g) in animal studies.

1.4.2: Microstructure of bone

The base unit of cortical bone is the osteon, approximately 200µm in diameter, as demonstrated in Figure 1.2. At the centre of each osteon lies a Haversian canal which allows the neurovascular supply to the osteon. Around this lies concentric layers of bone, termed lamellae. Lamellae are predominantly constituted of an extracellular matrix based on an array of parallel but branching Type 1 collagen fibres which knit and network together with bone maturity. This collagen matrix facilitates the strength in bone absorbing tensile, compressive and shearing forces [17, 19].

The bone matrix within each osteon is also highly mineralised with 50-70% of mass attributable to inorganic mineral salts such as hydroxyapatite, making it hard, dense and relatively inelastic, and thus resistant to fracturing [17]. Other ions containing denser minerals such as citrate, magnesium, sodium, potassium, and fluoride may be found

in trace quantities. These inorganic materials are typically in crystal-like form and slot into gaps left in the collagen networking of the bone matrix [19].

Osteons generally run parallel with each other and with the long axis of a bone, but they may spiral, branch or deviate. Haversian canals are anastomosed together via vessels in Volkmann's canals. These canals inter connect Haversian canals and run obliquely or perpendicularly to osteons. They also connect the osteon network with the microvascular blood supply provided via the periosteum and bone marrow [19].

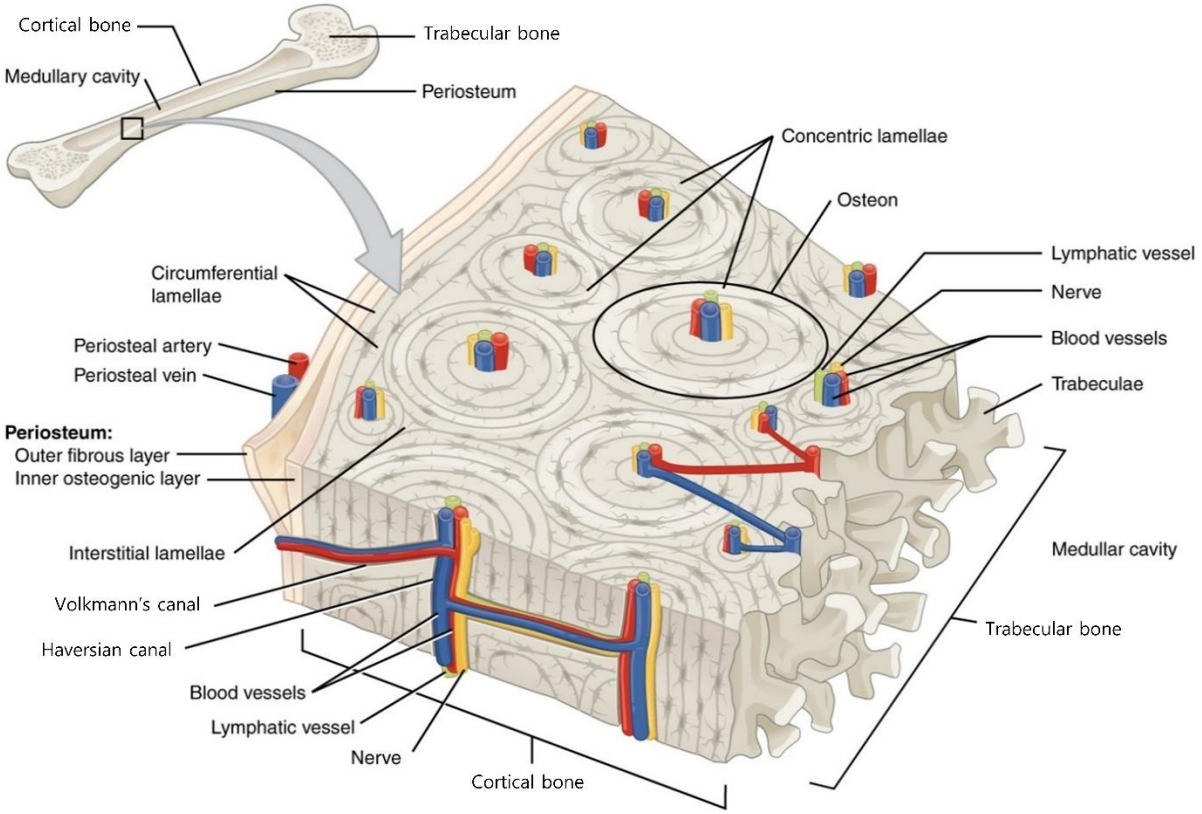

Figure 1.2: Typical microstructure of osteon systems within cortical bone. Reprinted with permissions from Betts et al 2013 [21].

Within each osteon are osteocytes, organic cells locked within the bone matrix. These cells are derived from osteoblasts (discussed below) and although comparatively spaced by the bone matrix (typically 20-30µm), they form a cellular network through dendritic processes with each other within osteons, and with the osteoblasts situated on bone surfaces. These dendrites allow electrical and metabolic connections as well as a route for the diffusion of nutrients and waste products between osteocytes and adjacent blood supply [19].

Functionally osteocytes do not contribute to new bone formation or resorption, nor do these cells divide or replicate. As they are placed within a rigid bone matrix, bone

cannot be remodelled from within the bone matrix, only from the peripheries of each osteon. Osteocytes survive for a long period within the matrix (in the range of several years) but cannot be replaced once they die until bone resorption and replacement occurs as the osteon reaches the surface of the bone/trabecula. Dead osteocytes are more commonly found in bone after the third decade of life and effectively reduce the efficiency of the osteocyte network, affecting diffusion through bone tissue [17, 19].

On the surface of bone can be found two primary cell types, osteoblasts and osteoclasts, responsible for the remodelling of bone through continual synthesis and resorption, respectively. Osteoblasts differentiate from osteoprogenitor stem cells present in bone marrow. They are responsible for synthesising collagen and organic macro molecules such as osteonectin, osteocalcin and various growth factors and proteases. As such osteoblasts are pivotal for the building and remodelling of bone as they lay down the organic matrix (termed osteoid) for the establishment of new compact bone. Osteoblasts also help promote mineralisation of osteoid by locally concentrating minerals such as calcium and phosphate ions using mechanisms such as osteocalcin production, and release of cellular vesicles containing bone-specific alkaline phosphatase, which can aid in the formation of hydroxyapatite [19].

Osteoblasts can be typically found on surfaces of forming or remodelling bone (including at the periosteum, endosteum or within vascular canals) or at the outer layers of osteons undergoing remodelling (see Figure 1.3). Once surrounded and locked in by the bone matrix they have constructed, they form into osteocytes [17, 19].

Along with exogenous factors such as mechanical loading, osteoblasts also regulate bone formation and turnover hormonally in a wide variety of mechanisms. Examples include producing receptors for parathyroid hormone and other promoters of bone resorption such as calcitriol (derived from Vitamin D_3).

Osteoblasts also regulate osteoclast differentiation and therefore influence bone resorption rates. For example, osteoblasts produce osteoprotegerin which restricts the development of osteoclasts. However, in the presence of parathyroid hormone, osteoblasts produce less osteoprotegerin and increase production of RANKL, a protein which binds with cell surface RANK on immature osteoclasts and encourages differentiation of more mature osteoclasts.

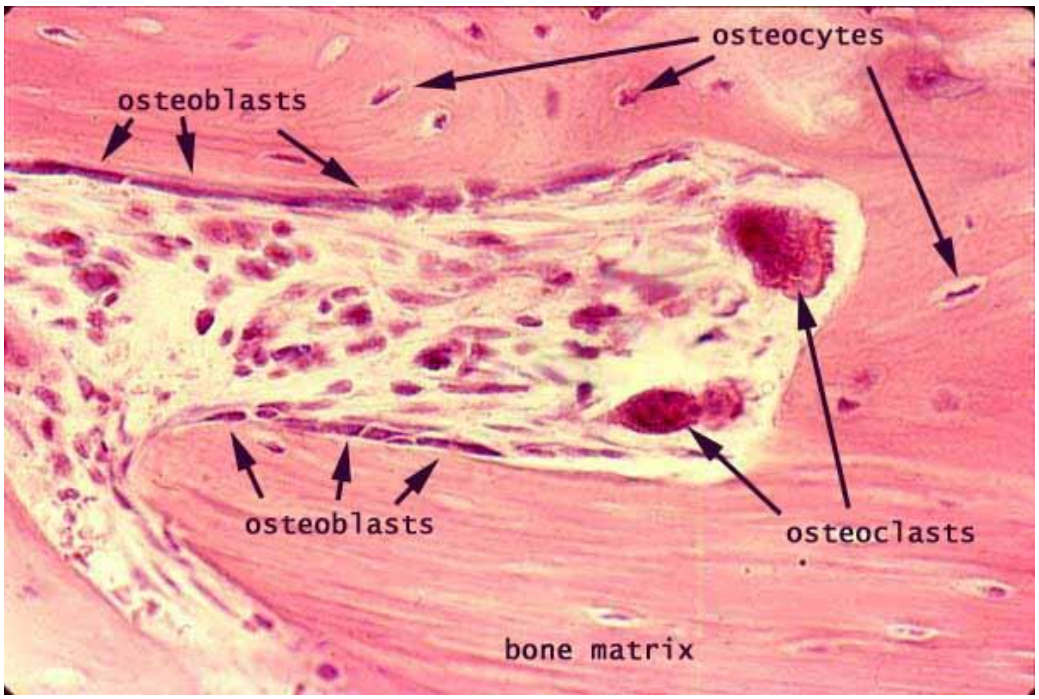

Figure 1.3: Micrograph of a typical "cutting cone" of cortical bone remodelling with osteoclasts resorbing bone and osteoblasts laying new bone matrix. Osteocytes are also seen contained within the bone matrix. Image sourced with permissions [24].

Osteoclasts are responsible for bone resorption and are also found on the surfaces of bone where bone remodelling occurs (See Figure 1.3). Osteoclasts play an important role in allowing bone remodelling by osteoblasts after resorption has occurred, initiated by the release of demineralising enzymes [25]. Osteoclast activity is controlled by various metabolic mechanisms including osteoblastic mediated signals and blood borne factors such as parathyroid hormone, calcitriol and calcitonin. Osteoclasts are formed from the fusion of monocytes in bone marrow, following a similar but distinct differentiation pathway to macrophages [17].

1.5: Vascular supply to bone

Blood flow within bone is critical just as in any other organ. In particular, blood supply to bone allows for transportation of key minerals and exportation of newly derived blood cells from haematopoietic marrow. Blood-borne hormones and signalling proteins also regulate bone turnover and play an important role in homeostasis [8].

Blood flow through cortical bone is primarily centrifugal (see Figure 1.4) [23]. Typically in long bone there is a primary vascular supply through a nutrient artery entering the diaphysis via a nutrient foramen in the cortical bone. Once in the medullary cavity the nutrient vessel bifurcates into ascending and descending branches towards the epiphyseal regions of the long bone with branching tributaries supplying the endosteal

surface [19]. Tributaries can then divide into cortical bone via Volkmann's canals and supply Haversian systems. Some larger canals will contain arterioles and venules, but most just have one capillary tributary [5].

The microvessels of cortical bone are typically continuous capillaries with transcapillary exchange diffusion limited rather than flow limited. Within cortical bone there is typically relatively wide differences between capillaries and osteocytes of up to 100µm. Microvessels are fenestrated sinusoids within the marrow of the medullary cavity, allowing newly derived blood cells and serum proteins to enter the microcirculation [23]. Microvascular density within bone is rarely reported quantitatively in either human or animal studies and is likely to be heterogenous both between bones of the body and within bones (such as between cortical bone, red marrow and yellow marrow). Oikawa et al 2010 also reports localised variability of microvessel density within haemopoetic marrow [26].

Towards the epiphysis, anastomosis of the terminal nutrient branches form with centripetal metaphyseal and epiphyseal vessels. These are generally supplied via local systemic and articular arterial branches with various nutrient foramen often visible in the non-articulating areas of the epiphysis, forming a richer blood supply then is found in the diaphysis [23]. Arteriole networks also form within the periosteum serving the outer lamellae and osteons of cortical bone centripetally. As such articulating surfaces and those areas of bone without a periosteal layer have comparatively poorer microvascular supply [5]. Irregular bones without a diaphysis such as the vertebrae may still have nutrient arteries supplying cancellous bone. Alternatively smaller bones may be supplied completely via periosteal centripetal supply [5].

Draining venules also follow Haversian and Volkmann canals and drain centripetally into venous sinusoids within the medullary cavity which supply a central venous sinus, which in turn drains into a central vein usually accompanying the nutrient artery through the nutrient foramen. Venous sinusoids play an important role in regulating intramedullary pressure within the rigid framework of cortical bone in combination with the presence of vasomotion and mechanical stressors on bone [18]. Alternatively, venules may drain centrifugally to the periosteal surface draining through venous plexuses in the periosteum [5].

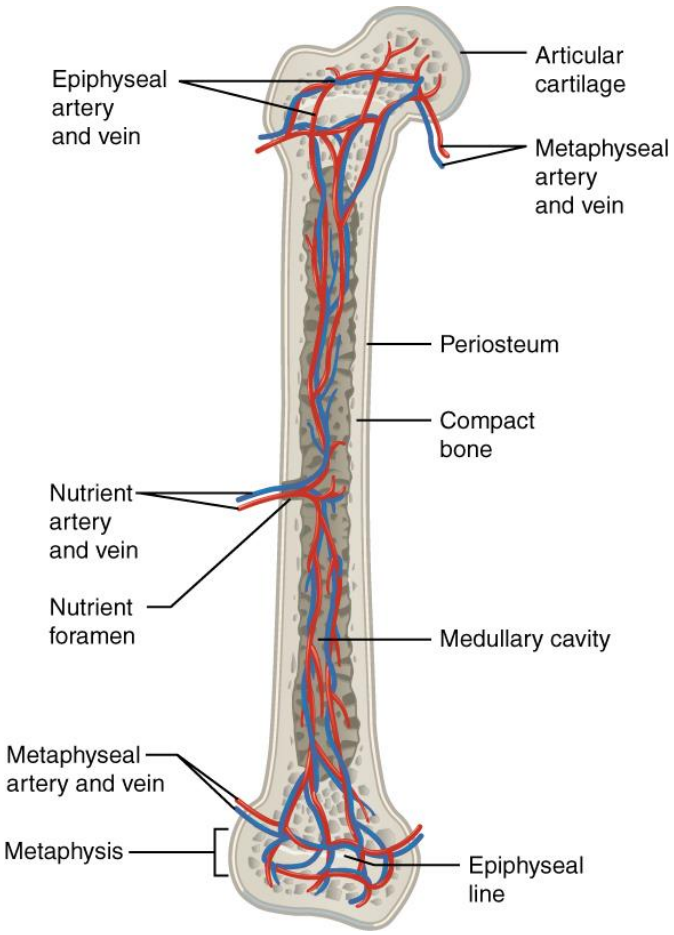

Figure 1.4: Typical blood supply to long bones. Reprinted with permissions from Betts et al 2013 [21].

1.5.1: Microvascular regulation of oxygen supply

Supplied by the vascular network described above, it is the role of the microvasculature to provide a constant supply of oxygenated red blood cells to supply oxygen to tissue through diffusion from capillaries to surrounding interstitial tissue. Cells will use this oxygen supply in the production of adenosine triphosphate (ATP) within mitochondria, providing energy for constant cell function. As a result it is vital that the microvasculature can regulate itself flexibly both systemically and locally in order to maintain its oxygen-providing homeostasis under a variety of conditions [27]. This is predominantly controlled through vasomotion (i.e. the dilation and contraction of microvessels) which in turn mediates the flow and volume of blood cells (and therefore oxygen) reaching tissue [28].

Laroche 2002 contends that intraosseous vessels are particularly distensible, particularly the venous circulation, having similar structure to the microvasculature of other parts of the body despite being within a rigid organ, allowing the critical homeostasis of intraosseous pressure [5]. Similarly the central sinus of the diaphysis

can distend fivefold in terms of volume before being drained by veins that essentially run parallel with the arterial network, including metaphyseal, epiphyseal and central medullary veins [5].

Systemically, vascular regulation is typically triggered by neural or humoral mechanisms [27]. Vasodilation and vasoconstriction in intraosseous vessels is in part mediated by sympathetic and parasympathetic nerve systems which run alongside vessels within Haversian canals [5]. For example, stimulation of sympathetic efferent fibres can trigger the release of norepinephrine leading to vasoconstriction, which decreases blood supply and drops intramedullary pressure [27].

Humoral mechanisms include vasoconstrictive responses to blood-borne hormones such as epinephrine and angiotensin [27]. Conversely hormonal factors such as the presence of parathyroid hormone (PTH) in blood can trigger vasodilation [5]. Both humoral and neural mechanisms will cause systemic effects in association with potential cardiac and respiratory changes [28].

Local changes in vascular supply to tissue can be categorised broadly into myogenic and metabolic responses. Myogenic responses involve reactions from the smooth muscle cells in arteriole walls responding to increases in intramural pressure with vasoconstriction. Conversely shear stress on the endothelium from blood flow may induce nitric oxide (NO) release from the endothelial lining causing smooth muscle relaxation and vasodilation [29]. NO also inhibits cytochrome c-oxidase, reducing the rate of oxygen consumption by mitochondria [27].

There are a number of metabolic pathways that trigger vasodilation when increased oxygen supply is required. For example, a lack of oxidative phosphorylation processes in tissue can lead to cellular production of adenosine, causing local vasodilation. During hypoxia, glycolysis occurs in the absence of adequate ATP production, with increased lactate as a by-product, also triggering local vasodilation. Increased carbon dioxide production as a by-product of oxygen consumption also vasodilates [27].

The nature of bone microstructure appears reliant on relatively high interstitial pressures. Movement of interstitial fluid is important for diffusion in bone given the relatively wide spacing of osteocytes within bone. Movement is driven by both mechanical stresses and this relatively high interstitial pressure [18]. In particular, mechanical loading causes increased interstitial pressures during compression and then decompression, promoting interstitial flow. This also causes shear stress on

osteocytes which have been shown to trigger osteogenesis in response via the release of NO and ATP, which suppresses osteoclast activity and aides osteoblast differentiation [8].

Whilst intraosseous microvessels are in a relatively unique environment within the body, evidence suggests that many typical vascular regulatory processes still apply. However, there are also unique physiological features of the intraosseous microcirculation being identified. It is theorised that angiogenesis and endothelial cells may be precursors to osteoblast cell differentiation [18]. Conversely, there is also evidence that osteoblasts can also trigger angiogenesis, strengthening the evidence that vascular function and bone self-regulation are inherently inter linked [8].

1.5.2: Altered states of bone metabolism

The strong link between vascular blood supply to bone and healthy bone metabolism is well established. Laroche 2002 contends that intraosseous vessels are comparable with the vasculature of any other organ, an exception being the increased distensibility of venules and venous sinusoids that allow regulation of intramedullary pressure. However, there may be unique mechanisms of vascular control in bone that are not fully understood (mainly due to the difficulty in measuring *in vivo* bone haemodynamics) and may contribute to bone pathologies [18]. It stands to reason that the vasculature of bone is also just as susceptible to vascular diseases such as atherosclerosis and thrombosis, which can lead to secondary effects on bone such as avascular bone necrosis if acute, or osteoporosis in more chronic pathogenesis [5].

What is known is that vascular supply to bone plays a key part in the regulation of bone formation and resorption. For example, it is known that those mechanisms which control angiogenesis within bone (triggers such as cytokines and growth factors) also trigger bone regulation metabolism [18]. Likewise arterioles lie at the centre of bone resorption bays suggesting they play the primary role in mediating resorption first, before reformative osteoblastic activity [5]. With respect to normal homeostasis, intraosseous blood flow may regulate by adjustments to flow in existing vessels or by angiogenesis of new vessels [5]. Kristensen et al 2013 observed an increased capillary density on the surface of cortical bone where active remodelling is taking place, demonstrating the importance of direct proximity of vascular supply with active cells, and the potential stimulus for osteoblast differentiation [30].

Relationships between altered vasomotion and blood flow with metabolic bone disease have been established, but the underlying mechanisms are not fully understood. Some examples relevant to this project are explored more in the following sub sections.

1.5.2.1: Osteoporosis

Osteoporosis is a chronic progressive bone disease characterized by a loss of bone mineral density (BMD) and structural integrity resulting in fragility fractures, defined as fracture occurring from a standing height fall or less. It is currently clinically diagnosed using dual energy X-ray absorptiometry (DXA) as a loss of BMD of more than 2.5 times less than the mean peak bone density for sex (i.e. a T-score of -2.5) [31]. The resulting increased risk of fragility fractures has wide ranging and increasing socioeconomic, morbidity, and mortality effects. The most common fracture sites are vertebral, at the hip, and distal radius. Indeed, there are approximately 300,000 fragility fractures in the UK each year, and with the growing elderly population, fragility fractures are predicted to cost the UK healthcare economy up to £2.2 billion by 2025 [32].

There is an epidemiological link between arteriosclerotic disease, reduced BMD and fracture incidence. The two occurrences have shared environmental risk factors such as poor diet, sedentary lifestyle and smoking [5]. However, there is also more direct evidence suggesting a causal link. Laroche et al. 1994 found significantly reduced unilateral BMD where peripheral arterial disease was identified in only one leg [33]. Several studies have demonstrated increased fatty involution and loss of arterioles in osteoporotic bone [5] including reduced capillary density at remodelling sites in osteoporotic bone [30]. Similarly Karampinos et al 2017 reported a corresponding higher fat fraction in many regions of long bones in those with osteoporosis, identified using MRI spectroscopy [22]. A higher fat fraction, and increased yellow marrow is conducive to reduced marrow perfusion and a lower capillary density. A number of MRI based studies have concluded an association between reduced bone perfusion, increased marrow fat percentage, and reduced BMD [34-37]. Mesenchymal stem cell production is also reduced in yellow marrow, reducing the potential development of formative osteoblasts [22]. McCarthy 2006 postulates that osteoclasts are sensitive to hypoxia, and therefore increased bone resorption may also be linked with poor vascular supply to bone [23].

1.5.2.2: Ageing

Natural ageing has been associated with a number of different intraosseous vascular changes, including decreased endothelial response, reduced capillary density, as well as increased risk of atherosclerosis and vascular calcification [18]. MRI has highlighted decreased haemodynamic markers and increased marrow fat percentage with age [34, 36]. There is also evidence from human bone biopsies that atherosclerotic processes may occur in intraosseous vessels first, and that these vessels are more prone to calcification, producing potential microvascular "dead space" that leads to areas of reduced bone health due to decreased regional vasomotion and microvascular permeability [38]. Reduced perfusion within the diaphysis of long bones has been reported to be associated with increased age, and this is believed to be suggestive that intraosseous vessels may be first affected, with older long bones having been shown to be more reliant on periosteal blood supply [38, 39] .

Whilst the physiological pathway is not definitively established, it is generally accepted that angiogenesis is a key trigger for osteogenesis and normal bone turnover, so it follows that with reduced age-related vascular function, reduced bone health may follow [18]. Findings from Bousson et al. 2012 support this with trabecular bone scores (a marker of architectural bone quality discussed in more detail in Section 2.4.2) observed to drop at an accelerated rate from the age of 65 [40].

1.5.2.3: Sex

Accelerated bone resorption in post-menopausal females is a commonly accepted phenomena that is widely agreed to be related to reduced oestrogen levels post menopause. Oestrogen reductions associated with menopause have been linked to both reduced BMD and the risk of cardiovascular disease [41]. Prisby et al 2017 argues a lack of oestrogen can degrade bone health by a failure of two key roles of oestrogen: 1) reducing osteoclast resorption activity, and 2) protection of vasomotor function in microvascular endothelial cells [8]. With regards to the latter, whilst endothelial dysfunction is linked with ageing, it may also be further accelerated in post-menopausal females, with studies demonstrating reduced vascular function with oestrogen depletion [42], and eventual decreases in capillary density [8]. Murine studies involving oophorectomy have demonstrated more directly that reduction of oestrogen levels may precipitate vascular dysfunction and reduced capillary density before changes to bone quality, suggesting a causal pathway [43, 44].

1.5.2.4: Type 2 Diabetes Mellitus (T2DM)

T2DM, although considered a disease of glucose regulation, is associated with wide-ranging derangement of metabolic and vascular homeostasis. Worldwide in 2014, approximately 422 million people had diabetes, of which approximately 90% had type two [45]. The prevalence of T2DM increases dramatically in ageing populations with around two-thirds of cases in those aged over 60 [32].

It is generally accepted that T2DM diagnosis confers an increased fragility fracture risk which has been shown to be dependent on the duration and severity of T2DM and different medications involved [46]. This is often an underestimated secondary effect of T2DM despite the increased morbidity and associated costs of fragility fracture, and the delayed healing and increased complication risk of those with T2DM [32].

Some of the increased fracture risk in those with T2DM may be accounted for by the increased risk of falling due to, for example, hypoglycaemia, peripheral neuropathy, nocturia, retinopathy or impaired vascular homeostasis leading to postural hypotension [32]. However, even allowing for increased falls risk, there does still appear to be a physiological link between reduced bone health and T2DM. This association is likely to be linked with bone metabolism and architectural bone quality, as T2DM appears not to affect BMD, and may even be protective of BMD (although this is likely to be confounded by increased BMI in people with T2DM) [32, 46].

People with T2DM have been shown to have poorer quality collagen fibres, increased bone porosity [47] and slower mineral apposition rates [46]. Leslie 2012 argues this decline is preferential in cortical bone, explaining increased fracture risk and poorer bone healing in the long bone extremities such as the radius and tibia [48]. Burghardt et al 2010 found that those with T2DM had increased cortical porosity, but increased trabecular thickness suggesting pathophysiological changes in distribution on bone mass, which may lead to impaired bone strength [49].

Potential physiological links between T2DM and bone health include reduced bone turnover and flawed bone matrix remodelling caused by reduced microvascular function associated with T2DM, which may prohibit the angiogenetic driven processes of osteogenesis. Chronic hyperglycaemia can lead to an increase in advanced glycation end-products, which is linked with decreased bone-forming osteocalcin production, osteoblast apoptosis, and increased osteoclastic activity. Hyperglycaemia may also increase oxidative stress and inflammatory processes within bone, and

glycosuria is associated with hypercalcuria, which can lower calcium levels, affecting bone quality [32].

Treatment of T2DM with thiazolidiones has been shown to increase the risk of osteoporosis by suppressing the differentiation of mesenchymal stem cells into osteoblasts. Treatment with insulin is associated with increased fracture risk and may have the unwanted secondary effect of stimulating osteoclasts [46]. However, metformin is generally considered to increase bone mass [50].

Many people with T2DM are prescribed statins to protect against the associated increased risk of cardiovascular disease and stroke. Statins are generally considered to provide a small but significant benefit to bone health [51], although this may be dose dependent and those at high risk of osteoporosis should be monitored in cases where higher doses of statin are prescribed [52].

T2DM is characterised by systemic microvascular disease, raising the question whether poor microvascular blood supply to bone reduces bone metabolism and bone strength, and if this predisposes people with T2DM to fracture, independent of BMD. Given the increasing incidence of T2DM in an ageing population, and the associated mortality and morbidity of fragility fracture, NIRS could play an important role in understanding this under researched mechanism of disease, informing better preventative treatment options and improving early prediction of those “at-risk” of fragility fracture in this sub-population. Lasschuit et al 2019 argues there is a demand for simple testing methods for those at risk of poor bone health independent of BMD [53]. This is especially important, as those with T2DM may not respond as well to current preventative osteoporosis treatments as those without T2DM [32].

1.6: The tibia

The tibia is of particular interest for this PhD project, being the predominant site of NIRS measurements. The tibia (see Figure 1.5) is the second longest bone in the body, second only to the femur. Its dimensions expand at either end, facilitating articulations with the ankle and knee joints, with the narrowest part of the tibial shaft around the junction of the middle and distal third [19].

The proximal tibia is expanded with two condyles forming superior articulations with the medial and lateral condyles of the femur. The proximal tibia also articulates postero-laterally with the fibula at the proximal tibiofibular joint. Between the tibial condyles superiorly is an irregular intercondylar area. Anteriorly between the condyles

is the easily palpable tibial tuberosity, which is a roughening of the bone where the patellar tendon attaches. This is roughly triangular in shape with the apex pointing distally. The apex of the tibial tuberosity is then continuous distally with the sharp anterior border of the tibial shaft [19].

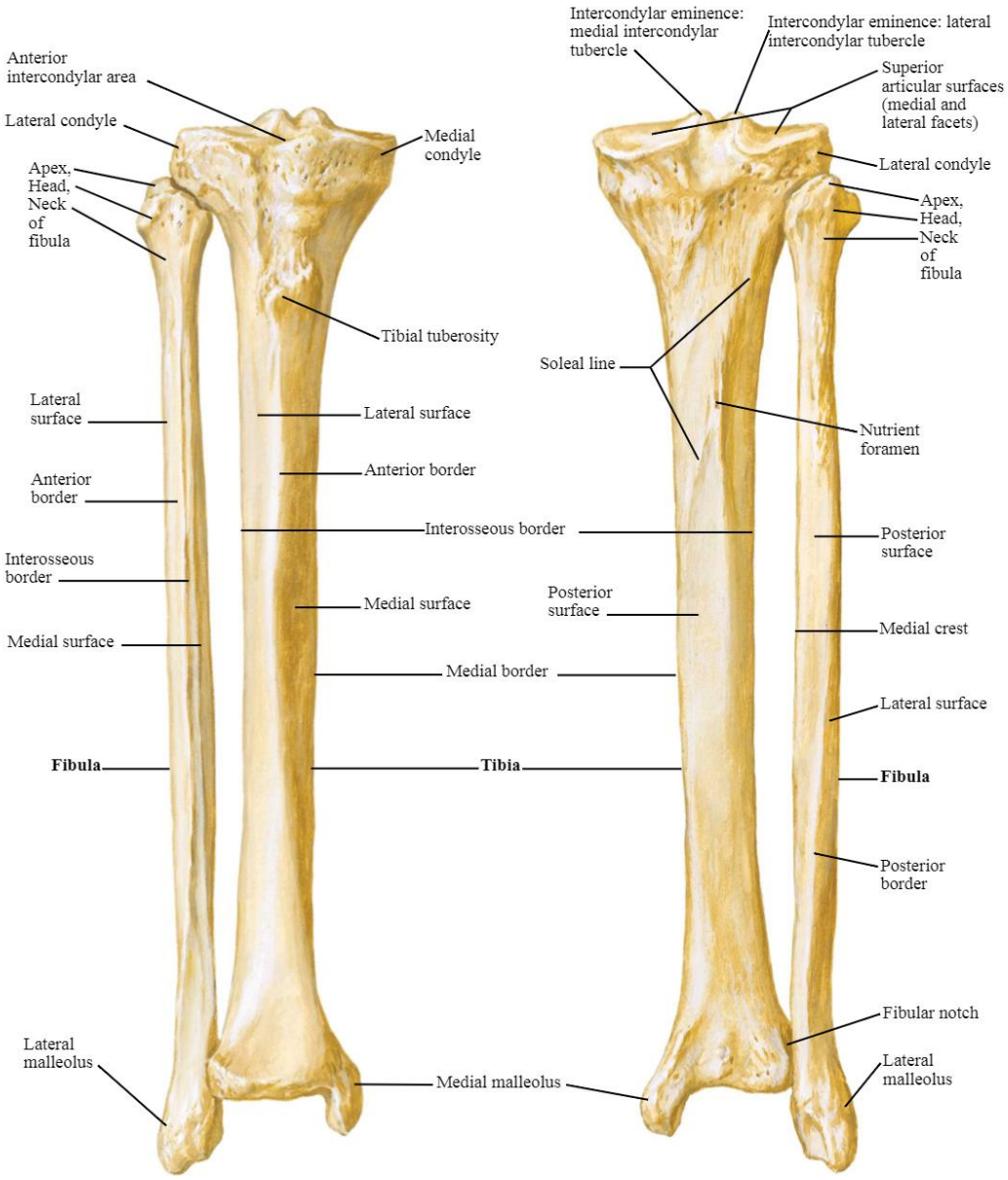

Figure 1.5: Anatomical landmarks of the tibia. Reproduced with permissions from Netter 2014 [54].

The shaft or diaphysis of the tibia is broadly triangular with anteromedial, anterolateral and posterior facing surfaces. These are demarcated by anterior, medial, and lateral (interosseous) borders. The lateral border is the attachment point for the interosseous membrane connecting the tibia and fibula for most of its length. The anterior border is easily palpable and continuous with the anterior margin of the medial malleolus. Both the anterior border and anteromedial surface are subcutaneous with the anteromedial

surface forming a broad and smooth plane. The medial border is also palpable on most individuals. It begins at the medial surface of the medial condyle and continues to form the posterior margin of the medial malleolus. The posterior surface has a distal-medial line running at the point of attachment of the soleus (marked as the soleal line on Figure 1.5), with the nutrient foramen of the tibia usually on the posterior surface at the distal end of this line, around where the proximal third of the tibia meets the middle third [19].

The distal third of the tibia again begins to expand forming anterior, medial, posterior, lateral, and distal surfaces. The lateral surface facilitates distal articulation with the fibula via the fibular notch concavity. The distal surface is saddle shaped and articulates directly with the talus. The anteromedial surface of the tibia is continuous with the medial surface of the distal tibia which becomes prominent at the medial malleolus. The medial malleolus is the most distal extension of the distal tibia. It is subcutaneous and articulates with the medial surface of the talus as well as being a point of attachment for the deltoid ligament [19].

1.6.1: Relevant tibial vasculature

Figure 1.6 demonstrates the main arterial supply of the tibia. The popliteal artery is continuous distally with the femoral artery and passes through the intercondylar fossa of the femur before branching into the anterior and posterior tibial arteries at the level of the proximal tibial metaphysis. It also gives rise distally to various genicular branches that anastomose to supply the proximal tibia, distal femur and patella. Local muscle and cutaneous tissue posterior to the knee are supplied by cutaneous, sural and muscular branches [19].

As the anterior tibial artery is a branch of the popliteal artery, it initially starts posteriorly before traversing through the oval aperture at the proximal interosseous membrane and travelling anteriorly to the intraosseous membrane closest to the anterolateral surface of the tibia, and beneath the tibialis anterior muscle. Distally it goes on to become the dorsalis pedis artery. The anterior tibial artery has several branches. The posterior tibial recurrent artery and anterior tibial recurrent artery help supply the proximal tibiofibular joint and the knee joint, also anastomosing with genicular branches of the popliteal artery. Distally anterior medial and lateral malleolar arteries supply the ankle joint. Several muscular branches and perforating branches also supply local muscle and skin tissue [19].

The posterior tibial artery is the other major branch arising from the popliteal artery. It courses closely with the tibial nerve, running distally through the flexor compartment, medio-posteriorly within the lower leg, and posterior to the tibialis posterior muscle and posterior surface of the tibia. Distally it diverts into the medial and lateral plantar arteries of the foot. Superficially covering the posterior tibial artery lies the soleus and gastrocnemius muscles [19].

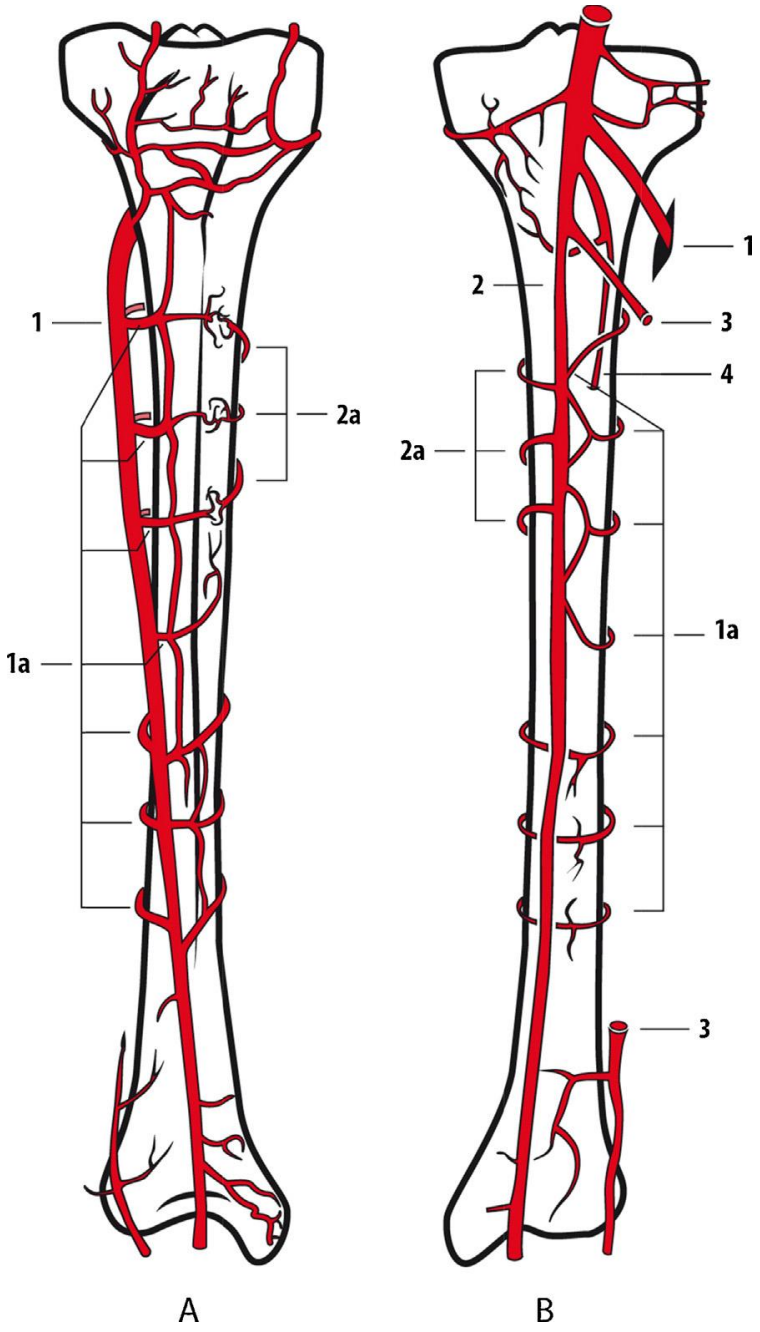

Figure 1.6: Anterior view (A) and posterior view (B) of the lower leg arterial blood supply. This figure demonstrates the anterior tibial artery (1) and branches (1a); the posterior tibial artery (2) and branches (2a); the peroneal artery (3); and, the nutrient artery (4) prior to entering the medullary cavity through the cortex of the tibia. Reproduced with permissions from Santolini et al 2014 [55].

The posterior tibial artery gives rise to the nutrient artery of the tibia soon after its origin. This enters the tibia at the posterior surface around where the proximal and middle thirds of the tibia meet, landmarked by the distal extent of the soleal line. Some normal variants include branches of the anterior tibial artery or branches at the level of the popliteal bifurcation becoming the nutrient artery of the tibia. Once entering the shaft of the tibia this nutrient artery bifurcates into ascending and descending branches [(55)].

The circumflex fibular artery also supplies the proximal tibia and knee joint structures. It passes around the neck of the fibula and also anastomoses with genicular arteries arising from the popliteal. The posterior tibial artery also gives rise to several muscular and perforator branches to supply local muscle, fascia and cutaneous tissue. Distally, medial malleolar and calcaneal branches anastomose to supply soft tissue in this area [(19)].

The peroneal artery is a branch of the posterior tibial artery that runs obliquely along the medial crest of the fibula, deep to the soleus and posterior to the intraosseous membrane, towards the distal tibiofibular joint where it branches into calcaneal branches supplying the tarsal, and posterior and lateral areas of the calcaneus and surrounding soft tissue. Again the peroneal artery has muscular and perforator branches. It also provides a nutrient artery supplying the fibula and entering at the middle third of the fibula [(19)].

Deep venous return follows the anterior and posterior tibial arteries with anterior and posterior tibial veins. These communicate via perforator veins with superficial venous return facilitated by the greater and lesser saphenous veins. The greater saphenous vein runs the length of the leg medially over the medial malleolus and medial condyle of the femur to drain into the common femoral vein. The small saphenous vein runs laterally around the lateral malleolus and then courses posteriorly between the heads of the gastrocnemius muscle to typically drain into the popliteal vein around the level of the knee joint [(19)].

1.6.2: Superficial muscles of the leg

The gastrocnemius is a dual headed bipennate muscle. It has a medial and lateral head which attaches at the medial and lateral condyle of the femur, respectively. Both heads merge distally to form the Achilles tendon which attaches at the posterior calcaneus at the calcaneal tuberosity. The soleus muscle also forms part of this tendon distally as well as attaching to the posterior surface of the tibia at the soleus line. These

two muscles form the bulk of the muscular volume of the lower leg and are demonstrated in Figure 1.7. The tibialis anterior is also often observable lateral to the anterior border of the tibia [19].

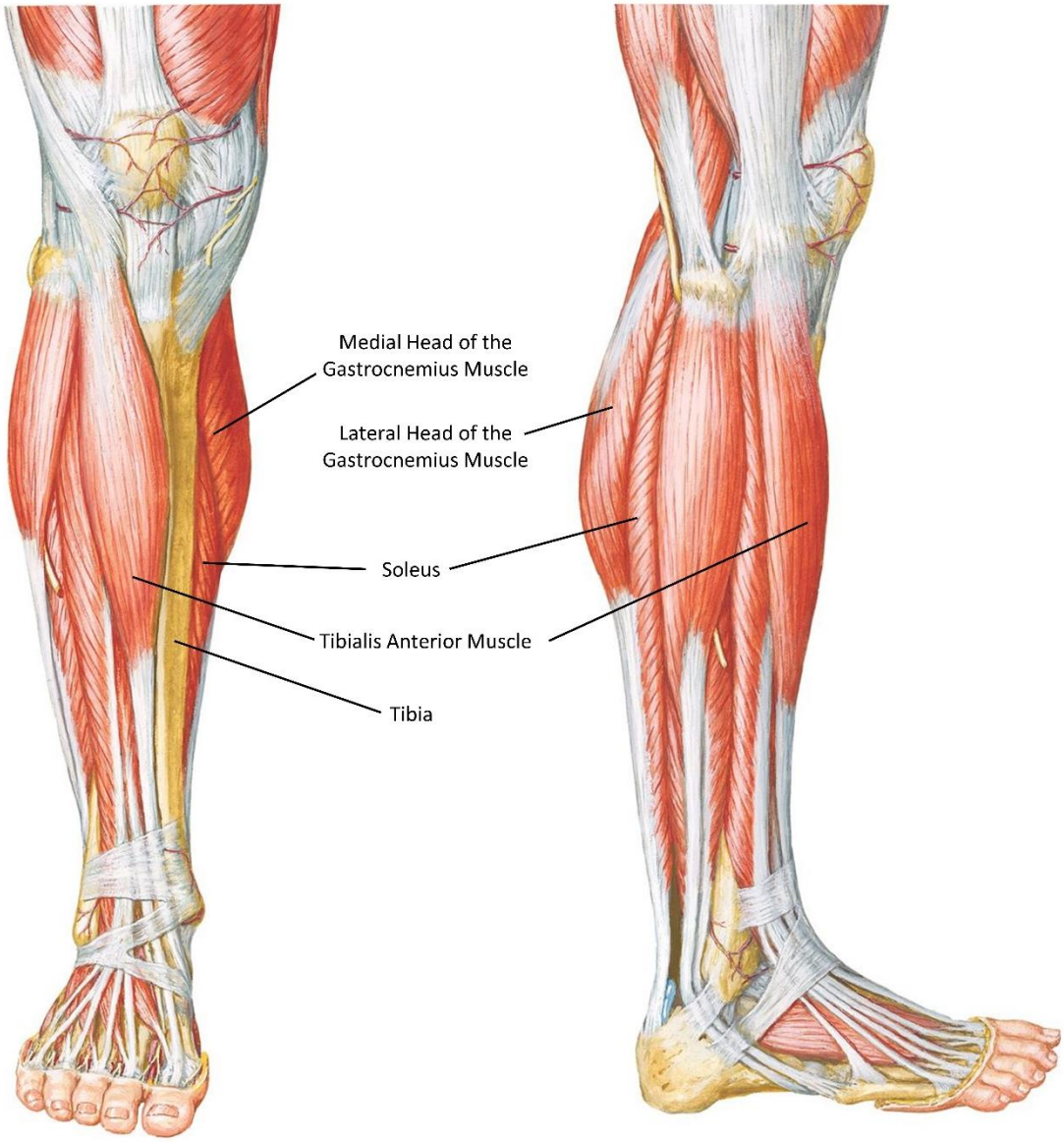

Figure 1.7: Illustration of relevant muscles of the lower leg. Reproduced with permissions from Netter 2014 [54].

1.7: Rationale for the PhD project

As discussed in this chapter, there is a clear rationale for further research into the vascular supply of bone tissue, with indirect evidence that poor vascular supply in bone is associated with poor bone health [18]. At the same time, it is evident that measuring bone haemodynamics is difficult [6], and the limitations of existing methods are discussed in more detail in Chapter 2. If successful, NIRS technology has the potential to become an inexpensive, fast and effective way to measure blood supply to bone

that is safe for the participant. This could be useful when researching common bone diseases like osteoporosis, poor fracture healing, arthritis and potentially blood-borne cancers like leukaemia [6, 13, 56].

The structure and methodological approach of this PhD project has been designed in consideration with the Medical Research Council (MRC) Complex Interventions Framework [57]. This suggests development of an intervention or test by four main stages: development; feasibility/piloting; evaluation; and, implementation (outlined in Figure 1.8).

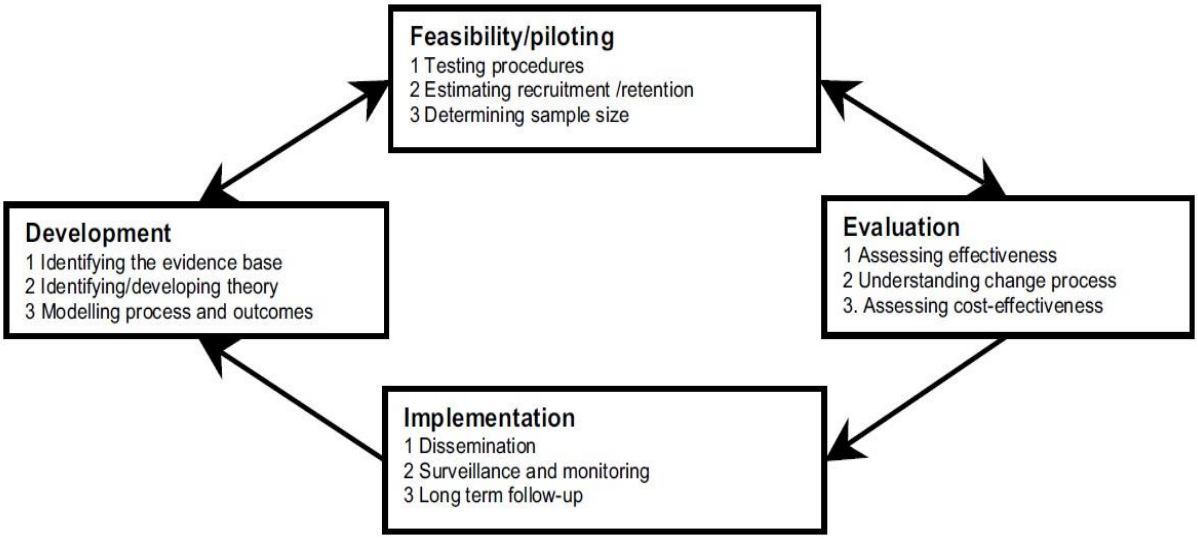

Figure 1.8: Key elements of the development and evaluation process from the Medical Research Council Complex Interventions Framework 2008 [57] (reproduced from Craig et al 2008 with permission).

Using this model, "development" has taken the form of a systematic review of the use of near infrared (NIR) technologies when measuring haemodynamic markers in human bone tissue *in vivo* in order to establish existing knowledge on the topic and guide further studies.

This process fed into "feasibility" in the form of protocol development to demonstrate whether the available NIRS equipment (Hamamatsu NIRO-200NX, discussed in Section 2.2.1) could be used in a way that warranted further evaluation. This included establishing preliminary evidence that NIRS measurements are able to potentially represent bone tissue haemodynamics, the ideal anatomical location for measurements, that protocols that are tolerable to participants, and that protocols appear potentially reliable enough to warrant formal evaluation. Suitable protocols were developed that are in line with existing local use of the equipment at the University

of Exeter Diabetes and Vascular Research Centre (DVRC) and the existing evidence base.

"Evaluation" was then undertaken in a representative population using NIRS via the validation and reliability aspects reported in this PhD thesis [57]. Reliability evaluation includes inter and intra operator reproducibility assessments. Validation of NIRS was also attempted through evaluation of NIRS results against MRI sequences including dynamic contrast enhanced MRI (DCE-MRI). This will assess for any correlation between NIRS measurements and this reference standard measuring markers of gross perfusion and blood volume in bone. NIRS results were also compared against other markers of bone health including bone density, blood markers of global bone metabolism and trabecular bone scoring (TBS).

The discussion in this thesis includes consideration of the required improvements and research required before "implementation" of NIRS in further post-doctoral research [57]. Feasibility data for the recruitment of participants with T2DM for the potential research applications of NIRS for measuring bone health in this sub-population has also been considered via recruitment of participants with and without T2DM (matched for age, sex, BMI and ethnicity).

1.8: Overview of PhD Project

Chapter 2 of the thesis explores in detail the current available methods of measuring *in vivo* haemodynamics in bone tissue using NIR and imaging modalities, with particular focus on NIRS technology. This chapter also describes the other measures of bone health utilised in this project.

Chapter 3 presents a systematic review of the existing evidence base around the use of NIR technologies for measuring *in vivo* haemodynamics in bone tissue. This work sets the foundation for the PhD project by outlining the gaps in the evidence base that require addressing.

Chapter 4 provides the methodological detail for the protocol development component of the PhD project. This includes the development of suitable protocols for NIRS testing of the tibia, the results of which are presented in Chapter 5.

Chapter 6 presents the methodological approach taken for the reliability assessment of NIRS measurements taken at the proximal tibia (with results presented in Chapter 7) and the approach to validating NIRS measurements against external comparators

of bone health. Chapters 8, 9 and 10 present results on this attempted validation. As feasibility work, this allows judgement on whether there is potential for NIRS to be a useful research tool warranting further investigation. Chapter 11 summarises the thesis and draws conclusions relating to the initial aims and objectives of the project discussed above in Section 1.2. This includes recommendations for future research on the topic.

Chapter 2: Measuring bone health

2.1: Overview

Chapter 1 has outlined the anatomy and physiology of bone tissue and the role of macro and micro vascular function in the metabolism of bone tissue. This chapter will outline existing methods for measuring bone tissue haemodynamics using near infrared (NIR) systems (Section 2.2) and imaging modalities (Section 2.3), as well as other commonly used tests of bone health relevant to this thesis (Section 2.4).

2.2: Measuring bone haemodynamics with NIR systems

This section will explore current research methods for measuring haemodynamic markers of bone tissue in humans *in vivo* utilizing three commonly used approaches involving NIR light systems: Near Infrared Spectroscopy (NIRS; Section 2.2.1); Photoplethysmography (PPG, Section 2.2.2); and, laser Doppler flowmetry (LDF; Section 2.2.3). Although not used in the experimental components of this PhD project, PPG and LDF are introduced as they are relevant to the systematic review presented in Chapter 3.

2.2.1: Near infrared spectroscopy (NIRS)

In the broadest sense, NIRS involves the use of multiple near infrared (NIR) wavelengths to provide spectroscopic information on the concentrations of chromophores that contribute to a material of interest. In this context, a chromophore is any compound that attenuates (i.e. absorbs and scatters) different NIR wavelengths of light in a predictable manner [(2)]. The NIR range is a small window of infrared wavelengths (700-1000nm) near visible red light on the electromagnetic spectrum (hence “near infrared”), whereby most tissue types are comparatively less attenuating and more “transparent” to these wavelengths [(58)].

The ability of NIRS to measure compounds with known attenuation characteristics means NIRS has quality control applications in agriculture, pharmaceuticals and manufacturing [(58)]. In particular the ability of NIRS to measure dynamic changes in haemoglobin oxygenation status has made NIRS attractive as a medical research tool. This use of NIRS systems was first described in 1977 by Jobsis for use in measuring cerebral oxygenation [(59)]. There are now wide ranging medical research applications using NIRS, predominantly including cerebral oxygenation monitoring, muscle physiology research, and microvascular studies of the skin [(58)].

NIRS offers a medical research tool that allows relatively inexpensive, portable, safe, non-invasive haemodynamic measurements that can be taken in continuous real time on *in vivo* tissue during interventions. This offers advantages over the inherent logistical and analytical limitations of other methods of measuring haemodynamics involving medical imaging modalities (outlined in Section 2.3). Unlike these modalities, NIRS also offers oxygenation information otherwise only identifiable via blood samples, which are typically invasive to obtain [6].

Figure 2.1 presents the Hamamatsu NIRO-200NX system that was used in this PhD project. This NIRS system essentially comprises a central processing unit and two optodes. The first optode is capable of producing several monochromatic wavelengths of NIR light using semiconducting LED laser diodes. Pulses of different wavelengths can be applied rapidly (i.e. less than 100 nanoseconds in duration) providing virtually simultaneous measurements [2]. The second optode detects NIR light photons that have been transmitted through tissue using two photodiodes. Photodiodes are ideal as they are small and compact with high quantum efficiency, sampling at frequencies of up to 20 Hz [60].

(a)

(b)

(c)

Figure 2.1: These images demonstrate the Hamamatsu NIRO-200NX equipment that the PhD project used. (a) demonstrates the near infrared emitting sensor optode (left) and the detector optode (right) housed in a optode holder; (b) shows the optodes connected with the system components; (c) demonstrates typical positioning of the optodes for measurement of the tibial diaphysis.

When applied to tissue, light from the source optode may be absorbed by tissue (with energy transferred to thermal energy), scattered within tissue (typically elastically without energy loss), or transmitted through tissue without interaction. When probes are placed in "reflectance" mode (as per this PhD), with probes placed in parallel a short distance apart (typically up to 5cm maximum [61]), photons detected by the receiving optode will be those which have scattered within the "banana shaped" tissue volume between the probes [6]. As such NIRS measurements are representative of this volume of tissue. This is schematically represented in Figure 2.2 below.

NIRS technology itself poses no appreciable risk to the participant as it uses near infrared non-ionising wavelengths of light. The Hamamatsu NIRO-200NX system is a class 1M laser, meaning tissue heating caused by laser use is negligible, and minimal specific safety requirements are required for its usage [61]. Section 2.2.1.2 below describes in more depth how NIRS systems calculate haemodynamic markers based on the absorption spectrum of oxygenated haemoglobin (O_2Hb) and deoxygenated haemoglobin (HHb).

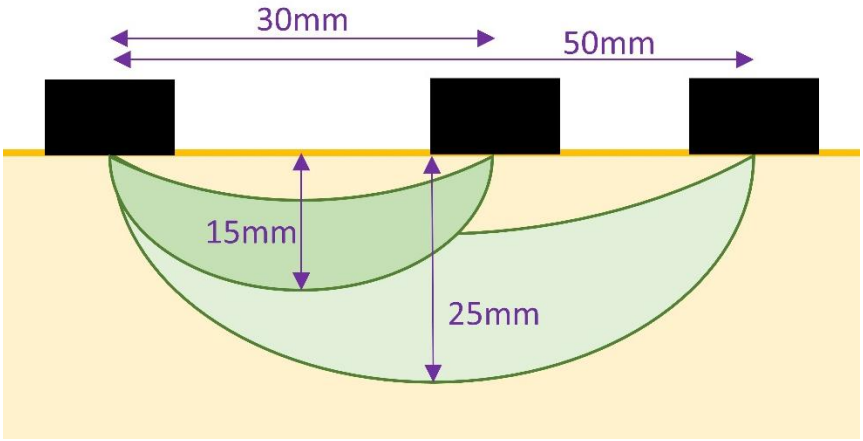

Figure 2.2: When the source optode is applied to tissue, light will be scattered in all directions, but the detector optode will detect photons from the "banana-shaped" volume between the two optodes [6]. Increased distance between the optodes will increase the depth of measurements but lead to greater attenuation of the emitted NIR light. The maximum depth measured has been evidenced to be around half the interoptode spacing [2, 10].

2.2.1.1: Relevant chromophores

Prior to explaining the methodological approaches NIRS uses to measure haemodynamics in more depth, it is important to consider the properties of those organic chromophores of interest that will contribute to the attenuation of NIR light. NIRS can take advantage of the known differences in scattering and absorption

characteristics of different chromophores to measure changes in their concentration within tissue so long as there is an abundance of the chromophore in the tissue sampled. The absorption and scattering characteristics of the chromophore also need to be well defined, and can be quantifiably represented with the specific extinction coefficient of the chromophore [2]. This coefficient is also dependent on the specific wavelength of NIR light employed [62].

NIRS becomes particularly useful when assessing chromophores which vary in concentration in relatively short spans of real time, such as O_2Hb and HHb [62]. Haemoglobin is a protein found abundantly in red blood cells, with the primary function of transporting oxygen. Each haemoglobin unit has four reversible binding points for oxygen molecules [27]. Red blood cells (RBC) make up 40-45% of blood by volume, with haemoglobin making up around 33% of RBC mass. Thus, haemoglobin is a suitable indicator for blood haemodynamics. Both types of haemoglobin are mostly transparent to light between 650-1000nm, however crucially there is differences in the attenuation profile of O_2Hb and HHb at different wavelengths of NIR light (see Figure 2.3). This allows NIRS systems to tease out the differing contributions of each chromophore to attenuation of each wavelength of NIR light applied, using the methods outlined below in Section 2.2.1.2 [2, 62].

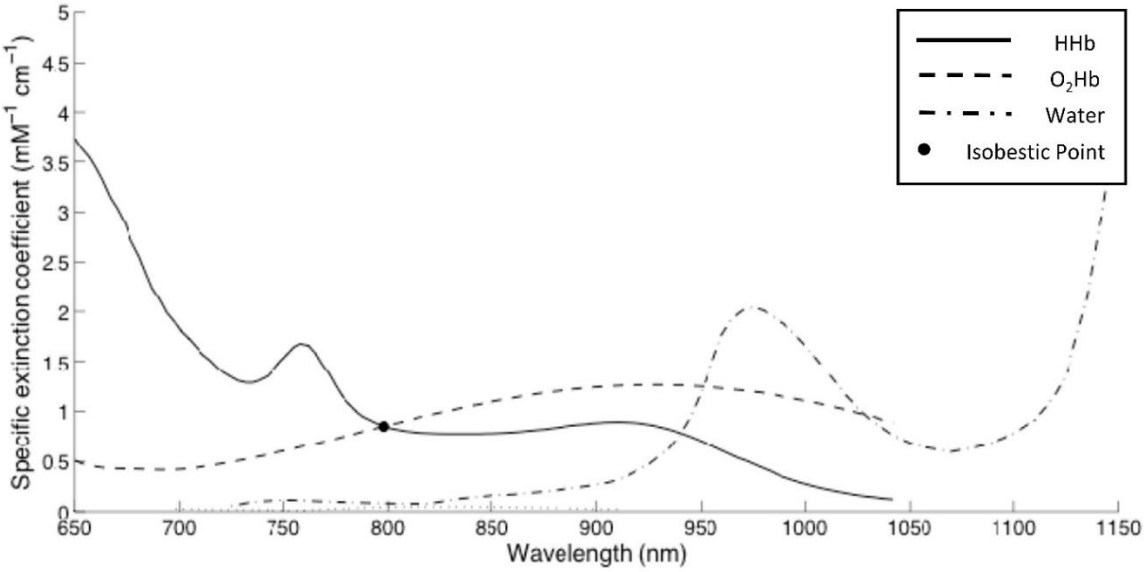

Figure 2.3: Specific extinction coefficients of deoxygenated haemoglobin (HHb), oxygenated haemoglobin (O_2Hb) and water at different wavelengths of NIR light. The specific extinction coefficient of HHb and O_2Hb are equal (i.e. isobestic) around 800nm. Water increasingly attenuates NIR light greater than 900nm, making NIRS less feasible at these greater wavelengths. Reproduced from Bakker et al 2012 with permissions [62].

It can be seen from Figure 2.3 that HHb has a higher specific extinction coefficient than oxygenated haemoglobin at the frequencies of red visible light (~680nm). This explains why arterial blood is predominantly bright red (i.e. it is relatively transparent to red wavelengths) whilst venous blood is more tinged blue/purple (as it attenuates red wavelengths more efficiently) [58]. This colour difference can be used as an analogy for how NIRS differentiates between chromophores based on differences in attenuation of NIR wavelengths either side of the isobestic point of approximately 800nm (i.e. the wavelength where attenuation is comparable between both oxygenated and deoxygenated haemoglobin). Utilising the 800nm isobestic wavelength can also be used to calculate total haemoglobin concentration independent of oxygenation status [63].

It should be noted that other related forms of haemoglobin exist, such as carboxyhaemoglobin, haemiglobin, and sulfhaemoglobin. However these are all found in low concentrations in human blood and are estimated to contribute less than 1% to NIR attenuation [2].

Cytochrome c-oxidase (CCO) is also a potential chromophore of interest as it has oxygenated and deoxygenated forms, and is an essential component of the oxygen metabolism cycle of mitochondria [27]. Thus obtaining measurements of changes in CCO concentration could provide indications of direct cellular oxygen consumption, as opposed to the indirect haemoglobin markers of vascular oxygen supply to tissue [62]. Unfortunately, CCO is difficult to monitor as it is less abundant (contributing approximately one tenth of the attenuation to NIR signal) and with a less distinctive attenuation spectrum across NIR wavelengths [64]. Monitoring CCO remains an area of interest for future NIRS technology development, and is discussed further in Chapter 11.

Myoglobin is another potentially relevant chromophore for NIRS measurements as a protein responsible for storing oxygen in muscle tissue. The absorption spectrum of oxygenated and deoxygenated myoglobin are indistinguishable from O_2Hb and HHb, however oxygenation concentrations within myoglobin will only change with oxygen saturation (sO_2) values typically below 25%. It is generally accepted myoglobin does not contribute significantly to NIRS signal changes in muscle, and remains constant even during ischaemic muscle challenges such as exercise or induced occlusions [65, 66]. This has been confirmed using NIRS alongside MRI spectroscopy [63].

There are a number of other chromophores which contribute to the attenuation of NIR wavelengths, but are not affected by oxygenation status. Vascular NIRS measurements are based on an assumption that the attenuation of NIR light by tissue is expected to be constant and unaffected by oxygenation changes, outside of vascular related changes. This includes chromophores such as water, lipids, and melanin.

Water and lipids have a relative window of transparency of 200nm to 900nm. As human tissue has such a high combined concentration of both, this effectively limits NIRS to a maximum 900nm wavelength. However between 200nm-900nm wavelengths the absorption profile of water and lipids is effectively constant, and not expected to change dynamically [(2)].

Melanin is another relevant attenuating compound found in the epidermis of the skin. This will be constant for within subject measurements but may need considering when comparing participant results of different ethnicity (although all participants in this project were Caucasian) [(62, 67)].

2.2.1.2: Principles of NIRS

As introduced in Section 2.2.1, NIRS utilizes NIR wavelengths that are comparatively transparent in tissue. However even at NIR wavelengths, attenuation is dominant with an approximate 1.0×10^{-6} % transmission rate (i.e. one photon of NIR light is transmitted through tissue for every 100 million photons based on typical reflectance NIRS usage as in this project) [(2)].

With respect to attenuation, the ability of a specific tissue within a volume to absorb and scatter NIR light will be dependent on the specific wavelength of light and the properties of the tissue's inherent chromophores (such as the concentration of the chromophores in tissue and their molecular mass and surface area). Elastic scattering is generally the more dominant photon interaction, attributing around 80% of interactions in tissue. However, as photons are scattered in essentially random directions a NIRS light detector will receive less photons, with the result being an effective contribution to attenuation that is greater than absorption interactions alone [(2)].

Table 2.1 presents representative absorption and reduced scattering coefficients of different tissue types found in the evidence base, although it should be stressed that these values can differ depending on the wavelength of NIR light, between individuals, and even within individuals at different anatomical sites [(68)]. Table 2.1 demonstrates

that bone (i.e. skull) is comparatively transparent compared with other tissue types (as indicated by the absorption coefficients demonstrated). This is evidenced in practice by the common use of NIRS for non-invasive cerebral measurements despite the need for NIR light to travel through two layers of cortical skull bone. This suggests the use of NIRS for measuring bone tissue is feasible in principle.

Table 2.1 also demonstrates that bone does have a comparatively high reduced scattering coefficient. This is partly explained by the probability of scattering events also incorporating the influence of different densities within tissue, causing light refraction. Thus light photons travelling through bone tissue are more prone to scattering events due to the relative heterogeneity of this tissue type [2].

Table 2.1: Summary table of the absorption and reduced scattering coefficient of different tissue types used by Niwayama et al 2018 in their modelling study. Reproduced with permissions [68].

Tissue	Reduced scattering coefficient μ_s' (mm^{-1})	Absorption coefficient μ_a (mm^{-1})
Scalp	1.3	0.020
Skull	2.0	0.010
Cerebrospinal fluid	0.3	0.002
Gray matter	1.6	0.035
White matter	5.0	0.015
Skin	1.3	0.020
Fat	1.2	0.003
Muscle	0.7	0.025

With the known attenuation properties of different chromophores of interest, NIRS technology can quantify changes in haemoglobin concentration using several different approaches. Measurements made by the Hamamatsu NIRO-200NX used in this study are primarily based on two approaches; the Modified Beer Lambert Law (MBL; discussed in Section 2.2.1.3), and Spatially Resolved Spectroscopy (SRS; discussed in Section 2.2.1.4). Some other emerging approaches to NIRS measurements relevant

to the systematic review presented in Chapter 3 will also be briefly described in Section 2.2.1.6, including frequency domain, time resolved, and diffuse correlation spectroscopy systems.

2.2.1.3: The modified Beer Lambert (MBL) law

The MBL law is an approach to deriving NIRS measurements adapted from the Beer Lambert Law, which calculates the intensity of light that remains (or that should be detected) due to absorption after an incident intensity of light is directed at a volume of interest. It is intuitive that if an intensity of NIR light (I_o) was directed at a volume containing only one chromophore capable of only absorbing NIR light (and not scattering), then the intensity of light leaving the volume (I) would be dependent on:

- The absorption properties of the chromophore, as indicated by a specific extinction coefficient for a specific wavelength of NIR light (ε) measured in $\mu M^{-1}cm^{-1}$;

- The concentration of the chromophore in the volume (c), in µMolar; and,

- The thickness of the volume (i.e. the distance between the light source and detector), in centimetres (d).

As such the Beer Lambert Law states:

$$A = log_{10}\left(\frac{I}{I_o}\right) = \varepsilon.c.d \qquad \text{[Eq. 2.1]}$$

Where A represents the amount of absorption of light from the volume in arbitrary units of optical density. This is a logarithmic unit demonstrating the magnitude of the reduction in light intensity, and is therefore unitless. It is worth noting that with a known volume thickness and specific extinction coefficient, the concentration of the chromophore can easily be derived from the recorded change in intensity caused by attenuation [(2)].

In the more complex case of several different NIR attenuating chromophores being present in the volume, total absorption is simply calculated using a sum of the absorption caused by each chromophore:

$$A = [\varepsilon_1 . c_1 + \varepsilon_2 . c_2 + \cdots \varepsilon_n . c_n]d \qquad \text{[Eq. 2.2]}$$

However, adding to the complication of measurements using the Beer Lambert Law is that both scattering and absorption interactions occur within human tissue, with scattering much more probable than absorption in human tissues (approximately 80%

of interactions) [2]. To allow for this high scattering, the Beer Lambert law is modified (i.e. the Modified Beer Lambert (MBL) Law) to include an additive term (G) to allow for the attenuation effect of scattering, and a multiplier to allow for the added distance travelled by photons due to multiple elastic scattering events. The latter is called the differential pathlength factor (B) and again is dependent on the specific wavelength of NIR light used [62]. Calculations for B in soft tissues such as brain and muscle have produced results for B ranging approximately from 3.57 to 6.26 [2], meaning photons travel approximately 3 to 6 times further on average then the direct pathlength between source and detector.

So the Modified Beer Lambert Law applied for attenuation in a homogenous material becomes:

$$A = log_{10}\left(\frac{I}{I_o}\right) = \varepsilon.c.d.B + G \qquad \text{[Eq. 2.3]}$$

Where the specific extinction coefficient (ε) of attenuation now incorporates both absorption and scattering properties of a specific chromophore [16].

A notable limitation of the modified Beer Lambert Law is that G cannot be reliably calculated without knowing the reduced scattering coefficient of the medium and the precise measurement geometry of photon pathways. This is rarely achievable *in vivo* outside of controlled conditions. As such, absolute concentration of chromophores can no longer be derived using Equation 2.3. However if G is assumed to remain constant during measurements then absolute changes in chromophore concentration can still be calculated relative to the starting point of measurements. For example, if more of a chromophore (such as O_2Hb) is added to a volume, and factors ε, d, B and G are assumed to remain constant, the change in attenuation of NIR light will be proportional to the absolute change in chromophore concentration [2]. Therefore,

$$\Delta A = \varepsilon.\Delta c.d.B \qquad \text{[Eq. 2.4]}$$

Should G and B be estimated prior in controlled conditions, calculating absolute chromophore concentration is still possible, but this remains rarely reported in the literature, and so limited reference information on the scattering properties of different tissue types and their interactions with NIR light exist. Specifically, calculating B in bone tissue will be very complex due to the heterogeneity of bone (and is yet to be done as far as literature searches indicate). Even in homogenous tissue types differential pathlength is variable and depends on a number of factors including the

wavelength used, the reduced scattering coefficient of tissue, optode geometry, and is also likely to change with dynamic blood volume changes [62, 69].

When trying to calculate the changes in chromophore concentration of several chromophores (such as oxygenated and deoxygenated haemoglobin), the attenuation changes at several wavelengths (e.g. 735, 810 and 850nm using the Hamamatsu NIRO-200NX system [60]) can be utilised to produce simultaneous computations involving a matrix algorithm. Whilst absolute concentrations of chromophores are not able to be calculated, absolute changes in chromophore can be expressed (in µMolar) from an arbitrary zero point set by the user at the start of the measurement period. With use of the Hamamatsu NIRO-200NX in this project, measurements have been made without a differential pathlength factor being indicated, meaning measurements are taken in µMolar.cm. This is because an accepted differential pathlength in bone tissue has not been agreed, and may even vary between participants. However with the same interoptode separation used between participants, comparison of results between participants is still warranted [2].

2.2.1.4: Spatially resolved spectroscopy (SRS)

SRS utilises a fundamentally different approach to deriving haemodynamic markers than MBL. SRS requires a light source with two detectors in parallel, one slightly further from the light source than the other. SRS relies on the principle that the difference in attenuation recorded by each detector is inherently linked with the difference in distance of the detectors from the light source (see Figure 2.4). This is intuitive as photons reaching the detector further away from the light source are more likely to be attenuated, and hence a decreased intensity is expected at the most distant detector [62]. A limitation of SRS compared with MBL is that it inherently can only work in reflectance mode, and not in transmission through tissue, as both detectors would be equal distance from the light source [61].

With the Hamamatsu NIRO-200NX, SRS detectors will compare the change in attenuation at the differently spaced detectors for three different wavelengths (735, 810 and 850nm). By calculating the rate of change in the received detector amplitude with interoptode distance, at multiple wavelengths, relative absorption from oxygenated and deoxygenated haemoglobin can be calculated using simultaneous computations using a matrix algorithm (akin to MBL calculations). In order to do this, the scattering of light is assumed constant for both oxygenated and deoxygenated haemoglobin, leaving

differences to be attributable to absorption alone [61]. The absolute absorption coefficients are not calculated, only relative contributions of absorption between oxygenated haemoglobin and deoxygenated haemoglobin are derived [62]. Therefore, absolute haemoglobin concentrations can still not be calculated, as for MBL.

Two main SRS-derived haemodynamic markers are produced using the Hamamatsu NIRO-200NX. As the relative concentrations of oxygenated and deoxygenated haemoglobin are known, "Tissue oxygenation index" (TOI) percentage can be calculated using the equation:

$$TOI\ (\%) = O_2Hb / (O_2Hb + HHb) * 100 \qquad [Eq.\ 2.5]$$

This is representative of the oxygen saturation (sO_2) of the sampled tissue and is presented as a percentage. Likewise relative changes in total haemoglobin concentration (termed "normalised total haemoglobin index" (nTHI)) can be calculated as the sum of oxygenated and deoxygenated haemoglobin relative to the initial total haemoglobin concentration, expressed as a unitless ratio. SRS offers an advantage over MBL-derived parameters as TOI and nTHI are both ratio values, and therefore effectively normalised for comparison between participants [61]. As can be seen from Equation 2.4, comparisons of MBL concentration changes between participants could be influenced by between-participant differences in differential pathlength factors or the inherent attenuation properties of tissue.

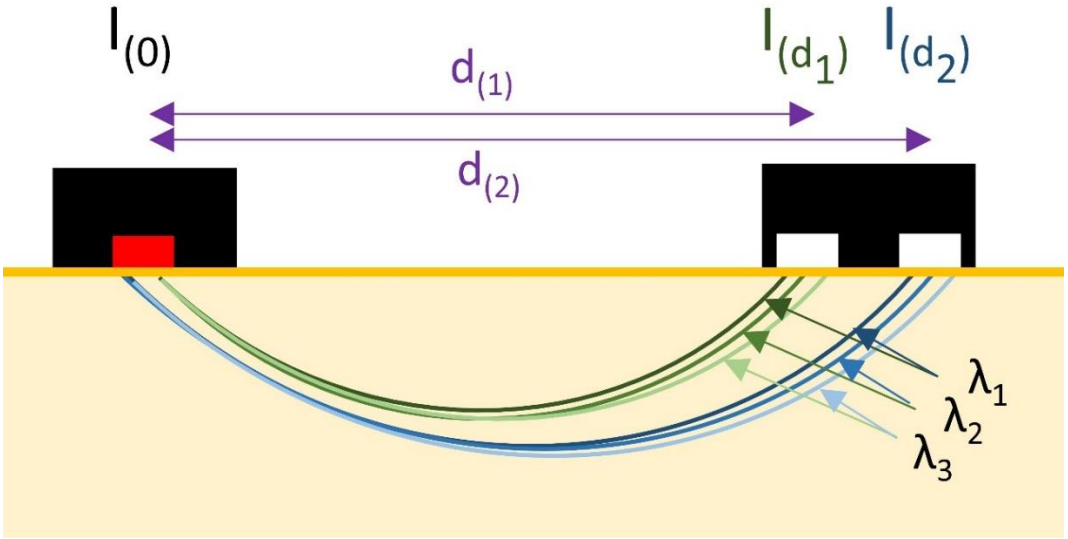

Figure 2.4: Schematic diagram of spatially resolved spectroscopy. The difference in intensity of three different wavelengths (λ) incident on two detectors set at different distances from the NIR source (in red) can be used to calculate the relative contribution to attenuation by oxygenated and deoxygenated haemoglobin.

For both MBL and SRS measurement approaches, the optode spacing will determine the depth of tissue sampled, with the deepest measurement depth being half the internode spacing, with the tissue sampled considered to be a "banana shaped" volume [16]. It is important to also note that haemoglobin influencing NIRS measurements could be in arterioles, capillaries or venules. Ferrari et al 2004 reports that in most soft tissues around 5% of blood is in capillaries with about 20% arterial and 75% venous [69].

2.2.1.5: NIRS parameters relevant to this PhD project

Utilizing the MBL and SRS approaches to measurement outlined above, the Hamamatsu NIRO-200NX system allows measurement of several parameters as outlined in Table 2.2. Measurements in this project were taken at a sampling interval of 1 second. The system was "zeroed" prior to commencing measurements, as many parameters are relative to the initial starting measurement when measuring haemodynamic changes to a stimulus.

Table 2.2: Table of haemodynamic parameters measurable with the Hamamatsu NIRO-200NX NIRS system (SRS = spatially resolved spectroscopy; MBL = modified Beer Lambert) [2, 61].

Haemodynamic Marker	Measurement Approach	Description
Tissue Oxygenation Index (TOI)	SRS	The ratio of oxygenated haemoglobin to total haemoglobin, presented as a percentage.
Normalised Total Haemoglobin Index (nTHI)	SRS	The relative change in total haemoglobin concentration within the measured volume from the initial haemoglobin concentration at the commencement of measurements.
Oxygenated Haemoglobin Concentration Change (O_2Hb)	MBL	The absolute change in concentration of oxygenated haemoglobin from the initial measured zero point within the measured volume sampled (in µM.cm).
Deoxygenated Haemoglobin Concentration Change (HHb)	MBL	The absolute change in concentration of deoxygenated haemoglobin from the initial measured zero point within the measured volume sampled (in µM.cm).
Total Haemoglobin Concentration Change (cHb)	MBL	The absolute change in total concentration of haemoglobin from the initial measured zero point within the measured volume sampled, equal to O_2Hb + HHb (in µM.cm).

2.2.1.6: Other NIRS Systems:

Both SRS and MBL rely on the intensity of light incident on the detector as an indicator on the amount of NIR photons attenuated, and therefore the concentration of O_2Hb and HHb present. Systems utilising SRS and MBL methods are typically coined continuous wave (CW) systems. There are alternative ways being developed for NIRS systems to measure relevant haemodynamics that offer advantages over the existing SRS and MBL techniques. However, these systems are still relatively new and typically not commercially available.

Time resolved spectroscopy (TRS) systems measure the time taken for photons to travel from light source to detector (i.e. time-of-flight) using ultra short laser pulses (in picoseconds). By doing this differential path length factors can be estimated and data on the attenuation and variation of photon time-of-flight can lead to calculation of absorption and scattering coefficients, allowing calculation of absolute concentrations of oxygenated and deoxygenated haemoglobin [6, 64]. Lange et al 2018 report on a new multichannel, time domain NIRS system utilising 16 different wavelengths that can measure absolute concentrations of oxygenated and deoxygenated haemoglobin as well as cytochrome-c-oxidase [64]. Such systems offer definite advantages but a current limitation is increased sampling time, which typically takes a few minutes per reading. The development of photonics equipment means there is a trade-off between acquisition time and the number of wavelengths sampled [9, 70]. TRS systems are also typically more expensive and bulkier units [62].

Frequency domain (FD) systems (or intensity modulated spectroscopy) rely on modulation of the amplitude and phase of the laser light source, and measures of the resultant output light detected at the photodetector can determine absolute oxygenated and deoxygenated haemoglobin concentrations [6]. Frequency shifts dependent on the distance of the photon pathlength can be detected, which allows calculation of absorption and reduced scattering coefficients, and therefore absolute chromophore concentrations [2, 71].

TRS and FD systems have a distinct advantage in that they can calculate attenuation coefficients for each individual participant, which may differ between individuals based on tissue characteristics and/or potential pathological changes, where many current studies utilising CW systems assume uniform differential pathlength factors for their calculations based on previous studies [68, 72]. In Van Beekvelt et al 2000, this was

estimated to introduce a potential variation between individuals of up to 12% when studying muscle [73]. This is likely to be higher in a heterogeneous tissue such as bone.

Diffuse Correlation Spectroscopy (DCS) systems use a continuous source of monochromatic NIR light and observe fluctuations in the photon detection count at the detector. These fluctuations are attributable to photon scattering produced from interactions with moving chromophores (i.e. haemoglobin within RBC) which alter the pathlength of these photons. As such, DCS can produce a blood flow index representing blood flux changes (i.e. changes in velocity and/or number of moving RBC) relative to the starting point of the measurement. DCS is a relatively new technology that can be used in parallel with TRS or FD systems to provide complimentary blood flow information. It has the advantage of sampling deeper tissues than existing alternative PPG and LDF systems which also measure blood flux indices, discussed in Section 2.2.2 and 2.2.3 [74, 75].

Table 2.3 outlines a number of parameters also relevant to this thesis, but not measurable with the Hamamatsu NIRO-200NX. These parameters are typically identifiable with more advanced TRS, FD or DCS NIRS systems.

2.2.1.7: Interventions for NIRS measurements

As has been summarised in Table 2.2, there are a number of parameters measurable with the Hamamatsu NIRO-200NX system used in this PhD project. However, all but one of these parameters (i.e. TOI) rely on measuring temporal changes. So to facilitate their use in research, and allow comparison between participants, CW-NIRS measurements typically need to be taken during a measurement intervention.

There are a number of different approaches to stimulating changes in O_2Hb and HHb concentration. Cerebral research studies often rely on controlled changes in inspired oxygen levels [2] or functional activity changing blood flow demands in the brain [62]. Studies investigating microvascular health in muscle often use variations in activity and recovery through exercise protocols [76]. Alternative approaches may be local or systemic use of a vasodilatory or vasoconstricting medication or stimulus [28, 77], or changes in external pressure using positional changes or hyperbaric chamber systems [78]. This PhD project predominantly relies on arterial occlusion of tissue using a high pressure cuff system to occlude proximal blood vessels and induce distal ischaemia to tissue, with observation of the subsequent recovery post occlusion release as well. This protocol is outlined in more detail in Section 4.4.1.

Table 2.3: Table of haemodynamic parameters measurable with time-resolved, frequency domain, and/or diffuse correlation spectroscopy NIRS systems [1, 62].

Haemodynamic Marker	Units	Description
Specific Extinction Coefficient (ε)	$\mu M^{-1}cm^{-1}$	A constant value representing how efficient a chromophore is at attenuating NIR light of a specific wavelength.
Absorption Coefficient (μ(a))	cm^{-1}	Representative value of a tissue type representing the sum of absorption contributed by all chromophores within the tissue. As such this incorporates both the concentration and absorptive properties of each chromophore. This is also NIR wavelength dependent.
Reduced Scattering Coefficient (μ(s)')	cm^{-1}	Representative value of a tissue type representing the sum of scattering losses contributed by all chromophores within the tissue. As such this incorporates both the concentration and the scattering properties of each chromophore, as well as adjusting for the anisotropy of scattering. This is also NIR wavelength dependent.
Absolute Haemoglobin Concentration	μM	The absolute concentration of haemoglobin (total, oxygenated or deoxygenated) within the measured volume sampled by NIRS.
Blood Flow Index (BFI)	cm^2/s	Marker of blood flux proportional to the rate of temporal NIR photon light fluctuations, which are caused by moving scatterers (and therefore most likely representative of moving red blood cells). Where μ(a) and μ(s)' are unknown, results are presented as relative BFI change from an initial measurement, expressed as a percentage.

The choice of intervention or stimulus is influenced by the tissue of interest, key NIRS parameters being adopted, the perceived reliability of the technique across different participants, and logistical considerations around availability of the required equipment. Thorn et al 2016 argues the most established method of obtaining markers of oxygen extraction from blood to tissue is through use of occlusion techniques, based around the rate that O_2Hb is converted to HHb within the occluded tissue. With a well

performed arterial occlusion the total blood volume will be constant, and blood flux should be negated, representing a closed system, unlike exercise protocols and stimulus responses, where changes in blood volume and blood flow can be confounding variables. Therefore changes to NIRS measurements during arterial occlusions are typically interpreted as being representative of the oxygen extraction metabolism of tissue, and not changes in haemodynamics [65].

Another advantage of arterial occlusion is that in principle it should only demonstrate local functional responses in the tissue sampled, representative of the tissue health of the volume sampled by NIRS. Unlike exercise, arterial occlusion should be minimally confounded by systemic changes such as pulse and respiratory changes triggered by humoral responses (such as epinephrine production) or neural responses via the sympathetic nervous system (although the discomfort of the occlusion may involuntarily induce some changes) [27].

During occlusion, in response to ischaemia, vasodilation of arterioles and microvessels typically occurs in response to hypoxia in attempts to increase blood flow (although in reality this is restricted by the occlusion) [79]. This is triggered by the production of vasodilatory agents (such as CO_2, lactate, and adenosine) from hypoxic local tissue and increased production of vasodilatory nitrous oxide (NO) triggered from the endothelium of the vascular supply itself (as discussed in Section 1.5.1), which continue to build up locally during occlusion [65]. Meanwhile, without new arterial blood supply, NIRS can observe the rate of oxygen extracted from RBC by tissue by observing the drop in O_2Hb and synchronised increase in HHb concentrations [65].

Occlusion protocols will also observe the rate and extent of increased blood perfusion in recovery following release of the occlusion cuff, termed post occlusive reactive hyperaemia (PORH). Following arterial occlusion release in soft tissues, the vasodilated state of microvessels facilitates a rapid hyperaemic response, typically seen involving elevated blood flow and increased tissue oxygen saturation “overshooting” initial pre-occlusion baseline measurements, followed by a slower recovery period back to baseline measurements (see Figure 2.5) [27, 80].

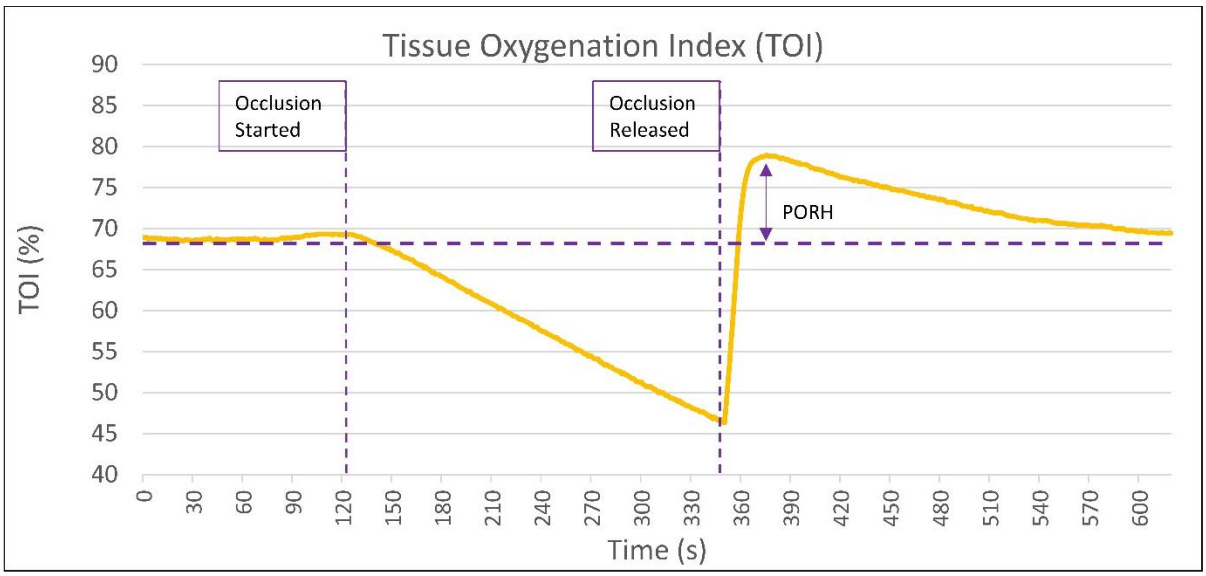

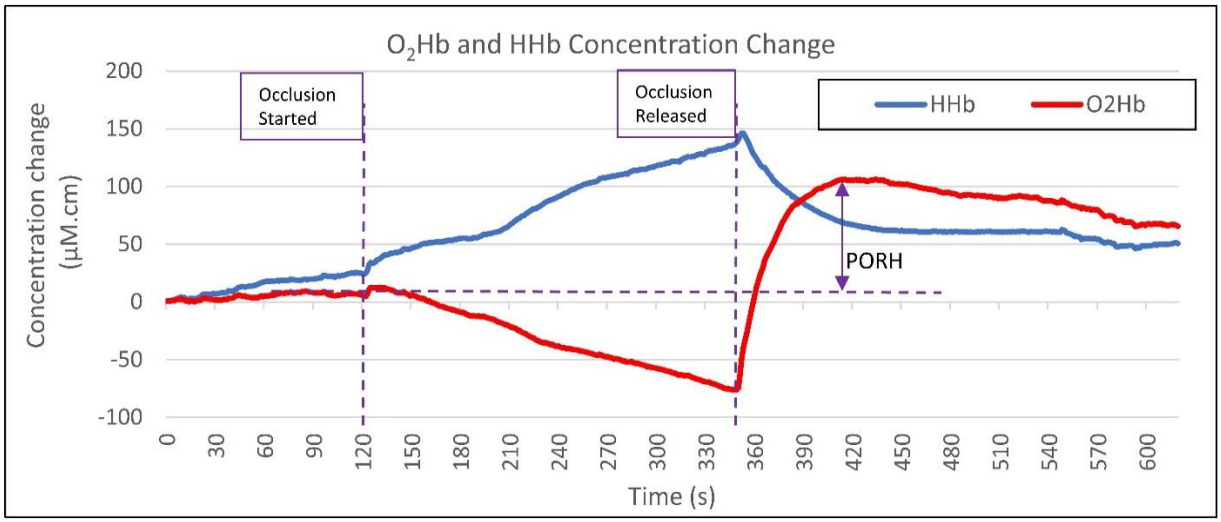

Figure 2.5: An example of NIRS parameters during an arterial occlusion. TOI (yellow) drops during the occlusion as local tissue uses oxygen within the closed system. This is also represented by a mirrored drop in oxygenated haemoglobin (O_2Hb; red) and increase in deoxygenated haemoglobin (HHb; blue). When the occlusion is released, TOI and O_2Hb rapidly recover and "overshoot" initial baseline values in a post occlusive reactive hyperaemic (PORH) response, before slowly returning to resting baseline conditions.

Rosenberry et al 2018 describes that dilation of arterioles occurs during ischaemia alongside build-up of vasodilatory mediators. When the cuff is released, vascular resistance is also reduced, leading to hyperaemia with increased shear stress on larger supply arteries also encouraging proximal flow mediated dilation [79]. Previously closed capillaries may also open in attempts to increase the proximity of tissue to oxygen supply and increase the potential surface area for diffusion of oxygen [27].

The PORH response is not fully understood, and there are several potential autonomic, myogenic and metabolic mechanisms that contribute. As such, PORH response can

only be considered an overall marker of microvascular function, but with many potential underlining contributory mechanisms [81]. A strong PORH response is generally considered a marker of good vascular health in the tissue sampled, suggesting strong endothelial reactivity and high capillary density. However, Clough et al 2016 argues PORH is confounded by the oxygen metabolism demands of cells, which may differ between participants or different tissue types [28]. Pereira et al. 2007 supports this with evidence that PORH response has been shown to correlate with aerobic cellular activity in muscle during exercise protocols [63]. Rosenberry et al 2018 demonstrates the extent of PORH response in muscle is also associated with the pre-occlusion blood flow markers taken at rest [79].

There are also variations in the application of arterial occlusion protocols and PORH results observed. Roustit et al 2012 describes a lack of consensus with how PORH is investigated in terms of occlusive cuff pressure used (ranging between 160-250 mmHg), the duration of the occlusion (typically between 3 and 5 minutes), and quantitative representative markers used. PORH can be quantified in many different ways including peak values, time to peak response, or area under the curve analysis [81]. The approaches to quantifying NIRS haemodynamics during and after arterial occlusion taken in this PhD project are outlined in Section 4.5.

2.2.2: Photoplethysmography

Photoplethysmography (PPG) uses a single wavelength of NIR light to measure haemodynamic markers in tissue. As such, PPG systems involve two optodes; a source of monochromatic NIR light (typically a light emitting diode (LED)) and a detector optode (such as a photodetector). Measurements are based on the intensity of NIR attenuation as indicated by the light intensity incident upon the photodetector, relative to the initial intensity of light imparted on tissue. As previously discussed with NIRS, the detector optode is placed adjacent to the source optode to detect the intensity of light attenuated through the “banana shaped” tissue volume [82]. The distance between optodes will determine the thickness of tissue sampled. PPG can sample similar depths as NIRS although this has not been validated in bone tissue [77].

With the assumption that all other tissue within the sampled volume is constant, PPG measurements are based on the change in total haemoglobin concentration. Hence only one wavelength is required, and typically an isobestic wavelength of around 800nm (or 560nm for measuring superficial skin) is most appropriate, as attenuation is

equally probable for both oxygenated and deoxygenated haemoglobin and so measurements are independent of tissue oxygen saturation [82]. Recordings are derived from the relative attenuation of haemoglobin as it enters and leaves the tissue sampled. PPG measurements include an AC component representative of the pulsatile flow in tissue as well as a quasi-static DC component representative of blood volume in tissue (see Figure 2.6). The DC component may be influenced by factors including respiration, thermoregulation and sympathetic vascular regulation [82]. This DC component has been found to be unreliable as a marker of blood volume for essentially unknown reasons, although possibly due to natural biological temporal variability in tissue and/or fluctuations in ambient background light [77]. As such the AC component is typically reported in PPG studies, presented as the "peak to peak" amplitude during systole (measured in Volts, or as "arbitrary units" with some systems).

The advantages of PPG are that the AC component of PPG signal can measure pulsatile changes in blood flow in real time at a fast sampling frequency owing to its simple, inexpensive design. PPG is relatively simple compared to other optical techniques allowing faster acquisition times and within-pulse information [6]. As such, PPG is an established technique for muscle and skin readings [82].

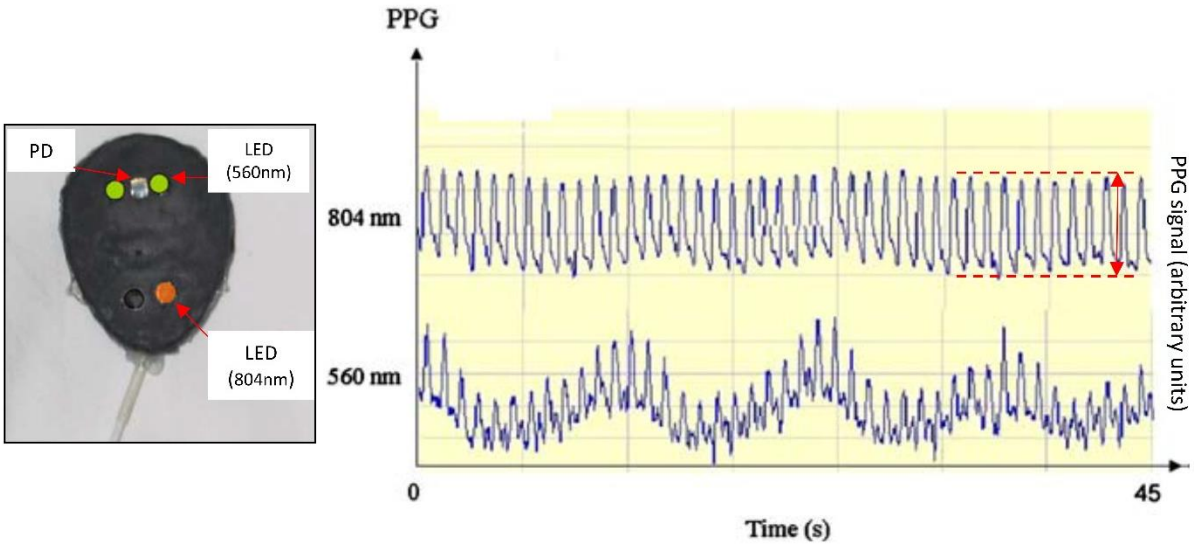

Figure 2.6: Photoplethysmography (PPG) probe and associated example measurement trace (reproduced from Naslund et al 2006 with permissions) [83]. The probe has a NIR optode (804nm) spaced 25mm from a photodetector (PD) for measuring bone, and green light optodes (560nm) spaced 3.5mm from the PD for measuring skin. The measurement trace shows recording of the "peak to peak" AC signal (in red). It can be seen that DC changes are greater in the 560nm trace, most likely representing the greater auto-regulation of skin compared with bone.

However there are a number of limitations to consider when interpreting PPG results. AC signal can be influenced by a number of haemodynamic factors including vascular tone, blood velocity, pulse rate, intravascular volume and intravascular pressure. It is not possible to distinguish the contribution of each factor to a change in PPG AC signal. However, it has been shown that PPG signal can be useful as a general marker of perfusion into tissue, as all these factors are likely to influence overall tissue perfusion and AC signal in tandem [77].

Like some NIRS markers, PPG measurements cannot be used as absolute measures to be compared across participants, nor are PPG amplitude results clinically tangible in their own right. Rather it is the relative change in PPG signal in response to a stimulus (such as positional changes, occlusion or vaso-altering medications) that is compared between subjects [84]. Comparing PPG measurements between participants can be complicated by differences in calibration of PPG for each participant based on skin pigmentation, inevitable variations in optode placement (including variations in anatomical site, optode pressure, and background ambient light), and high within-subject variations in baseline measurements at rest [82]. Biological variability is affected by temperature, acclimatization protocols, resting pulse and blood pressure variability. Often the average AC signal across a set period (for example 60 seconds) is used to obtain a measurement in an attempt to improve reliability [82]. Compared with NIRS, PPG also has the limitation of not being able to measure tissue oxygenation saturation levels. The application of PPG for measuring bone is discussed in greater depth in Chapter 3.

2.2.3: Laser Doppler flowmetry

Laser Doppler flowmetry (LDF) also provides a marker of blood perfusion akin to PPG, albeit with data acquired in a different way. LDF measures blood cell flux, which represents the number of red blood cells present in the tissue sampled multiplied by their velocity. As such LDF measurements will be influenced by both blood volume and blood velocity, however cannot differentiate between these two parameters contributing to LDF signal [84].

LDF systems also utilise a source and detector arrangement but work by detecting the frequency (or “Doppler”) shift of a monochromatic source light returned to the photodetector. When NIR light photons interacts with moving red blood cells (RBC) there is a Doppler shift in their wavelength and therefore spectral analysis of the

scattered light returned to a photodetector will be indicative of RBC flux, based on the assumption that other tissue within the sampled volume is non-moving.

LDF is constrained by its depth of measurements (typically only up to 8mm) and the resultant small tissue volume measured (up to a few cubic millimetres). In the context of measuring bone tissue this means LDF is generally confined to intraoperative measurements in order to remove any overlying superficial tissue (see Figure 2.7). Some technological advances making LDF measurements of deeper tissue feasible (and thus non-invasive) are emerging [84].

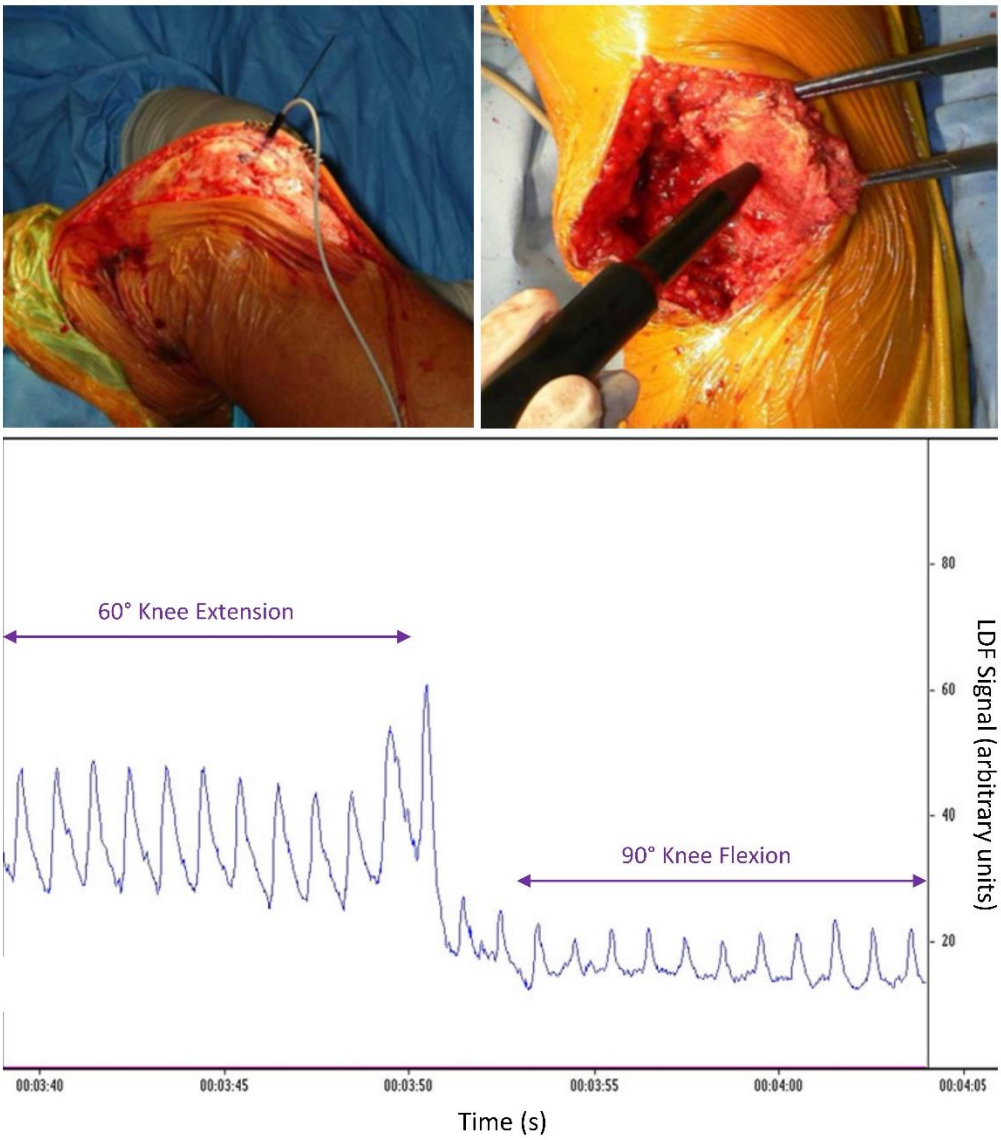

Figure 2.7: Examples of LDF use for measuring blood flux at the patella using intraosseous LDF probes and hand held LDF probes. The LDF signal shows an example of a decrease in the mean LDF signal, and pulsatile range of signal, when moving the knee from extension to flexion of the knee. Images have been reproduced with permissions [85-87].

Like PPG there are some limitations with LDF to be aware of. As photons of NIR light undergo multiple elastic scattering events it is assumed that the angle that photons interact with RBCs is random. Therefore the direction of blood flow is not determinable using LDF, only the magnitude of flux present. Frequency shift is greatest when the velocity of blood flow is orthogonal/perpendicular to the orientation of the LDF optode. Thus positioning of the LDF optode relative to the direction of blood flux can be important and will affect the signal received [88].

LDF measures represent RBC flux but absolute units should be used cautiously for between participant comparisons as the volume of the sampled tissue is not clearly defined [6]. As such LDF derived blood flux is often not presented as absolute measures, but rather in arbitrary units derived from the signal received from the LDF system. Like PPG, LDF is also typically used in conjunction with a microvascular challenge such as delivery of vasoactive drugs, iontophoresis, temperature based response, or post occlusive response in order to provide relative responses to stimuli, allowing more appropriate comparison between participants [81].

Reliability of LDF is also complicated by a number of factors. Due to the small tissue volume sampled and the known heterogeneity of vascular beds, variation in results can occur, even when sampling very close tissue volumes on the same organ [81]. Likewise, should an unexpected larger vessel be present in the sample volume then signal will be altered by the large difference in RBC concentration and velocity that these contain. This is arguably an even more pronounced risk in bone, given its known structural heterogeneity [88].

Also, even when measuring a static system with LDF there is some noise which can lead to signal (i.e. a biological zero). These could represent thermal changes to vessel walls or random Brownian type motion. Likewise, signal detected will be dependent on the initial source energy, so calibration is important when making longitudinal measurements. As the Doppler effect is non selective, LDF systems are also sensitive to movement artefact. As such the measured volume and optode need to be held securely, also being mindful that the optode does not change perfusion dynamics if held directly on to the volume of interest with pressure [88].

Table 2.4 below is a summary of the NIR based technologies discussed in Section 2.2, all of which will be mentioned in the Chapter 3 systematic review.

Table 2.4: Summary table of near infrared (NIR) based technologies relevant to this thesis, adapted from Binzoni et al 2015 [6].

NIR based method	Number of light wavelengths	Application of light source	Measured parameters
Continuous Wave Near Infrared Spectroscopy (CW-NIRS) utilising the Modified Beer Lambert (MBL) approach	Multiple, typically three	Continuous	- Deoxygenated Haemoglobin Concentration Change (HHb; µM.cm) - Oxygenated Haemoglobin Concentration Change (O_2Hb; µM.cm) - Total Haemoglobin Concentration Change (cHb; µM.cm)
Continuous Wave Near Infrared Spectroscopy (CW-NIRS) utilising the Spatially Resolved Spectroscopy (SRS) approach	Multiple, typically three	Continuous	- Tissue Oxygenation Index (TOI; %); - Normalised Total Haemoglobin Index (nTHI; unitless)
Time Resolved NIR Spectroscopy (TRS)	Multiple	Pulsed	- Absolute Haemoglobin Concentration (µM) - Tissue Oxygenation Index (TOI; %); - Absorption Coefficient (µ(a)) - Reduced Scattering Coefficient (µ(s)')
Frequency Domain Near Infrared Spectroscopy (FD-NIRS)	Multiple, typically three	Amplitude and phase altered	- Absolute Haemoglobin Concentration (µM) - Tissue Oxygenation Index (TOI; %); - Absorption Coefficient (µ(a)) - Reduced Scattering Coefficient (µ(s)')
Diffuse Correlation Spectroscopy (DCS)	One	Continuous	Blood Flow Index (BFI; cm^2/s or expressed as relative change)
Photoplethysmography (PPG)	One	Continuous	Change in blood flux (presented in mV, relative change or arbitrary units)
Laser Doppler Flowmetry (LDF)	One	Continuous	Change in blood flux (presented in mV, relative change or arbitrary units)

2.3: Imaging modalities for measuring bone haemodynamics

This section will outline the most commonly used methods to measure bone haemodynamics using diagnostic imaging modalities. This predominantly involves magnetic resonance imaging (Section 2.3.1) and nuclear medicine protocols (Section 2.3.2). Less common examples are also briefly discussed in Section 2.3.3.

2.3.1: Magnetic resonance imaging (MRI)

MRI has been used for a variety of different applications around haemodynamic measurements of bone tissue *in vivo* in humans. For example, previous MRI studies have shown a correlation between reduced bone mineral density (BMD), increased marrow fat and reduced bone perfusion [36, 89, 90]. These associations have been linked with type 2 diabetes mellitus (T2DM) [91], oophorectomy [43], cardiovascular disease and peripheral arterial disease [36], smoking [11] and the natural aging process [89, 92, 93]. Chen et al 2001 found bone perfusion in vertebral bodies decreased with age, more markedly in females, and in line with BMD changes [94]. Similarly Biffar et al 2011 found perfusion in vertebral bodies decreased in those with lower BMD. Significant changes in bone perfusion were also seen in vertebral bodies with compression fractures [95]. In a longitudinal study, Ma et al 2013 found a link with poor bone perfusion and a faster consequential loss of BMD [92]. Griffith et al 2011 also found that people with poorer bone perfusion and higher fat marrow content on MRI lost BMD more rapidly over a four year period [37].

There are a number of proposed theories to explain these links between bone haemodynamics, marrow fat content and BMD, but the true underpinning physiological relationships are still undetermined. However, the associations demonstrated strengthen the case for investigating bone haemodynamics as a predictive tool for BMD changes and/or susceptibility to fracture [37, 96].

Despite the existing precedence for the use of MRI to investigate bone haemodynamics, there is no consensus on the most suitable approach for these types of investigations. This section will explore some of the MRI protocols applicable to this project, including justification for the approach adopted.

2.3.1.1: Blood oxygen level dependent (BOLD) protocols

BOLD protocols use T2* scanning parameters to take advantage of the paramagnetic properties of deoxygenated haemoglobin and diamagnetic properties of oxygenated

haemoglobin in order to demonstrate oxygenation changes as T2* signal change during temporal scanning of a volume [97, 98].

BOLD imaging is recognised as an established imaging technique for perfusion in the brain [99] and has been used to investigate disease states in skeletal muscle due to conditions such as peripheral arterial disease [100]. BOLD protocols have been shown to be reproducible is soft tissues [101, 102]. In principle BOLD protocols are ideal for validation of NIRS haemodynamic markers as they can similarly demonstrate oxygenation changes in real time with temporal imaging during an intervention such as an arterial occlusion protocol [103]. BOLD protocols have been used to demonstrate strong correlations with cerebral NIRS measurements obtained during motor-task related activities [104, 105]. Likewise BOLD protocols have been used to compare NIRS-measured changes in skeletal muscle at the calf during exercise protocols [106].

Unfortunately, there was no previous studies identified using this protocol in bone. Given the potential advantages of BOLD as a validation tool, a T2* BOLD protocol was trialled as part of protocol development work for this PhD project but was unsuccessful, most likely due to susceptibility artefact and low signal intensity received from the tibial region of interest during imaging with the available 1.5 Tesla MRI scanner. This failed protocol is discussed in more detail in Section 4.9.

2.3.1.2: Dynamic contrast enhanced MRI (DCE-MRI)

DCE-MRI protocols are the most commonly reported MRI-based method to measure bone haemodynamics [89]. DCE-MRI protocols involve scanning a volume of tissue temporally during an intravenous Gadolinium contrast injection in order to observe markers of Gadolinium uptake, representative of the haemodynamic vascular blood supply in the tissue region of interest (ROI) [107]. Gadolinium contrast is paramagnetic and therefore works by changing the magnetic spin (and therefore MRI signal) in the Hydrogen nuclei immediately surrounding it. Therefore when Gadolinium is injected in the bloodstream via venous injection, measures of the signal change in Hydrogen nuclei in the ROI will be representative of its blood perfusion [99].

DCE-MRI imaging has been shown to be a useful way of demonstrating haemodynamics in bone tissue in a number of different bony sites (such as vertebrae [43, 95], neck of femur (NOF) [108, 109], mandible [110], wrist [111, 112], and tibia [113, 114]) and to investigate a number of different pathologies (such as osteoporosis [92, 95], compression fractures [89], avascular necrosis and NOF fracture [108, 115], Paget's

disease [116, 117], types of arthritis [111, 118], medial tibial pain [114], and bone-related cancers such as leukaemia, multiple myeloma, primary tumours and metastases [119-122]).

When analysing DCE-MRI scans, a time-signal intensity curve is generated graphing the enhancement of signal in the predetermined ROI over time (Figure 2.8 provides an example). From this a number of quantitative measures can be used as haemodynamic markers, including:

- The time to first enhancement, which can be influenced by a number of factors such as the rate of contrast injection, cardiac output and/or distance of the ROI from the heart;

- The rate of contrast uptake post injection, considered to represent vascular perfusion (incorporating blood flow velocity, capillary permeability and interstitial diffusion [123]) within the ROI. Measurement protocols here may vary (for example taking the steepest point of enhancement, or the initial period of the enhancement curve [43]);

- Time to peak enhancement, also considered to represent vascular perfusion within the ROI;

- Maximum amplitude of Gadolinium signal reached compared with baseline signal. This associates with blood volume, capillary capacitance and permeability, and interstitial space volume, which influence the ability of tissue to hold larger concentrations of contrast within the ROI [124];

- Area under the curve (AUC) of the time-signal enhancement curve can also be used as an alternative marker of maximum amplitude [108]; and,

- Washout rates or time taken for signal to return towards baseline post enhancement may be used to represent venous outflow [99].

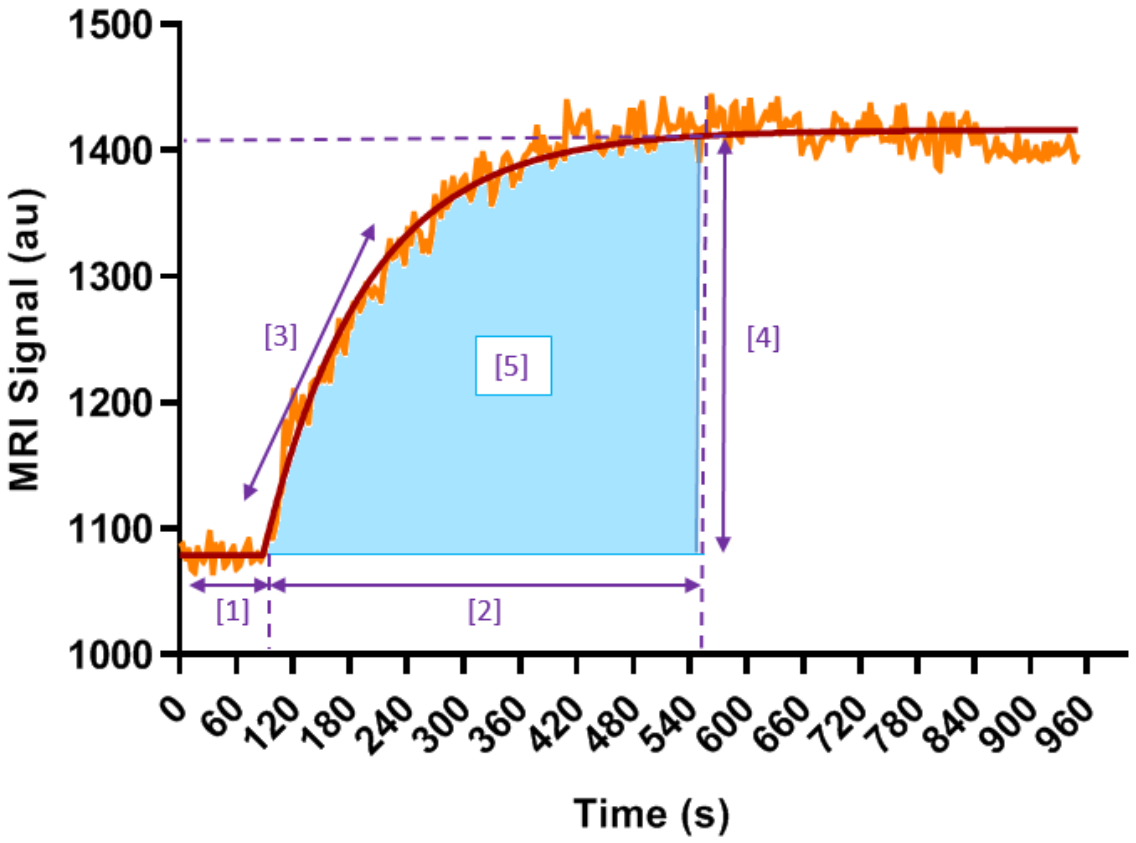

Figure 2.8: An illustrative example of commonly used quantitative markers of DCE-MRI time-signal curves (in purple). Quantitative markers are calculated following curve fitting of raw data (represented by the orange line) with appropriate nonlinear regression (demonstrated in red).
[1] Onset time to first enhancement post injection
[2] Time to peak enhancement
[3] Initial slope of Gadolinium uptake
[4] Amplitude of maximum enhancement
[5] Area under the curve to peak enhancement

The markers in Figure 2.8 are considered indirect descriptive quantitative representations of the haemodynamic properties of the ROI. These are relatively easy to calculate but are not directly physiologically applicable, but rather simply quantitative descriptions of the time-signal curves obtained, which may be presumed to be associated with the haemodynamics of the ROI. These markers are likely to be affected inherently by a combination of factors such as the participant's cardiovascular function, absolute blood volume, tissue perfusion, capillary permeability, and extravascular space. However, the individual contribution of each of these factors to the quantitative markers derived is not easily distinguished [35, 107].

Also, due to these being inherently based around MRI signal changes, they may be susceptible to influence from the scanning parameters used and inherent features of

the MRI scanner itself. In the case of this project, all participants have been scanned on the same scanner with identical scan protocols, so this does not affect comparison within the cohort of participants [107].

It is possible to make more analytical physiological measurements that are directly relatable to the haemodynamics of the ROI using pharmacokinetic modelling of the tissue of interest, such as absolute measures of capillary permeability, extravascular space, blood volume, and blood perfusion rates. However, this is more complex analysis requiring physiological assumptions on the tissue of interest, such as the arterial input rate to the volume of interest, and assumptions around uniform contrast concentration and contrast transfer within the volume. There are a number of approaches to pharmacokinetic modelling, with potential error introduced if adopting an inappropriate model [99, 107]. A consensus on pharmacokinetic modelling for measuring bone haemodynamics has not been sufficiently developed and so pharmacokinetic modelling of DCE-MRI data was not attempted for this PhD project.

Given its established use in measuring bone haemodynamics, DCE-MRI appears to be a sensible scanning protocol to use as a reference standard to attempt to validate NIRS, and was logistically feasible using the MRI facilities available.

2.3.1.3: MRI proton spectroscopy (MRS)

MRS does not directly image bone haemodynamics but it can be useful for measuring the relative fat content of bone marrow, which is known to increase in those with osteoporosis, and to negatively correlate with bone mineral density [34, 125]. Using an MRS scanning protocol, spectroscopic data can be acquired on water and lipid concentration leading to calculation of a marrow fat fraction [22, 43]. Yellow marrow is known to consist of around 80% lipids, while red marrow typically consists of 40-60% (See Figure 2.9) [22].

Fat content within bone marrow has also been found to negatively correlate with bone perfusion [126]. Increased marrow fat suggests a decrease in red erythropoetic marrow, as expected with the observed negative correlation with bone perfusion [43, 127]. This reduction in red marrow occurs with age [22] but also may be accelerated with pathology such as osteoporosis [94]. MRS can also be sensitive to different types of fat, and not just total fat content [128]. For example, Patsch et al 2013 indicated using MRS that there were differences in fat composition within vertebral bone marrow in those with

fragility fracture, and those with T2DM, both having higher proportional saturated fat content compared with controls [91, 129].

MRS techniques of measuring bone have been validated against histological results, and both DCE-MRI and MRS parameters have been shown to be acceptably reliable for research purposes [22]. Griffith et al 2009 found DCE-MRI and MRS parameters for the femoral shaft, neck and head to be reproducible with intra class correlations (ICC) generally above 0.75. ICC was better in areas of high perfusion (red marrow) for DCE-MRI, and fat content (yellow marrow) for MRS, as signal is increased in both cases [130]. Padhani et al 2002 used a pharmacokinetic model to calculate maximum contrast medium accumulation in the ischial bone marrow with a within subject coefficient of variation of 23.1%. This was similar to results in adjacent muscle [131]. Yang 2009 also used a pharmacokinetic model to look at DCE-MRI of bone metastases. Using different models, within-participant coefficient of variation ranged between 9% and 15% for markers of contrast agent transfer rates to tissue [132].

An MRS protocol was attempted in this study as part of MRI imaging in order to potentially corroborate MRS results with bone haemodynamic results found with DCE-MRI and NIRS, and also to observe any differences in marrow fat content between sexes, and those participants with and without T2DM.

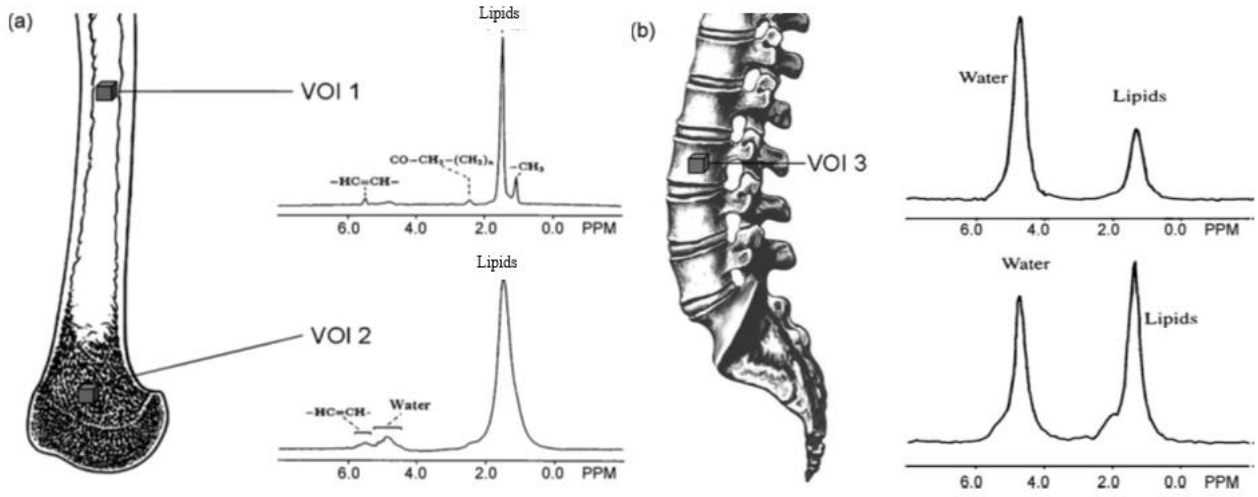

Figure 2.9: Example MRI spectroscopy data from the yellow marrow of the femoral diaphysis (VOI 1); the trabeculae bone of the distal femur with yellow marrow (VOI 2); and the vertebral body of L3 (VOI 3). The yellow marrow of VOI 2 has a much smaller water peak (relative to fat peak) then at the red marrow of L3. VOI 3 displays two example spectra, one from a healthy 24 year old female demonstrating a lower relative fat fraction than the second healthy 46 year old female. Reproduced with permissions from Machann et al 2008 [133].

2.3.1.4: Alternative MRI protocols

There are a number of alternative MRI protocols that also have the ability to take representative haemodynamic measurements of tissue. However, these were not applied in this project, mostly due to a lack of established precedence in the evidence base and/or the requirement of a more advanced MRI system than was available. Ryan et al 2013 used Phosphorus MRI spectroscopy to investigate for association between phosphocreatine levels (as a marker of muscle metabolism) and arterial occlusion NIRS markers in skeletal muscle at the calf [134]. However, Phosphorus MRI is unlikely to produce enough signal to image temporally in bone.

MRI based diffuse correlation spectroscopy (DCS) protocols are based around imaging representative of the random Brownian motion of water molecules in the tissue of interest. If microvascular perfusion is also assumed to be a pseudo-random motion of molecules given the intricate and pseudo-random orientation of capillaries, changes in signal caused by altered perfusion can be derived from diffusion weighted imaging [89, 135]. DCS protocols have been used for bone marrow tumours, although the technique is still new and mainly based in neurological imaging [89]. Some initial studies on osteoporosis and diffusion imaging were identified but findings remain unclear and conflicting [35, 89, 136].

Arterial Spin Labelling (ASL) works by effectively "labelling" red blood cells that are proximal to the ROI. This is done with a radio frequency excitation to an area proximal to the ROI. By then scanning the area of interest after this radio frequency excitation, the signal change recorded within the ROI will be a marker of the rate of flow of the "labelled" RBCs to the area of interest [100]. This protocol has the advantage of not requiring contrast, but has disadvantages in that it relies on the efficiency of the labelling process [97]. ASL has been documented to reliably measure brain, muscle (including use of occlusion protocols), and renal tissue, among others [97, 100, 137, 138]. ASL was used to validate the use of NIRS for measuring oxygenation changes in newborns with hypoxic-ischemic encephalopathy [138]. However, no evidence was found of the use of ASL in bone tissue. As the T2* signal in bone is low and seemingly untested it was deemed infeasible to use this type of MRI imaging in this PhD project.

Ultrashort-TE (UTE) MRI is another relatively new protocol allowing better T1 and T2* signal delineation in cortical bone, also facilitating more reliable DCE-MRI

measurements specifically in cortical bone [139]. However, this type of scan protocol was not possible on the MRI scanner available.

2.3.2: Nuclear medicine

Bone seeking radiopharmaceuticals such as ^{99m}Tc-labeled methylene diphosphonate (^{99m}Tc-MDP) can be used for a variety of dynamic nuclear medicine scan protocols to investigate bone perfusion and metabolic rates of turnover [140]. When injected intravenously, ^{99m}Tc-MDP is absorbed by the inorganic matrix of bone, and this process is more likely in areas of mineralisation and anabolic remodelling [141]. Thus in the first few minutes post injection, the rate and extent of uptake of ^{99m}Tc-MDP will reflect the vascularity supplying bone tissue at each specific anatomical site of interest, or as a whole body scan [123]. Specifically this could be influenced by the rate of blood flow, the density of capillary supply, and permeability of capillary exchange, although quantitative results won't be able to distinguish between these factors. Uptake rates in bone during delayed phases (a few hours after injection) will also reflect the mineral apposition rates of bone. Venous blood sampling can also compliment this by examining the plasma clearance rates of the injected radiopharmaceutical, indicative of bone metabolism activity [142]. Nuclear medicine imaging has the advantage of acquiring data at specific bony sites and/or the whole body, unlike blood markers of bone metabolism (discussed in Section 2.4.4) [141]. 18F-labeled sodium fluoride (18F-NaF) is also a PET/CT compatible radiopharmaceutical allowing higher spatial resolution and 3D tomographic imaging utilising dynamic protocols typically only taking up to 60 minutes [11].

Nuclear medicine scans can be subject to error, predominantly from the assumptions required for quantitative kinetic modelling of blood flow in bone (such as assuming uniform capillary diffusion capabilities between participants, assumptions around soft tissue uptake, and assuming normal renal clearance) [141]. Reproducibility is difficult to establish for scan protocols given the time and radiation burden for participants. Wassberg et al 2017 reports repeatability coefficients of quantitative standardised uptake markers of 18F-flouride in the range of 23-35% relative to mean results, comparable with other metabolic bone blood markers taken in the same 10 participants [143]. Using comparable scan protocols, Siddique et al 2011 report coefficients of variation ranging between 10.1% and 14.8% [144]

Nuclear medicine scanning has been used to research bone vascularity in humans *in vivo*, to investigate for a number of metabolic bone diseases (e.g. Paget's disease, bone metastases, and non-union of fractures) [141]. However it was not a viable logistical option for this project. It is felt the project is not severely limited by this methodological choice to use DCE-MRI, which appears to have comparable reliability and equitable use in the existing evidence base.

2.3.3: Other methods for measuring bone haemodynamics

There were numerous alternative testing methods identified in the literature for exploring vascular parameters in bone, especially in studies involving animal testing. Lafage-Proust et al 2015 describes multiple methods of staining blood vessels in murine models using molecules captured by endothelial cells or smooth muscle cells for capillary density counting histologically. Barium based agents can be used to fill microvascular spaces and allow histological or x-ray based microtomography [145]. Radioactive particle tracers can also be used, however these methods typically involve sacrificing tested animals [146]. *In vivo* murine studies can be performed using NIR systems with fluorescent contrast agents and/or microscopy under anaesthetic [145].

There are examples in the evidence base of selective angiography [147] and Doppler ultrasound [76] imaging in humans measuring blood flow of nutrient vessels into bone. However, this is limited to representing the supply of blood to bone and will not represent the microvascular function of small vessels within bone tissue [76]. Contrast enhanced ultrasound has been applied to measurements of *in vivo* human bone tissue including applications such as monitoring osteocutaneous fibular grafting of the mandible [148, 149], and monitoring of non-union at the tibia [150, 151]. However, the application of this technique remains in its infancy with a limited evidence base and so was not included as a comparator for NIR technologies in the systematic review presented in Chapter 3.

Bone biopsy, typically of the iliac crest, can provide histological and structural information on the quality of trabecular and cortical bone. When used in conjunction with tetracycline as a tagging agent it can also be used to investigate bone metabolism. However, this is a painful procedure for the participant, and longitudinal monitoring is restricted due to its invasive nature [152].

2.4: Common tests of bone health

This section will discuss some of the commonly utilised research tools relevant to this PhD project that address different measures of bone health, alternative to measuring haemodynamics.

2.4.1: Dual energy x-ray absorptiometry (DXA)

DXA testing is the clinical mainstay of bone health testing, having been in clinical use since 1987. It has been demonstrated to have high precision when measuring bone mineral density (BMD) at multiple sites, but clinically the lumbar spine (L1-L4) and hips (including femoral head, neck of femur and intertrochanteric regions) are of most interest as sites of common fragility fracture that show the earliest signs of BMD loss [(153)].

DXA is a quantitative x-ray based test that uses x-ray beams of two energy levels (typically 30-50 and 70-140 keV) to distinguish the differential attenuation of x-rays by bone, fat, or lean tissue within the region of interest scanned, and can thus give a measurement of BMD [(153)]. Because DXA is a two dimensional scan of a three dimensional body, BMD measurements are reported as an areal density in g/cm^2. However, clinically T-score results are most commonly reported, indicating the number of standard deviations that a patient's BMD differs from a young adult reference population, matched for sex and ethnicity (see Figure 2.10) [(153)].

The World Health Organisation's diagnostic threshold for an osteoporosis diagnosis is a T-score ≤ -2.5, with osteopenia indicated with T-scores between -1.0 and -2.49 [(31)]. An accepted limitation of DXA is that it is not a sole predictor of fragility fracture with more than 50% of fragility fractures occurring in patients who do not belong to the osteoporosis category by DXA testing alone [(154)]. Here alternative diagnostic methods indicating bone micro architectural quality (such as trabecular bone scoring) and clinically relevant risk factors (such as the Fracture Risk Assessment Tool) can play a role. These are discussed in Section 2.4.2 and Section 2.4.3 respectively.

Limitations of DXA are that it provides two dimensional imaging, unlike peripheral quantitative computed tomography (pQCT) scans which are able to provide higher resolution volumetric imaging and analysis of cortical and trabecular bone, albeit with a greater associated radiation burden for the participant. Areal bone density is also susceptible to overestimating fracture risk in those with small bone volume [(153)] and has reduced precision in obese populations [(155)]. Volumetric adjustment of areal BMD

measurements are possible to adjust for differences in bone volume if required, often applied in paediatric testing. Low resolution imaging is produced with DXA imaging to rule out degenerative changes or calcification of the aorta which can lead to over estimations of true BMD [153].

El Maghraoui et al 2005 demonstrate DXA has good reliability with a coefficient of variation of 2.02% at the lumbar spine and 1.29% for total hip measurements. This facilitates a "least significant change" in BMD of 5.60% and 3.56% at the lumbar spine and hip respectively, which would be within the expectant scale of changes over a biannual period for patients undergoing abnormal physiological BMD loss [156].

(a)

(b)

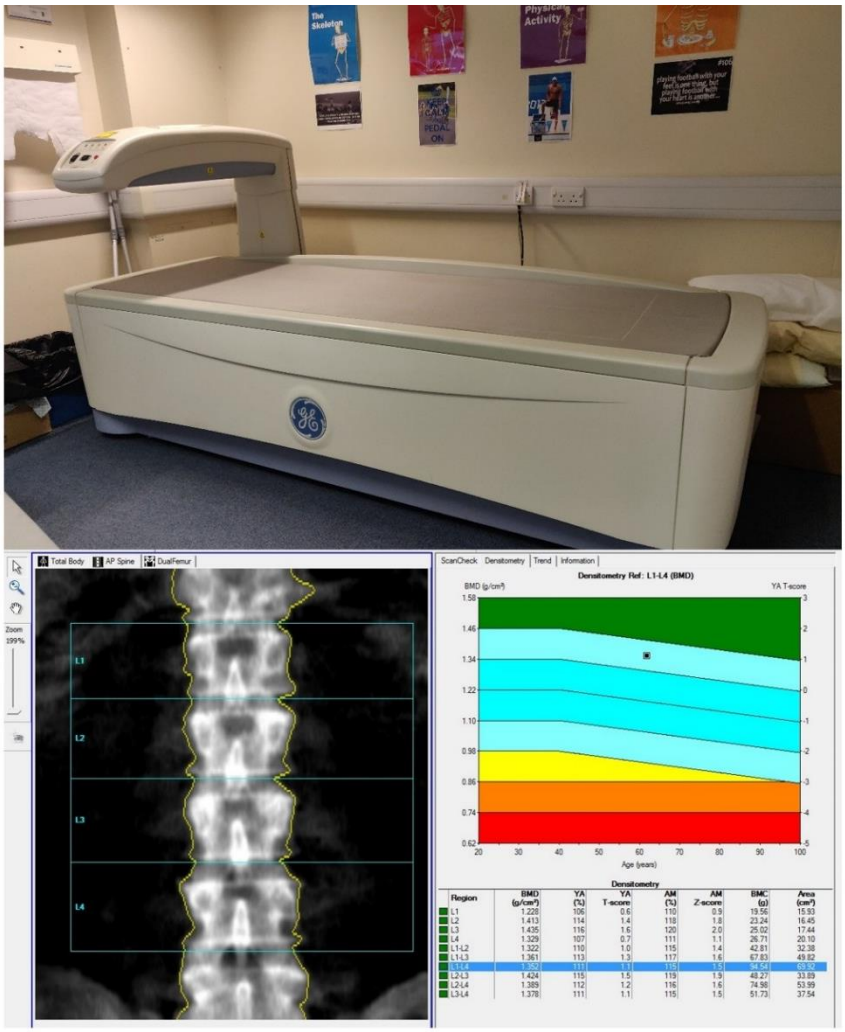

Figure 2.10: (a) Image of the GE Lunar Prodigy Advance dual x-ray absorptiometry (DXA) scanner used in this thesis. (b) Illustrative example of the typical output of bone mineral density (BMD) measurements taken from L1 to L4. The low resolution image of the lumbar spine allows region of interest (ROI) placement for each vertebrae as well as assessment for obvious influence from degenerative spinal changes or overlying aortic calcification. T-scores derived from L1-L4 BMD measurements are graphically presented to show result comparisons with age related norms and with longitudinal changes (where applicable).

DXA has been utilised in this project to obtain measurements representative of BMD. DXA is the most common clinically performed test of bone health and is generally easy for participants who can lie supine. The test also has a small radiation burden (less than 50µSv). pQCT was not available and has a much higher radiation burden (typically 1.5-2.9 mSv) [153]. It is of interest to investigate for relationships between BMD and vascular markers obtained with NIRS, as associations have been demonstrated between BMD measured with DXA and DCE-MRI parameters [36]. Similar associations between BMD and NIRS would give confidence in NIRS as a future research tool.

2.4.2: Trabecular bone scoring (TBS)

TBS is a post processing application of DXA scans of the lumbar spine which gives an indicator of bone quality via assessment of the homogeneity of trabecular bone within vertebrae (coined “textural analysis” of trabecular bone) [157]. TBS scores of lumbar vertebrae represent, and can be influenced by, the number of trabeculae, their thickness, their separation from adjacent trabeculae, and their connectivity with adjacent trabeculae, as well as the bone volume fraction relative to total volume within each vertebrae. A limitation of TBS is that it does not image the trabecular matrix of lumbar vertebrae directly, so it cannot distinguish between these contributory parameters, unlike histology or high resolution pQCT [158]. This would be impossible for a 2D imaging application such as TBS due to the micro resolution and complexity of trabecular bone structure. Rather TBS provides a marker of “bone texture” and assesses the relative heterogeneity of data points obtained from the DXA lumbar spine as a marker of porosity in bone [40].

Despite the relatively poor spatial resolution of DXA (pixel size is reported as four times greater than mean trabecular size [159]), TBS assessment of trabecular bone quality has been shown to have significant correlations with pQCT results on the micro-architectural histomorphometric parameters of bone [157]. TBS achieves this by using mathematical algorithms that can represent averaged bone quality information despite resolution poorer than individual components of trabecular bone. TBS is based around the spatial variability of pixel values by calculating the sum of squared adjacent pixel differences [157].

Similar to BMD, TBS results can be compared with a population database matched for sex, ethnicity and ages between 40 to 90 years. Data are presented on a reference graph which demonstrates the normative curve for population results and colour codes

for fracture risk (see Figure 2.11). As for BMD measurements, TBS T-scores can be calculated by finding the difference between a participant's TBS value and the typical TBS peak within the population of interest (matched for sex and ethnicity), and dividing this by the standard deviation of the population [153].

Although not yet clinically adopted in the UK, TBS has been shown to be an independent predictor of fracture risk [160], including in T2DM populations [161]. TBS has been shown to improve fracture risk prediction when combined with DXA BMD data, and can now contribute to estimates of fragility fracture using the Fracture Risk Assessment Tool (FRAX; discussed more in Section 2.4.3) [162]. The precision of TBS has been shown to be comparable with DXA for demonstrating longitudinal change. Bandirali et al 2015 quotes a coefficient of variation of up to 2.0% and least significant change of up to 5.4% for TBS measurements (depending on scan mode), which is clinically comparable with DXA BMD measurements [163].

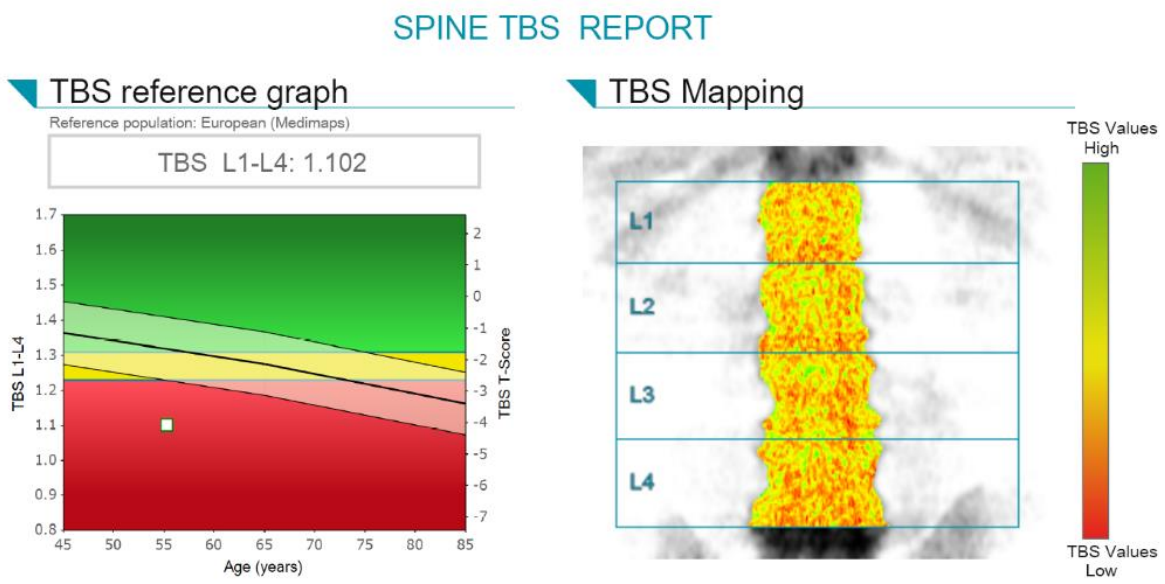

Figure 2.11: An example output of trabecular bone scoring (TBS). TBS is a quantitative test but the image shows graphical representation of how the TBS algorithm assesses the heterogeneity and porosity of bone.

In the absence of pQCT availability as the gold standard in assessing the microarchitecture of bone, TBS was deemed an appropriate tool for use in this project as a bone health comparator for NIRS haemodynamic markers. As a post processing application there is no further radiation burden to participants in addition to DXA. There is evidence of associations between trabecular bone quality and vascular properties of bone [5, 8] which suggests investigating for associations between NIRS markers of haemodynamics in bone and TBS scores of bone quality would be appropriate for this

project. Specifically, Biffar et al 2011 demonstrate a significant correlation between DCE-MRI derived haemodynamic markers of the lumbar vertebrae and markers of trabecular bone quality acquired using high resolution computed tomography [95]. Similarly, Prisby et al 2012 demonstrate correlations in the reduction of both endothelial microvessel function and trabecular bone volume with both age and/or oophorectomy in a murine study [42].

2.4.3: The fracture risk assessment tool (FRAX)

FRAX is a predictive algorithm that primarily calculates the ten year risk of any fragility fracture, or alternatively any hip fracture, based on prioritised clinically associated risk factors. These include the participant's age, sex, country of residence, weight, height, personal and family history of fracture, smoking status, glucocorticoid usage, alcohol consumption and history of rheumatoid arthritis or secondary osteoporosis [164]. The participant's femoral neck BMD and TBS score can also be entered as part of the scoring algorithm [162]. In the absence of BMD measurements, the risk of fragility fracture probability in women can range from 3.5% in 50 year olds, to 31% in 80 year olds, assuming a BMI of 25 kg/m^2 [164].

FRAX was developed in order to capture the complexities of clinical decision making around treatment of osteoporosis and associated fracture risk, which lack sensitivity if based on BMD alone, and is known to be dependent on a wide range of clinical factors [164]. FRAX has limitations such as the omission of other clinical risk factors such as bone metabolism markers, BMD at other sites, and indicators of falls risk. Likewise, the omission of T2DM has been topical with an evidenced increased fracture incidence in those with T2DM for a given FRAX score or BMD based T-score [48, 165].

QFracture is a similar algorithm that has been developed in parallel including a wider range of clinical risk factors, especially useful where BMD is not available [166]. Both are now integral to the recommended pathways for assessing the risk of fragility fracture and osteoporosis as per National Institute for Health and Care Excellence (NICE) guidance (CG146) [167].

2.4.4: Blood markers of bone metabolism

As discussed in Section 1.4, bone remodelling is a constant process within the human skeleton, and is a cohesive action between resorptive osteoclasts and anabolic osteoblasts. It is when the balance between these actions is disturbed that bone loss

can occur, the most common example being osteoporosis where resorption is dominant [168].

Use of blood markers to diagnose and monitor bone metabolism can be useful, providing an indication of the turnover rate of bone, unlike bone mineral densitometry. They can also indicate response to treatment for osteoporosis at an earlier stage [169]. The use of bone metabolism markers is established in research applications such as monitoring therapy, predicting BMD loss, or predicting fragility fracture risk (in some cases independently of BMD) as they are easily repeated, relatively inexpensive, and can be sensitive to metabolic changes [25, 168].

There are a number of available bone markers, and these can be broadly split into two categories: formative (based around outputs of osteoblast activity) and resorptive (representative of osteoclast activity and collagen degradation). Here focus is only on those used in this project: N-terminal propeptide of type 1 procollagen (P1NP) and C-terminal telopeptide of type I collagen (CTX). These two markers are recommended by the International Federation of Clinical Chemistry (IFCC) Bone Marker Standards Working Group as being most responsive to longitudinal change [170].

P1NP and other propeptides of collagen are elevated in the presence of increased collagen production by osteoblasts, as type 1 collagen makes up 90% of the inorganic bone matrix. However collagen plays a role in various tissue types around the body, which is a potential confounder. Use of P1NP has been shown to be most sensitive for use in monitoring anabolic treatments [168].

CTX is left in blood as a waste product of resorptive activity and the breakdown of type 1 collagen. As such it is a marker of osteoclast activity and has been found to inversely correlate with BMD in post-menopausal women [168]. Post menopause, females have generally been shown to have sharp increases in resorptive markers such as CTX (circa 50-150%). Formative markers also increase (osteoblast activity is triggered by resorption) but not to the same extent (circa 50-100%) meaning a net bone loss with age [171].

A limitation of bone metabolism markers are the various sources of biological and analytical variability, which has limited their acceptability in clinical usage. In particular, CTX varies with circadian rhythm and after eating, so testing is protocolled with a fasting early morning sample. Variability can also be introduced age, sex, ethnicity, seasonal effects, renal function, and some medications [168]. In particular recent

fracture can be a confounder as increased bone metabolism markers are expected with fracture healing [170].

With the identified sources of variability, the precision of CTX and P1NP should be kept in context with the expected clinical differences. There are documented within-participant coefficient of variations for repeated longitudinal measurements of 8.4% and 7.5% in pre and post-menopausal women respectively, and 7.9% for CTX in post-menopausal women [172].

Likewise, given the wide sources of variability, "normal" ranges of these markers should be applied tentatively with consideration of sub groups based on age, sex, menopausal status, and the testing protocol used [172]. With wide normal ranges across the population, markers tend to be used in the context of intra participant longitudinal changes over time, such as during treatment.

Blood markers of bone metabolism were deemed useful in this study to compare with bone haemodynamics for any correlation in results. There was some precedence identified for comparison of bone metabolism blood markers with haemodynamic markers. Libicher et al 2008 found statistically significant positive associations between the formative alkaline phosphatase marker and DCE-MRI markers of blood perfusion in those with Paget's disease [117] which subsequently both decreased with treatment [116]. Wu et al. 2012 found participants with heart failure had raised bone resorption markers. After treatment with ventricular assist devices, there was a drop in resorption markers and increase in formative markers, suggesting improved circulation stimulating improved anabolic bone formation [173].

2.5: Chapter summary

This chapter has outlined the underlying principles of the NIR based technologies relevant to this PhD project, as well as other associated tests that can measure haemodynamics in bone tissue *in vivo*, and relevant alternative tests of bone health. Chapter 3 will present a systematic review of the NIR technologies mentioned and the existing evidence base around their use for measuring *in vivo* haemodynamics in human bone tissue.

Chapter 3: Systematic review

3.1: Overview

This chapter presents the rationale, methods and results of a systematic review carried out prior to the commencement of the experimental work reported in Chapter 4 onwards. The protocol for this systematic review was submitted to the International Prospective Register of Systematic Reviews (PROSPERO; Study ID: CRD42015024463) [174] and updated upon completion with a published paper [14]. This chapter is structured around the "preferred reporting items for systematic reviews and meta-analyses" (PRISMA) guidelines for systematic review reporting [175].

3.2: Rationale

Chapters 1 and 2 have outlined the vascular physiology of bone tissue and the existing technologies available to measure various haemodynamic parameters. As introduced, a range of technologies using near infrared (NIR) light have shown promise at providing real time measurements of haemodynamic markers in bone tissue *in vivo*. These technologies have the potential to measure markers of vascular supply to bone including blood oxygenation, oxygen extraction rates, and perfusion rates. NIR technologies also overcome some of the logistical and safety concerns of existing MRI, nuclear medicine and interventional testing methods, being non-invasive, non-destructive, non-ionising, inexpensive and allowing repeat or continuous measurements. This could benefit research in a range of bone pathologies with suspected vascular elements to their pathogenesis, such as the earlier detection, prevention and monitoring of haematopoietic malignancies, osteoporosis, non-osteoporotic fragility fractures, and slow fracture healing.

There are currently no established clinical applications of near infrared spectroscopy (NIRS) for measuring bone tissue despite research in this field. An initial review on the topic suggested there was established but limited research on the use of NIRS for measuring haemodynamics in bone tissue. However, a systematic review on the topic had not been performed to date. Such a review would serve as useful to guide further feasibility work and ensure future research effectively adds knowledge to the existing evidence base. Before proceeding to experimental work with the available Hamamatsu NIRO-200NX system, it was essential to have a context for the existing evidence base around the use of NIR systems for measuring haemodynamics in human bone tissue *in vivo*.

3.3: Aim and objectives of the systematic review

The primary aim of this systematic review was to gauge the existing knowledge base on the ability of NIRS and similar NIR-based optical techniques for measuring haemodynamic markers of blood supply to *in vivo* bone tissue in humans, and to investigate the potential of NIRS as a diagnostic tool in this field. The systematic review was also performed to guide further development of NIRS as part of this PhD project.

To achieve this aim, the following objectives were to be investigated through the literature identified:

- Whether NIRS (or similar technologies) has been shown to measure haemodynamics exclusively in bone tissue (and the potential influence of overlying tissue);

- What types of haemodynamic markers are used to represent the vascular blood supply within bone;

- What anatomical sites are ideal for obtaining such haemodynamic markers;

- How accurate these haemodynamic markers are when compared to reference standards for measuring the haemodynamics of bone;

- Whether measurements of bone are reproducible and precise across different operators and different participants;

- Whether measurements are tolerable for participants; and,

- Whether the use of NIRS (or similar technologies) can be optimised in terms of measurement protocols developed for research use.

Secondary objectives also included:

- Observing what types of bone pathologies have been investigated using NIR technology, with a specific mind to any diabetes related research.

- Observing methodological approaches and gaps in the existing evidence to guide further research as part of this PhD project.

- To observe any methodological weaknesses in the existing evidence base.

3.4 Methods

3.4.1: Eligibility criteria

This systematic review looked to assess the effectiveness and diagnostic accuracy with which NIRS (or similar technologies) measures haemodynamic markers of the vascular blood supply to bone, and compare identified results with existing comparators. As such, eligibility criteria were based on diagnostic test accuracy eligibility criteria including participants, target condition, index test, and reference standard/comparators; as well as study design and report characteristics. However, much of the pre identified literature was in the form of investigative feasibility work and as such emphasis on eligibility for the review was on the target condition and index test categories as outlined below. Studies were still eligible for inclusion without a detailed comparator or reference standard. A diverse but relatively small evidence base was expected and as such broad search criteria were established as outlined below.

3.4.1.1: Participants

Only human studies were considered for the review involving either healthy and/or diseased participants. Studies involving children were considered eligible.

3.4.1.2: Target conditions

A scoping review of the topic suggested a relatively small yet wide ranging evidence base on the use of NIRS at measuring the vasculature of bone. As such the "target condition" criteria was kept broad to include any *in vivo* haemodynamic monitoring of healthy or diseased bone tissue vasculature, including any bony anatomical site. This could be for the purposes of diagnosis, prognostic assessment, longitudinal monitoring or screening purposes. Any logical choice of a superficial bony anatomical site was considered, as NIRS is limited to measuring tissue depths of several centimetres [(176)].

Any haemodynamic measurements of bone tissue vasculature was considered eligible, and was expected to be in line with the haemodynamic measurements discussed in Section 2.2; including TOI, haemoglobin concentration changes, and markers of blood flux and blood volume. Other haemodynamic markers not previously identified were considered if they gave insight to the haemodynamic state of the bone tissue measured.

3.4.1.3: Index tests

The primary index test of interest was NIRS. As an index test NIRS could include a wide variety of diagnostic techniques that use near infrared wavelengths (700 to 1000nm) of light to measure the target condition. NIRS can utilize selected wavelengths for spectroscopy measurements or may also be “broadband” incorporating a wide or continuous range of wavelengths. In addition, any adaptation of NIR-based technology was considered eligible for this review. The main range of systems expected was NIRS, laser Doppler flowmetry (LDF) and photoplethysmography (PPG).

3.4.1.4: Reference standards or comparators

Given the broad scope of the target condition, there are a number of reference standards that could apply. Again, given the small number of expected eligible studies and the broad target condition, any suitable comparator would be considered. Also, given many included studies will be pilot or feasibility work, the absence of a comparator or reference standard test did not prohibit inclusion in the review. Example comparator tests are described in Section 2.3 and could include bone biopsy, nuclear medicine scans, positron emission tomography (PET) or magnetic resonance imaging (MRI) protocols.

3.4.1.5: Report characteristics

There were no restrictions on the geographical location of publication, nor the year of publication. Only studies in English were included.

3.4.1.6: Types of studies

Case studies of individual participants were excluded, as were opinion pieces and editorials. Given the small number of expected studies, any other empirical research meeting all other eligibility criteria was considered eligible.

3.4.2: Information sources

An initial search of online databases including MEDLINE, EMBASE, the Cochrane Library, NICE Evidence Search, PROSPERO and the Centre for Reviews and Dissemination (CRD) database indicated this systematic review was yet to be attempted. MEDLINE and EMBASE online databases were searched using the OVID search platform, along with CINAHL using the EBSCO platform. Grey literature databases including conference abstracts and unpublished works were also searched,

including Web of Science, OpenSIGLE, OpenGrey, Clinicaltrials.gov, the WHO International Clinical Trials Registry Platform, and the National Technical Information Service (NTIS) database. Previous theses on eligible topics were searched for using the British Library EThOS database and the Proquest Dissertation and Theses Database. The reference list and further citations of any eligible studies were hand searched. Authors were contacted for full texts or for further information pertaining to study design or interpretation of results when required.

3.4.3: Search strategy

Search strategies were developed with consultation from a search methodologist and available experts in the field for suitable and exhaustive search terms. There were no search filters used, such as those for study design, date, or language of publication. Medical subject headings (MeSH) and text words were used as part of the search strategy. MEDLINE and EMBASE search strategies are included in Appendix A. Once finalised these were adapted for other search sources accordingly. Searches were performed in September 2015, with a repeated addendum search of MEDLINE and EMBASE performed in July 2019.

3.4.4: Study selection

Upon agreement of the search strategies, searches were executed and exported to Endnote (Version 8.0; Clarivate Analytics, Philadelphia). Duplicates were then removed if matched by title and authors. The title and abstract of results were then screened for meeting the inclusion criteria. Given there was only one person screening titles and abstracts, if there was any doubt over an individual study it was included for full text eligibility assessment.

The remaining studies were considered for inclusion in the systematic review based on assessment of their full text using the aforementioned eligibility criteria. This was carried out independently by two reviewers, blinded to each other's decision making. Full text eligibility assessment was carried out using the proforma included in Appendix B which had been piloted on two previously identified eligible studies. Any disagreements with respect to eligibility were planned to be mediated by a third reviewer, but this was not required. Reasons for exclusion were documented. The search process was summarised with a PRISMA flow chart (see Figure 3.1).

3.4.5: Data collection process

Upon agreement of eligible studies, relevant data were extracted from the included studies by the primary author using the data extraction proforma included in Appendix C, which was piloted on two previously identified eligible studies. If multiple studies were found addressing the same data, the most comprehensive source was adopted and the other source excluded.

3.4.6: Data items

Key data were extracted on study design and publication status, report characteristics (geographical location, language and date of study), sample size, participant demographics (age, sex, BMI), anatomical bony sites used, application of the index test, target conditions addressed, results reported, and comparators employed. A wide range of applications of the index test were expected along with different approaches to measuring the outcomes of target conditions. Other outcomes were also included such as comparison with the comparator/reference standard used, reporting of participant tolerability, preferred anatomical bony sites, measures of precision or reproducibility, and evidence that measurements are exclusively of bone tissue.

3.4.7: Risk of bias in individual studies

Quality assessments of included studies were carried out with a sample of ten studies double assessed independently for validation of the approach used. Any other concerns or queries were discussed with the wider supervisory team during the process. No studies were to be removed from the review on the basis of having a high risk of bias. Initially it was planned that identified studies would be scrutinised for potential bias or methodological weaknesses using the QUADAS-2 tool based on current guidance from the Cochrane Handbook for Systematic Reviews of Diagnostic Test Accuracy [(177)]. This covers four broad domains including participant selection, index test, reference standard/comparator and “flow and timing”. Pre stated signalling questions were designed to investigate “applicability” and “risk of bias” for each domain and were piloted on two previously identified eligible studies.

However, after the search strategy was carried out it became apparent that the majority of included studies were not diagnostic test accuracy study designs and that there was a wide range of study designs reflected in the included literature. As such a more flexible approach was adopted. Studies were quality assessed using the quality assessment tools provided by the National Heart, Lung and Blood Institute [(178)]. This

package presents a checklist of reporting components to consider when assessing reporting quality for different study designs (such as case series, case-control, cross-sectional, or pre-post study designs). The use of these checklists allowed quality assessment judgements using the six domain-based intrinsic bias assessment recommendations from the Cochrane Collaboration for investigating risk of bias within individual studies (see Table 3.1 below) [179]. As these criteria were designed with interventional trials in mind, adaptations to the interpretation of these internal biases were made based on the "Risk of Bias Assessment Tool for Nonrandomized Studies" (RoBANS) suggested by Kim et al. 2013 [180].

Table 3.1: The six domain-based internal biases that included studies were judged on in the systematic review [179, 180]

Type of Internal Bias	Description
Selection Bias	Risk of bias caused by the inadequate selection of participants and/or by the inadequate confirmation and consideration of confounding variables
Performance Bias	Risk of bias caused by the inadequate measurement of exposure and/or due to knowledge of the allocated interventions by participants and personnel during the study.
Detection Bias	Detection bias caused by the inadequate performance and/or blinding of outcome assessments by those performing analyses.
Attrition Bias	Attrition bias caused by the amount, or inadequate handling, of incomplete outcome data
Reporting Bias	Risk of bias caused by the selective reporting of outcomes
Other Biases	Risk of bias due to problems not covered elsewhere by the other five domains

Responses to the six domain-based assessment signalling questions lead to categorising the study as "low risk" or "high risk" for each domain overall. Where there was not enough information provided, an "unclear" rating was given. An overall judgement of reporting quality as either "good", "fair" or "poor" was made for each study. "External applicability" and "generalisability" of studies were also assessed using these categorical criteria [177]. Methodological patterns or trends for "unclear" or

“high risk” areas of bias were identified and their potential effect on results discussed in context within the discussion of the review.

3.4.8: Summary measures

As discussed in Section 2.2, differing NIR systems can measure different relative and absolute quantitative outcomes of haemodynamics including changes in haemoglobin concentrations, tissue oxygenation, blood flux, and blood volume. These quantitative markers were the primary outcome measures reported.

3.4.9 Synthesis of results

Due to the heterogeneity in the identified literature, the primary approach of this review was a narrative synthesis of studies. Studies were primarily grouped based on the NIR testing system adopted and discussed in context of the differing applications of the index test, participants used, comparators employed and anatomical sites of interest. Results from studies were compared in context to the methodological limitations identified from the risk of bias assessment described above in Section 3.4.7. Data were labelled as missing or incomplete when this was encountered, and where contact with authors was unsuccessful.

3.4.10: Statistical analysis and data synthesis

Due to methodological heterogeneity, meta-analysis was not performed. Narrative synthesis of the primary outcomes mentioned in Section 3.4.8 was completed. Throughout the narrative synthesis, sub groups of eligible studies were described according to common methodological approaches, including studies:

- Investigating similar participants (for example post-menopausal women or elderly populations), anatomical bony sites or disease states;

- Investigating similar NIRS technologies (e.g. continuous wave, time-resolved or frequency domain based NIRS systems);

- Measuring similar haemodynamic markers of microvascular blood supply to bone (such as oxygenation, perfusion or blood volume); and,

- Adopting a feasibility or validation methodology of NIR technologies, or using NIR technologies for physiological research.

3.4.11: Risk of bias across studies

Statistical analysis of reporting bias such as using funnel plots were unlikely to be meaningful with the heterogeneity of study designs and outcome measures in the included studies. Sub group analysis of published and unpublished "grey" data identified can be performed to indicate a potential for publication bias. Likewise, sub group analysis of studies with small sample sizes can suggest the presence of "small study effect" biases. However, these approaches were not adopted due to the heterogeneity of study designs and NIR applications compromising the validity of these assessments of bias [181].

The review includes a discussion on the strength of the evidence accumulated in the systematic review. This includes consideration of the risk of bias of individual studies, patterns in biases (such as common methodological weaknesses across studies), the consistency of results across studies, and the applicability and generalisability of results across the general population. These are kept in context with the strengths and limitations of the review process.

3.5 Results

3.5.1: Study selection

A summary of search results is presented in the PRISMA diagram below (Figure 3.1). Ninety studies were included for full text analysis. A summary of extracted data is available in an online supplementary resource (available at http://tiny.cc/1ybljz) presenting all data extracted by the primary author. Study publication dates ranged from 1987 to 2019 and there was wide geographical variation with publications based in 13 different countries. These were predominantly peer reviewed journal articles along with five conference proceedings [70, 182-185] and two theses [186, 187].

Twenty-two studies were identified using NIRS [9, 10, 15, 16, 56, 70, 72, 75, 78, 183, 185, 186, 188-196] and eleven studies were identified using PPG non-invasively on *in vivo* bone sites [77, 78, 83, 197-204]. Two of these studies used both NIRS and PPG [78, 204]. Fifty nine studies were identified using LDF *in vivo* [85-87, 147, 182, 184, 187, 205-256] of which 58 were used intra operatively during surgical procedures. Only one study using LDF attempted to measure bone non-invasively [254]. Most studies were in adult populations with only 7 of the 59 LDF studies including paediatric populations [207, 212, 234-236, 241, 253].

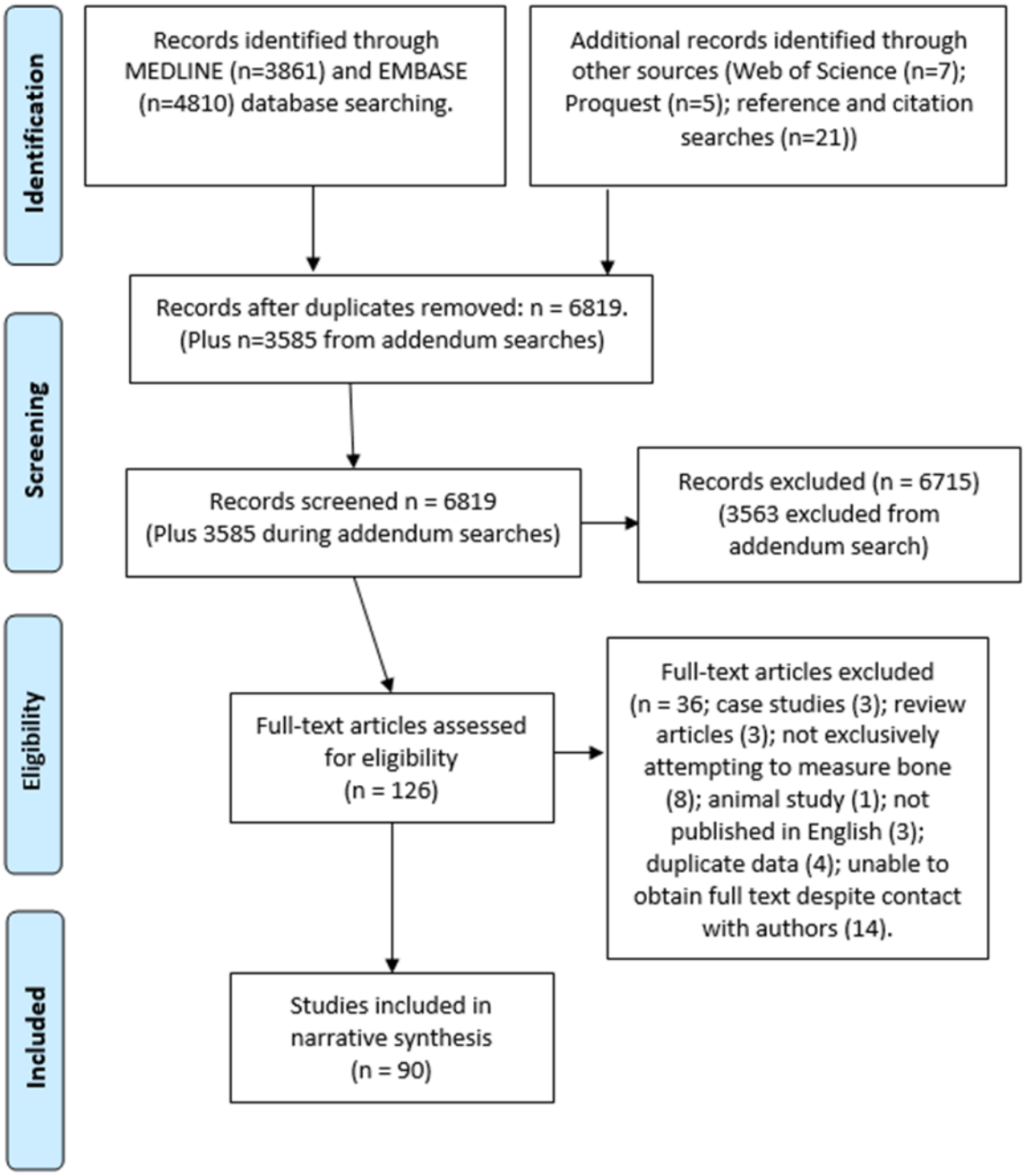

Figure 3.1: PRISMA flow chart of search strategy.

3.5.2: System characteristics

3.5.2.1: Near infrared spectroscopy (NIRS)

Studies most commonly utilised continuous wave (CW) NIRS systems using spatially resolved (SRS) or modified Beer Lambert (MBL) law algorithms, comparable with the Hamamatsu NIRO-200NX used in the experimental research presented in this thesis. These systems utilised at least two or three discrete wavelengths of NIR light in the first NIR window (700 nm-1000 nm), and either side of the NIR isobestic point of ~800nm, to detect changes in oxygenated haemoglobin (O_2Hb) and deoxygenated

haemoglobin (HHb) concentrations, taking advantage of their different attenuation properties at these wavelengths. This also allows these systems to measure oxygen saturation and total haemoglobin concentration changes in the tissue sampled. All were using reflectance spectroscopy (light scattered back from tissue) apart from studies utilising transmission spectroscopy (light scattered through tissue) to investigate the calcaneus [9, 70, 75] and mandible [191, 192].

For reflectance spectroscopy, probe spacing (affecting the depth of tissue measured) varied including 10 mm [15, 186, 193], 20 mm [186], 25 mm [56, 70], 30 mm [10, 185, 188-190], and 40 mm [16, 190, 196]. Temporal resolution typically ranged from 1 second [10] to 12 seconds [56, 75]. Exceptions were Farzam et al 2013, which reported an ECG gated system capable of measuring 14 data points per cardiac cycle [15]. Pifferi et al 2004 reported a ten minute acquisition time with the time resolved system used with the participant at rest [9].

Use of bespoke time resolved spectroscopy (TRS) systems is reported in five studies [9, 56, 70, 75, 195]. For example, Farzam et al. 2014 uses 687nm, 785nm, 830nm wavelengths at pulse widths of 400, 350, 450ps with a 50MHz repetition rate. As these systems record photon time of flight information, they allow measurements of absorption and reduced scattering coefficients for bone tissue and therefore absolute concentrations of O_2Hb and HHb are calculated at the manubrium with participants at rest (in µM) [9, 15, 56, 70, 192]. Farzam et al. 2013 also reports on use of a bespoke frequency domain based NIRS system measuring the same absolute haemoglobin concentration outcomes utilising 15 NIR laser sources (5 each at 3 different wavelengths) based around two photomultiplier detectors at the patella [15].

Six studies used bespoke NIRS systems utilising a broadband spectrum of NIR light enabling the system to calculate absolute concentrations of haemoglobin and in some cases also water, collagen, mineral and lipid content in the bone tissues sampled [9, 56, 70, 72, 75, 192, 195]. Additionally, four studies also measured markers of blood flow rates utilising emerging diffuse correlation spectroscopy (DCS) NIRS technology which can calculate additional markers of blood flow by assessing the impact of moving red blood cells on the scattered path length of NIR photons [56, 70, 75, 194].

3.5.2.2: Photoplethysmography (PPG)

Eleven PPG studies were identified originating from two research groups investigating the patella [83, 198, 201, 202], tibia [77, 78, 197, 199, 203, 204] and sternum [200]. These studies

utilised bespoke PPG systems utilising an isobestic 800 nm NIR wavelength to measure the amplitude of pulsatile flow in bone tissue based on attenuation changes in reflected signal. When reported, inter-probe spacing ranged from 15-25 mm. Some studies also measured overlying skin tissue, utilising a less penetrative wavelength in the visible range (either 526 nm, 560 nm or 660 nm). Studies involving PPG had small adult participant samples (ranging from 6-42 participants).

Studies generally used "peak to peak" amplitude during pulsatile flow as their primary outcome measure, typically measured and averaged over a 30-60 second period to gain a mean value representing the strength of pulsatile flow. Changes were then typically compared to baseline measurements during and/or after an intervention in either relative (i.e. percentage change) or absolute terms (in Volts). An exception was Naslund et al. 2019 which used linear regression to model PPG amplitude readings as a marker of oxygen saturation at the sternum, based on corresponding CO-oximetry results [200].

3.5.2.3: Laser Doppler flowmetry (LDF)

Most studies reported the use of a commercial LDF system utilising a monochromatic wavelength typically at 632 nm, 780 nm, 785 nm, or 830 nm. LDF systems derive a measure of flowmetry from the Doppler frequency shift induced by the moving red blood cells. Changes in the frequency power spectrum of the reflected light provide a measure of the concentration of moving red blood cells (blood flux or flowmetry) in arbitrary units (described as perfusion units, flux units, or detector signal measured in milliVolts). A mean amplitude of pulsatile flow is calculated over a set period (typically 60s or less). Comparison of these values across participants should be done cautiously (as discussed in Section 2.2.3), and typically these values are used to assess relative changes following a vascular challenge (either expressed as absolute change or relative percentage change).

LDF systems only measure to a depth typically less than 4 mm [257], and therefore 58 of 59 studies involve intra operative use of LDF with probe placement directly on bone or intra-osseous measurements. Two studies utilised laser speckle techniques involving laser light interference from a tissue surface and then subsequently mapping blood flux to produce a 2D flowgraphy "heat" map. These were used intra-operatively to study the flux in the surface of the bone tissue up to a depth of 2mm, namely the femoral head [216] and the cochlea promontory [237]. Two studies used the Oxygen-To-

See (O2C; LEA Medizintechnik, Geissen) system inter-operatively on the sternum. This system primarily provides blood flux measurements, but by using multiple wavelengths can also provide tissue oxygenation saturation percentages at shallow depths of 2mm and 8mm [224, 225].

3.5.3: Study characteristics

Studies looking to investigate bone tissue non-invasively used a wide range of superficial anatomical bone sites including the tibia, calcaneus, radius, ulna, greater trochanter of the femur, patella, mandible and manubrium/sternum. In addition, invasive LDF procedures also investigated deeper bone tissue including the proximal femur, acetabulum, cochlea, maxilla, metatarsal, humerus and lumbar vertebrae. Studies could broadly be split into two categories. Firstly, studies investigating the feasibility of NIR technologies for measuring bone tissue in healthy adults (discussed in Section 3.5.3.1). Secondly, studies that used previous evidence to defend the validation of NIR technologies, and applied these systems for a physiological research purpose (discussed in Section 3.5.3.2).

3.5.3.1: Feasibility studies

The most substantial work demonstrating NIRS and PPG could truly measure haemodynamic markers of bone tissue non-invasively was based around studies that demonstrated significantly lower oxygen extraction rates and reperfusion rates in bone tissue compared to adjacent muscle tissue. These two parameters were derived during and after extended arterial occlusions of the leg respectively, reflecting bone's lower oxygen metabolism and vascular responsivity compared to muscle [15, 183, 185, 188, 189].

Three studies demonstrated a non-significant contribution of superficial tissue to PPG and NIRS measurements of the patella and tibia by selectively altering superficial tissue haemodynamics either through the localised introduction of vasodilating or vasoconstricting elements such as gentle compression [77], cold packs [186], nitro-glycerine patches [77] and liniment [83]. Whilst only illustrating that superficial tissue does not significantly contribute to measurements, these studies concluded that their systems were a suitable tool for measuring haemodynamics in superficial bone tissue. Conversely, Klasing et al. 2003 does report a significant negative correlation between superficial tissue thickness and markers of oxygen consumption taken at the tibia using a NIRS system [185]. However, this study also suggests the tibia is truly being sampled

as haemoglobin concentration demonstrates a minimal increase during muscle contraction exercises, relative to what is observed at the adjacent tibialis anterior.

Binzoni et al. 2013 was the only study focusing purely on non-invasive LDF measurements in bone through the skin surface. Feasibility work was undertaken in healthy participants with a source/detector spacing of 1.5 cm giving enough penetrative depth to measure superficial bone *in vivo* at four anatomical sites [254]. NIRS based DCS technology also provides blood flux information non-invasively but at greater tissue depths and may supersede LDF here given the added advantages of NIRS systems [56, 75]. Alneami 2015 also describes *in vitro* work demonstrating NIRS can penetrate through 7mm of cortical bone tissue [186].

Other applications of NIRS and PPG systems applied to healthy populations included haemodynamic measurements taken during positional changes such as leg extension, or head up/down tilt to demonstrate oxygen saturation and blood volume changes [10, 78, 186, 197, 203, 204]. Four studies examined the effects of positive and negative external pressure changes (using lower body pressure chambers) on the amplitude of PPG pulsatile flow and NIRS oxygen saturation [78, 198, 199, 204]. In the case of Larsson et al. 2014, the use of hyperbaric chambers and variable respired oxygen levels were also used to observe their effects on bone haemodynamics at the patella [198].

Figure 3.2: Example of NIRS testing used with head down tilt, and with use of a lower extremity pressure chamber to study the effects of negative pressure. Reproduced with permissions from Siamwala et al 2015 [78].

These studies concluded that the use of pressure alterations may have applications for therapy by mimicking weight-bearing physiology in a microgravity environment, or

for potential therapeutic applications involving vascular mechanisms in bone. However, there are numerous variables involved, requiring further investigation including optimising the timing, magnitude, and application method of pressure use, and the risk of potentially unpredictable responses in disease states.

Three studies investigated the response of NIR systems and the effects of exercise on tibia and patella haemodynamics using exercise bikes [186], rowing machines [72, 186] or high intensity quadriceps workloads [201]. Sorensen et al 2017 investigated the effect of phenylephrine on oxygen saturation of the proximal tibia [196]. For TRS NIRS systems, absolute measurements could be taken on healthy adult participants simply at rest [9, 56, 70, 75, 195].

In terms of validating LDF for use in bone, there were some studies which used fairly basic approaches to illustrating LDF may be a useful intra operative diagnostic tool. This included observing a response to stimuli intra operatively [233], or following up and associating intra operative LDF results with patient outcomes post operatively [207, 226, 250]. Importantly none of these studies attempts to validate LDF as a research tool for measuring blood flux in bone by comparing LDF blood flux results with a direct reference standard that also measures markers of blood flux in tissue. This is most likely due to the lack of comparator options, with only intra operative observations, angiographic studies, MRI perfusion studies, and nuclear medicine studies likely to be appropriate *in vivo* in humans.

Exceptions included Fukuoka et al 1999 which looked at the use of LDF “laser speckle” imaging at the femoral head intraoperatively. This method takes the principles of LDF but involves exposing the scanned femoral head with a monochromatic infrared laser and mapping the blood flux, producing a colour coded blood flow map across the femoral head. This study sought to validate laser speckle “flowgraphy” by correlating results against pre-operative T1 MRI scans and intra operative observation of necrotic collapse at the femoral head in 100 cases undergoing surgery. Laser speckle identified necrotic areas in 75 of 81 scans where MRI found necrosis. In 19 cases where MRI was inconclusive, laser speckle identified necrotic areas in 16 cases. It was concluded that these results showed promise for guiding surgical approach in osteotomies, but were obviously limited being intra operative, as they could not be pre-operatively diagnostic [216].

Sugamoto et al 1998 also sought to compare the presence of LDF signal within the femoral head with the microselective angiographic presence of extraosseous vessels around the femoral head in 44 cases. All cases without LDF signal also had no angiographic visualisation. 9 cases without angiographic visualisation did have LDF pulsatile readings and all 9 cases went on without developing osteonecrosis, giving potential claims to the use of LDF for predicting poor surgical outcomes at the hip [147].

These studies take a more rigorous approach to validation by comparing results with other markers of blood flux, however with small numbers and methodological weaknesses, further studies are still required to build the case for LDF as a valid method of measuring blood flux in *in vivo* human bone tissue, especially when used for novel applications investigating diseased states. As discussed further below in Section 3.5.7.1, further work demonstrating reproducibility and overcoming logistical barriers to intra operative use of LDF is also needed.

3.5.3.2: Physiology research applications

Studies using NIR optical systems for physiological research in diseased populations were predominantly LDF studies, focusing on dynamic flux changes in response to fixed stimuli or during various stages of a surgical intervention. Some studies used case-control designs to correlate these results with other clinically relevant observations assessing the predictive role of intra-operative LDF on outcomes.

The proximal femur and hip joint represented one of the biggest areas of interest for research involving LDF in bone tissue, with 19 studies [147, 182, 205, 207-210, 214-216, 219, 223, 229-231, 239, 240, 246, 253] found investigating a range of clinical applications including osteonecrosis (either idiopathic, steroid induced, or following neck of femur fracture) [147, 216, 229, 246], approaches to hip resurfacing arthroplasty [182, 205, 208, 231, 240] or total hip replacement following arthritis [147, 210, 214, 215, 223, 230], femur-acetabular impingement [209], hip joint debridement [239], and congenital developmental problems [207, 219, 253]. Specifically most studies took measurements from the femoral head and neck, but others also looked at intra-trochanteric regions [229, 246], the greater trochanter [214, 223, 230], proximal femoral shaft [223], medial calcar [223], or acetabulum [215, 219].

There were six studies identified that used LDF intraoperatively to investigate patellar blood flux changes before and after positional changes or different surgical manoeuvres in adult patients having total knee arthroplasty [85-87, 220, 222, 244]. Five studies used LDF technology to measure blood flux in the manubrium [206] or sternum

[217, 224, 225, 238] during and following open cardiac surgery involving the internal mammary arteries. Seven studies looked at the use of LDF to measure blood flux in the mandible [187, 226, 250], maxilla [252, 255, 258] or both [227, 251] for patients undergoing maxilla-facial or dental surgery including wisdom tooth removal [187], dental implants [226, 250, 255], osteomyelitis [251] or corrective maxillary surgery [227, 252, 258]. Eleven studies reported on the use of LDF to assess blood flow in the bony wall of the cochlea [211, 212, 232-237, 242, 243, 249] to investigate a range of inner ear pathologies including otosclerosis [237, 243], Meniere's disease [242], curative treatment for uncontrolled drooling [232, 233] or idiopathic or congenital hearing loss and surgical implantation of hearing aid devices [212, 234-236]. Four studies from the same research group investigated the use of LDF technology for assessing bone perfusion during the surgical debridement of bone tissue in adult patients compromised by acute trauma (such as open fracture) and/or osseous infections such as osteomyelitis [213, 245, 247, 248].

LDF has also been used to investigate successful post-operative monitoring of fibular bone grafts [241]; intra-osseous haemodynamic measurements of thoracic and lumbar vertebral bodies during mimicked unilateral and bilateral ligation [218]; for investigating the predictive ability of humeral head fracture patterns for determining the risk of humeral ischemia [221]; and for investigating the blood flux in the first metatarsal head during corrective surgery [184, 228].

The clinical utility of NIRS has been explored in the mandible [190-192] and sternum [193]. In a case-control manner, mandibular conditions such as osteoradionecrosis post radiotherapy [191, 192], and fibular grafting post tumour removal [190], as well as chest wall measurements taken post cardiac surgery [193] were explored. Results showed potential for the use of NIRS for post-operative monitoring using oxygen saturation (TOI) measurements, however the small sample sizes and shortage of adverse outcomes precluded the ability to identify a diagnostic predictive threshold.

Naslund et al 2007 [202] used PPG to investigate haemodynamic differences between cases of Patello-Femoral Pain Syndrome (PFPS) with age, sex, and body mass index (BMI) matched controls. This study demonstrated cases of PFPS had significantly reduced PPG pulsatile amplitude when flexing their affected knee to 90 degrees for five minutes, supporting the hypothesised ischaemic element to pathogenesis. Naslund et al. 2019 used a PPG based wireless device to demonstrate its utility in hypoxia monitoring at the sternum by comparing PPG readings with CO-oximetry whilst participants breathed modified air supply of varying oxygenation [200].

3.5.4: Risk of bias within studies

An overview of quality assessment ratings for all included studies is presented in Appendix D using the approach outlined in Section 3.4.7. Summaries of the six domains of intrinsic risk of bias are presented in Figure 3.3.

A general methodological issue with many studies was the poor description of recruitment strategies, including inclusion and exclusion criteria. There was often poor detail provided on the demographic details of the participants, with mainly only age and sex described. Especially in feasibility work, more detail on potential confounders such as superficial tissue thickness or BMI are useful, as well as other physiological markers such as heart rate, blood pressure, and ankle-brachial index. In the absence of specific details, selection biases cannot be definitively discussed.

Similarly, most feasibility studies involved small cohorts of healthy, young and predominantly normal BMI participants, raising concerns around the generalisability of non-invasive applications of NIR systems in wider demographics and disease states. Many studies also included small sample sizes of participants without sample size justification, presumably using convenience sampling.

Attrition or incomplete results were rarely directly addressed. How incomplete results are handled can lead to biases in results and it is important these are reported in context with study findings. This is especially relevant at the early stages of the technological development of NIR optical systems in order to better understand why results may not be obtained, or are erroneous, from some participants.

Generally, most studies had a low risk of performance and reporting bias as testing protocols were clearly pre-stated and all participants received the same testing. In the case of studies investigating the potential feasibility of NIR optical systems on healthy participants, detection bias was considered generally low, despite studies not always reporting if testing and data analysis was strictly protocoled, or if acquisition and data analysis was blinded to participant information/status.

Figure 3.3: Intrinsic risk of bias summaries for included studies based on primary NIR technology used.

However, in studies investigating different sub populations for physiological differences, this was deemed a more significant potential bias risk, especially when LDF or oxygen saturation with NIRS was used as an outcome measure, where probe placement can be easily adjusted in real time for minor subjective corrections in results, or the most suitable data could be selectively sampled for data analysis. It is acknowledged that for most intra operative LDF studies, LDF operators were not blinded to their participant status as they were likely performing the surgical procedures. As such, detection biases are hard to avoid.

Studies were also deemed at “unclear” risk of “other biases” as there are inherent unknowns around the use of NIR optical systems for these applications in bone tissue, as relatively weak validation exists. Along similar lines many studies involving NIRS and PPG systems reported use of bespoke made systems, reducing the applicability of results. For example, there is evidence of systematic differences in haemodynamic measurements across commercial systems from different manufacturers [(259)]. Many studies demonstrated wide variability in haemodynamic results, even within healthy cohorts, which may indicate unknown sources of physiological variability or measurement error. Most feasibility studies only involved one measurement before and after an intervention for each participant, or just one representative measurement in the absence of an intervention protocol. When the restricted use of repeated measurements is incorporated with the use of small healthy cohorts, this reduces the confidence in results and the applicability of results for further use of NIRS testing.

There was also an applicability issue evident when considering intra-operative LDF findings to guide clinical practice or normal physiology. Often studies found reduced blood flux at various stages during surgical interventions, but without the ability to take pre and post-operative readings the clinical importance of these findings is hard to distinguish. Likewise, obtaining healthy control data is also ethically difficult given the invasive approach taken. Similarly, some studies only presented relative percentage changes in haemodynamic markers with time. Whilst this demonstrates the responsiveness of NIR optical systems in bone, the applicability of these results is limited without development of absolute haemodynamic quantitative markers and threshold results for normal physiology that can guide research into diseased states.

3.5.5: Results of individual studies

A summary of data extracted for all individual studies is available at http://tiny.cc/1ybljz. For brevity this section will discuss the results of those studies with direct relevance to the experimental work presented in this thesis, in context with the potential risks of bias discussed in Section 3.5.4.

3.5.5.1: Measurements at rest

Three studies provided results that were directly relevant to the resting TOI measurements taken at the proximal tibia in this PhD project. Siamwala et al. 2015 reports a mean proximal tibia TOI of 81.3% (SD 5.5) with 11 participants in the supine position. Siamwala et al. 2017 looks at sex differences in microvascular responses between nine male and nine female participants. This study reports resting mean TOI values at the proximal tibia of 73.5% (SD 7.2) for females and 76.8% (SD 6.3) for men, although this was in a sitting position. Sorensen et al 2017 reports a median supine resting tibial TOI of 81% (IQR 69% to 87%) [196]. Binzoni et al. 2003 reports a mean TOI value of 84.9% (SD 2.8) at the tibial diaphysis [189].

Farzam et al. 2013 presents data on the mean patella TOI at rest (65% SD 9) [15]. Farzam et al 2014 looks at the manubrium, taking repeated measurements at four sites. This was feasibility work prior to a potential application for NIRS screening for haematological malignancies in young populations. The median and inter quartile range values for TOI of the manubrium were reported as 71.1% (IQR 69.5% to 72.3%) [56].

Takami et al 2008 describes the use of NIRS to monitor haemodynamics in the chest wall (including the sternum) continuously for up to 5 days post cardiac surgery in order to investigate the effects of coronary artery bypass grafts utilising skeletonised *in situ* left internal mammary artery grafts, and any subsequent effects on the left sided chest wall compared to the right. Initial TOI values are not presented, only differences pre and post-surgery. However, it is of relevance to this study to report there was significantly decreased mean TOI (3.74% SD 2.47% vs. 1.98% SD 1.67%, $p = 0.036$) and increased mean nTHI change (0.28 SD 0.19 vs. 0.13 SD 0.13, $p = 0.020$) in diabetic cases post-operatively versus non-diabetic cases. The study concludes diabetes appears to be a risk factor for post-operative sternal ischaemic complications, and that NIRS may play a future role in post-operative monitoring [193].

Cai et al 2008 investigated the use of NIRS for monitoring the mandible following fibular graft transplantation post mandibular tumour removal. In controls, there were no statistically significant differences in TOI between sides of the mandible or between what times of day measurements were taken. Mean TOI values at bilateral measurement sites at the mandibular body and ramus ranged between 68.38% (SD 3.24) and 70.49% (SD 3.83) respectively. Post operatively it was found that the grafted side was in the range of 1.33%-4.2% less than the normal side in cases. A trend emerged where TOI was worst four to twelve hours post operatively but then recovered, although always just below the normal side's TOI. The study showed a promising application of NIRS, but more examples in failed cases are required to set a threshold for when grafts may require revision (there was only one failed case) [190].

Table 3.2: Summary of reported TOI values on healthy participants at anatomical bone sites (CW=continuous wave; m/f=male/female; SRS=spatially resolved spectroscopy; TRS=time resolved spectroscopy). Results are means unless otherwise stated.

Study	NIRS System	Anatomical Location	Demographics	TOI values
Binzoni et al 2003	Broadband CW	Tibial diaphysis	N=13 (m/f not stated; age range 25-72)	84.9% (SD 2.8)
Cai et al 2008	SRS	Mandibular body and ramus	N=40 (m/f 20/20; age range 21-70)	74.2% (SD 4.1)
Farzam et al 2013	Frequency domain	Patella	N=8 (all male; mean age 34.4 (SD 9.6))	65% (SD 9)
Farzam et al 2014	TRS	Manubrium	N=32 (m/f 15/17; age range 24-42)	Median 71.1% (IQR 69.5% to 72.3%)
Sekar et al 2015	Broadband TRS	Distal radius and ulna; proximal radius and ulna; greater trochanter; calcaneus	N=53 (m/f not stated; age range 20-78)	Distal radius (98%) Distal ulna (91%) Proximal radius (98%) Proximal ulna (74%) Greater trochanter (55%) Calcaneus (54%) (SD not reported)
Sekar et al 2016	Broadband TRS	Manubrium; forehead	N not reported	Manubrium 72% Forehead 81% (SD not reported)
Siamwala et al 2015	SRS	Proximal tibia	N=11 (m/f 8/3; age range 20-40)	81.3% (SD 5.5)
Siamwala et al 2017	SRS	Proximal tibia	N=18 (m/f 9/9; age range 20-40)	Females: 73.5% (SD 7.2) Males: 76.8% (SD 6.3)
Sorensen et al 2017	SRS	Proximal tibia	N=17 (all males; age range 19-38)	Median 81% (IQR 69% to 87%)

Sekar et al. 2015 presents mean TOI values at various superficial bone sites. Results varied from 54% at the calcaneus, to 98% at the radius [70]. A follow up study by the same group using a different NIRS system graphically demonstrated resting median TOIs of around 80% at the calcaneus, and radius, however wide variability amongst the sample of 17 participants is graphically evident, and quantitative data are not presented [75]. A summary of TOI results is presented in Table 3.2.

Some studies presented absorption and reduced scattering coefficients for bone [9, 15, 56, 75, 195], and/or absolute measures of haemoglobin concentration (in µM) [9, 15, 56, 70, 75, 195] at rest using more advanced frequency domain or time resolved spectroscopy NIRS systems. No studies reported comparisons with muscle or other soft tissue types for these parameters. A summary table of quantitative data from these studies is presented in Table 3.3. Two of these studies presented DCS-derived blood flow index (BFI) measures in bone tissue. Farzam et al 2014 reports a median BFI at the manubrium of 5.0×10^{-9} cm^2/s (IQR 4.2×10^{-9} to 7.4×10^{-9}) [56]. Sekar et al 2016b presents BFI data at six bony anatomical sites with values highly variable ranging from $2.0x10^{-9}$ to $8.0x10^{-9}$ cm^2/s [75]. This variability is in keeping with the variation in blood flow indices presented in animal studies, which may be dependent on different anatomical bone sites, and different tissue types within bone (such as red marrow, yellow marrow and cortical bone) [23, 260].

Overall this section demonstrates the wide variation in resting TOI values as well as the more advanced NIRS markers reported in bone tissue that can be measured at rest. This is perhaps understandable given the range of bespoke and commercially available NIRS systems used, and the variation in anatomical sites. However it also raises concerns over the applicability of using NIRS at rest as a research tool.

Table 3.3: Summary of reported NIRS parameters from healthy participants utilising more advanced NIRS systems at anatomical bone sites (m/f=male/female; TRS=time resolved spectroscopy; μ(a)=absorption coefficient; μ(s)'=reduced scattering coefficient). Results are means unless otherwise stated.

Study	NIRS system	Anatomical Site and Demographics	Absorption and Reduced Scattering coefficients (cm^{-1})	Absolute Haemoglobin Concentration (μM)
Farzam et al 2013	Frequency domain	Patella N=8 (all male; mean age 34.4 (SD 9.6))	λ 690 nm: μ(a) 0.038 (SD 0.009) μ(s)' 7.4 (SD 0.8) λ 785 nm: μ(a) 0.035 (SD 0.009) μ(s)' 5.4 (SD 0.8) λ 830 nm: μ(a) 0.044 (SD 0.009) μ(s)' 4.4 (SD 0.8)	18μM (SD 4)
Farzam et al 2014	TRS	Manubrium N=32 (m/f 15/17; age range 24-42)	Median λ 690 nm: μ(a) 0.14 (IQR 0.12, 0.17) μ(s)' 10.1 (IQR 9.7, 10.9) Median λ 785 nm: μ(a) 0.15 (IQR 0.12, 0.17) μ(s)' 9.6 (IQR 9.0, 10.2) Median λ 830 nm: μ(a) 0.16 (IQR 0.13, 0.18) μ(s)' 8.7 (IQR 8.3, 9.5)	Median 77.3 μM (IQR 62.2, 88.6)
Pifferi et al 2004	Broadband TRS	Calcaneus N=7 (all females; age range 26-82)	μ(a) individual ranges from 0.05-0.20 cm^{-1} and μ(s)' individual ranges between 10-16 cm^{-1} between wavelengths of 650-1000nm	Individual participant range between 17-28 μM
Sekar et al 2015	Broadband TRS	Radius and ulna; greater trochanter; calcaneus N=53 (m/f not stated; age range 20-78)	Not presented	Distal radius (28.3 μM) Distal ulna (25.3 μM) Proximal radius (19.2 μM) Proximal ulna (52.0 μM) Greater trochanter (17.7 μM) Calcaneus (20.5 μM) (SD not reported)
Sekar et al 2016a	Broadband TRS	Manubrium; forehead (N not reported)	μ(a) individual ranges from 0.1-0.7 cm^{-1} and μ(s)' individual ranges between 6-13 cm^{-1} between wavelengths of 600-1000nm	Manubrium 58.6 μM Forehead 29.8 μM (SD not reported)
Sekar et al 2016b	Broadband TRS	Radius and ulna; greater trochanter; calcaneus N=17 (m/f not stated; age range 25-50)	μ(a) ranges from 0.05-0.45 cm^{-1} and μ(s)' individual ranges between 4-12 cm^{-1} across anatomical sites between wavelengths of 700-1000nm	Not presented

3.5.5.2: Arterial protocol markers

Binzoni et al. 2002 and Binzoni et al. 2003 were the first studies to report arterial occlusion haemodynamic data in bone tissue at the tibia. These studies claimed

confidence that bone was truly being measured based on the observed smaller reperfusion rates of recovery in bone tissue post arterial occlusion release, compared with muscle. These studies quantify this using a “perfusion index” based on derivatives of haemoglobin time signal curves.

Aziz et al. 2010 did not present quantitative data, but demonstrated mirrored changes in HHb and O_2Hb concentration (in µM.cm) at the proximal tibia during and after arterial occlusion of the distal femur using a bespoke NIRS device on five participants [16]. Likewise, Klasing et al. 2003 does not present quantitative data on haemoglobin concentration changes at the tibia during arterial occlusion (AO). However, an interesting finding is presented with resting oxygen consumption rates pre arterial occlusion reported as fivefold greater in muscle tissue than at the tibia. This study also finds oxygen consumption rates do not significantly change at the tibia during a protocol of calf muscle contraction, arguing that this provides confidence that bone is being sampled [185].

Farzam et al. 2013 makes use of frequency domain NIRS to look at changes in bone haemodynamics within a cardiac cycle. This looked at confirming whether microvessels in the bone have the ability to display pulsatile vasodilation and constriction despite their location in rigid bone tissue. The study found an AC mean fluctuation of 0.7% TOI and 3.1% total haemoglobin concentration during the cardiac cycle at rest, suggesting pulsatile vasodilation occurs. The absorption coefficient also varied throughout the cardiac cycle, suggestive of blood volume changes. These changes are confirmed to be physiological as they are not present during arterial occlusion. These results conflict earlier theories that microvessels in bone were restricted in their pulsatile vasodilation and that therefore NIR signal from PPG or LDF was only influenced by blood flow/velocity changes [83, 254].

Farzam et al. 2013 [15] also reports a mean 8.2% (95% CI 7.6% to 8.8%) drop in TOI at the patella during a 5 minute occlusion. The authors argue this demonstrates a slower rate of oxygen extraction compared with previous findings by Yu et al. 2005 [261] describing a 16.4% (SD 4.4) mean reduction in TOI for muscle tissue at the calf during a three minute arterial occlusion.

3.5.5.3: Other relevant results

Alneami 2015 showed the responsiveness of NIRS to exercise, recording tibial blood volume increases in the range of 19%-33%, restoring to baseline at rest. This study

also used NIRS to monitor haemodynamic changes at the tibia of paraplegic participants using a modified rowing machine, citing this as a potential application of NIRS, however results were reported descriptively from two participants [186].

Binzoni et al. 2006 showed NIRS was responsive to blood volume changes in response to head up tilt whilst in the supine position, and sensitive to changes from as little as 15 degrees tilt change. Total haemoglobin concentration in the tibial diaphysis increased on average 120.7% (SD 9.7) with 75 degrees of head up tilt [10]. Siamwala et al. 2015 showed statistically non-significant changes in TOI with 15 degrees of positional tilting of the supine participant. These manoeuvres did however produce statistically significant changes in blood volume (measured with strain-gauge plethysmography) and microvascular flow (measured with PPG) [78].

3.5.6: Synthesis of results

As expected there was too much methodological heterogeneity in NIR systems used, anatomical sites, and approaches to haemodynamic measurements to combine any study results in a meta-analysis.

3.5.7: Additional analyses

3.5.7.1: Reliability of NIR systems

Broadly speaking, study results using NIR systems longitudinally were suggestive of the expected haemodynamic changes during interventions. However, across most studies wide variability in results between participants was evident, especially across applications of LDF. Crucially, no studies were identified specifically addressing the reliability or reproducibility of NIR optical systems. Studies that did attempt to assess reliability typically did this in a superficial or *ad hoc* way in small samples without rigorous statistical analysis of agreement or reliability. Approaches included comparing anatomical contralateral results, describing repeat measurements in terms of their variability (either in the same or different sessions), or simple comparison of results with existing literature in animal studies or involving different tissue types.

Specifically within NIRS studies, Reher et al 2011 reports wide variability in results on one patient where measurements were taken 6 times over three months. This was despite using the mean of 5 repeated measurements as one data point. Likewise there was no statistically significant difference between left and right mandible measurements in controls, however wide variability was observed and the study

concluded this would restrict the potential diagnostic applications of NIRS in the mandible [192]. Farzam et al 2013 looks at comparing total haemoglobin concentration in absolute measures against other literature, but results have large uncertainty due to small sample sizes [15]. Likewise, Farzam et al 2014 [56] compares absorption and reduced scattering co-efficients to wide ranging results from previous literature such as Pifferi et al 2004 [9]. Sekar et al 2015 also presents wide ranging results of TOI, cHb and scattering and absorption co-efficients across bone sites when sampling 53 participants [70].

This wide variation in results may prohibit the development of useful diagnostic thresholds for NIR optical systems [225, 239]. Wide biological variability in vascular measurements is a known barrier to research in this field [81] and this is also reflected in suboptimal reproducibility in alternative modalities for measuring bone tissue haemodynamic markers, such as with DCE-MRI protocols [130, 131].

Variability is likely to be affected by the heterogeneity of bone tissue and the small sampling volume of NIR optical systems (particularly LDF) with sampling of small arterioles, variations in marrow composition, or less vascular trabecular striate potentially altering readings. It is important to tease out what variation in results is attributable to measurement error and what reflects normal physiological ranges. Likewise, most studies typically used only one, or a small group, of operators. Few studies took repeat measurements, or multiple readings at adjacent sites, which is recommended due to this small penetration depth and sampling volume of NIR optical systems, especially with LDF.

Other factors requiring more investigation on potential reliability specific effects to LDF studies include the comparison of results in studies where the probe is placed non-invasively, directly on the bone surface, or intra-osseously. The sensitivity of probes to movement also means stable probe placements during surgical operations is important and some studies reported holding probes by hand or using bespoke probe holders [206, 217]. Some study designs involved having to move probes in between measurements to facilitate surgery, which can introduce measurement error given the small sampling volume and potential for measuring a different vascular bed when probes are repositioned [240, 244]. In addition, as these LDF studies were intra operative the effects of anaesthesia, blood loss during surgery and direct impact of surgery cannot be discounted as sources of error [207]. When placing probes intra-osseously, the effect of drilling on intra-osseous blood flow is unknown and flushing of the probes

is required to remove clotting around the measurement site, which could otherwise prohibit flow and affect readings.

3.5.8: Risk of bias across studies

Formal statistical analyses of potential publication bias have not been possible due to the methodological heterogeneity of the included studies. The majority of studies presented NIR technologies in a positive light or with significant results, however it should be noted that most studies were from published journal articles or conference proceedings, which may mean collective results are prone to publication biases. However the two sources of grey literature (both theses) identified similar positive findings to the published evidence identified.

The identified studies also generally involved small participant sample sizes putting the collective interpretation of results at risk of "small study effects". This term is used to describe the potential of increased effect sizes being presented in studies with small sample sizes, either because of a potential association between small sample sizes and poor methodological quality, or potential heterogeneity in the sample population chosen [262]. Given included studies generally reported the recruitment of participants poorly, small study effects cannot be ruled out and should be considered when judging the strength of evidence from the review. Likewise the difficulties in blinding assessors from detection biases and inconsistent handling of attrition or incomplete results also needs to be kept in context with the conclusions of the review.

The assessment of internal biases of individual studies has identified that reporting bias was generally low minimising the risk of selective reporting biases across the evidence base.

3.6 Discussion

3.6.1: Summary of evidence

A large number of studies have been identified utilising NIRS, PPG and LDF systems to investigate bone tissue either non-invasively or intra-operatively. The wide heterogeneity in anatomical sites and investigated applications demonstrates the demand for the types of information NIR technology promises. The studies identified are predominantly early stage studies which often illustrate the promise for future clinical and research applications. However, there are a wide range of challenges that require addressing to advance this field of research in bone health.

There is yet to be conclusive evidence that haemodynamics markers obtained non-invasively truly represent the bone tissue that is being sampled. As outlined in Section 3.5.3.1 some studies investigated the contribution of superficial tissue to NIRS signal. Other studies compared NIRS results taken at bony anatomical locations to muscle readings, but results from these types of direct comparisons should be interpreted with caution in context with the differing attenuation properties and capillary densities of different tissue types, which may potentially confound comparative results of markers such as oxygen extraction rates [65].

Validation of NIRS measurements against an external reference of comparable haemodynamic markers could provide further confidence that haemodynamic markers truly reflect bone tissue. No studies used a reference standard or comparator to compare results to validate this application of NIRS. Potential reference standards are discussed such as DCE-MRI, Nuclear Medicine, Doppler and PET [56, 192], and DXA (in the case of absolute measurements of collagen and mineral content) [9, 258]. Scintigraphy of the sternum is mentioned by Takami et al 2008 but can only be done one week post-surgery [193].

The need for further work on the reliability and reproducibility of NIR optical systems for repeat measurements across different operators and participants has been identified. There was a wide variation of NIRS systems and technological approaches used, with differing approaches to data collection, probe spacing, anatomical sites and microvascular challenges. Likewise, continued investigation around whether variability is physiological or equipment based (or both) is important, as this is still not clear from the literature. If physiological variability is wide at an individual level even in healthy participants, NIR optical systems may be unhelpful for development of individual diagnostic thresholds, but NIR research could perhaps still elucidate important haemodynamic differences between sub populations of interest given the current lack of alternative research tools. Reliability investigations of NIR technologies should also be kept in context with the reliability of other existing comparator tests measuring bone tissue haemodynamics *in vivo.*

There is a small body of evidence that suggests there is disparity between NIRS manufacturers when measuring TOI at rest for other tissue types. This is another potential source of error to consider for future research, particularly if multi-site. Hyttel-Sorenson et al. 2011 found similar reproducibility results across three different sets of commercially available spatially resolved NIRS systems when measuring muscle at

the forearm, but different resting mean TOIs ranging between 60.8% (SD 3.6%) and 70.2% (SD 6.7%) [263]. Ye Yang et al. 2007 presents similar variation in baseline TOI at the forearm between different studies [264]. There was very little information provided in the included studies on calibration protocols or quality assurance techniques used to ensure accurate measurements, even where bespoke equipment is presented.

A small number of studies attempted to validate LDF results against an external comparator or reference standard, such as microangiography, MRI protocols, nuclear medicine and PET protocols. However, those that did presented promising results [147, 216, 221]. External validation remains crucial to give credence to future NIRS optical systems. Alternatively, confidence could be gained through correlation with other relevant indicators of bone health, such as bone density, blood markers of bone metabolism, or longitudinal patient follow up when used to guide operative cases.

Establishing the generalisability of results is also crucial to the development of these technologies. This includes gauging the expected normal physiological variability between different ethnicities, ages, sexes and body habitus, as well as during the operative state in the case of LDF. Al-Kassab 1995 reflects that differences in ethnicity and bone structure are not accounted for with NIRS measurements and their individual effects remain unknown [187]. Alneami 2015 also discusses the potential effects of melanin levels on non-invasive NIRS measurements [186]. Ethnic differences in microvascular function of the skin have been previously identified [265] and so may be expected in bone. It appears the influence of overlying tissue on non-invasive measurements also requires careful consideration. Most feasibility studies used non-obese volunteers to overcome this, which limits generalisability due to the potential effects of greater depths of superficial tissue on NIRS measurements [56, 77, 83, 189].

As always, participant tolerability of protocols should also be considered, as well as ruling out any potential negative impact of intra-operative use of LDF, which was not addressed by the studies identified. There was very little discussion of the participant tolerability of testing. Siamwala et al. 2015 was one exception stating minimal discomfort with no adverse effects, and that all participants completed the study [78]. Consideration of participant tolerability is an important aspect, primarily from an ethical perspective, but also because measurements may be confounded by a stress response if uncomfortable or unfamiliar microvascular challenges are being applied.

Technological advances in NIR optical systems also show promise in the future of this application. The development of TRS NIRS systems promises the ability to measure absolute concentrations of oxygenated and deoxygenated haemoglobin non-invasively with the participant at rest. This facilitates easier measurement protocols and more appropriate data comparison between participants. Likewise, the possible development of commercially available broadband NIRS systems can allow the potential measurement of other relevant components of bone tissue such as mineral, lipid, collagen, and water concentration [9, 70, 75, 195]. With improved probe design and detector sensitivity, the ability to measure deeper tissues may also be feasible in the future. These developments are discussed further in Chapter 11.

3.6.2: Limitations

Sections of the review process including title and abstract searches, data extraction, and risk of bias assessments were carried out primarily by one reviewer. This may have introduced some error or subconscious biases, but steps were taken to minimise this subjectivity, and concerns or queries were raised with the supervisory team as required.

After executing the search strategy, the searches used for MEDLINE and EMBASE were retrospectively audited. All additional included studies identified by reference list and citation tracking were retrospectively checked on the search returns of MEDLINE and EMBASE searches. Two studies were identified that had been included in database search returns but excluded incorrectly. One other study, Pifferi et al. 2004, was not identified in database searches despite undertaking spectroscopy of the calcaneus. It was likely this study was missed as the focus and terminology of the article is on absorption spectra of the calcaneus (rather than haemodynamic markers) including water, lipid and bone mineral concentration, as well as haemoglobin concentrations [9]. Seven studies were indexed on MEDLINE but not returned in the search used. All seven studies were primarily investigating the cochlea with LDF and were likely to be missed by the search as cochlea was not a specific search term used, as it was an unexpected field of research.

A protocol change was made to the approach for the intrinsic risk of bias assessment of included studies. Whilst deviations from pre stated protocols may introduce biases to the review process, it was felt this change was necessary to allow for the unexpected range of study designs encountered.

3.6.3: Conclusions

Further work is required before NIR optical systems can be considered a valid and reliable research tool of vascular bone health. However, the wide and varied literature base identified in this review ultimately highlights the strong promise of this application of NIR optical systems, which potentially offers real time, safe and inexpensive measurements of bone tissue haemodynamics.

This thesis will aim to address some of the most pressing gaps in the evidence base around the use of NIRS for measuring haemodynamics in human bone tissue *in vivo.* This includes development of an arterial occlusion protocol and a formal assessment of reliability for related NIRS measurements. It also includes an attempt to validate NIRS measurements with comparison of results with other tests of bone haemodynamics using a dynamic contrast enhanced MRI (DCE-MRI) protocol, and other indicators of bone health including bone mineral density measurements and trabecular bone scoring, as well as blood markers of bone metabolism.

Chapter 4: Methodology of protocol development

The outcomes of the systematic review in Chapter 3 have highlighted the potential applications of NIRS for measuring haemodynamic markers of bone tissue, but also the current gaps in the evidence base around reliability, and validation against external markers of bone health. This leads to the experimental component of this PhD project hoping to address these concerns around this application of NIRS. The experimental work involved three main stages and are presented in the following order:

Chapter 4: Methodology of protocol development for obtaining *in vivo* NIRS measurements in human bone, with results from the adopted protocols presented in Chapter 5.

Section 6.1: Methodology for the reliability assessment of the adopted protocols, with associated results presented in Chapter 7.

Section 6.2: Methodology for the validation assessment of the adopted protocols against other markers of bone health, with associated results presented in Chapters 8, 9 and 10.

4.1: Aim and objectives of protocol development

The systematic review in Chapter 3 identified a number of feasibility studies with small sample sizes and a variety of methodological approaches, which indicate that NIRS has the potential for providing useful haemodynamic information for *in vivo* bone tissue. Building on this, the aim of this protocol development work was to demonstrate if the available NIRS equipment (Hamamatsu NIRO-200NX, outlined in Section 2.2.1) could be used to develop protocols for use in bone that were worthy of more rigorous assessments of reliability and validation.

Ethical approval for protocol development was obtained from the University of Exeter Medical School (UEMS) Research Ethics Committee to carry out testing on healthy volunteers recruited internally from UEMS (application 14/11/063). Recruitment of participants involved recruiting volunteers from the Diabetes and Vascular Research Centre (where the research was carried out) and at the University of Exeter St Luke's campus, using convenience sampling. This primarily included staff volunteers and stage 3 undergraduate student volunteers from the Medical Imaging programme. Recruitment was non-intrusive and involved selected email addresses, visiting

teaching sessions, and word of mouth. There were no incentivisations or pressure put on potential participants to participate.

Protocol development included answering the following key objectives, with justification of methods addressed further in the following sub sections:

4.2: Determining the best anatomical location for measurements;

4.3: Optimising placement of NIRS optodes;

4.4: Establishing NIRS protocols to be adopted for reliability and validation evaluation;

4.5: Establishing appropriate haemodynamic markers from protocols;

4.6: Confirming haemodynamic markers derived from proposed protocols are representative of bone tissue and can detect changes in real time;

4.7: Ensuring protocols are tolerable for participants;

4.8: Determining initial impressions of reliability to justify further investigation; and,

4.9: MRI protocol development for potential validation against NIRS.

4.2: Determining the best anatomical location for measurements

As discussed in Section 2.2.1, only anatomically superficial bony sites are suitable for NIRS measurements. Previous studies have measured bone haemodynamics at a variety of superficial bony sites including the tibia [10, 16, 78, 186, 188, 189], calcaneus [9, 70], radius and ulna [70], greater trochanter of the femur [70], patella [266] and manubrium [56].

A number of anatomical sites were ruled out initially following consideration:

- Frontal bone/skull vault: The anticipated variation in frontal sinuses across participants was considered a risk. There was also concerns of controlling the depth of measurements (since NIRS is used routinely for measuring deeper cerebral tissue).

- Calcaneus: Due to the variation in foot size and overlying soft tissue in the population, it was considered that the calcaneus could be too small for some participants and its irregular shape may prohibit reliable reflectance spectroscopy measurement. There is potential to measure the calcaneus using transmission mode NIRS [9], but this option would prohibit use of spatially resolved NIRS markers which rely on reflectance spectroscopy (as described in Section 2.2.1.4).

- Metatarsal and metacarpals: Were considered too small to guarantee sampling of bone tissue.

- Sternum: Was excluded due to logistical and ethical considerations of measuring female participants and also the potential variability in overlying soft tissue. Also, given its anatomical location, interventions to simulate haemodynamic changes are limited.

- Distal Radius and Ulna: This would be a site of interest given its susceptibility to fragility fracture [167]. However, there were concerns over whether bone tissue alone would be sampled given the relatively small bone volume of these two bones and the various different tissue types passing through the wrist (including nervous tissue and connective tissue such as large blood vessels, ligaments and tendons).

- Olecranon: Excluded due to positioning difficulties keeping optodes in parallel, as required using the spatially resolved system available.

As such, it was decided to focus on the following four anatomical sites (with optode positioning demonstrated in Figure 4.1) for further protocol development:

- Patella: Optodes were placed transversely across both superior angles of this approximately triangular shaped bone. The patella is generally very superficial, easily palpated and generally large enough to allow optode separation of 4 cm.

- Proximal Tibia (TP): The proximal optode was placed just medial to the palpable tibial tuberosity with both optodes on the medial plane of the tibia, medial to the anterior tibial ridge.

- Diaphysis of Tibia (TD): Optodes were placed at the mid shaft at the tibial diaphysis on the medial plane of the tibia at a point mid-way between the medial malleolus and the tibial tuberosity.

- Medial Malleolus: Optodes were placed just proximal to the bony prominence of the medial malleolus, on the distal medial plane of the tibia.

For the assessment of potential protocols involving monitoring haemodynamic changes during occlusion interventions it was decided to focus on the proximal tibia and tibial diaphysis, given that there was anecdotal optode positioning issues with the patella and medial malleolus leading to the most variability at these two sites (discussed further in Section 5.3.1). The proximal tibia and tibial diaphysis are both superficial bony landmarks, with a comparatively large bone volume to sample, best suited for reliability of optode placement and ensuring bone tissue is predominantly

sampled. Both sites are also in weight bearing bone that is likely to be representative of poor systemic bone health, with the tibia a relatively common site for fragility fracture [267]. Popp et al 2009 identified tibial BMD changes were as predictive of clinical fracture risk as traditional BMD measurement sites at the hip and lumbar vertebrae [268].

These two sites are potentially measuring two predominantly different types of bone (trabecular bone at the proximal tibia, as opposed to yellow marrow in the diaphysis) [55]. For comparison measurements of the lateral calf were also obtained, likely to represent the lateral head of the gastrocnemius muscle and soleus muscle, which is a more established site of measurement in the scientific literature [269, 270].

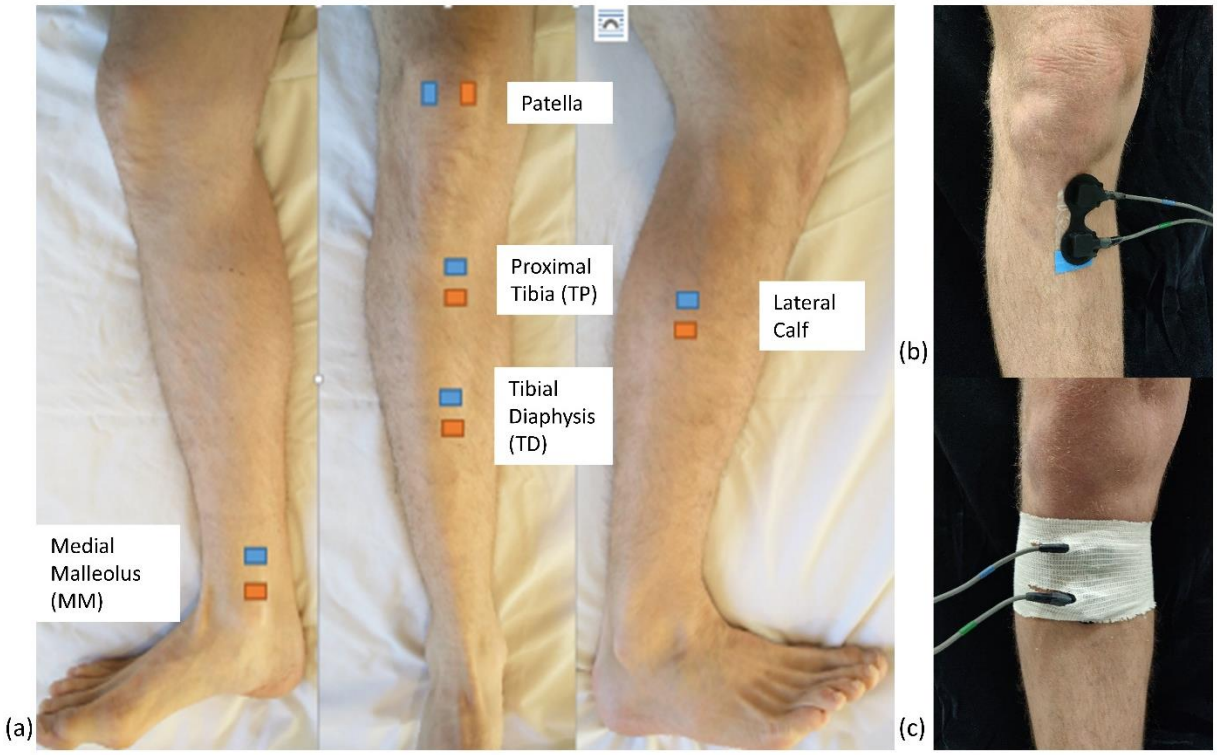

Figure 4.1: (a) Typical placement of NIRS laser optode (orange) and detector optode (blue) at relevant anatomical sites. (b) positioning at the proximal tibia using double sided adhesive and the 4cm optode "hood" for light shielding and ensuring consistent spacing between optodes. (c) demonstrates the same positioning at the proximal tibia using the preferred method of stabilisation using tubular bandages.

4.3: Optimising placement of NIRS optodes

4.3.1: Securing optodes

Initially optodes were placed on the skin at the above anatomical locations using double sided adhesives provided by the manufacturer. However these were designed with soft tissue measurements in mind and initial testing found these hard to make small adjustments when positioning optodes more precisely on bony anatomy. They also proved difficult to ensure adequate pressure for stable readings over a long period

of up to 15 minutes for some of the proposed intervention protocols. The adhesive was also unpleasant for the participant, as it pulled hair when being removed.

An alternative solution was to use tubular bandages which could hold the optodes in a stable position and allow small adjustments more easily. This also had the advantage of shielding external light from the optodes and applying a small amount of pressure to the optodes on the skin surface. Small incisions were cut into the bandage to allow the optode to be inserted and held underneath whilst allowing space for optode cabling (see Figure 4.1).

With soft tissue measurements, too much skin pressure may lead to partial occlusion of superficial micro vessels, thus altering readings. However this is less of a concern with bone readings where bone tissue haemodynamics are expected to be minimally affected by pressure put on the skin surface. Conversely, gentle pressure is proposed to be beneficial by reducing the superficial soft tissue thickness being sampled [56, 77, 191]. There is precedence of using bandages to aid optode placement, and previous evidence supports that applying optodes with pressure can aid measurement of deeper tissue types [77, 254]. Anecdotally, subjects preferred the bandage to the use of adhesives, which can cause discomfort to remove. Operators also found positioning optodes easier using the bandages without adhesives.

4.3.2: Shielding light

Previous studies recommend covering optodes with a black blanket to shield any surrounding light from affecting detector readings [3, 4]. Upon trialling this it was found that the weight of the cloth had potential to move optode position. Instead, by using a combination of the manufacturer's optode holders and tubular bandages to secure optode position (as per Figure 4.1), external light sources were suitably shielded from the detectors. Lighting in the room was also kept consistent in the testing lab.

Anecdotal testing was performed using this optode set up to test for any effect from external light pollution. Once a rest baseline was established, continuous measurements were taken on one participant with normal lighting, then using a black cloth to cover optodes, then without the cloth but with room lights off, and finally shining a torch directly on the optode set up from a distance of 10cm. There was no observable systematic changes in any NIRS measurement parameters as external light was varied. This gave confidence that the optode set up was adequately shielding from external light sources, without using a black cloth.

4.3.3: Optode spacing

As discussed in Section 2.2.1, when using continuous wave NIRS the light emitting optode is placed a set distance from the light detecting optode, and the distance set will determine the volume and depth of tissue sampled. Aziz et al. 2010 demonstrates a maximum depth measured of half the internode spacing [16]. The Hamamatsu system comes with 3cm and 4cm premanufactured optode "hoods" to shield external light and ensure consistency with optode spacing (demonstrated in Figure 4.1). As spatially resolved spectroscopy relies on parallel optode placement, any potential anatomical protocols need to consider the parallel spacing of optodes to ensure it facilitates sampling of bone tissue and is logistically feasible.

For use of NIRS at superficial bony sites, it was initially considered whether optode spacing should be altered depending on participant size or superficial tissue thickness, allowing for these differences in superficial tissue or cortical bone thickness. However, without reliable data on how much variation exists in overlying soft tissue depths across the population, it was decided to keep optode spacing consistent, with any systematic confounding based on superficial tissue thickness to be investigated during data analysis.

As such, measurements of leg circumference were taken at the knee, calf and ankle, along with skin calliper measurements at measurement sites at the patella, proximal tibia, tibial diaphysis and medial malleolus. Previous studies have also performed such analysis on the effects of superficial tissue variation on measurements at the tibia and patella, demonstrating negligible effects of variations in superficial tissue in healthy participants with normal BMI [56, 77].

Some feasibility work was undertaken to investigate for any systematic effects of optode spacing between 2.5cm and 5cm, as the existing literature mentions using a variety of spacing distances within this range, as discussed in Section 3.5.2.1. Results of this work are presented in Appendix E. Given these observations it was decided to use a 4cm spacing between optode and detector using the premanufactured light hood. This was considered the best balance between penetrating tissue depth and the decreased signal to noise ratio attributable to wider inter optode separations [2].

Anecdotal feasibility work was also carried out to ensure the arrangement of light source and detector did not alter readings depending on which was placed proximally

and distally on the anatomy in question. No obvious trends were noticed, but for consistency, the laser light source optode was kept proximal for all participants.

4.4: Establishing NIRS protocols for reliability and validation evaluation

Several protocols were explored before deciding on the eventual AO protocol developed for further reliability and validation assessment in this thesis. These protocols were predominantly guided by the evidence base identified in Chapter 3 and past studies looking at skin and muscle tissue performed at the Diabetes and Vascular Research Centre (DVRC).

Three protocols were attempted that were promising, but turned out to be unlikely to be reliable enough for further reliability evaluation. This included a mid-calf occlusion protocol, a venous occlusion protocol, and replicating a study that looked at NIRS response to gravitational positional changes. These protocols all showed differences between proposed bone haemodynamics and measurements at the lateral calf, giving confidence that a different tissue type was being measured. However, these protocols were clearly not reliable enough to pursue more rigorous reliability and validation assessment. Details of the methods and results of these three protocols are presented in Appendix F.

4.4.1: Arterial occlusion protocol

Of the protocols that were attempted and considered for further reliability and validation assessment, it was decided an AO protocol was most appropriate, and as such this will be explained in more detail in this section. The AO protocol was observed as the most likely to be objectively and consistently applied as a protocol, and therefore most likely to be reproducible. As a technique it also has the most precedence in the existing NIRS evidence base involving *in vivo* bone haemodynamic measurements [16, 56, 185, 188, 189]. AO protocols are also established for NIRS studies of muscle and skin and are used routinely at the DVRC where this PhD is based [65, 271].

The AO protocol involved simultaneously taking NIRS measurements of a tibial site and the lateral calf before, during and after occluding blood flow to the leg proximally at the distal femur. Recordings were zeroed at the commencement of the protocol and a sampling rate of one second was used. Only one leg was measured, but occlusions were repeated so both the TP and TD site could be measured on each participant, with optode placement as outlined above in Section 4.2.

Positioning pads were considered to stabilise the leg, however these did not appear to offer any advantages over supine positioning. Feet were kept in a relaxed position without dorsiflexion and care was taken to ensure feet were not overhanging the mattress, which could cause compression over the course of testing. Supine positioning was preferred to avoid gravitational effects and compression changes to lower limb perfusion over the course of testing [272].

Figure 4.2: Arterial occlusion set up. The blood pressure cuff is around the distal femur. NIRS optodes are positioned at the proximal tibia (TP) and lateral calf muscle, secured by bandages. A temperature optode and O2C white light optode is placed at the foot to observe any systemic changes and to check for the effectiveness of the arterial occlusion. Occlusion is rapidly applied and released using the pictured occlusion system.

Participants were required to lie supine for 15 minutes to allow acclimatisation prior to commencement of the AO [272]. Two minutes of baseline readings were then taken with

the participant at rest. Arterial occlusions were performed using a blood pressure cuff around the distal femur with a second non inflatable cuff placed around it to prevent any movement or loosening of the cuff during inflation (see Figure 4.2). A quick inflation system was connected to the cuff to allow for a rapid and smooth AO inflation (see Figure 4.2). The blood pressure cuff was typically inflated to 200mmg of pressure [65]. If higher resting blood pressure was recorded for a participant, a higher pressure was considered if the participant could tolerate this. The integrity of the occlusion using the blood pressure cuff was assessed during testing using laser Doppler flowmetry of the skin distal to the occlusion site on the dorsal surface of the foot. A successful AO was confirmed by a reduction in blood flow to biological zero during occlusion [273].

Four minutes of arterial occlusion was sustained as is standard practice in vascular occlusion studies carried out at the DVRC alongside evidence suggesting typical use of AO between three to five minutes [65, 79, 272]. NIRS measurements were then taken for five minutes following instantaneous release of the occlusion. Arterial occlusion has been demonstrated to be very low risk in terms of inducing irreversible ischaemia or any other adverse effects [272]. Some moderate discomfort may be experienced by participants but the cuff can be quickly released if requested with any discomfort quickly alleviated.

The integrity of the inflation was also assessed using the resulting readings taken using NIRS. This typically results in simultaneous and matched increases in deoxygenated haemoglobin (HHb) and decreases in oxygenated haemoglobin (O_2Hb) concentration as oxygen extraction continues in the occluded leg, with a mirrored return to baseline once the cuff is released [65]. An acceptable AO was also required to have a change of total haemoglobin concentration (nTHI) of less than +/- 15%, suggesting a valid arterial occlusion with stable blood volume during the occlusion [80]. Due to the non-instantaneous inflation of the cuff, it is expected that there may be some change in nTHI as the cuff is inflated, as venous flow is occluded prior to arterial flow (which flows at a greater pressure). As such there is sometimes a momentary change in blood volume going into the leg prior to full AO [266]. However, this should plateau post occlusion and was considered a successful occlusion if this plateau was within +/-15% of the pre-occlusion nTHI (see Figure 4.3 for an example).

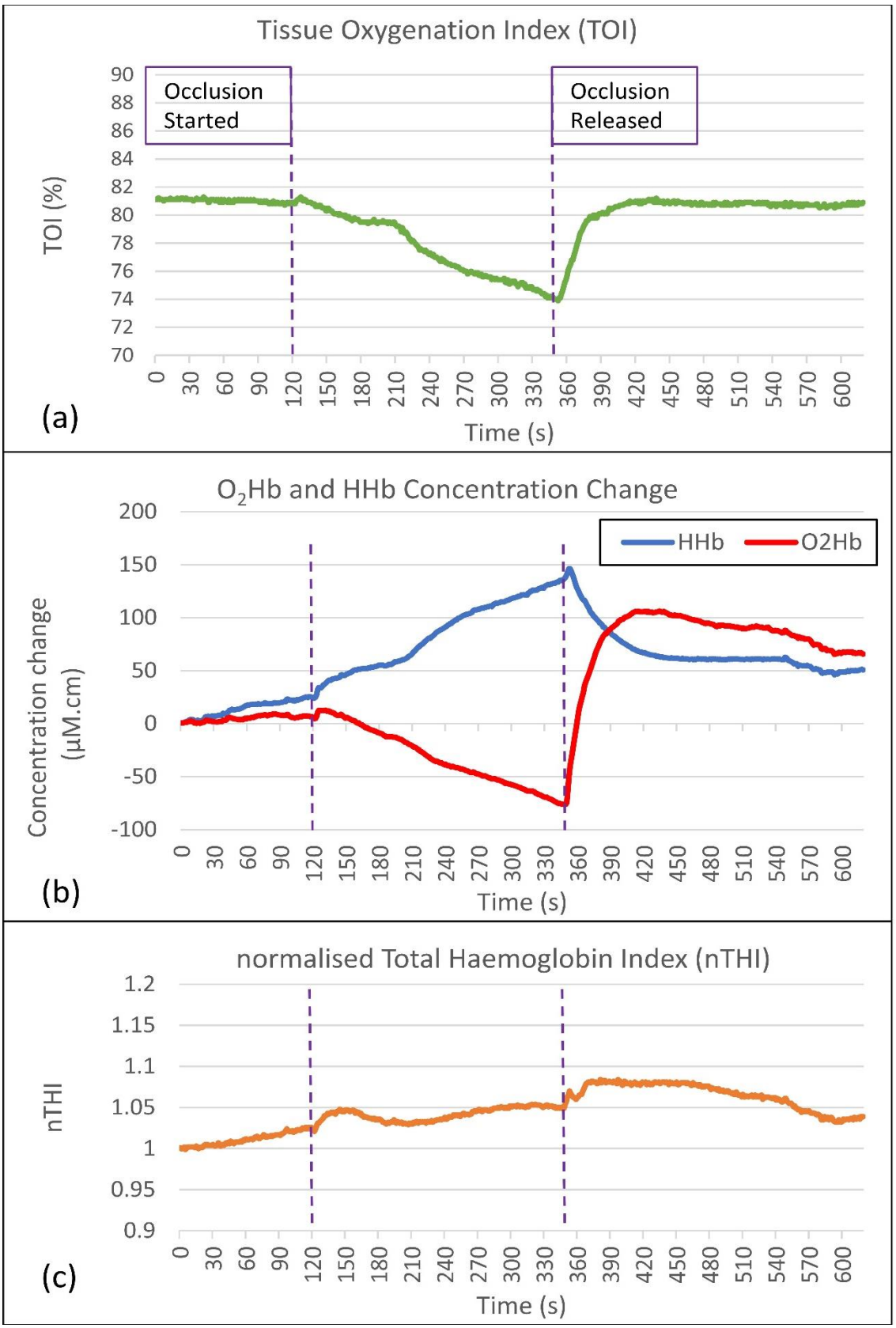

Figure 4.3: An individual example of acceptable arterial occlusion data for bone. (a) the overall TOI drops during occlusion and responds upon occlusion release; (b) O_2Hb and HHb experience equal and opposite changes during occlusion; (c) nTHI remains +/- 15% during occlusion (i.e. between 0.85 and 1.15). Some nTHI change is expected during inflation of the cuff as pressure will momentarily occlude venous blood return but not arterial inflow.

Systemic arterial oxygen saturation readings, pulse readings, and foot temperature were also monitored throughout the process to observe any systemic changes to oxygenation or body temperature during the course of the experiment, in order to rule out any confounding systemic changes during the testing period. The testing labs used have a controlled temperature of 22.5 +/-0.5 ºC [65]. Using the data collected, potential haemodynamic markers were investigated, as outlined below in Section 4.5. Data were downloaded from the NIRO-200NX system software and imported into Microsoft Excel (Microsoft Office, Professional Plus 2013) for data analysis.

4.5: Justification of the haemodynamic markers to be assessed

As discussed in Section 3.5.5.2, there is a lack of consensus on how the changes observed during and after arterial occlusion should be quantified. As this project aims for validation of the use of NIRS in bone tissue, it is important to identify which approach to quantifying the haemodynamic changes observed during occlusion is most appropriate, both from a physiological and reliability standpoint. This choice of markers investigated is discussed in this section and was determined by examining data from AO protocol development, as well as from studies identified utilising AO protocols for investigation of bone, skin and muscle tissue haemodynamics.

As previously introduced in Section 2.2.1, NIRS can measure several parameters in real time including tissue oxygenation index (TOI), absolute oxygenated haemoglobin concentration change (O_2Hb), absolute deoxygenated haemoglobin concentration change (HHb), and normalised total haemoglobin index (nTHI). This section will outline and justify a range of haemodynamic markers based on the above parameters that are physiologically warranted, and therefore had statistical assessment of their reliability. There are a number of markers considered, which leaves the statistical analysis open to criticism of multiple testing. However, given the context of early feasibility investigations of this potential application of NIRS, it was felt this was warranted in order to investigate the most reliable parameters to take forward.

4.5.1: During occlusion (DO) haemodynamic markers

In order for AO data to be included in analysis, it was essential that blood volume in the leg was observed to be relatively constant during the four minute occlusion period (i.e. an nTHI +/-15% from baseline). In this context, measurements of nTHI are only of interest for establishing that a closed system has been achieved by occlusion. When blood volume is constant, changes in HHb and O_2Hb are physiologically relevant

during this phase, as they are representative of oxygen extraction metabolism in a closed physiological system [65]. TOI naturally reflects this too as a ratio of O_2Hb to total haemoglobin concentration. It should be noted that this only represents the extraction of oxygen from haemoglobin. However, the rate that oxygen is extracted from haemoglobin could be influenced by the oxygen consumption metabolism and health of cellular tissue, the capillary density of tissue, and/or the microcirculatory function within the measured volume [272]. Stronger measures of oxygen extraction are generally considered to indirectly represent better microvascular health [65, 272].

Investigation of the rates of change in O_2Hb and HHb is potentially useful and physiologically representative of oxygen extraction rates during the occlusion. There is precedence for looking at the first 60 seconds of occlusion [65, 274]. However based on this protocol development process, it was observed this initial period was potentially prone to sources of variability including participant movement, and the short time to inflate the cuff, with nTHI changes most volatile in the first minute of occlusion [275]. If blood volume (as measured by nTHI) is changing during measurements, then there cannot be confidence that the rates measured are representative of oxygen extraction alone [276].

As such, the last 120s and the last 60s of oxygen extraction rates during occlusion were investigated, as this is the period most likely to have a stable blood volume, and continuous linear rates of change, whilst still providing a sufficient period of data to allow potentially reliable calculations of rates. Hence data were assessed for the rate of change during the last 120s and 60s for all three relevant parameters (TOI, HHb, and O_2Hb). This was conditional on an nTHI change of less than 5% within the 60s/120s period of measurement to ensure blood volume changes do not confound these measurements of oxygen extraction rates. Again, data were also not included if nTHI fluctuated more than +/-15% during the whole four minute occlusion. Data were also excluded if they were non-linear as indicated by a Pearson's r-value of <0.90 [65]. These parameters are represented in Figure 4.4.

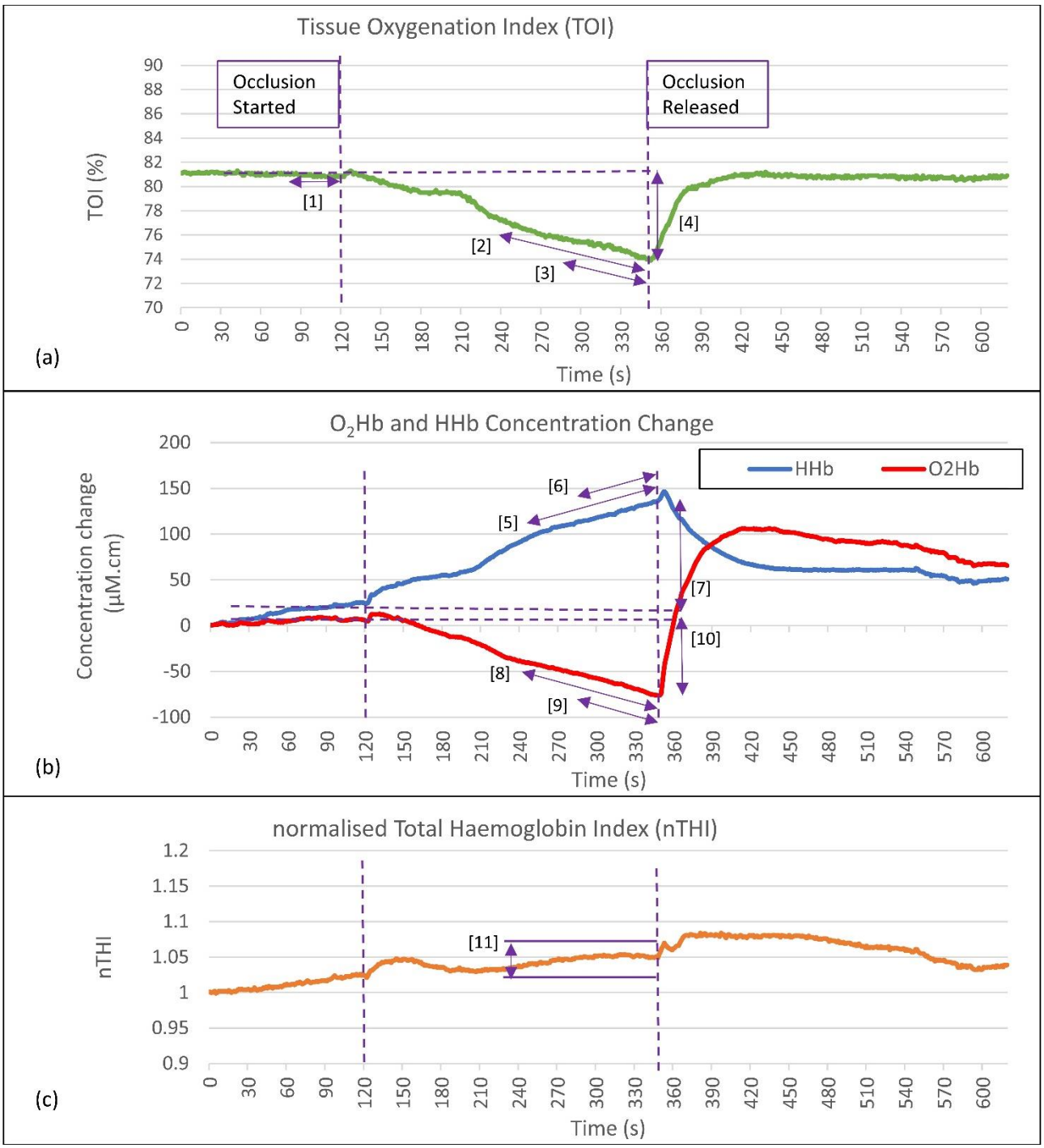

Figure 4.4: Graphical representation of proposed haemodynamic markers for NIRS analysis during occlusion (DO).

[1] Baseline TOI at rest prior to the occlusion (TOI_rest; (%))
[2] Rate of TOI decrease in the last 120s of occlusion (TOI_DO_120s (%/s))
[3] Rate of TOI decrease in the last 60s of occlusion (TOI_DO_ 60s (%/s))
[4] Absolute change in TOI DO (TOI_DO_absΔ (%))
[5] Rate of HHb increase in the last 120s of occlusion (HHb_DO_120s (µM.cm/s))
[6] Rate of HHb increase in the last 60s of occlusion (HHb_DO_60s (µM.cm/s))
[7] Absolute change in HHb DO (HHb_DO_absΔ (µM.cm))
[8] Rate of O_2Hb decrease in the last 120s of occlusion (O_2Hb_DO_120s (µM.cm/s))
[9] Rate of O_2Hb decrease in the last 60s of occlusion (O_2Hb_DO_60s (µM.cm/s))
[10] Absolute change in O_2Hb DO (O_2Hb_DO_absΔ (µM.cm))
[11] Observation that the change in nTHI is less than 5% during the 120s period

The absolute changes in concentration of O_2Hb and HHb during occlusion over the four minute occlusion period (measured in µM.cm) were also investigated as a potential marker of oxygen extraction in a closed system. There is some precedence for investigating changes across the full four minute occlusion time [277], however these may also potentially be non-linear and confounded by the first minute of "settling" of nTHI. These markers also need to be approached with some caution, because these are taken from an arbitrary baseline of zero. Hence a change of a certain absolute concentration of O_2Hb or HHb in a participant could represent any range of relative change when there is an unknown initial haemoglobin concentration for comparison [272]. The total TOI percentage change during occlusion was also recorded. These markers are also represented in Figure 4.4.

4.5.2: Post occlusion release (PO) haemodynamic markers

Chapter 3 has identified no meaningful consensus for quantitative analysis of haemodynamic markers post AO based on NIRS studies of bone tissue. Other studies using NIRS in muscle or skin rely on markers based primarily on the extent of the post occlusive reactive hyperaemic (PORH) response (such as maximal response relative to baseline measurements, recovery rates to maximum values, or time to full recovery), as introduced in Section 2.2.1.7 [76, 274, 276]. These were considered unlikely to be transferable for use in bone tissue, as this pattern of PORH response was not observed during AO observations of TOI at the tibia during protocol development testing. Figure 4.5 provides an illustrative example of the typical differences in PORH response between the lateral calf and tibia. As reported in Section 5.3.2, this difference was quantifiably confirmed with respect to the hyperaemic response upon occlusion release. This was performed by measuring the maximum TOI and O_2Hb differences past initial baseline values post cuff release ([4] and [8] on Figure 4.6).

When considering bone health, NIRS markers of arterial inflow and reperfusion rates are of interest and may be directly related to DCE-MRI perfusion markers. Physiologically, O_2Hb haemodynamic markers post occlusion release should intuitively resemble the rate of arterial inflow and be heavily influenced by endothelial vasodilatory function, although are also likely to be influenced by the initial blood volume and capillary density of tissue [272]. The rate of TOI recovery also could be representative of this and is commonly used in other studies using AO, However, it also inherently incorporates total haemoglobin concentration, so will be influenced by venous changes post occlusion release [61].

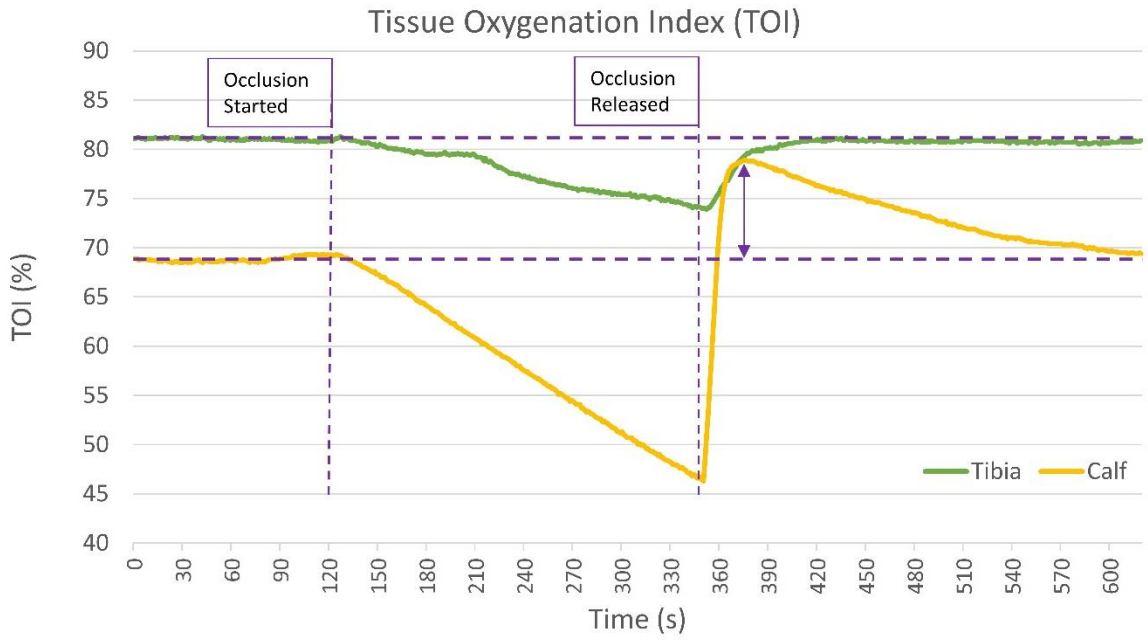

Figure 4.5: Graphical demonstration of the minimal post occlusive reactive hyperaemic (PORH) response seen at the tibia compared with the calf. Unlike the tibia, the TOI of the calf is seen to "overshoot" the baseline TOI measurement indicated by the purple arrow.

Following observation of AO on 15 participants in protocol development work, the time period post occlusion release which appears to be most useful is around the first 10 to 20 seconds post occlusion release. Data after 20 seconds post occlusion risks becoming non-linear. Precedence also exists for rates of change in TOI and O_2Hb around 10s [278] and 20s post occlusion [279].

As such it was decided to assess the resaturation rates of TOI and O_2Hb during the first 10s and 20s post occlusion release, taken from the time of cuff release (represented by the lowest data point). All data were tested for linearity with a statistically significant Pearson correlation of r-value ≥0.90 required. These parameters are represented in Figure 4.6. The absolute change in TOI and O_2Hb post occlusion release from the point of cuff release, and relative to initial resting baseline, was also investigated, as demonstrated in Figure 4.6.

Rates or absolute amounts of total haemoglobin concentration increase post occlusion release (such as indicated by nTHI) could also theoretically be relevant, representing the blood volume increase post occlusion release (and therefore a marker of perfusion). However, this could also be confounded by differing levels of venous drainage or high venous pressure following the occlusion release, as it also incorporates deoxygenated haemoglobin. Similarly, as nTHI is a relative measure, a

10% increase in blood volume could mean very different rates of reperfusion in different participants relative to the baseline absolute blood volume (which is unknown with the NIRO-200NX system) [61]. HHb markers are not considered physiologically relevant post occlusion as they mainly represent venous vascularity as well as HHb derived from oxygen extraction, as opposed to tissue reperfusion during PO recovery.

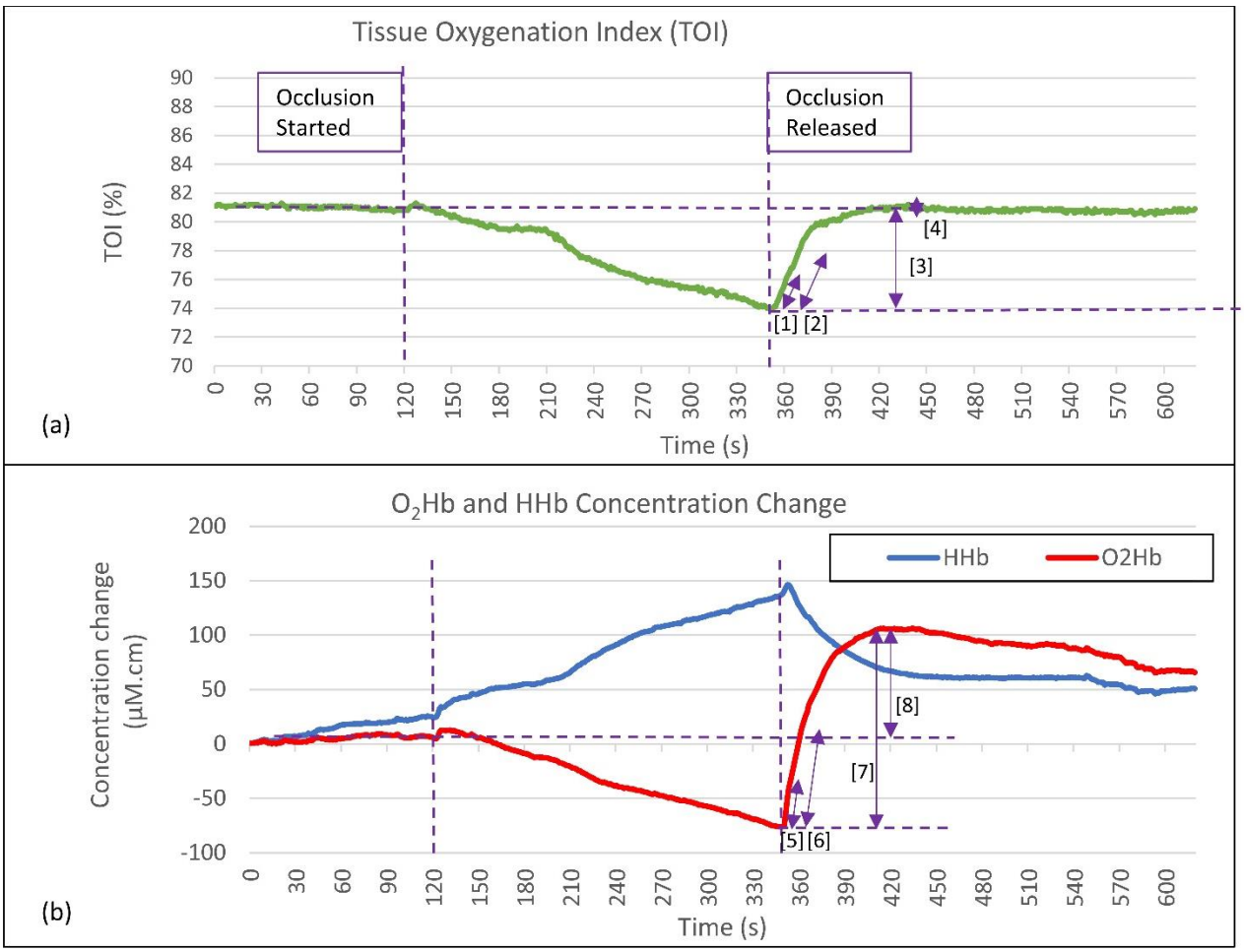

Figure 4.6: Graphical representation of proposed haemodynamic markers for NIRS analysis post occlusion release (PO).
[1] Rate of TOI increase in first 10s post occlusion release (TOI_PO_10s (%/s))
[2] Rate of TOI increase in first 20s post occlusion release (TOI_PO_20s (%/s))
[3] Maximal absolute change in TOI post occlusion (TOI_PO_absΔ (%))
[4] Absolute hyperaemic change in TOI post occlusion (TOI_PO_hyperΔ (%)). Note this is small in bone but can be observed in muscle by the purple arrow in Figure 4.5.
[5] Rate of O_2Hb increase in first 10s post occlusion release (O_2Hb_PO_10s (µM.cm/s))
[6] Rate of O_2Hb increase in first 20s post occlusion release (O_2Hb_PO_20s (µM.cm/s))
[7] Maximal absolute change in O_2Hb post occlusion (O_2Hb_PO_absΔ (µM.cm))
[8] Absolute hyperaemic change in O_2Hb post occlusion (O_2Hb_PO_hyperΔ (µM.cm))

Another approach could be to use markers that are relative to baseline values. Here there is precedence with muscle tissue studies that use time taken and/or rate of change up to recovery of 25%, 50% and/or 75% of baseline values [274, 280-282]. However, given the short time intervals of recovery identified during protocol development, this approach does not appear to offer any real benefit, as there needs to be enough time to sample data for a meaningful rate, yet still ensuring linearity.

There is also some precedence for looking at non-linear markers of post occlusion response in studies performed on muscle tissue using non-linear modelling [80, 280, 283, 284]. As demonstrated in Figure 4.6, data on TOI and O_2Hb presented as time-signal curves suggests the potential for non-linear modelling to provide quantitative markers of PO tissue recovery. However there are no existing data proposing the type of non-linear response that should be physiologically expected in bone tissue post occlusion release. As such, one phase exponential modelling of TOI and O_2Hb response was considered based on its observed close fit with PO response in both muscle and bone. This modelling provides data on the time constant and amplitude of the recovery observed [285]. Non-linear post occlusion markers were explored but found to be less reproducible than linear markers and were therefore not adopted. For brevity the work around assessment of non-linear markers is presented in Appendix G.

4.6: Confirming haemodynamic markers are representative of bone tissue

One of the important steps in protocol development work was to demonstrate that the Hamamatsu NIRO-200NX NIRS equipment available may truly represent haemodynamics in bone tissue, and that it is receptive to changes in oxygenation to bone tissue in real time. Previous studies presented in Chapter 3 have concluded that NIRS can take measurements representative of superficial bone tissue [10, 56, 186, 189]. However this remains a small body of evidence, using a variety of methods that only compare results with soft tissue comparators, and only in small studies of 13 participants or less. As such, the methods used in previous studies to demonstrate bone tissue is being measured are not conclusive, and only demonstrate measurement of a deep tissue that produces different readings to muscle or overlying skin, rather than definitively demonstrating that it is truly bone tissue being measured. Because bone and muscle are different tissue types, with different capillary densities, conclusions drawn from direct comparison of oxygen extraction and perfusion using NIRS should be tentative. Likewise, muscle and bone have different absorption and scattering properties which can confound results [1, 65]. As such it can only be concluded

that the measurements taken on what is proposed to be bone are significantly different to muscle readings.

Confirmation that NIRS is truly representing bone tissue cannot be confirmed without comparison of NIRS results with an external reference that also produces comparable and reliable measures of bone haemodynamics. This is yet to be published in the evidence base but is attempted in the methodology outlined in Section 6.2 of this thesis.

As the AO protocol used in protocol development work involves optode placement directly onto superficial bone, and that bone is likely to make up most of the sampled tissue volume from NIRS measurements, a suggestion may be made that bone tissue is being represented if statistically significant differences between tissue types are observed for the haemodynamic markers proposed, in line with the existing evidence base. This would then justify further more rigorous validation that bone is truly being measured with assessment against external tests of bone health, as presented in Chapters 8, 9 and 10.

This has been best achieved with data from the AO protocol and relies primarily on comparison of simultaneous measurements taken at tibial sites and over the lateral calf for haemodynamic markers taken at rest, during occlusion, and post occlusion release. Paired t-tests of muscle and bone haemodynamics at these sites have been performed to assess for statistically significant differences based on a threshold p-value of 0.05 using StataSE software (Version 14.0, StataCorp, Texas). Before using t-tests the assumptions of this statistical approach were considered, including normality assessment of paired differences, assessed descriptively using boxplots and using a Shapiro-Wilks test, and assessment of comparable variance between groups using the Levene test, including consideration of any outliers [286].

4.6.1: Recruitment

Recruitment of healthy participants was undertaken in order to develop the arterial occlusion protocol and perform a preliminary assessment that NIRS was taking representative measurements of bone tissue, under the ethical approval outlined in Section 4.1.

Sample size calculations were performed on expected differences based on previous literature. As identified in Chapter 3, such previous evidence is sparse. Siamwala et al. 2015 provides mean TOI results of the tibia (81.3% (SD 5.5)) using similar supine

positioning and a healthy population of 11 participants [78]. Comerota et al. 2003 reports a resting mean TOI at the calf of 65% (SD 19) in 35 healthy participants [287]. A sample size calculator using StataSE software (Version 14.0, StataCorp, Texas) was used to calculate that based on these data a sample size of 14 participants is required to demonstrate a statistically significant difference between tissue types for NIRS-derived resting TOI markers, using a t-test with a significance threshold of 0.05 and power of 0.80.

Mean and standard deviation of during and post occlusion AO markers are not presented in those NIRS studies identified investigating both bone and muscle tissue. However, Klasing et al. 2003 reports a resting molar oxygen extraction rate of 11.16 µmol/(Litre.min) (SD 3.99) at rest, compared with a resting molar oxygen extraction rate of 2.04 µmol/(Litre.min) (SD 1.08) in bone tissue [185]. It was determined that similar magnitudes of difference in the haemodynamic markers proposed in AO protocol development work would also be identifiable as statistically significantly different, using paired t-tests with a significance threshold of 0.05 and power of 0.80 utilising 14 participants.

All participants were consented before starting and had the right to withdraw at any stage. It was expected that the methods used in the AO protocol would be low risk with some moderate discomfort only when AO occurred, as outlined in Section 4.7. Participants were generally in good health and were screened prior to participation for any history of serious injury or pathology affecting the vascularisation of their legs. This was to ensure their safety and avoid any potential confounding of results caused by health status. Participants were also screened for any history of smoking, osteoporosis, diabetes, arthritis, any current medications and menopausal status (if female). Participants were advised not to smoke, eat or have caffeinated drinks two hours prior to testing as high sugar content and caffeine can cause vasodilation and affect haemodynamic measurements [65, 201].

4.6.2: Initial physiological measurements

Physiological measurements were taken in order to investigate any potential confounders. Measurements included height and weight (and henceforth body mass index (BMI)) and initial baseline blood pressure and pulse. Measurements of leg circumference were also taken at the knee, calf and ankle, along with skin calliper measurements at measurement sites at the patella, proximal tibia, tibial diaphysis and

medial malleolus. Intra operator reproducibility assessment was carried out prior to recruitment to ensure the reproducibility of my ability to precisely take these physiological measurements. This was achieved by taking three repeated measurements on three participants on three separate occasions, in line with DVRC policy. At this stage it was observed that leg circumference measurements were noticeably more reproducible than skin calliper measurements, and so were adopted moving forward.

At baseline and during testing, pulse rates, arterial oxygen saturation, and foot temperature were monitored. Cutaneous blood TOI and blood flow measurements were also continuously monitored at the dorsal surface of the foot of the leg of interest using the O2C system (Oxygen to See; LEA Medizintechnik, Gießen, Germany), which utilises white light to take superficial measurements of cutaneous tissue. This allowed real time data when assessing the success of applying the AO (see Appendix H for example data).

Results are presented in two parts: comparison of differences in TOI between the lateral calf and tibia taken at rest, and differences in the lateral calf and tibial response to AO. Methods for both approaches are outlined in more detail below in Sections 4.6.3 and 4.6.4. Corresponding results are presented in Section 5.3.1 and 5.3.2.

4.6.3 Initial differences in TOI between the lateral calf and bone sites

Prior to AO protocols and after 15 minutes of supine rest, initial measurements of TOI were taken on each participant at the four bony sites described in Section 4.2 in a randomised order. Once optode position was stable, sample measurements were taken at a one second sampling rate for 20 seconds, with TOI results averaged to produce a mean TOI value.

A simultaneous oxygen saturation measurement was taken postero-laterally over the lateral calf muscle. It was expected that if NIRS was measuring oxygenation of bone tissue then the oxygen saturation levels will differ markedly from those taken at the lateral calf based on the previous evidence used to inform sample size calculations [78, 287]. Results were obtained from 15 participants and are presented in Section 5.3.1.

4.6.4: Differences in the lateral calf and bone sites during AO protocol

Two arterial occlusions were performed on each participant whilst measuring at the TD and TP sites, with corresponding measurements of the lateral calf muscle also taken

during both AO. Only one leg was measured per participant but this was alternated between right and left using a predetermined randomisation template. One participant had testing on both legs and both sets of data were included, as they had revealed a unilateral sympathectomy that was of interest and later published as a case report [288]. Likewise, the order of occlusions was alternated to avoid any systematic confounding with leg laterality or the order of occlusions.

Arterial occlusions followed the protocol outlined in 4.4.1. If NIRS is truly representing bone tissue it would be expected that there would be differences in the oxygen extraction of both bone and muscle being measured simultaneously, as has been observed in the evidence base [185, 188, 189]. Based on this literature, it was expected that deoxygenation should occur at a slower rate in bone compared with muscle. Likewise upon occlusion release, the return of O_2Hb and HHb to baseline levels should take longer, without the hyperaemic response of TOI that is known to be observed when measuring muscle. Results are presented in Section 5.3.2.

4.7: Ensuring protocols are tolerable for participants

Arterial protocols are known to be potentially painful, which in turn may have varying physiological effects on the microcirculation of participants, especially in response to cardiac and respiratory changes [272]. Serious adverse effects are reported to be rare anecdotally in the DVRC, and there is little documented evidence of risk with AO occlusion protocols. A national survey of Kaatsu training in Japan reported a very low occurrence of side effects such as venous thrombus (0.055%), pulmonary embolism (0.008%), and rhabdomyolysis (0.008%) based on records of 12,642 participants. Subcutaneous haemorrhage at the site of occlusion had a higher incidence of 13.1%, but this is in the context of AO protocols to the limb sustained during exercise, for potential extended periods greater than five minutes, and regularly repeated as part of a Kaatsu training protocol [289].

Participants were asked to rate how uncomfortable they found the AO at its worst point using a pain scale of 1-10 (with 10 being the worst pain they had experienced) as well as whether they thought the testing they had undergone would be feasible in the wider population for clinical testing. Results are discussed descriptively in Section 5.4.

4.8: Determining initial estimates of reliability

Some initial work was also carried out around the reliability of the AO protocol. This was intra operator reproducibility testing with the primary author taking all

measurements. Three participants underwent repeated TP arterial occlusions on three different days. The aim of this initial work was to gauge initial impressions around whether the reproducibility of AO was worth further investigation in a larger, more representative reliability study as outlined in Section 6.1 (with results presented in Chapter 7).

Upon graphing these repeated occlusions, the reproducibility within participants of repeated results at tibial sites and the lateral calf was assessed graphically and appeared acceptable enough to warrant further investigation in a larger sample (graphs are presented in Appendix I). Intra participant coefficients of variation supported this and are presented in Section 5.4, although statistical analysis of these three initial participants was considered tentatively, as the sample size was too small for meaningful reproducibility assessment. Their data have contributed to the reliability results presented in Chapter 7 which utilises a larger sample size.

4.9: MRI protocol development

As discussed in Section 2.3.1, there are a number of MRI techniques available to measure haemodynamic markers in bone tissue. As a result of this literature review, a number of potential protocols were ruled out due to the technical limitations of the 1.5T MRI scanner available. However, one promising MRI protocol was tested for feasibility. This blood oxygen level dependent (BOLD) non-contrast MRI protocol could potentially provide temporal scanning of a participants leg during AO whilst in the MRI scanner, with signal changes representing changes in oxygenation status of bone tissue, thus potentially providing a direct comparison with the NIRS arterial occlusion protocol [97].

This type of temporal BOLD protocol has been performed successfully in studies on muscle and brain tissue [98], but without precedence in bone tissue. Previous studies have also used BOLD protocols to validate NIRS measurements (or vice versa) during exercise interventions of skeletal muscle [106] and brain function [104, 105]. There are known limitations with BOLD protocols including the need for a high signal to noise ratio (due to the small changes in signal indicating oxygenation changes) and susceptibility to field inhomogeneities, such as between cortical bone interfaces [98]. It was clear from this feasibility work on four participants that MRI signal was too low in bone tissue for this protocol to be feasible, and so it was not adopted moving forward. Results are presented in Appendix J.

As a result, a dynamic contrast enhanced MRI protocol was adopted instead, which has precedence for reliable use in bone tissue [89]. This protocol is outlined in more detail in Section 6.2.4. This protocol does give information on the perfusion of Gadolinium at the calf and tibia, but with the disadvantage of measuring tissue at rest and not during ischaemic conditions, as per the BOLD protocol and NIRS arterial occlusion protocol.

4.10: Summary of protocol development

Table 4.1 presents a summary of the different protocol development activities undertaken as part of this PhD project and described in Chapter 4, including where corresponding results can be found.

Table 4.1: Summary of protocol development work carried out.

Protocol	Participants Enrolled	Main Outcome	Link to Section
Mid-calf occlusion protocol	6	Protocol Abandoned: confounding results	Appendix F
Positional protocol	3	Protocol Abandoned: replicates one study but small existing evidence base	Appendix F
Venous occlusion protocol	14	Protocol Abandoned: poor reliability of obtaining true venous occlusions	Appendix F
Arterial occlusion (AO) protocol	15	Protocol adopted for further evaluation in Chapters 8,9&10	5.3.2
TOI at rest for different anatomical sties	15	Protocol adopted for further evaluation in Chapter 8,9&10	5.3.1
Intra operator different day AO test/retest feasibility	3	Adopted for further reliability evaluation in Chapter 7	5.4 and Appendix I
MRI BOLD arterial occlusion protocol feasibility	4	Protocol abandoned due to low bone signal	Appendix J

Chapter 5: Protocol development of NIRS

5.1: Chapter overview

This chapter presents results of the first stage of experimental work for the PhD project. The primary aim was to develop an arterial occlusion (AO) protocol using the Hamamatsu NIRO 200NX near infrared spectrometer available. This protocol needed to build on the existing evidence base and provide sufficient rigour to warrant further assessment of reliability and validation.

This chapter represents protocol development results in line with the following objectives presented in Chapter 4:

- Gaining confidence that haemodynamic markers derived from proposed protocols are representative of bone tissue and can detect changes in real time;

- Establishing appropriate haemodynamic markers from protocols;

- Ensuring protocols are tolerable for participants;

- Determining initial impressions of reliability to justify further investigation; and,

- Determining the best anatomical location for measurements and optimising placement of NIRS probes.

5.2: Demographics

Fifteen healthy participants were recruited to assist with protocol development work. A summary of demographic information is presented in Table 5.1. All participants were current non-smokers and reported good general health. Two participants had T2DM, one of which also had osteoporosis but unfortunately did not contribute AO data as they could not tolerate the occlusion. Three participants reported mild osteoarthritis that was not being treated medically. One participant was taking Dextroamphetamine as treatment for idiopathic hypersomnia. Of the seven female participants, three were pre-menopausal, one was peri-menopausal, and three were post-menopausal.

Table 5.1: Summary of key demographics for recruited participants (N=15) in protocol development work (mean values presented with standard deviation in parentheses).

Demographic	Mean (SD)
Age (years)	40.3 (16.9)
Sex (m/f)	8/7
Height (m)	1.74 (0.08)
Weight (kg)	76.0 (15.4)
BMI (kg/m^2)	25.4 (4.5)
Systolic Blood Pressure (mmHg)	125 (12)
Diastolic Blood Pressure (mmHg)	75 (10)
Resting Pulse Rate (beats/min)	71 (15)
Resting Arterial Oxygen Saturation (%)	97 (2)
Foot Temperature (°C)	30.1 (1.9)
Knee Circumference (mm)	380 (28)
Calf Circumference (mm)	368 (40)
Ankle Circumference (mm)	244 (12)

5.3 Establishing if NIRS is representative of bone tissue

One of the primary objectives of using the protocols outlined in Chapter 4 was to gain confidence that NIRS was measuring haemodynamic markers representative of bone tissue based on the known physiological differences between bone and muscle. This was based on investigating initial differences in resting tissue oxygenation index (TOI) between the lateral calf muscle and anatomical bone sites (presented in Section 5.3.1). Differences were also investigated between the lateral calf muscle and tibial sites in response to arterial occlusion at the distal femur, with simultaneous measurements taken at tibial sites and over the lateral calf (presented in Section 5.3.2).

5.3.1: Resting TOI results

Participants initially rested supine on a bed for 15 minutes to acclimatise to the room conditions and reach a relaxed baseline for consistency in results. Initial measurements of TOI were taken on each participant at four bony sites (as outlined in Section 4.2) in a randomised order. Anatomical sites included the patella; the proximal tibia (TP); midway on the tibial diaphysis (TD); and, the medial malleolus (MM). Once probe position was stable, sample TOI measurements were taken every second for 20

seconds, with mean results obtained. The use of 20 second samples enabled investigation of the variability of the TOI signal being recorded (an indicator of signal to noise), as indicated by the "within reading" coefficient of variation for these measurements presented in Table 5.2. Results were obtained from all 15 participants. All data and paired differences were tested for normality using a Shapiro-Wilks parametric test, confirming parametric statistics were appropriate.

Summary results are presented in Table 5.2 below, indicating statistically significant differences in resting TOI at all four bony anatomical sites compared with the lateral calf muscle using paired t-tests. The "within reading" coefficient of variation (CV) also indicates how variable readings were within the 20 second sample used to calculate mean TOI. It can be seen that the proximal tibia site is most comparable with the lateral calf in terms of the stability of readings taken during 20 second samples. These data supported anecdotal findings that the medial malleolus and patella were the most difficult sites to position NIRS probes. This was likely a contributor to the increased variability at these sites, as opposed to increased physiological variability between participants.

Table 5.2: Summary of mean resting TOI results (N=15) for each anatomical site. Mean difference (%), 95% confidence intervals of differences, and p-values from paired t-tests are also presented for each bone site versus lateral calf muscle measurements.

Anatomical Site	"Within Reading" Coefficient of Variation (%)	Mean TOI % (SD)	Paired t-test mean difference (95% CI) vs lateral calf
TP	0.19	83.0 (4.1)	11.8 (5.9-13.5); p<0.001
TD	0.22	80.6 (4.6)	9.7 (5.9-13.5); p<0.001
MM	0.33	81.2 (6.1)	9.5 (5.4-13.5); p<0.001
Patella	0.25	82.2 (8.4)	10.3 (3.7-16.9); p=0.005
Lateral Calf	0.16	70.9 (4.8)	

5.3.2: Tibial and lateral calf response to arterial occlusion

Two arterial occlusions (AO) were performed on each of the 15 participants. Measurements were taken at the medial surface of the midshaft of the tibia (tibial diaphysis (TD)) and the proximal tibia slightly medial and distal to the tibial tuberosity (TP) for each occlusion, with corresponding readings taken at the lateral calf in all

occlusions. From the 15 participants, 12 pairs of paired AO data were obtained for the TP site, and 11 for the TD site. Two participants were unable to tolerate the arterial occlusion and the other excluded data were due to the conditions of the AO not being met (i.e. an nTHI change >15% and O_2Hb not decreasing during occlusion as expected). There were no obvious reasons for the failure of the AO in these cases. The most plausible explanation is an inadequate occlusion due to inadequate application of the cuff or for physiological and/or anatomical reasons (for example, calcified arteries not compressing, or deep arteries not affected by the external cuff).

The haemodynamic markers outlined in Section 4.5 were calculated for all participants. Shapiro-Wilks testing of variables and paired differences confirmed parametric testing was appropriate for all markers. Of the usable data obtained, there was a significant statistical difference demonstrated using paired t-tests between tibial bone sites and the simultaneous lateral calf muscle data for all haemodynamic parameters measured (p-values <0.05). For paired data between bone (at both TP and TD sites) and the lateral calf there were clear trends demonstrating bone sites had slower and weaker haemodynamic responses to arterial occlusion compared with simultaneous lateral calf tissue data obtained. This included both the rates of oxygen extraction and absolute haemoglobin concentration changes during occlusion, and the rates of recovery and absolute haemoglobin concentration changes upon release of the occlusion. Figures 5.1 and 5.2 graphically present these results.

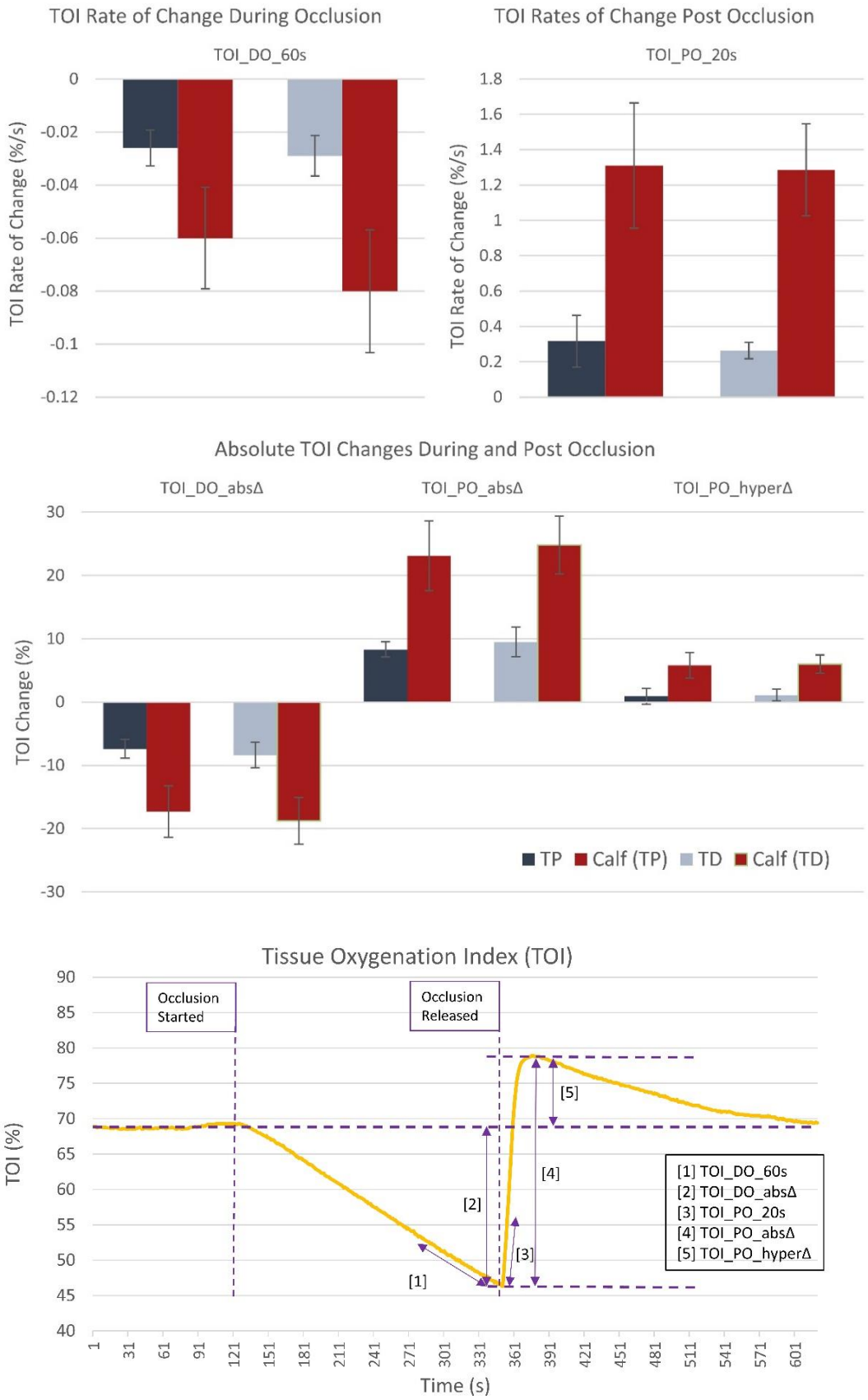

Figure 5.1: Graphs of mean rates of change and mean absolute change in tissue oxygenation index (TOI) during and post arterial occlusion for each measurement site (N=15). Error bars represent 95% confidence intervals. Calf measurements are presented twice corresponding with the arterial occlusions of the proximal tibia (TP) and tibial diaphysis (TD).

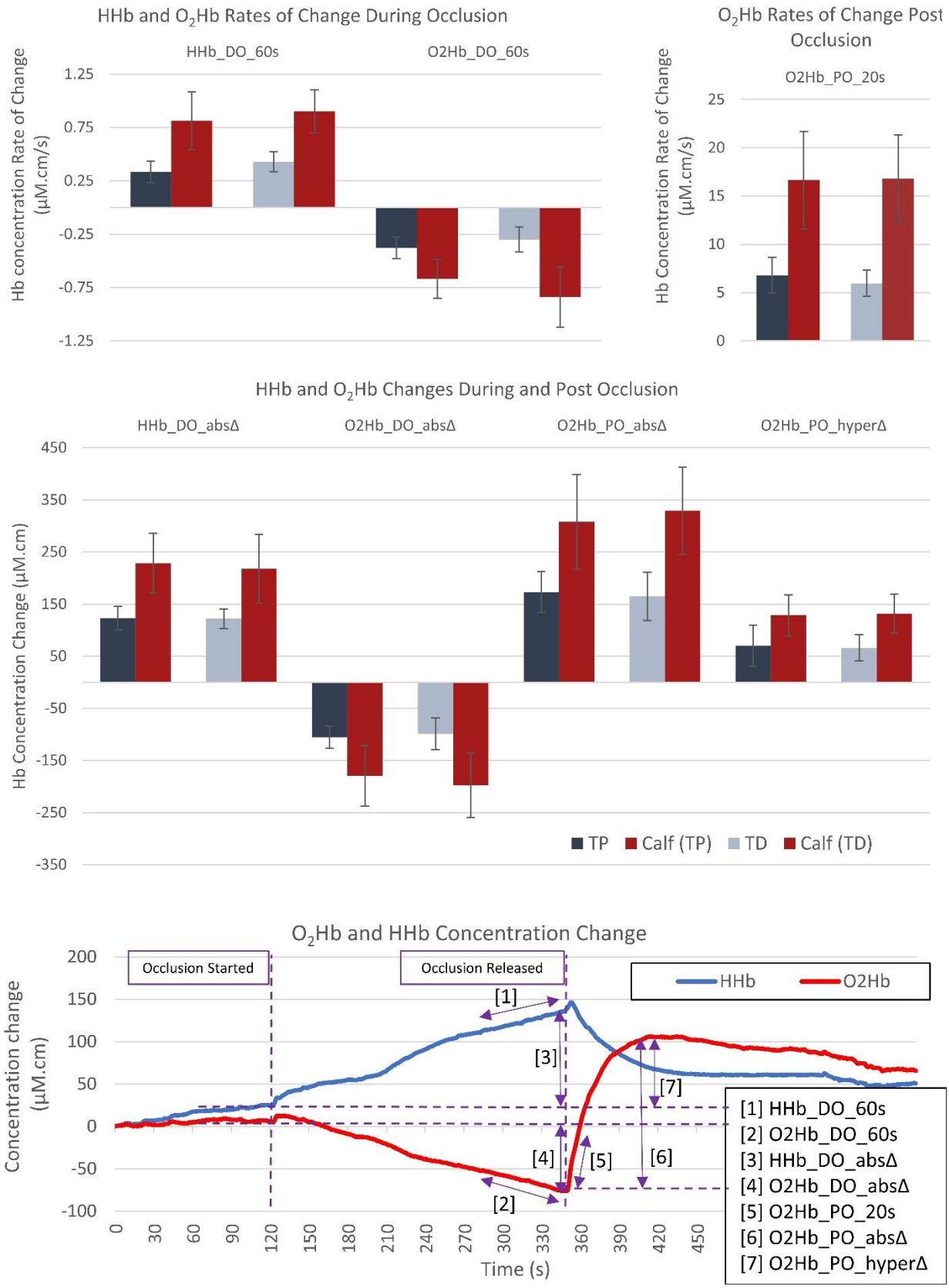

Figure 5.2: Graphs of the mean rates of change and mean absolute change in oxygenated haemoglobin (O_2Hb) and deoxygenated haemoglobin (HHb) during and post arterial occlusion for each measurement site (N=15). Error bars represent 95% confidence intervals. Calf measurements are presented twice as these were recorded during both arterial occlusions for the proximal tibia (TP) and tibial diaphysis (TD).

5.4: Participant tolerability

Pain scale scores from the 15 participants varied widely from 3 to 10 (mean 6.5; SD 2.0). However, most stated they could see the test potentially being used as a screening test or research tool if it could lead to a clinically important finding. Two participants commented that the experience was analogous to the discomfort of mammography, which could be endured if clinically useful outcomes were obtained.

It was noted that most participants found the second occlusion easier and this may be related to psychological factors during the first occlusion, with participants being more familiar with the process in the second inflation. Experience of the cuff also varied in terms of being described as painful, alternatively being described as "pressure", a "continuous dull ache" and "pins and needles". Koch et al 2011 [290] asked participants to rate their pain using a visual analogue scale (VAS) from 0-10 following a therapeutic ischaemic pre conditioning protocol involving three repeated five minute AO protocols at the thigh. This was repeated for a mean 7.7 sessions for each of 21 participants. Mean VAS scores were 3.6 (SD 3.4). These scores were lower and may support familiarisation with multiple occlusions lowering the perceived discomfort for participants.

Adverse feelings were quickly alleviated post cuff removal in all cases. Some red skin marks of the leg did result in some instances, resolving without bruising. Two participants out of the 15 who undertook arterial occlusions throughout protocol development work could not tolerate the occlusion. It was felt this was an acceptable rate of tolerance in terms of adopting the protocol for further research given the advantages that the AO protocol offered, and previous experiences using AO at the DVRC research facility.

5.5: Initial impressions of reliability

As discussed in Section 4.8, three participants volunteered to undertake repeat arterial occlusion protocols on three different occasions. These participants were all healthy young males between the ages of 21 and 26. Figure 5.3 presents intra participant coefficients of variation for proposed NIRS haemodynamic markers at baseline, during occlusion, and post occlusion release. It was felt these data showed enough potential for producing reproducible haemodynamic parameters for further investigation in a larger sample of participants, which is presented in Chapter 7. Graphical examples of the repeated arterial occlusions for all three participants is presented in Appendix I.

NIRS marker	Intra Participant Coefficient of Variation (%)		
	Participant 1	Participant 2	Participant 3
[1] TOI_rest; (%)	0.5	1.9	0.4
[2] TOI_DO_ 60s (%/s)	27.6	11.3	6.0
[3] TOI_DO_absΔ (%)	13.7	12.0	19.9
[4] TOI_PO_20s (%/s)	7.8	15.9	24.7
[5] TOI_PO_absΔ (%)	16.2	18.4	10.7
[6] HHb_DO_60s (µM.cm/s)	23.7	49.5	9.4
[7] HHb_DO_absΔ (µM.cm)	11.0	10.7	24.3
[8] O_2Hb_DO_60s (µM.cm/s)	27.1	27.7	10.4
[9] O_2Hb_DO_absΔ (µM.cm)	5.9	15.4	27.1
[10] O_2Hb_PO_20s (µM.cm/s)	4.6	4.7	28.2
[11] O_2Hb_PO_absΔ (µM.cm)	17.2	9.5	7.7

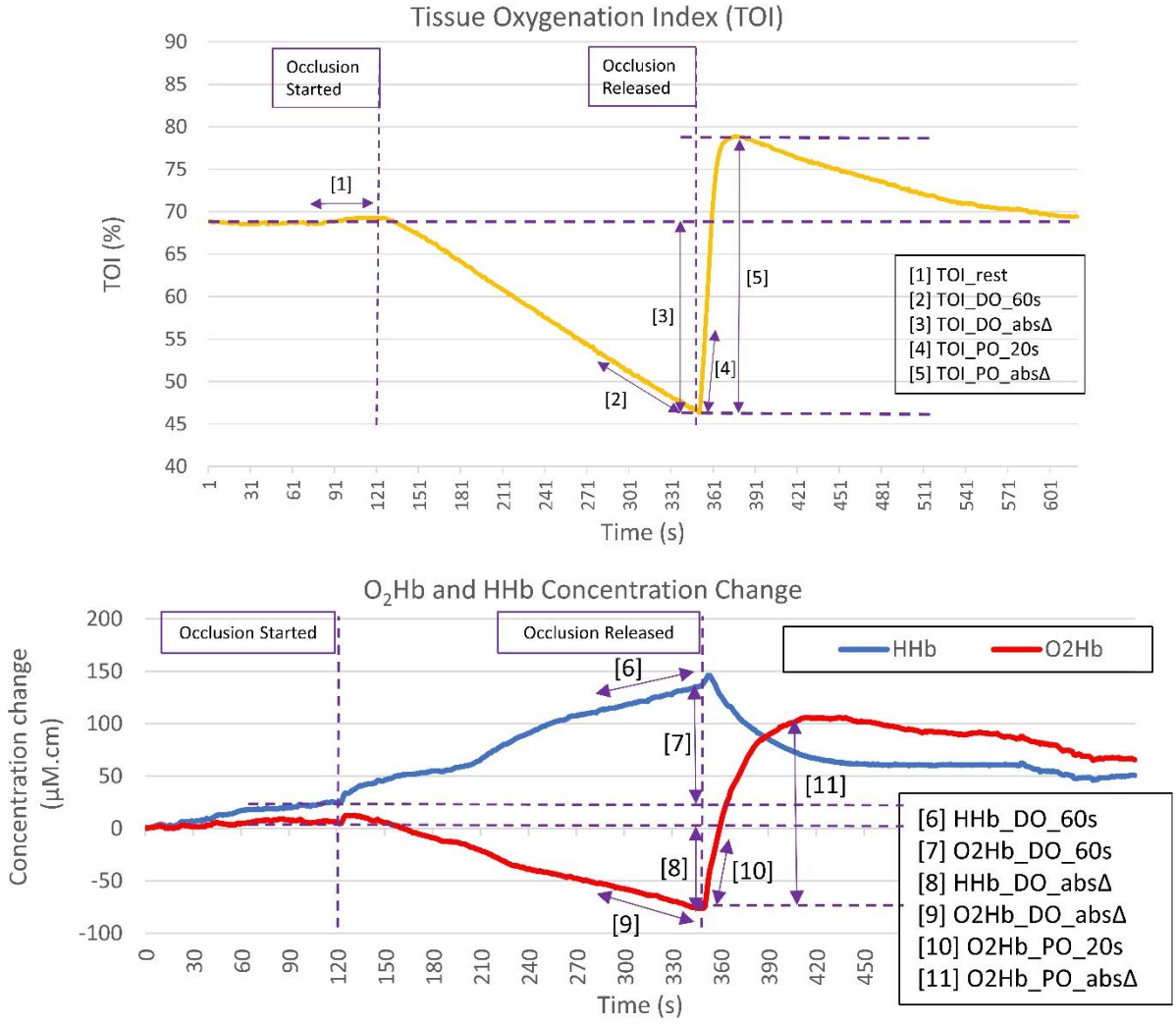

Figure 5.3: Intra participant coefficients of variation for three repeat arterial occlusions on three participants. All occlusions were performed on separate days. Results for eleven haemodynamic markers from the parameters of interest (TOI, HHb, and O_2Hb) are presented, which are also demonstrated on the corresponding graphical figures.

5.6: Discussion

5.6.1: TOI measurements at rest

Simultaneous TOI measurements were taken at four anatomical bony sites and postero-laterally over the lateral calf. As was expected based on previous evidence [189], TOI was significantly higher at all four bony sites compared with the muscular site. It was also identified that TOI measurements at the tibia were comparable in mean value and inter participant variability with the most methodologically comparable studies (see Table 5.3) [78, 196]. Likewise, TOI values at the lateral head of the calf are similar to previously published literature [270, 287]. Binzoni et al 2003 argue that the higher resting TOI observed at the tibia compared with the calf may be explained by the lower metabolic rate of bone leading to lower oxygen extraction [189]. Likewise, this will result in higher venous oxygen saturation, which has been estimated to contribute up to 70% of the sampled volume in NIRS when measuring muscle [62]. Klasing 2003 [185] supports this reporting a resting oxygen extraction rate that is five-fold lower in tibial bone compared with the tibialis anterior muscle. As TOI is a ratio of oxygenated haemoglobin to total haemoglobin, relatively smaller microvascular venous reservoirs within bone could also increase TOI [189].

Table 5.3: Summary table of TOI results from protocol development work (N=15) in comparison with relevant existing evidence.

Anatomical Location	Mean TOI (SD) from protocol development	Comparator Study	NIRS System	TOI values
Proximal tibia	83.0% (4.1)	Siamwala et al 2015 [78]	SRS	81.3% (SD 5.5; N=11)
		Siamwala et al 2017 [204]	SRS	Females: 73.5% (SD 7.2; N=9) Males: 76.8% (SD 6.3; N=9)
		Sorensen et al 2017 [196]	SRS	Median 81% (IQR 69 to 87; N=17)
Tibial diaphysis	80.6% (4.6)	Binzoni et al 2003 [189]	Broadband CW	84.9% (SD 2.8; N=13)
Patella	82.2 (8.4)	Farzam et al 2013 [15]	Frequency domain	65% (SD 9; N=8)
Lateral Calf	70.9 (4.8)	Torricelli et al 2004 [270]	TRS	70.5% (SD 1.7; N=5)
		Comerota et al 2003 [287]	SRS	65% (SD 19; N=35)

Statistical analyses supported anecdotal findings that the proximal tibia and tibial diaphysis were the most reliable and stable bony measurement sites. Amongst the four bony sites these had the lowest standard deviation amongst participants, comparable to the muscle readings of the more established measurement site of the calf. Likewise, within the 20 second samples taken, the "within reading" CV of samples were lower than the MM and patella readings, and again comparable with the muscle readings taken at the calf, suggesting a more stable monitoring site. It was also noted that TOI values at the patella varied widely from the single study identified in the Chapter 3 systematic review investigating the TOI of the patella (see Table 5.3) [15].

It was of interest to note a statistically significant difference in resting TOI between the proximal tibia and tibial diaphysis using a paired t-test (p=0.02), although the clinical significance of this difference is likely to be small. There was little evidence of differences in AO haemodynamic markers between the TD and TP sites. It may be that there is better arterial blood supply leading to more oxygenation in the trabecular bone of TP compared with TD. But this may also be confounded by the TP site being more proximal to the central arterial blood supply. Santolini et al 2014 reports that anatomically the proximal tibia is the most vascularised part of the tibia, with the distal third of the tibia least vascularised [55]. As TOI is a ratio of oxygenated haemoglobin to total haemoglobin, it may also be that the tibial shaft has greater venous reserves leading to a decreased TOI [5].

Results in this chapter support taking proximal tibia measurements forward to the next stages of the PhD. The proximal tibia was superior in terms of reduced variability and stability of TOI readings compared with other bone sites. The proximal tibia appears to be the most stable site with the largest bone volume. It is also more likely to represent trabecular bone than the tibial diaphysis, making it arguably more relevant to exploration of bone strength and potential future research applications, especially around prediction of fragility fracture.

5.6.2: Arterial occlusion measurements

In consideration of arterial occlusion results, expected differences in haemodynamic markers at both the tibial diaphysis and proximal tibia sites were observed when compared with the lateral calf muscle being measured simultaneously. It was expected the tibia would have a slower resting metabolic rate than muscle [185, 291], so deoxygenation should occur at a slower rate than in muscle during occlusion, as

measured by the rate of increase in deoxygenated haemoglobin, and the rate of TOI reduction. Klasing 2003 [185] reports mean muscle VO_2 (a marker of oxygen consumption) increased twenty-fold during muscle contraction, whereas mean bone VO_2 only increased 16%. Nagasawa et al 2003 demonstrates that oxygen consumption rates with NIRS are typically associated with oxidative capacity of muscle tissue, despite not being directly representative [284]. These results are in keeping with the reduced oxygen extraction NIRS markers at the tibia observed in this PhD project, and the previously documented reduced oxidative capacity of bone tissue when compared with muscle sites [185, 291].

The results presented in this chapter are also in line with the previously demonstrated differences between bone and muscle during arterial occlusion [188, 189]. The magnitude of TOI reduction during arterial occlusion is comparable with the 8.2% (95% CI 7.6% to 8.8%) mean reduction in TOI reported at the patella by Farzam et al 2013 [15]. Yu et al 2005 reports a mean TOI reduction of 16.4% (SD 4.4) at the calf during occlusion, and a PORH “overshoot” of mean 3.8% (SD 1.7), in line with the results presented in this chapter [261].

Results from this chapter have demonstrated that there was typically a negligible post occlusive reactive hyperaemic (PORH) response in TOI at the tibia, despite strong PORH responses seen when measuring the calf. This strengthens the argument that bone is being sampled by NIRS at the tibia, and that the contribution of overlying soft tissue is minimal, as PORH has been observed in both cutaneous and adipose tissue as well as muscle [65, 292]. This is supported by TOI data collected from cutaneous tissue at the dorsal surface of the foot using O2C during AO testing, further discussed in Appendix H.

It is expected that reduced oxygen extraction rates during occlusion should lead to reduced PORH [79], but it is possible with the rigid structure of bone and relatively high intraosseous pressures within bone tissue, that reactive vasodilation of intraosseous microvessels is further limited [5]. Reduced capillary density in bone may also be an explanator for reduced PORH response. Direct comparisons of capillary density between bone and muscle could not be found in the evidence base in either animal or human studies. However comparison of unrelated murine studies utilising similar immunohistochemistry techniques have reported microvessel density in plantaris muscle [293] and femora [26] demonstrating a fivefold greater capillary density in muscle.

Furthermore, Laughlin et al 2011 reports large animal studies have shown that vascular resistance can increase in bone marrow during acute exercise-induced ischaemia, with a potential mammalian response of vasoconstriction in bone to redirect blood to skeletal muscle during exercise, driven by sympathetic response [294]. This may also potentially explain the lack of post occlusive hyperaemic response in bone observed in this PhD project, but further research is required to confirm this unique response in bone.

Heinonen et al 2013 [295] reports response in the femur of 15 human participants to a ten minute exercise intervention measured using positron emission tomography (PET). Mean blood flow does increase from 1.8 mL/100 g/min (SD 0.6) to 4.1 mL/100 g/min (SD 1.5; p=0.01) with low intensity exercise, however appears to then be physiologically limited in the presence of further increased exercise intensity, despite a fivefold increase in glucose metabolism. This again supports a potential unique vaso-regulatory response in bone in line with the lack of PORH response seen at the tibia in this study.

It is generally accepted that the microvascular supply to bone is affected by the same neural, humoral, myogenic and metabolic parameters as the rest of the body, responding to most vasoconstricting and vasodilatory substances [23]. A case report related to this PhD project also supports this, with observed reduced vascular response in the leg of a participant suffering from unilateral lumbar sympathectomy [288]. However, unique vaso-regulatory mechanisms within bone may exist and this idea is supported by the data in this chapter.

5.6.3: Limitations

These comparisons in 15 participants have shown that when measuring the tibial bone sites described, there is a statistically significant difference between haemodynamic markers recorded and corresponding measurements taken at the lateral calf. However, some caution needs to be taken before concluding that measurements are truly representative of bone tissue alone. Although statistically significant physiological differences have been identified, the physiological relevance of these remains essentially unknown. Likewise there is no evidence base identified for which to directly externally validate these results against known haemodynamics for bone tissue (this is attempted in Chapters 8, 9 and 10).

An important limitation of NIRS is that during occlusion it only represents oxygen extraction from haemoglobin. This is assumed to represent the efficiency and responsiveness of the microvascular system. However when comparing between different tissue types such as the tibia and the calf, comparison may also be influenced by differences in the oxygen consumption demand from cellular tissue being supplied, the inherent rate of oxygen diffusion within the tissue, and the arrangement and density of capillaries [27]. Although no direct evidence was found quantifying capillary density between tissue types, it is assumed this is different given the active metabolic requirements of muscle. Capillary density has indirectly been reported as up to fivefold greater in muscle than bone [26, 293], and eightfold higher in muscle than in skin [65] meaning a different volume of surrounding tissue is supplied by each capillary. Likewise, Klasing et al 2003 reports that resting oxygen consumption was more than five times greater in muscle at the tibialis anterior then at the tibia, suggesting a more metabolically active cellular basis [185].

As such it remains a limitation of NIRS that the reasons for differences between the calf and tibia cannot be definitively elucidated. For example, slower oxygen extraction during occlusion could be representative of a lower oxygen demand from surrounding tissue and/or lower capillary density supplying this tissue. Future time-resolved and frequency domain NIRS systems may be able to gain more insight by investigating cytochrome-c-oxidase levels, directly indicative of cellular oxygen consumption, and by taking total haemoglobin concentration measurements indicative of blood volume within the sampled tissue (discussed further in Chapter 11).

Likewise the differing scattering properties of differing tissue types can also affect the differential path lengths of which modified Beer Lambert (MBL) calculations are based on, confounding direct comparison of haemodynamic markers between different tissue types [1, 65]. Although in this chapter differences between measurement sites were consistent between MBL derived parameters and spatially resolved TOI parameters.

An inherent limitation of the continuous wave NIRS system used in this PhD project is that markers are not indicative of total blood volume, which is of interest for bone research. Existing studies using time resolved NIRS suggest a higher capillary density and higher concentration of haemoglobin in the measured NIRS volume at the calf compared to the tibia. Toricelli et al 2004 reports a mean resting total haemoglobin at the lateral head of the gastrocnemius of 135.9 μM (SD 8.2) [270]. Table 3.3 has previously reported the variability of total haemoglobin concentration results across

bony sites (ranging from 17.7 µM to 77.3 µM), however all are much lower than what has been reported at the calf [9, 15, 56, 70, 75, 195]. As such it cannot be elucidated whether differences in PO markers between tibial sites and the lateral calf are due to blood volume differences, differences in capillary density, or differences in vaso-function in response to ischaemia.

Likewise, indices of resting blood flow cannot be measured by the Hamamatsu NIRO-200NX. Only two studies from Chapter 3 presented diffusion correlated spectroscopy derived blood flow index (BFI) measures in bone tissue. Farzam et al 2014 reports a median BFI at the manubrium of 5.0×10^{-9} cm^2/s (IQR 4.2×10^{-9} cm^2/s to 7.4×10^{-9} cm^2/s) [56]. Sekar et al 2016b presents BFI data at six bony anatomical sites with mean values highly variable ranging from $2.0x10^{-9}$ to $8.0x10^{-9}$ cm^2/s [75]. Baker et al 2017 reports a similar mean BFI at the calf at rest of $5.3x10^{-9}$ cm^2/s (SD $5.07x10^{-9}$ cm^2/s). However it is likely that it is the greater ability of the microvascularity of the calf to increase BFI when required that is different to bone. No human studies directly identifying these differences in BFI response to induced ischaemia were identified, however Gross et al 1979 illustrate these differences in an animal study [260]. With high intensity exercise, mean blood flow increased from 11 ml/min/100g (SD 5) to 119 ml/min/100g (SD 47) at the vastus lateralis muscle in 8 dogs tested using microsphere techniques. Mean blood flow in the red marrow of the femur only increased from 26 ml/min/100g (SD 11) to 30 ml/min/100g (SD 17) [260].

A potential criticism of this protocol development work is the multiple comparisons that have been made across different anatomical sites and potential haemodynamic markers. It is possible to correct for multiple testing using methods such as Bonferroni corrections, which make allowances for the increased likelihood of a significant result when multiple comparisons are made. However such corrections may be too conservative, and are inappropriate when many of the comparisons made are inherently linked [296]. As such the approach suggested by Perneger 1998 has been adopted [297]. This involves reporting significance levels tentatively, and in the context of the biological plausibility of individual associations. It is felt this is justified by the exploratory nature of this PhD project. It has been observed that the interpretational trends of these multiple comparisons appear to be consistent, with bone sites consistently showing differences with muscle, and these differences being consistent with the existing evidence base.

With these limitations in mind, the difference in haemodynamics results strongly suggest a different tissue type other than muscle is being measured. With evidence to suggest that superficial tissue contributes minimally with haemodynamic measurements [77], and knowledge that the depth of measurements at 4cm internode spacing is up to 2cm depth, its seems plausible that haemodynamic measurements are representing bone tissue using the TP and TD probe placement sites, where bone tissue is very superficial and occupies a relatively large volume. Validation work presented in Chapters 8, 9 and 10 of the project was attempted to further help confirm this by comparing AO haemodynamic results with external measurements of bone haemodynamics acquired using a DCE-MRI protocol.

5.7: Conclusion

Protocol development work outlined in this chapter has built on evidence based AO protocols to add enough justification that, using the AO protocol developed, NIRS can potentially take measurements representative of bone tissue in real time, and that this was worthy of further investigations in reliability (Chapter 7) and validation (Chapter 8, 9 and 10) using a comparison of NIRS results against other markers of bone health (such as bone density, trabecular bone scoring, and bone metabolism blood markers), and other markers of bone haemodynamics (provided by DCE-MRI). An AO protocol has been developed that is tolerable for participants and appears to utilise the most reliable and relevant anatomical sites available.

Chapter 6: Methodology for reliability and validation assessments of NIRS

This chapter will outline the methodological approach to assessing the reliability of haemodynamic NIRS markers at the proximal tibia and lateral calf derived from the arterial occlusion (AO) protocol discussed in Chapters 4 and 5 (see Section 6.1). The methodological approach to assessing the validity of NIRS AO haemodynamic markers with comparison against relevant markers of bone health is outlined in Section 6.2.

6.1: Methodology for reliability assessment of NIRS

6.1.1: Background and aims of reliability assessment

An important aspect of determining the potential of NIRS for measuring haemodynamics in bone tissue is to assess the reliability of the observations made. In this context, reliability can be defined as the ability of a test to produce similar results when measuring the same thing [3]. This can be reflected by the reproducibility of a test and/or the repeatability of a test. Definitions of these terms are varied in the evidence base, but for this thesis reproducibility refers to the variability of repeated measures obtained by a test when repeated on the same participant longitudinally (assuming no appreciable change to the participant being measured). Repeatability refers to the variability of measurements taken during the same testing session [3]. In the context of NIRS it is important that when measurements are taken longitudinally on the same participant, changes in observations can be attributed to a change in the participant's haemodynamics, and not measurement error from the NIRS protocol used. Higher reproducibility will therefore also make a test measure more sensitive to smaller real clinical changes in the participant's haemodynamics [3, 298].

Accordingly, as part of feasibility work on NIRS use in bone, the within participant reproducibility and repeatability of NIRS measurements taken on participants was based around the AO protocol outlined in Section 4.4.1. The approach to assessing reproducibility needs to take into account the following potential sources of measurement error to the AO protocol:

- Biological variations: including natural variations in microvascular haemodynamics caused by the time of day, recent diet, recent exercise, body temperature and stress levels [65, 272]. Familiarity with the AO protocol for the second AO measurements could also be a potential source of systematic error. Biological variation was minimised by testing participants using protocols that controlled for time of day, room temperature,

participant diet before testing, exercise and smoking status (discussed further in Section 6.2.1.3).

- Optode placement: including the ability to follow anatomical protocols for placing optodes, and minimising variations in optode spacing. A protocol for optode placement was developed and is described in Section 4.2, and a commercially available optode holder was used to minimise variation in optode spacing.

- Execution of arterial occlusion: including potential variations in cuff pressures used and speed of delivery of cuff execution. A pre-inflation cuff system was used to standardise and minimise the time of AO delivery.

- Inherent inaccuracies in the NIRS equipment's ability to produce and detect photons, and produce corresponding measurements.

- Data analysis: There are potentially subjective aspects to how data are analysed, despite data analysis being designed to be as objective as possible.

6.1.2: Outline of reliability assessments

To investigate these potential sources of error, the reliability aspect of the project included three primary approaches outlined in the following sections:

6.1.4: Intra operator reliability of AO protocol measurements on both same day repeatability and different day reproducibility test/retest measurements, incorporating the DO and PO NIRS markers justified in Section 4.5.

6.1.5: Inter operator repeatability of optode placement to obtain resting TOI measurements.

6.1.6: Inter operator reproducibility of data analysis of AO haemodynamic markers.

The best reproducibility results could be expected when the same participant is measured in the same session, by the same operator, using the same equipment (i.e. the repeatability of the test) [298]. By performing this same session analysis, the best possible indication of how much error is attributable inherently to the NIRS system and the operator can be gained, as the participant and equipment are kept as close to consistent as possible (although in practice when measuring precision in living tissue, it is very difficult to completely separate biological variation and measurement error from the testing system [299]).

If NIRS is to be a useful research tool it is also important to estimate the biological variation of results on different days, despite participants following the same protocol (i.e. the reproducibility of the test) [298]. This will give some indication of how different future measurements would need to be before an operator could be confident that changes in haemodynamic measurements were attributable to a real change in the participants test status, as opposed to expected biological variation and/or measurement error. This was investigated by measuring participants on different days, with the same operator, protocol and equipment. This testing should give insight into how much variability can be attributed to normal biological variation when measurements are taken longitudinally, in context with the variability represented by same day test/retest repeatability data, were error is primarily inherent within the NIRS system and protocol used [3].

A limitation of the above approach is results will only apply to one operator, with different operators being another potential source of error. It is also important to assess the variability introduced by having measurements taken by different operators and using different equipment. Here a compromise was made in order to not over burden participants with too much repeat testing with an AO protocol. As inter operator variability is likely to be attributable to subjective elements of optode placement and subsequent data analysis, these two aspects alone were assessed for their inter operator repeatability. It is not feasible to undertake reliability work using different NIRS systems, with only one NIRS system available, and therefore this will remain a limitation of this research project.

Some participants recruited for reliability assessments were recruited under the same ethical approval of the University of Exeter Medical School Research Ethics Committee (application 14/11/063) as the protocol development work outlined in Section 4.1 involving recruitment of staff and students internally from the University. Volunteers were recruited as participants but also as operators in some instances, following tuition on the principles of NIRS and practical instruction on how to use the equipment.

Additionally to aid in the generalisability of intra operator reliability assessment outlined in Section 6.1.4, further recruitment of participants from the general public was carried out with ethical approval from the NHS Health Research Authority via the Integrated Research Application System process (REC ref:16/SW/0254). Recruitment was carried out via the existing “Exeter Ten Thousand (EXTEND)” research register. This recruitment process is outlined in more detail in Section 6.2.3.

6.1.3: Statistical approaches to reliability analysis

There are a number of possible approaches to assessing the reliability of a test statistically. In reality no one measure is appropriate on its own due to the limited scope of each measure. As such, a number of approaches will be used to assess the reliability of results derived in the three reliability assessments performed, as there is a lack of consensus on which combination is appropriate [298]. An overview of the data analysis techniques adopted is provided in this section. All analysis was carried out after reliability testing protocols were completed, ensuring blinding of all results during reliability assessments.

6.1.3.1: Descriptive analysis of variation

In the context of test/retest data, the dispersion of results from within participant measurements can be presented as a within participant root mean square standard deviation (RMSSD) by calculating the root of the mean squared standard deviation of within participant results [300]. RMSSD represents the variability of a repeated measurement from an individual participant, with a low RMSSD indicating little dispersion of results from the mean test result obtained. However presenting RMSSD alone has its limitations, including difficulty comparing it as a measure of variability against tests using different units (as is the case when comparing different haemodynamic markers). Also variation may change depending on the mean value and this is not reflected by RMSSD [299, 301].

6.1.3.2: Root mean square coefficient of variation (RMSCV)

Root mean square coefficient of variation (RMSCV) represents the ratio of the within participant RMSSD of a repeated measure relative to the within participant mean value of that measure [302]. As such RMSCV will be used to represent reliability for within participant measurements. It can be more useful than measuring RMSSD alone as it provides an indication of how much variability there is in measurements, independent of the mean value (i.e. not just in absolute terms). Being a percentage measure, RMSCV also allows more meaningful comparison of precision across different measures or test systems [299].

6.1.3.3: Intra Class Correlation (ICC)

ICC is a measure of reliability that provides a correlation result (with 95% confidence intervals) between -1 and 1. ICC represents the ratio of true variation in measurements

(i.e. the “real” difference between measurements) to the total variability between measurements (i.e. true variation plus measurement error combined). As such an ICC of 1 means any difference between two results is attributable to “real” differences with no contribution of measurement error. An ICC of 0.6 would indicate 40% of the variability between results was due to measurement error and 60% was attributable to “real” participant differences [298].

There are several approaches to ICC analysis. For intra operator analysis in this project, one way random effects ICC analysis is appropriate, as error is attributable to either random error or true variability between measurements on participants (i.e. there is no error attributable to different operators). For inter operator analysis, two way random effects ICC analysis is appropriate as results should incorporate error attributable to random error and error attributable to differences in the operators who acquired measurement results [303].

A weakness of ICC is that it is dependent on the variability of the measure, with wider variability across a measured population more likely to increase ICC, since the variability inherently attributable to the population increases, relative to the fixed measurement error of the test [298]. This means it is important to undertake any reproducibility testing in a representative population. Likewise, ICC is a unitless measure and defining a threshold of an acceptable ICC is essentially arbitrary. For this thesis the criterion proposed by Evans 1996 will be adopted, which describes commonly adopted thresholds of an ICC of 0.8-1.00 as “very strong”, with ICC higher than 0.60 described as “strong”, and an ICC of 0.4-0.6 as “moderate” [304].

6.1.3.4: Bland-Altman plots

Bland-Altman plots allow visualisation of the difference between test/retest measurements plotted against the mean of the two repeated measurements. They can help to assess whether the differences between measurements follow a normal distribution, and whether there is systematic bias in the differences between test/retest measurements. Bland-Altman plots can also demonstrate any changes in the variance of differences as the mean measurement value increases [305, 306]. Bland-Altman plots were produced for the haemodynamic markers assessed in test/retest reliability work in Chapter 7 in order to rule out any systematic changes between test/retest measurements. Examples are presented in Appendix K.

6.1.3.5: Repeatability coefficient

In the case of test/retest measurements where Bland-Altman plots have confirmed no systematic biases and normally distributed differences in test/retest results, Bland and Altman 2003 propose the use of a repeatability coefficient. This measure represents the difference in repeat measurements that will only be exceeded by 5% of repeat measurements, assuming no physiological change in the participant. This value is calculated by multiplying the standard deviation of the mean difference between test/retest measurements by 1.96 [(305)].

Whilst there is no clinically accepted threshold for repeatability coefficients, it may still give useful context to the error of the measurement in question, especially if compared with the typical mean measurement taken across the sample population [(305)]. This can then be compared with what might be considered the minimum clinically important difference to determine if the test may be a useful research or clinical tool for identifying the desired clinical change of interest.

6.1.3.6: Paired t-tests

Paired t-tests of initial test results with retest results were performed to rule out a statistically significant systematic difference between test/retest measurements [(286)]. A threshold p-value of 0.05 was adopted to indicate a statistically significant difference.

6.1.3.7: Testing for normality

All reproducibility datasets were continuous variables and so were inspected for normality to meet the assumptions of the above statistical methods adopted. This was carried out by observational comparison of mean and median data, via observation of boxplots, and via Shapiro-Wilk testing of normality. In the case of the repeatability coefficient and paired t-tests, it was the differences between within participant test/retest results that were assessed for normality.

6.1.4: Intra operator reliability of AO protocol measurements

The AO protocol outlined in Section 4.4.1 was adopted. All testing was carried out by the same operator using the same equipment. Same day repeatability involved carrying out the AO protocol within the same testing session concurrently, allowing for recovery time back to baseline between application of the AO protocol for at least 10 minutes.

Different day reproducibility involved test/retest measurements using the AO protocols on two separate days within a four week period. It was felt four weeks was a suitable period to allow flexibility for participants whilst minimising any contribution of any confounding pathological changes, as bone pathologies are generally chronic in nature. Testing was carried out after the same 15 minute rest period, at the same time of day, and with protocolled participant preparation outlined below in Section 6.2.1.

Sample size was based on key outcome measures. Test-retest measurements on 30 participants will allow identification of an ICC of 0.8 with a 95% confidence interval width of 0.28 [307]. McAlinden et al 2015 reports that precision studies obtaining repeat measurements in 30 participants can identify if repeat measurements are likely to fall within 25% of the initial measured value, providing a reliability estimate with 25% uncertainty [3]. In the context of the aims of this project, this was seen as acceptable for allowing judgement of whether further investigation of using NIRS as a tool for measurement in bone haemodynamics is warranted. This sample size is also in line with the International Society of Clinical Densitometry recommendation of 30 test/retest scans to assess intra operator precision for DXA BMD measurements [308].

Ultimately, sample size calculations for recruitment for this project were primarily based around validation assessments (discussed in Section 6.2.9.1) which were greater than the 30 participants required in the above estimate. This resulted in a target sample of 36 participants. With 36 participants in addition to the reproducibility data already obtained from participants as part of initial protocol development work (as discussed in Section 4.8), reaching 30 sets of test/retest data was achievable, even allowing for data loss from participants unable to tolerate the arterial occlusion, or producing data not suitable for inclusion.

6.1.5: Inter operator repeatability of optode placement

As a compromise on the burden of repeat AO on participants, inter operator repeatability was assessed on the main suspected source of inter operator error: optode placement. Previous evidence with NIR technologies such as laser Doppler flowmetry has identified heterogeneity in microvascular beds can contribute to variability in results, even when testing vascular beds adjacent to each other on the same participant [81]. Differences in optode pressure applied, application of the bandages and optode holder, and subjective variations in interpretation of the optode positioning protocol could all lead to potential sources of error [14].

This protocol involved five operators placing optodes on 16 participants within the same session to assess inter operator repeatability. Resting TOI was used as the haemodynamic marker of interest as it is the only measure provided by NIRS data that does not require an arterial occlusion to provide meaningful data. Inter operator repeatability was assessed using the statistical approaches outlined in Section 6.1.3, including use of a two way random effects ICC analysis. Using five operators to repeat measurements on 16 participants can allow demonstration of an ICC of 0.80 or higher with confidence interval width of 0.30 [307]. Operators for this work were identified and data collection was carried out over a two week period.

Operators were asked to carry out their optode positioning twice on each participant within the same session. This allowed each operator's intra-operator repeatability to also be assessed using a one way random effects ICC analysis. By carrying out measurements in the same session for each participant, variation caused by biological variation was minimised. As error inherent to the NIRS equipment is assumed constant, and by having each operator's intra-operator repeatability as well, this testing will give the best assessment of how much error might be attributable to different operators alone.

6.1.6: Inter operator reproducibility of data analysis

Analysis of AO data has been protocolled to be as objective as possible. Data are predominantly obtained through use of a template and macro actions making the process predominantly objective, so there was an expectation that agreement should be high between data analysts. However there is still some subjective decision making inherent to data analysis, which is making the decision on the end point of the occlusion and the start point of the post occlusion release markers. This is typically easily identified as the lowest (or highest as applicable) point of data before the occlusion release, but there is some subjectivity owing to noise and potential movement artefact at the point of occlusion release.

As this is another potential source of inter operator error, an inter operator reliability analysis of NIRS data analysis was carried out. It was planned that this would involve three operators' data analysing 20 sets of previously obtained arterial occlusion data using the Microsoft Excel template constructed during development of the AO protocol described in Section 4.5. Inter operator reproducibility was assessed using a one way random effects ICC analysis, as in this case error can only be attributed to the data

analysts, and not participants. Using three operators to repeat measurements on 20 participants will allow demonstration of an ICC of 0.80 or higher with a 95% confidence interval width of 0.30 [307].

6.1.7: Summary of reliability assessment

Table 6.2 below summarises the activities undertaken to assess the reliability of NIRS parameters in this PhD project, and the corresponding sections where results can be found.

Table 6.2: Summary of reliability evaluations.

Protocol	Intra operator same day AO repeatability	Intra operator different day AO reproducibility	Inter operator optode placement reproducibility	Inter operator data analysis reproducibility
Link to Section	7.2	7.2	7.3	7.4

6.2: Methodology for the validation assessment of NIRS

Following successful determination of a NIRS protocol, an important aspect of establishing the potential of NIRS for measuring haemodynamics in bone tissue is to assess not only the reliability of NIRS measurements, but also the validity of the observations made. In this context, validity refers to the ability for a test measure to represent the "true" value that it aims to measure [299]. This is difficult to demonstrate in the context of NIRS, where there are limited options for obtaining a gold standard value for directly comparable haemodynamics with which to compare NIRS observations [6].

However, attempts of validating NIRS were made in this project by comparison of NIRS measurements against other tests measuring markers of haemodynamics and health in bone tissue. Although not using an established gold standard, if NIRS measurements were to show an association with corresponding measures of bone health on the same participants, more confidence could be gained in the potential ability of NIRS to reflect "true" bone tissue haemodynamics.

This type of comparison of NIRS results against external reference standards is also yet to be attempted for this application of NIRS in bone tissue, as identified in the systematic review in Chapter 3. Comparison of NIRS results against other markers of bone health could also give early indications of where NIRS may be potentially useful as a research tool.

The approach adopted for validation of NIRS for the measurement of haemodynamics in bone tissue is discussed in this section. The methodology used for the appropriate tests are outlined in the following sub sections:

6.2.1: Recruitment of participants and testing regime

6.2.2: Baseline data and physiological testing

6.2.3: NIRS testing

6.2.4: MRI testing

6.2.5: Dual X-ray Absorptiometry (DXA) testing

6.2.6: Trabecular Bone Scoring (TBS)

6.2.7: Use of the Fracture Risk Assessment (FRAX) Tool

6.2.8: Blood and urine testing

6.2.9: Data analysis

During the recruitment approach to this validation assessment, the opportunity was also taken to observe any potential significant difference in bone haemodynamics in participants with and without T2DM as a secondary objective. This offers a novel feasibility investigation into an established and expanding healthcare problem, i.e. the susceptibility of those with T2DM to suffer fragility fracture [32], as discussed earlier in Section 1.5.2.4. Differences between the sexes of participants was also investigated. This could also potentially illustrate the ability of NIRS to distinguish differences between sub groups, given the known sex-based differences in bone aging, discussed earlier in Section 1.5.2.3 [8].

6.2.1: Recruitment of participants and testing regime

Participants were recruited from a variety of age ranges and from both sexes in order to strengthen the generalisability of results to the wider population. Recruitment of participants from the general public was carried out under ethical approval from the NHS Health Research Authority via the Integrated Research Application System process (REC ref: 16/SW/0254). This also allowed for approval for the research to be undertaken in conjunction with the Royal Devon and Exeter Research and Development department and for inclusion in the National Institute of Health Research Clinical Research Network Portfolio, utilising the Exeter Clinical Research Facility.

Recruitment was carried out using the existing “Exeter Ten Thousand” (EXTEND) research register. This register includes the details of potential volunteers who have pre consented for approach in Exeter CRF research projects. There was no other advertising of the study, incentives, or pressure put on potential participants to volunteer. This approach to recruitment also allowed for the recruitment of participants with and without T2DM, matched for age, sex, BMI and ethnicity, as this information was available via the EXTEND database.

6.2.1.1: Eligibility criteria

Potential participants were considered if they were generally healthy non-smoking adults with a BMI of <35 kg/m^2, with capacity to consent, and if not meeting any of the exclusion criteria mentioned below. Participants were matched against T2DM status and controlled for age (within 3 years), sex, ethnicity, and BMI (within 3 kg/m^2). For this study a participant with T2DM was defined as someone who has been formally diagnosed with T2DM by a medical practitioner. Participants with either diet controlled or medically dependent T2DM were considered. During analysis, participants were assessed on the severity of their T2DM based on markers of nephropathy, neuropathy and HbA1c results (discussed below in Section 6.2.2).

Exclusion criteria were:

- Those with type 1 diabetes mellitus. It was felt this could confound the secondary objective of looking for differences in those with T2DM.

- Any contraindications to MRI such as severe claustrophobia, an inability to lie flat, or metallic or electrical implants (for example pacemakers, internal cardio-defibrillators, cranial aneurysm clips or metallic ocular foreign bodies) identified using an MRI screening questionnaire.

- Known allergies to Gadolinium contrast or established poor renal function.

- Women who were breast feeding, pregnant or planning to become pregnant.

- Any history of recent serious injury or disease in the legs in the past twelve months that could prohibit the use of the NIRS arterial occlusion protocol, including symptomatic deep vein thrombosis, or active claudication.

- Active participation in another research study that may affect results in either study;

- Undergoing medical treatment or supplementation for osteoporosis or any bone related health condition (including bisphosphonates, hormone replacement therapy, or calcium and/or vitamin D supplementation).

- Use of glucocorticoids at a daily dose of 2.5mg or greater for three or more months in 2 years prior to the study, as this may affect bone health and confound results [167].

- Any other significant disease or disorder which, in the opinion of the investigators, may have put the participant at risk because of participation in the study, or may have influenced the result of the study, or the participants' ability to participate in the study.

6.2.1.2: Recruitment process

The EXTEND database was filtered by Exeter CRF staff using identifiable eligibility criteria data already available in order to produce a shortlisted database of potential participants. These potential participants were then contacted in batches via post with a brief overview of the study and a request slip to return if interested in participating. Batches were used to manage workload and to also allow better matching, with T2DM participants typically contacted first to enable easier matching with a non-diabetic control.

Once returned "expression of interest" slips were collated, a phone call was made to the participant by the primary author to provide further basic information on the study, answer any initial queries, and provide a background check for eligibility in the study. If the participant was still interested and eligible for the study, a participant information sheet (Appendix L) was sent with further information on the study. This was followed up by another phone call around a week later to answer any queries and confirm if the participant was still interested in participating. If they were, it was confirmed that the participant would like to book an initial appointment and a letter was sent in the post for the initial appointment. Informed pre consent was also obtained verbally over the phone for a fasting blood test at this initial consultation, with a pre-consent form (Appendix M) completed upon attendance prior to the blood test. This was because this blood test involves a 10 hour fast prior to testing (discussed further in Section 6.2.8).

At the initial appointment, participants of this research programme underwent a full consent process (Appendix N) outlining the rationale behind the testing; the duration of the study; the risks involved with participation; confidentiality and data storage; and,

their right to withdraw consent at any time. Consent was rechecked at every attendance with the participant free to withdraw at any stage.

6.2.1.3: Testing regime

The tests outlined below were performed over at least two appointments, with the possibility of a third should the participant prefer it. Repeat testing of NIRS needed to be carried out within a four week period. NIRS and MRI testing needed to be carried out on the same day, with NIRS testing performed first.

Each participant was asked to limit strenuous exercise for 48 hours prior to testing (described as any exercise resulting in a raised heart rate for more than 20 minutes). The first appointment involved a ten hour fast for blood testing, so caffeine and dietary requirements were inherently restricted. For the second attendance participants were instructed to avoid food and caffeinated drinks two hours prior to attendance. All appointments were scheduled as early morning appointments to control for biological variation during the day.

Figure 6.1 shows the intended pathway for testing during validation work (and including intra operator AO reliability work described in Section 6.1.4). The first attendance involved consent, fasting blood tests (including bone metabolism markers and diabetic profiling), obtaining medical history, and NIRS testing including a first attempt at the AO protocol.

The second attendance involved retesting participants undergoing the AO NIRS protocols (twice for same day repeatability). Participants then underwent MRI protocols and DXA scanning on the same day. This approach minimised any participant related changes in bone health during the testing period. All DXA, NIRS and MRI analysis was performed blinded to other test results.

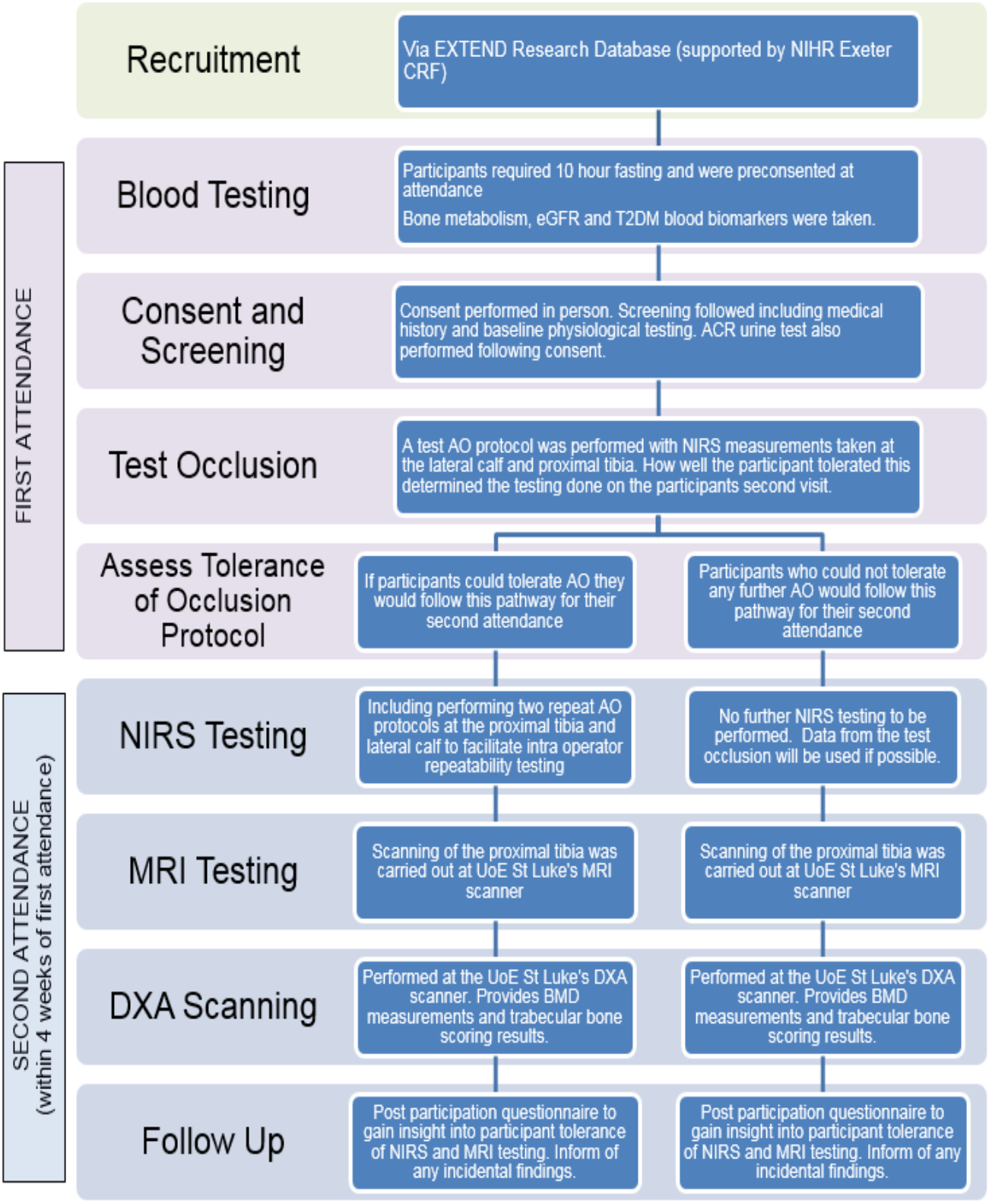

Figure 6.1: Flowchart of validation study testing regime (ACR=albumin to creatinine ratio; AO=arterial occlusion; BMD=bone mineral density; CRF=clinical research facility; DXA=dual x-ray absorptiometry; eGFR=estimated glomerular filtration rate; EXTEND=Exeter Ten Thousand Research Register; NIHR=National Institute for Health Research; NIRS=near infrared spectroscopy; MRI=magnetic resonance imaging; T2DM= Type 2 Diabetes Mellitus; UoE=University of Exeter).

6.2.2 Baseline data and physiological testing

Following informed consent, participants were asked to complete a screening questionnaire of medical history (Appendix O) as well as a pre MRI safety questionnaire (Appendix P). This was used for data analysis and ensuring eligibility criteria were met. Data were also taken on relevant medical history such as duration of T2DM (as appropriate), arthritis or fracture history, menopausal status, and current medications. Physiological measurements were taken, including:

- Basic observations such as brachial blood pressure, pulse rate, arterial oxygen saturations, and height and weight measurements measured using standard equipment;

- Measurements of leg circumference taken around the knee, widest aspect of the calf, and the ankle as a marker of the amount of soft tissue overlying the tibia;

- Peripheral neuropathy tests including monofilament sensation testing and vibration sensitometry testing using a neurothesiometer; and,

- Ankle brachial index (ABI) in order to rule out any obvious unexpected vascular pathology in the legs and to gauge lower limb systolic blood pressure prior to commencing the AO NIRS protocol.

6.2.3: NIRS testing

At the first attendance after physiological measurements were taken and a supine rest period of at least 15 minutes, NIRS measurements were taken at the left leg unless contraindicated. The left leg was chose for consistency, and for pragmatic reasons when preparing for the DCE-MRI examination. Resting mean TOI measurements based on a 20 second sample were taken at the lateral calf muscle and TP as outlined in Section 4.2.

Following this an AO protocol was performed as outlined in Section 4.4.1. Measurements were taken at the lateral calf and TP sites for all AO protocols. This contributed towards different day intra operator reproducibility work (outlined in Section 6.1.4) and also ensured the participant could tolerate arterial occlusions used during testing to ensure better participant compliance during testing at the second attendance. This also allowed an opt out point should the participant not want to undergo any more arterial occlusion testing, with the option to still undergo the second attendance in an abbreviated form, as shown in the trial flowchart in Figure 6.1. Alternatively if the

participant wanted to stop participation in the study they could avoid unnecessary preparation (and wasted laboratory/MRI scanner time) should they not wish to tolerate further leg occlusions. Arterial occlusions lasted for four minutes with a pressure of 200mmHg adopted. In cases where blood pressure was recorded as high (i.e. greater than 140mmHg systolic), arterial occlusion pressure may have been increased where participants could tolerate this to ensure a satisfactory arterial occlusion.

Assuming the participant tolerated the test arterial occlusion at the first attendance, the participant would attend for repeated NIRS testing at their second attendance. Following the minimum 15 minute supine rest period, participants would undergo some repeated physiological testing to monitor for biological variation (blood pressure, pulse, arterial oxygen saturation, and peripheral neuropathy testing). Testing would then proceed with more resting TOI measurements and two repeated arterial occlusion protocols. The first AO data would be used for validation analysis and both sets of AO data would contribute to the intra operator repeatability work outlined in Section 6.1.4. Should the data from the first AO protocol fail to meet the required inclusion criteria for analysis outlined in Section 4.5, the second arterial occlusion data could be adopted for validation analysis if meeting the required inclusion criteria.

After completing testing for the study, participants were asked to complete a questionnaire reflecting on their experience during testing (Appendix Q). This was primarily designed to help optimise the NIRS test for potential future clinical use. As per previous protocol development work, participants were asked to rate the pain of an arterial occlusion on a scale of 1-10, with one being no pain and 10 being the worst pain they had experienced. Participants were asked for any feedback on the experience, including how it was described at consent and how it was carried out. Participants were also asked for their thoughts on undergoing the AO protocol if it were to become a clinically utilised test for bone health.

6.2.4: MRI testing

Participants underwent MRI scanning on their second attendance. Undertaking MRI scanning as a participant involves some risk of injury due to the high magnetic field subjected to the participant and the potential attraction of metallic implants or items (such as wallets, keys etc.) or potential damage to electronic implants. However risk was minimised by initiation of established MRI safety standards and thorough pre-screening of the participant prior to entering the MRI scanner (Appendix P).

There was also risk of participant discomfort psychologically in terms of the closed in nature and noise produced by the MRI scanner. The participant was also required to remain lying still for up to an hour. Again, pre-screening and thorough prior description of the test helped to ensure compliance and participant comfort. All MRI scans were reported by a consultant radiologist for any incidental clinically relevant findings which were reported back to the participant and to the participant's GP (where consent had been given to do so).

Scanning was performed using a Phillips Intera (1.5T) scanner with a dual element "Sense-Flex" coil. Initially, sagittal and axial anatomical scans of the proximal tibia tested with NIRS were taken using proton density protocols with fat suppression. Coronal scans were then taken using a T1 spoiled gradient echo protocol with water selective excitation. A cod liver oil tablet was placed at a point marked on the skin of the proximal tibia, representing the inter optode point from the previously obtained NIRS measurements.

An MRI spectroscopy (MRS) protocol was used to attempt to assess relative fat content in marrow at the proximal tibia, as introduced in Section 2.3.1.3. This was attempted as part of the MRI imaging protocol in order to investigate for potential associations between bone marrow fat fraction, haemodynamic markers measured with NIRS, DCE-MRI results, and BMD measurements taken with DXA using Pearson's correlation. MRS data could also be used to investigate for potential differences between sub groups of interest: sex and T2DM status, using independent t-tests. A point resolved spectroscopy sequence (PRESS) was adopted with a volume of interest 10mm x 10mm x 30mm within the bone marrow, repetition time of 2000ms, and echo time of 46ms with 96 acquisitions. Using the spectroscopic data obtained a percentage fat fraction was calculated by dividing the integral of the fat peak (representing the area under the curve) by the sum of the water and fat peak integrals [22, 43].

A DCE-MRI protocol of the proximal tibia was then employed using a fat supressed 3D T1 weighted gradient echo sequence with a 12 sequential 3mm slice sagittal volume, utilising a 200x164mm field of view and 156x130 matrix size, resulting in 0.78mm x 0.79mm x 3mm voxel size. A flip angle of 10 degrees was used with repetition time (TR) of 3.4ms and echo time (TE) of 1.76ms. A 15 minute temporal scanning sequence was employed including a 30 second pre contrast scan time. A Gadolinium-based injection (Gadovist; 1.0mmol/mL concentration) was given intravenously at the cubital fossa at an injection rate of 2.0 mL/s. The contrast volume delivered was 0.1mmol per

kilogram of the participant's weight, with a standard 20 mL bolus of saline delivered immediately after.

Gadolinium contrast has a small reaction rate (around 1 in 100) and this can include nausea, dizziness, coldness at the injection site or headaches. More serious allergic reactions are even rarer (around 1 in 1000). However, risk is further reduced by screening the participant for any previous adverse reactions to Gadolinium, for any previous anaphylactic reactions in general, for pregnancy, and/or poor renal function [99]. Estimated glomerular filtration rate (eGFR) was also tested on all participants as a marker of renal function within four weeks prior to scanning, as nephrogenic systemic fibrosis is an uncommon but serious side effect of Gadolinium contrast which predominantly only occurs in those with poor renal function [99]. MRI scanning was also carried out under the direct supervision of a medical doctor with emergency response equipment in the scanner area.

The DCE-MRI scans were reformatted to obtain a non-orthogonal sagittal slice of 5mm thickness that contained the cod liver oil tablet and ran through the centre of the tibial shaft (see Figure 6.2). Regions of interest (ROI) of 600mm^2 were used at the proximal tibia within the bone marrow of the tibia and over the muscular tissue of the calf to produce time signal curve data for the two tissue types of interest.

There was no existing evidence based consensus for analysis of time-signal curve data in bone obtained from the DCE-MRI protocol. Likewise there is no evidenced physiological model for the "typical" enhancement of bone marrow at the tibia identified. As such, non-linear analysis was performed using GraphPad Prism software (Version 8.1.0; GraphPad Software, San Diego) by fitting a non-linear curve, applied using the "plateau followed by one phase association" settings using a least squares fit approach (see Figure 6.2). This approach was adopted as it appeared to fit data well with all data returning an R-squared value of greater than 0.8 for muscle, and greater than 0.6 for the tibia (the difference owing to increased signal noise in tibial data).

Markers of interest included the amplitude of signal change within the ROI as a marker of absolute signal enhancement and extracellular space incorporating both intra vascular volume and interstitial space. A linear model was also applied for the first 60 seconds of signal enhancement post Gadolinium injection as a marker of initial perfusion, vascular permeability and vascular density [116]. These two markers are generally considered the most robust without using pharmacokinetic modelling [123].

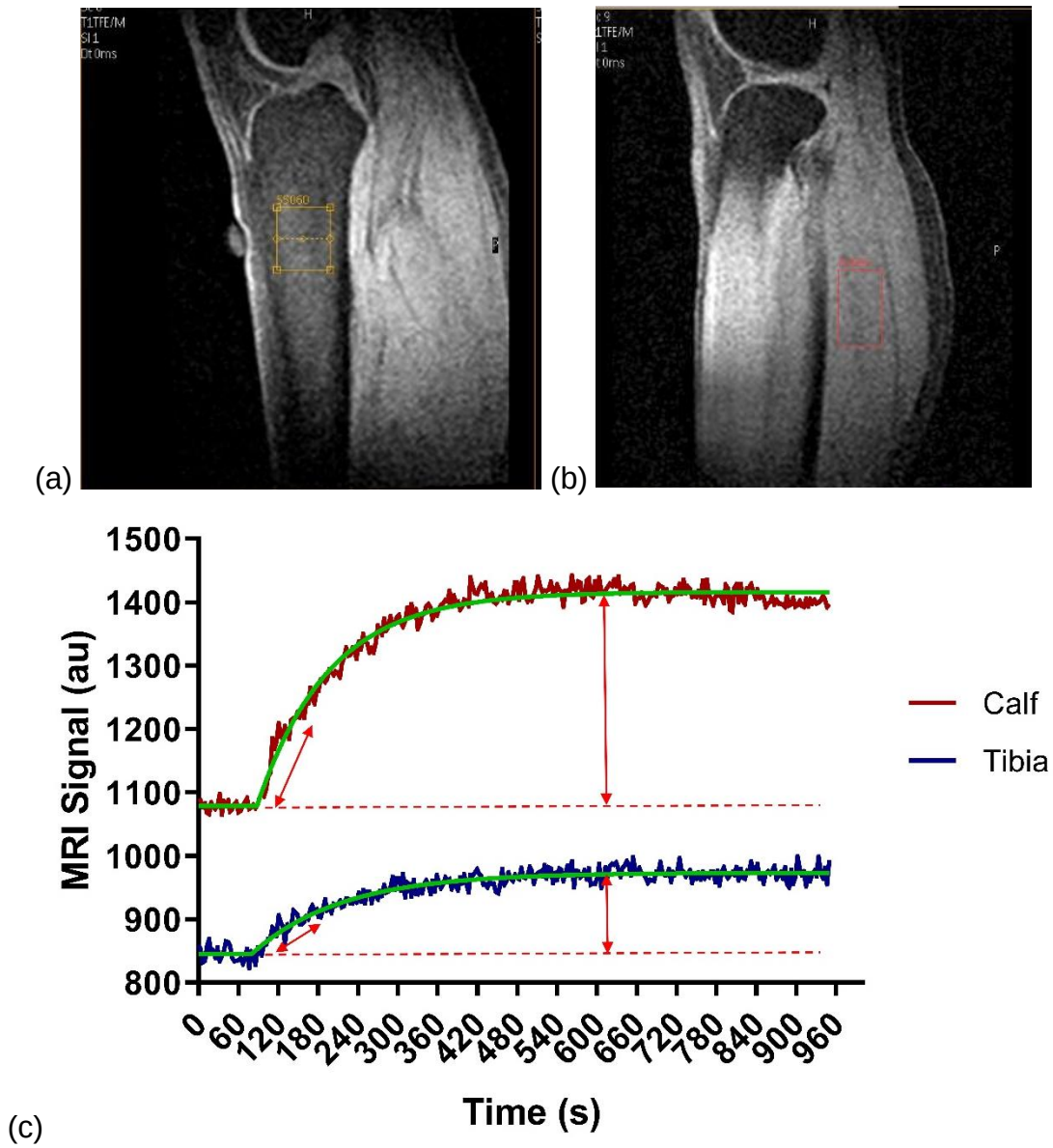

Figure 6.2: Examples of DCE-MRI region of interest for (a) the proximal tibia, and (b) the calf muscle. (c) demonstrates time signal data from both the calf and tibia including the two markers of interest: the linear initial rate of uptake over the initial 60 seconds of contrast uptake, and the amplitude of maximum signal enhancement from baseline.

Axial images of cortical bone area were used to calculate a marker of cortical bone thickness *post hoc*. It was decided not to directly measure cortical thickness as there would likely be error introduced because this is a small measurement. It would therefore be difficult to ensure this measurement was accurately taken from the internal and external borders of the cortex. Likewise it would be impossible to ensure measurements were taken in parallel with the plane of NIRS measurements. As such it was decided to calculate total bone area and cortical bone area as general markers of volume at the proximal tibia, and the contribution of cortical bone to NIRS and DXA measurements taken at the proximal tibia [309]. This was performed using freehand ROI placement (see Figure 6.3 for an example).

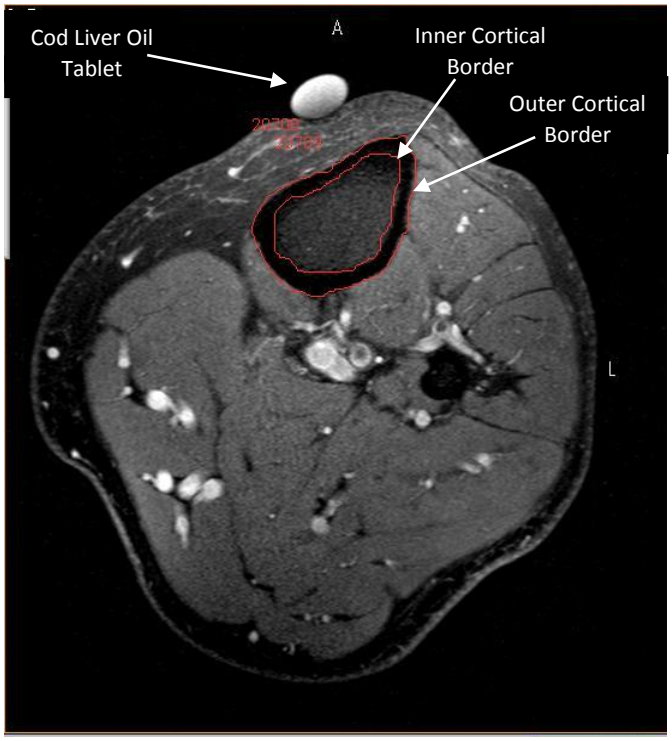

Figure 6.3: Example of total bone area measurements (i.e. the area within the outer cortical border) and cortical bone area measurements (i.e. the difference between the area within outer and inner cortical borders). A cod liver oil tablet is present to indicate the position of NIRS optodes.

6.2.5: Dual X-ray absorptiometry (DXA) testing

DXA scans were performed on all participants using a GE Lunar Prodigy Advance 2005 DXA scanner, using Encore 11.40.004 software. All scans were performed by the same technician. Protocols involved whole body scans and dedicated scan protocols of the hip and lumbar spine as per accepted clinical positioning standards [310]. From the whole body scans, areal bone mineral density (BMD; g/cm^2) measurements of the whole body, both legs combined, and the measured lower leg were taken. Whole body and lower leg composition was also taken including measures of percentage bone, lean tissue and fat body mass. Lumbar spine BMD of L1-L4 was recorded with omission of vertebral data if affected by degenerative changes. Total hip and femoral neck BMD were recorded. All BMD measurements were reported in areal density (g/cm^2) to allow comparison within the cohort of participants, as opposed to population based T-scores.

The proximal tibia of the leg measured with NIRS was also scanned with DXA. The participant was positioned supine with the leg extended with minor internal rotation to achieve a true anatomical antero-posterior (AP) position. Without dedicated lower limb software, DXA analysis was performed using an AP lumbar spine protocol on a “thin”

scan setting, designed where tissue thickness is expected to be less than 13cm. Because of this it was vital that sandbags were positioned either side of the calf to mimic soft tissue that the DXA algorithm would anticipate for a lumbar spine scan. For BMD analysis of the tibia, two ROI were placed, with a standardised 3x10cm size. One on the proximal tibia resting just under the articulating surface of the tibia, and a second just below this representing the likely position of NIRS optodes during NIRS measurements (see Figure 6.4 for an example).

All DXA scans were reported by a qualified DXA reporter. Any relevant clinical findings were reported back to the participant and to the participant's GP (where consent had been given to do so). This whole process involved one hour maximum of DXA scanning time for the participant.

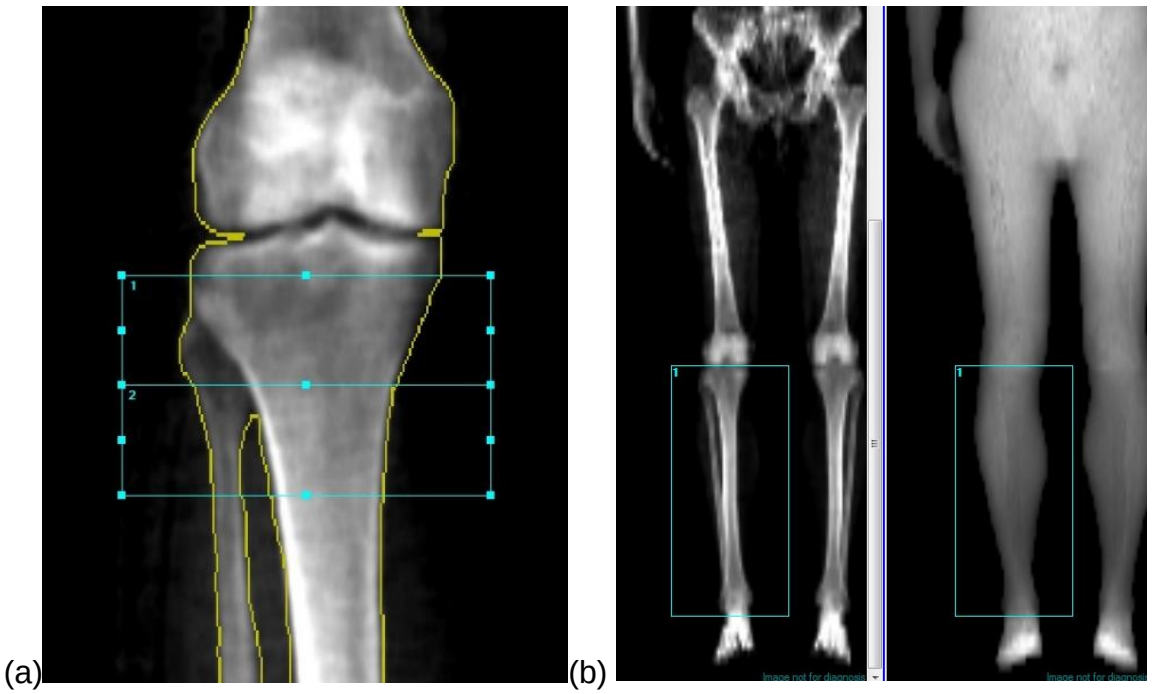

Figure 6.4: (a) Illustrative example of the two regions of interest (ROI) for measuring areal bone mineral densitometry measurements for the proximal tibia, one placed just under the articulating surface of the tibia and a second immediately below this representing the likely position of NIRS optodes during NIRS measurements. (b) Illustrative example of the ROI placement for measurements of the lower leg including the entire tibia.

6.2.6: Trabecular bone scoring (TBS)

TBS was also performed using TBS iNsight software (Medimaps Group, Geneva, Switzerland). This is a software-based post processing application that provides a marker of bone architectural strength, which is an indicator of fracture risk, independent of bone mineral density, as discussed in Section 2.4.2. TBS software analyses L1-L4

vertebral bodies as identified in the corresponding DXA scan, although vertebrae are excluded if previously excluded from BMD measurement. TBS algorithms allow for BMI ranges between 15-37 kg/m^2, meaning all participants were eligible for analysis.

As our DXA has not been calibrated for TBS using the required scanning of a phantom, values were only comparable within the cohort (as all had the same scan protocol), and not against population normative data. As such only raw unitless TBS scores were used, as opposed to population based T-scores. Figure 6.5 provides an example of TBS outputs.

(a)

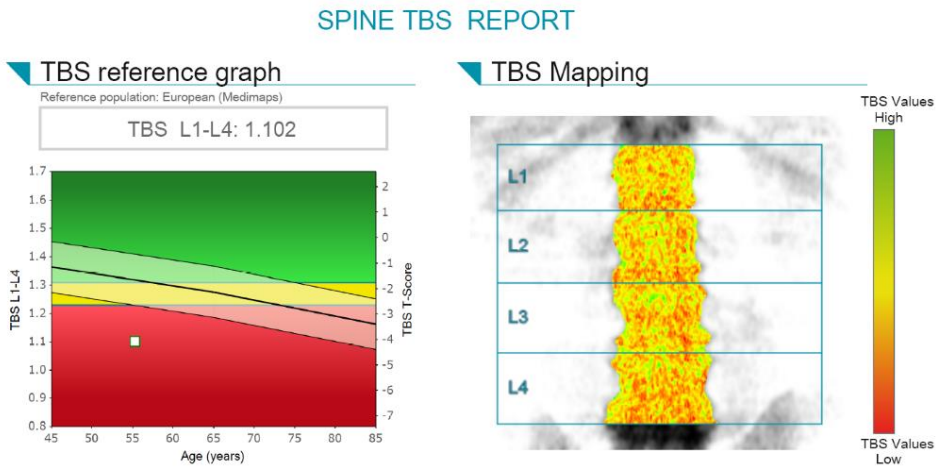

(b)

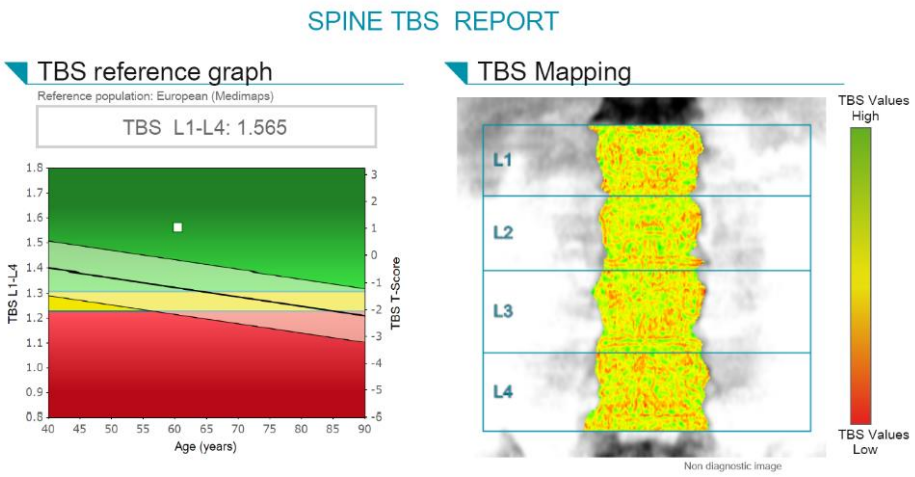

Figure 6.5: Example outputs from iNsight TBS software. (a) demonstrates the lowest TBS results from the cohort, and (b) the highest. The images demonstrate graphically the assessment of heterogeneity and porosity in bone.

6.2.7: Fracture risk assessment tool

It was decided that utilisation of the clinical tool for assessing fragility fracture would be useful to assess for an association with NIRS markers, as introduced in Section 2.4.3. As DXA and TBS data were available for all participants, FRAX was chosen over

QFracture as the predictive algorithm. FRAX scores were calculated for all participants utilising their TBS and femoral neck BMD results, and the medical history provided, to provide a percentage estimation of a fragility fracture in the next ten years. As this was *post hoc* analysis, medical history had not been taken on alcohol consumption and family history of fracture. As such, these conditions were entered as a negative for these two questions, as this was the approach adopted for missing data during the initial development stages of the FRAX algorithm [311].

6.2.8: Blood and urine testing

Participants had blood samples taken to test for blood markers of bone metabolism, namely N-terminal propeptide of type 1 procollagen (P1NP) and C-terminal telopeptide of type I collagen (CTX). Measurements were made using the Elecsys total P1NP and Elecsys b-CrossLaps/serum CTX assays utilising a Cobas e411 analyser (Roche Diagnostics). Blood samples for CTX were required to be taken after 10 hours fasting so were performed initially at presentation at the first appointment, early in the morning after an overnight 10 hour fast. To facilitate the participant, pre consenting for blood testing was attempted so this could be carried out at the first appointment with fasting.

Blood samples were immediately labelled with the participant's personal details with some samples stored at -80°C as required using existing CRF facilities. Once all blood samples were obtained from participants, serum samples were sent and batch processed by the Metabolic Bone Centre, (Northern General Hospital, Herries Road, Sheffield, South Yorkshire). The remainder of blood testing was processed at the Exeter Clinical Research Facility.

A number of tests were performed to provide background data on participants' T2DM severity and microvascular health including liver function tests, lipid profiling, and HbA1c. Testing methods are reported in Appendix R. A urine albumin to creatinine ratio (ACR) test was performed post consent to assess for nephropathy linked with T2DM microvascular disease. This involves a simple urine sample provided by the participant without any specific preparation required. Urine samples were tested immediately at the CRF testing site.

An eGFR test (utilising the Chronic Kidney Disease Epidemiology Collaboration (CKD-EPI) equation) was also performed to assess renal function for consideration of using Gadolinium based MRI contrast. The second attendance was booked in within four weeks of blood samples being taken at the first attendance to ensure eGFR results

were current, and that blood marker results remain medically relevant to MRI, NIRS and DXA results.

Vitamin D and parathyroid hormone (PTH) levels were also tested to rule out potential confounders on bone health. Vitamin D deficiency can affect the ability of the body to absorb and store calcium [8]. PTH plays an important role in activating Vitamin D to aid calcium absorption. PTH also triggers bone resorption by bonding to osteoblasts and triggering RANKL release and suppression of osteoprotegerin. Increased levels of PTH linked to conditions such as hyperparathyroidism are linked with low bone mineral density (i.e. secondary osteoporosis) [312]. Interestingly, PTH also can stimulate angiogenesis and improve vasodilatory response, whilst Vitamin D also plays a dual role in bone as it helps regulate vasomotion in small vessels [8].

6.2.9: Statistical analysis

The primary objective of the validation aspect of this PhD project is to investigate the association between NIRS haemodynamic results and external markers of bone health obtained from the same participants using the methods described above. This validation process would ideally be a diagnostic test validation study aiming to validate the use of NIRS for measuring bone tissue haemodynamics against existing tests measuring the same outcome. Typically a diagnostic test accuracy study would compare the sensitivity and specificity of a new test (in this case NIRS) at diagnosing a disease compared with a reference standard (in this case DCE-MRI) based on a threshold score that indicates the presence or absence of disease [177]. Since there is no pre-existing threshold of what constitutes pathologically poor bone perfusion, and testing involves different outcome measures, Pearson's correlation of NIRS results with other bone health markers is more appropriate. This will assess the strength of any association between the haemodynamics measured in bone by NIRS and the external markers of bone health indicating bone metabolism, bone strength and BMD.

The use of Pearson's correlation for data analysis has limitations. Linear relationships are assumed but this may not be the case as there is no precedence for comparison of these markers. Data were examined graphically using scatterplots to rule out any obvious non-linear associations. Lines of best fit are presented on scatterplots, calculated using simple linear regression using a least squares method. However, this is not for the purpose of generating regression equations, but rather to use lines of best fit to illustrate possible linear trends in the data presented [9].

Whilst correlation demonstrates association, it does not indicate agreement. If one marker was systematically over estimating a value it could still correlate well with other markers [305]. Correlation values are also inherently dependent on the range and distribution of the sample population [286]. Steps have been made to ensure participants are obtained from range of representative ages and sexes, but are unlikely to represent the ethnic mix of the wider population, or the incidence of some of the key pathologies of interest (i.e. T2DM, osteoporosis, or other metabolic bone conditions) [305]. However, with the primary aim of the project to investigate the feasibility of NIRS for measuring bone tissue, Pearson's correlation should demonstrate the expected associations between microvascular haemodynamics and other markers of bone health if NIRS is reliably measuring the proximal tibia.

In cases where there was a suspected confounding variable(s) behind an observed association, *post hoc* partial correlation analysis was performed to investigate the association whilst controlling for the suspected confounder [313]. All analysis was performed using Stata V16.0 (StataCorp, Texas).

In order to meet the statistical assumptions of Pearson's correlation, the normality of all continuous variables was assessed by examining boxplots and using the Shapiro-Wilk test for each continuous variable. Where outliers have been identified, data have been checked for analytical error. Assuming no error, outliers have been assumed to be genuine results, but findings may be presented with and without the outlying data in some instances.

Sub group analysis was also performed using independent t-tests on continuous variables comparing NIRS and bone health markers between groups according to T2DM status and sex. Before using t-tests, the normality of all continuous variables was assessed and outliers considered as above. The variance of measurements in sub groups were also compared using Levene's test of equal variance between sub groups [286].

6.2.9.1: Sample size

In order to meet the primary aim of validation, giving confidence in NIRS as a test and to justify further study in this area, a Pearson's correlation co-efficient of 0.8 or higher was desired between NIRS haemodynamic markers and external markers of bone health. A sample size of 26 participants will allow a statistically significant correlation coefficient of 0.8 to be estimated with a 95% confidence interval of 0.60 to 0.91 [307].

Similar measurements of the lateral calf will also be taken to further validate correlation between NIRS and DCE-MRI, as well as re-confirming any metabolic differences in bone and muscle tissue types.

Protocol development involved 15 volunteer participants. Successful baseline TOI readings were obtained from all 15 participants, however there were 4 failed arterial occlusions when measuring the proximal tibia from the 15 participants. This was due to issues with compliance or with executing arterial occlusions. With this 73% success rate, 36 participants would be required to obtain 26 successful datasets. Any withdrawn or missing data, or participants lost to follow up, have been narratively reported to give context and consider any systematic biases they may have introduced. Any adverse events experienced have also been reported.

It was felt appropriate to only consider sample size calculations for the primary objective of validation (i.e. the correlation of NIRS markers with other markers of bone health). Given the nature of the project as a feasibility study, it was acknowledged that sub group analyses between participants with and without T2DM, and between sexes, would potentially be underpowered. As secondary objectives of the project, these analyses were interpreted tentatively and in the context of their biological plausibility, based on the existing evidence base. This was seen as justified given the exploratory nature of the project, which has been designed to inform further research.

6.3: Chapter Summary

This chapter has presented the experimental methodology for an assessment of the reliability of AO haemodynamic markers obtained with NIRS, with corresponding results presented in Chapter 7. Chapters 8, 9 and 10 will present results comparing NIRS-derived haemodynamic markers of the proximal tibia against other recognised tests of bone health using the methods outlined in Section 6.2 of this chapter.

Chapter 7: Reliability assessment of NIRS

This chapter presents data on the reliability assessment of the AO protocol developed and outlined in Chapters 4 and 5. It is important to have confidence that haemodynamic markers are acceptably reliable alongside attempts to validate them against external markers of bone health, as is done in Chapters 8, 9 and 10. Reliability has been assessed in three primary ways:

Section 7.1 outlines intra operator reliability results for the arterial occlusion (AO) protocol developed. This assesses the repeatability of same day measurements and the reproducibility of measurements taken on different days (but within a four week period) by the same operator.

Section 7.2 outlines inter operator reliability results for obtaining baseline TOI measurements at rest. This highlights the ability of different operators to place NIRS probes using the protocols developed.

Section 7.3 outlines inter operator reliability results on the data analysis approach used to derive the haemodynamic parameters associated with the AO protocol developed.

7.1: Intra operator reliability of AO protocol measurements

7.1.1: Demographics

Table 7.1 shows the demographics of participants who undertook same day repeatability and different day reproducibility measurements. Participants were free from any history of metabolic bone disease, stroke or transient ischaemic attack (TIA), arrhythmias, cardiovascular disease, renal disease, peripheral artery disease, or deep vein thrombosis. Eighteen participants had T2DM and their case-control recruitment is discussed in more depth in Section 8.2.1.1.

In terms of bone health, none of the participants had a diagnosis of osteoporosis or history of recent low impact fracture, except one participant reporting a low impact neck of humerus fracture leading to a diagnosis of osteopenia and subsequent calcium and cholecalciferol (iCalD3) supplementation on prescription for 4 years. In eight instances participants did report osteoarthritis, but all cases were mild and not being medically treated. One participant reported early onset arthritis secondary to chemotherapy treatment at age 25 and a fibromyalgia diagnosis. One participant reported rheumatoid arthritis diagnosed from age 21, but again these conditions were not medically treated.

The age of participants ranged from 21-77 years. All participants were generally in good health and all participants were currently non-smokers for at least the past 5 years, with 14 having never smoked (7 of which had T2DM). Three participants had successfully been treated for cancer (2 breast, 1 eye) in the past but had ceased treatment for at least 12 months. All participants reported being normotensive with normal resting pulse at consent, however eight participants presented with high systolic blood pressure. It should be acknowledged that this could be caused by psychological factors whilst obtaining blood pressure readings in an unfamiliar research environment [314]. All 14 female participants were post-menopausal for a mean of 14.4 years (range 6 months to 35 years), with one participant with a history of hysterectomy at age 40.

Table 7.1: Summary of key demographics for recruited participants in same day repeatability and different day reproducibility testing (mean values presented with standard deviation in parentheses).

Demographic	Same day repeatability (N=38)	Different day reproducibility (N=41)
Age (years)	60.4 (10.7)	57.7 (14.2)
Height (m)	1.70 (0.09)	1.71 (0.09)
Weight (kg)	77.9 (12.1)	77.7 (11.9)
BMI (kg/m^2)	26.8 (3.1)	26.6 (3.2)
Sex	24m/14f	27m/14f
Diastolic Blood Pressure (mmHg)	76 (8.3)	76 (8.1)
Systolic Blood Pressure (mmHg)	132 (18.1)	132 (17.8)
Pulse (beats/min)	64 (9.7)	66 (11.8)
Resting Arterial Oxygen Saturation (%)	97 (1.4)	97 (1.6)
Resting Foot Temperature (°C)	28.2 (1.7)	29.1(2.0)
Knee Circumference (mm)	380 (25)	380 (25)
Calf Circumference (mm)	373 (26)	373 (25)
Ankle Circumference (mm)	252 (17)	251 (17)

7.1.2 Intra operator reproducibility of AO protocol measurements

Demographic data and data for each haemodynamic marker of the tibia and calf were assessed for normality using the methods described in Section 6.1.3.7. There was no evidence of non-normality, meaning parametric statistical analysis was appropriate for all analyses.

Reproducibility results of measurements taken on separate occasions were prioritised over repeatability results when assessing haemodynamic markers for adoption in further analysis against external markers of bone health. This is because these will incorporate typical biological variation and pragmatically replicates the potential future longitudinal use of NIRS for measuring bone haemodynamics. Same day repeatability results are still affected by some biological variability, but this is minimised as much as possible by testing within the same session, so results predominantly reflect the amount of variability inherent to the testing method and NIRS equipment alone.

Tables 7.2-7.9 present the measures of reliability, calculated using the statistical methods outlined in Section 6.1.3 and the NIRS haemodynamic markers graphically demonstrated in Figures 4.4 and 4.6. When selecting the most reliable markers to take forward, root mean square coefficient of variation (RMSCV) was considered the priority marker of consideration. RMSCV allows comparisons of reproducibility across different units of measure and by its nature objectively compares the variability of individual measurements against the typical (i.e. mean) results obtained.

Repeatability Coefficients (RC) are also of interest as these demonstrate the minimally detectable clinical change that the haemodynamic marker will be able to detect. It is therefore possible to get a feel for the sensitivity of a marker to clinical change by comparing the RC to the mean value of the marker.

Intraclass correlation (ICC) is also of interest as it represents the ability of a marker to distinguish between real clinical changes in the context of longitudinal measurements, relative to the differences in results caused by measurement error. However, ICC has been used cautiously for determining haemodynamic markers of choice moving forward. This is because the cohort of participants is essentially a healthy population and therefore there may be little variance between participants. As such, ICC may underestimate the potential of some markers in these situations despite having acceptable precision in terms of RMSCV values [298]. Examples of this are illustrated

within this chapter. More appropriate assessment of ICC would involve the use of NIRS amongst inherently different/diseased populations of interest.

7.1.2.1 Different day reproducibility at the proximal tibia

Tables 7.2 and 7.3 summarise the different day reproducibility data of haemodynamic markers of the proximal tibia during occlusion (DO) and post occlusion (PO). There was a mean of 12 days between testing (SD 7 days). Of the 41 participants tested for different day reproducibility, usable test/retest data were achieved from 26 participants. Reasons for missing data included twelve instances where data were excluded due to nTHI changes of >15% during an occlusion (including three instances where this affected both occlusions); one instance where HHb did not meet the criteria for inclusion in one AO (as it did not mirror O_2Hb changes); one instance of equipment error where nTHI data were not recording; and, one withdrawal due to the discomfort of occlusions. In addition, within the 26 participants who provided usable test/retest data, there were some individual haemodynamic markers assessing rates of change that were removed when not meeting the straight line condition of a Pearson's r-value of >0.9 and/or where the condition of a <5% change in nTHI within the measurement period was not met. The "paired data" rows of Tables 7.2 and 7.3 indicate the final number of paired data for each haemodynamic marker.

When assessing DO markers of the proximal tibia it can be seen in Table 7.2 that TOI_rest and TOI_DO_60s have the best performing RMSCV values. The RC values of these two markers are the smallest, relative to the mean values for their respective markers. The next most reliable markers during occlusion were the HHb_DO_120s and HHb_DO_60s markers.

In terms of post occlusion (PO) markers, O_2Hb_PO_20s and O_2Hb_PO_absΔ were clearly the best in terms of RMSCV and when comparing the magnitude of RC relative to the typical mean score across the cohort. These markers also had strong ICC results of greater than 0.8.

Table 7.2: Different day test/retest reproducibility data on haemodynamic markers of the proximal tibia during occlusion. Markers in green were used for validation analysis into Chapters 8, 9 and 10. (DO=During Occlusion; SD=Standard Deviation; RMS=Root Mean Square; CV=Coefficient of Variation; ICC=intra class correlation).

DIFFERENT DAY DATA DURING OCCLUSION (TIBIA)	TOI_rest (%)	TOI_DO_120s (%/s)	TOI_DO_60s (%/s)	TOI_DO_absΔ (%)
Paired data (N)	26	21	22	26
Mean	78.4	-0.028	-0.026	-7.3
Between Participant SD	4.2	0.009	0.005	2.2
Within Participant RMSSD	2.3	0.009	0.004	1.9
Within Participant RMSCV (%, with 95% CI)	3.0 (0-6.0)	30.8 (0-68.8)	16.3 (0-36.3)	24.8 (0.1-49.4)
Repeatability Coefficient	6.4	0.025	0.011	5.2
ICC (with 95% CI)	0.71 (0.46-0.86)	-0.18 (-0.55-0.26)	0.28 (-0.14-0.62)	0.36 (0.0-0.65)

DIFFERENT DAY DATA DURING OCCLUSION (TIBIA)	HHb_DO_120s (µM.cm/s)	HHb_DO_60s (µM.cm/s)	HHb_DO_absΔ (µM.cm)	O_2Hb_DO_120s (µM.cm/s)	O_2Hb_DO_60s (µM.cm/s)	O_2Hb_DO_absΔ (µM.cm)
Paired data (N)	21	26	26	21	26	26
Mean	0.356	0.326	98.9	-0.357	-0.329	-99.2
Between Participant SD	0.119	0.107	36.1	0.131	0.110	55.8
Within Participant RMSSD	0.073	0.074	24.7	0.095	0.094	23.9
Within Participant RMSCV (%, with 95% CI)	21.3 (1.3-41.4)	25.9 (0-56.1)	31.4 (0-73.1)	27.8 (0-56.7)	29.9 (0-62.1)	27.7 (0-58.6)
Repeatability Coefficient	0.203	0.204	68.4	0.264	0.261	66.2
ICC (with 95% CI)	0.65 (0.32-0.84)	0.53 (0.19-0.76)	0.55 (0.21-0.77)	0.51 (0.12-0.77)	0.33 (-0.05-0.63)	0.83 (0.67-0.92)

Table 7.3: Different day test/retest reproducibility data on haemodynamic markers of the proximal tibia post arterial occlusion release. Markers in green were used for validation analysis into Chapters 8, 9 and 10. (PO=Post Occlusion Release; SD=Standard Deviation; RMS=Root Mean Square; CV=Coefficient of Variation; ICC=intra class correlation).

DIFFERENT DAY DATA POST OCCLUSION (TIBIA)	TOI_PO_20s (%/s)	TOI_PO_10s (%/s)	TOI_PO_absΔ (%)	TOI_PO_hyperΔ (%)
Paired data (N)	23	20	26	26
Mean	0.256	0.355	7.8	0.6
Between Participant SD	0.117	0.175	2.6	1.8
Within Participant RMSSD	0.100	0.128	2.3	1.2
Within Participant RMSCV (%, with 95% CI)	43.0 (3.8-82.1)	45.1 (2.1-88.1)	27.6 (0-57.6)	837.7 (0.0-2138.9)
Repeatability Coefficient	0.278	0.353	6.4	3.3
ICC (with 95% CI)	0.15 (-0.26-0.52)	0.47 (0.06-0.75)	0.30 (0.0-0.61)	0.53 (0.19-0.76)

DIFFERENT DAY DATA POST OCCLUSION (TIBIA)	O_2Hb_PO_20s (µM.cm/s)	O_2Hb_PO_10s (µM.cm/s)	O_2Hb_PO_absΔ (µM.cm)	O_2Hb_PO_hyperΔ (µM.cm)
Paired data (N)	26	26	26	26
Mean	7.328	10.81	186.2	87.0
Between Participant SD	2.803	5.009	59.5	47.7
Within Participant RMSSD	1.114	2.589	24.8	21.2
Within Participant RMSCV (%, with 95% CI)	19.1 (0.0-39.7)	28.3 (0-58.8)	18.6 (0-41.0)	50.9 (0-133.5)
Repeatability Coefficient	3.086	7.17	68.8	58.7
ICC (with 95% CI)	0.86 (0.71-0.93)	0.76 (0.54-0.88)	0.85 (0.69-0.93)	0.82 (0.64-0.91)

7.1.2.2: Different day reproducibility at the lateral calf

Tables 7.4 and 7.5 summarise the different day reproducibility data of haemodynamic markers of the lateral calf DO and PO. Of the 41 participants tested for different day reproducibility, usable test/retest data were achieved from 30 participants. Reasons for missing data included eight instances where data were excluded due to nTHI changes of >15% during an occlusion (including one instance where this affected both occlusions); two instances of probe movement; and, one participant withdrawal due to the discomfort of occlusions. In addition, within the 30 participants who provided usable test/retest data, there were some individual haemodynamic marker results for rates of change that were removed when not meeting the straight line condition of a Pearson's r-value of >0.9 and/or where the condition of a <5% change in nTHI within the measurement period was not met, as indicated on Tables 7.4 and 7.5 in the "paired data" row.

Table 7.4: Different day test/retest reproducibility data on haemodynamic markers of the calf muscle during occlusion. Markers in green were used for validation analysis into Chapters 8, 9 and 10. (DO=During Occlusion; SD=Standard Deviation; RMS=Root Mean Square; CV=Coefficient of Variation; ICC=intra class correlation).

DIFFERENT DAY DATA DURING OCCLUSION (CALF)	TOI_rest (%)	TOI_DO_120s (%/s)	TOI_DO_60s (%/s)	TOI_DO_absΔ (%)
Paired data (N)	29	22	27	29
Mean	68.8	-0.065	-0.060	-17.0
Between Participant SD	4.3	0.024	0.023	9.6
Within Participant RMSSD	2.1	0.011	0.011	8.5
Within Participant RMSCV (%, with 95% CI)	3.1 (0-6.9)	14.6 (0-30.2)	17.2 (1.2-33.2)	22.8 (0-55.5)
Repeatability Coefficient	5.8	0.031	0.032	23.5
ICC (with 95% CI)	0.78 (0.58-0.89)	0.73 (0.45-0.88)	0.74 (0.51-0.87)	0.29 (0.0-0.59)

DIFFERENT DAY DATA DURING OCCLUSION (CALF)	HHb_DO_120s (µM.cm/s)	HHb_DO_60s (µM.cm/s)	HHb_DO_absΔ (µM.cm)	O_2Hb_DO_120s (µM.cm/s)	O_2Hb_DO_60s (µM.cm/s)	O_2Hb_DO_absΔ (µM.cm)
Paired data (N)	22	29	29	22	28	28
Mean	0.925	0.874	246.7	-0.786	-0.755	-182.3
Between Participant SD	0.432	0.431	104.3	0.377	0.364	88.5
Within Participant RMSSD	0.202	0.176	47.0	0.158	0.176	37.1
Within Participant RMSCV (%, with 95% CI)	22.0 (1.1-43.0)	18.5 (1.8-35.2)	19.9 (0-40.0)	24.4 (0-53.9)	27.6 (0-56.6)	21.3 (0.7-42.0)
Repeatability Coefficient	0.558	0.487	130.2	0.437	0.487	102.6
ICC (with 95% CI)	0.77 (0.52-0.89)	0.84 (0.69-0.92)	0.81 (0.63-0.90)	0.83 (0.64-0.92)	0.79 (0.59-0.89)	0.80 (0.62-0.90)

Table 7.5: Different day test/retest reproducibility data on haemodynamic markers of the calf muscle post arterial occlusion release. Markers in green were used for validation analysis into Chapters 8, 9 and 10. (PO=Post Occlusion Release; SD=Standard Deviation; RMS=Root Mean Square; CV=Coefficient of Variation; ICC=intra class correlation).

DIFFERENT DAY DATA POST OCCLUSION (CALF)	TOI_PO_20s (%/s)	TOI_PO_10s (%/s)	TOI_PO_absΔ (%)	TOI_PO_hyperΔ (%)
Paired data (N)	30	29	29	29
Mean	1.232	1.416	22.9	6.8
Between Participant SD	0.439	0.584	7.7	3.1
Within Participant RMSSD	0.249	0.430	3.1	1.6
Within Participant RMSCV (%, with 95% CI)	29.1 (0-77.3)	34.2 (0-83.3)	13.7 (0-28.4)	34.6 (0.0-84.7)
Repeatability Coefficient	0.689	1.190	8.6	4.4
ICC (with 95% CI)	0.78 (0.60-0.89)	0.61 (0.32-0.79)	0.35 (0.0-0.63)	0.73 (0.51-0.87)

DIFFERENT DAY DATA POST OCCLUSION (CALF)	O_2Hb_PO_20s (µM.cm/s)	O_2Hb_PO_10s (µM.cm/s)	O_2Hb_PO_absΔ (µM.cm)	O_2Hb_PO_hyperΔ (µM.cm)
Paired data (N)	29	30	28	28
Mean	18.92	24.10	354.4	172.1
Between Participant SD	7.92	10.20	133.5	67.6
Within Participant RMSSD	3.14	4.34	51.3	30.8
Within Participant RMSCV (%, with 95% CI)	17.0 (0.3-33.7)	19.1 (0.4-37.9)	13.9 (0-28.3)	19.4 (1.7-37.2)
Repeatability Coefficient	8.71	12.02	142.2	85.3
ICC (with 95% CI)	0.84 (0.69-0.92)	0.79 (0.60-0.89)	0.84 (0.69-0.92)	0.77 (0.58-0.89)

Results for the lateral calf demonstrate similar trends to the proximal tibia results presented in Tables 7.2 and 7.3. TOI_rest is the best performing marker and TOI_DO_60s is the second best performing marker in terms of RMSCV. Therefore it is sensible to use these markers moving forward to validation work. It can be seen that the TOIs_DO_60s marker has similar RMSCV values at the tibia and the calf (16.3% (95%CI 0% to 36.3%) versus 17.2% (95%CI 1.2% to 33.3%), respectively). However these two markers have markedly different ICC values (0.28 (95%CI -0.14 to 0.62) versus 0.74 (95%CI 0.51 to 0.87)). The reason for this is best illustrated graphically in Figure 7.1. This demonstrates that despite comparable precision with RMSCV, the range of TOI_DO_60s values at the tibia is very narrow compared with the lateral calf. As a result ICC is lower for the proximal tibia because between participant differences are small compared with the wider range of between participant values evident at the lateral calf [298]. As only relatively healthy participants have been recruited, it would be unwise to exclude TOI_DO_60s at this stage based on a low ICC value, in light of comparable RMSCV values with the calf.

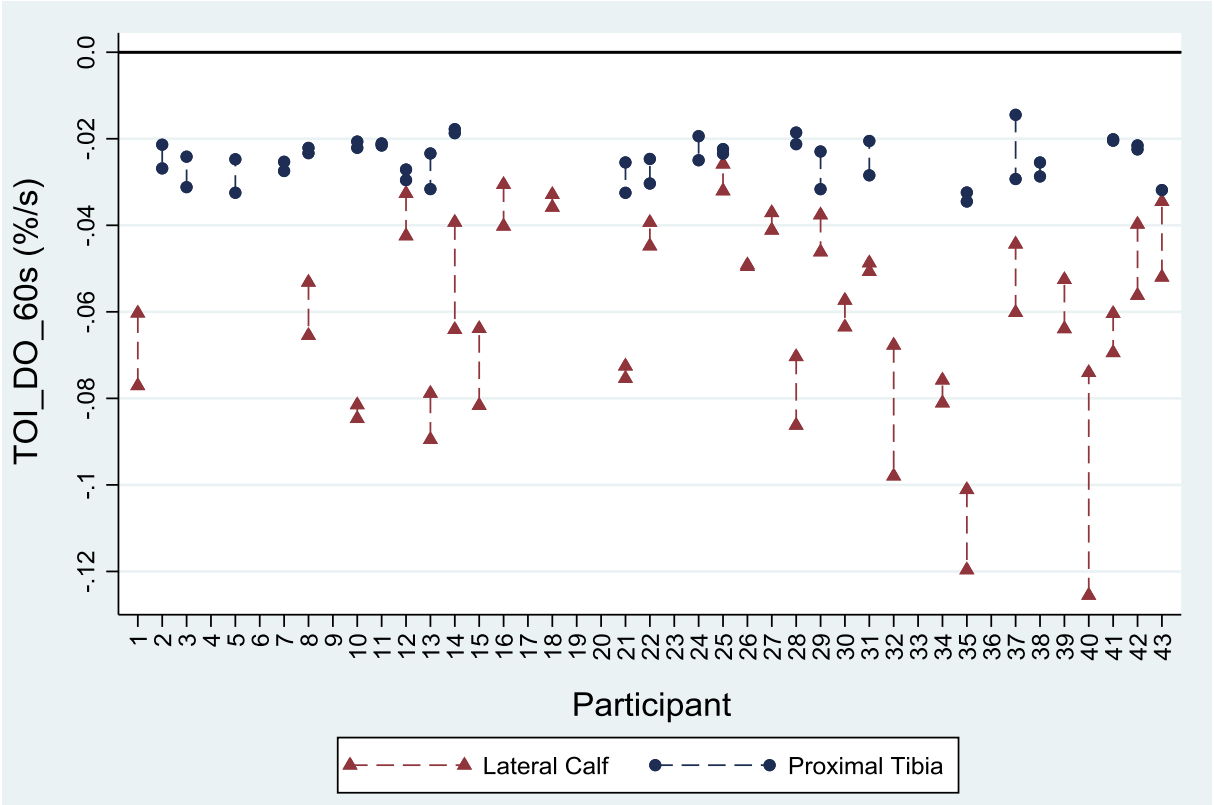

Figure 7.1: Graphical demonstration of different day reproducibility test/retest scores of the TOI_DO_60s marker for the proximal tibia and lateral calf representing the rate of TOI reduction during the last 60 seconds of arterial occlusion. This demonstrates the relatively low between-participant variation at the proximal tibia contributing to a lower ICC score, despite comparable RMSCV% with the lateral calf.

In light of this potential limitation of TOI_DO_60s as a haemodynamic marker at the tibia it was also decided to take the HHb_DO_60s marker moving forward. This was the next best alternative DO marker identified in muscle, with less data loss compared with HHb_DO_120s. This is likely due to the shorter sampling time leading to more stable nTHI during the measured time period and less data loss. Similarly, the O_2Hb_DO_absΔ marker was also taken forward for validation in Chapter 7 as the best performing DO O_2Hb marker for both the proximal tibia and lateral calf.

In terms of post occlusion markers, as for the proximal tibia, O_2Hb_PO_20s and O_2Hb_PO_absΔ were clearly the best in terms of RMSCV and when comparing the magnitude of RC relative to the typical mean score across the cohort. These markers also had strong ICC results of greater than 0.8. As such it was decided to use these markers for validation analysis. The TOI_PO_absΔ was also used in validation work as the best performing TOI marker PO at both the proximal tibia and the lateral calf.

Results presented are in line with the sparse existing evidence base around reliability of NIRS use in muscle tissue. Rosenberry et al 2018 reports a similarly low CV of 4.9% for repeated resting TOI measurements at the forearm in 14 participants [79]. Crenshaw et al. 2012 found comparable ICC reproducibility in inter day test/retest DO data for HHb rates representing oxygen extraction of muscles in the forearm (ICC 0.83 (95% CI 0.64 to 0.92)) [279].

Kragelj et al. 2000 reports mean within participant CV results ranging from 6%-30% (n=6) for DO and PO arterial occlusion parameters of the calf, arguing these are still acceptable for research applications [274]. Willingham et al. 2016 also investigated O_2Hb rates of recovery in the calf PO, adopting multiple haemodynamic markers. The most reproducible parameter (comparable with O_2Hb_PO_20s) produced a coefficient of variation of 7.12% (SD 3.95; N=20) [281]. Lacroix et al. 2012 also concluded O_2Hb recovery time was reproducible with an ICC of 0.63 and CV of 6.68% (CI not presented; N=24) [282]. McLay et al. 2016 reported high reproducibility of TOI recovery 10s post AO release at the tibialis anterior muscle with a CV of 14% (SD 5%). This study involved 9 healthy participants being tested on five different days [278].

Results from the evidence base are in keeping with those achieved in the presented reliability work and generally support the choices of haemodynamic markers moving forward to Chapter 8.

7.1.3: Intra operator repeatability assessment of AO protocol

7.1.3.1 Same day repeatability of the proximal tibia

Tables 7.6 and 7.7 summarise the same day repeatability data of haemodynamic markers of the proximal tibia DO and PO. Of the 38 participants tested for same day repeatability, usable test/retest data were achieved from 28 participants. Reasons for missing data included five instances where data were excluded due to nTHI changes of >15% during an occlusion (including one instance where this affected both occlusions); one instance where HHb did not meet the criteria for inclusion in one AO (as it did not mirror O_2Hb changes); one instance of equipment error where nTHI was not recording; and, three withdrawals due to the discomfort of occlusions. In addition, within the 28 participants who provided usable test/retest data, there were some individual haemodynamic marker results removed involving rates of change not meeting the straight line condition of a Pearson's r-value of >0.9 and/or where the condition of a <5% change in nTHI within the measurement period was not met, as indicated on Tables 7.6 and 7.7 in the "paired data" row.

There is generally lower RMSCV values at the tibia for same day repeatability across all haemodynamic markers when compared with the different day reproducibility results presented in Table 7.2 and 7.3. This is expected without the contribution of "different day" biological variation and probe repositioning as potential sources of error. However the markers already identified as best performing across different days are still amongst the best performing markers for repeatability at the proximal tibia.

Table 7.6: Same day test/retest repeatability data on haemodynamic markers of the proximal tibia during occlusion. Markers in green were used for validation analysis into Chapters 8, 9 and 10. (DO=During Occlusion; SD=Standard Deviation; RMS=Root Mean Square; CV=Coefficient of Variation; ICC=intra class correlation).

SAME DAY DATA DURING OCCLUSION (TIBIA)	TOI_rest (%)	TOI_DO_120s (%/s)	TOI_DO_60s (%/s)	TOI_DO_absΔ (%)
Paired data (N)	28	23	25	28
Mean	77.1	-0.028	-0.027	-7.4
Between Participant SD	4.1	0.007	0.005	1.7
Within Participant RMSSD	1.1	0.005	0.004	0.8
Within Participant RMSCV (%, with 95% CI)	1.4 (0-3.0)	16.7 (0-37.8)	14.2 (0-30.4)	10.6 (0-23.0)
Repeatability Coefficient	3.0	0.013	0.011	2.1
ICC (with 95% CI)	0.93 (0.86-0.97)	0.58 (0.23-0.79)	0.42 (0.05-0.70)	0.79 (0.60-0.90)

SAME DAY DATA DURING OCCLUSION (TIBIA)	HHb_DO_120s (μM.cm/s)	HHb_DO_60s (μM.cm/s)	HHb_DO_absΔ (μM.cm)	ΔO_2Hb_DO_120s (μM.cm/s)	ΔO_2Hb_DO_60s (μM.cm/s)	O_2Hb_DO_absΔ (μM.cm)
Paired data (N)	23	28	28	23	28	28
Mean	0.356	0.313	95.8	-0.383	-0.363	-105.0
Between Participant SD	0.105	0.096	28.2	0.122	0.123	52.5
Within Participant RMSSD	0.048	0.061	12.4	0.075	0.078	17.2
Within Participant RMSCV (%, with 95% CI)	14.9 (0-31.8)	21.9 (0-48.6)	18.3 (0-42.8)	20.6 (0-41.0)	23.3 (0.5-46.1)	27.4 (0-63.3)
Repeatability Coefficient	0.133	0.170	34.3	0.207	0.216	47.5
ICC (with 95% CI)	0.82 (0.62-0.92)	0.61 (0.32-0.80)	0.81 (0.63-0.91)	0.66 (0.36-0.84)	0.63 (0.35-0.81)	0.89 (0.79-0.95)

Table 7.7: Same day test/retest repeatability data on haemodynamic markers of the proximal tibia post arterial occlusion release. Markers in green were used for validation analysis into Chapters 8, 9 and 10. (PO=Post Occlusion Release; SD=Standard Deviation; RMS=Root Mean Square; CV=Coefficient of Variation; ICC=intra class correlation).

SAME DAY DATA POST OCCLUSION (TIBIA)	TOI_PO_20s (%/s)	TOI_PO_10s (%/s)	TOI_PO_absΔ (%)	TOI_PO_hyperΔ (%)
Paired data (N)	22	22	28	28
Mean	0.272	0.379	7.9	0.5
Between Participant SD	0.107	0.160	2.0	1.8
Within Participant RMSSD	0.037	0.062	1.0	0.8
Within Participant RMSCV (%, with 95% CI)	15.7 (0-33.4)	17.8 (0-36.8)	13.1 (0-26.3)	276.6 (0-692.9)
Repeatability Coefficient	0.101	0.172	2.9	2.1
ICC (with 95% CI)	0.85 (0.67-0.93)	0.77 (0.52-0.90)	0.71 (0.47-0.86)	0.78 (0.58-0.89)

SAME DAY DATA POST OCCLUSION (TIBIA)	ΔO_2Hb_PO_20s (µM.cm/s)	ΔO_2Hb_PO_10s (µM.cm/s)	O_2Hb_PO_absΔ (µM.cm)	O_2Hb_PO_hyperΔ (µM.cm)
Paired data (N)	28	28	28	28
Mean	7.58	11.36	184.7	79.7
Between Participant SD	2.85	5.21	56.9	42.5
Within Participant RMSSD	0.77	1.47	17.6	25.0
Within Participant RMSCV (%, with 95% CI)	11.2 (0.2-22.2)	14.5 (0.0-29.1)	9.3 (0-19.5)	29.7 (1.4-57.9)
Repeatability Coefficient	2.13	4.08	48.6	69.1
ICC (with 95% CI)	0.93 (0.86-0.97)	0.92 (0.85-0.96)	0.91 (0.82-0.96)	0.66 (0.39-0.82)

7.1.3.2: Same day repeatability of the lateral calf

Tables 7.8 and 7.9 summarise the same day repeatability data of haemodynamic markers of the lateral calf DO and PO. Of the 38 participants who were tested for same day repeatability, 31 contributed usable test/retest data. Reasons for missing data included two participants where data were excluded due to nTHI changes of >15% during an occlusion (including one where this affected both occlusions); two instances where there was probe movement during one attempt; and, three withdrawals due to the discomfort of occlusions. In addition, within the 31 participants who provided usable test/retest data, there were some individual haemodynamic marker results removed involving rates of change not meeting the straight line condition of a Pearson's r-value of >0.9 and/or where the condition of a <5% change in nTHI within the measurement period was not met, as indicated on Tables 7.8 and 7.9 in the "paired data" row.

With respect to same day repeatability for haemodynamic markers of the lateral calf, most markers appeared to be reliable with RMSCV below 10% and ICC of greater than 0.8. Same day repeatability results for haemodynamic markers at the proximal tibia were generally not as reliable as those at the lateral calf. However, RMSCV results at the tibia were below 20% and ICC results were generally within the "strong" categories of 0.6 and above proposed by Evans 1996 [304]. Similarly, different day reproducibility results at the proximal tibia were generally not as reliable as at the lateral calf. However, RMSCV results of the markers identified as best performing for reproducibility in both bone and muscle were also mostly less than 20%.

Table 7.8: Same day test/retest repeatability data on haemodynamic markers of the calf muscle during occlusion. Markers in green were used for validation analysis into Chapters 8, 9 and 10. (DO=During Occlusion; SD=Standard Deviation; RMS=Root Mean Square; CV=Coefficient of Variation; ICC=intra class correlation).

SAME DAY DATA DURING OCCLUSION (CALF)	TOI_rest (%)	TOI_DO_120s (%/s)	TOI_DO_60s (%/s)	TOI_DO_absΔ (%)
Paired data (N)	30	29	28	30
Mean	68.3	-0.065	-0.060	-16.3
Between Participant SD	3.5	0.023	0.023	5.7
Within Participant RMSSD	0.8	0.005	0.006	1.2
Within Participant RMSCV (%, with 95% CI)	1.2 (0.0-2.5)	9.2 (0-24.3)	11.0 (0-29.3)	6.4 (0.0-15.6)
Repeatability Coefficient	2.2	0.015	0.016	3.5
ICC (with 95% CI)	0.95 (0.90-0.98)	0.94 (0.88-0.97)	0.93 (0.86-0.97)	0.95 (0.90-0.98)

SAME DAY DATA DURING OCCLUSION (CALF)	HHb_DO_120s (μM.cm/s)	HHb_DO_60s (μM.cm/s)	HHb_DO_absΔ (μM.cm)	O_2Hb_DO_120s (μM.cm/s)	O_2Hb_DO_60s (μM.cm/s)	O_2Hb_DO_absΔ (μM.cm)
Paired data (N)	29	30	30	29	29	29
Mean	0.951	0.891	253.2	-0.828	-0.802	-191.8
Between Participant SD	0.483	0.473	114.7	0.403	0.392	99.4
Within Participant RMSSD	0.062	0.067	14.3	0.064	0.068	19.8
Within Participant RMSCV (%, with 95% CI)	8.0 (0-19.8)	9.7 (0-22.9)	6.4 (0.0-14.1)	8.8 (0-18.5)	12.3 (0-26.3)	12.7 (0.0-26.6)
Repeatability Coefficient	0.171	0.186	39.5	0.178	0.188	54.8
ICC (with 95% CI)	0.98 (0.97-0.99)	0.98 (0.96-0.99)	0.98 (0.97-0.99)	0.98 (0.95-0.99)	0.97 (0.94-0.99)	0.96 (0.92-0.98)

Table 7.9: Same day test/retest repeatability data on haemodynamic markers of the calf muscle post arterial occlusion release. Markers in green were used for validation analysis into Chapters 8, 9 and 10. (PO=Post Occlusion Release; SD=Standard Deviation; RMS=Root Mean Square; CV=Coefficient of Variation; ICC=intra class correlation).

SAME DAY DATA POST OCCLUSION (CALF)	TOI_PO_20s (%/s)	TOI_PO_10s (%/s)	TOI_PO_absΔ (%)	TOI_PO_hyperΔ (%)
Paired data (N)	31	31	30	30
Mean	1.245	1.394	23.4	7.1
Between Participant SD	0.435	0.561	7.8	2.9
Within Participant RMSSD	0.203	0.192	1.1	1.1
Within Participant RMSCV (%, with 95% CI)	25.4 (0-73.2)	25.5 (0-71.7)	5.1 (0-10.5)	16.9 (0-37.8)
Repeatability Coefficient	0.563	0.533	3.2	3.0
ICC (with 95% CI)	0.96 (0.93- 0.98)	0.95 (0.90 - 0.98)	0.98 (0.95-0.99)	0.86 (0.72-0.93)

SAME DAY DATA POST OCCLUSION (CALF)	O_2Hb_PO_20s (µM.cm/s)	O_2Hb_PO_10s (µM.cm/s)	O_2Hb_PO_absΔ (µM.cm)	O_2Hb_PO_hyperΔ (µM.cm)
Paired data (N)	30	31	30	30
Mean	19.47	24.52	365.2	173.4
Between Participant SD	8.69	11.15	146.1	64.2
Within Participant RMSSD	1.36	2.06	22.5	16.8
Within Participant RMSCV (%, with 95% CI)	9.4 (0-22.2)	10.3 (0-22.5)	6.0 (0.03-12.1)	11.6 (0.0-28.1)
Repeatability Coefficient	3.77	5.70	62.3	46.6
ICC (with 95% CI)	0.97 (0.95 - 0.99)	0.96 (0.92 - 0.98)	0.97 (0.95-0.99)	0.92 (0.84-0.96)

7.1.4: Discussion of intra operator reliability of AO protocol measurements

7.1.4.1: Comparison with existing evidence

When judging if the reliability results presented for NIRS at the proximal tibia are acceptable, two main factors have been considered:

1) How does reliability compare to accepted norms and comparable evidence in this field of research?

2) Is reliability sufficient to identify real changes in bone haemodynamics that could justify NIRS usage for future research applications?

With regards to the first question, as identified by the systematic review in Chapter 3, no studies have carried out a meaningful analysis on the reliability of NIRS for measuring bone haemodynamics in any capacity, let alone for arterial occlusions. However arterial occlusions have been used as a protocol for studies of skin and muscle tissue, and there is some evidence from which to draw comparison for reliability. Unfortunately, few studies identified reported repeatability coefficients of similar units for comparison, but most studies presented RMSCV or ICC data (or both). Direct comparison with reproducibility results are presented above in Section 7.1.2.2.

Similar conclusions are drawn when investigating reliability of alternative NIR systems, such as LDF, with reliability particularly affected in microvascular studies by susceptibility to biological variations from a wide range of potential sources. One specific example is the small sampling volume and heterogeneity of vascular beds, where even measuring a small distance away from the first site can produce variation in results [81]. A comprehensive review by Roustit et al. 2012 describes iontophoresis with laser speckle imaging reproducibility as good with a 22% CV, and 0.72 ICC (CI not included). This paper also describes use of LDF for measurement of PORH in a variety of contexts, stating acceptable reproducibility at 25% CV for the finger pad, and poor CV at 45% or higher [81].

Reliability results are also in line with the alternative imaging modalities that may be applicable to measuring haemodynamic markers in bone. Griffith et al 2009 found DCE-MRI parameters for the femoral shaft, neck and head to be reproducible with ICC generally above 0.75 [130]. Padhani et al 2002 used a pharmacokinetic model to calculate maximum contrast medium accumulation in the ischial bone marrow using DCE-MRI with a within participant coefficient of variation of 23.1%. This was similar to

results in adjacent muscle [131]. Yang 2009 also used a pharmacokinetic model to look at DCE-MRI of bone metastases. Using different models, within participant coefficient of variation ranged between 9% and 15% for markers of contrast agent transfer rates to tissue [132]. Wassberg et al 2017 reports repeatability coefficients of quantitative standardised uptake markers of 18F-NaF using PET/CT in the range of 23%-35% relative to mean results [143].

Whilst the results obtained may fall outside ranges of reproducibility considered ideal for clinical tests at an individual participant level, it is reassuring that reliability results are comparable with the existing evidence base of systems that measure differences in haemodynamics between sub groups of interest. Buchheit et al. 2011 makes the point that when assessing new research tests, the presence of reliability results outside ideal ranges (such as CV>10%) should not necessarily condemn the test for future research use. Reliability results should be kept in context with the expected "minimum clinically important difference" (MCID) of interest for the research application [277]. This of course does not excuse less than ideal reliability. However, it does give context to reliability results in the field of measuring microvascular haemodynamics, where reproducibility is known to be difficult.

The second question to consider is whether the reliability of NIRS is sufficient for detecting the expected physiological differences between disease states. In particular the repeatability coefficient represents the maximum absolute difference expected between two repeated measurements 95% of the time. This is useful as an absolute measure of reliability when compared with the MCID using the same method during longitudinal testing [305].

The systematic review carried out in Chapter 3 has not identified any NIRS based assessments of clinically important differences in bone haemodynamics during AO (or comparable microvascular challenges). Likewise, there is a paucity of research around bone haemodynamics due to the inherent difficulties in measuring it reliably. However there are some studies that suggest reliability results in keeping with the presented reliability data in this Chapter could still allow useful research of *in vivo* bone haemodynamics with NIRS.

For example, in murine studies mean bone perfusion at the tibia was found to be reduced from 0.18 (SD 0.03) mL/min/g in controls to 0.11(SD 0.01) mL/min/g in mice with T1DM using fluorescent microspheres, representing a 38.9% reduction [26].

Stabley et al. 2015 also demonstrated reduced femoral blood flow in mice with T2DM compared with controls using radiolabelled microspheres, with 30-50% reductions observed across various sites of the femur [315].

No human studies on bone perfusion were found pertaining directly to diabetes. However, Griffith et al. 2008 has demonstrated that in those with osteoporosis, maximum signal enhancement and enhancement rates using DCE-MRI were reduced around 50% compared with healthy controls [36]. Libicher et al. 2008 also demonstrated using DCE-MRI that areas of Pagetic bone had markers of signal enhancement and rates of enhancement more than double that of healthy bone sites [117].

This evidence suggests that based on the repeatability coefficient results reported in Tables 7.2 and 7.3, meaningful clinical differences of similar magnitude between groups of interest (such as those with T2DM or osteoporosis) could potentially be identified using NIRS assessment of bone haemodynamics. Given the advantages NIRS holds as a safe and inexpensive test, and the lack of alternative options for measuring bone haemodynamics in bone tissue, this warrants further investigation of NIRS validation in Chapters 8, 9 and 10.

7.1.4.2: Justification of haemodynamic markers for validation

It was noted that TOI data typically had lower ICCs compared with HHb and O_2Hb measurements at the same stage of the occlusion, despite having similar or even better RMSCVs. Section 7.1.2.2 and Figure 7.1 discusses an example of this. Brandmaier et al. 2018 illustrates how this is possible given that RMSCV represents the relative error of a marker to its mean value, whilst ICC calculations incorporate the ratio of between participant variance to within participant variance [316]. Since it is desirable for NIRS to be able to identify useful haemodynamic differences between participants, or clinically important changes longitudinally within participants, opting for HHb and O_2Hb markers with better ICC results is sensible, however TOI markers have also been included in validation work to ensure that markers achieved using both the modified Beer Lambert law (MBL) and spatially resolved spectroscopy (SRS) are taken forward.

HHb_DO_60s and TOI_DO_60s provide physiologically relevant markers. It would be expected that increased rates of these markers would be greater in those participants where oxygen is extracted more rapidly in the closed system provided by AO. Binzoni et al. 2003 also found HHb to be a more reliable marker that is less sensitive to small blood volume changes when compared with O_2Hb [189]. Measuring O_2Hb_PO_20s post

occlusion release also makes physiological sense as this represents the rate of increase in oxygenated haemoglobin following release of occlusion, which may be representative of microvascular reperfusion function. $O_2Hb\_DO\_abs\Delta$ and $O_2Hb\_PO\_abs\Delta$ also are physiologically relevant representing the absolute maximum concentration change from oxygen extraction DO, and the absolute maximal increase in O_2Hb concentration following the release of the occlusion. Likewise TOI_PO_absΔ represents the maximum increase in oxygen saturation in tissue during the post occlusive period. Pragmatically, there was less data loss for these DO marker rates taken over 60s, PO marker rates over 20s, and markers looking at absolute changes of O_2Hb and TOI DO and PO.

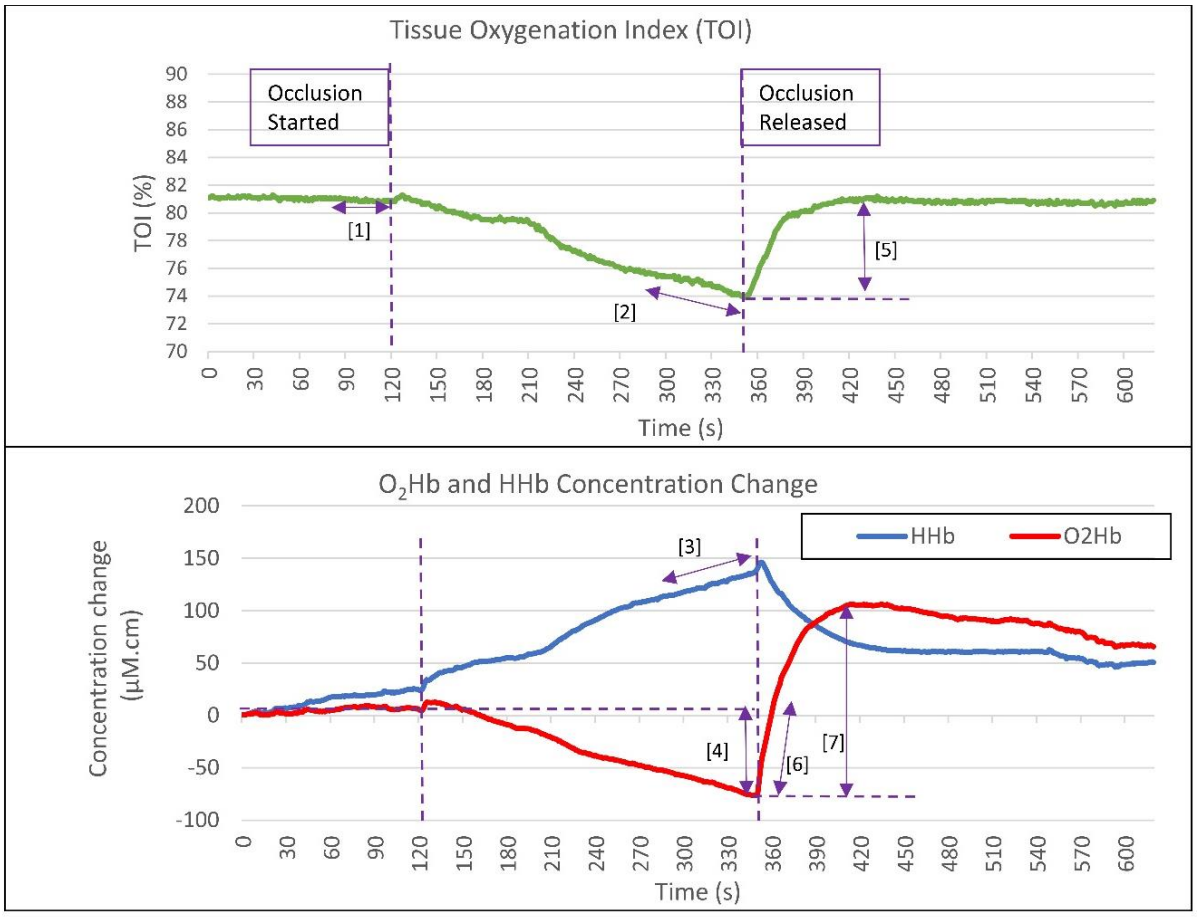

Figure 7.2: Graphical display of the haemodynamic parameters adopted for analysis in Chapters 8, 9 and 10.

[1] Baseline TOI at rest prior to the occlusion (TOI_rest; (%))

[2] Rate of TOI decrease in the last 60s of occlusion (TOI_DO_ 60s (%/s))

[3] Rate of HHb increase in the last 60s of occlusion (HHb_DO_60s (µM.cm/s))

[4] Absolute change in O_2Hb during the occlusion (µM.cm; $O_2Hb\_DO\_abs\Delta$)

[5] Maximal absolute change in TOI post occlusion (TOI_PO_absΔ (%))

[6] Rate of O_2Hb increase in first 20s post occlusion release ($O_2Hb\_PO\_20s$ (µM.cm/s))

[7] Maximal absolute change in O_2Hb post occlusion ($O_2Hb\_PO\_abs\Delta$ (µM.cm))

These seven haemodynamic markers are used for validation comparisons in Chapters 8, 9 and 10 and are presented in Figure 7.2. They are deemed to offer the most reliable and physiologically relevant indicators of *in vivo* bone haemodynamics of those markers investigated.

As discussed in more detail in Appendix G, a non-linear modelling approach to PO markers was also attempted, but was not taken forward as results did not offer any clear reliability advantages over the markers presented here in Chapter 7. Markers looking solely at the hyperaemic response were also abandoned as they produced high RMSCV values that are unlikely to be acceptable. This is due to the small magnitude of hyperaemic response at the tibia, which was also negative in some individual cases.

7.1.4.3: Sources of Error

As discussed above in Section 7.1.4.1, reliability testing of the lateral calf has shown results generally in keeping with the wider literature base on this more established use of NIRS. Results from testing at the tibia have shown this measurement site generally to be not as reliable as the calf, with more missing data. However, some markers (see Figure 7.2) have still been identified that have produced reliability results in line with the more established use of NIRS at the calf.

Differences between the lateral calf and proximal tibia may be attributable to the heterogeneity of bone tissue leading to a higher reduced scattering coefficient of near infrared light [1, 2]. A suggestive example of this is that RMSCV values of the same day repeatability at the proximal tibia were typically poorer than at the calf. This suggests an inherent increased error due to the tissue type, as measurements were taken with the same probe positioning in the same session, and with no other obvious systematic error contributing. In terms of different day reproducibility, there is also generally a smaller target volume at the tibia compared with the lateral calf, potentially increasing the effects of probe placement differences on repeated measurements taken longitudinally [9].

Figure 7.3 and 7.4 below demonstrate the test/retest scores of the HHb_DO_60s, O_2Hb_DO_absΔ, O_2Hb_PO_20s and O_2Hb_PO_absΔ markers across all participants. It was noted across both proximal tibia and lateral calf measurements that there was wide variability in results between participants for these markers. This is also indicated by the magnitude of the between participant SD relative to the mean for each

haemodynamic marker presented in Tables 7.2-7.9 above. It is interesting to note the wider between participant variation at the proximal tibia for these markers derived using MBL conflicts with the earlier example in Section 7.1.2.2 (including Figure 7.1) based on the SRS-derived TOI_DO_60s marker. This variability between participants may be explained by the differences in NIRS algorithms used to derive MBL and SRS calculations. This is discussed in more detail in Section 10.2.2.1.

There is also noticeable variation between the differences in test/retest scores in some individual cases illustrated in Figures 7.2 and 7.3. Retrospective investigation of those participants with larger differences between test/retest scores was carried out on potential explanatory factors such as predisposing medical conditions, how well occlusions were tolerated, or increased calf circumference (and therefore increased overlying superficial tissue). There was no obvious explanation as to why these participants may have been susceptible to poorer reliability. It was also noted that these instances of poorer reliability were typically isolated to one tissue type and/or one marker for each participant. As such it was deemed suitable to keep these results in the analysis with these wide differences interpreted as measurement error, rather than rule them out as confounded or outliers. Sub group analysis was also carried out looking for any differences in reliability between sex and T2DM sub groups with no obvious differences identified.

a)

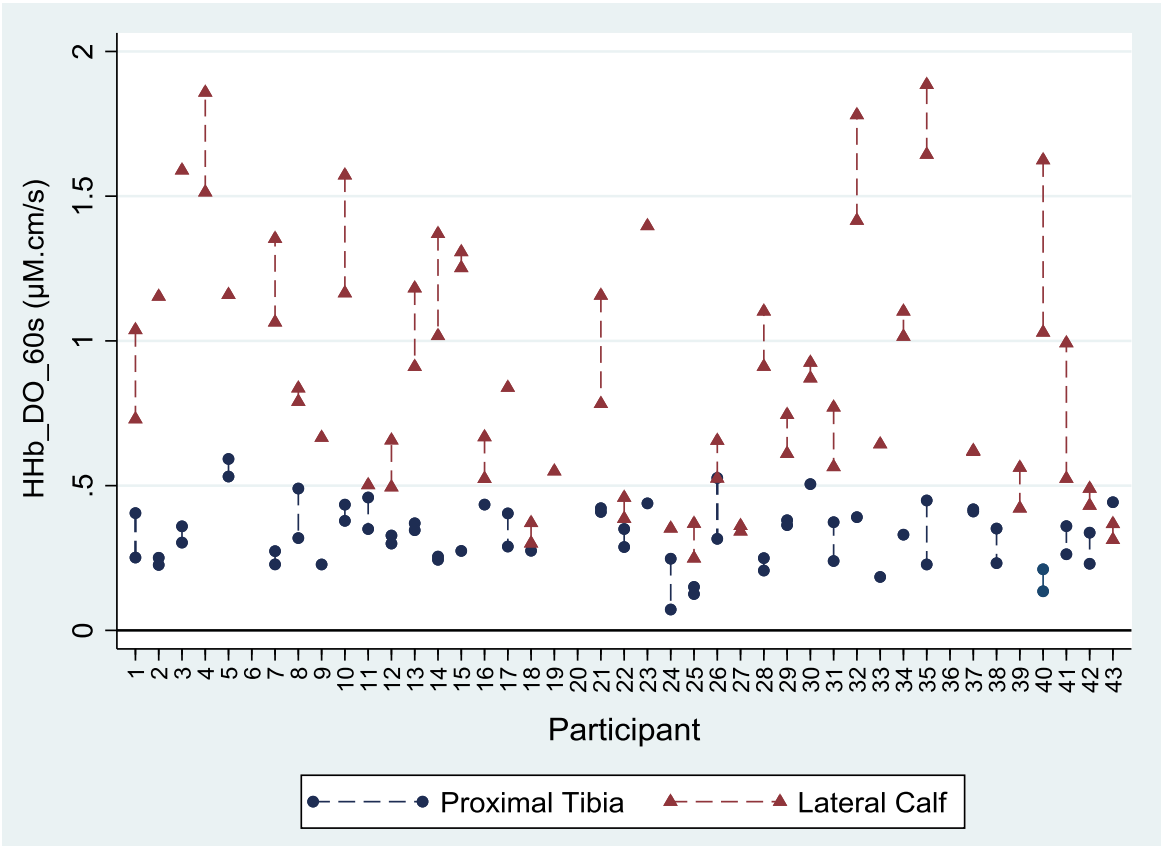

b)

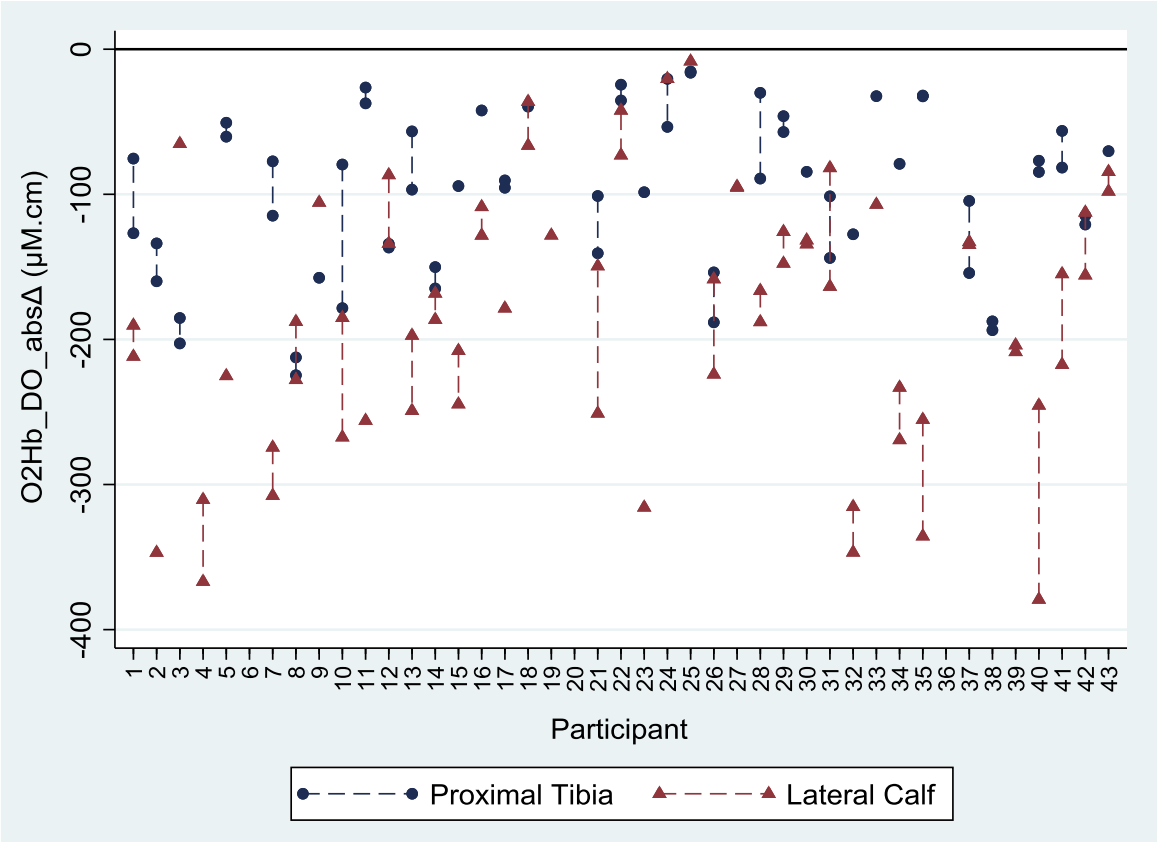

Figure 7.3: Different day proximal tibia and lateral calf test/retest results of two favoured MBL based DO markers (a) HHb_DO_60s and (b) O_2Hb_DO_absΔ.

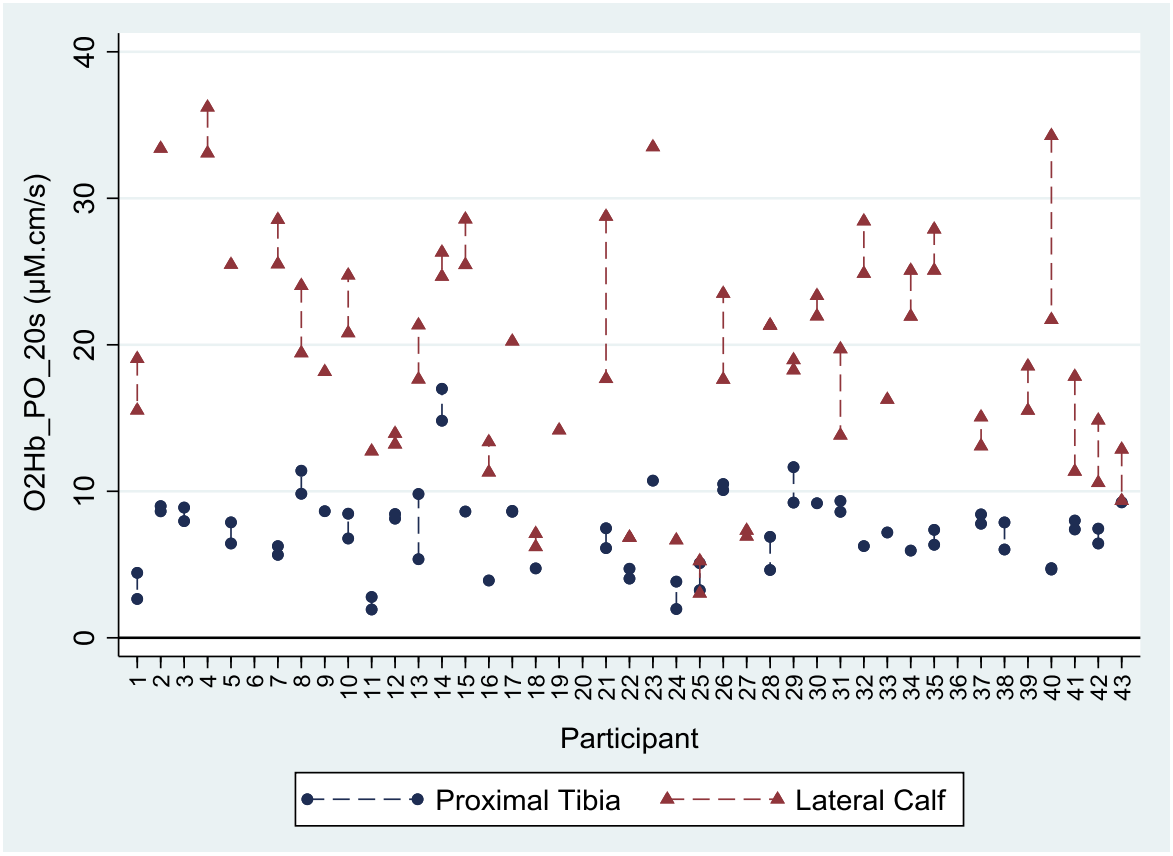

a)

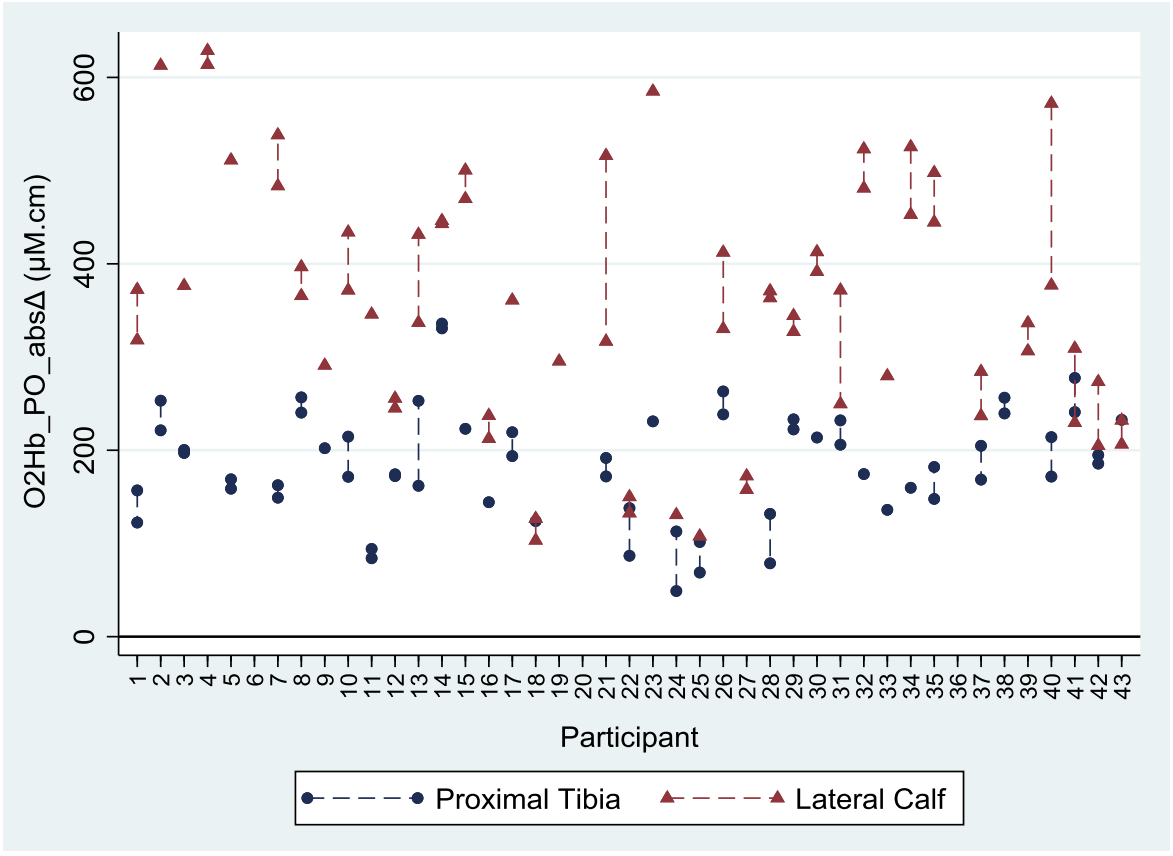

b)

Figure 7.4: Different day proximal tibia and lateral calf test/retest results of two favoured MBL based PO markers (a) O_2Hb_PO_20s and (b) O_2Hb_PO_absΔ.

7.1.4.4: Potential for systematic error

Paired t-tests and Bland-Altman plots were inspected for any systematic differences between test/retest results. It was noted that there were potential systematic differences observed in the same day test/retest measurements. At the lateral calf, PO measurements demonstrated statistically significant faster (O_2Hb_PO_20s) and stronger (O_2Hb_PO_absΔ) PO results for the retest measurements. This could suggest increased reperfusion following the release of the second occlusion due to a cumulative hypoxic effect of the two occlusion protocols in the same session. It is unlikely that this was a psychological effect of the second occlusion being better tolerated, as the same effect was not observed for tibial PO measurements. Despite the statistically significant differences, and in context of the strong repeatability results obtained, the clinical relevance of any systematic change between the test/retest means for this marker was considered likely to be small. Harris et al 2006 support that repeat arterial occlusions taken within the same testing session is appropriate without accounting for systematic effects [317].

No other obvious systematic differences in test/retest measurements were found for different day repeated measurements at the calf or tibia, generally suggesting no learned response from the participant.

7.1.4.5: Limitations of intra operator reliability testing

The results presented should be kept in context of the limitations of this reliability assessment. By nature of being an intra operator assessment, only one operator and one piece of NIRS equipment has been used. As a feasibility study it was considered unethical to request participants undergo the number of arterial occlusions that would be required to assess inter operator reliability of several operators.

The use of different NIRS systems was not pragmatically possible, with only one system available. However, use of multiple systems could be of potential interest in the future, given the previously documented disparities in NIRS results obtained from systems from different manufacturers, particularly if considering multi-site studies. Hyttel-Sorenson et al. 2011 found similar reproducibility results across three different sets of commercially available SRS NIRS systems when measuring resting TOI for muscle at the forearm, but significantly different resting mean TOI values were obtained of 60.8% (SD 3.6%) and 70.2% (SD 6.7%) [263]. Yang et al. 2007 present similar variation in resting TOI at the forearm between different studies [264]. Matcher

et al. 1995 discusses the differences in results that may occur during interventional protocols due to the differences in algorithms and the associated assumptions used to derive continuous wave NIRS parameters [318].

The loss of data due to inadequate arterial occlusion conditions also requires consideration. This is a source of potential attrition bias, although there was no obvious predictor for which participants would be more likely to be unable to tolerate occlusions, or produce data meeting the pre-stated conditions for data inclusion. Likewise there was no obvious changes to the arterial protocol that could have minimised this loss of data.

Ideally reliability work should be carried out in a varied and representative population of those who are likely to benefit from the test. For example Maggio et al 1998 found reproducibility of BMD measurements of the hip were decreased in the elderly, owing to degenerative change and more variability when positioning participants [319]. This reliability study has a wide age range including both sexes from a potential target population of those who may benefit from bone health testing.

Similarly, a suitable population for reliability testing should include those with pathological conditions that may be predictive from the test of interest. The sampled population includes those with T2DM as per the rationale outlined in Section 4.5.2.4. Participants of varying osteoporotic status are also included. Despite this, as discussed in Section 7.1.2.2, there was small variation in the TOI_DO_60s marker observed between participants. This is considered an unforeseeable limitation as there was variation observed between participants at the calf as expected, and within the MBL-derived haemodynamic markers.

As this study was part of feasibility work, participants had a BMI of less than 35 kg/m^2 in order to minimise the potential effect of overlying tissue at the tibia. As such, the effect of obesity on the reliability of NIRS measurements remains unexplored (although there was no obvious effects from within the sampled population). A pragmatic decision was also made to recruit only Caucasian participants given the ethnic distribution of the recruitment catchment in the South West of England. Skin pigmentation can have a potential effect on NIRS measurements [2] although this is likely to only affect variation between participants.

7.1.4.6: Potential improvement of reliability

Many steps were taken in order to maximise the reliability of the NIRS arterial occlusion protocol used. It is felt that inherent biological variability has been minimised as participants were tested at the same time of day following the same fasting protocol. Laboratory conditions and acclimatisation protocols were standardised as per all vascular testing performed at the DVRC. The arterial occlusion and probe placement protocols were also consistently used, benefitting from the protocol development work previously discussed in Chapter 5.

There were few modifications identified that could improve reliability. One potential suggestion is development of a designated probe holder for the proximal tibia. There is precedence with DXA around the importance of strict protocol adherence for improved longitudinal testing reliability [310]. Although probe placement in this work followed a pre-stated objective protocol, perhaps improvements here are the most likely way to improve reliability results as even small differences in probe placement may lead to different volumes of tissue being sampled and error being introduced.

A range of approaches to deriving haemodynamic markers from time-signal data have been attempted including linear and non-linear methods. However it is acknowledged that there may be more advanced modelling algorithms that may produce more reliable haemodynamic markers from the time-signal data produced by the NIRS system. Likewise with the further advances in optical technologies, inherent inaccuracies within future NIRS systems may be reduced, although this is beyond the scope of this thesis.

7.1.4.7: Conclusions of intra operator reliability

The main conclusion of this reliability analysis is that results support the potential of seven haemodynamic markers derived from arterial occlusions for further investigation and validation in Chapters 8, 9 and 10. These AO markers have demonstrated reliability in line with existing comparable tests, suggesting they may potentially prove useful for research applications investigating the haemodynamics of bone tissue. This should also be kept in context with the lack of alternative options for measuring haemodynamics in bone tissue, and the convenience and practicality of NIRS systems compared with current techniques.

7.2: Inter operator repeatability of probe placement

7.2.1: Overview

This section presents inter operator repeatability of resting TOI measurements taken by five operators on participants. It was considered unethical to take multiple arterial occlusions on participants to facilitate inter operator repeatability assessment of the AO protocol, and so it was considered a suitable compromise to consider the repeatability of resting TOI measurements, which should reflect the potential error from probe placement of different operators, with minimised biological variation from participants.

7.2.2: Results of inter operator repeatability of probe placement

Table 7.10 shows the demographics of the 12 participants who undertook testing by five operators. The target of 16 participants was not reached due to time constraints of the availability of the operators, who were undergraduate medical imaging students. All participants were generally healthy with a BMI within a range of 22-36 kg/m^2 and an age range of 20 to 32 years. All participants had stable peripheral arterial SO_2 readings at rest of 97% or higher. Temperature at the foot was monitored with a mean change of -2.2°C (range -0.2°C to -6.5°C) during the testing session, which typically took around 60 minutes. All variables were considered normally distributed after following the approach described in Section 6.1.3.7.

Table 7.10: Demographics of participants (N=12) for inter operator reproducibility (mean with standard deviation in parenthesis).

Demographic	Mean (SD)
Age (years)	22.1 (3.6)
Height (m)	1.704 (0.076)
Weight (kg)	79.1 (12.9)
BMI (kg/m^2)	27.5 (4.8)
Sex (m/f)	5/7
Maximum calf circumference (mm)	385 (41.4)
Calf circumference at level of tibial tuberosity (mm)	368 (34.4)

Table 7.11 shows a summary of inter operator repeatability outcomes for both the proximal tibia and lateral calf across five operators. Measurements were 20s samples of TOI percentage taken at rest after 15 minutes acclimatisation. In the last five minutes of acclimatisation, TOI was constantly monitored in order to gauge the natural biological variability of TOI, which may be affected by homeostatic regulation of the vascular system (as discussed in Section 1.5.1). Mean TOI variability during this five minute period at the proximal tibia was 1.7% (SD 0.4%; range 1.0%-2.4%) and 2.3% (SD 1.2%; range 1.3%-5.1%) at the lateral calf.

Table 7.11: Summary of inter operator probe placement repeatability results for measurements of resting TOI. (RMS= Root Mean Square; SD= Standard Deviation; CV=Coefficient of Variation; ICC=intra class correlation).

	Proximal Tibia	Lateral Calf
Number of measurements (N=12)	60	60
Mean TOI (%)	81.6	73.7
Between Participant TOI SD (%)	4.0	4.5
Within Participant TOI RMSSD (%)	3.1	2.0
Within Participant RMSCV (%, with 95% CI)	3.8 (0.4-7.1)	2.7 (0-5.5)
Repeatability Coefficient (%)	8.5	5.5
ICC (with 95% CI)	0.28 (0.06-0.62)	0.77 (0.57-0.91)

When looking at the intra operator results of the five operators (presented in Table 7.12 and 7.13) it can be seen that, as expected, RMSCV and ICC reproducibility results are improved marginally compared with inter operator results, without the potential source of inter operator differences in probe placement. As for inter operator results, lateral calf TOI measurements had better repeatability than the proximal tibia for most operators with regards to RMSCV, with results generally in line with inter operator results across the five operators.

Table 7.12: Same day test/retest repeatability data on TOI measurements of the proximal tibia at rest. (RMS= Root Mean Square; SD= Standard Deviation; CV=Coefficient of Variation; ICC=intra class correlation).

INTRA-OPERATOR PROBE PLACEMENT (TIBIA)	Operator 1	Operator 2	Operator 3	Operator 4	Operator 5
Paired data (N)	12	12	12	12	12
Mean (%)	81.0	80.8	82.7	81.6	80.7
Between Participant SD (%)	4.1	4.1	3.8	4.1	3.8
Within Participant RMSSD (%)	2.0	2.4	1.9	1.8	2.6
Within Participant RMSCV (%, with 95% CI)	2.5 (0-5.0)	3.1 (0-7.1)	2.3 (0-5.3)	2.1 (0-5.2)	3.1 (0-7.1)
Repeatability Coefficient (%)	5.5	6.7	5.2	4.8	7.1
ICC (with 95% CI)	0.53 (0.00-0.84)	0.30 (-0.28-0.73)	0.53 (-0.01-0.83)	0.65 (0.17-0.88)	0.12 (-0.45-0.63)

Table 7.13: Same day test/retest repeatability data on TOI measurements of the lateral calf at rest. (RMS= Root Mean Square; SD= Standard Deviation; CV=Coefficient of Variation; ICC=intra class correlation).

INTRA-OPERATOR PROBE PLACEMENT (CALF)	Operator 1	Operator 2	Operator 3	Operator 4	Operator 5
Paired data (N)	12	12	12	12	12
Mean (%)	73.7	73.1	73.2	73.9	73.9
Between Participant SD (%)	4.7	4.3	4.4	4.2	5.0
Within Participant RMSSD (%)	2.0	0.9	0.8	1.1	0.7
Within Participant RMSCV (%, with 95% CI)	2.8 (0-6.8)	1.2 (0-2.6)	1.2 (0-2.3)	1.6 (0-3.4)	1.0 (0-2.1)
Repeatability Coefficient (%)	5.5	2.3	2.3	3.1	2.0
ICC (with 95% CI)	0.66 (0.20-0.89)	0.93 (0.77-0.98)	0.93 (0.78-0.98)	0.86 (0.59-0.96)	0.96 (0.87-0.99)

7.2.3: Discussion of inter operator repeatability of probe placement

As discussed in Chapter 3, there was no existing evidence base on NIRS reliability in bone to compare results with. However, reliability results for calf measurements were in line with existing evidence. Adami et al. 2017 found a mean resting TOI of 68% (SD 5%) at the medial head of the gastrocnemius using a comparable SRS NIRS system [320]. Re et al. 2018 also demonstrated CVs <3% when repeating calf measurements 30 times on one participant during one session (with probes replaced between measurements) using a time domain NIRS system [321]. Ubbink et al. 2006 found very good reproducibility at the calf when investigating test/retest TOI at rest on different testing days using a comparable NIRS system (ICC 0.91; 95% CI 0.77 to 0.96) and reproducibility was also higher than other comparable vascular measurements such as transcutaneous oxygen pressure, ankle-brachial blood pressure index, and toe systolic blood pressure [322].

Regarding other muscular sites, Fulford et al. 2014 found different day repeated measures on 10 participants repeated 3 times at the paraspinal muscles had a CV of 5% (95% CI 2% to 7%) and ICC of 0.75 (95% CI 0.46 to 0.92) [323]. Choo et al. 2017 measured test/retest TOI recordings of the vastus lateralis on nine healthy males using comparable NIRS equipment and recorded a CV of 3.9% (95% CI 2.6% to 7.7%) and ICC of 0.75 (95% CI 0.23 to 0.94) [324]. Lucero et al. 2018 performed baseline TOI measurements on the vastus lateralis muscle on 12 participants on four separate days using a comparable NIRS system. Resting TOI was found to be reproducible with an ICC of 0.71 (90%CI 0.44 to 0.88) and CV of 2.4% (90%CI 1.9% to 3.5%), comparable with the results presented in Table 7.11 [325]. Niemeijer et al. 2017 reported on test/retest measurements at the same site on 28 healthy participants using a SRS NIRS system with similar ICC of 0.74 (95% CI 0.51 to 0.87) and CV of 4.7% (CI not reported) [326]. None of these studies specifically reported the number of operators, so are assumed to represent intra operator reliability.

This suggests probe placement has been carried out with comparable reliability to the existing evidence base despite the relative novice status of four of five operators. The results at the proximal tibia appear to generally be more variable, with higher within participant standard deviation and RMSCV. However, results are comparable to that of the lateral calf and the evidence base around muscular data.

The exception is the inferior performance of the proximal tibia with respect to ICC, rated as “poor” with an ICC <0.4 [304]. As ICC calculations incorporate between participant variation and within participant variation of repeated measurements, it is suspected the ICC is lower at the proximal tibia due to relatively low between participant variation in resting TOI amongst the 12 participants, and comparatively high within participant variation (relative to between participant variation) compared with results at the lateral calf [316]. Figure 7.5 demonstrates the wider between participant variability for the lateral calf measurements when compared with the proximal tibia. It is known that in instances where mean results between participants are close, ICC will be lower as it inherently reflects the ability of a test to identify real variance between measurements from error [327].

The repeatability coefficients presented in Table 7.11 are of interest as these suggest the minimum detectable clinical difference. There was no identified existing evidence of what TOI change may indicate a specific type of pathology, but a repeatability coefficient of 8.5% suggests only large physiological changes in TOI could be definitively identifiable at the proximal tibia. In line with the discussion of AO haemodynamic markers above, this suggests TOI is unlikely to be useful at an individual level bearing in mind the cyclical variation of TOI that also occurred even at rest during the same session (with a range of 1.0%-2.4% in the sampled population). The repeatability coefficient could also likely be worse with biological variation if measurements had been taken on separate days.

Upon looking at those participants with the poorest precision, anecdotally there was no obvious predictor in terms of participants with higher BMI, smaller or larger calf circumference, or who had more variable TOI measurements observed during the initial 5 minute measuring period at rest, although the small number of participants prohibits any formal statistical analysis of these potential sources of error.

This inter operator repeatability study has similar methodological limitations to those already identified in Section 7.1.4.5. Only one NIRS system was available for use and the small sample of participants were healthy and under 32 years of age, with a maximum BMI of 36 kg/m^2.

a)

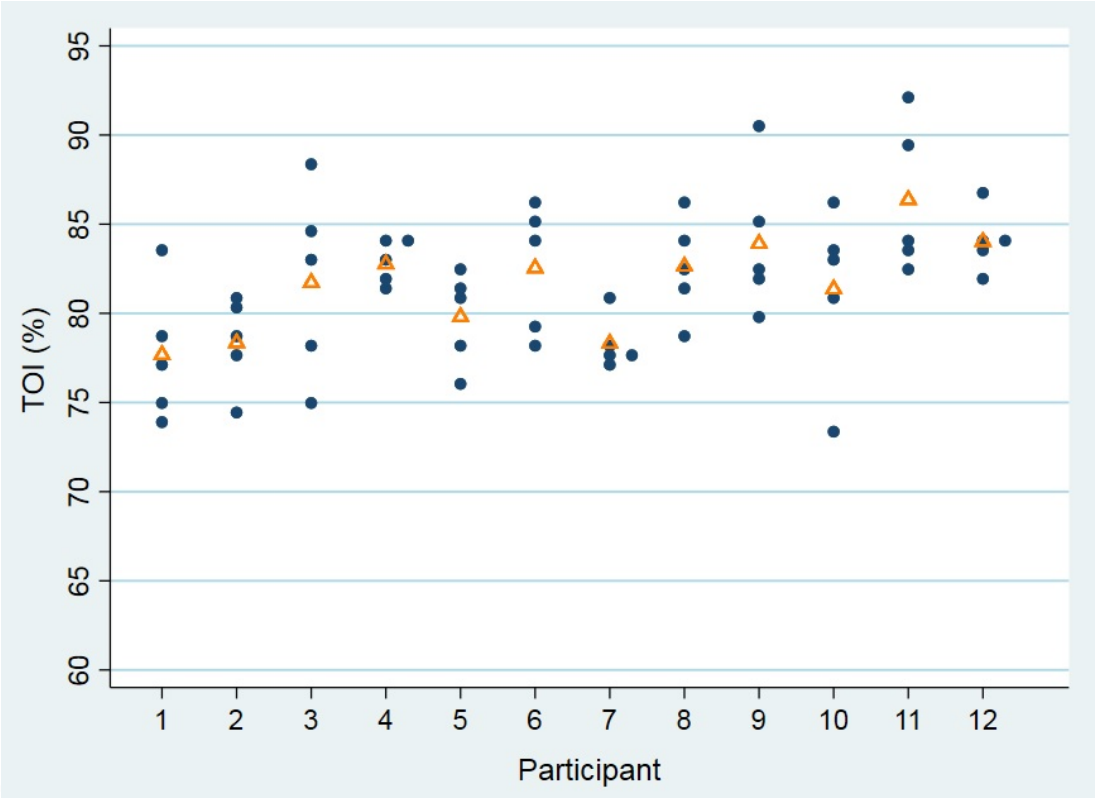

b)

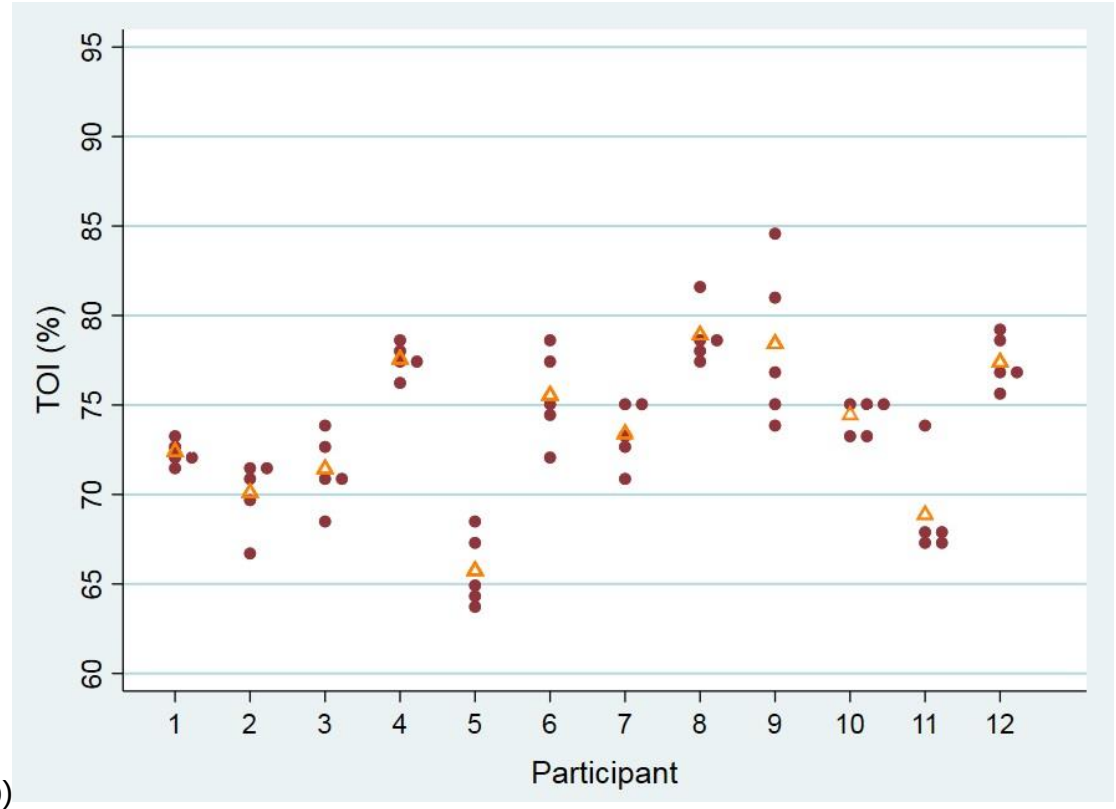

Figure 7.5: Dot plots of repeated inter operator TOI measurements from five operators for the proximal tibia (a) and lateral calf (b). Orange triangles represent the mean value for each participant. Dot plots demonstrate greater between participant variance and lower within participant variance at the lateral calf, explaining the higher ICC values at the lateral calf compared to the proximal tibia.

7.2.4: Conclusion of inter operator reliability

This exercise in investigating inter operator repeatability of baseline TOI measurements suggests that some variability in probe placement technique between operators is present but is not a significant contributor to measurement error. This is mainly evident in inter operator repeatability markers being only slightly inferior to the intra operator results obtained by the participating operators.

The exercise has highlighted the limitations of using resting TOI as a marker of tibial health, given its natural cyclical variation, low ICC, and relatively high minimum detectable difference produced (as indicated by the repeatability coefficient of 8.5%).

Despite this, RMSCV reliability results are in line with the published evidence base for similar studies in muscle tissue and provide reassurance that reliability and validation studies carried out by one operator may still be representative in terms of probe placement, in the absence of any significant potential variation in technique that may be caused by different operators.

7.3: Inter operator reliability of data analysis

Using the approach outlined in Section 6.1.6, an investigation was carried out to ensure data analysis of haemodynamic markers undertaken from the arterial oclusion protocol was reproducible. The results obtained from two independent blinded assessors were compared and quantified using one way random effects ICC. One assessor was the author and the second assessor was a novice medical student who had been trained to analyse NIRS data. The reproduciblity of two haemodynamic markers, HHb_DO_60s, and O_2Hb_PO_20s, were assessed. 17 datasets were analysed, falling short of the initial 20 planned due to time limitations around the availability of the medical student.

Initial analysis demonstrated an ICC of 0.68 (95% CI 0.31 to 0.88) for calculation of O_2Hb_PO_20s markers. 13 of 17 results were matched perfectly. On inspection of the four discrepancies, four were due to data input errors from the novice user. Correcting these meant 100% agreement and demonstrated that deriving the O_2Hb_PO_20s marker was not prone to subjectivity. However, the potential for data input error was flagged. It was agreed this could be improved with clearer instructions if the data analysis was to be carried out by mulitple users.

Analysis demonstrated an ICC of 0.62 (95% CI 0.22 to 0.84) for calculation of HHb_60s_DO markers. 8 of 17 results were matched perfectly. On inspection of the nine discrepancies, it was observed these were due to differences in interpetation of what was considered the end point of the occlusion. The novice user objectively took the highest HHb value as the end point. However this was confounded by a commonly observed spike in HHb at the point of occlusion release (see Figure 7.6 below for an example). The author had been adjusting for this by taking the end point as the last HHb reading before the sudden upturn of this PO spike. This exercise in data analysis reproducibility demonstrated the importance of visualising arterial occlusion data graphically for signal artefact, rather than a fully automated data analysis approach. Correcting for this difference in interpretation lead to perfect agreement.

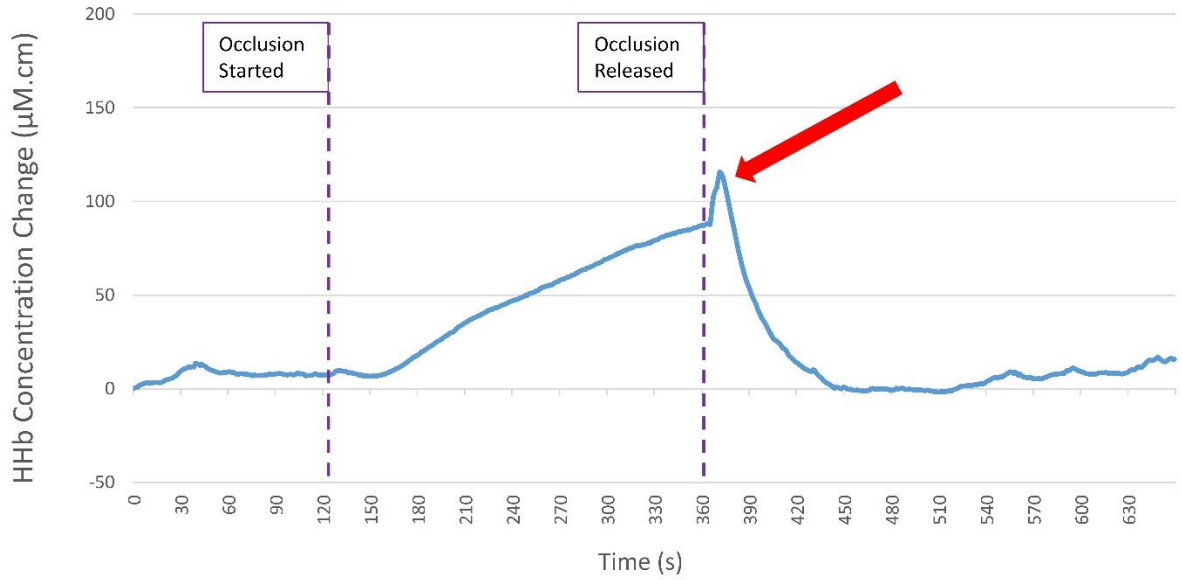

Figure 7.6: Demonstration of a common spike in HHb following occlusion release (signalled by the red arrow) which could lead to error in calculation of HHb_DO_60s measurements.

This artefact in HHb upon occlusion release has been observed in previous papers where graphical raw data are presented for ischaemic protocols in both bone [16] and muscle [277] tissue, however the reasons behind this occurrence are not discussed. A potential explanation is that following the removal of ischaemic stimuli, such as an AO cuff or exercise, there is a sudden muscular and/or vascular recovery response causing a short surge in pooled venous deoxygenated blood in response to the suddenly improved arterial inflow. When examining the microcirculation of the skin, Adingupu et al 2015 [271] report a sub group of participants who demonstrate a sudden rapid increase in blood flow immediately following the release of an arterial occlusion,

that is subsequently quickly overcome by vasoconstriction, presumed to be a myogenic response.

It should be noted that it was felt that analysis by a third reviewer was not required as initially planned as there was perfect agreement allowing for data input errors or misinterpretation from the novice user. Overall this exercise demonstrated the potential of the data analysis approach to be adopted by mulitple users, but also the importance of initial piloting to identify any potential misunderstandings in approach.

7.4: Chapter conclusion

This chapter has identified haemodynamic markers from the arterial occlusion protocol developed in Chapter 5 that have comparable reliability with the wider evidence base around NIRS usage. These are also considered physiologically relevant for comparisons against alternative tests of bone health that will be reported in Chapters 9 and 10. Reliability work around inter operator positioning of NIRS probes and data analysis have also been performed, with acceptable reliability demonstrated.

Chapter 8: NIRS validation results

8.1 Overview

This chapter will present a descriptive summary of participant recruitment for the validation of NIRS in Section 8.2. Descriptive summaries of NIRS haemodynamic parameters taken from 36 participants at both the proximal tibia and the lateral calf are presented in in Section 8.3, with discussion of results including comparison with the existing evidence base in Section 8.4.

8.2: Recruitment summary

Stage 3 recruitment successfully reached its target of 36 participants, 18 with T2DM and 18 without. Table 8.1 presents the summary demographic data for the recruited participants. Despite a slightly smaller sample population than was used for reliability work, the description of participants for validation work is consistent with Section 7.1.1. Participants were free from any other history of metabolic bone disease, type 1 diabetes, stroke or TIA, arrhythmias, cardiovascular disease, renal disease, peripheral artery disease, or deep vein thrombosis. In some cases participants did report osteoarthritis which was mild and not being medically treated. There was one participant with early onset arthritis secondary to chemotherapy treatment at age 25 and a fibromyalgia diagnosis. One participant reported rheumatoid arthritis diagnosed from age 21, but again these conditions were not medically treated.

The age of participants ranged from 41 to 77 years. BMI ranged from 20.4 to 32.5 kg/m^2. All 14 female participants were post-menopausal for a mean of 14.4 years (range 6 months to 35 years), with one participant having a history of hysterectomy at age 40. All participants were currently non-smokers for at least the past 5 years, with 14 having never smoked (7 of which had T2DM). All participants were generally in good health. Three participants had successfully been treated for cancer (two for breast cancer, one ophthalmological cancer).

In terms of bone health, no participants had a previous diagnosis of osteoporosis or history of recent low impact fracture, with one exception. This participant reported a low impact neck of humerus fracture leading to a diagnosis of osteopenia and subsequent calcium and cholecalciferol (iCalD3) supplementation on prescription for four years.

All participants reported being normotensive with normal resting pulse rates at consent, however eight participants presented with high systolic blood pressure. It should be acknowledged that this could be influenced by the unfamiliar research environment at the time of measurement [314]. Testing was carried out on the left leg by default but on nine occasions the right leg was tested due to previous injury, surgery or varicose veins in the left leg.

Table 8.1: Summary of key demographics for recruited participants, including sub group data for those with and without T2DM. Results presented are means with standard deviation in parentheses. *p*-values are from independent t-tests between those with and without T2DM (* denotes statistical significance).

	Total (N=36)	T2DM (n=18)	Non-T2DM (n=18)	*p*-value between sub groups
Age (years)	62.0 (8.4)	62.6 (7.3)	61.7 (9.7)	0.86
Height (m)	1.70 (0.09)	1.70 (0.09)	1.70 (0.10)	0.87
Weight (kg)	76.8 (11.3)	76.0 (12.1)	77.6 (10.8)	0.67
BMI (kg/m^2)	26.5 (2.9)	26.3 (3.1)	26.7 (2.7)	0.63
Sex (m/f)	22/14	11/7	11/7	n/a
Diastolic Blood Pressure (mmHg)	77 (9)	78 (7)	76 (7)	0.52
Systolic Blood Pressure (mmHg)	133 (17)	138 (19)	128 (14)	0.08
Pulse (beats/min)	64 (9)	67 (8)	62 (9)	0.16
Resting Arterial Oxygen Saturation (%)	97 (1)	97 (1)	97 (1)	1.00
Resting Foot Temperature (°C)	28.8 (2.1)	28.8 (2.2)	28.7 (2.0)	0.83
Knee Circumference (mm)	379 (26)	374 (24)	384 (27)	0.24
Calf Circumference (mm)	372 (26)	372 (25)	371 (27)	0.97
Ankle Circumference (mm)	251 (16)	250 (17)	253 (17)	0.65
Right Ankle Brachial Index	1.26 (0.16)	1.29 (0.16)	1.23 (0.15)	0.25
Left Ankle Brachial Index	1.24 (0.13)	1.24 (0.13)	1.23 (0.14)	0.78
Tibial Length (cm)	37.9 (3.1)	37.9 (3.8)	37.9 (2.4)	0.99
Lower Leg Fat Content (%)	25.2 (9.8)	23.4 (7.5)	27.1 (11.6)	0.26
HbA1c (mmol/mol)	45 (10)	53 (7)	36 (3)	<0.001*
Vitamin D (nmol/L)	61 (25)	57 (21)	65 (29)	0.38
Parathyroid Hormone (pmol/L)	4.2 (1.2)	4.1 (1.3)	4.2 (1.1)	0.78
Estimated Glomerular Filtration Rate (ml/min/1.73m²)	77.7 (11.9)	77.0 (13.7)	78.4 (10.2)	0.73
Menopausal Duration (years)	14.4 (10.4) (n=14)	11.6 (10.1) (n=7)	17.1 (10.7) (n=7)	0.34

8.2.1: Sub group demographics

8.2.1.1 Diabetes status

In terms of case-control matching between those with and without T2DM, participants were successfully matched for sex (11 male pairs and 7 female pairs) and ethnicity (all "white British"). All case-control pairs were matched for BMI to within 4.2 kg/m^2. Most pairs were matched within 2 years of age, although this had to be widened to find matches in six recruitment pairs where there was difficulty matching younger participants with normal BMI and T2DM. As demonstrated in Table 8.1, there was no statistically significant difference between those with and without T2DM in any of the presented demographic data (apart from HbA1c, as expected).

Of those 18 participants with T2DM, four were diet controlled and the mean duration since diagnosis was 6.2 years (range 1-16 years). It is noted that the sub group of those with T2DM is likely to have a lower mean time since diagnosis then the general population of those with T2DM. As research participants, these participants are also likely to have better controlled diabetes and this is reflected by HbA1c results in the T2DM group (mean 53 mmol/mol; SD 7.2; range 41 to 68) generally being close to the diagnostic threshold for T2DM of 48 mmol/mol [328]. Similarly only one participant with T2DM demonstrated neuropathy using microfilament and neurothesiometry assessment on the plantar surface of the foot. There was also very little indication of nephropathy amongst the T2DM sub group, with only three participants with T2DM returning urine ACR results above the commonly used threshold of 3mg/mmol, and with the lowest eGFR result 50 ml/min/1.73m². Eight participants with T2DM were on statin medications to reduce cholesterol, with three also on anti-hypertensive drugs (Ramipril or Amlodipine). No non-diabetics were on these medications.

Nevertheless, there was a statistically significant difference in HbA1c (p<0.001; independent t-test) to allow comparison between subgroups, whilst there was little evidence of differences between sub groups for some of the key potential confounders in bone health (such as Vitamin D levels, parathyroid hormone levels, age, sex, BMI, and ethnicity), as demonstrated in Table 8.1.

8.2.1.2 Sex

There was little evidence of differences between sexes for most key demographics. Exceptions were significant differences with shorter height and lower weight in females

(but with no significant difference in BMI), and smaller ankle circumference but higher percentage fat content at the lower leg in females (as measured with DXA). Results are presented in Table 8.2.

Table 8.2: Summary of key demographics for recruited participants, including sub group date based on sex. Results presented are means with standard deviation in parentheses. *p*-values are from independent t-tests between sexes (* denotes statistical significance).

	Total (N=36)	Male (n=22)	Female (n=14)	p-value between sub groups
Age (years)	62.0 (8.4)	61.8 (9.4)	62.3 (7.0)	0.86
Height (m)	1.70 (0.09)	1.74 (0.08)	1.63 (0.06)	<0.001*
Weight (kg)	76.8 (11.3)	80.2 (9.5)	71.54 (12.3)	0.02*
BMI (kg/m^2)	26.5 (2.9)	26.3 (2.4)	26.7 (3.6)	0.72
Diastolic Blood Pressure (mmHg)	77 (9)	77 (7)	77 (7)	0.92
Systolic Blood Pressure (mmHg)	133 (17)	134 (17)	131 (17)	0.60
Pulse (beats/min)	64 (9)	62 (9)	68 (7)	0.05*
Resting Arterial Oxygen Saturation (%)	97 (1)	97 (1)	98 (2)	0.06
Resting Foot Temperature (°C)	28.8 (2.1)	28.7 (2.0)	28.9 (2.2)	0.80
Knee Circumference (mm)	379 (26)	378 (20)	382 (33)	0.63
Calf Circumference (mm)	372 (26)	373 (22)	369 (31)	0.62
Ankle Circumference (mm)	251 (16)	257 (13)	242 (17)	0.01*
Right Ankle Brachial Index	1.26 (0.16)	1.26 (0.17)	1.26 (0.14)	0.91
Left Ankle Brachial Index	1.24 (0.13)	1.23 (0.14)	1.24 (0.12)	0.82
Tibial Length (cm)	37.9 (3.1)	38.7 (3.5)	36.7 (2.0)	0.07
Lower Leg Fat Content (%)	25.2 (9.8)	19.1 (3.9)	34.9 (8.4)	<0.001*
HbA1c (mmol/mol)	45 (10)	45 (11)	44 (9)	0.83
Vitamin D (nmol/L)	61 (25)	62 (28)	60 (21)	0.85
Parathyroid Hormone (pmol/L)	4.2 (1.2)	4.4 (1.3)	3.8 (1.1)	0.21
T2DM Duration (years)	6.2 (4.5) (n=18)	7.2 (5.1) (n=11)	4.7 (3.2) (n=7)	0.27
Estimated Glomerular Filtration Rate (ml/min/1.73m^2)	77.7 (11.9)	78.7 (11.5)	76.1 (12.9)	0.54
Menopausal Duration (years)	n/a	n/a	14.4 (10.4)	n/a

8.3 NIRS results

8.3.1: Statistical assumptions

Pearson's correlations have been used for comparing NIRS haemodynamic markers with other demographic variables and tests of bone health, as any relationships observed are expected to be linear (as will be confirmed by observing scatterplots). All r-values reported in Chapters 8, 9 and 10 are from Pearson's correlation analysis. The following statistical assumptions [329] for the use of Pearson's correlation have been met for its use throughout Chapters 8, 9 and 10:

- All data are continuous.
- Outliers have been assessed and results are presented with and without the outlier in cases where outliers are believed not to be resulting from measurement error, but are influencing associations disproportionately.
- All variables are normally distributed. This has been confirmed using the Shapiro Wilk test for each continuous variable.

Sub group analysis has also been performed using independent t-tests comparing continuous variables of NIRS and bone health markers against categorical variables T2DM status and sex. The following statistical assumptions [286] have been met:

- Groups are independent without overlap and as such all observations are independent.
- Variance is similar in the sub-groups being compared, confirmed using Levene's test and as demonstrated in Tables 8.1 and 8.2.
- All continuous data are normally distributed, again confirmed with use of the Shapiro-Wilk test for each continuous variable sub group.

For analysis of differences between the lateral calf and proximal tibia, paired t-tests have been used with the above assumptions regarding variance and normality met, with the difference between paired measurements also assessed for normality using Shapiro-Wilk tests [286].

8.3.2: Summary of NIRS markers

As discussed in Chapter 7.1, the seven arterial occlusion (AO) haemodynamic markers presented in Figure 8.1 have been adopted for further analysis in Chapters 8, 9 and 10, based on physiological relevance and having demonstrated suitable reliability in Chapter 7.

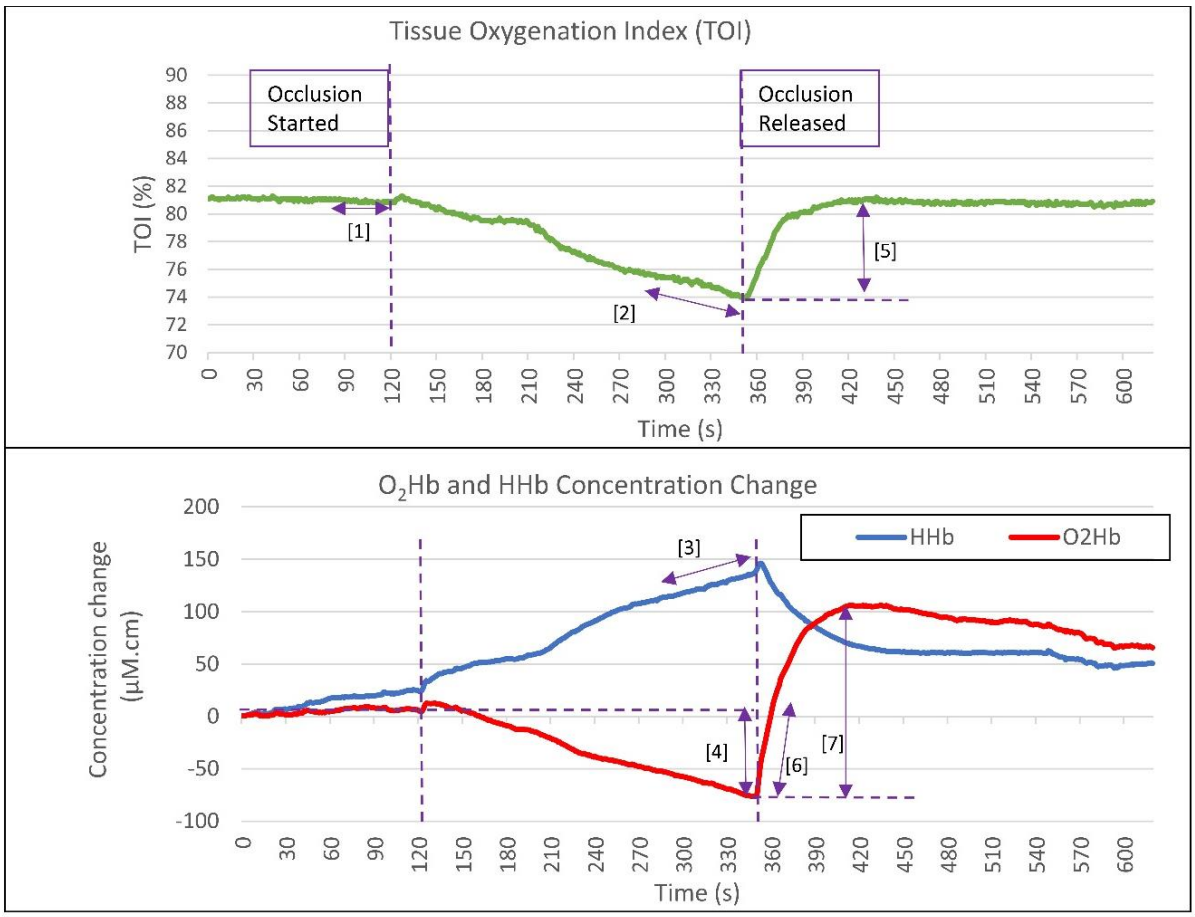

Figure 8.1: Graphical display of the haemodynamic parameters adopted for analysis in Chapters 8, 9 and 10.
[1] Baseline TOI at rest prior to the occlusion (TOI_rest; (%))
[2] Rate of TOI decrease in the last 60s of occlusion (TOI_DO_ 60s (%/s))
[3] Rate of HHb increase in the last 60s of occlusion (HHb_DO_60s (µM.cm/s))
[4] Absolute change in O_2Hb during the occlusion (µM.cm; O_2Hb_DO_absΔ)
[5] Maximal absolute change in TOI post occlusion (TOI_PO_absΔ (%))
[6] Rate of O_2Hb increase in first 20s post occlusion release (O_2Hb_PO_20s (µM.cm/s))
[7] Maximal absolute change in O_2Hb post occlusion (O_2Hb_PO_absΔ (µM.cm))

8.3.3: Summary of NIRS results

Table 8.3 presents the summary statistics of NIRS haemodynamic markers at the proximal tibia and lateral calf. As was identified in Chapter 5, there was a strong statistically significant difference between measurements taken at the proximal tibia and lateral calf, with the calf demonstrating stronger during occlusion (DO) and post occlusion (PO) responses. Of the 36 participants, 34 contributed AO data. One participant could not tolerate the arterial occlusions. For the tibia, one participant's data were removed due to a system error affecting all data (the system was not recording nTHI data). For the lateral calf, one participant had all data excluded as all AO attempts resulted in data with nTHI changes greater than 15%.

Table 8.3: Summary of NIRS haemodynamic markers. Results presented are means with standard deviation in parentheses. Mean difference, 95% confidence intervals of differences, and p-values from paired t-tests between anatomical sites are also presented for each NIRS marker (* denotes statistical significance of p–value <0.05).

NIRS Marker	Proximal Tibia (N=34)	Lateral Calf Muscle (N=34)	Paired t-test mean difference (95% CI)
TOI_rest (%)	77.1 (4.0)	68.0 (3.5)	9.2 (7.3-11.0); p<0.001*
TOI_DO_60s (%/s)	-0.027 (0.007)	-0.063 (0.024)	0.036 (0.026-0.046); p<0.001*
HHb_DO_60s (µM.cm/s)	0.321 (0.104)	0.957 (0.463)	0.636 (0.473-0.799); p<0.001*
O_2Hb_DO_absΔ (µM.cm)	-102.8 (53.8)	-194.7 (99.1)	91.9 (53.3-130.5); p<0.001*
TOI_PO_absΔ (%)	8.2 (2.3)	24.0 (7.7)	15.9 (12.9-18.9); p<0.001*
O_2Hb_PO_20s (µM.cm/s)	7.56 (2.99)	20.20 (8.45)	12.64 (9.87-15.41); p<0.001*
O_2Hb_PO_absΔ (µM.cm)	188.7 (55.9)	381.5 (136.8)	192.8 (147.1-238.6); p<0.001*

Figure 8.2 also demonstrates these markers graphically for both the proximal tibia and lateral calf, stratified by sex. Females had significantly reduced oxygen extraction during occlusion at the lateral calf as indicated by statistically significant differences for all three DO markers based on independent t-tests (p<0.05). These were also reduced at the proximal tibia but only statistically significant for the O_2Hb_DO_absΔ marker (p<0.001*)*. Both O_2Hb_PO_20s and O_2Hb_PO_absΔ markers demonstrated statistically significant differences between sexes at both the proximal tibia and the lateral calf (p<0.05), with a reduced PORH response in females compared with males, whilst TOI_PO_absΔ was only significantly different at the lateral calf.

There was little evidence of differences between those with and without T2DM for any markers at either the lateral calf or the proximal tibia.

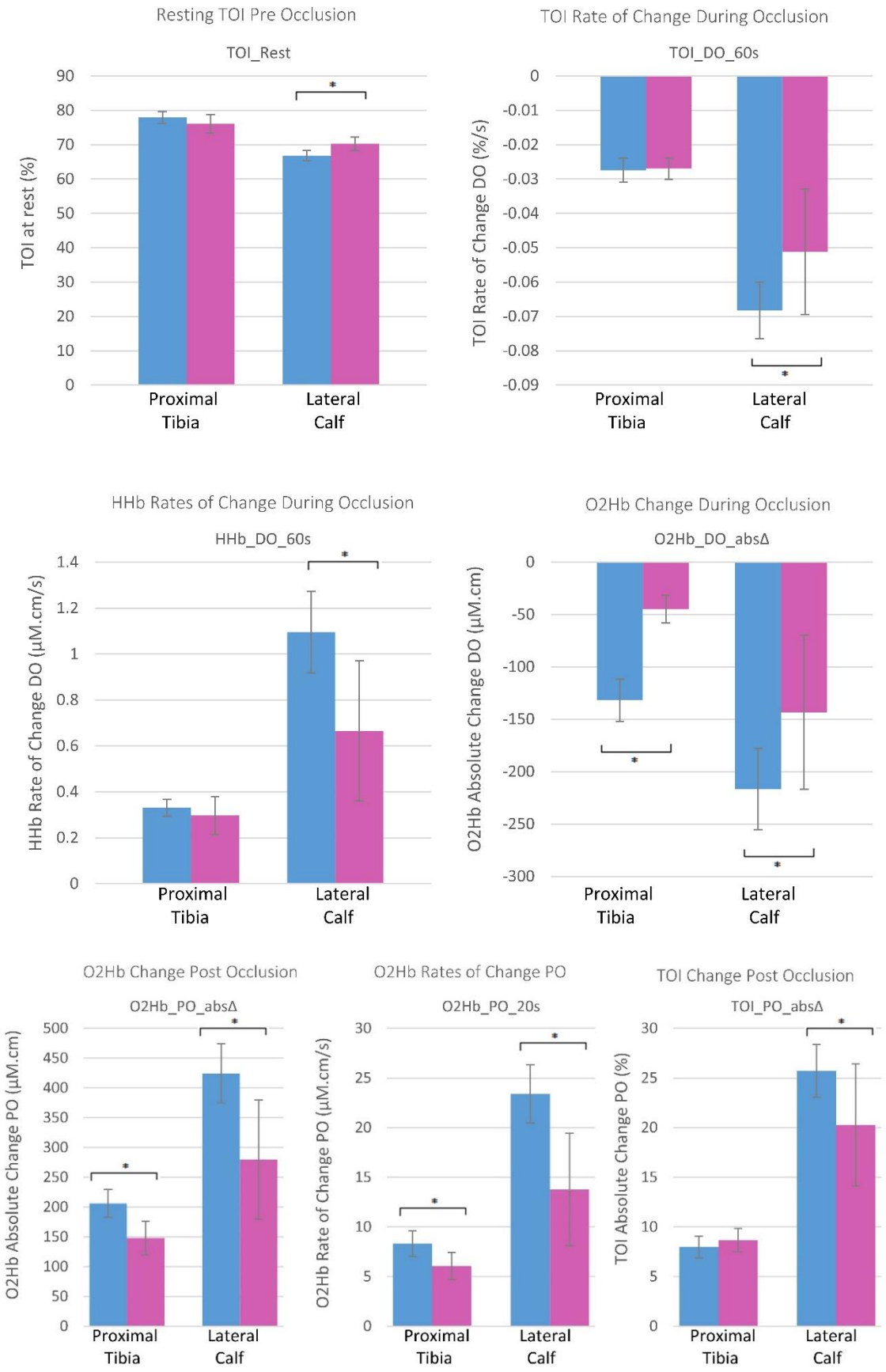

Figure 8.2: Summary of mean haemodynamic markers for both the proximal tibia and lateral calf stratified by sex (male = blue (n=22); female = pink (n=14)). Error bars represent 95% confidence intervals of mean values, * denotes statistically significant differences (p-value <0.05) based on independent t-tests between sexes.

There were some statistically significant associations of interest between haemodynamic NIRS markers and the demographics presented in Table 8.1. There was a statistically significant positive association between percentage fat content in the lower leg and resting TOI at the lateral calf (r=0.54; p=0.001). Percentage fat content in the lower leg was also significantly negatively associated with all DO and PO NIRS markers taken at the lateral calf, with Pearson's r-values ranging in magnitude from 0.61-0.79 ($p<0.001$), meaning higher percentage fat content in the lower leg associated with lower oxygen extraction response DO, and lower PO response upon occlusion release. Similar significant associations were also seen with DO and PO O_2Hb markers at the proximal tibia (Pearson's r-values ranged in magnitude from 0.44 to 0.63; $p \leq 0.01$; see Table 8.4), but not for TOI and HHb markers.

However, higher fat content in the leg may be confounding for sex-dependent effects as there was also significant differences in percentage fat content in the lower leg between males and females ($p<0.001$, independent t-test). Partial correlation analysis indicates that sex does confound associations between DO and PO O_2Hb markers of the proximal tibia and percentage fat content at the lower leg. These associations become non-significant when adjusting for the influence of sex. However significant negative associations still exist between AO markers at the lateral calf and percentage fat content at the lower leg, even controlling for sex (see Table 8.4).

Table 8.4: Pearson correlation r-values between lower leg percentage fat content and O_2Hb DO and PO NIRS markers taken at the proximal tibia and lateral calf. Partial correlation coefficients are also presented adjusting for sex. Asterisks indicate a statistically significant correlation with *p*-value <0.05 (N=34).

Proximal Tibia	O_2Hb_DO_absΔ	O_2Hb_PO_20s	O_2Hb_PO_absΔ
Lower Leg % Fat Content	0.63*	-0.44*	-0.57*
Lower Leg % Fat Content (partial correlation adjusting for sex)	0.12	-0.33	-0.06

Lateral Calf	O_2Hb_DO_absΔ	O_2Hb_PO_20s	O_2Hb_PO_absΔ
Lower Leg % Fat Content	0.61*	-0.79*	-0.76*
Lower Leg % Fat Content (partial correlation adjusting for sex)	0.57*	-0.68*	-0.59*

Associations between age and NIRS markers were also of interest. As the healthy participants testing as part of protocol development work (presented in Chapter 5) were generally of a younger age, it was deemed appropriate to merge these data to look at a wider age range (21-71 years; N=51). None of the AO parameters were significantly associated with age. However, interestingly age was significantly negatively associated with resting TOI values at both the proximal tibia (r=-0.45; p=0.001) and the lateral calf (r=-0.51; p=<0.001). It appears resting TOI is reduced with age in both tissues, as demonstrated in Figure 8.3.

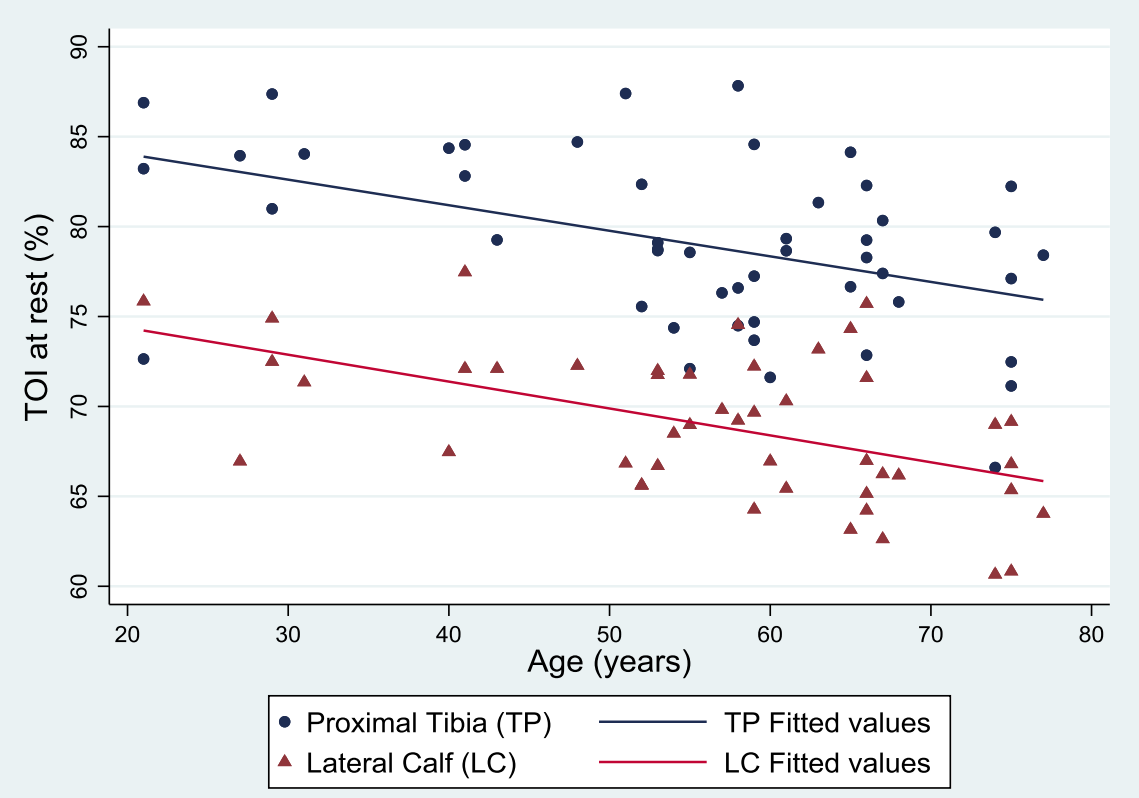

Figure 8.3: Association between resting TOI and age at the proximal tibia (r=-0.45; p=0.001) and the calf (r=-0.51; p=<0.001) with associated lines of best fit.

8.3.3.1: During occlusion (DO) versus post occlusion (PO) NIRS results

At the lateral calf, the rate of reoxygenation upon occlusion release (O_2Hb_PO_20s) strongly correlated with the two markers representing rates of deoxygenation during occlusion (TOI_DO_60s and HHb_DO_60s; r=-0.84 (p<0.001) and r=0.90 (p<0.001) respectively). Non-significant weak associations with O_2Hb_PO_20s were seen at the proximal tibia between TOI_DO_60s (r=0.04; p=0.85) and HHb_DO_60s (r=0.16; p=0.37). These relationships are demonstrated graphically in Figure 8.4. It appears the weak associations at the proximal tibia are influenced by the relatively low variance within the cohort for these two DO markers.

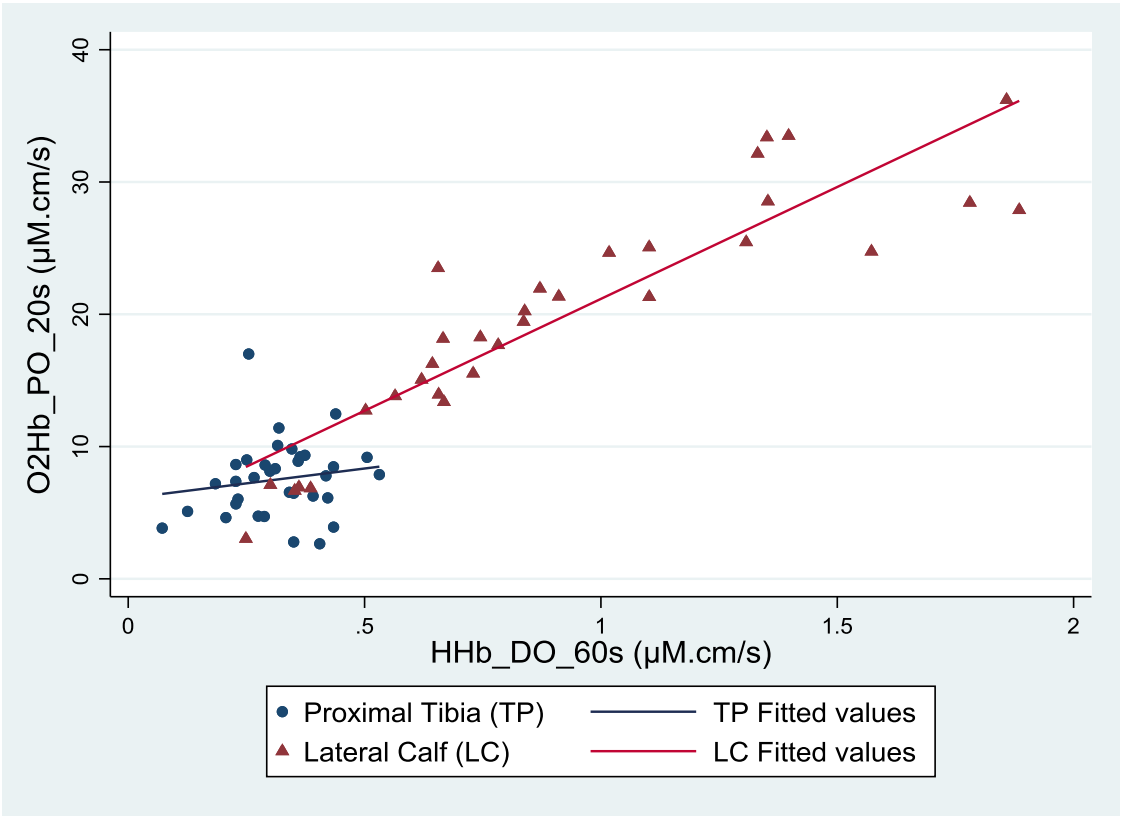

(a)

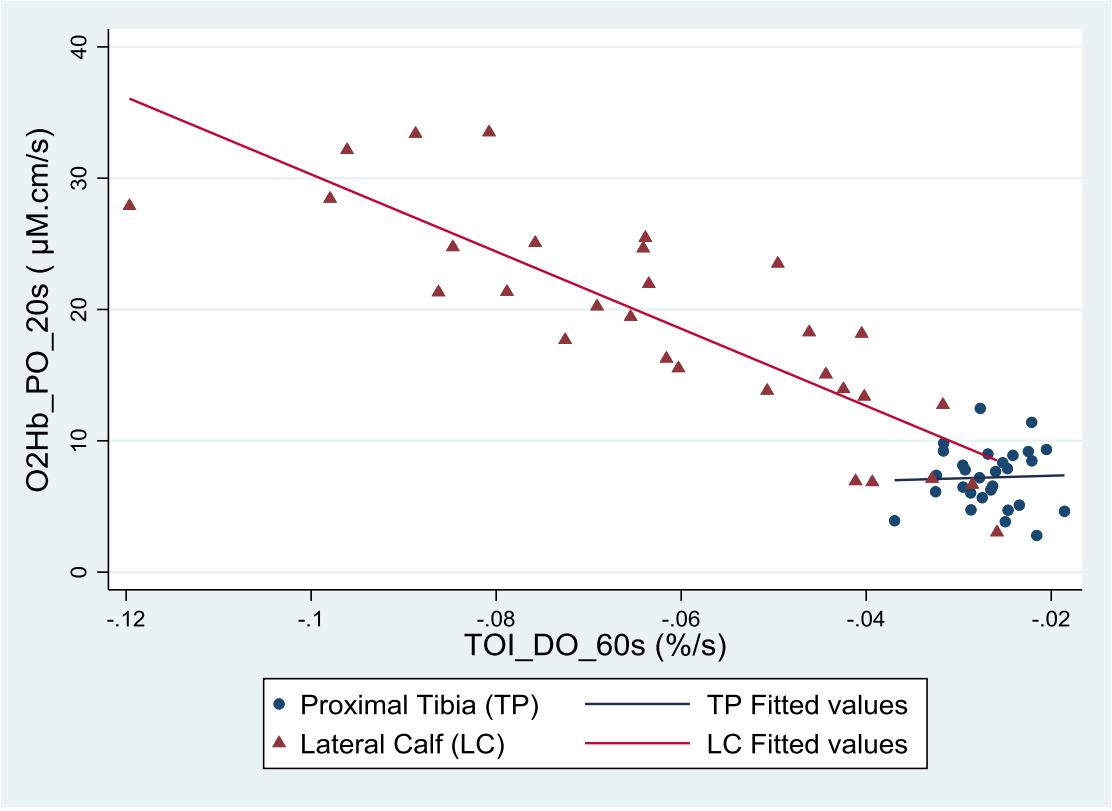

(b)

Figure 8.4: (a) Graph demonstrating weak non-significant correlation at the proximal tibia between O_2Hb_PO_20s and HHb_DO_60s (r=0.16; p=0.37). The correlation at the lateral calf is strong and statistically significant (r=0.90; p<0.001). (b) Graph demonstrating weak non-significant correlation at the proximal tibia between O_2Hb_PO_20s and TOI_DO_60s (r=0.04; p=0.85). The correlation at the lateral calf is strong and statistically significant (r=-0.84; p<0.001).

The absolute change in O_2Hb concentration during occlusion ($O_2Hb\_DO\_absΔ$) correlated strongly with the absolute change in O_2Hb concentration post occlusion release ($O_2Hb\_PO\_absΔ$; (r=-0.91; p<0.001) at the lateral calf. Although weaker, this correlation was statistically significant at the proximal tibia (r=-0.70; p<0.001). These associations are presented in Figure 8.5.

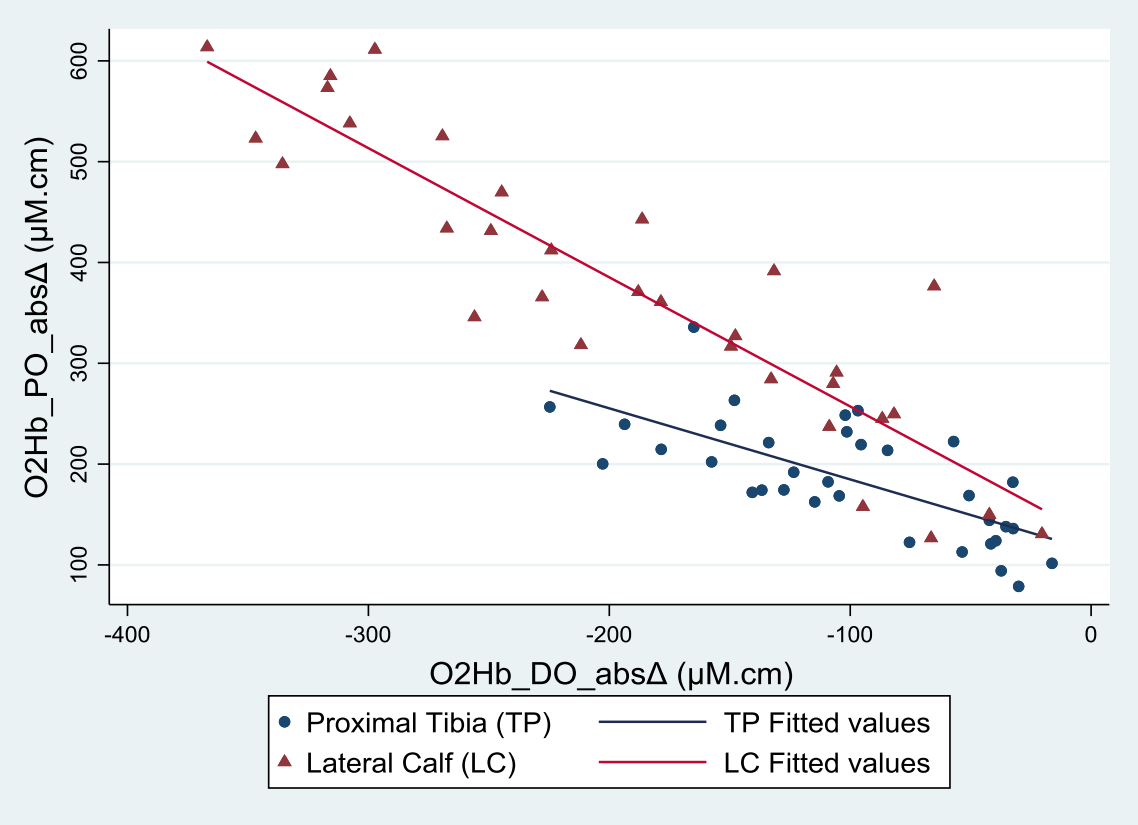

Figure 8.5: Graph demonstrating the strong correlation of both the proximal tibia (r=-0.70; p<0.001) and lateral calf data (r=-0.91; p<0.001) between $O_2Hb\_DO\_absΔ$ and $O_2Hb\_PO\_absΔ$ with associated lines of best fit.

As expected, after occlusion release in both the tibia and calf, the rate of O_2Hb recovery ($O_2Hb\_PO\_20s$) correlated strongly with the absolute O_2Hb concentration change ($O_2Hb\_PO\_absΔ$) (r= 0.88; p<0.001 and r=0.98; p<0.001, respectively). This suggests that the rate and extent of reoxygenation are linked during recovery from ischaemic events.

8.3.3.2: Proximal tibia versus lateral calf NIRS results

NIRS results at the lateral calf during occlusion generally correlated weakly with the proximal tibia, with the strongest association found for HHb_DO_60s (r=0.21; p=0.24). There was a moderate correlation between the tibia and calf for post occlusion markers $O_2Hb\_PO\_20s$ (r=0.46; p=0.009) and $O_2Hb\_PO\_absΔ$ (r=0.41; p=0.02). These associations are presented in Figure 8.6.

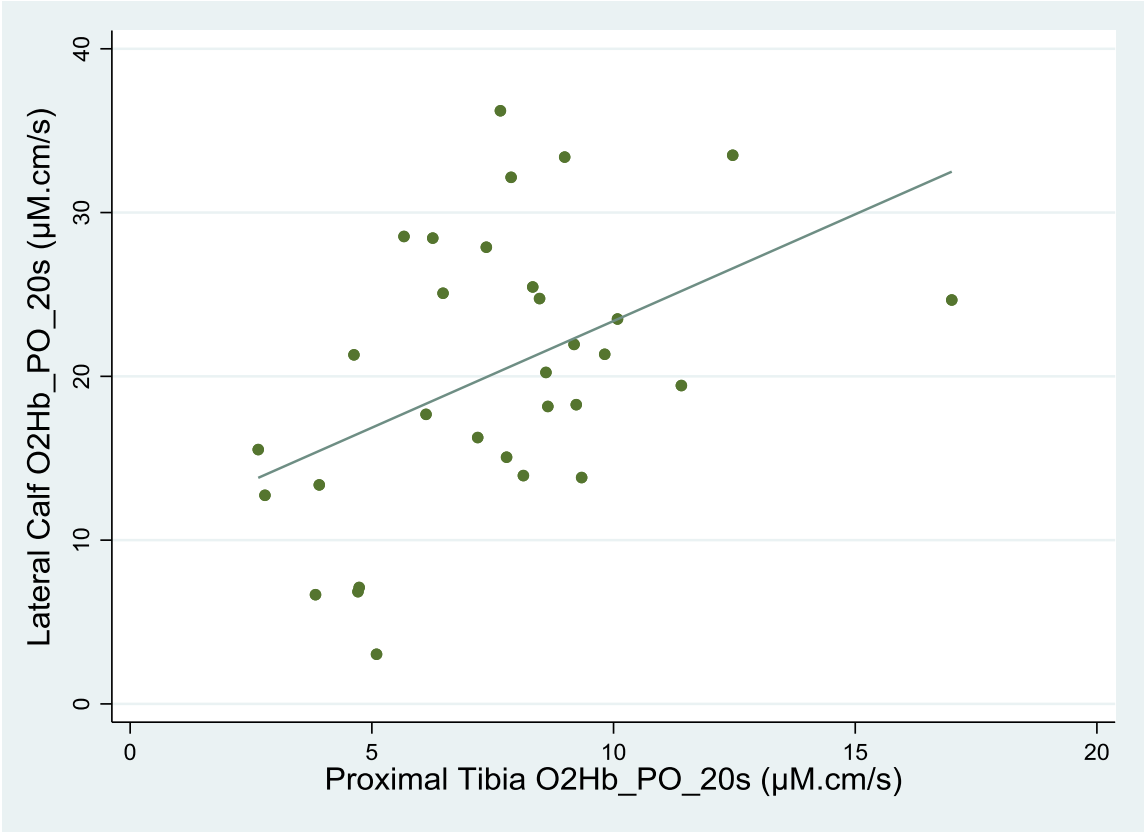

(a)

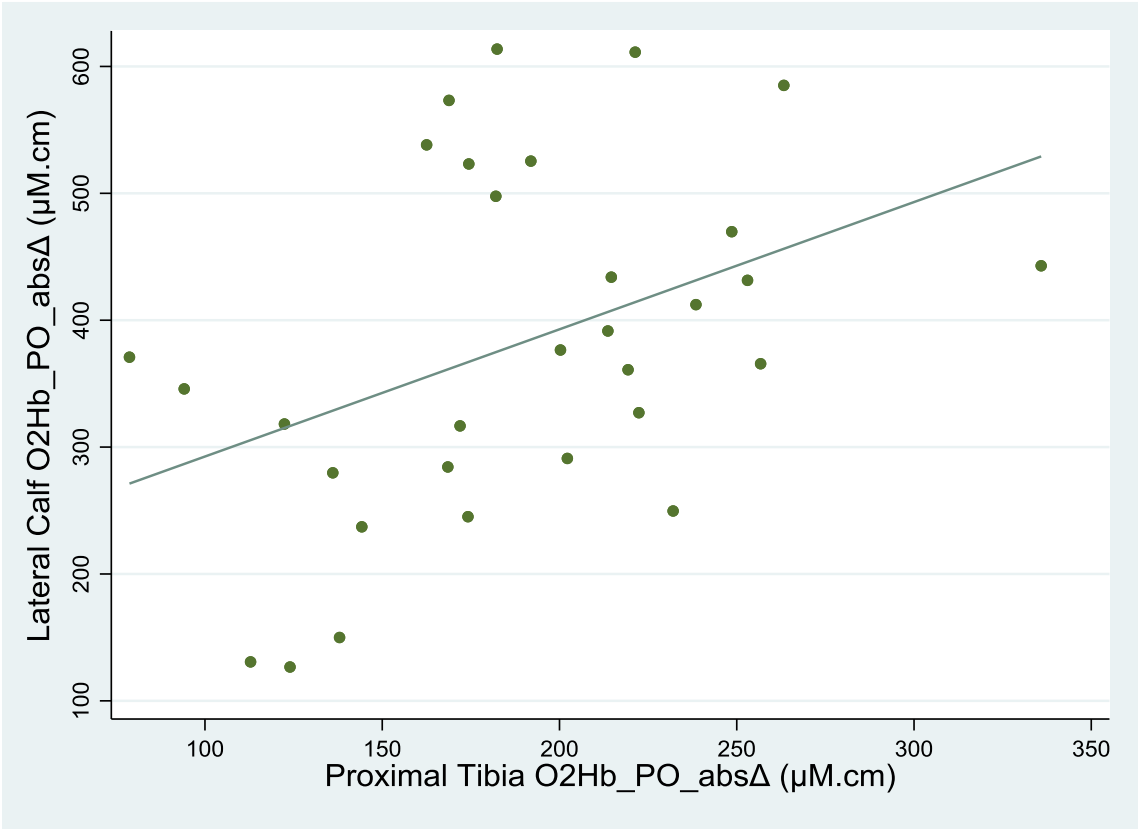

(b)

Figure 8.6: Scatter plots with associated lines of best fit demonstrating the moderate but statistically significant correlations between the proximal tibia and lateral calf for the (a) O_2Hb_PO_20s marker (r=0.46; p=0.009) and (b) the O_2Hb_PO_absΔ (r=0.41; p=0.02) marker.

8.3.4: Participant acceptability of arterial occlusion protocol

No serious complications were observed resulting from the AO protocols carried out on participants, although the protocol could leave temporary red marks on the skin due to compression, and participants were pre warned about this. Participants were asked about their thoughts on the AO protocol following participation in the study. Specifically, participants were asked to score the occlusion at its most painful using a pain scale of 0-10, with 10 being the worst pain they had experienced. This question highlighted the high variability in subjective experience from participants observed during testing. Scores ranged from 1-9 with a mean score of 6.4 (SD 2.4).

There are a number of possible contributing explanations to this variability in experience. Pain scoring systems may be more suited for monitoring longitudinal changes in pain within participants rather than comparing pain experienced between participants. How a participant scores pain can be influenced by many factors including their past experiences with pain and general anxiety levels relating to participation in the study. There is some evidence also suggesting differing pain thresholds based on physiological differences based around age and sex [330, 331].

Anecdotally, most participants were generally more comfortable with the arterial occlusions on the second attendance, suggesting there is a psychological element to experiencing more pain during an arterial occlusion when it is an unfamiliar experience. Participants also suggested some distraction techniques that could help such as listening to music, reading or mindfulness techniques. These may help, but caution needs to be exercised that the participant remains in a resting state for testing and does not inadvertently move their leg.

Participants were also asked to comment on whether they thought they would participate in an AO test if it would provide information on their bone health in a screening situation. Most participants agreed they would, provided they considered the potential clinical gain was worth the discomfort. This feedback is confounded by the sample being those who are willing to volunteer for such research, and some participants commented that they knew others who would not tolerate the protocol. The fact the protocol was uncomfortable but not potentially harmful was an important consideration highlighted by one participant. Another participant commented that a thorough explanation at the point of consent was also important (and had been provided).

8.4: Discussion of NIRS results

Figure 8.7 presents a summary of key trends from the NIRS results reported in Section 8.3. The results in this section have reiterated the significant differences identified in Chapter 5 between haemodynamic markers from what is likely to represent both muscle and bone tissue haemodynamics at the lateral calf and proximal tibia respectively. Furthermore, analysis presented in this chapter has also given confidence in the application of NIRS in this project, as results were generally in keeping with the existing evidence base, which is more established when looking at the lateral calf muscle and which will be discussed in this section.

Variable	Tibia (vs Calf)	T2DM (vs non-T2DM)	Female (vs Male)	Increasing Fat % in Lower Leg	Increasing Age
NIRS DO Markers	↓	↔	↓	↓	↔
NIRS PO Markers	↓	↔	↓	↓	↔
Resting TOI	↑	↔	↓	↑ (calf only)	↓
Fat % in Lower Leg		↔	↑		↔

Figure 8.7: Summary trends from Section 8.3. Arrows indicate statistically significant differences between groups, or associations between continuous variables of interest.

Both the rate and extent of O_2Hb response post occlusion release were strongly correlated at both the proximal tibia and the lateral calf as expected, and as also demonstrated at the calf by Rosenberry et al. 2018 [79] using occlusion protocols. This study makes an interesting point that if future research is interested specifically in PORH response differences between participants, it may be worth controlling for the metabolic use of oxygen during the occlusion. This way post occlusive response will not be confounded by differences in the metabolic oxidative capacity of different participants. Rosenberry et al. 2018 showed that when controlling for increased oxygen extraction in younger participants by using a shorter occlusion time, there was little evidence of differences between elderly participants in terms of PORH response [79].

At the proximal tibia, DO NIRS parameters were weakly associated with PO markers. This may be expected with the weaker magnitude of responses in bone, but may also

be due to potential unique regulatory mechanisms in bone, limiting increased blood flow capabilities in physiological response to ischaemia in bone, as previously discussed previously in Section 5.6.2 [294, 332].

At the lateral calf, DO NIRS parameters correlated strongly with PO markers. The evidence base seems to support healthier tissue having a stronger response both DO and PO. Literature looking at runners suggests oxygen extraction rates increase with increased general fitness [283, 333]. Conversely, studies have demonstrated reduced oxygen consumption rates and hyperaemic response in those with sepsis, and in smokers [272]. Adelnia et al 2019 concludes that reduced oxidative capacity may be influenced by reduced mitochondrial function and density, or potentially a reduced microvascular blood volume and capillary density at rest [334]. A murine study by Frikha-Benayed et al 2016 suggests similar variation in oxidative capacity may exist within bone, where mitochondrial density and the function of osteocytes was variable depending on cell age and location within the cortex [335].

Duteil et al 2004 [336] reports that trained athletes had a higher concentration of myoglobin in skeletal muscle, which was associated with more efficient oxidative metabolism (i.e. creatine phosphorylation) and greater vascular reactivity during exercise. Although the role of myoglobin is generally considered not definitively understood, the results of Duteil et al 2004 suggest an improved efficiency in oxygen regulation in healthier muscle tissue during ischaemic challenge.

There also has been demonstrated to be a higher capillary density in muscle of athletes, which may explain the stronger and faster PORH of those with a lower fat percentage in the lower leg [337]. There is some encouraging research that similar results may extend to bone tissue. Stabley et al 2014 demonstrated in a murine model that exercise training led to a stronger hyperaemic response in the femoral diaphysis [338]. Rats have also shown increased capillary density in muscle [293] and cortical bone [8] with exercise, with the latter found to precede positive changes to BMD.

8.4.1: Sex

Whilst sex-based differences to AO response in muscle were not found in the evidence base, studies comparing sex-based differences to ischaemia-inducing exercise have found a stronger desaturation response in males using NIRS [339-341] , in line with results found at the lateral calf in this chapter. In particular, the rationale for one of these studies (Paradis-Deschenes et al. 2017) is based on the known reduced response

observed in females during ischaemia-inducing exercise [340]. Sader et al 2002 argue that oestrogen has been shown to stimulate NO synthase, meaning females may have physiologically different coping mechanisms for ischaemic events, leading to lower DO and PO responses indicated by NIRS [29].

There is no existing evidence specifically addressing sex differences to ischaemic response in bone tissue. However Siamwala et al 2017 observed greater response in males when undergoing positional changes (head down tilt) and lower body negative pressure for 10 minutes [204]. Differences observed in resting TOI at the proximal tibia between sexes in this chapter were also in line with Siamwala et al. 2017, which reports resting mean TOI values at the proximal tibia of 73.5% (SD 7.2) for females and 76.8% (SD 6.3) for males [204]. Farzam et al 2014 found resting TOI at the manubrium was 2% higher in males [56].

Mantooth et al 2018 demonstrated sex-specific differences with greater deoxygenation in males than females during forearm exercises of comparable intensity. The authors contend this may be due to differences in muscle mass and/or morphology [339]. Kao and Sun 2015 also postulate that differences in muscle to fat ratios in the sampled tissue may contribute to sex-based differences. This study found males were two-fold more vaso-reactive to superficial temperature changes induced using far-infrared illumination [342]. Unfortunately indicators of muscle morphology, including exercise levels or general fitness, were not recorded in this study.

8.4.2: Percentage fat content in the lower leg

Sex-based differences at the proximal tibia and lateral calf may be partially explained by the significantly higher percentage fat content in the lower leg of female participants, either directly influencing NIRS measurements within the measured volume, or indirectly if related to reduced muscle strength and/or cardiovascular health in female participants. It is expected that females may have a greater proportion of fat in the lower limbs due to the known sexual dimorphism of fat distribution [343], and that females may have a greater total body fat percentage even when controlling for activity levels [344]. On the other hand, Lorbergs et al 2015 [313] presents data demonstrating negative associations between increased intra and inter muscular fat and markers of physical performance and activity within an all-female cohort. This study also demonstrates a negative association between increased intra-muscular fat at the calf, and markers of tibial bone health [313]. Gomes et al 2017 demonstrate capillary

rarefaction at the soleus muscle in sedentary rats with increased intramuscular fat, likely to reduce the efficiency of oxygen extraction DO and reduce the extent of PORH response [345]. Karampinos et al 2017 also discusses evidence that increases in visceral fat can lead to increased fat fraction in bone marrow, impacting negatively on bone health [22].

It is possible that the increased fat content observed in females may not be intra muscular but may be related to increased superficial fat thickness at measurement sites with NIRS, systematically reducing NIRS changes due to the reduced metabolism of adipose tissue [346]. However, there was no obvious associations between NIRS markers and calf circumference or BMI. Taking more objective measurements of superficial tissue thickness at the proximal tibia with callipers was abandoned in this study at the protocol development phase, predominantly because these were difficult measurements to take on healthy participants, as there was often a very small superficial thickness to measure, and because compression was likely anyway with probe placement. Superficial tissue thickness could be observed on axial MRI scans and it was observed that when the skin marker was applied with tape, using similar gentle pressure to the bandage used to stabilise NIRS probe placement, that superficial tissue thickness generally became very small (circa up to 8-10 millimetres maximum). This analysis was not formalised as it was felt there were too many potentially influential variables such as error in replicating the exact location and pressure of NIRS probes used in testing. However, examples are presented in Figure 8.8.

The evidence base is divided on how much superficial tissue might influence NIRS measurements taken on bone. As discussed in Chapter 3, three studies conducted small experiments to rule out the confounding effects of overlying tissue by selectively altering superficial tissue haemodynamics either through the localised introduction of vasodilating or vasoconstricting elements such as gentle compression [77], cold packs [186], nitro-glycerine patches [77] and liniment [83]. Whilst only illustrating that superficial tissue does not significantly contribute to measurements, these studies concluded that their systems were a suitable tool for measuring haemodynamics in superficial bone tissue. Farzam et al 2014 also found little evidence of association between skin tissue thickness and NIRS measurements taken [56]. Conversely, Klasing et al. 2003 does report a significant negative correlation between superficial tissue thickness and markers of oxygen consumption taken at the tibia using a NIRS system [185]. However,

in the latter study there is difficulty in teasing out whether systematic differences are directly related to increased superficial tissue layers or reflect a systemic decrease in microvascular function and health that may relate with increased systemic adiposity.

a) 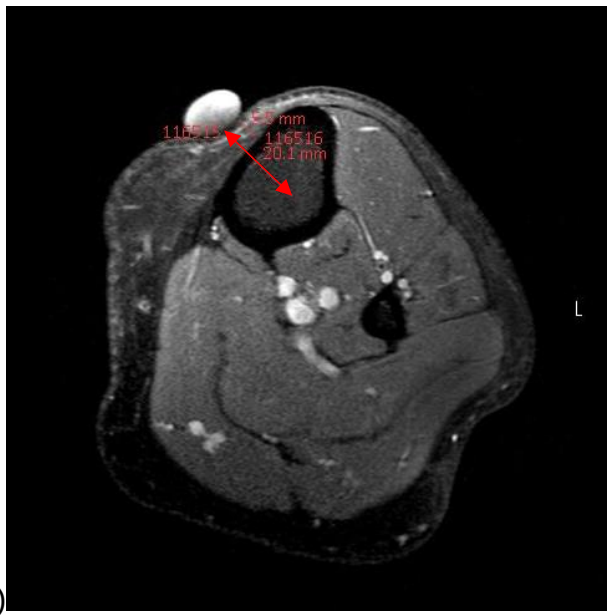

b) 

Figure 8.8: Examples of soft tissue thickness in the participants with the (a) smallest (314mm) and (b) greatest (412mm) calf circumference measured. With the probe spacing of 40mm used, NIRS measurements reflect a depth of up to 20mm [16], which is indicated on the images with red arrows, demonstrating NIRS penetration to the centre of the tibia.

Elwell 1995 argues the reduced absorption coefficient of fat relative to muscle (0.003 mm^{-1} versus 0.025 mm^{-1} [68]) is also suggestive of minimal attenuation effects of superficial adipose tissue to measurements of deeper tissue [2]. In the context of cerebral NIRS, Kohri et al 2002 calculated using time resolved NIRS that with interoptode spacing of four centimetres, 69% of signal detected would be attributable to cerebral tissue despite overlying skin and skull tissue [347].

It was felt in this PhD project that recruiting healthy weight participants (and observing only non-significant associations between NIRS measurements and calf circumference or BMI) was enough to rule out significant influence from overlying soft tissue. This decision also took consideration of previous evidence supporting that firm pressure with probes is a sensible approach to removing the influence of overlying tissue on measurements [56]. As discussed in Section 5.6.2 and Appendix H, the absence of a PORH response in NIRS TOI measurements at the tibia also suggests minimal contribution from overlying soft tissue, as both skin and adipose tissue have been evidenced to show PORH response [65, 292].

8.4.3: Age

It was of interest to investigate for any associations between NIRS markers and age. Age has been found to be associated with increased endothelial dysfunction with lower levels of endothelium derived nitric oxide (NO) and lower levels of endothelial derived dilatory prostaglandins during ischaemic events, reducing vasodilatory response and the extent of reactive hyperaemia [29, 79]. However, occlusion protocols at the calf and proximal tibia presented in this chapter found little evidence of associations between NIRS markers and age for any DO or PO markers. Olive et al 2002 also found older participants (>60 years) had no difference in post ischaemic recovery at the calf compared with younger participants (<40 years) and identified that activity levels and general fitness may be more influential than age for preserving vascular function [348]. Moderate physical activity is proposed to be protective of cardiovascular function and so in our cohort of relatively healthy, non-obese participants, any age related differences may not have been as prominent.

Significant negative correlations were observed between age and resting TOI at both the lateral calf and the proximal tibia. This conflicts with Binzoni et al 2003, which only found this association at the calf and not the tibia, although this study used a smaller cohort of 13 participants [189]. Costes et al 1999 also found lower resting TOI at the vastus lateralis muscle with aging, despite little evidence of differences with age in ischaemic recovery post AO. Without impaired vascular regulation, it was concluded by the authors that reduced TOI is most likely related to reduced capillary density and/or lower blood flow rates, meaning muscle at rest has reduced arterial oxygen supply leading to a reduced resting TOI, independent of vascular reactivity to ischaemic events [349]. Binzoni et al 2003 supports this, arguing that resting TOI in muscle may be more effected by aging due to its faster resting metabolism than bone [189].

8.4.4: T2DM

Perhaps one expected observation that did not eventuate was a difference in DO and PO markers between those with and without T2DM. There was no existing evidence identified utilising NIRS regarding differences in bone tissue in those with and without T2DM. However differences in bone marrow microvascular density and perfusion associated with diabetes have been identified in murine studies [26, 315]. Significant differences in NIRS-derived parameters in muscle between those with and without

T2DM are well documented in the evidence base whilst undergoing ischaemic inducing exercise, particularly with slower recovery post-ischaemia expected in those with T2DM [350-352]. Thorn et al. 2016 argues that oxygen extraction DO NIRS markers may be altered in those with T2DM in muscle and skin if endothelial response or mitochondrial function is impaired [65]. It may be that in our case, the sampled population of T2DM participants was too small to observe a significant difference. Perhaps more likely is that the T2DM population sampled generally had well controlled T2DM with relatively short duration and a lack of relevant co-morbidities (such as obesity or diagnosed peripheral arterial disease).

8.5: Conclusion

The NIRS results presented in this chapter suggest some DO and PO NIRS markers taken at the proximal tibia are associated with each other. Likewise the rate and extent of post ischaemic response has shown to be associated as expected. NIRS results identified significant differences between calf muscle and the proximal tibia, whilst also still showing associations between measurements at the two anatomical sites. Differences between sexes were demonstrated at both anatomical sites, although failed to identify any significant differences between those with and without T2DM. Results from the seven haemodynamic markers presented in this chapter will now be compared with DCE-MRI parameters in Chapter 9, and markers of bone health in Chapter 10.

Chapter 9: MRI validation results

This chapter will summarise MRI spectroscopy results (Section 9.1) and dynamic contrast enhanced MRI (DCE-MRI) results (Section 9.2). Comparison of DCE-MRI results with NIRS-derived haemodynamic markers will also be presented in Section 9.3. Associations of interest will be presented with discussion of potential explanatory relationships based on the results obtained, and the existing related evidence base, in Section 9.4.

9.1: MRI spectroscopy (MRS) results

Thirty-five participants contributed MRS data. There was one set of missing data as the participant was unexpectedly not suitable for MRI due to an anterior cruciate ligament knee repair that unexpectedly caused too much artefact on MRI scans. Table 9.1 presents summary data of bone marrow fat fraction amongst participants, including for subgroups of interest based on sex and T2DM status. This table demonstrates there was little evidence of differences between sub-groups using independent t-tests. Likewise no statistically significant associations were observed between MRS fat fraction and any haemodynamic markers obtained with NIRS; nor between fat fraction and other markers of bone health such as DXA measurements, TBS, FRAX, age, CTX, or P1NP. Figure 9.1 provides an example of the output data from the MRS protocol.

Table 9.1: Summary of mean MRS percentage fat fraction (%) of bone marrow at the proximal tibial site of NIRS measurements, including sub groups based on T2DM and sex status (standard deviation in parentheses). *p*-values are from independent t-tests of the corresponding subgroups.

	Total (N=35)	T2DM (n=18)	Non-T2DM (n=17)	*p*-value between sub groups
MRS Fat Fraction (%)	96.1 (1.8)	96.1 (1.8)	96.1 (1.9)	0.93

	Total (N=35)	Males (n=21)	Females (n=14)	*p*-value between sub groups
MRS Fat Fraction (%)	96.1 (1.8)	96.1 (2.0)	96.1 (1.4)	0.84

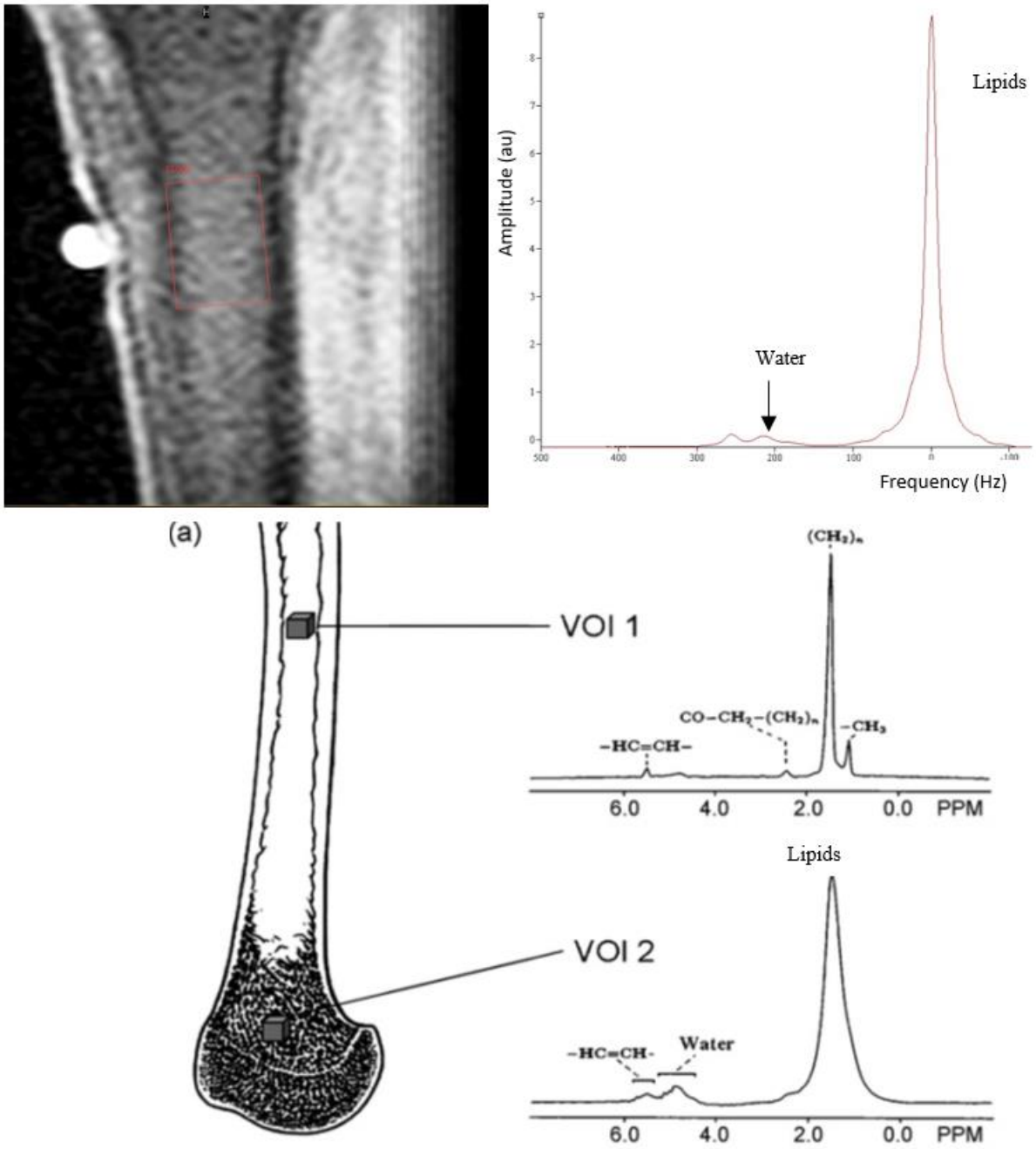

Figure 9.1: Example MRI spectroscopy data from the proximal tibia demonstrates comparable spectra to the trabecular bone of the distal femur (VOI 2) reproduced with permissions from Machann et al 2008 [133].

9.1.1: Discussion of MRS results

Although MRS does not directly image bone haemodynamics, results were of interest to investigate the relative fat content (i.e. fat fraction) of the bone marrow within the volume of tissue measured with NIRS. It has been demonstrated in the evidence base that increases in the fat fraction of bone marrow is known to associate with reduced bone mineral density [34, 125]. Fat fraction within bone marrow has also been found to negatively correlate with bone perfusion [126]. Relative increases in marrow fat suggests

a corresponding decrease in red erythropoetic marrow, tying in with the observed negative correlation in reduced bone perfusion in previous studies [43, 127].

MRS data could also be used to elucidate the type of marrow being sampled within the NIRS volume based on the fat fraction obtained. Yellow marrow is known to chemically constitute of around 80% lipids, with red marrow typically 40-60% lipids, with the remaining tissue consisting predominantly of water, as well as protein (including haemoglobin) [22, 353]. Water signal stems predominantly from fluid in cellular tissue, interstitial fluid, and blood within the circulation of the marrow [133].

The MRS results presented in Table 9.1 have demonstrated a very high fat fraction in all participants with a narrow range of results (from 91.2% to 98.5%). As such, MRS data has proven useful in determining that NIRS has likely been sampling yellow marrow at the proximal tibia for all participants. This was one of the initial objectives for including an MRS sequence into MRI data collection. This finding supports the observations that DCE-MRI enhancement patterns also follow that of yellow marrow, discussed in Section 9.4.5 with reference to Budvik et al 2014 [109], who found that red bone marrow in the hip had faster perfusion, earlier washout of contrast, and greater blood volume than yellow bone marrow.

The initial selection of the proximal tibia over the tibial diaphysis as the primary anatomical site of interest for NIRS measurements was partly justified in that it may better represent trabecular bone and potentially red marrow at the metaphysis of this long bone. The bone marrow of peripheral long bones is known to be predominantly red marrow in infancy [133], with conversion to yellow marrow into adulthood, occurring initially in the diaphysis and epiphyses, and finally in the metaphyseal areas [22]. As such, red marrow would be most likely found at the proximal tibia site around the metaphyseal area of the proximal tibia. However, the MRS results presented support Vandeberg et al 1998 [353], who report changes in the location of red marrow with maturity culminating typically to negligible red marrow in the distal femur and entire tibia after 25 years of age. From this age onwards, red marrow is typically concentrated in the axial skeleton. Future research into the anatomically superficial sternum may be of interest in the future, allowing direct comparison between NIRS measurements and a known red marrow site prevailing through adulthood. Although the proximal tibia has been shown to represent yellow marrow, it is still arguably the optimal site for comparison in this PhD study, as it still represents trabecular bone and has other advantages in terms of the ease of positioning, suitability for the arterial occlusion

protocol, precedence in the evidence base, and greater bone volume for NIRS sampling relative to the tibial diaphysis.

The small range of fat fraction amongst the sample population may also be beneficial when considering DCE-MRI results. Biffer et al 2010a [354] suggests marrow fat fraction is a potential confounder for DCE-MRI parameters and proposes consideration of correction factors based on fat fraction, which may be highly variable at red marrow sites. This may be particularly important for longitudinal studies where changes in DCE-MRI parameters may be confounded by physiological changes in marrow composition. McCarthy 2006 reports a wide variation in blood flow rates between cancellous bone containing red marrow (approximately 20mL/min/100g) and yellow marrow (approximately 1mL/min/100g) in microsphere-based animal studies [23].

Moorthi et al 2015 reports a marrow fat percentage at the tibial diaphysis of 84.8% (SD 2.6) in five healthy controls of similar age using a comparable MRS protocol [355]. This is more in keeping with the wider published literature estimating lipid chemical composition to be approximately 80% in yellow marrow [22, 353]. However Jensen et al 1990 has previously reported tibial fat fractions of mean 94% (range 92-99%) in 19 normal adult controls, more closely replicating results from this PhD study [356]. Furthermore, two studies were identified reporting negligible water peaks with MRS when assessing the differences in lipid characteristics in tibial bone marrow in adult populations [357, 358].

MRS data has not been successful at demonstrating correlations with NIRS markers (or any other measurements of interest). This is likely to be explained by the small range of fat fraction results within the cohort, with correlation results known to be reduced by sample populations with small variance [298]. Associations are also complicated by the physiological comparisons being made. MRS presents the chemical composition of the measured volume of bone marrow, where BMD is predominantly representative of cortical bone, and NIRS is representative of vascular reactivity with influence from blood volume and/or capillary density. Whilst it may be hypothesised these measurements would be indirectly linked, and there is previously discussed precedence for the association between fat fraction, bone density, and microvascular haemodynamics in bone; it remains that they measure fundamentally different elements of bone health.

It was observed that there was little evidence of differences between sexes in sub group analysis. There are evidenced differences in the onset and rate of age-related changes in marrow conversion from red marrow to yellow marrow. Initially during adulthood, marrow fat is 10-15% more abundant in males due to conversion of red marrow, however post menopause red marrow is rapidly converted in females [22, 123]. With all females in the sample population post-menopausal, and the mean age 62 years (SD 8) it seems plausible that sex-dependent differences were negligible in the sampled population.

9.1.2: Limitations of MRS protocol

There are a number of reasons why the MRS results presented should be considered tentatively, despite existing evidence that MRS of long bones can be a reproducible technique [109, 130]. As the bone marrow volume sampled had small water peaks, small variations and measurement error of integrals are potentially enhanced by the fat fraction calculation. MRS relies on the differing chemical shift caused by different chemical components within the region of interest and a large volume of interest is required due to the relatively poor spatial resolution of MRS [123]. However the volume of bone marrow available at the proximal tibia is anatomically restricted [355]. MRS is also sensitive to susceptibility artefacts which is relevant to the analysis of bone marrow, which lies close to cortical bone interfaces, introducing potential local magnetic field inhomogeneity [353]. MRS is also inherently limited in that it demonstrates chemical composition, which may be indicative, but not necessarily representative, of cellularity or associated physiological function [133].

Another limitation of PRESS MRS sequences is that only one volume of interest can be explored during one scan sequence (which takes approximately ten minutes of scanning time), and analysis cannot be performed retrospectively on imaging data sets [355]. This ruled out the potentially interesting *post hoc* analysis of fat infiltration at the calf muscles. It was observed that participants with a higher percentage fat content in the lower leg (as measured by DXA) also had lower tibial bone density (Pearson's r=-0.49; p=0.002). MRS data may have been able to provide more specific information on the distribution of fat within the lower leg [133]. Lorbergs et al 2015 [313] investigated associations between intramuscular fat percentage and BMD at the tibia in a comparable cohort of 35 post-menopausal women, adjusting for age, BMI, and activity levels. This study found that increased intramuscular fat percentage was negatively

associated with markers of tibial bone density and bone strength measured with peripheral quantitative CT.

MRS data obtained was not able to distinguish between different types of fat present within bone marrow due to low signal to noise using a 1.5T MRI scanner. Lidell and Enerback report in their 2015 review that there is research interest into the properties of bone marrow fat and associated adipocytes. It is proposed that brown adipocytes with increased mitochondria and nearby microcirculation may be more conducive to osteogenesis, whilst also improving glucose metabolism [359]. This may have particular application in investigations of bone health in those with T2DM, where pathophysiological mechanisms are suspected to be independent of BMD. For example, evidence suggests that there may be MRS detectable increases in the relative proportion of saturated lipids in bone marrow in those with T2DM, also associated with increased risk of fracture. These differences in lipid composition may be a useful predictor of poor bone health [91, 129].

Grey et al 2012 also found that treatment for T2DM with Pioglitazone (a type of thiazolidinedione) increased marrow fat fraction significantly within a six month period to the detriment of bone health. It is believed this drug modulates mesenchymal stem cells to prioritise adipogenesis over osteogenesis [360]. Sheu et al 2017 found men with T2DM who were not taking thiazolidinediones still had a significantly higher bone marrow fat fraction than those without diabetes in a cohort of 156 men over 74 years of age [361]. Patsch et al 2013 [91] found no significant difference in marrow fat fraction in those with and without T2DM, but did find that those with T2DM had proportionally higher saturated fat, as did those with recent vertebral fracture. The authors link this with existing epidemiological data stating diets high in saturated fat are linked with fragility fracture, however reflecting that proving direct pathophysiological mechanisms requires more research.

9.2: DCE-MRI results

As discussed in Section 6.2.4, analysis in this section focuses on the initial slope of signal enhancement of Gadolinium, and the amplitude of Gadolinium enhancement at the proximal tibia and calf during a dynamic T1 DCE-MRI scan protocol. These parameters are illustrated in Figure 9.2.

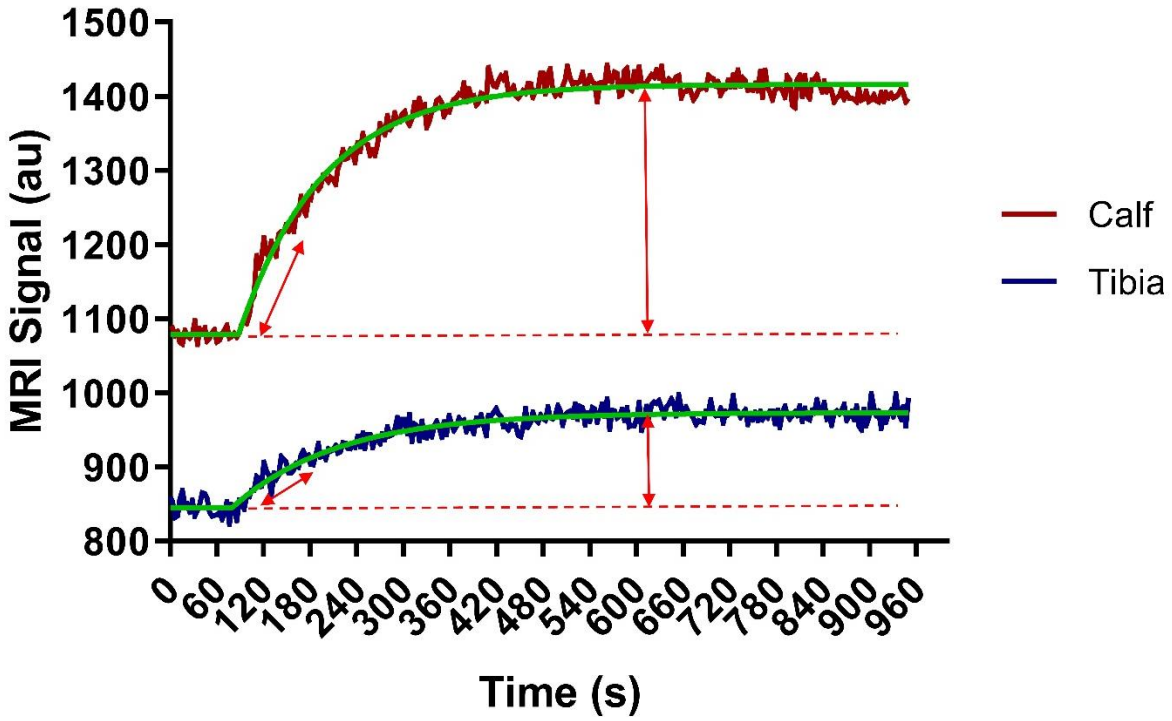

Figure 9.2: DCE-MRI haemodynamic markers reported in this chapter. This includes the linear rate of signal enhancement in the first 60 seconds of Gadolinium uptake, and the maximum span of Gadolinium enhancement after curve fitting with a one phase exponential association.

Thirty four of the 36 participants underwent DCE-MRI scans. One participant did not undergo the scan due to a logistical issue with the scan (no available medical supervision), whilst one other had an anterior cruciate ligament knee repair that unexpectedly caused too much artefact on MRI scans.

There were five other instances of data not being included for analysis of tibial DCE-MRI parameters as there was no obvious pattern of enhancement in these cases. In one instance, data from the calf was also removed as there was also no typical pattern of enhancement, meaning the Gadolinium injection may have failed (possibly due to extravasation). However, in the four other cases muscle enhancement was as expected. In these latter cases it was assumed that enhancement in bone was negligible to the noise in the time signal curve produced.

Figure 9.3 presents descriptive data of the primary DCE-MRI haemodynamic markers of interest taken at the proximal tibia and the calf muscle, stratified by sex. As for NIRS results, there are statistically significant differences between the two tissue types for both DCE-MRI markers using independent t-tests ($p<0.001$), with muscle having faster and greater Gadolinium enhancement in both sexes.

Females had a statistically significant faster uptake of Gadolinium than males at the tibia (p=0.03) and the calf (p=0.005) based on independent t-test results. Females also had a greater amplitude of Gadolinium enhancement at both these sites, although differences in enhancement were not statistically significant with independent t-tests.

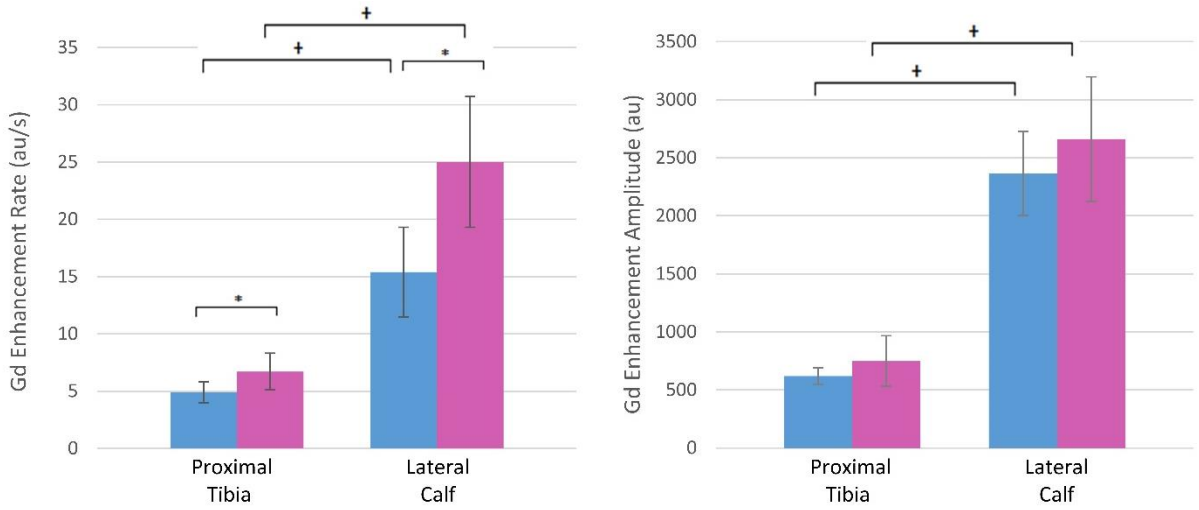

Figure 9.3: Summary of mean DCE-MRI haemodynamic markers for both the proximal tibia and calf stratified by sex (male = blue (n=20); female = pink (n=14)). Error bars represent 95% confidence intervals of mean values, * denotes statistically significant differences based on independent t-tests between sexes, + denotes statistically significant differences between tissue types.

Similar to NIRS, DCE-MRI based parameters at both the calf and proximal tibia also had some statistically significant correlations with percentage fat content in the lower leg, presented in Table 9.2. These were positive associations with r-values ranging between 0.43-0.51 ($p<0.05$) suggesting increased percentage fat content in the lower leg was associated with increased Gadolinium rate and amplitude of enhancement. Again, there may be confounding here, as females generally had increased DCE-MRI markers and also had significantly increased percentage fat content in the lower leg compared to males (mean in females 34.9% (SD8.4) versus mean in males 19.1% (SD3.9); $p<0.001$; independent t-test). Partial correlation analysis was performed to adjust for the effect of sex, and these associations between DCE-MRI markers and percentage fat in the lower leg became weaker (results presented in Table 9.2).

There were no other associations between DCE-MRI parameters at either the proximal tibia or calf and the demographic data presented in Table 8.1. As for NIRS there was little evidence of differences between those with and without T2DM for any DCE-MRI

markers at either the calf or the proximal tibia. There were also little evidence of associations between age and DCE-MRI markers at either anatomical site.

Table 9.2: Pearson correlation r-values between lower leg percentage fat content and DCE-MRI haemodynamic markers taken at the proximal tibia and lateral calf. Partial correlation coefficients are also presented adjusting for sex. Asterisks indicate a statistically significant correlation with *p*-value <0.05.

Proximal Tibia (N=29)	Gd enhancement Rate (au/s)	Gd enhancement Amplitude (au)
Lower Leg % Fat Content	0.46*	0.43*
Lower Leg % Fat Content (partial correlation adjusting for sex)	0.24	0.37*

Lateral Calf (N=33)	Gd enhancement Rate (au/s)	Gd enhancement Amplitude (au)
Lower Leg % Fat Content	0.51*	0.33
Lower Leg % Fat Content (partial correlation adjusting for sex)	0.23	0.32

9.2.1: Enhancement rate and amplitude of Gadolinium enhancement

There were positive statistically significant associations between the rate of gadolinium enhancement and amplitude of gadolinium enhancement at both the calf (r=0.64; p<0.001) and the proximal tibia (r=0.52; p=0.004). This is comparable with NIRS results where the rate of O_2Hb increase post occlusion release was strongly associated with the amplitude of O_2Hb increase post occlusion release. Figure 9.4 demonstrates these relationships.

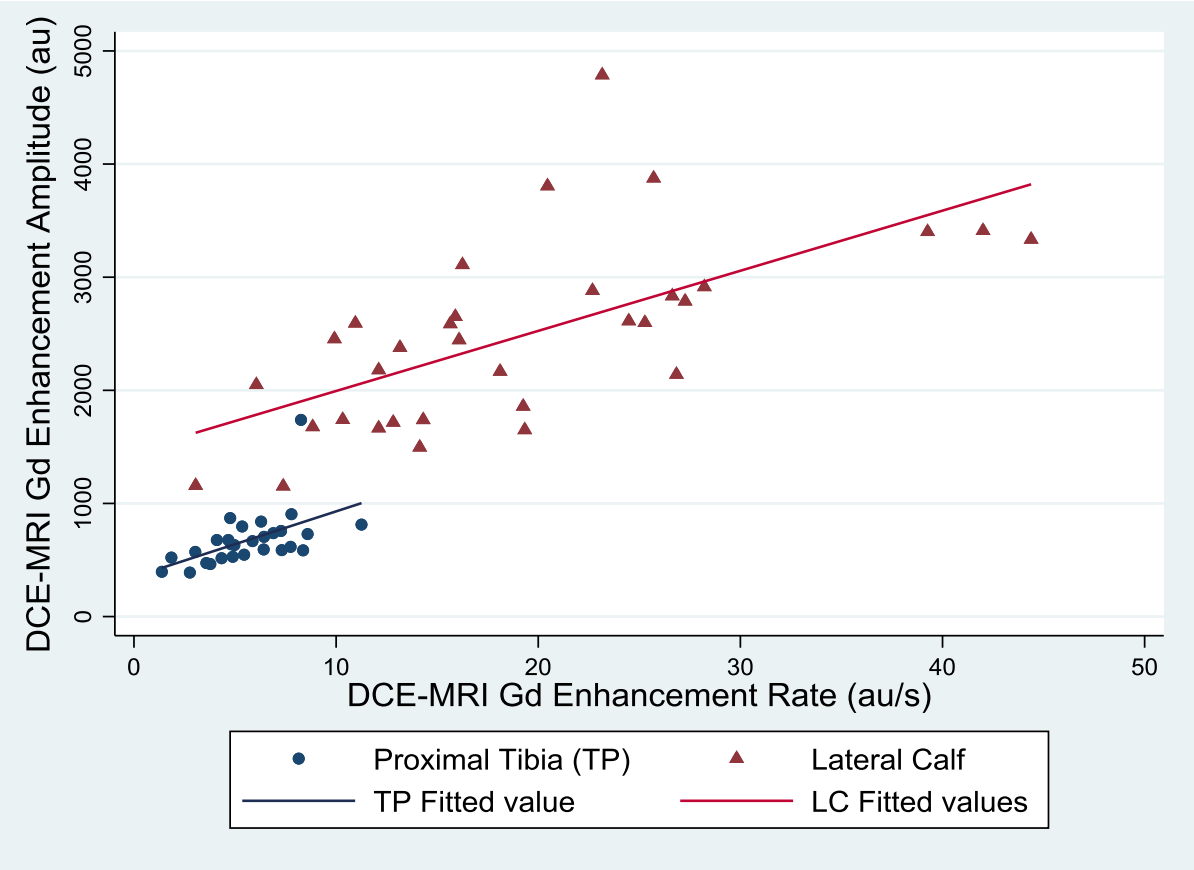

Figure 9.4: Graph demonstrating the associations between the rate of Gadolinium enhancement and amplitude of Gadolinium enhancement at both the calf (r=0.64; p<0.001) and the proximal tibia (r=0.52; p=0.004) with associated lines of best fit.

9.2.2: Proximal tibia versus calf DCE-MRI results

Analogous with NIRS results, the rate and amplitude of signal enhancement with DCE-MRI was significantly greater at the calf than at the proximal tibia. With respect to the amplitude of Gadolinium enhancement, enhancement at the proximal tibia and calf were strongly associated (r=0.60; p=<0.001). This is demonstrated graphically in Figure 9.5. It is clear there is an outlier data point which is enhancing the correlation coefficient. Without the outlier data point the correlation is weaker but still approaching statistical significance (r=0.36; p=0.06). This outlying data point has not been excluded from analysis in this section as there has been no obvious error or confounding contributor to explain it, so has been assumed to be physiologically representative of the participant. The association between the rate of enhancement at the calf and the proximal tibia was weak and non-significant (r=0.29; p=0.13). This is graphically demonstrated in Figure 9.6.

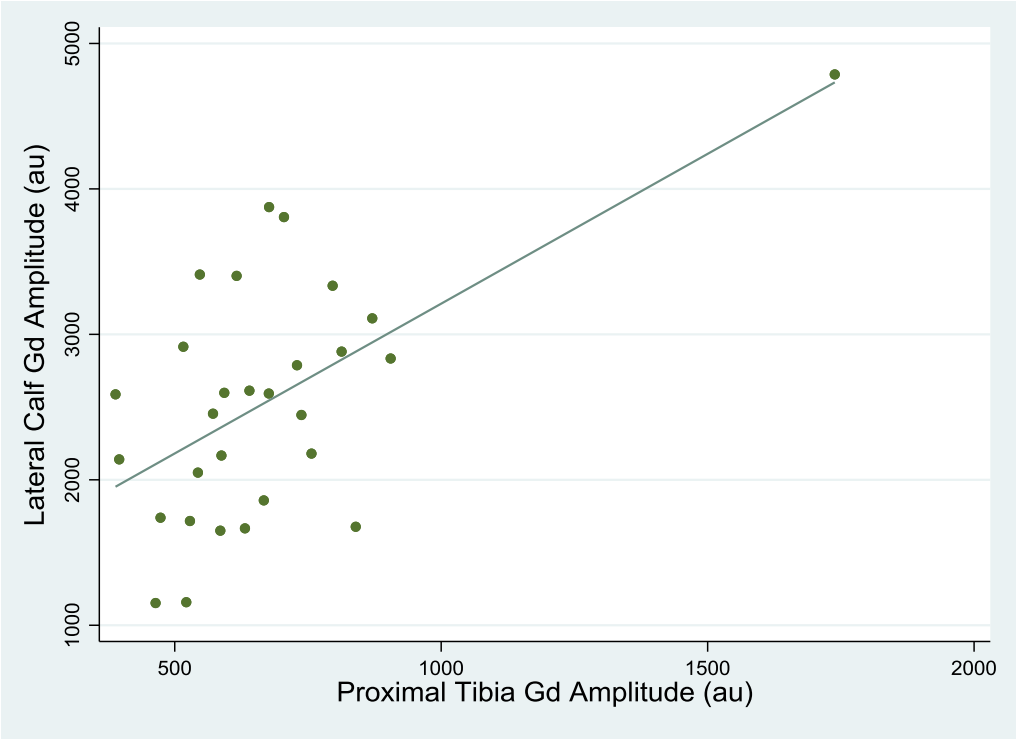

Figure 9.5: Scatterplot demonstrating the association between the amplitude of Gadolinium enhancement with DCE-MRI at the proximal tibia and calf (r=0.60; p=<0.001) and an associated line of best fit. Without the outlying data point the association is weaker (r=0.36; p=0.06).

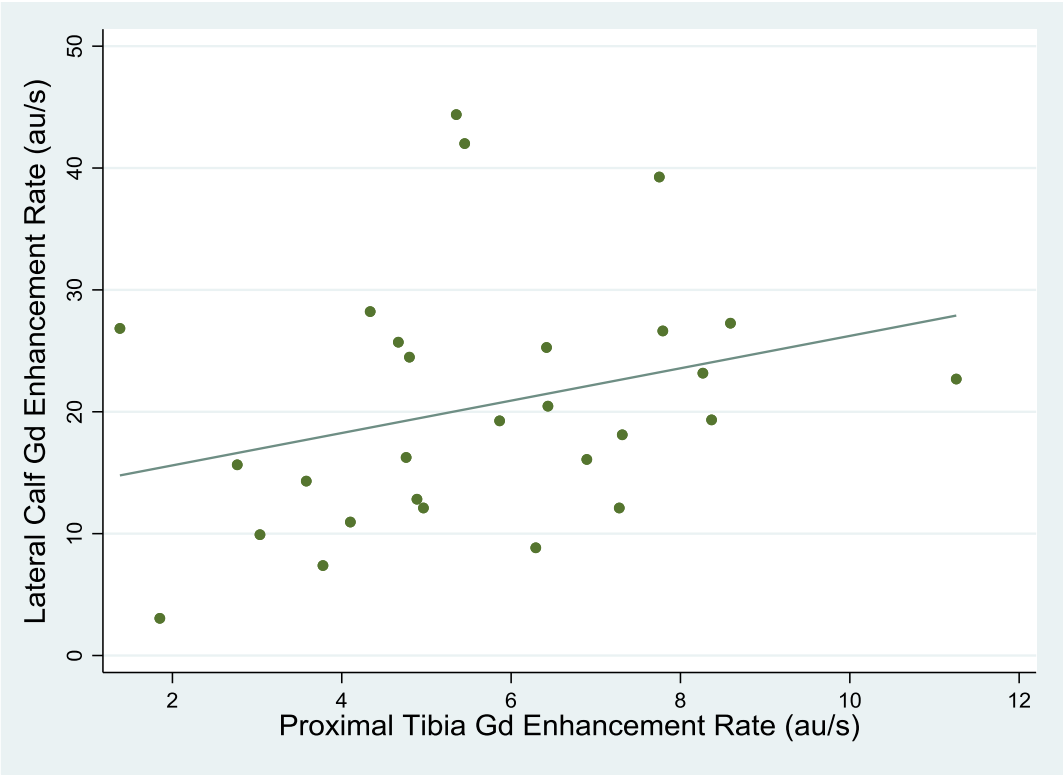

Figure 9.6: Scatterplot demonstrating the association between the rate of Gadolinium enhancement with DCE-MRI at the proximal tibia and calf (r=0.29; p=0.13) and an associated line of best fit.

9.3: NIRS versus DCE-MRI results

It is of interest to investigate whether haemodynamic markers obtained through the use of NIRS associate with those haemodynamic markers obtained with DCE-MRI in the same participants. As discussed in Section 4.9, these two tests do not measure markers of the same haemodynamic properties of tissue, but are a compromise given the existing scarcity in available techniques for measuring bone haemodynamics *in vivo.* Intuitively, if NIRS is representing bone tissue, an association between the reperfusion markers of NIRS post arterial occlusion release and the Gadolinium enhancement markers obtained at rest with DCE-MRI may be expected. This section presents the associations between these markers at both the proximal tibia (Section 9.3.1) and the calf (Section 9.3.2).

9.3.1: NIRS versus DCE-MRI at the proximal tibia

A weak negative correlation is demonstrated between the NIRS PO reperfusion rate (O_2Hb_PO_20s) and the rate of Gadolinium enhancement at the proximal tibia during DCE-MRI (r=-0.35; p=0.08). There is a similar association between the absolute concentration change of O_2Hb post occlusion release (O_2Hb_PO_absΔ) and the amplitude of Gadolinium enhancement (r=-0.27; p=0.17). These associations are presented in Figure 9.7. There was a weak non-significant association between the absolute change in TOI post occlusion release (TOI_PO_absΔ) and the amplitude of Gadolinium enhancement (r=0.10; p=0.59).

9.3.2: NIRS versus DCE-MRI at the calf

A moderate statistically significant negative correlation is demonstrated between the O_2Hb_PO_20s NIRS marker and the rate of Gadolinium enhancement at the calf during DCE-MRI (r=-0.58; p=0.001). There is a similar association between the absolute concentration change of O_2Hb post occlusion release (O_2Hb_PO_absΔ) and the amplitude of Gadolinium enhancement (r=-0.42; p=0.02). These associations are presented in Figure 9.7. There was also a significant association between the absolute change in TOI post occlusion release (TOI_PO_absΔ) and the amplitude of Gadolinium enhancement (r=-0.49; p=0.006).

(a)

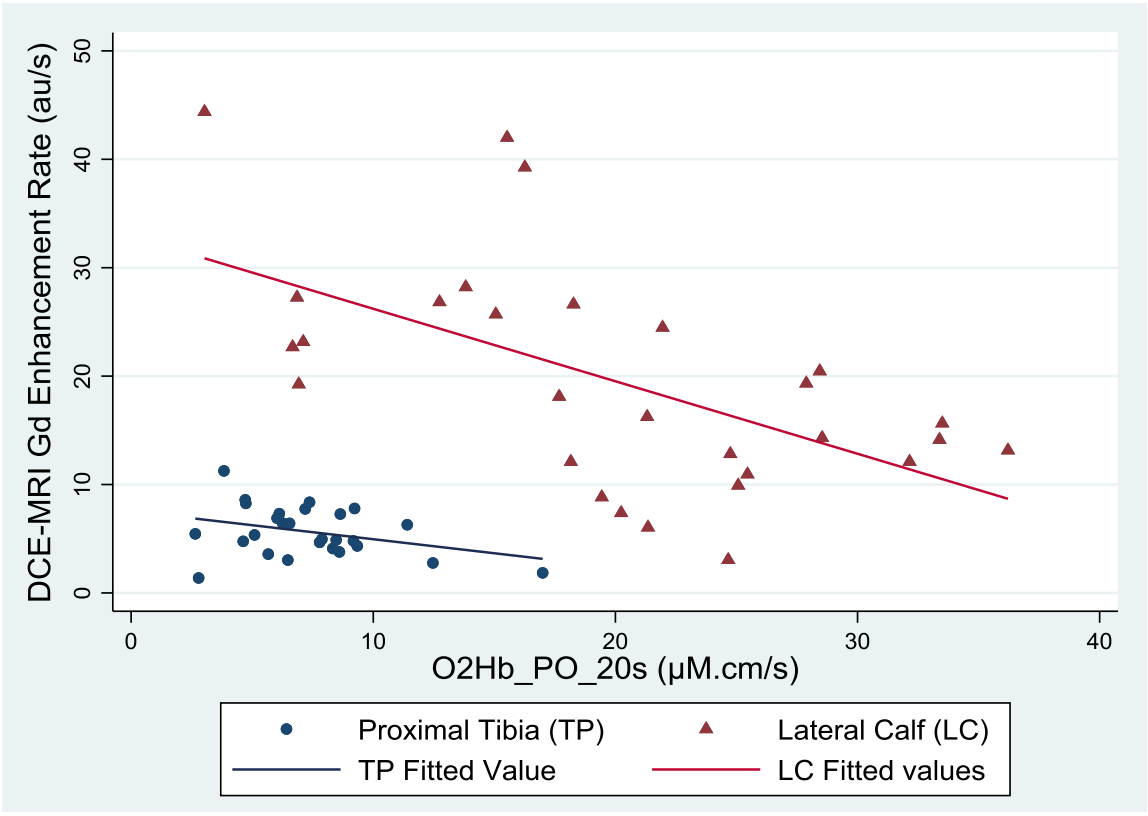

(b)

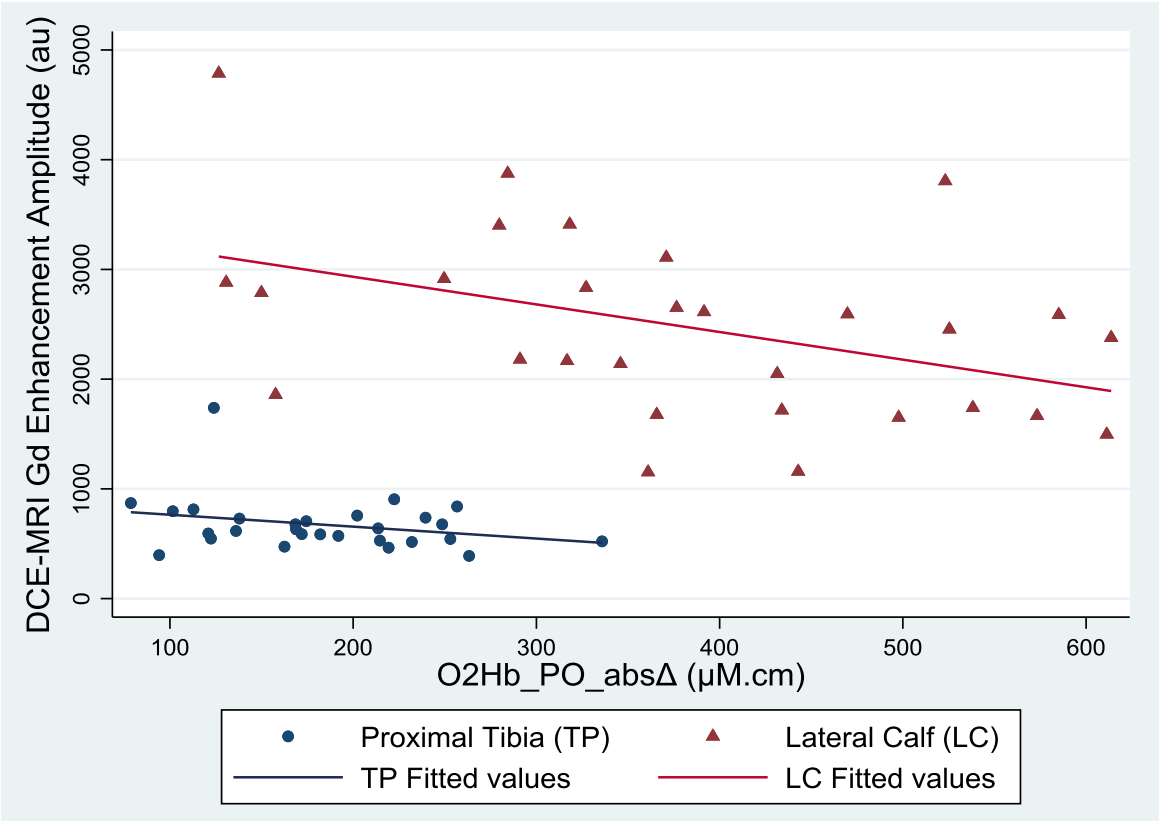

Figure 9.7: Scatter plots with associated lines of best fit demonstrating the associations between (a) O_2Hb_PO_20s NIRS marker and the rate of Gadolinium enhancement during DCE-MRI (proximal tibia r=-0.35; p=0.08; calf r=-0.58; p=0.001) (b) O_2Hb_PO_absΔ and the amplitude of Gadolinium enhancement (proximal tibia r=-0.27; p=0.17; calf r=-0.42; p=0.02).

9.4: Discussion of DCE-MRI results

Figure 9.8 presents a summary of key trends from Chapters 8 and 9. DCE-MRI results were reassuring in that they shared similar trends with NIRS data. Compared with the proximal tibia, the calf demonstrated significantly stronger results for haemodynamic markers derived from both NIRS and DCE-MRI. Analogous markers of DCE-MRI and NIRS correlated significantly at the calf, and in the same direction as associations at the tibia, although these associations were weaker at the tibia. Haemodynamic markers taken at the tibia and the calf were significantly associated with each other with both modalities. Enhancement rate and amplitude of Gadolinium enhancement were associated at both the calf and tibia, just as post occlusion markers of rate and absolute change in O_2Hb were with NIRS. Whilst not conclusive, and whilst the underlying physiological explanations for these observations cannot be definitively determined from these results, the observed results generally support that NIRS measurements may be representative of the vascular health of the proximal tibia.

Variable	Tibia (vs Calf)	T2DM (vs non T2DM)	Female (vs Male)	Increasing Fat % in Lower Leg	Increasing Age
NIRS DO Markers	↓	↔	↓	↓	↔
NIRS PO Markers	↓	↔	↓	↓	↔
Resting TOI	↑	↔	↓	↑ (calf only)	↓
Fat % in Lower Leg		↔	↑		↔
DCE-MRI Gd Uptake Rate at Rest	↓	↔	↑	↑	↔
DCE-MRI Gd Amplitude at Rest	↓	↔	↑*	↑	↔

Figure 9.8: Summary trends from Chapter 8 and 9. Arrows indicate statistically significant differences between groups, or associations between continuous variables of interest (* denotes association not statistically significant but considered clinically relevant).

The observed correlation between PO recovery rate and absolute change in O_2Hb with NIRS, as well as between the rate and amplitude of Gadolinium enhancement at rest with DCE-MRI, is consistent with the findings of Farzam et al 2014 [56]. This study found statistically significant positive correlations between total haemoglobin concentration and blood flow rates using time resolved NIRS at rest at the manubrium [56].

9.4.1: Sex

Just as for NIRS results, there were significant differences observed between the sexes with DCE-MRI haemodynamic markers. However, it was unexpected that in the case of DCE-MRI, females had a faster rate and greater enhancement of Gadolinium than males, when with NIRS females had slower DO oxygen extraction rates and weaker PO hyperaemic reactivity. This may be explained by the difference in what vascular properties these markers represent. DCE-MRI markers represent the resting blood flux, capillary density, blood volume and interstitial space within tissue that allows Gadolinium to enhance the region of interest. Whereas NIRS markers represent the oxygen extraction demand and capabilities of tissue during ischaemia, and vascular function in recovery post ischaemia.

DCE-MRI results are in line with El Rafei et al 2018, who found the initial slope of Gadolinium enhancement in muscle was over double in females compared with males in a middle aged population [362]. Savvopoulou et al 2008 identified faster Gadolinium uptake in the lumbar spine of females over 50 years of age, compared with males in the same age bracket [93]. Libicher et al 2008 found increased vascularity with DCE-MRI in areas of increased bone turnover in those with Paget's disease [117], and the post-menopausal female cohort in this PhD project also have higher bone turnover than males (markers of bone metabolism are presented in Section 10.5). Likewise Kristensen et al 2013 identified increased capillary density in areas of increased bone turnover using bone biopsies from the iliac crest [30]. As such, it may be expected that those participants with anticipated higher bone turnover (i.e. post-menopausal women) had greater Gadolinium enhancement.

This potential relationship between resting haemodynamics measured with DCE-MRI and bone metabolism may be independent of the ischaemic vascular reactivity represented by NIRS. Prisby et al 2015 identifies micro calcification of blood vessels in murine blood vessels as an example of bone tissue that may still have blood flow,

but has impaired microvascular regulatory capacity [38]. The authors propose that these microvessels in bone may be the first to calcify in the body.

Conversely, there is evidence that supports a relationship of reduced DCE-MRI markers at rest in females with lower bone mineral density [34, 36, 37]. These studies investigate the spine and hip, arguing that reductions in bone mineral density are associated with increased fatty marrow with reduced vascularity. These studies differ in that they typically had cohorts of participants diagnosed with more severe osteoporosis. It is clear that whilst significant associations between DCE-MRI and NIRS markers have been identified, the underlying microvascular explanation remains undetermined and requires more research.

9.4.2: Percentage fat content in the lower leg

The results between sexes may also partially be explained by confounding relating to the percentage fat content of the lower leg. This was significantly higher in females and also positively correlated with DCE-MRI markers of interest (as presented in Table 9.2). Gadolinium contrast was injected at a concentration determined per kilogram of body mass. Given that contrast entering the leg was therefore theoretically equalised for body mass with each participant, those with greater percentage fat may be expected to have greater signal enhancement in the calf and tibia, as fat is relatively less vascularised compared to these tissue types (demonstrated in Figure 9.9), and proportionately more concentrated Gadolinium may therefore be distributed to the remaining muscle and bone tissue.

Tyml et al. 1995 observed in a murine model that induced muscle atrophy led to a relative increase in capillary density within muscle tissue, and a subsequent increase in blood velocity caused by reduced vascular resistance. In the case of the DCE-MRI data, this may also be accentuated by increased relative percentage fat content effectively concentrating more Gadolinium in muscle tissue. This would explain greater (and faster) uptake of Gadolinium at rest, independent of reduced oxygen extraction metabolism and reduced post ischaemic response as observed by NIRS as a result of poorer muscle tone and/or vascular health [363]. A review by the same authors also provided evidence of poorer hyperaemic response associated with disuse or muscle atrophy [364].

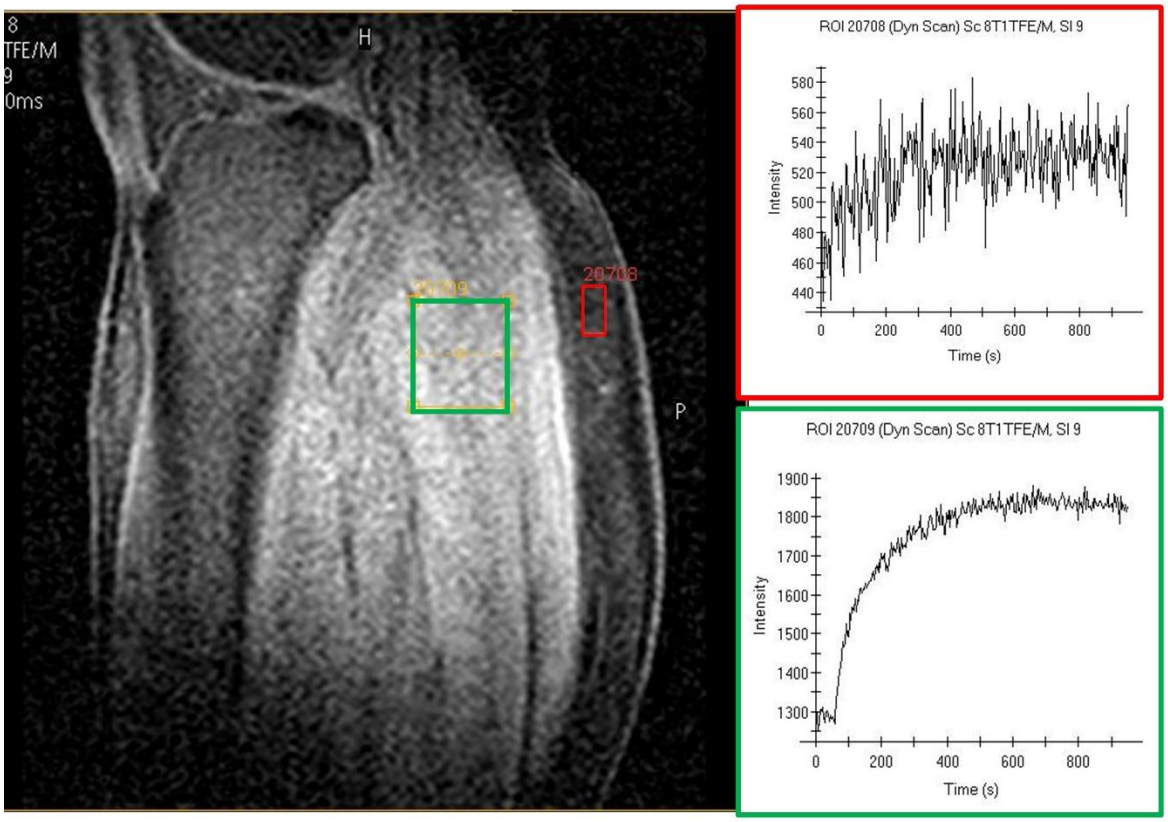

Figure 9.9: DCE-MRI enhancement curves for adipose tissue (red) and calf muscle (green) demonstrates the relatively minimal Gadolinium enhancement of adipose tissue.

Alternatively, if assumed to be a marker of poor general cardiovascular health [313], increased percentage fat content in the leg may also explain faster and greater uptake of Gadolinium at rest. Thorn et al 2016 argues increased oxygen extraction requirements at rest may be a result of mitochondrial dysfunction in those who are obese or have T2DM [65]. There is evidence within diabetes research to support this with Jan et al 2019 [365] demonstrating faster resting skin blood flow in those with T2DM compared with controls. Tibirica et al 2009 [366] demonstrates greater capillary density in skin at rest in those with T1DM compared with controls, yet impaired capillary recruitment which weakens PORH response after AO. Both articles cite impaired mechanical and myogenic vasoregulation as potential causes. Although these articles are in the context of diabetes research, they demonstrate a relationship where haemodynamic markers may be increased at rest, yet impaired with ischaemic challenge. Adingupu et al 2015 supports this with data suggesting higher resting perfusion in the skin of participants with altered microvascular reactivity during post occlusive response [271]. This could support the observations in this chapter for those

with increased relative fat content in the leg, if taken as a marker of poorer cardiovascular health.

Similarly, those with low AO responses (as a marker of poorer vascular reactivity) may also be expected to be showing signs of increased irregular microvascular permeability. van Hinseberg 1997 [367] reports increased vascular permeability being related to other indicators of poor microvascular health such as hypercholesterolemia and atherosclerosis. This pattern could also be expected in both post-menopausal females (due to the protective effect of oestrogen on endothelial health being withdrawn [368]) and those with poorer cardiovascular health (represented by increased percentage fat content in the lower leg) [369]. As such, those requiring more oxygen extraction at rest may also expect to have increased capillary permeability, which would also lead to increased uptake of Gadolinium contrast in the interstitium of tissue.

As mentioned in Section 8.4, conversely there is evidence to support that healthier tissue has increased efficiency in metabolising oxygen supply during ischaemia [336]. This may support lower resting perfusion at rest in healthier tissue (as demonstrated by slower enhancement rates of Gadolinium with DCE-MRI in those with lower percentage lower leg fat) with reduced demand for systemic oxygen supply to maintain homeostasis, yet stronger vascular regulatory responses during ischaemic events. Brizendine et al 2013 supports this potential interpretation, demonstrating a lower resting oxygen extraction rate in endurance-trained athletes [283]. Jones et al 2017 also demonstrated a reduction in resting oxygen extraction rates in participants following an endurance training regime [333].

9.4.3: Missing data

Considering the above suggestion that increased percentage fat content is associated with greater resting DCE-MRI parameters, it was of interest to note that three of the participants' data who were excluded from data analysis due to no perceivable signal enhancement in bone were males with the lowest percentage fat content (ranging between 14.8% and 16.6%). The fourth remaining participant was female with a higher percentage fat content (32.2%), but was diagnosed with osteoporosis in the lumbar spine and had the lowest tibial BMD within the cohort. It was noted that these four participants were all older (age range 61-68) with low trabecular bone scores (T-score range -1.0 to -2.2). It is unclear how missing data from these four participants may have affected the associations observed, had any minimal signal enhancement been

detectable and contributed to the data sets analysed, but this remains a potential source of attrition bias.

9.4.4: T2DM

As for NIRS results, there was little evidence of differences between those with and without T2DM for any DCE-MRI markers at either the calf or the proximal tibia. There is very little prior evidence with DCE-MRI to compare these observations with. Zheng et al. 2014 found those with T2DM had a significantly reduced oxygen extraction response and reduced muscle perfusion response to exercise when scanned using a non-contrast arterial spin labelled MRI protocol. However this was a small study of participants with a long duration of T2DM and secondary complications such as cardiovascular disease and peripheral neuropathy [370]. Two MRI-based studies cite increased marrow fat in those with T2DM, but haemodynamic parameters are not reported [22, 91].

9.4.5: Limitations

As discussed in Section 4.9 and Appendix J, the use of a BOLD MRI protocol that observes oxygenation changes in real time during AO was the initial comparator of choice. This protocol would have allowed direct comparison between BOLD MRI and NIRS AO haemodynamic markers, but was not feasible using the MRI equipment available. DCE-MRI allows measurement of haemodynamic markers representative of tissue health at rest, however these are not directly relatable to NIRS markers, which are based around changes in tissue during ischaemic challenge.

There were also a number of unavoidable limitations with the DCE-MRI protocol that may have affected the reliability of the data collected, and the ability to discern low levels of signal in the aforementioned participants with missing data. Some inaccuracies may be introduced by fixed magnetic field (B0) inhomogeneities inherent within the MRI scanner. It is not possible to quantify this error but it is likely to have been minimised as a smaller field of view was used for imaging the lower leg. Likewise, application of the radiofrequency field (B1) was likely to be imperfect with the positioning of the coil around the lower leg, leading to potential localised field inhomogeneities [99].

Imaging of cortical bone, and adjacent tissue, presents a challenge with MRI as the density of bone introduces the potential for magnetic susceptibility artefact where

differences in the local magnetic properties of adjacent tissue types can cause misregistration of signal [22, 139]. Using a higher field strength than the 1.5T scanner available for DCE-MRI protocols may improve signal to noise ratios, although tissue interface magnetic susceptibility artefacts around cortical bone could also be enhanced [109]. Perhaps more importantly, newer scanners can use faster "ultra-short" T1 sequences that can improve signal detection in bone [139]. Such developments with newer scanners could improve the temporal resolution and signal to noise ratio of DCE-MRI protocols, improving reliability [362].

Regions of interest for DCE-MRI analysis were standardised for size, but placement within the bone marrow inevitably varied between participants due to the different shape and volume of the tibia. Similar to many of the NIRS markers, it was also observed that DCE-MRI markers appeared highly variable across participants. El Rafei et al 2018 [362] also reflects that haemodynamic parameters taken in muscle using DCE-MRI were highly variable, and that variability exists even within different muscles at the hip. This has also been demonstrated using contrast enhanced ultrasound at the calf at rest [371]. Padhani et al 2002 [131] also notes a high within participant variability in DCE-MRI results and argues that this means longitudinal monitoring with DCE-MRI should be used cautiously, with a reliability component recommended inherently with any future work. This study also comments that the use of DCE-MRI may only be suitable for between group comparisons, not at an individual level [131].

Yang et al 2009 used a pharmacokinetic model to look at DCE-MRI of bone metastases [132]. This article reports wide variability within and between participants for arterial input functions which are representative of cardiac function and may affect the rate at which Gadolinium is transported by the circulatory system around the body. This is not accounted for in our non-pharmacokinetic DCE-MRI analysis.

The above markers are considered indirect descriptive quantitative representations of the haemodynamic properties of the ROI. These are not directly physiologically applicable, but rather simply quantitative descriptions of the time-signal curves obtained, which are likely to be associated with the haemodynamics of the ROI. These markers are likely to be affected inherently by a combination of factors such as the participant's cardiovascular function, blood volume, tissue perfusion and capillary permeability, but the contribution of each of these factors to the quantitative markers derived are not easily distinguished [35].

Also, due to these being inherently based around MRI signal changes, they may be susceptible to influence from the scanning parameters used and inherent features of the MRI scanner itself. In the case of this project, all participants have been scanned on the same scanner with identical scan protocols, so this does not affect comparison within the cohort of participants [107].

It is possible to make more analytical physiological measurements that are directly relatable to the haemodynamics of the ROI using pharmacokinetic modelling of the tissue of interest, such as absolute measures of capillary permeability, extravascular space, blood volume, and blood perfusion rates. However, this is much more complex analysis requiring physiological assumptions on the tissue of interest [107]. This has not been developed sufficiently in the case of bone tissue and has ruled out this approach to DCE-MRI analysis in this project. For example, El Rafei 2018 found pharmacokinetic markers had reduced reliability compared with indirect descriptive markers when assessing DCE-MRI data for muscles at the hip [362].

One inherent potential source of variability between participants is the properties of bone marrow within the measured ROI and whether the bone marrow sampled is haematopoietic red marrow or fatty yellow marrow, which are known to have varied fat composition, blood volume and blood flow rates [8, 22, 260]. Biffer et al 2010a suggests correcting signal readings based on initial fat content as water/fat content influences signal and can be highly variable depending on age, sex, bone health, and marrow type [354]. However, all participants were over the age of 40, and therefore past the age of peak bone mass, and with standardised positioning of NIRS probes at the proximal tibia, the risk of different marrow types being sampled between participants is believed to be minimised. This was confirmed by the low variance in bone marrow fat fraction reported in MRS results presented in Section 9.1.

Typical enhancement patterns with DCE-MRI were similar with all participants regardless of BMD, demonstrating a fast initial uptake and then slower continuous uptake or eventual plateau (see Figure 9.10). Budvik et al 2014 supports that this pattern of enhancement is suggestive of yellow marrow being measured, as red marrow typically displays a contrast “washout” phase due to a faster blood flow and more extensive and dynamic capillary bed [109, 260]. Ma et al 2010 argues that slow washout may be induced by increased presence of fat in marrow, which may limit interstitial diffusion and potentially increase intraosseous pressure [372]. This is supported by the MRS results presented in Section 9.1 which report consistently high

relative fat content in the sampled area of bone marrow across all participants (fat fraction range 91.2% to 98.5%), suggesting fatty yellow marrow was present in the measured ROI. As such, it is considered unlikely that the relative adiposity of bone marrow was a confounding factor in DCE-MRI results for the sampled population.

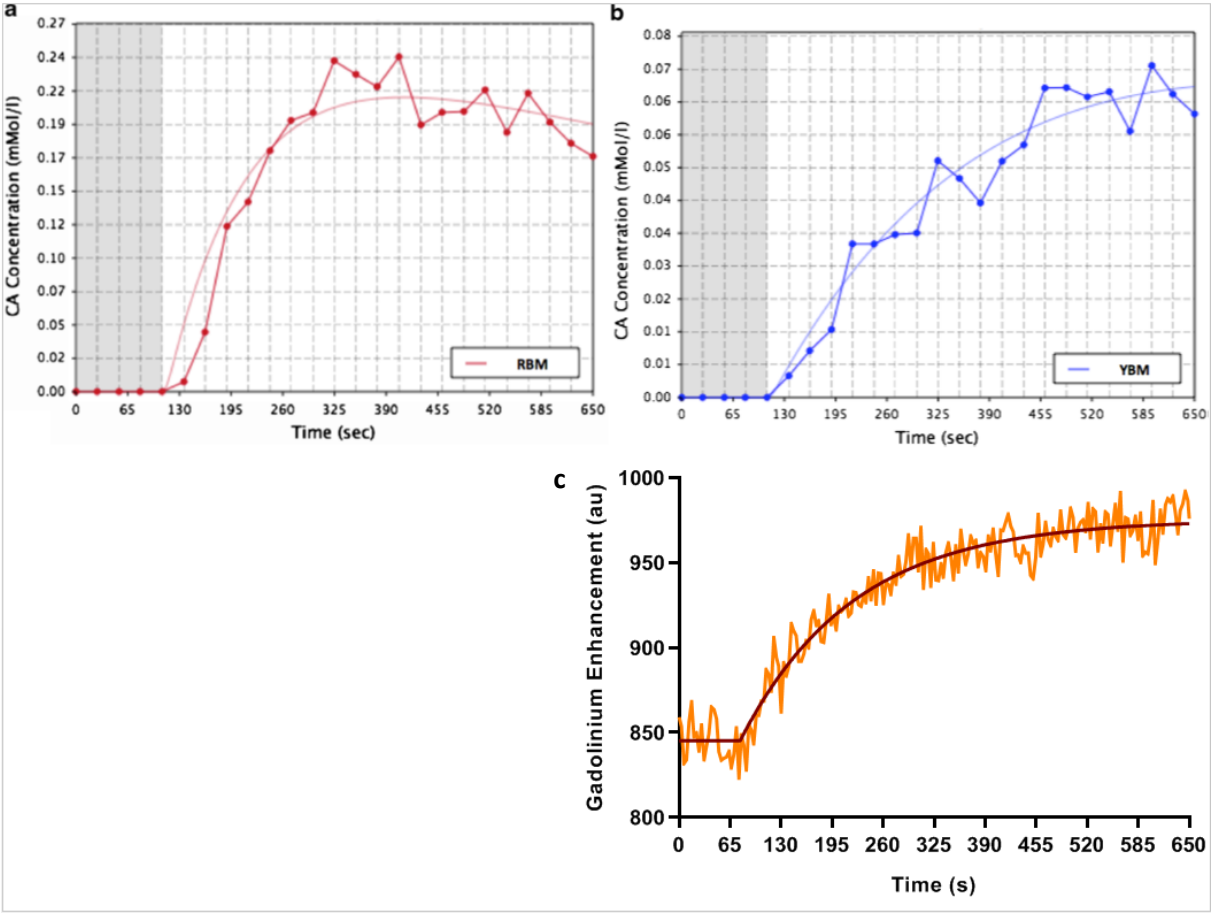

Figure 9.10: Enhancement curves, reproduced with permissions from Budvik et al 2014 [109] typical of (a) red marrow demonstrating Gadolinium washout, and (b) yellow marrow demonstrating more gradual enhancement in keeping with the observed enhancement profiles at the proximal tibia in this PhD study, demonstrated in (c).

The proximal tibia was selected as a weight bearing bone site that represents trabecular bone, which is typically associated with the presence of red marrow at axial and proximal long bone sites [353]. However, MRS results suggest yellow marrow is being sampled. This remains a limitation of the study as sampling more vascular dynamic red marrow is desirable. This remains difficult with the limitation of measurement depth with NIRS and ideal red marrow sites such as vertebrae and the proximal femur. The sternum offers a red marrow site, however simulating ischaemic challenges at this central site is difficult. Despite this, the results obtained still facilitate the primary aim of the project, i.e. associating NIRS haemodynamics markers with other markers of bone health, including DCE-MRI analysis at the same anatomical site.

9.5: Chapter summary

This chapter has outlined the results obtained with MRS and DCE-MRI protocols taken at the same anatomical sites as NIRS measurements. Comparison has been made with reliable NIRS haemodynamic markers taken at the lateral calf and the proximal tibia during and after an arterial occlusion protocol applied at the distal thigh.

MRS results confirmed that yellow marrow was being sampled by NIRS in all participants. NIRS markers were associated with analogous DCE-MRI markers, however this was an unexpected negative association. Identifying potential causal explanations for these associations is difficult with a small but varied existing evidence base to consider. There are also inherent limitations to the two vascular testing methods, and potential confounding variables (such as sex-dependent differences and percentage fat content in the lower leg), as well as other bone health markers to consider (e.g. bone mineral density, trabecular bone score, and bone metabolism) discussed further in Chapter 10.

Whilst the haemodynamic results presented leave a number of questions around the vascular physiology of bone unanswered, the results in this chapter have identified the potential merit in further exploration of NIRS as a research tool for investigating haemodynamics in bone.

Chapter 10: Validation of NIRS against markers of bone health

10.1: Overview

This chapter will provide a descriptive summary of the bone health markers obtained from participants including bone mineral densitometry measurements (Section 10.2); trabecular bone scoring (Section 10.3); FRAX scores (Section 10.4); and, blood markers of bone metabolism (Section 10.5). These sections will also include associations between NIRS markers and discussion of potential explanatory relationships.

10.2: Bone mineral densitometry

Table 10.1 presents the descriptive results of areal bone mineral density (BMD) measurements and related DXA results taken at various different anatomical sites, as per the protocol outlined in Section 6.2.5.

Table 10.1: Summary of mean areal bone mineral densitometry (BMD in g/cm^2) and associated DXA results, including sub groups based on type 2 diabetes mellitus (T2DM) status (standard deviation in parentheses). *p*-values are from independent t-tests between those with and without T2DM.

	Total (N=36)	T2DM (n=18)	Non-T2DM (n=18)	*p*-value between sub groups
L1-L4 BMD	1.168 (0.150)	1.198 (0.125)	1.138 (0.170)	0.24
Average Hip BMD	1.049 (0.124)	1.074 (0.111)	1.025 (0.135)	0.24
Total Body % Bone	3.847 (0.447)	3.850 (0.417)	3.843 (0.487)	0.96
Total Body % Fat	31.56 (7.70)	30.86 (6.60)	32.26 (8.81)	0.59
Total Body BMD	1.237 (0.096)	1.245 (0.081)	1.229 (0.110)	0.62
Both Legs BMD	1.369 (0.142)	1.377 (0.107)	1.361 (0.173)	0.75
Whole Tibia BMD (measured leg)	1.251 (0.144)	1.253 (0.125)	1.250 (0.165)	0.94
Proximal Tibia BMD (measured leg)	0.982 (0.112)	0.984 (0.107)	0.979 (0.120)	0.91
Lower Leg % Fat Content	25.2 (9.8)	23.4 (7.5)	27.1 (11.6)	0.26

There was little evidence of differences between those with and without T2DM for all DXA measurements (see Table 10.1), although it can be seen that those with T2DM typically have higher BMD results across most measurement sites. There were some expected associations observed such as positive associations between BMI and BMD at all sites (r-values ranging between 0.01 and 0.27). These were weak and statistically non-significant, likely influenced by the small overall sample size of participants, all with BMI less than 35 kg/m^2. There was also weak to moderate negative correlations between menopausal duration and BMD at all lower limb sites, as expected (r-values ranging between -0.32 to -0.58; p-values ranging between 0.27 to 0.03).

Table 10.2 shows that males had higher BMD across all sites, and statistically significant higher total body BMD, leg BMD, tibial BMD, and overall percentage bone tissue. This was expected with the known sex-dependent BMD changes associated with the post-menopausal women recruited in this study [8]. Males also had significantly reduced total body fat percentage and lower leg fat percentage.

Table 10.2: Summary of mean areal bone mineral densitometry (BMD in g/cm^2) and associated DXA results including sub groups based on sex status (standard deviation in parentheses). *p*-values are from independent t-tests between sexes, * denotes statistical significance of *p*-value <0.05.

	Total (N=36)	Males (n=22)	Females (n=14)	*p*-value between sub groups
L1-L4 BMD	1.168 (0.150)	1.189 (0.152)	1.135 (0.146)	0.30
Average Hip BMD	1.049 (0.124)	1.068 (0.103)	1.019 (0.151)	0.25
Total Body % Bone	3.847 (0.447)	4.008 (0.307)	3.594 (0.522)	0.005*
Total Body % Fat	31.56 (7.70)	26.85 (3.74)	38.96 (6.38)	<0.001*
Total Body BMD	1.237 (0.096)	1.273 (0.080)	1.179 (0.091)	0.003*
Both Legs BMD	1.369 (0.142)	1.441 (0.102)	1.256 (0.123)	<0.001*
Whole Tibia BMD (measured leg)	1.251 (0.144)	1.320 (0.123)	1.144 (0.106)	<0.001*
Proximal Tibia BMD (measured leg)	0.982 (0.112)	0.999 (0.117)	0.957 (0.105)	0.30
Lower Leg % Fat Content	25.2 (9.8)	19.1 (3.9)	34.9 (8.4)	<0.001*

Supplementary data were collected on the cortical area of bone, acquired from axial MRI scans as outlined in Section 6.2.4. Table 10.3 presents these results. It can be seen that there was no significant difference between those with and without T2DM. As expected, males had a significantly larger cross sectional area of bone at the proximal tibia, in line with their significantly greater height (reported in Table 8.2).

Table 10.3: Summary of mean total bone area and cortical bone area (in mm^2) of the axial plane of the proximal tibia at the site of NIRS measurements including sub groups based on T2DM and sex status (standard deviation in parentheses). *p*-values are from independent t-tests between sub groups, * denotes statistical significance of *p*-value <0.05.

	Total (N=35)	T2DM (n=18)	Non-T2DM (n=17)	*p*-value between sub groups
Total Bone Area (mm^2)	939.9 (243.1)	871.8 (170.0)	1012.0 (290.1)	0.09
Cortical Bone Area (mm^2)	320.7 (59.2)	317.0 (46.9)	325.0 (73.0)	0.74

	Total (N=35)	Males (n=21)	Females (n=14)	*p*-value between sub groups
Total Bone Area (mm^2)	939.9 (243.1)	1030.2 (255.2)	804.3 (146.3)	0.005*
Cortical Bone Area (mm^2)	320.7 (59.2)	350.3 (44.6)	280.4 (53.6)	0.001*

10.2.1: NIRS results versus BMD

There were a number of statistically significant moderate positive associations between NIRS markers and BMD at various measurement sites. Table 10.4 presents a matrix of these associations. As discussed in Section 8.3.5, it is generally accepted that stronger DO and PO responses are indicators of better vascular health, and this appears consistent with the results in Table 10.4 as increased response in AO NIRS markers are significantly associated with higher BMD at several anatomical sites, and cortical area at the proximal tibia. Conversely, several NIRS markers show a reduced NIRS response is significantly correlated with higher body fat and lower limb fat percentages.

Table 10.4: Pearson correlation r-values between haemodynamic NIRS markers taken at the proximal tibia and areal bone mineral density (BMD in g/cm^2) results at different measurement sites. Measurements of percentage tissue composition and cross-sectional area (in mm^2) are also presented. Asterisks indicate a statistically significant correlation with *p*-value <0.05. Associations colour coded were statistically significant and considered poor (<0.40; orange), moderate (0.4-0.6; yellow) and strong (>0.60; green) based on the criteria set out in Evans 1996 [304].

	TOI_rest	TOI_DO_60s	HHb_DO_60s	O_2Hb_DO_absΔ	TOI_PO_absΔ	O_2Hb_PO_20s	O_2Hb_PO_absΔ
L1-L4 BMD	0.09	0.17	0.22	-0.24	0.25	0.38*	0.45*
Total Hip BMD	0.03	-0.08	0.39*	-0.16	0.00	0.30	0.38*
Total Body % Bone	0.00	0.07	0.46*	-0.41*	-0.03	0.38*	0.39*
Total Body % Fat	-0.12	0.12	-0.34*	0.63*	0.11	-0.34*	-0.42*
Total body BMD	0.08	0.02	0.43*	-0.51*	0.01	0.42*	0.56*
Both legs BMD	0.16	-0.01	0.44*	-0.63*	-0.05	0.45*	0.57*
Whole Tibia BMD (measured leg)	0.20	-0.03	0.33	-0.55*	0.02	0.37*	0.44*
Proximal Tibia BMD (measured leg)	-0.01	0.14	0.44*	-0.09	-0.22	0.24	0.28
Lower Leg % Fat Content	-0.13	0.15	-0.31	0.63*	0.08	-0.44*	-0.57*
Total Bone Area (mm^2)	0.26	-0.39*	0.26	-0.33	-0.16	0.08	0.13
Cortical Bone Area (mm^2)	0.15	-0.06	0.39*	-0.63*	-0.08	0.42*	0.59*

Bearing in mind there was little evidence of differences in BMD between those with and without T2DM (demonstrated in Table 10.1), Figure 10.1 explores the T2DM status with respect to one of the strongest correlations identified in Table 10.3 between $\Delta O_2Hb\_DO\_abs\Delta$ and BMD of both legs (r=-0.63; p<0.001); Correlations in those with and without T2DM appear to be comparable.

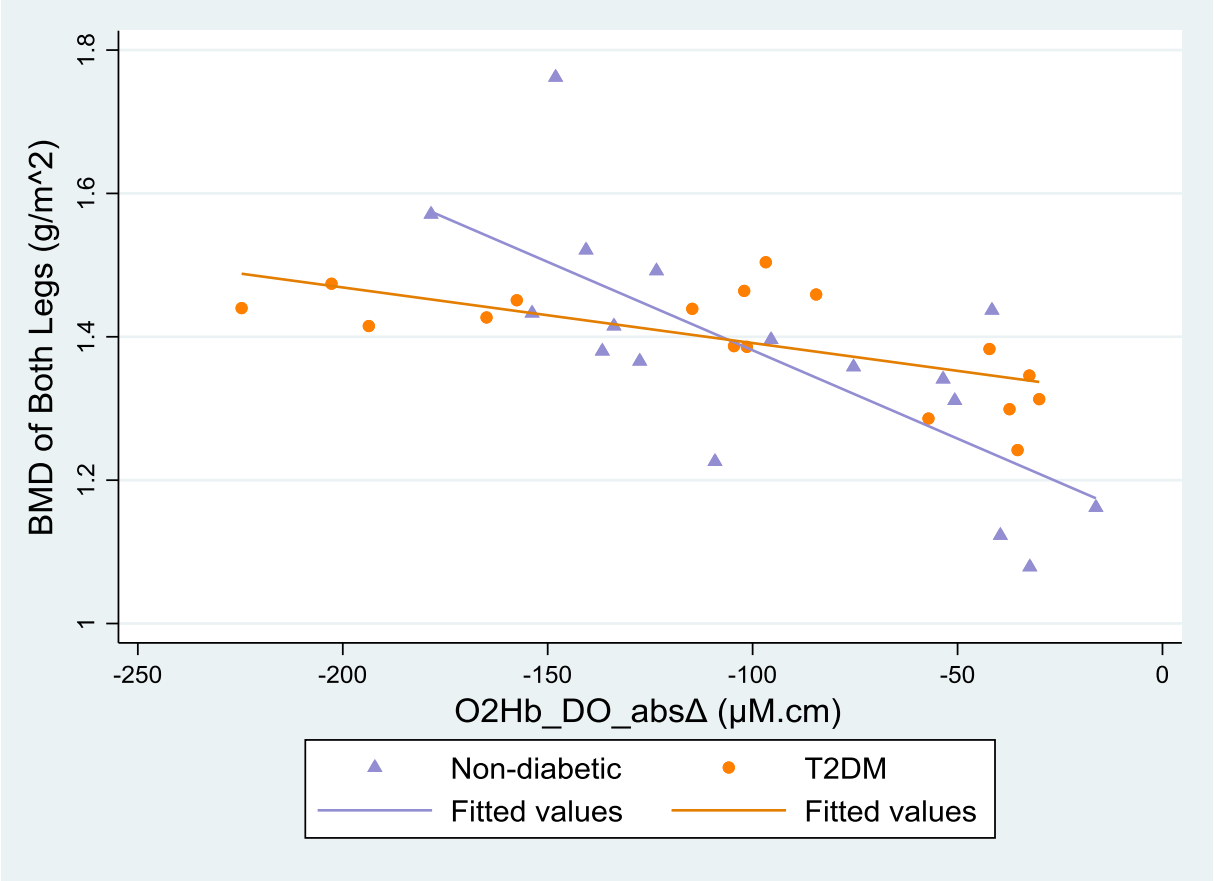

Figure 10.1: Scatter plot of $O_2Hb\_DO\_abs\Delta$ at the proximal tibia and BMD of both legs (r=-0.63; p<0.001). Sub group associations and lines of best fit are presented for those with T2DM (r=-0.66; p=0.003) and those without T2DM (r=-0.74; p=<0.001).

Figures 10.2 and 10.3 explore sex subgroups with respect to two of the strongest BMD correlations identified in Table 10.4: $\Delta O_2Hb\_DO\_abs\Delta$ and BMD of both legs (r=-0.63; p<0.001); and, $O_2Hb\_PO\_abs\Delta$ and total body BMD (r=0.56; p<0.001). Correlations in males appear to be slightly weaker. However perhaps more interestingly, these figures show an obvious difference between sexes in terms of absolute values.

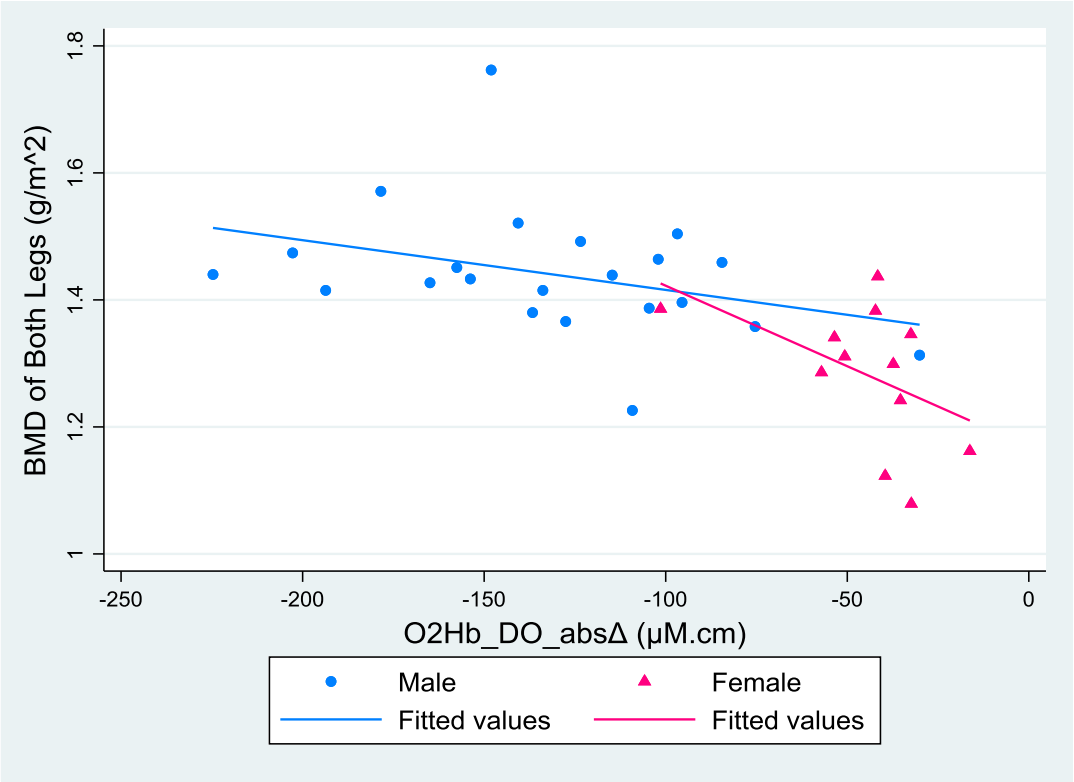

Figure 10.2: Scatterplot of O_2Hb_DO_absΔ of the proximal tibia and BMD of both legs (r=-0.63; p<0.001). Sub group associations and lines of best fit are presented for males (r=-0.35; p=0.11) and females (r=-0.47; p=0.01).

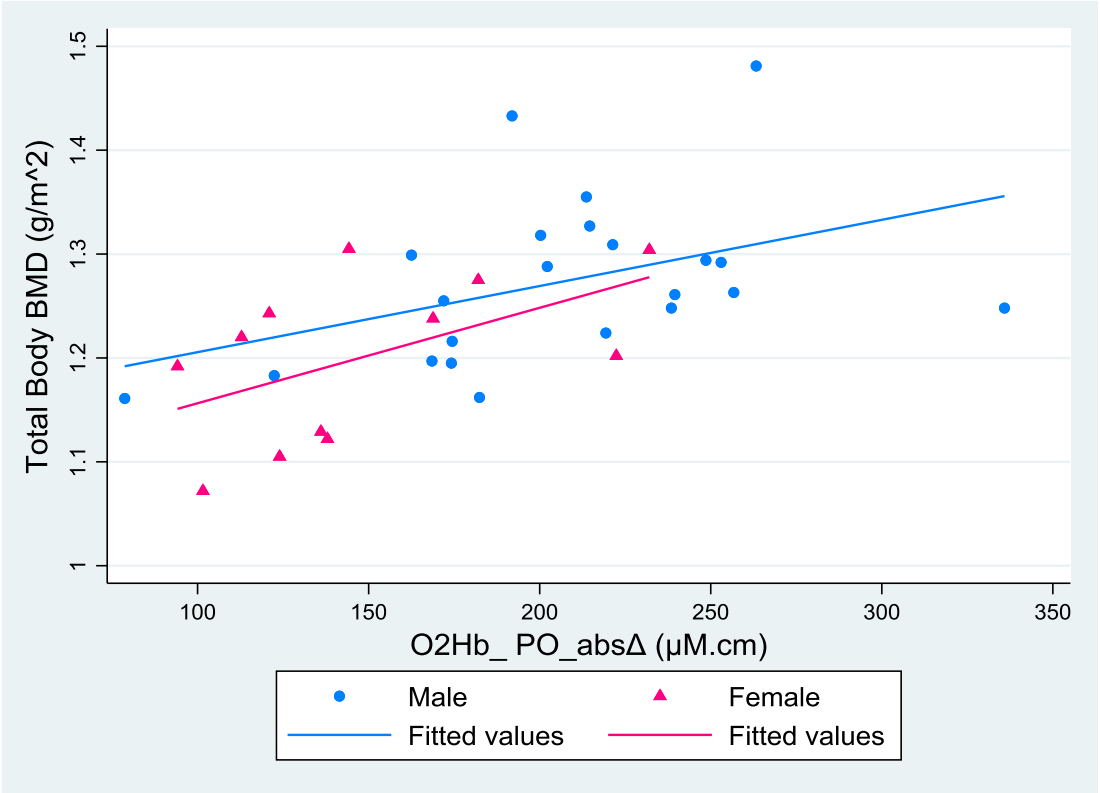

Figure 10.3: Scatter plot of O_2Hb_PO_absΔ at the proximal tibia and total body BMD (r=0.56; p<0.001). Sub group associations and lines of best fit are presented for males (r=0.42; p=0.05) and females (r=0.52; p=0.08).

10.2.2: Discussion

Statistically significant correlations were identified between DO and PO markers of NIRS and BMD measurements of the whole body, legs, lower leg, and proximal tibia measurement site. These suggest that stronger AO responses, indicative of stronger oxygen extraction DO and better microvascular regulatory function PO, associate with higher BMD. Associations of a similar magnitude were also evident between DCE-MRI haemodynamic markers and BMD measurements taken at multiple sites. For brevity, these results are presented and discussed in Appendix S.

Associations were often statistically significant but weaker for the clinically relevant spine and hip, but this is perhaps to be expected as they are different regions of the body, and regional variation in BMD and bone composition at specific anatomical sites is known to exist. For example, Clarke 2008 reports the ratio of cortical bone to trabecular bone may vary highly from 1:3 at vertebral bodies to 19:1 at the long bone diaphysis [(17)].

Associations were also generally weaker at the proximal tibia site, despite being the most closely aligned anatomical site with NIRS measurements. This may be due to increased error introduced by the smaller volume from which BMD measurements were calculated. Knapp et al 2012 also observed precision error was close to double when measuring the femoral neck, compared to the total hip [(300)]. In keeping with this it may be expected that BMD measurements of the whole tibia and legs were more reliable for comparisons with NIRS, incorporating a wider bone volume.

It is physiologically intuitive that poor microvascular function may precede poor bone density as regulatory bone metabolism is inherently linked with microvascular processes, as discussed in Section 1.5.2. However, to date there is little direct evidence of this causal pathway *in vivo* in humans, in part due to the difficulties of measuring haemodynamics in bone tissue that this study seeks to investigate. As the results presented in this section only represent association between NIRS markers and BMD (as opposed to causation), it is pertinent to consider potential confounding variables. For example, even if not truly directly associated, positive associations between microvascular health and bone density may be expected given the number of shared environmental and lifestyle factors that promote (or are a risk) to both positive cardiovascular health and bone health. For example, high levels of weight bearing

exercise would independently promote both improved cardiovascular fitness, whilst also stimulating increased BMD [373].

10.2.2.1: Bone attenuation properties as a confounder

It is observed from Table 10.4 that there were no significant associations between TOI markers and BMD at any anatomical site. This may be an important technical observation requiring consideration for future research. As identified in Chapter 7, TOI markers had low ICC results at the proximal tibia, most likely due to relatively small between-participant variance. It is therefore not surprising to see lower correlation results with BMD if TOI markers have small variance across the sampled participants.

Appendix S supports that haemodynamic differences between participants did truly exist, with DCE-MRI haemodynamic results also correlating with BMD measurements. This raises the question why TOI markers (which are derived using spatially resolved spectroscopy (SRS) methods) do not have significant associations, whilst modified Beer Lambert (MBL) derived markers have produced moderate statistically significant associations.

This may be explained in part by the differences in how NIRS markers are derived. As previously discussed in Section 2.2.1.3, Equation 2.4 (restated below) outlines how MBL parameters are derived:

$$\Delta A = \varepsilon . \Delta c . d . B$$

MBL parameters such as HHb and O_2Hb concentration change are measured by changes in light intensity (ΔA) that indicate changes in the concentration of oxygenated or deoxygenated haemoglobin (Δc), based on the assumption that the attenuation properties of the volume (represented by the specific extinction coefficient (ε)) are constant, as is the distance between the optodes (d) and the differential pathlength factor (B) of NIR photons [2]. This assumption is more likely to hold for longitudinal within-participant comparisons, but when between-participant comparisons are made, as with the results in this chapter, changes in HHb and O_2Hb may potentially be confounded by differences in the attenuation properties of bone. It may be that the associations between MBL derived parameters and BMD measurements are confounded by the differences in attenuation properties of bone between participants, which intuitively would be likely to also be linked with BMD and cortical cross-sectional area at the proximal tibia. Takeuchi et al 1997 has demonstrated in an *ex vivo* study

that absorption and reduced scattering coefficients of bone are directly associated with BMD using a time resolved spectroscopy system [374].

There is very little evidence around representative absorption and scattering properties of bone in the existing evidence base. Examples previously presented in Table 3.3 demonstrate a wide range of obtained values, which may be indicative of methodological variation (and the difficulties of obtaining these data using existing methods) or a true wide range of attenuation properties of bone across the population (or both). For example, Farzam et al 2014 presents a highly variable range in absorption coefficients at the manubrium between 0.06 cm^{-1} and 0.22 cm^{-1} and a reduced scattering coefficient range between 8.3 cm^{-1} and 12.6 cm^{-1} across 32 participants [56]. Table 3.3 results also highlight the potential differences in attenuation properties of different bone sites.

Another complicating factor is that different participants also have a different thickness of cortical bone within the measured NIRS volume. This variable thickness of denser bone could also alter NIR attenuation, independent of inherent differences in the attenuating properties of cortical bone between participants. Changes in SRS parameters involving TOI were not affected by the same confounding as these indicate a change in oxygenation status calculated independent of the scattering properties of bone, as described in Section 2.2.1.4. Binzoni et al 2003 also argues differences in cortical thickness should still be normalised in the case of SRS-derived NIRS measurements [189]. The lack of variation between participants may also be explained by TOI parameters being a ratio value of oxygenated to total haemoglobin, and therefore normalised for blood volume changes. This may limit TOI parameters at distinguishing response between participants if absolute concentration changes in O_2Hb and/or HHb are being normalised for between-participant comparisons [61].

If the use of NIRS in bone is to be developed, future research will need to involve determination of how much variation in attenuation properties exists in bone, and how this can be compensated for when trying to produce NIRS measurements solely representing haemodynamic changes. Attenuation properties of tissue are also dynamic and will be affected by fluid shifts within the measured volume. Farzam et al 2013 demonstrated up to 3.5% variation in the absorption coefficient of the patella during pulsatile flow, attributing this to the 3.1% change in total haemoglobin concentration during pulsatile blood volume changes [15].

This issue is not unique to bone tissue and there is evidence of variation in muscle and skin attenuation properties across the general population [1]. These tissue types should in principle have less variation as they are more homogenous in structure than bone, however there has still been shown to be significant variation across participants. Van Beekvelt et al 2017 [73] assumed constant attenuation properties between participants in their investigation of NIRS derived haemodynamics at the forearm, adopting a constant differential pathlength factor of 4.0 between participants. The authors estimated differences in attenuation properties in muscle may have attributed to up to 12% variation in between-participant results based on the published range of differential path length factors for muscle (ranging between 3.59 and 4.57).

Section 11.3 discusses future technological improvements in NIRS utilising frequency domain and time resolved NIRS systems that are able to determine the absorption and scattering properties of sampled bone tissue in real time, providing markers of haemoglobin change independent of changes in attenuation properties of the volume sampled.

In the case of this study, the inability to rule out confounding from changes in attenuation properties is a limitation. However given the demonstrated association with BMD, the results in this section still show the potential utility of NIRS. With potential improvements in NIRS technology, discussed further in Chapter 11, NIRS systems could facilitate both bone density and microvascular information in a point of care diagnostic device, and explore if differences in bone properties are confounding MBL derived NIRS parameters.

10.2.2.2: Other potential limitations of NIRS markers

It was observed that the strongest associations were demonstrated involving the two O_2Hb markers based on absolute concentration change DO and PO. This was interesting to note and was not expected, as the total change in concentration should be closely linked with the rate of change, if assuming linear observations. A potential explanation is that as the O_2Hb_DO_absΔ marker is taken over the full four minute occlusion period, and the O_2Hb_PO_absΔ marker taken up to maximum hyperaemia, and these two markers may better represent these periods during and post induced ischaemia, than the rate markers taken over 60 seconds (DO) and 20 seconds (PO).

Previous evidence in muscle and skin has demonstrated differing periods of response during 3-5 minute occlusions, with initial oxygen extraction in the first 60 seconds

occurring faster than the final 60 seconds [65, 276]. Corretti et al 2002 reports that vasodilation does not peak until around three to four minutes, remaining relatively constant only after reaching this maximal dilation [375]. The influence of different phases of ischaemic response mediated by different physiological regulatory responses (such as endothelial, myogenic or neurogenic responses) also regulate at different frequencies [28, 376]. Clough et al 2017 demonstrated using LDF that the time constant of myogenic and sympathetic response is quicker than endothelial-derived responses, and as such vascular response to occlusion induced ischaemia may be phased or non-linear, although it is very difficult to demonstrate the individual contributions of these different physiological responses in the artificial conditions of an arterial occlusion [28].

Alternatively oxygen extraction rates may also vary as the available oxygenated haemoglobin levels and localised cellular demand of oxygen dynamically change during the occlusion. As such, NIRS measurements within the last 60 seconds of the occlusion period, and first 20 seconds post occlusion may not be representative of the full time period in terms of ischaemic response in tissue.

10.2.2.3: T2DM

As discussed in Chapter 8, there was little evidence of differences between those with and without T2DM for any NIRS parameter. Likewise, there was little evidence of differences in BMD, although those with T2DM typically had higher BMD and lower TBS (presented below in Section 10.3) as expected [32, 46]. A review by Moayeri et al 2017 reports that fracture risk was positively associated with T2DM of duration greater than 10 years, insulin therapy and corticosteroid use, which was generally not applicable to the participants in this study. The review found T2DM was a predictive risk factor for fracture risk with a relative risk of 1.20 (95% CI 1.17 to 1.23). However, 8 of 30 studies included in the review found no difference between fracture risk in those with and without T2DM, suggesting there may be regional genetic or lifestyle variations that are potentially unexplored confounders [377]. Lasschuit et al 2019 found those with T2DM with fragility fracture were more likely to have dyslipidaemia, cerebrovascular disease and/or chronic renal disease than those without T2DM with fragility fracture, which again did not generally apply to the sample of those with T2DM included in this PhD project [53]. It has been proposed that those with T2DM may even have reduced risk in the initial years following diagnosis (although this may be confounded by increased BMI) [50]. The recruited sample of participants with T2DM may have had a mean T2DM duration that was too short (mean 6.2 years SD 4.5) to identify significant

differences, or their well-controlled diabetes and general lack of co-morbidities may have introduced bias.

10.2.2.4: Sex

Although the strength of associations between NIRS and BMD measurements were similar between sexes, there was an obvious difference between sexes in absolute terms. As a sub group, female participants had lower BMD at all anatomical sites, and lower NIRS-derived haemodynamic markers.

This may be explained by post-menopausal changes, with evidence to suggest reduced oestrogen levels can affect both BMD and microvascular function. Majmudar et al 2000 reports post-menopausal women have reduced flow mediated vessel dilation, representative of reduced endothelial response, associated with reduced vaso-protective oestrogen levels [(378)]. Prisby et al 2017 outlines the role of oestrogen in regulating normal bone turnover, promoting osteoblast activity and inhibiting bone resorption [(8)]. Prisby et al 2012 demonstrates a close association between these two oestrogen dependent effects, demonstrating reduced vascular endothelial function and reduced trabecular bone volume in an experimental murine study design [(42)].

However, given the observed greater relative fat content in the whole body and the lower limbs of females, lifestyle factors around fitness and exercise levels may also be confounding here, as this would be expected to affect both vascular NIRS measurements and BMD levels [(313)]. Unfortunately, this information was not gathered from participants but it is deemed more likely that sex-based differences are likely to cause the observed differences than a higher percentage fat content in the leg. Bradbury et al 2017 demonstrates that females are expected to have a greater percentage fat content than males when controlling for activities levels. The mean percentage body fat and BMI recorded for males and females in the sampled population place both sexes in the low activity categories presented in Bradbury et al 2017 [(344)]. Section 8.3.3 outlines that associations between NIRS markers and percentage fat content became non-significant when adjusted for sex, suggesting sex is the more influential variable on NIRS markers at the tibia.

Another consideration was potential confounding from differences in bone volume between sexes at the proximal tibia and BMD, as females were significantly shorter. A known limitation of areal BMD measurements taken with DXA is that smaller bone volume may lead to underestimated BMD [(379)]. However no significant association was

observed between bone area at the proximal tibia and tibial BMD, meaning corrections such as bone mineral apparent density (BMAD) were not adopted.

Likewise with smaller bone volume and lower BMD as a sub group, it is plausible that NIRS results from female participants had a relatively smaller cortical bone contribution. As discussed above in Section 10.2.2.1, relatively thinner dense cortical bone may have contributed to less attenuation of NIRS photons, underestimating MBL-derived NIRS parameters.

10.3: Trabecular bone scoring

Table 10.5 presents descriptive results of TBS scores taken from L1 to L4 for each participant, and includes sub group results for those with and without T2DM, and based on sex. There was little evidence of an association between TBS results and BMD measurements taken at any site. This is expected and is inherently the rationale for including TBS as an indicator of bone health. TBS has been shown to be representative of bone strength inherently through the architectural integrity of bone, independent of bone density. As such both BMD and TBS are complimentary as they indicate fracture risk through different risk factors of poor bone health [40, 160].

Table 10.5: Mean trabecular bone scores (TBS) taken from L1 to L4, including sub group results for those with and without T2DM, and based on sex (standard deviation in parentheses). *p*-values are from independent t-tests between sub groups, * denotes statistical significance of *p*-value <0.05.

	Total (N=36)	T2DM (n=18)	Non-T2DM (n=18)	*p*-value between sub groups
Mean TBS	1.329 (0.087)	1.325 (0.095)	1.333 (0.080)	0.79
	Total (N=36)	Males (n=22)	Females (n=14)	*p*-value between sub groups
Mean TBS	1.329 (0.087)	1.339 (0.093)	1.314 (0.076)	0.42

There was also little evidence of associations between NIRS parameters and TBS results. It was anticipated that a decrease in bone strength and increased porosity in bone, with a representative lower TBS score, may have associated with poor ischaemic response in bone, as indicated by NIRS. Whilst there is evidence of an association between poor vascular supply and bone quality [8], there was no existing evidence found for comparison directly between TBS and markers of vascular supply in bone with any haemodynamic testing method.

There may be a number of reasons why this association has not been identified in this study. It may be that there is only a weak association between microvascular function and bone quality. TBS is based on measurements taken at the lumbar spine and regional variations in bone quality exist, although are typically associated. NIRS parameters taken at the proximal tibia compared with peripheral QCT would have been a more direct comparison, if this had been available. TBS is only measured at the spine as this anatomical site has been shown to respond most quickly to treatment and is more predictive of future osteoporotic fractures than other sites, such as the hip. The hip is also more prone to positioning variability, and TBS analysis has proven to be more complex at this anatomical site [380].

NIRS measurements taken at the proximal tibia must incorporate the tibial cortical bone as well as trabecular bone. The blood flow rates between these two types of bone are likely to vary, and this has been demonstrated in murine studies [8]. TBS does not represent cortical porosity, and trabecular bone is likely to be more influential to TBS results at the spine, with a documented ratio of trabecular to cortical bone of 3:1 [40, 157].

Bousson et al 2012 argues TBS has been shown to help prediction of fragility fracture based on bone quality, but may not reflect microarchitecture directly, which is a limitation of its usage in the context of this project. A number of studies have shown associations between microarchitectural features and TBS, however the effect of each microarchitectural property (i.e. trabecular size, connectivity, and spacing) on TBS individually, and in relation with each other, still requires elucidation. Likewise TBS results are influenced by other external factors such as soft tissue composition over the lumbar spine and inherent image noise [159].

It is possible the small relatively healthy sample may have hindered demonstration of associations in the wider population of interest. However it is noted that there was a wide range of TBS results recorded (1.130-1.565), with four participants having “high risk” TBS results below 1.23, and ten at “intermediate risk” according to thresholds outlined in McCloskey et al 2016 [162].

10.3.1: Sub group analysis

Table 10.3 has demonstrated a lower TBS score in those with T2DM compared to those without, as is consistent with the literature [381], although differences were statistically non-significant. Table 10.1 also demonstrates higher BMD results across

most measurement sites in those with T2DM, controlled for BMI. Although differences are non-significant, this finding is also consistent with the evidence base [32, 46].

Leslie et al 2013 found that TBS was an independent predictor of fragility fracture in those with T2DM and more effective than BMD at predicting diabetes associated fracture risk [381]. Dhaliwal et al 2014 and Kim et al 2015 both found higher BMD but lower TBS in those with T2DM in US and Korean populations respectively [382, 383]. Both studies found an association between glycaemic control and TBS which may explain why TBS did not differ significantly in this study's sample population, who generally had relatively good glycaemic control amongst those with T2DM. Zhukouskaya et al 2015 found that BMD and TBS scores were not significantly different between those with and without T2DM, although those with T2DM had higher BMD. This is more in keeping with the results observed in Table 10.5, and is likely explained by comparable cohorts, both generally having well controlled T2DM [384].

Males had slightly higher TBS than females. Leib et al 2014 reports a number of studies which typically found TBS lower in males then females [158]. However, sex comparisons are complex and age dependent, as two studies report a faster reduction of TBS with age in females post-menopause [158, 383]. Apart from the established physiological differences in bone health between sexes with aging, it is also not entirely clear how the typically larger vertebral size of men affects the textural analysis of TBS and if this relates to sex-based differences in results. More research has been suggested to explore sex-based differences in TBS [157, 158].

10.4: Fracture risk assessment tool (FRAX):

As described in Section 6.2.7, FRAX scores were calculated for all participants based on their TBS and DXA results, and the medical history provided, to provide a percentage estimation of a fragility fracture in the next ten years. Descriptive results are presented in Table 10.6. As expected females had a significantly higher fracture risk than males using FRAX based on independent t-tests ($p<0.001$). This is primarily because FRAX uses female sex as a risk factor for fragility fracture based on the well documented post-menopausal influence on bone health and epidemiological differences in sex, observed during the development of FRAX [164]. There was little evidence of difference between FRAX score for those with and without T2DM ($p=0.29$; independent t-test).

Table 10.6: Mean fracture risk assessment (FRAX) scores for the percentage risk of fragility fracture within the next ten years, including sub group results for those with and without T2DM, and based on sex (standard deviation in parentheses). *p*-values are from independent t-tests between sub groups, * denotes statistical significance of *p*-value <0.05.

	Total (N=36)	T2DM (n=18)	Non-T2DM (n=18)	*p*-value between sub groups
FRAX (%)	5.5 (2.7)	5.1 (2.0)	6.0 (3.2)	0.29
	Total (N=36)	Males (n=22)	Females (n=14)	*p*-value between sub groups
FRAX (%)	5.5 (2.7)	4.3 (1.2)	7.4 (3.2)	<0.001*

10.4.1: NIRS versus FRAX results

There were significant associations between FRAX scores with the O_2Hb_DO_absΔ marker (r=0.45; p=0.008), and the O_2Hb_PO_absΔ marker (r=-0.41; p=0.02). No other statistically significant associations were found. It is perhaps not surprising that associations were not quite as strong between FRAX score and NIRS markers, when compared with associations between BMD results and FRAX markers. This is because FRAX also inherently considers TBS scores, where no associations were found with NIRS markers.

Likewise as the sampled cohort were generally healthy with a BMI less than 35 kg/m^2, and environmental factors such as smoking, glucocorticoid use, previous fracture, secondary osteoporosis and rheumatoid arthritis were almost uniformly answered no, these factors had minimal impact on FRAX scores within the sampled population. Section 10.2.2.1 above has discussed possible reasons why the O_2Hb_DO_absΔ marker and the O_2Hb_PO_absΔ marker may be the most likely to associate with BMD, and the same principles apply here with FRAX.

When looking at the correlations between FRAX and the O_2Hb_DO_absΔ marker and between FRAX and the O_2Hb_PO_absΔ marker for those with and without T2DM, no obvious differences between these two sub groups were observed. These data are presented in Figure 10.4.

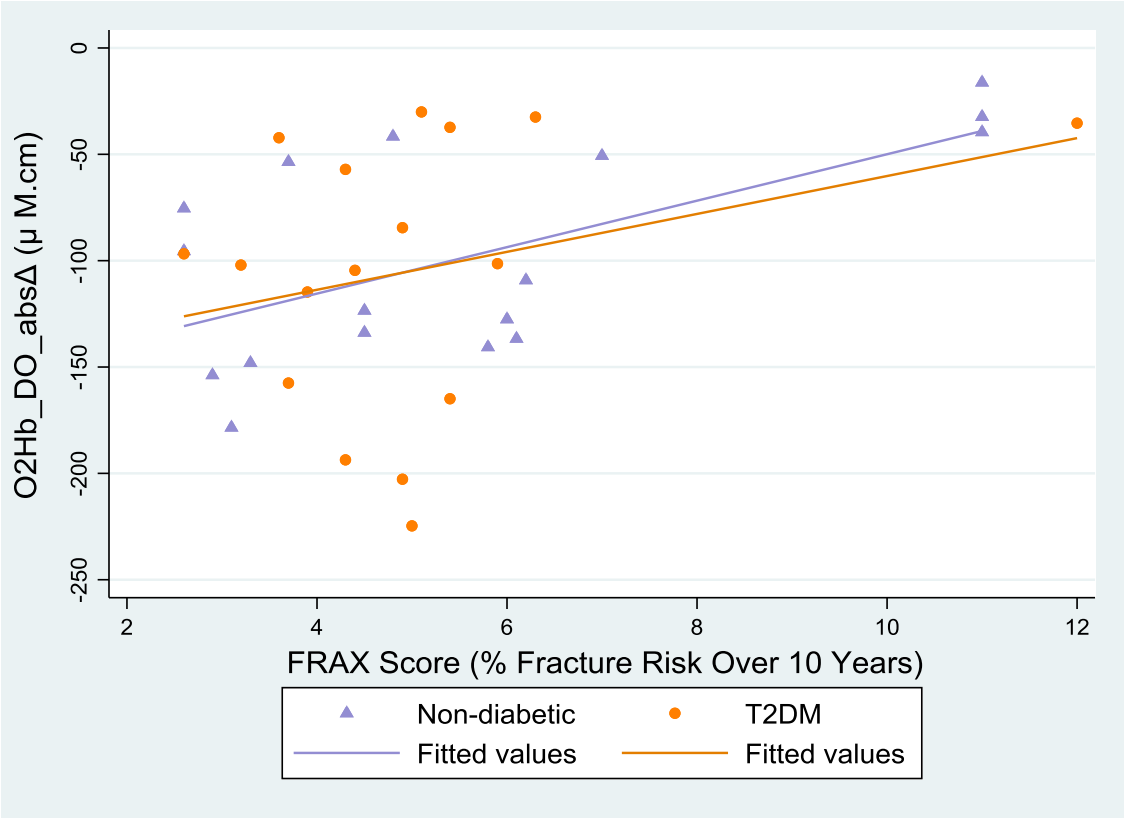

(a)

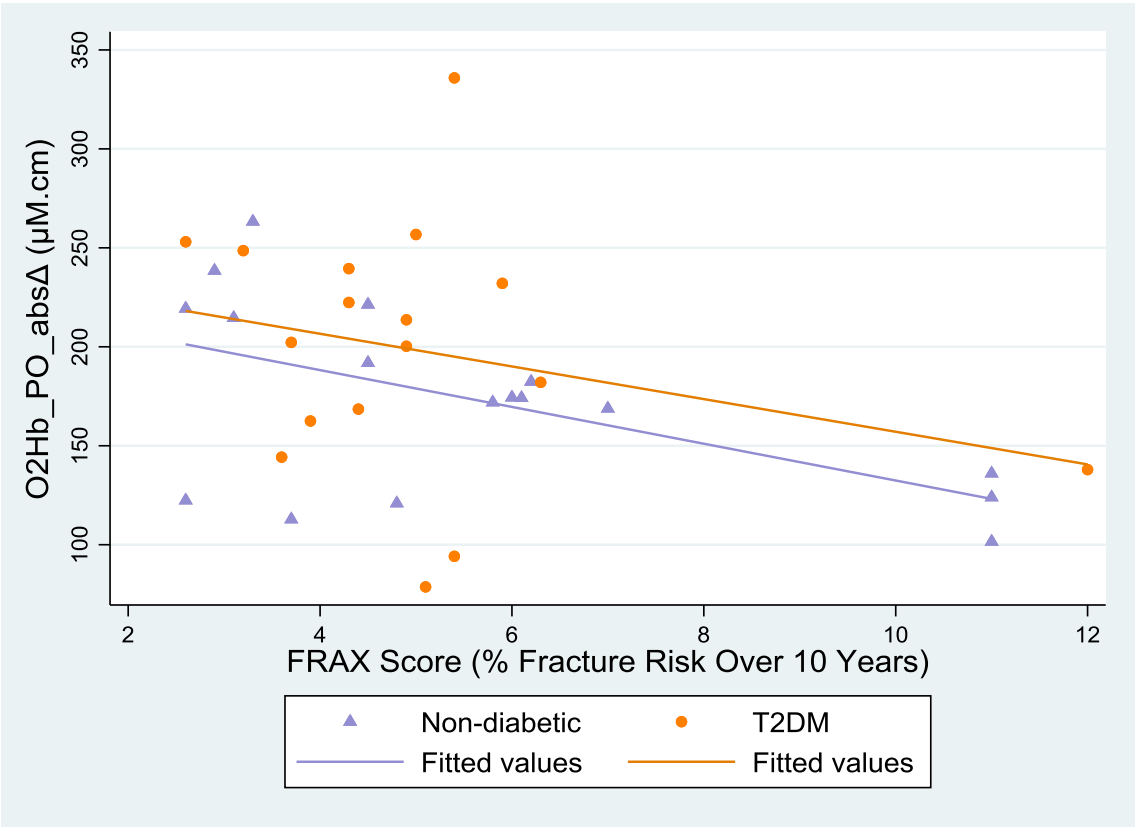

(b)

Figure 10.4: Demonstrations of the associations and lines of best fit between FRAX scores of the percentage risk of fragility fracture in the next ten years with (a) $O_2Hb\_DO\_absΔ$ (r=0.45; p=0.008) and (b) $O_2Hb\_PO\_absΔ$ (r=-0.41; p=0.02) at the proximal tibia, stratified by those with T2DM ((a) r=0.29; p=0.27; (b) r=-0.26; p=0.31), and those without ((a) r=0.63; p=0.007 (b) r=-0.56; p=0.02))

Figure 10.5 presents data on FRAX with the O_2Hb_DO_absΔ and O_2Hb_PO_absΔ markers stratified by sex. Although associations are weak, there is a clear difference in the overall levels of these markers between sexes. This is mainly attributable to post-menopausal females having a higher fragility fracture risk assigned [164]. Figure 10.5 also clearly shows females have lower DO and PO responses than males. This may be indicative of a relationship between poor vascular function and higher fracture risk in females but this needs more investigation outside the scope of this exploratory project to confirm this relationship in a larger representative population, and to elucidate the underlying reasons why this sex-dependent association may exist.

As discussed in Section 10.2.2, potential confounding variables relating to cortical thickness and attenuation properties in bone also need considering when investigating sex-based differences. There is also evidence suggestive of indirect associations between poor bone health, low bone density and cardiovascular disease in post-menopausal women, with proposed shared mechanisms from the effects of low oestrogen levels. However there is limited definitive causal evidence between these factors [90, 385, 386].

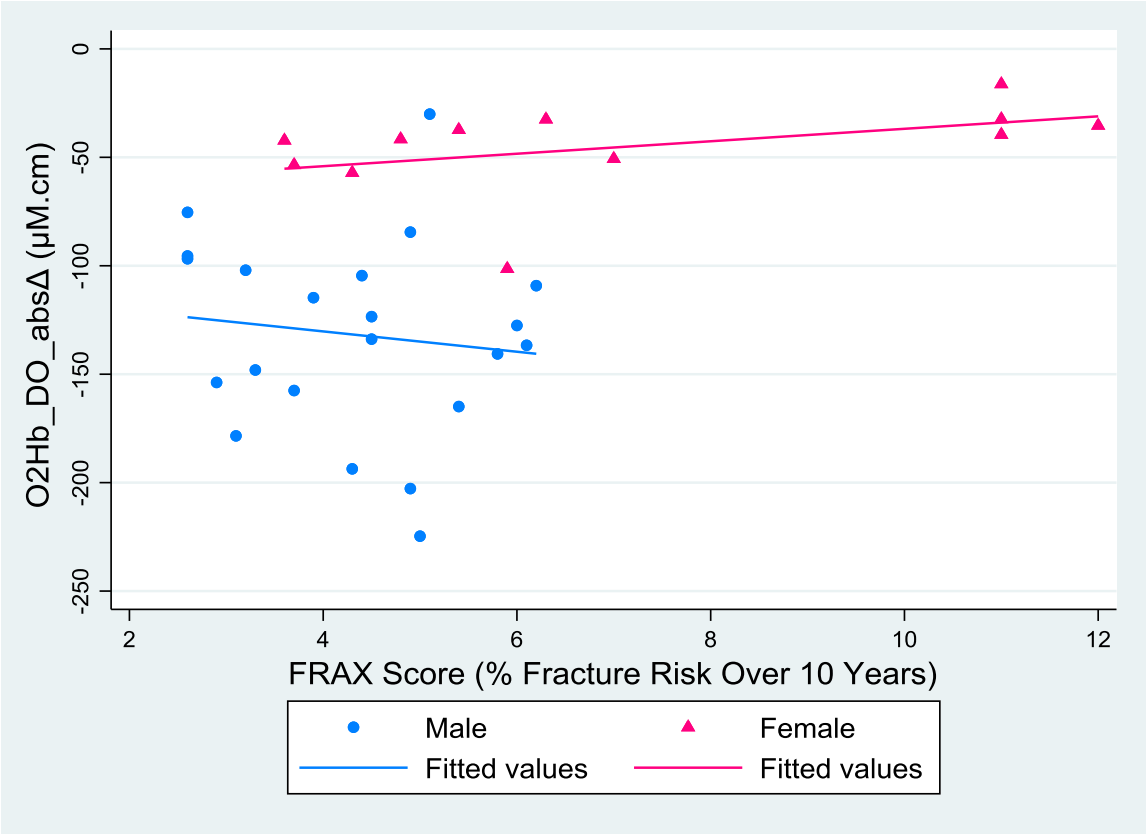

(a)

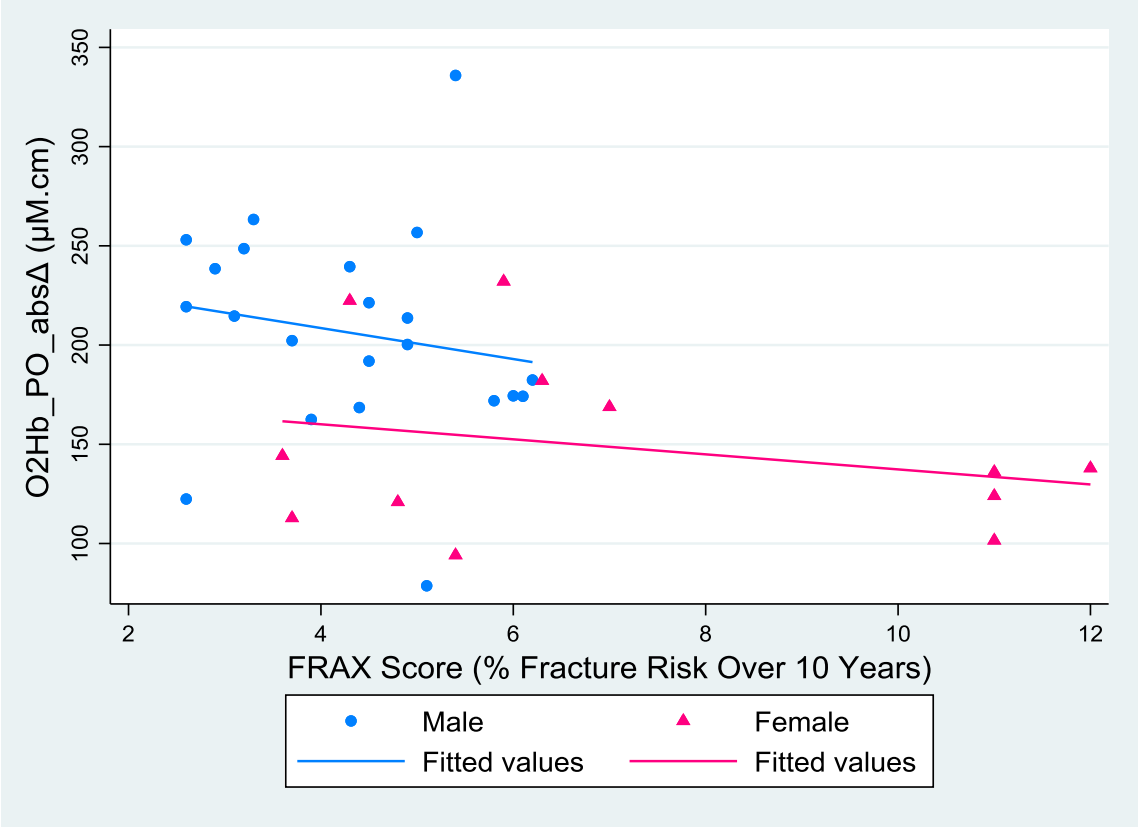

(b)

Figure 10.5: Demonstrations of the associations and lines of best fit between FRAX scores of the percentage risk of fragility fracture in the next ten years with (a) O_2Hb_DO_absΔ (r=0.45; p=0.008) and (b) O_2Hb_PO_absΔ (r=-0.41; p=0.02), at the proximal tibia, stratified by males ((a) r=-0.12; p=0.58; (b) r=-0.17; p=0.44) and females ((a) r=0.44; p=0.15; (b) r=-0.27; p=0.40).

10.5: Blood turnover markers of bone metabolism

Descriptive results of CTX and P1NP are presented in Table 10.7 and Figure 10.6. Results between CTX and P1NP were strongly correlated as expected (r=0.75; p<0.001). However CTX and P1NP did not significantly correlate with any of the demographic variables previously presented in Table 8.1. Nor did CTX and P1NP significantly correlate with any DXA, TBS or FRAX results. All correlations with NIRS markers were non-significant except with O_2Hb_PO_absΔ, which had weak associations with CTX (r=-0.34; p=0.05) and P1NP (r=-0.34; p=0.05). However, these became non-significant when performed without one outlying data point (r=-0.19; p=0.30 and r=-0.13; p=0.48 respectively).

Table 10.7: Summary table of mean CTX and P1NP results including sub group results for those with and without T2DM, and based on sex (standard deviation in parentheses). *p*-values are from independent t-tests between sub groups, * denotes statistical significance of *p*-value <0.05.

	Total (N=36)	T2DM (n=18)	Non-T2DM (n=18)	*p*-value between sub groups
CTX (ng/mL)	0.34 (0.14)	0.28 (0.12)	0.41 (0.14)	0.006*
P1NP (ng/mL)	44.9 (15.5)	37.7 (12.6)	52.1 (15.0)	0.004*
	Total (N=36)	Males (n=22)	Females (n=14)	*p*-value between sub groups
CTX (ng/mL)	0.34 (0.14)	0.31 (0.11)	0.39 (0.17)	0.10
P1NP (ng/mL)	44.9 (15.5)	40.2 (12.4)	52.3 (17.4)	0.02*

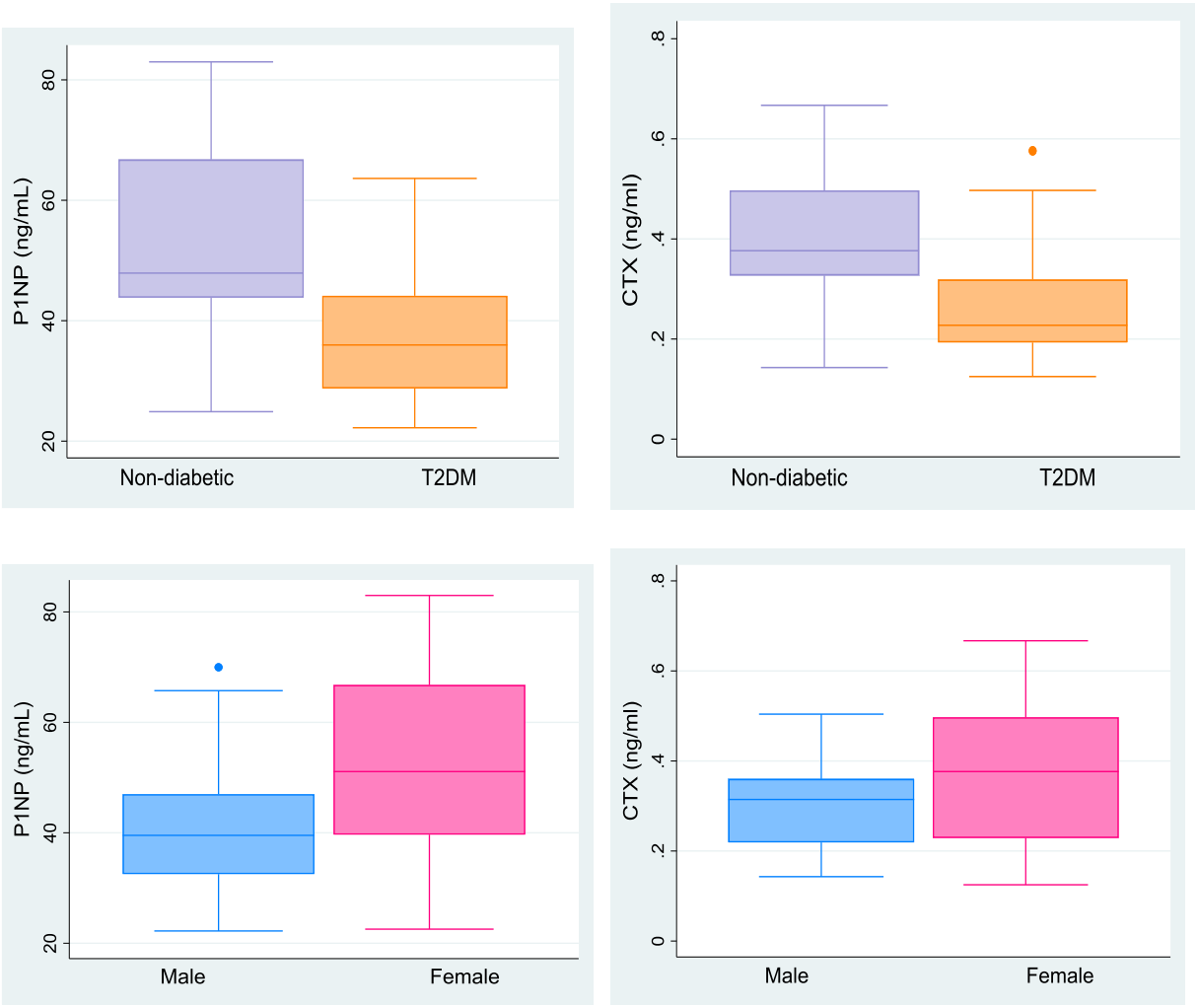

Figure 10.6: Box plots of CTX and P1NP results according to T2DM status and sex.

10.5.1: T2DM and sex sub groups

CTX and P1NP were significantly lower in those with T2DM, supporting the idea that T2DM may suppress bone metabolism. Likewise, HbA1c was moderately negatively correlated with CTX (r=-0.45; p=0.006) and P1NP (r=-0.40; p=0.01). These results are in line with the systematic review of Starup-Linde 2013 regarding bone metabolism markers in those with diabetes. This review indicated reduced bone turnover in those with T2DM (with reduced CTX, P1NP, and several other markers of bone metabolism), concluding that altered glucose metabolism and associated microvascular dysfunction may alter normal bone remodelling [(387)].

CTX and P1NP were both higher in females. In females there were also weak positive correlations between years since menopause and CTX (r=0.32; p=0.27) and P1NP (r=0.26; p=0.36). As oestrogen plays a role in suppressing bone resorption, higher bone metabolism markers were expected in the post-menopausal females recruited, as previously reported [(172)].

10.5.2: Discussion

Confidence can be taken that CTX and P1NP results are representative of the sampled population, as there was expected statistically significant associations between CTX and P1NP, and expected differences in CTX and P1NP observed between T2DM and sex sub groups. However, it is perhaps surprising that bone metabolism markers did not correlate with any of the other bone health markers obtained. This may be due to the small range of CTX and P1NP results obtained, despite recruiting participants of varying age, sex, T2DM status and BMD. In particular, CTX results representing bone resorption rates in females were generally lower than the range of results presented in Naylor et al. 2016 for post-menopausal females being medically treated for osteoporosis [169]. A wider range of CTX and P1NP results may have demonstrated associations more representative of the population of interest.

Previous research synthesised in a systematic review by Burch et al. 2014 also found numerous studies generally demonstrating weak correlations between bone mineral density and bone metabolism marker response to different medical treatments for osteoporosis, raising concerns over the suitability of bone metabolism markers for monitoring osteoporosis treatment [388]. As discussed in Section 2.4.4, the wide range of physiological factors affecting bone metabolism markers (including age, sex and ethnicity) may mean that observation of longitudinal changes within participants is more appropriate than the cross sectional design utilised in this project, with wide "normal" ranges observed across the population [172].

10.6: Chapter summary

Figure 10.7 presents a summary of results from Chapters 8, 9 and 10. Alongside the acceptable reproducibility of NIRS markers demonstrated in Chapter 7, confidence is also taken from the significant associations demonstrated in Chapter 8 between DO and PO NIRS markers, and between tibial and calf NIRS markers taken simultaneously. Likewise DCE-MRI showed similar associations between tibial and calf measurements, albeit slightly weaker. This chapter has demonstrated statistically significant associations between NIRS markers and BMD and FRAX results, supporting that NIRS is taking representative measurements of bone tissue that may have useful predictive research applications. Whilst demonstrating the potential utility of NIRS, these associations should be interpreted tentatively, as potential confounding factors such as cortical thickness and inter participant variation in the attenuation

properties of bone need further investigation. Chapter 11 will discuss potential future research applications to address this.

Variable	Tibia (vs Calf)	T2DM (vs non T2DM)	Female (vs Male)	Increasing Fat % in Lower Leg	Increasing Age	Decreasing BMD
NIRS DO Markers	↓	↔	↓	↓	↔	↓
NIRS PO Markers	↓	↔	↓	↓	↔	↓
Resting TOI	↑	↔	↓	↑ (calf only)	↓	↔
Fat % in Lower Leg		↔	↑		↔	↑
DCE-MRI Uptake Rate at Rest	↓	↔	↑	↑	↔	↑
DCE-MRI Amplitude at Rest	↓	↔	↑*	↑	↔	↑
BMD		↔	↓	↓	↓*	
Cortical Area		↔	↓	↓	↓*	↓
TBS		↔	↔	↔	↔	↔
FRAX		↔	↑	↑	↑	↑
CTX		↓	↑	↔	↔	↔
P1NP		↓	↑	↔	↔	↔
Potential NIRS Confounder		Volunteer sampling in this study may have underestimated T2DM effects	Female sex potentially confounding with significantly higher fat % in the lower leg	Female sex potentially confounding with significantly higher fat % in the lower leg	Volunteer sampling in this study may have underestimated ageing effects	Scattering and absorption properties of bone

Figure 10.7: Summary of key results from Chapters 8, 9 and 10. Arrows represent statistically significant differences or associations between variables (* denotes result not statistically significant but considered clinically relevant).

Blood markers of bone metabolism and TBS had weak associations with all other measures of bone health. However both are known to have wide variability in the healthy population and are ideally used for monitoring within-participant change, rather than cross sectional comparison between participants.

A limitation of this PhD project is the multiple hypothesis testing that has been carried out, seeking to find associations between various indicators of bone health, and a number of NIRS markers. It is possible to correct for multiple testing using methods

such as Bonferroni corrections, which make allowances for the increased likelihood of a significant result when multiple comparisons are made. However such corrections may be too conservative, and are inappropriate when many of the comparisons made are inherently linked [296]. As such the approach suggested by Perneger 1998 has been adopted [297]. This involves reporting significance levels tentatively, and in the context of the biological plausibility of individual associations, as well as their consistency across what trends might be expected across comparisons between different testing methods. This was seen as justified given the exploratory nature of the project, which has been designed to inform further research.

Sub groups of interest (T2DM and sex status) were generally well controlled for potential confounding variables such as ethnicity, age and BMI. Those with T2DM did not significantly differ from non-diabetics in terms of DXA, TBS, FRAX, MRI or NIRS markers. Associations were generally comparable when split into sub groups of those with and without T2DM. However, there was significantly reduced bone metabolism blood markers, and non-significant reductions in TBS, in those with T2DM suggesting there may be differences in bone metabolism within this subgroup. This feasibility study may be underpowered to demonstrate other associated effects on bone health related with this. There is also potential recruitment bias in the sampled population of those with T2DM.

Females demonstrated significantly reduced vascular markers with NIRS compared with males during ischaemic conditions. This related to significantly increased markers of enhancement with DCE-MRI at rest. Females also had significantly lower BMD than males at the tibia, significantly higher risk of fracture through FRAX scoring, and higher blood markers of bone metabolism. By demonstrating differences in post-menopausal females with NIRS that are in keeping with other markers of bone health, there is optimism that NIRS may be a useful research tool in investigating associations between bone vascularity and clinical measures of bone health, and observing differences between relevant sub groups, or monitoring longitudinal change.

Chapter 11 will further summarise the PhD project, with reference to the initial aim and objectives stated in Section 1.2. Chapter 11 will also propose future directions in research around the applications of NIRS for measuring *in vivo* bone tissue, building on the exploratory results of this project.

Chapter 11: Thesis summary

This chapter will summarise the findings of this PhD project in the context of its strengths and limitations. Potential future research will also be explored.

11.1: Summary of findings

When summarising the findings of this thesis, it is pertinent to refer back to the aims and objectives stated in Section 1.2. The primary aim of exploring the potential feasibility of NIRS as a diagnostic research tool in the measurement of *in vivo* vascular haemodynamics in human bone tissue has been achieved.

The systematic review presented in Chapter 3 highlighted the breadth of applications for NIR technologies, and the demand for testing methods of bone haemodynamics that are safe, inexpensive, non-invasive, and logistically feasible. But this review also highlighted the need for more rigorous assessment of the reliability of NIRS, and for validation of NIRS by comparison of results against suitable comparator tests. The experimental work in this PhD project has made the first contributions towards these gaps in the existing evidence base.

An arterial occlusion (AO) protocol utilising NIRS was developed using a continuous wave NIRS spectrometer. This involved selecting haemodynamic markers of oxygen extraction during AO, and post occlusive markers representative of microvascular response to ischaemic conditions. This project represents the first study to rigorously assess the reliability of haemodynamic NIRS markers for measuring bone *in vivo* in humans. A sub selection of these markers has been demonstrated to be suitably reliable compared with NIRS based markers used in the evidence base for measuring muscle and skin, as well as alternative imaging tests obtaining markers of bone haemodynamics. This AO protocol has been shown to be generally tolerable for participants, and likely to be reliably performed by different operators.

The AO protocol has been demonstrated to be highly likely to be representing bone tissue at the proximal tibia, as significant differences were identified with the lateral calf, and a unique post occlusive response (i.e. a lack of TOI post occlusive reactive hyperaemia (PORH)) has been demonstrated. Likewise haemodynamic markers at the proximal tibia have demonstrated significant associations with DCE-MRI haemodynamic markers and DXA based measurements of bone health, the first attempt in the evidence base to make such comparisons. There were limitations to the methodological approach taken to obtain these associations (discussed in Section

11.2), but overall the merit of further investigation into NIRS based technology for the assessment of bone haemodynamics has been further strengthened by the novel components of this PhD project.

The thesis did not identify differences between those with and without T2DM, most likely because of selection bias leading to a sampled population of participants with well controlled and shorter duration of T2DM. However, sex-based differences have been illustrated, highlighting the potential of NIRS for researching differences in bone haemodynamics between sub groups of interest.

11.2: Limitations and risk of bias

In order to consider the limitations of this PhD project, the six domain-based intrinsic biases (presented in Table 3.1) used to assess included studies in the systematic review of Chapter 3 were considered.

Like many of the studies on NIR technologies, this thesis reports on a feasibility project with a small sample population recruited using convenience sampling. This leaves the results susceptible to selection biases. Again this may have led to an underestimation of differences between those with and without T2DM, as participants were otherwise generally healthy with few co-morbidities. The approach to recruitment has also reduced the generalisability of results, with eligibility restrictions on BMI greater than 35 kg/m^2 and with only Caucasians recruited. When assessing the tolerability of the AO protocol, it is also more likely that volunteers for research are able to withstand the pressure applied to the distal thigh.

Although participants of different sexes and from a wide age range were recruited, there is a likelihood that associations have been affected by reduced variability within the sampled population. It is recommended that further studies involve diseased sub groups. The promising reliability and validation results in this thesis would support this research being pursued, as is discussed further in Section 11.3.

There is a low risk of performance bias for the experimental results presented, as all participants received the same testing. NIRS protocols were performed using an objective pre-stated protocol, with only one operator in the case of all AO data. Likewise detection bias is also low. Data analysis was performed by the same operator who carried out testing and was therefore not performed blinded, however was performed using predominantly objective measures that were shown to be reproducible when performed by different analysts in Section 7.3. Reporting biases are

also believed to have been minimised. The systematic review followed a pre stated protocol, made publically available via PROSPERO [174]. Likewise, experimental studies were conducted using pre stated protocols.

The number of missing data points has been reported throughout the thesis, with description of the underlying reasons. There is a risk of attritional biases with the results presented in this thesis that should be considered in context. For example when assessing different day reproducibility of NIRS markers at the proximal tibia, 15 of 41 participants did not contribute successful test and retest data. These participants are potentially more likely to be participants who struggled to tolerate the AO or may have had physiological differences that led to their data not meeting the inclusion criteria for analysis. Thus reliability of NIRS markers may be overestimated due to attrition bias. Likewise for DCE-MRI data there was four participants who had data excluded due to low signal to noise, and these participants were identified as having poor bone health compared to the rest of the sampled cohort of participants. Thus their exclusion may have introduced a bias to the association of NIRS results with DCE-MRI.

As feasibility work, the study designs of the experimental aspects of the PhD do have limitations. The desired comparator offering direct comparison of AO NIRS-derived haemodynamic markers was attempted but deemed to be unreliable (BOLD MRI; discussed in Appendix J). Attempts to validate NIRS against other external comparators used a cross sectional design looking at association only. As such, there are potential confounding variables which cannot be ruled out but have been discussed throughout the thesis. In particular, it appears the variability in bone attenuation properties between participants may be affecting MBL-derived NIRS measurements. This is an important consideration for future research, and technological developments with NIRS may help here, discussed further in Section 11.3.

The study looked at comparisons between multiple haemodynamic markers derived by NIRS and DCE-MRI, and multiple indicative tests of bone health. This was considered a justifiable approach to a feasibility study, but results should be considered more tentative in light of these multiple comparisons [297].

Although the thesis reinforces the potential of NIRS for measuring bone haemodynamics *in* vivo, the project has raised issues with the applicability of the AO protocol, and the future use of continuous wave NIRS systems. NIRS is inherently restricted to superficial bone sites, but the AO protocol is further restricted to peripheral

sites which facilitate proximal cuffing. In adult populations over the age of 40, this restricts NIRS measurements to sites of yellow marrow [353], although trabecular bone such as at the proximal tibia is still of interest.

The protocol is restricted to those who can tolerate the four minutes of AO. AO is also a forced experimental protocol, which does not facilitate haemodynamic measurements that may be more representative of normal physiology, such as measurements taken at rest or during exercise.

The CW-NIRS system used also has inherent limitations attributable to the MBL and SRS derived parameters that it can measure. Although the Hamamatsu NIRO-200NX benefits from being a commercially available and relatively inexpensive system, the applicability of MBL results are hampered by representing concentration change which remains relative to an unknown initial blood volume. Likewise, SRS-derived nTHI measurements monitor blood volume change relative to an initial unknown blood volume, and TOI measurements represent a ratio value independent of blood volume. Similarly, although post occlusion markers using CW-NIRS systems broadly represent the reperfusion characteristics of tissue experiencing ischaemia, they are influenced by multiple factors which cannot be distinguished. This includes the vaso-regulatory function of the microvessels, the blood volume and capillary density of the measured tissue [366], the prior rate of perfusion [65], and the extent of oxygen extraction during the occlusion [79]. Direct measurements of blood flux are not possible with CW-NIRS and it is clear this is clinically desirable from the breadth of research utilising LDF and PPG technology outlined in the systematic review of Chapter 3.

CW-NIRS markers have been shown to be reliable, and associated with other markers of bone health. However, a primary recommendation for future research on this topic would be to investigate technological advancements with NIRS equipment given the inherent restrictions of the applicability of the AO protocol developed in this thesis, in terms of the anatomical sites and haemodynamic markers that are measurable. Such technologies are discussed in Section 11.3.1 and have the potential to build on the results of this thesis. Section 11.3.2 will also discuss parallel recommendations for further development of CW-NIRS.

11.3: Further research

11.3.1: Technological advances

11.3.1.1: Facilitating absolute haemodynamic measurements at rest

As discussed in Section 11.2, the inherent limitations of CW-NIRS systems reduce the applicability of testing options due to the inherent need for an intervention such as AO, and the limitations of not observing absolute markers of blood volume and/or blood flux that might facilitate comparison between participants with measurements taken at rest.

Section 2.2.1.6 introduced alternative time-resolved spectroscopy (TRS) [195, 321] and frequency domain (FD) NIRS systems [266] that are emerging in more recent literature that can obtain absorption and reduced scattering coefficients of the volume measured. This allows calculation of absolute haemoglobin (total, oxygenated or deoxygenated) concentration within the measured volume. Although the measured volume is not definitively measurable, this can be assumed to be constant between participants if the same inter optode spacing is used [2, 62].

Calculation of absorption and reduced scattering coefficients for each individual participant should also improve the accuracy of absolute haemoglobin measurements for between-participant comparisons. Typically in muscle studies utilising NIRS to calculate maximal oxygen consumption (VO_2 max) or absolute haemoglobin concentration, values for differential path length and attenuation factors are assumed constant between participants. This introduces error as all participants will have attenuation differences based on tissue properties and haemoglobin concentration [71]. Van Beekvelt et al 2000 estimated this error to be 12% when measuring oxygen consumption during AO at the forearm [73].

The use of constants for NIRS studies in muscle is based on the assumption of homogeneity in muscle tissue [2]. As discussed in Section 9.2.2.1, MBL-derived NIRS markers may be more confounded by individual differences in scattering properties when measuring bone tissue, due to the heterogeneity of the measured sample (including cortical bone, trabecular bone and bone marrow), as well the increased variability in BMD and bone marrow fat fraction across the population, relative to variability in muscle. It is for this reason that a primary recommendation for future research into the application of NIRS for measuring bone haemodynamics should be focussed on development of technologies that can calculate the absorption and

reduced scattering coefficients of individual participants, allowing adjustment for this potential confounding when measuring haemoglobin concentrations.

Section 2.2.1.6 also introduced diffuse correlation spectroscopy (DCS), which can work in parallel with TRS and FD-NIRS systems to provide a marker of blood flux by measuring temporal fluctuations in signal with a monochromatic wavelength of NIR light [74]. However, DCS is generally limited to measuring relative changes in blood flux, just as CW-NIRS, PPG and LDF systems are, although technological developments are being researched to incorporate TRS data with DCS to calculate absolute markers of blood flux [389]. DCS also has the distinct advantage over LDF and PPG in that it can take measurements from a deeper sampled volume, and offers the additional advantages of incorporation with a TRS or FD-NIRS system [75, 389].

Development of more advanced NIRS systems able to take measurements of bone tissue at rest would open the applicability of NIRS research to multiple uses. This could include further investigation for unique regulatory mechanisms in human bone, as has been hypothesised in animal studies [23] and in human *in vivo* studies [332]. With NIRS systems able to obtain absolute measurements of blood volume, more likely to be representative of capillary density, diagnosis and monitoring of metabolic bone conditions may become feasible. Farzam et al 2014 justifies its feasibility study of a TRS and DCS NIRS system for measurement of absolute haemoglobin concentration and blood flux at the manubrium as a potential anatomical testing site for increased vascularity in red marrow consistent with haematological malignancies [56]. Similarly, precedence exists with DCE-MRI for the monitoring of treatment for multiple myeloma with longitudinal assessment of reductions in haemodynamic markers of capillary density and blood volume in identified lesions [119]. NIRS could feasibly be a simple testing method for diagnosing or monitoring treatment in these diseased populations more regularly.

Previous studies also exist using DCE-MRI to monitor bisphosphonate treatment for Paget's disease. Paget's disease is a metabolic bone disease which results in excessive osteoclast activity, promoting overactive bone turnover and resultant disorganised bone micro architecture, leaving patients prone to bone pain and fracture. Increased angiogenesis is known to be correlated with disease development [116]. DCE-MRI markers of perfusion have been shown to be decreased with bisphosphonate treatment, in line with bone metabolism blood markers, suggesting that excessive perfusion in bone is a contributory element to Paget's disease [116, 117].

As such, again NIRS measurements at diseased bone sites could potentially be useful in diagnosis or treatment monitoring for patients with Paget's disease, with TRS and FD-NIRS systems able to monitor red marrow sites of the axial skeleton at rest [176].

There is evidence that bone pain associated with osteoarthritis (OA) is linked with high intraosseous pressure and altered bone perfusion, although the role of altered microvascular bone perfusion in OA is not fully understood [11, 113, 390]. NIRS systems with the technological advances discussed in this section could play a role investigating haemodynamics in subchondral bone (such as at the proximal tibia) at various stages of OA, to see if symptoms or progression of disease correlate with haemodynamic markers in bone. NIRS may also be useful for monitoring treatment methods.

11.3.1.2: Measuring additional properties of bone

The discussion of alternative NIRS systems above is in the context of a system with comparable use of up to three wavelengths of NIR light, as with CW-NIRS. However, there is also great potential with TRS and FD-NIRS systems that collect data from multiple wavelengths [9, 195, 391]. As introduced in Sections 2.2.1.3 and 2.2.1.4, MBL and SRS derived parameters rely on multiple wavelengths to calculate relative contributions of O_2Hb and HHb to attenuation, based on their different attenuation profiles across the NIR wavelength range. However, utilization of more wavelengths offers the potential to decipher the concentration of multiple chromophores of interest [2]. Collecting data with more wavelengths requires greater sampling and processing time, and increases the expense of the system, but could allow valuable information collection relevant to bone health [62].

Although the radiation burden of DXA is low for participants, it does add expense and logistical difficulty when providing services for measuring BMD. There is a demand for inexpensive point of care devices that can screen for BMD. Osteoporosis and subsequent fragility fracture has a large societal and economic effect, but effective screening for those at risk can lead to preventative lifestyle and medical interventions that can help [31]. A number of ultrasound based systems have been introduced measuring markers of BMD at the calcaneus [53], tibia [392], hip and lumbar spine [393]. Development of broadband NIRS systems could also contribute here, calculating markers of BMD with the added value of haemodynamic markers as well [9, 394]. The incorporation of TBS into fracture risk assessment tools such as FRAX demonstrates

the advantages of alternative measures of bone health, which may indicate pathophysiological change in bone, independent of BMD [157].

A number of studies have reported the use of NIR wavelengths to measure markers of bone density. These build on previous attempts to profile the absorption and scattering properties of *in vitro* cortical bone from equine [395] and porcine [396] bone samples. Takeuchi et al 1997 also used a TRS system to demonstrate associations between BMD and attenuation properties of *in vitro* bovine trabecular bone [374].

Pifferi et al 2004 [9] is the first identified study that obtains values for attenuation and scattering properties of *in* vivo human bone at the calcaneus across a broad spectrum of NIR wavelengths. Results are comparable with previously obtained *in vitro* data. By considering the known attenuation spectrums of water and lipids, the relative contribution of bone mineral to NIR attenuation was estimated and shown to decrease with age across a sample of seven female participants (age 26 to 82 years). Absolute concentrations of haemoglobin were also measurable using this system. It should be noted this system had a 10 minute sampling time, highlighting the need for further development in TRS systems. Sekar et al 2016 report outcomes from a comparable TRS broadband system measuring at multiple superficial bone sites, quoting a sampling time of one second per wavelength sampled [195].

Afara et al 2018 [397] also presents data on the attenuation profiles across NIR wavelengths of subchondral bone specimens taken from the femur and tibia of cadaveric knees. Data from NIRS was strongly associated with markers of bone strength (such as subchondral plate thickness, trabecular thickness and bone volume fraction) derived from peripheral quantitative computed tomography (pQCT). Although taken from specimens of subchondral bone, the authors contend that the findings could lead to the development of arthroscopic NIRS systems that could assess the integrity of cartilage and subchondral bone *in vivo.*

More recently, Chung et al 2018 demonstrated that attenuation of monochromatic 850nm NIR light transmitted posterior to anterior through the distal radius was strongly correlated with BMD at the same site measured with DXA [398]. Shanas et al 2020 presents pilot data of a broadband NIR system that profiles the shaft of the second metacarpal, producing spectral data on water, collagen, fat and protein which was found to be associated with other markers of bone health, based on projection

radiographs of the hand [399]. Although pilot studies, these show the potential of NIRS for screening multiple indicators of bone health.

There are also technological advances in NIRS research utilising multiple wavelengths of NIR light in order to measure cytochrome c-oxidase (CCO), particularly in the field of cerebral research. This chromophore forms part of cellular oxygen metabolism and as such it more directly represents oxygen metabolism in mitochondria from tissue within the sampled volume [2]. However, it is difficult to measure as it has a 10 fold weaker concentration than haemoglobin and a broad profile of absorption across the NIR spectrum, making it harder to distinguish from other chromophores [62]. However, TRS broadband systems can allow measurements of the change in concentration of CCO. Lange et al 2018 [64] report on a new multichannel, time domain NIRS system utilising 16 different wavelengths that can measure absolute concentrations of oxygenated and deoxygenated haemoglobin as well as absolute concentration changes in CCO. This technology has been used for cerebral monitoring of neonates, with CCO changes demonstrated as a better predictor of brain hypoxia and poor brain development (as indicated by MRI spectroscopy), compared with haemoglobin based markers [400]. Similar investigations with bone tissue may give better insight into the metabolic demands of cellular activity within bone marrow and cortical bone, instead of indirect markers of oxygen metabolism derived from haemoglobin oxygenation changes, which can be confounded by variables such as microvascular function and capillary density.

11.3.1.3: Wearables

Regardless of the acquisition mode of NIRS parameters, there is also interest in the development of smaller NIRS measurement devices that might facilitate NIRS to become a wearable, wireless testing tool. Likewise as light sources and detectors become smaller and cheaper, multi-channel devices are becoming more common. These developments could make NIRS more flexible as a monitoring or diagnostic device, taking real time measurements during everyday activities longitudinally and storing data remotely on a device, with the potential for data to be accessed by participants themselves [401, 402]. The use of multichannel devices also allows better differentiation of spatial resolution. Using different optode spacing and time-of-flight data from TRS systems can better delineate the depth of tissue which NIRS data represents [64].

Along with reduced size of NIRS monitoring, comes the potential of implantable NIRS devices, which could help to overcome the issues with sampling depth of non-invasive systems, and could facilitate more long term measurements. Goguin et al 2010 report on the implantation of a NIRS device saddled around the vertebral body of felines in order to measure haemodynamics of the spinal cord [403].

An interesting field of research involving the application of NIRS for measurement of bone haemodynamics is the effect of microgravity from longer term space travel on bone health, which is known to rapidly deteriorate BMD. Here NIRS offers portable inexpensive monitoring of bone health changes for astronauts, and has facilitated research into interventions to reverse the effects of microgravity on bone health, such as use of lower body negative pressure (LBNP) chambers. Using NIRS and PPG, Siamwala et al 2015 argue their results demonstrate that LBNP increases interstitial fluid pressure in the medullary cavity reducing blood velocity, increasing lower limb blood volume, and restoring the role of normal microvascular function in regulatory bone metabolism [78].

11.3.1.4: Use of contrast

The theoretical basis of NIRS systems relevant to this PhD has relied on a source of NIR light with detection of the attenuated photons through naturally occurring chromophores within tissue. An extension of this concept would be to introduce an artificial NIR-attenuating chromophore to the vascular system in order to measure markers of perfusion and blood volume. An example is Indocyanine Green (ICG) which has been used for this purpose in human *in* vivo studies within breast tissue and cerebral studies [404]. As it is non-toxic, inert and not naturally occurring, any relative changes observed with NIRS can be presented as absolute values for the purpose of between-participant comparison [62]. The intravenous injection of ICG could make a comparable protocol for validation of NIRS haemodynamics against DCE-MRI in bone, as both involve injection of a contrast agent at rest.

An alternative approach to using NIRS technology is taking advantage of the relative transparency of tissue at NIRS wavelengths with use of intravascular contrast agents which fluoresce NIR light, and would therefore be detectable with NIR photodetectors. In its simplest form, injection of a NIR emitting contrast agent (fluorophore) could be used for detecting a marker of blood perfusion in a volume of interest. However, more advanced fluorophores can be utilised that have changing properties depending on an

interaction of interest. For example, Le et al 2018 [405] report on use of an injectable subcutaneous hydrogel that contains glucose sensitive nanoparticles that are activated to fluoresce NIR light once interacting with glucose. Application of a non-invasive NIR detector can therefore detect a marker of glucose concentration proportional to the intensity of fluorescent light detected. Similar tagging of drugs with fluorophores could allow monitoring of targeted drug delivery where fluorophores are activated by chemical interactions at the target site [404].

11.3.2: Development of CW-NIRS

Section 11.3.1 has highlighted a number of future potential developments around NIRS equipment that may extend and improve the diagnostic capabilities of NIRS when measuring bone haemodynamics. However, this thesis has also highlighted the potential for CW-NIRS protocols to produce reliable haemodynamic markers associated with other comparators of bone health. Whilst the technological advances around NIRS continue, there is still a place for CW-NIRS and the AO protocol developed in this thesis, despite the limitations discussed in Section 11.2. However, as a feasibility study this thesis has also highlighted a number of recommendations that are required for further development of the CW-NIRS technology.

It is perhaps understandable that a variety of protocol variations and analytical approaches to quantifying NIRS markers were identified in the existing evidence base, given these studies were predominantly feasibility or pilot studies on small samples. This field of research would benefit from further networking and collaboration from like-minded researchers working towards a consensus on the approaches to collecting data with CW-NIRS, allowing better comparison of results between studies. There is precedence for this type of consensus, with guidance documents provided by working groups on the use of DCE-MRI [99] and DXA [31].

The results identified in Chapter 3 and presented in this thesis have highlighted the wide variability amongst the population when measuring haemodynamic markers, which is also complicated by the heterogeneity in testing methods and lack of established reliability data in this field. Whilst it is tempting to utilise NIRS technology solely for the investigation of diseased sub groups of interest, it is also imperative that more data representing the bounds of normal variability in bone haemodynamics are disseminated, given the known responsiveness and wide range of factors known to affect microvascular circulation in bone. This includes age and sex related differences

[29, 79, 339], ethnic differences [67], regional differences between different anatomical sites (e.g. axial vs appendicular skeleton; long bones vs flat bones) and bone tissue (e.g. cortical bone vs marrow; red marrow vs yellow marrow) [23]. Similarly, further investigation into the generalisability of NIRS measurements to the wider population is warranted, with special focus on the application of NIRS in obese populations and attempts to improve the tolerability of NIRS protocols. Once confidence is gained on the bounds on normal variation in bone vascular haemodynamics, more meaningful development of diagnostic thresholds for disease can be elucidated.

The ability of NIRS to monitor participants in real time with a safe inexpensive test appeals to applications of longitudinal monitoring for interventions on bone health. It is recommended that such studies utilising CW-NIRS should incorporate a reliability assessment similar to that presented in Chapter 7 of this thesis in order to assess the likelihood of longitudinal changes being attributable to reliability error.

An example of a potential application of existing commercially available CW-NIRS systems (such as the Hamamatsu NIRO-200NX) is for the current parallel field of research involving the use of repeated vascular occlusions (RVO) for therapeutic use to stimulate microvascular function and prevent muscle wastage in sedentary patients, and to promote healing of traumatic injury to limbs [406, 407]. Park et al 2008 demonstrated that RVO improved microvascular supply within bone tissue in rabbits, using intraosseous LDF probes [408]. Murine studies have also demonstrated RVO was associated with acceleration of fracture healing [409, 410]. The AO protocol used in this thesis could conveniently support measurement of NIRS haemodynamic changes in peripheral human bone in conjunction with the therapeutic RVO protocol.

If proven to be beneficial, RVO may offer a treatment option in patients with high risk of fracture non-union, such as those with a peripheral arterial disease or T2DM. Despite its limitations, CW-NIRS may still offer a potential monitoring tool for assessing vascular response to RVO treatment as a marker of the vascular component of fracture healing [77], which is known to heavily rely on angiogenesis to stimulate bone regeneration [8]. DCE-MRI sets precedence here with evidence of altered perfusion in vertebral bodies having suffered from compression fracture [89, 95]. The authors in these studies argue that DCE-MRI could be useful for diagnosing occult fractures, or longitudinally monitoring vertebral fracture healing.

11.4: Conclusion

This PhD project has contributed valuably to the existing evidence base. It has presented the first objective and comprehensive synthesis of the wide ranging literature available on the use of NIR based systems for the measurement of bone haemodynamics *in vivo,* highlighting the existing challenges and gaps in evidence around this topic. Development of an AO protocol has reinforced confidence in this technique, building on previously identified literature. This thesis also presents the first rigorous assessment of reliability for NIRS-derived haemodynamic markers measuring bone tissue *in vivo.* Likewise, it is the first attempt at comparison of NIRS-derived haemodynamic markers in bone against external comparator tests of bone health.

The results of this PhD have added confidence in this potential application of NIRS as a research tool in the field of bone health. However it is clear that further research on the application of NIRS should continue, including consideration of the imminent technological advancements in NIR based equipment, discussed in Section 11.3.

There remains a clear demand for testing methods that can take representative measures of bone haemodynamics in humans *in vivo* in order to explore the potential role of the intraosseous vasculature in normal bone regulation, and altered pathophysiological states. This thesis has contributed in part to a wider movement towards development of NIR testing methods that have desirable features for bone health research, including safe, inexpensive and real time protocols of measurement.

Appendix A: MEDLINE and EMBASE search terms

MEDLINE:

Index Test Terms: designed to identify the technology used to measure (ie NIR technologies)

1. NIRS.tw.
2. infrared.tw.
3. mid-wave.tw.7
4. near-wave.tw.
5. doppler.tw.
6. (light adj5 wavelength*).tw.
7. (light adj5 frequenc*).tw.
8. (optical adj5 (frequenc* or wavelength* or light*)).tw.
9. (visible adj5 (frequenc* or wavelength* or light*)).tw.
10. spectroscop*.tw.
11. photoplethysmograph*.tw.
12. spectrophotometr*.tw.
13. 1 or 2 or 3 or 4 or 5 or 6 or 7 or 8 or 9 or 10 or 11 or 12
14. exp Spectrum Analysis, Raman/
15. exp Laser-Doppler Flowmetry/
16. exp infrared rays/
17. exp luminescence/
18. exp Plethysmography/
19. exp Optical Imaging/
20. exp spectroscopy, near-infrared/
21. exp spectrometry, fluorescence/
22. exp Spectroscopy, Fourier Transform Infrared/
23. exp Spectrophotometry, Infrared/
24. 14 or 15 or 16 or 17 or 18 or 19 or 20 or 21 or 22 or 23
25. 13 or 24

“Participant” terms, which in this context is any bone tissue site

26. bone*.tw.
27. orthopaed*.tw.
28. orthoped*.tw.
29. calcan*.tw.
30. tibia*.tw.
31. patella*.tw.
32. femur*.tw.
33. femor*.tw.
34. radius.tw.
35. radial.tw.
36. ulna*.tw.
37. olecranon.tw.
38. manubrium.tw.
39. stern*.tw.
40. mandib*.tw.
41. skull.tw.
42. 26 or 27 or 28 or 29 or 30 or 31 or 32 or 33 or 34 or 35 or 36 or 37 or 38 or 39 or 40 or 41
43. exp "Bone and Bones"/
44. exp Orthopedics/
45. exp Bone Density/
46. exp Osteoporosis/
47. exp Bone Marrow/
48. exp Calcaneus/
49. exp Tibia/
50. exp Patella/
51. exp Femur Head/ or exp Femur/ or exp Femur Neck/
52. exp Radius/
53. exp Olecranon Process/
54. exp Ulna/
55. exp Manubrium/
56. exp Sternum/
57. exp Mandible/
58. exp Skull/
59. 43 or 44 or 45 or 46 or 47 or 48 or 49 or 50 or 51 or 52 or 53 or 54 or 55 or 56 or 57 or 58
60. 42 or 59

“Target condition” terms: any haemodynamic marker measured using NIR technology at a bone site

61. exp Oximetry/
62. exp Oxygen Consumption/
63. exp Blood Volume/
64. exp Perfusion Imaging/ or exp Perfusion/
65. exp Regional Blood Flow/
66. exp Blood Flow Velocity/
67. exp Microvessels/
68. exp Microcirculation/ or exp Capillaries/
69. exp Blood Volume Determination/
70. hemodynamics/ or exp vasoconstriction/ or exp vasodilation/ or exp vascular patency/
71. exp Pulsatile Flow/
72. 61 or 62 or 63 or 64 or 65 or 66 or 67 or 68 or 69 or 70 or 71
73. saturat*.tw.
74. TOI.tw.
75. nTHI.tw.
76. haemoglobin.tw.
77. hemoglobin.tw.
78. AC amplitude.tw.
79. perfusion.tw.
80. haemodynamic*.tw.
81. hemodynamic*.tw.
82. capillar*.tw.
83. microvascul*.tw.
84. microvessel*.tw.
85. (oxygen adj5 consumption).tw.
86. (oxygen adj5 metabolism).tw.

87. (blood adj5 flow).tw.
88. (blood adj5 volume).tw.
89. (blood adj5 velocity).tw.
90. oxygenat*.tw.
91. pulsatil*.tw.
92. 73 or 74 or 75 or 76 or 77 or 78 or 79 or 80 or 81 or 82 or 83 or 84 or 85 or 86 or 87 or 88 or 89 or 90 or 91
93. 72 or 92

The three sub categories are cross filtered with “AND” and I have used a human filter to exclude animal studies.
94. 25 and 60 and 93
95. human/
96. animal/
97. 95 not (95 and 96)
98. 94 and 97

EMBASE:

Index Test Terms: designed to identify the technology used to measure (ie NIR technologies)
1. NIRS.tw.
2. infrared.tw.
3. mid-wave.tw.
4. near-wave.tw.
5. doppler.tw.
6. (light adj5 wavelength*).tw.
7. (light adj5 frequenc*).tw.
8. (optical adj5 (frequenc* or wavelength* or light*)).tw.
9. (visible adj5 (frequenc* or wavelength* or light*)).tw.
10. spectroscop*.tw.
11. photoplethysmograph*.tw.
12. spectrophotometr*.tw.
13. 1 or 2 or 3 or 4 or 5 or 6 or 7 or 8 or 9 or 10 or 11 or 12
14. exp plethysmography/
15. exp spectroscopy/
16. exp laser Doppler flowmetry/ or exp Doppler flowmetry/
17. exp infrared radiation/ or exp infrared spectrometry/ or exp infrared spectrophotometry/ or exp infrared spectroscopy/ or exp infrared thermometer/
18. exp fluorescence correlation spectroscopy/ or exp fluorescence imaging/
19. exp Raman spectrometry/ or exp infrared spectrometry/
20. 14 or 15 or 16 or 17 or 18 or 19
21. 13 or 20

“Participant” terms, which in this context is any bone tissue site
22. bone*.tw.
23. orthopaed*.tw.
24. orthoped*.tw.
25. calcan*.tw.
26. tibia*.tw.
27. patella*.tw.
28. femur*.tw.
29. femor*.tw.
30. radius.tw.
31. radial.tw.
32. ulna*.tw.
33. olecranon.tw.
34. manubrium.tw.
35. stern*.tw.
36. mandib*.tw.
37. skull.tw.
38. 22 or 23 or 24 or 25 or 26 or 27 or 28 or 29 or 30 or 31 or 32 or 33 or 34 or 35 or 36 or 37
39. exp orthopedics/
40. exp bone marrow/
41. exp trabecular bone/
42. exp cortical bone/
43. exp calcaneus/
44. exp tibia/
45. exp patella/
46. exp femur/
47. exp radius/
48. exp olecranon/
49. exp ulna/
50. exp sternum/
51. exp mandible/
52. exp skull/
53. 39 or 40 or 41 or 42 or 43 or 44 or 45 or 46 or 47 or 48 or 49 or 50 or 51 or 52
54. 38 or 53

“Target condition” terms: any haemodynamic marker measured using NIR technology at a bone site
55. saturat*.tw.
56. TOI.tw.
57. nTHI.tw.
58. haemoglobin.tw.
59. hemoglobin.tw.
60. AC amplitude.tw.
61. perfusion.tw.
62. haemodynamic*.tw.
63. hemodynamic*.tw.
64. capillar*.tw.
65. microvascul*.tw.
66. microvessel*.tw.
67. (oxygen adj5 consumption).tw.
68. (oxygen adj5 metabolism).tw.
69. (blood adj5 flow).tw.
70. (blood adj5 volume).tw.
71. (blood adj5 velocity).tw.
72. oxygenat*.tw.
73. pulsatil*.tw.

74. 55 or 56 or 57 or 58 or 59 or 60 or 61 or 62 or 63 or 64 or 65 or 66 or 67 or 68 or 69 or 70 or 71 or 72 or 73
75. exp oximetry/
76. exp oxygen consumption/
77. exp blood volume/
78. exp artery perfusion/ or exp tissue perfusion/ or exp organ perfusion/
79. exp perfusion/
80. exp blood flow/
81. exp blood flow velocity/
82. exp microvasculature/
83. exp microcirculation/
84. exp capillary/
85. *hemodynamics/
86. exp vasoconstriction/
87. exp vasodilatation/
88. exp vascular patency/
89. exp pulsatile flow/
90. exp oxygen saturation/
91. exp hemoglobin determination/
92. exp oxyhemoglobin/
93. exp deoxyhemoglobin/
94. 75 or 76 or 77 or 78 or 79 or 80 or 81 or 82 or 83 or 84 or 85 or 86 or 87 or 88 or 89 or 90 or 91 or 92 or 93
95. 74 or 94

The three sub categories are cross filtered with “AND” and I have used a human filter to exclude animal studies.
96. 21 and 54 and 95
97. animal/
98. human/
99. 98 not (97 and 98)
100. 96 and 99

Appendix B: Full text eligibility screening form

Study	
Year of Publication	
Language of Publication	
Country of Publication	
Study Design	
Form of publication (peer reviewed, grey literature etc.)	
Sample Size	
Human/Animal Study?	
Adult/Paediatric Study?	
Healthy/diseased participants? If diseased, provide details.	
Does the index test utilise wavelengths between 400-25000nm?	
Index Test measuring a suitable haemodynamic marker of bone tissue? (If so, what?)	
Suitable bony anatomical site? (if so, what?)	
Reference Standard/comparator used	
INCLUDE/REJECT?	
If rejected, state why	

Appendix C: Data extraction template

Study	
Year of Publication	
Language of Publication	
Country of Publication	
Study Design	
Status of publication (peer reviewed, grey literature etc.)	
Sample Size	
Participant Demographics provided (e.g. age, BMI, sex)	
Adult/Paediatric Study?	
Healthy/diseased participants? If diseased, provide details.	
Did the study demonstrate NIRS measuring bone tissue exclusively, if so, how?	
Anatomical Sites Investigated	
Wavelengths utilised by the index test, (narrow or broadband NIRS?)	
Details on the application of the index test	
Types of Haemodynamic Markers measured (and if relative or absolute values)	
Corresponding results	
Reference Standard/ Comparators used and corresponding results	
Comments on patient tolerability	
Measurements or comments on reproducibility across operators	
Measurements or comments on applicability across the general population	
Suggested amendments and/or applications for clinical use	

Appendix D: Risk of bias assessment summary

NIRS STUDIES									
Study	Selection bias	Performance bias	Detection bias	Attrition bias	Reporting bias	Other bias	Applicability	Generalisability	Overall Quality
Alnaemi 2015	?	LOW	LOW	?	LOW	?	POOR	POOR	POOR
Aziz et al 2010	?	LOW	LOW	?	LOW	?	POOR	POOR	POOR
Binzoni et al 2002	?	LOW	LOW	?	LOW	?	FAIR	POOR	FAIR
Binzoni et al 2003	?	LOW	LOW	?	LOW	?	FAIR	POOR	FAIR
Binzoni et al 2006	?	LOW	LOW	?	LOW	?	FAIR	POOR	FAIR
Binzoni et al 2016	?	LOW	LOW	?	LOW	?	FAIR	POOR	FAIR
Cai et al 2008	?	LOW	HIGH	HIGH	LOW	?	POOR	FAIR	POOR
Draghici et al 2017	?	LOW	?	?	LOW	?	FAIR	POOR	POOR
Farzam et al 2013	?	LOW	LOW	?	LOW	?	FAIR	POOR	FAIR
Farzam et al 2014	?	LOW	LOW	?	LOW	?	POOR	POOR	FAIR
Hutchinson et al 1990	?	LOW	HIGH	?	LOW	?	POOR	FAIR	POOR
Klasing et al 2003	?	LOW	LOW	?	LOW	?	FAIR	POOR	FAIR
Meertens et al 2016	HIGH	LOW	LOW	HIGH	LOW	?	FAIR	FAIR	FAIR
Pifferi et al 2004	?	LOW	LOW	?	LOW	?	FAIR	POOR	FAIR
Reher et al 2011	?	LOW	?	?	LOW	?	POOR	FAIR	POOR
Sekar et al 2015	?	LOW	LOW	?	LOW	?	POOR	POOR	POOR
Sekar et al. 2016	?	LOW	LOW	?	LOW	?	POOR	POOR	FAIR
Sekar et al. 2016b	?	LOW	LOW	?	LOW	?	FAIR	POOR	FAIR
Siamwala et al 2015	?	LOW	LOW	LOW	LOW	?	FAIR	POOR	FAIR
Siamwala et al 2017	?	LOW	LOW	?	LOW	?	FAIR	FAIR	FAIR
Sorensen et al 2017	?	LOW	?	?	LOW	?	FAIR	POOR	FAIR
Takami et al 2008	?	LOW	?	?	LOW	?	POOR	FAIR	POOR

LDF STUDIES										
Study	Selection bias	Performance bias	Detection bias	Attrition bias	Reporting bias	Other bias		Applicability	Generalisability	Overall Quality
HIP/ACETABULAR LDF STUDIES										
Amarakesara et al. 2008	?	HIGH	?	?	LOW	?		POOR	FAIR	POOR
Bassett et al. 1997	?	?	?	LOW	LOW	?		POOR	FAIR	POOR
Beaule et al. 2006	?	LOW	?	LOW	LOW	?		POOR	FAIR	POOR
Beaule et al. 2007	?	LOW	?	LOW	LOW	?		POOR	FAIR	POOR
Beck et al. 2004	HIGH	LOW	?	LOW	LOW	?		POOR	POOR	POOR
Bogehoj et al. 2007	?	LOW	?	LOW	LOW	?		POOR	FAIR	POOR
El Maraghy et al. 1999	?	LOW	?	LOW	LOW	?		POOR	FAIR	POOR
El Maraghy et al. 2000	?	LOW	?	LOW	LOW	?		POOR	FAIR	POOR
Fukuoka et al. 1999	?	LOW	?	LOW	LOW	?		POOR	FAIR	FAIR
Halawi et al 2019	?	LOW	?	?	LOW	?		POOR	FAIR	FAIR
Hempfing et al. 2003	?	LOW	?	LOW	LOW	?		POOR	FAIR	POOR
Hupel et al. 2000	?	LOW	?	LOW	LOW	?		POOR	FAIR	POOR
Lausten et al. 1993b	?	?	?	?	LOW	?		POOR	FAIR	POOR
Lausten et al. 1993	?	LOW	?	LOW	LOW	?		POOR	POOR	POOR
Lorenzen et al. 2013	?	HIGH	HIGH	HIGH	LOW	?		POOR	FAIR	POOR
Notzli et al. 2002	?	LOW	?	?	LOW	?		POOR	FAIR	POOR
Schoeniger et al. 2009	?	LOW	?	?	LOW	?		POOR	FAIR	POOR
Sugamoto et al. 1998	?	LOW	?	LOW	LOW	?		POOR	POOR	POOR
Swiontkowski et al. 1987	?	LOW	?	LOW	LOW	?		POOR	POOR	POOR
Ziebarth et al. 2013	?	?	?	?	LOW	?		POOR	POOR	POOR
PATELLA LDF STUDIES										
Stoffel et al. 2007	?	LOW	?	?	LOW	?		POOR	FAIR	POOR
Nicholls et al. 2006	?	LOW	?	?	LOW	?		POOR	FAIR	POOR
Kohl et al. 2011	?	LOW	?	?	LOW	?		POOR	FAIR	POOR
Hughes et al. 1998	?	LOW	?	?	LOW	?		POOR	FAIR	POOR
Hempfing et al. 2007	?	LOW	?	?	LOW	?		POOR	FAIR	POOR
Hasegawa et al. 2009	?	LOW	?	LOW	LOW	?		POOR	FAIR	POOR
STERNUM LDF STUDIES										
Bahn et al. 1990	?	LOW	LOW	HIGH	LOW	?		POOR	FAIR	POOR
Green et al. 1993	?	LOW	?	LOW	LOW	?		POOR	FAIR	POOR
Kamiya et al. 2008	?	HIGH	HIGH	LOW	LOW	?		POOR	FAIR	POOR
Knobloch et al. 2003	?	LOW	?	?	LOW	?		POOR	FAIR	POOR
Nishi et al. 2011	?	LOW	?	LOW	LOW	?		POOR	FAIR	POOR
DEBRIDEMENT LDF STUDIES										
Duwelius et al. 1992	?	?	HIGH	?	LOW	?		POOR	POOR	POOR
Swiontkowski et al. 1999	?	LOW	?	?	LOW	?		FAIR	FAIR	FAIR
Swiontkowski 1989	?	?	HIGH	?	LOW	?		POOR	POOR	POOR
Swiontkowski et al. 1989b	?	?	HIGH	?	LOW	?		POOR	POOR	POOR

LDF STUDIES										
Study	Selection bias	Performance bias	Detection bias	Attrition bias	Reporting bias	Other bias		Applicability	Generalisability	Overall Quality
MANDIBLE/MAXILLA LDF STUDIES										
Al-Kassab 1995	LOW	LOW	?	LOW	LOW	?		FAIR	GOOD	FAIR
Kokovic et al. 2014	?	?	?	?	LOW	?		POOR	POOR	POOR
Kretschmer et al. 2009	?	LOW	?	LOW	LOW	?		POOR	FAIR	POOR
Verdonck et al. 2009	?	LOW	?	LOW	LOW	?		POOR	POOR	POOR
Wannfors et al. 1991	?	?	?	?	LOW	?		POOR	FAIR	POOR
Wong 2000	?	LOW	?	LOW	LOW	?		POOR	POOR	POOR
Vasovic et al. 2017	?	LOW	?	LOW	LOW	?		POOR	POOR	POOR
COCHLEA LDF STUDIES										
Degoute et al. 1997	?	LOW	?	LOW	LOW	?		POOR	POOR	POOR
Drinias et al. 2007	?	LOW	?	LOW	LOW	?		FAIR	FAIR	POOR
Miller et al. 1994	?	LOW	?	LOW	LOW	?		POOR	POOR	POOR
Miller et al. 1995	?	LOW	?	?	?	?		POOR	POOR	POOR
Nakashima et al. 2002	?	LOW	?	?	?	?		POOR	POOR	POOR
Nakashima et al. 2004	?	LOW	?	?	?	?		POOR	POOR	POOR
Nakashima et al. 2006	?	?	?	?	?	?		POOR	POOR	POOR
Nakashima et al. 2012	?	LOW	?	?	LOW	?		POOR	FAIR	POOR
Selmani et al. 2001	?	LOW	?	?	LOW	?		POOR	FAIR	POOR
Sone et al. 2013	?	LOW	?	?	LOW	?		POOR	FAIR	POOR
Tono et al. 1998	?	LOW	?	LOW	LOW	?		POOR	POOR	POOR
MISCELLANEOUS LDF STUDIES										
Schuurman et al. 1987	?	LOW	?	LOW	?	?		POOR	POOR	POOR
Hempfing et al. 2005	?	LOW	?	LOW	LOW	?		POOR	POOR	POOR
Hertel et al. 2004	?	LOW	?	LOW	LOW	?		POOR	FAIR	POOR
Kuhn et al. 2005	?	LOW	?	LOW	LOW	?		FAIR	FAIR	POOR
Minokawa et al. 2016	?	LOW	?	?	LOW	?		POOR	POOR	POOR
NON INVASIVE LDF STUDY										
Binzoni et al. 2013	HIGH	LOW	LOW	LOW	LOW	HIGH		FAIR	POOR	FAIR

PPG STUDIES										
Study	Selection bias	Performance bias	Detection bias	Attrition bias	Reporting bias	Other bias		Applicability	Generalisability	Overall Quality
Becker et al 2018	?	LOW	LOW	?	LOW	?		FAIR	FAIR	FAIR
Howden et al 2017	?	LOW	LOW	LOW	LOW	?		FAIR	FAIR	FAIR
Larsson et al 2014	?	LOW	LOW	LOW	LOW	?		FAIR	FAIR	FAIR
Mateus et al. 2012	?	LOW	LOW	LOW	LOW	?		FAIR	FAIR	FAIR
Mateus et al 2013	?	LOW	LOW	LOW	LOW	?		FAIR	FAIR	FAIR
Naslund 2006	?	LOW	LOW	?	LOW	?		FAIR	POOR	FAIR
Naslund et al. 2007	LOW	?	LOW	?	LOW	?		FAIR	POOR	FAIR
Naslund et al. 2011	?	LOW	LOW	?	LOW	?		FAIR	POOR	FAIR
Naslund et al. 2019	?	LOW	LOW	LOW	LOW	?		FAIR	POOR	FAIR
Siamwala et al. 2015	?	LOW	LOW	LOW	LOW	?		FAIR	FAIR	FAIR
Siamwala et al 2017	?	LOW	LOW	?	LOW	?		FAIR	FAIR	FAIR

Appendix E: Optode spacing experiment

An early protocol development experiment was undertaken to investigate any systematic effects of optode spacing between 2.5cm and 5cm, as the existing literature identified in the systematic review mentions using a variety of spacing distances within this range, as discussed in Section 3.5.2.1. Increasing inter optode spacing will increase the depth and volume of the tissue sampled, but at the expense of signal to noise ratio, as photons are more likely to be attenuated travelling a greater distance through tissue (see Figure E.1). It is generally accepted that the depth of tissue measured is approximately half the inter optode spacing [2, 10]. The experiment involved monitoring tissue oxygenation index (TOI) in real time. TOI was selected as the only parameter that is physiologically relevant at rest without any intervention protocol (as described in Section 2.2.1.4).

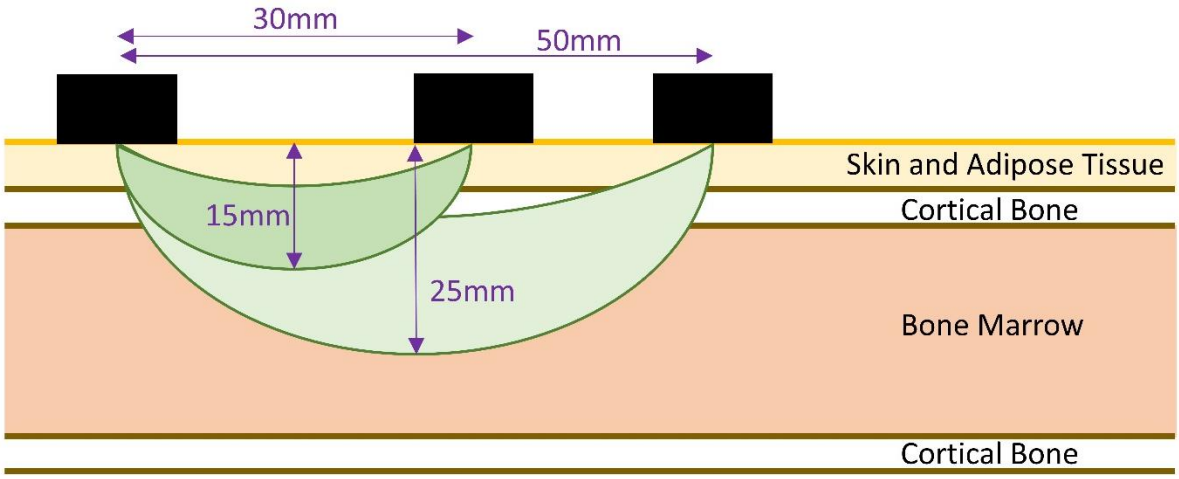

Figure E.1: Schematic diagram representing the increased volume and depth of measurements at the tibia with increased interoptode spacing.

Following a resting acclimatisation period of 15 minutes, the light emitting optode was placed at the proximal tibia medial to the tibial tuberosity. The light detecting optode was then initially placed 2.5cm away (from the centre of one optode to the other). Continuous monitoring was performed and after one minute the light detecting optode was placed a further 0.5cm apart. The system was zeroed with each new inter optode separation and a one second sampling rate was used. This sequence was continued up to an inter optode separation of 5cm. This test was performed twice each on three different participants.

Figure E.2 demonstrates that the trends in results were fairly consistent across all three participants. TOI generally peaked around 3.0cm to 3.5cm suggesting there may be

an interface where the system is more affected by cortical bone. From this point, as inter optode distance increased, TOI generally reduced slightly, presumably as more bone marrow was sampled at a greater depth.

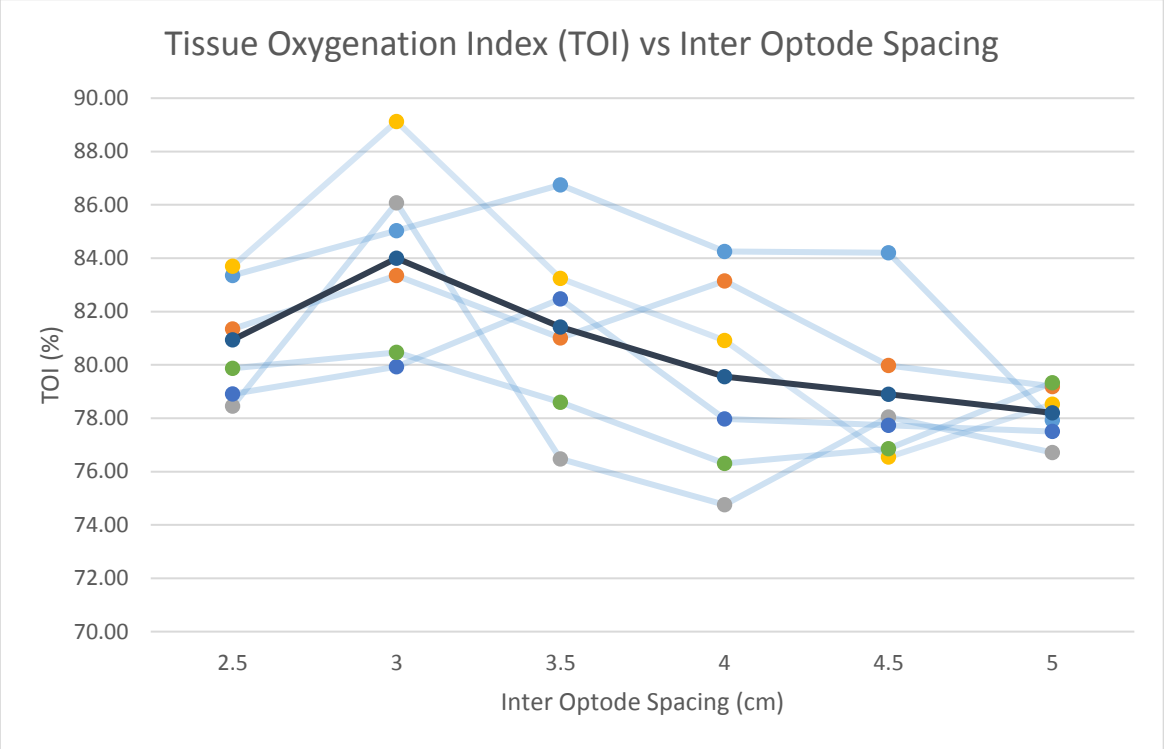

Figure E.2: Graph demonstrating the mean TOI of sample measurements taken at increasing increments of inter optode spacing (dark blue trendline). Individual trend lines of three participants measured twice each are shown with light blue trend lines.

At inter optode spacing of 4.5cm and 5cm, noise in the signal began to noticeably increase (see Figure E.3). The increased distance between source and detector means more attenuation of light photons before reaching the detector and thus a reduced signal to noise ratio. This was confirmed with the mean coefficient of variation (CV) within 50 second readings being 0.28% at 3cm, 0.46% at 4cm and 1.20% at 5cm. CV was calculated by dividing the standard deviation of the 50 individual measurements taken within the measurement period by the mean TOI measurement of the 50 second sample.

Given these observations it was decided to use a 4cm spacing between optode and detector. This was decided as a compromise between the potential inconsistency and unpredictability of cortical bone volume contributing more to measurements at 3cm inter optode spacing, and the decreased signal to noise ratio of 4.5cm and 5cm inter optode separations. The Hamamatsu NIRO-200NX also conveniently has a

premanufactured light hood for shielding light from optodes and maintaining a consistent 4cm spacing between participants.

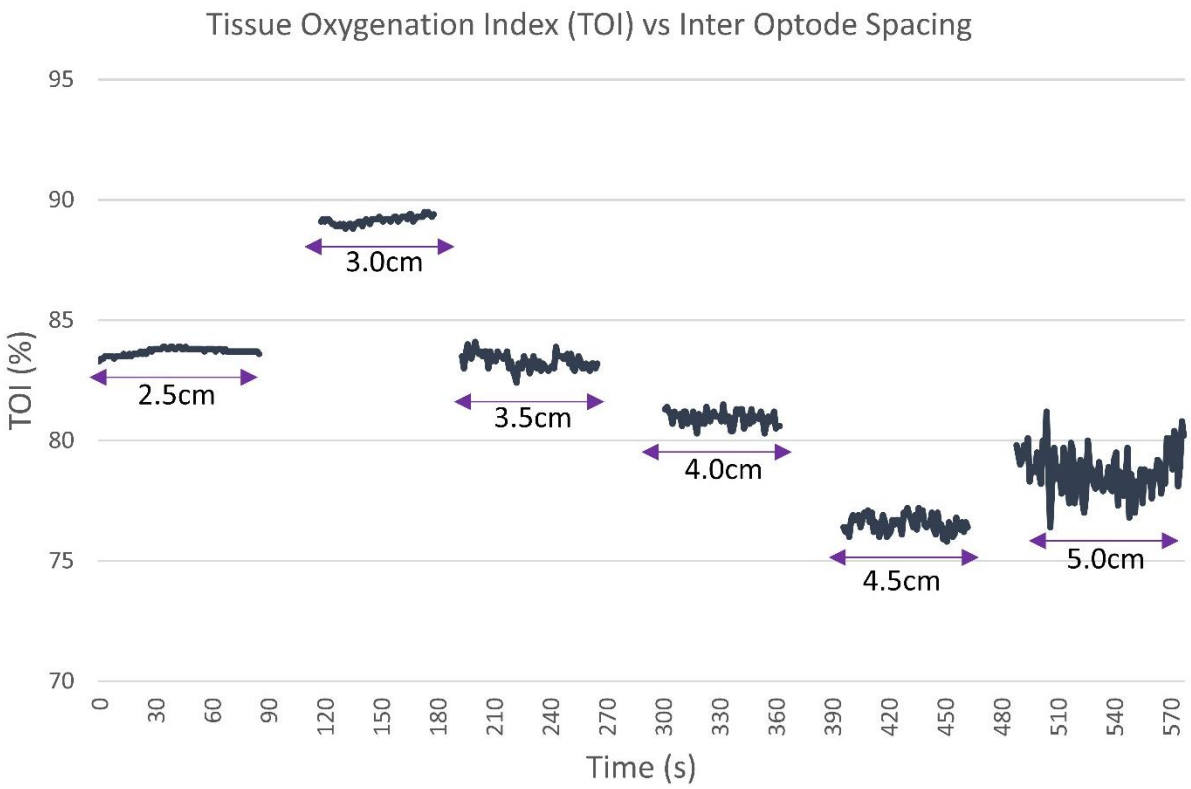

Figure E.3: Representative data from one participant, demonstrating the decreased signal to noise of TOI measurements as the inter optode spacing is increased.

Appendix F: Alternative NIRS intervention protocols

F.1: Mid-calf occlusion protocol

The aim of this protocol was primarily to demonstrate if NIRS optodes were taking measurements representative of bone tissue. NIRS measurements were taken at the medial malleolus of the tibia using the positioning outlined in Section 4.2. The medial malleolus was selected as a suitable measurement site as it is a superficial bony landmark in a weight bearing bone that is thick enough to suggest that NIRS signal will only travel through the tibia from optode to detector (apart from minimal overlying superficial tissue). Also the predominantly proximal vascularisation of the tibial medullary cavity via the tibial nutrient artery [55] allowed for an experimental design that could potentially observe if NIRS represented the vascular properties of bone, as further described below.

Two sets of NIRS measurement optodes were used. The first was placed at the medial malleolus and the second was placed over soft tissue laterally on the distal calf. After a resting period of 15 minutes, the vascular supply to the leg of the participant was then occluded at the midpoint of the lower leg using a blood pressure cuff inflated to 200mmHg for up to four minutes (see Figure F.1).

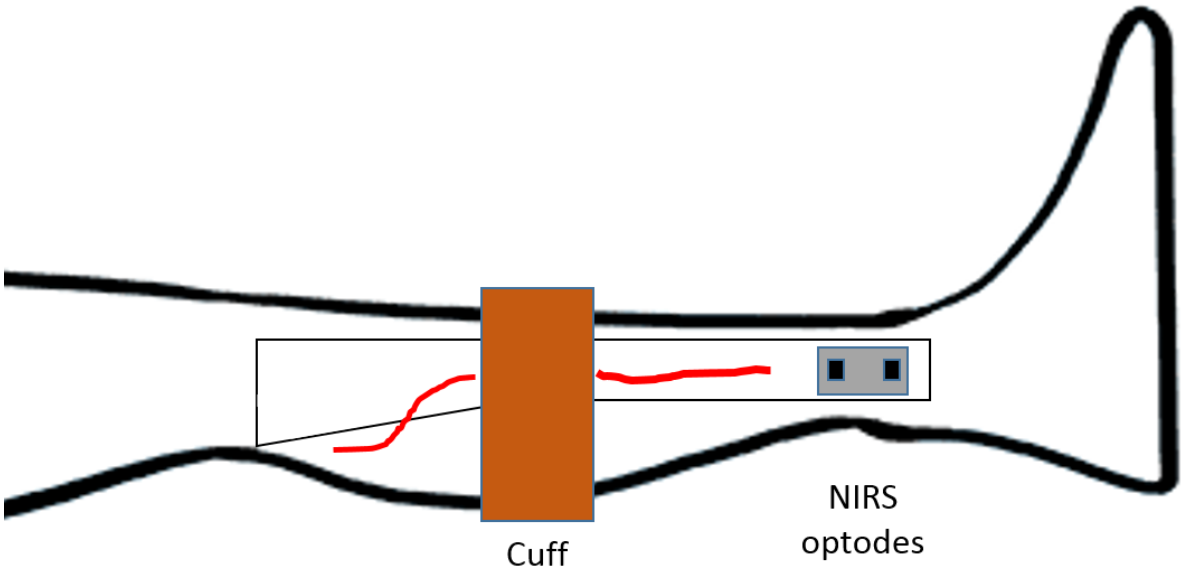

Figure F.1: Schematic of the mid-calf occlusion protocol set up. NIRS optodes are shown at the medial malleolus, and also placed at the lateral calf distal to the cuff around the mid-calf. The placement of the cuff should not occlude intraosseous blood supply from the nutrient artery.

It was hypothesised that if NIRS optodes were truly measuring bone oxygenation there would be minimal to no decrease in oxygenation at the medial malleolus when compared to the muscular site, as blood supply would be sustained through bone. This is because it was expected that the medullary cavity of the tibia predominantly receives its blood supply from a proximal artery supply through a nutrient foramen in the proximal end of the tibia, and being intraosseous should be protected from a mid-calf occlusion. It was expected that the oxygen saturation of the muscular site would still decrease due to inhibited arterial blood supply.

After a further rest period of ten minutes, a second occlusion was performed across the distal femur (using the same arterial occlusion protocol outlined in Section 4.4.1). Here both the muscular site and medial malleolus would be expected to deoxygenate, with occlusion of arterial blood supply at the distal femoral artery affecting both tissue sites.

This protocol was abandoned after six participants as no obvious differences between NIRS parameters at the medial malleolus were seen between the distal femur and mid-calf occlusions. Whilst this could potentially indicate NIRS was not truly measuring the medial malleolus, it was concluded that it was more likely that the influence of alternative blood supply to long bones via periosteal anastomosis had been potentially underestimated. McCarthy 2006 discusses the adaptability of long bone blood supply, citing examples of surgical reaming of the medullary cavity in sheep leading to no detectable change in cortical bone perfusion [23]. Santolini et al 2014 also argue that the distal third of the tibia and medial malleolus may be equally reliant on centripetal metaphyseal-epiphyseal vessels [55]. Likewise there may be variability amongst the population regarding the entry position of the tibial nutrient artery [55], and so there could not be certainty that this artery was not being inadvertently occluded during the mid-tibia occlusion. As mentioned in Section 5.3.1, the medial malleolus was also anecdotally more difficult to obtain stable optode placement, which may have contributed to measurement error.

F.2: Positional protocol

Testing was performed to demonstrate if NIRS was responsive to physiological haemodynamic changes caused by gravitational positional changes of the lower leg, as has previously been demonstrated in the literature [10, 78, 196, 204]. After 15 minutes supine rest, participants were continuously monitored at the proximal tibia and lateral

calf. With support of a tilting bed, participants raised and lowered their leg 15 degrees for 2 minutes each, with measurements at a neutral supine position taken before, between and after positional changes. This was repeated for three participants. Normalised total haemoglobin index (nTHI) was the NIRS parameter of interest as this can reflect relative changes in blood volume (as discussed in Section 2.2.1.4) that were expected due to the gravitational effects of differing leg positions. A mean nTHI was taken over 100 seconds for each position with a sampling rate of once per second.

Figure F.2: Representative image of NIRS measurements taken at the lateral calf and proximal tibia with leg up tilt.

Results are presented graphically in Figure F.3 below. During positional movements, total blood volume, as measured by nTHI, dropped in both the tibia (13.0% mean reduction; SD 6.0%) and lateral calf (4.0% mean reduction; SD 0.2%) when the leg was raised, as was expected with gravity. Likewise nTHI increased as the leg was dropped, again as expected with gravity, in both the tibia (16.2% mean increase; SD 16.4%) and the calf (2.2% mean increase, SD 3.7%). It would appear that bone had more marked relative changes in blood volume with positional changes than muscle. However this potentially highlights a limitation of the nTHI parameter. As discussed in Section 2.2.1.4, changes in nTHI represent relative changes in total haemoglobin concentration relative to the initial measurement point, with the initial absolute haemoglobin concentration unknown. It is expected that if the bone site has a smaller initial absolute blood volume (as is expected, see discussion in Section 5.6.3, page 153), then comparable changes in absolute haemoglobin concentration between the tibia and calf could be reflected as very different relative changes, with nTHI changes

at the tibia exaggerated compared with muscle due to a potentially smaller initial haemoglobin concentration.

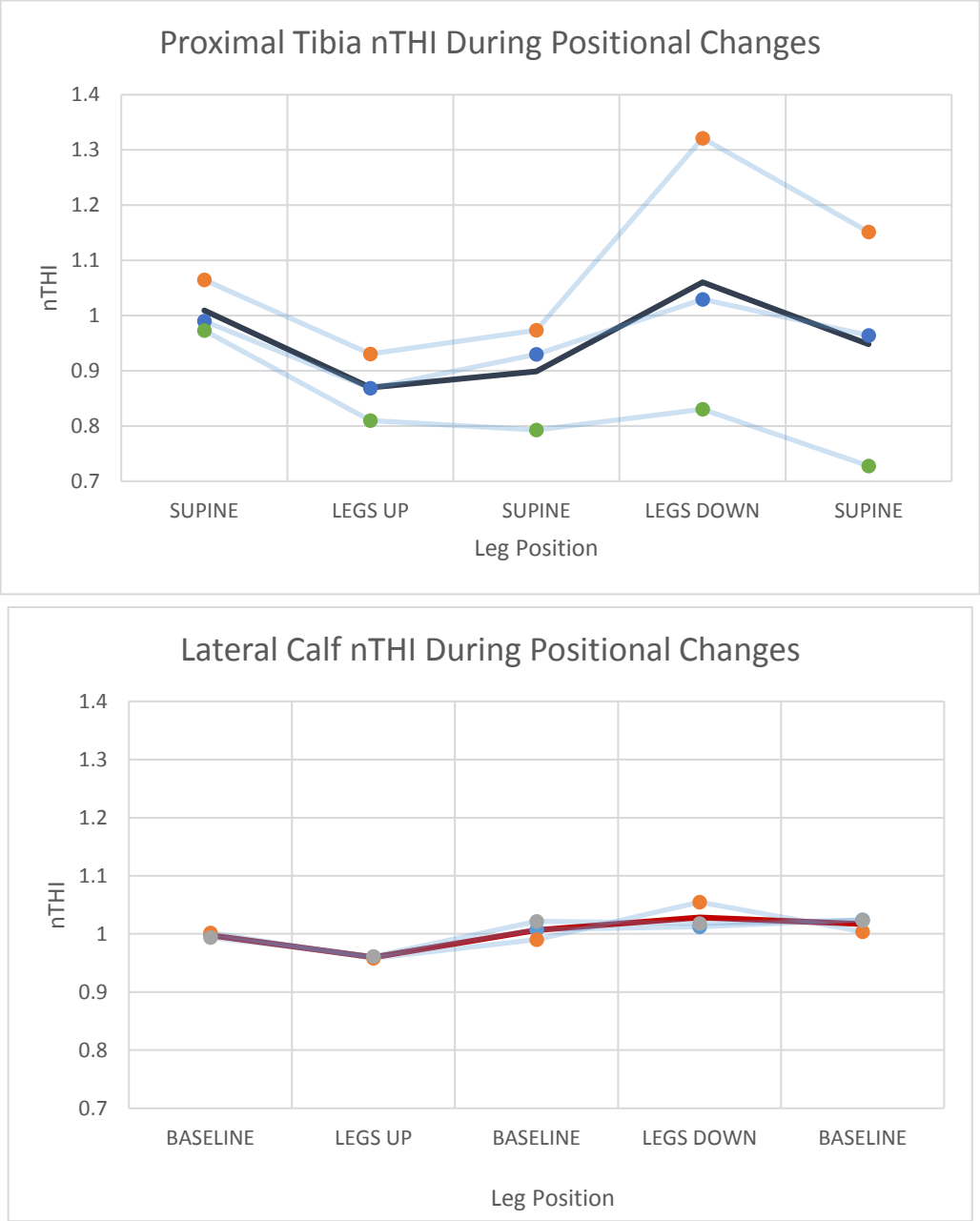

Figure F.3: nTHI changes (representative of relative blood volume changes) during positional movement of the proximal tibia and lateral calf with 15 degrees tilt of the leg up and down (N=3).

The results of this experiment were in keeping with previous similar feasibility work, demonstrating the responsiveness of NIRS to detect gravitational changes in blood volume, as represented by nTHI. Binzoni et al 2006 [(10)] discusses similar changes in NIRS parameters using similar positioning protocols. The authors reflect that the physiological vascular response underpinning the observed changes is unknown, and

may differ between muscle and bone, suggesting potentially unique vasoregulatory response at the tibia.

Siamwala et al 2015 [78] report a significant reduction in calf circumference with leg up tilt using strain-gauge plethysmography, suggestive of general blood volume reduction at the calf. This study also reported increases in blood flux at the tibial diaphysis measured using photoplethysmography (PPG). The authors were interested in applying lower body negative pressure using a pressure chamber (see Figure 3.2) in order to reverse these changes, as they hypothesised this may be a potential treatment option to reverse bone health changes in astronauts exposed to longer periods of microgravity. The authors also reflect that the physiological responses to positional changes are essentially unknown. Later work by the same author's also suggests sex-specific differences in response [204].

Despite these interesting observations, this protocol was not adopted further as there was only a small external evidence base around haemodynamic regulation in bone due to positional changes with which to compare results. This would prohibit validation of this protocol against external comparators, and make the clinical utility of NIRS results much harder to establish. Results also suggested wide variability in individual results despite similar trends in nTHI changes (as shown graphically in Figure F.3), suggesting the reproducibility of the testing may not be sufficient for further research.

F.3: Venous occlusion protocol

A venous occlusion protocol was attempted to assess if it would be a feasible protocol for obtaining haemodynamic measurements of bone tissue, and to try to demonstrate confidence that bone tissue was being measured at TP and TD sites, based on the differences between these sites and measurements taken at the lateral calf. This was achieved by applying an occlusion with only enough pressure to block venous return, but still allowing arterial inflow into the tissue being sampled. It was hypothesised there may be a difference between tissue types affecting the rate of inflow of arterial blood, detectable by NIRS. This could be because of differences in the size of feeder arteries or capillary density between tissue types, or differences in interstitial pressure within the differing tissue types [5].

A four minute femoral venous occlusion was performed at a personalised pressure midway between the previously observed diastolic and systolic brachial blood pressure of the participant. A venous occlusion was deemed successful if there was an increase

in both deoxygenated haemoglobin (HHb) and oxygenated haemoglobin (O_2Hb) during occlusion, with a corresponding increase in blood volume, as represented by normalised total haemoglobin index (nTHI) and total haemoglobin concentration change (cHb; equal to O_2Hb + HHb) [(275)]. With respect to blood volume changes, an increase during venous occlusion is expected as there is arterial inflow without venous outflow. As such, the rate of cHb increase can be used as a marker of blood flow into tissue [(73)]. Tissue oxygenation index (TOI) was also expected to decrease during occlusion as venous deoxygenated haemoglobin accumulates in tissue due to venous occlusion (see Figure F.4 for an example).

Gaining a true venous occlusion proved less reliable than for the arterial occlusion protocol outlined in Section 4.4.1. Six of 14 occlusions performed on participants did not meet the desired criteria. This may have been in part due to unknown differences between femoral and brachial blood pressures resulting in poor venous occlusion, or alternatively undesirable arterial occlusion. There was no obvious difference in complication rates between measurements taken at the proximal tibia and tibial diaphysis sites.

For the eight successful datasets obtained, analysis was performed on the rate of increase in cHb, HHb, O_2Hb and nTHI changes during the last 3 minutes of the occlusion (with the first minute of data excluded to allow for variable cuff inflation time and initial noise in data due to cuff inflation). cHb and HHb were the most reliable measures from the venous occlusions with linear change observed (represented by a Pearson's r-value of >0.9) for all eight successful venous occlusions, at both the tibia and calf. O_2Hb and nTHI changes were far less reliable, with non-linear change in either tibial and/or calf readings ruling out 50% of data for comparison between anatomical measurement sites for these two parameters amongst the eight successful venous occlusions.

Using paired t-tests, a significant difference in the mean rate of increase in HHb during occlusion was observed between the tibia and the lateral calf across the eight participants providing data (tibia 0.64 µM.cm/s (SD 0.36) vs lateral calf 1.28 µM.cm/s (SD 0.36); $p<0.01$). There was also a significant difference in the rate of increase in cHb during occlusion between the tibia and the lateral calf across the eight participants providing data (tibia 1.23 µM.cm/s (SD 0.43) vs muscle 1.82 µM.cm/s (SD 0.64); $p<0.01$).

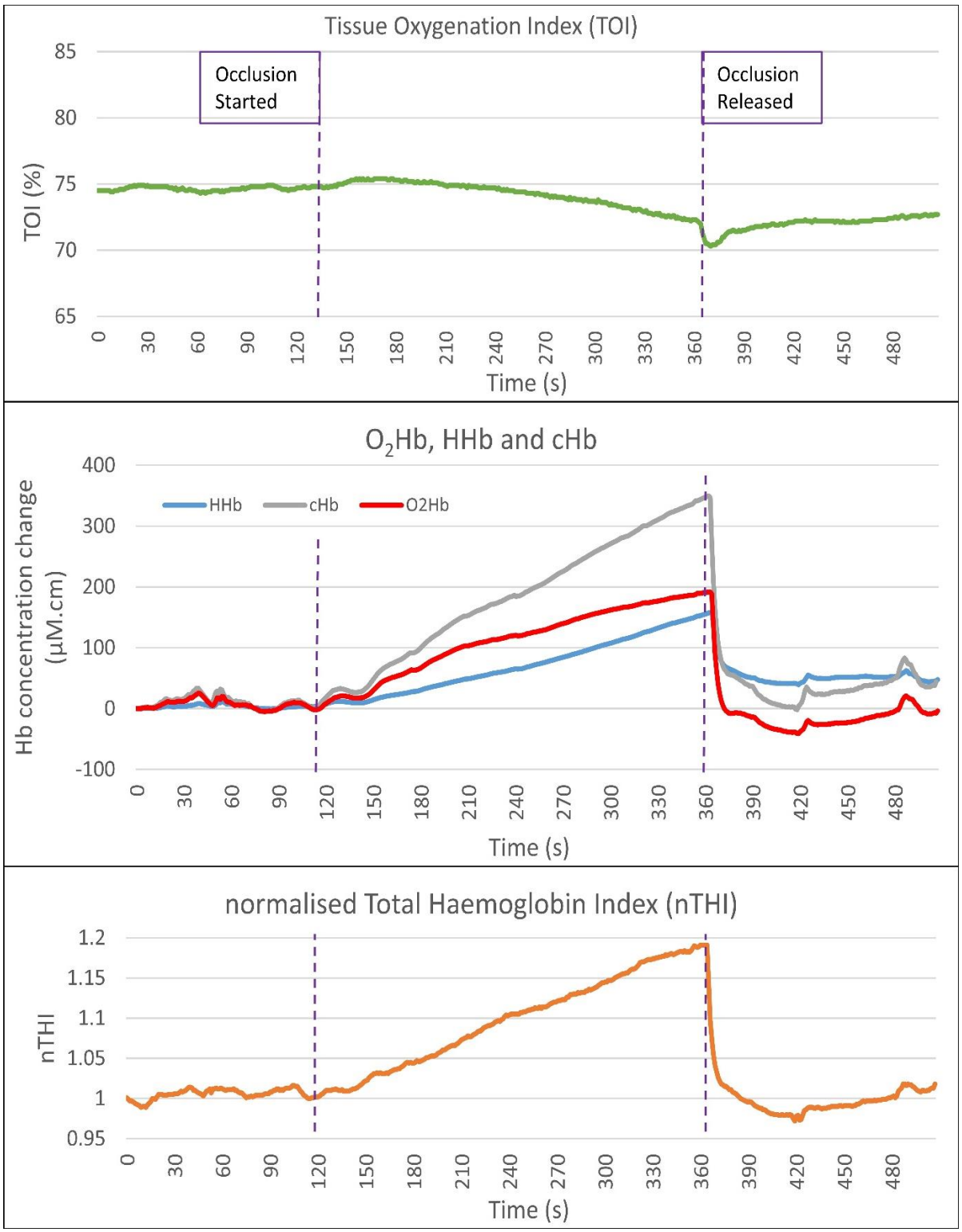

Figure F.4: An individual example of successful venous occlusion data at the proximal tibia. (a) The overall TOI drops during occlusion and responds upon occlusion release; (b) O_2Hb, HHb and cHb all increase as arterial inflow continues alongside venous pooling and oxygen extraction during occlusion. All return to approaching baseline during occlusion release; (c) nTHI increases during occlusion, again because of arterial inflow and venous pooling, returning to baseline once the occlusion is released.

Despite the statistically significant differences in results, the physiological importance of these differences is not possible to definitively determine. The results do support the arterial occlusion results presented in Section 5.3.2 that the lateral calf has a higher oxygen metabolism (as indicated by faster HHb rates of accumulation during occlusion), and greater tissue perfusion (as indicated by greater cHb rates of accumulation during occlusion). This supports the discussion in Section 5.6.2 that muscle has a higher physiological metabolism than bone, and that it has a greater blood volume capacity.

Venous occlusions were more tolerable for participants and provided some support that NIRS measurements at the tibia were responsive to microvascular change. Those changes were statistically significantly different to calf readings, and as such they could potentially represent tibial tissue. However, the venous occlusion protocol was not taken forward for reliability and validation assessment due to the poor success rate experienced when attempting adequate venous occlusions.

Van Beekvelt et al 2001 [73] also found venous occlusions unreliable compared with arterial occlusions of the upper limb when investigating forearm muscle with NIRS. The authors of this study made similar conclusions that venous occlusions may be more susceptible to localised changes to the limb being measured, whereas arterial occlusions offer a more definitive physiological change (i.e. total occlusion). Arterial occlusions were shown to be more reliable in Hassan et al 1999 [275] when examining peripheral oxygen utilisation in the forearm on neonates.

Venous occlusions also have other limitations. TOI data is by definition a ratio of O_2Hb and cHb and as such is affected by multiple confounding factors when measured during a period with changing blood volume, inherent during venous occlusion. Likewise using O_2Hb and HHb concentration changes as a marker of oxygen extraction is complicated by rising blood volume inherent with a venous occlusion. Venous occlusions also do not offer the same advantages of arterial occlusions when observing changes during cuff release and post occlusion recovery.

In principle, venous occlusions may be useful at observing the rate of O_2Hb increase during occlusion. In an occlusion system that does not allow outflow but only venous inflow, O_2Hb changes could be seen as a marker of the rate of arterial inflow into the tissue being sampled during occlusion. However, in practice O_2Hb was found to be an unreliable marker for venous occlusions.

Although cHb and HHb measurements were more reliable, they too have limitations. HHb and cHb readings measure absolute changes in haemoglobin concentration, but their value is relative to the initial readings taken at the time of first measurement, which remains unknown as a limitation of the continuous wave NIRS system used [2, 62]. It is likely that the rate at which HHb and cHb increases could be inherently dependent on the initial absolute blood volume at the time of measurement, the available space within tissue to facilitate increased blood volume, and the rate of arterial inflow during venous occlusion [275]. However it is impossible to distinguish between these potential variables, making comparison between individuals complex (especially when also considering the observed high failure rate of venous occlusion).

Measuring changes in HHb during venous occlusion has been previously attempted in NIRS research of the forearm and is most useful when considering oxygen metabolism (i.e. conversion of O_2Hb to HHb) [73, 275]. However, again this is a multifaceted haemodynamic marker during venous occlusion as oxygen metabolism will also be affected by differing rates of inter-participant arterial inflow and baseline arterial oxygenation [275]. As such it was decided that HHb changes would be more meaningful to be observed as a marker of oxygen extraction in the closed system of an arterial occlusion with constant blood volume. There was also no previous evidence identified investigating bone tissue through use of venous occlusion, unlike with arterial occlusions.

Appendix G: Non-linear modelling of post occlusion response

Non-linear modelling of time signal response curves is appropriate where linear responses are not observed. There are a number of different non-linear approaches possible (including variations of exponential and polynomial curves) but ideally the choice of non-linear model should be based on the physiological principles of the expected changes [286]. In this case, non-linear changes are evident in the NIRS-derived parameters of interest following the release of an arterial occlusion (see Figure G.1). These parameters are tissue oxygenation index (TOI), representing the percentage oxygenation of haemoglobin within the measured volume, and the change in oxygenated haemoglobin concentration (O_2Hb), representing the increase in O_2Hb concentration once arterial blood flow is restored.

Unfortunately there is no precedence for use of non-linear modelling for NIRS measurements of bone tissue and likewise no evidence based position on what type of non-linear response may be physiologically expected. However, there is some precedence for looking at non-linear markers of post occlusion response in studies performed on muscle tissue using non-linear modelling [80, 280, 283, 284].

These studies typically use exponential curve fitting to derive time constants (tau) that represent the time taken for the haemodynamic parameter to reach 63.2% of its recovery. Non-linear modelling using exponential modelling can also provide a measurement of amplitude or “span”, which in this context will provide the total maximum change in a haemodynamic parameter from the initial period of occlusion release to the maximum value obtained [286]. These markers of interest are graphically presented in Figure G.1.

Bopp et al 2014 used similar exponential curve fitting to investigate time constants of the change in total haemoglobin concentration in the forearm post occlusion release after arterial occlusion using a frequency domain NIRS system [80]. Nagasawa et al 2003 investigated the time constant of recovery in muscle oxygen consumption in muscles of the forearm of eight participants following hand grip exercise using a one phase exponential model [284]. Brizendine et al 2013 used a similar time constant of muscle oxygen consumption recovery to compare endurance athletes with controls, showing recovery rates two fold faster in athletes [283].

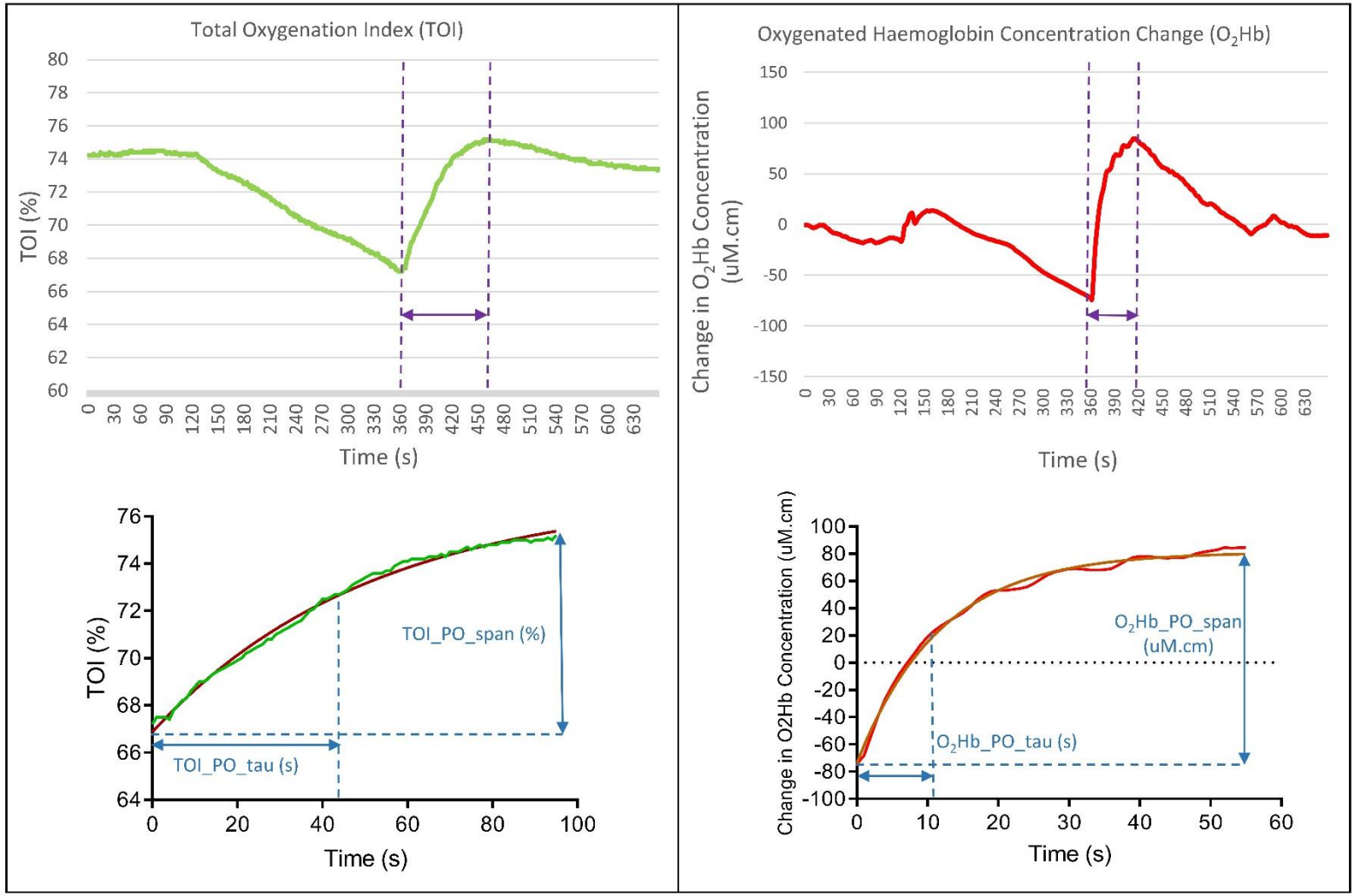

Figure G.1: Figure illustrating the sampling of the post occlusion period for non-linear one phase exponential analysis. The time period analysed is indicated by purple arrows and includes the start of the post occlusion period to the maximum value obtained. The four non-linear haemodynamic markers are presented in blue including span (amplitude) and tau (time constant) measurements for both tissue oxygenation index (TOI) and oxygenated haemoglobin concentration change (O_2Hb).

Based on the observation of exponential type responses post occlusion release, and the existing precedence in NIRS use of muscle, exponential curve fitting was explored. Non-linear analysis was performed using GraphPad Prism software (Version 8.1.0; GraphPad Software, San Diego) using the “one phase association” settings using a least squares fit approach [285]. Curves were fitted to data from the initial value of occlusion release to the maximum value observed (see Figure G.1 for examples), or for 120 seconds of recovery in instances were a typical post occlusive hyperaemic peak was not observed.

Non-linear markers were attempted for all participants who contributed to the intra operator reliability assessment presented in Section 7.1. Summary data are presented in Tables G.1 and G.2. This approach appeared to fit data well with all data returning an R-squared value of greater than 0.8, except for the tibial measurements in one participant. However, time constant markers (TOI_PO_tau and O_2Hb_PO_tau) demonstrated poorer reproducibility markers than comparable linear markers of the post occlusion recovery rate in the initial 20 seconds of the occlusion release (TOI_PO_20s and O_2Hb_PO_20s). The markers of span were analogous to the TOI_PO_absΔ and O_2Hb_PO_absΔ markers, with no clear advantage in reproducibility. As such, non-linear markers were abandoned for the validation analyses performed in Chapters 8, 9 and 10.

Table G.1: Same day test/retest repeatability data on non-linear haemodynamic markers of the proximal tibia and lateral calf post arterial occlusion release. (PO=Post Occlusion Release; SD=Standard Deviation; RMS=Root Mean Square; CV=Coefficient of Variation; ICC=Intra Class Correlation).

SAME DAY DATA POST OCCLUSION (TIBIA)	TOI_PO_span (%)	TOI_PO_tau (s)	O_2Hb_PO_span (μM.cm)	O_2Hb_PO_tau (s)
Paired data (N)	27	27	27	27
Mean	7.9	20.7	195.5	14.4
Between Participant SD	2.3	9.7	62.9	6.9
Within Participant RMSSD	1.1	5.8	15.2	3.8
Within Participant RMSCV (%, with 95% CI)	14.4 (0-29.2)	25.9 (0-59.4)	8.4 (0-17.1)	18.3 (0-37.2)
Repeatability Coefficient	3.0	16.1	42.0	10.5
ICC (with 95% CI)	0.76 (0.55-0.88)	0.63 (0.33-0.81)	0.95 (0.89-0.98)	0.72 (0.47-0.86)

SAME DAY DATA POST OCCLUSION (CALF)	TOI_PO_span (%)	TOI_PO_tau (s)	O_2Hb_PO_span (μM.cm)	O_2Hb_PO_tau (s)
Paired data (N)	31	31	31	31
Mean	33.5	16.7	500.95	14.16
Between Participant SD	13.7	14.0	244.78	8.94
Within Participant RMSSD	5.8	8.3	129.9	7.7
Within Participant RMSCV (%, with 95% CI)	13.7 (0-28.3)	21.9 (0-45.5)	21.0 (0-47.2)	28.3 (0-59.3)
Repeatability Coefficient	16.2	22.9	359.7	21.2
ICC (with 95% CI)	0.82 (0.66-0.91)	0.67 (0.42-0.82)	0.71 (0.48-0.85)	0.29 (0.0-0.58)

Table G.2: Different day test/retest reproducibility data on non-linear haemodynamic markers of the proximal tibia and lateral calf post occlusion release (DO=During Occlusion; PO=Post Occlusion Release; SD=Standard Deviation; RMS=Root Mean Square; CV=Coefficient of Variation; ICC=Intra Class Correlation).

DIFFERENT DAY DATA DURING OCCLUSION (TIBIA)	TOI_PO_span (%)	TOI_PO_tau (s)	O_2Hb_PO_span (μM.cm)	O_2Hb_PO_tau (s)
Paired data (N)	25	25	26	26
Mean	8.0	22.6	193.2	15.0
Between Participant SD	2.6	17.1	61.9	7.1
Within Participant RMSSD	2.4	17.3	26.3	4.6
Within Participant RMSCV (%, with 95% CI)	30.9 (0.0-62.2)	45.1 (3.4-86.7)	17.9 (0-39.6)	25.2 (0-55.6)
Repeatability Coefficient	6.6	48.0	72.7	12.6
ICC (with 95% CI)	0.21 (0.0-0.55)	0.12 (0.0-0.48)	0.83 (0.67-0.92)	0.62 (0.32-0.81)

DIFFERENT DAY DATA POST OCCLUSION (CALF)	TOI_PO_span (%)	TOI_PO_tau (s)	O_2Hb_PO_span (μM.cm)	O_2Hb_PO_tau (s)
Paired data (N)	30	30	30	30
Mean	31.5	14.9	458.7	12.3
Between Participant SD	12.5	12.2	199.3	4.3
Within Participant RMSSD	7.1	9.6	83.0	3.3
Within Participant RMSCV (%, with 95% CI)	17.9 (0-36.0)	25.9 (0-54.7)	20.3 (1.2-39.4)	24.9 (0-53.2)
Repeatability Coefficient	19.8	26.7	229.8	9.2
ICC (with 95% CI)	0.65 (0.39-0.82)	0.45 (0.11-0.69)	0.82 (0.66-0.91)	0.45 (0.11-0.69)

Appendix H: Oxygen to See (O2C) measurements

The Oxygen-To-See system (O2C; LEA Medizintechnik, Geissen) is an optical device designed to take non-invasive haemodynamic measurements of microcirculation within superficial tissue. This includes tissue oxygenation index (TOI) measurements representing the ratio of oxygenated haemoglobin to total haemoglobin using spectrometry methods discussed in Section 2.2.1. Markers of blood flow based on relative arbitrary units (au) are also possible using laser Doppler technology discussed in Section 2.2.3.

For measurements used in this appendix, data from the “deep” channel of the O2C probe have been used, primarily as it samples a larger tissue volume than the superficial channel. This involves a source to detector spacing of 8mm likely to represent cutaneous skin and some subcutaneous tissue of less than 4mm depth. Measurements were obtained with a two second sampling rate and utilising a range of optical wavelengths between 650-795nm for TOI measurements, and 830nm for blood flow measurements [224, 225].

Blood TOI and blood flow measurements were continuously monitored at the dorsal surface of the foot of the leg of interest. The primary rationale for this was to allow real time data when assessing the success of applying the arterial occlusion by assessing changes in blood flow to superficial tissue in the foot, which should become negligible with successful occlusion of pulsatile arterial flow. Figure H.1 provides an individual example of blood flow measurements of tissue at the dorsal surface of the foot, demonstrating the reduction of blood flow during arterial occlusion, with a rapid increase in blood flow upon occlusion release, as expected. It is noted blood flow does not reach zero during arterial occlusion, most likely due to Brownian motion of fluid within the sampled volume, termed biological zero [273]. TOI measurements taken at the foot using O2C, as well as at the proximal tibia with NIRS, are also presented in Figure H.1.

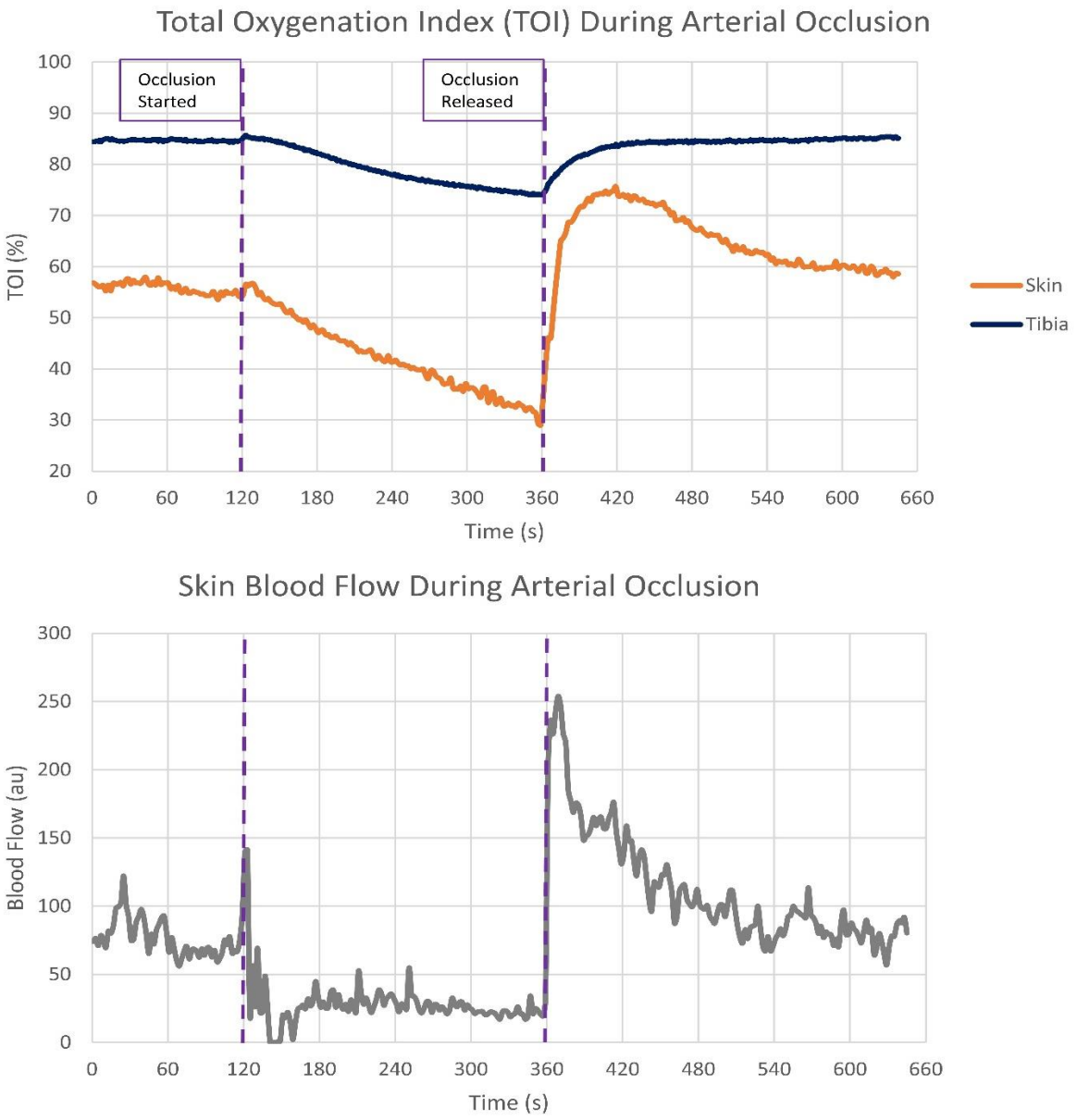

Figure H.1: Illustrative example of TOI and blood flow measurements taken from an individual participant during an arterial occlusion protocol. TOI data show clear differences in resting TOI between the tibial and foot measurement sites. There is also a difference in post occlusive reactive hyperaemia between tissue types when the occlusion is released. Blood flow data from the foot measurement site demonstrates a clear reduction in blood flow during arterial occlusion, with strong response, as expected, when the occlusion is released. This monitoring of blood flow was used in real time to help determine the integrity of the arterial occlusion applied.

Whilst the primary rationale for the use of O2C was for monitoring the integrity of arterial occlusions in real time, the data obtained from the O2C equipment also allowed for opportunistic *post hoc* analysis comparing the changes in TOI during arterial occlusion between NIRS and O2C equipment, where data are proposed to represent bone tissue at the tibia and superficial tissue at the foot, respectively. This was possible for 23 participants.

Figure H.2 demonstrates graphically the differences in resting TOI between sites, as well as the differences in TOI change during occlusion. Importantly, there is also a large difference in TOI response post occlusion release, with O2C measurements at the foot demonstrating a large PORH response, where there is negligible PORH response shown at the tibial measurement site with NIRS. Differences between measurement sites were confirmed to be statistically significant using paired t-tests ($p<0.05$) for all five haemodynamic markers of interest presented in Figure H.2.

Whilst it is acknowledged that potential confounders exist, such as the use of two different optical systems [259], the results gave confidence that NIRS and O2C data represent different tissue types. Similar observations were made in Figure 5.1 between NIRS measurements taken at tibial sites and over the lateral calf during arterial occlusion.

Whilst the results in this appendix cannot definitively rule out or quantify the contribution of overlying tissue to NIRS measurements taken at the proximal tibia, the results support the evidence based discussion presented in Section 8.4.2 around the likely minimal contribution of overlying superficial tissue to measurements of the proximal tibia in the data presented in this thesis.

Figure H.2: Graphs of tissue oxygenation index (TOI) haemodynamic markers obtained before, during and after arterial occlusion for measurement sites at the proximal tibia and at the dorsal surface of the foot (N=23). Error bars represent 95% confidence intervals.

Appendix I: Intra participant reproducibility pilot

This appendix graphically presents the TOI, HHb, and O2Hb data from arterial occlusion protocols repeated three times on three separate days, as described in Section 4.8. Data are presented for three participants. The graphs provide an example of the visual reproducibility of within-participant NIRS time signal curves, which as a pilot suggested further formal reliability assessment was warranted. These data also contributed to the quantitative assessment of reliability presented in Chapter 7.

Participant 1:

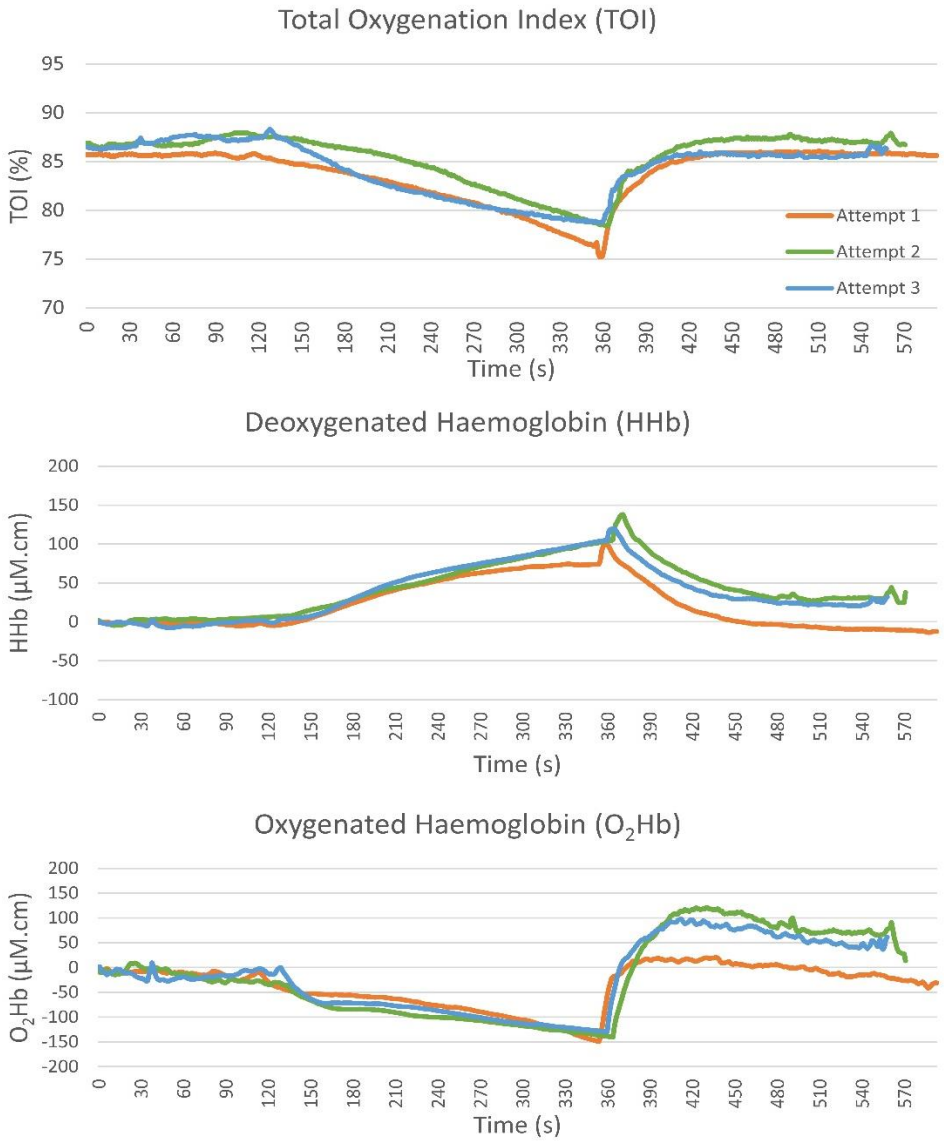

Participant 2:

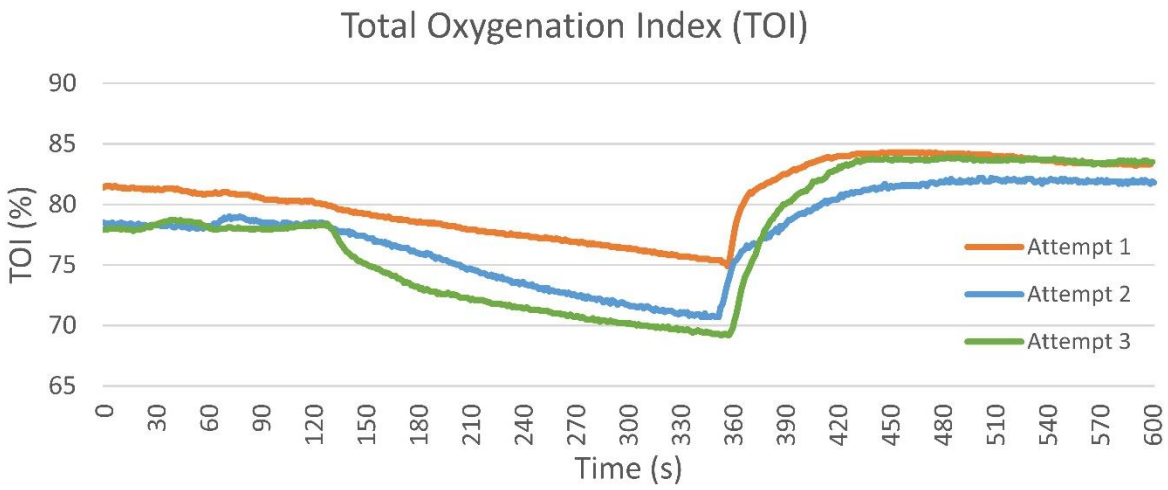

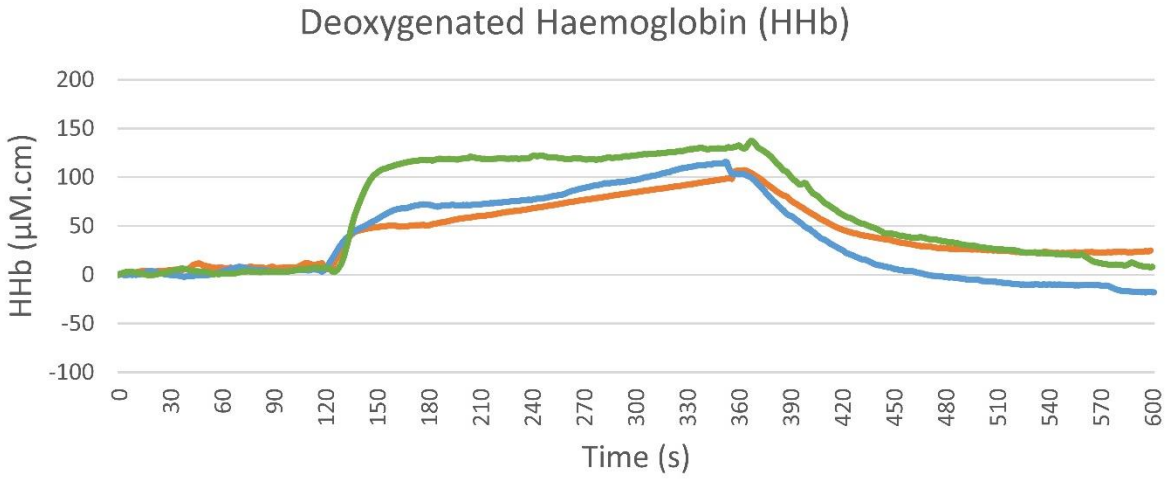

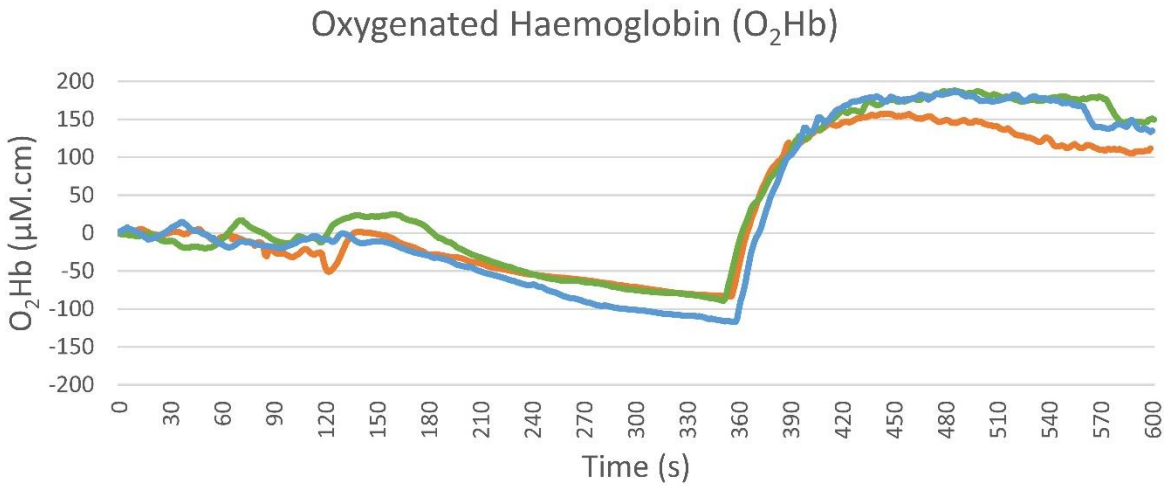

Participant 3:

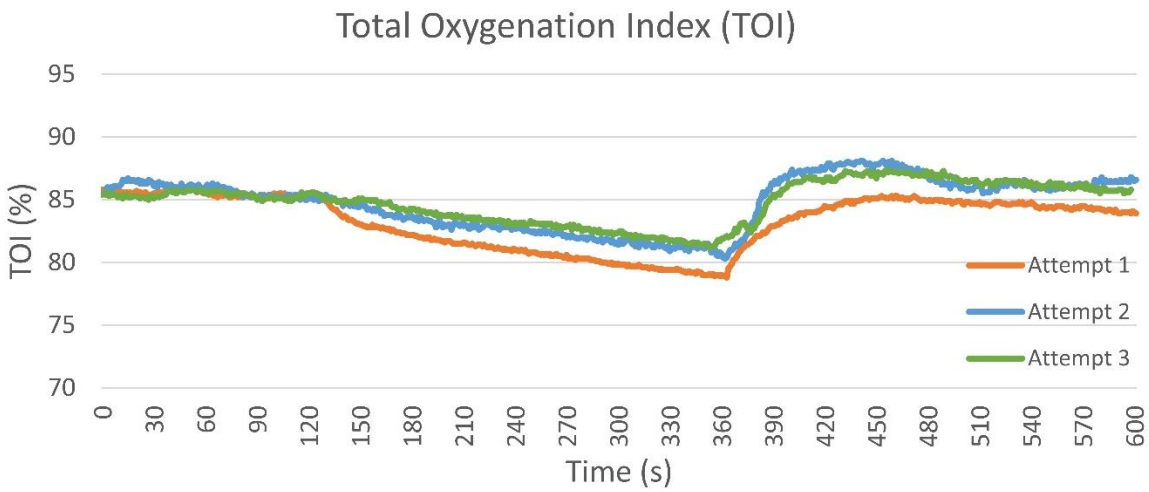

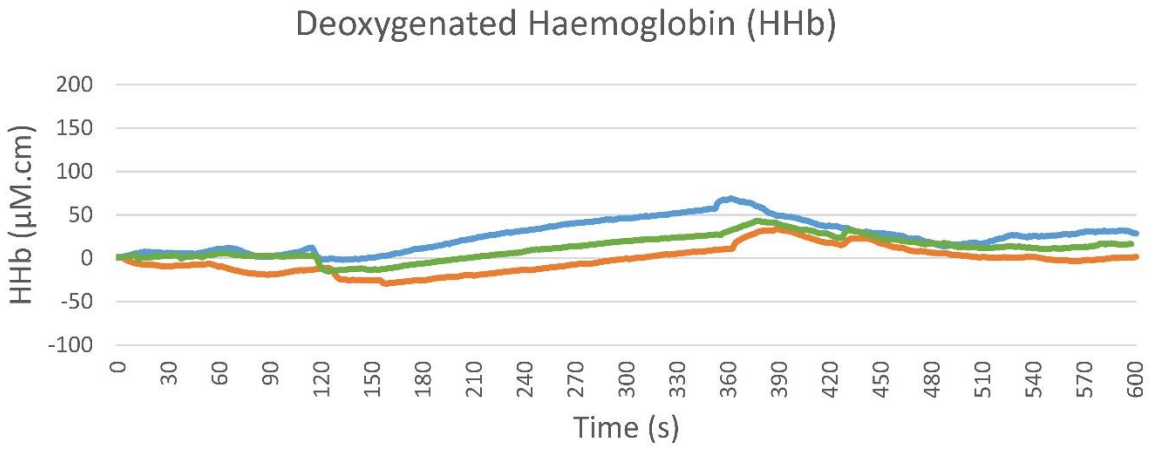

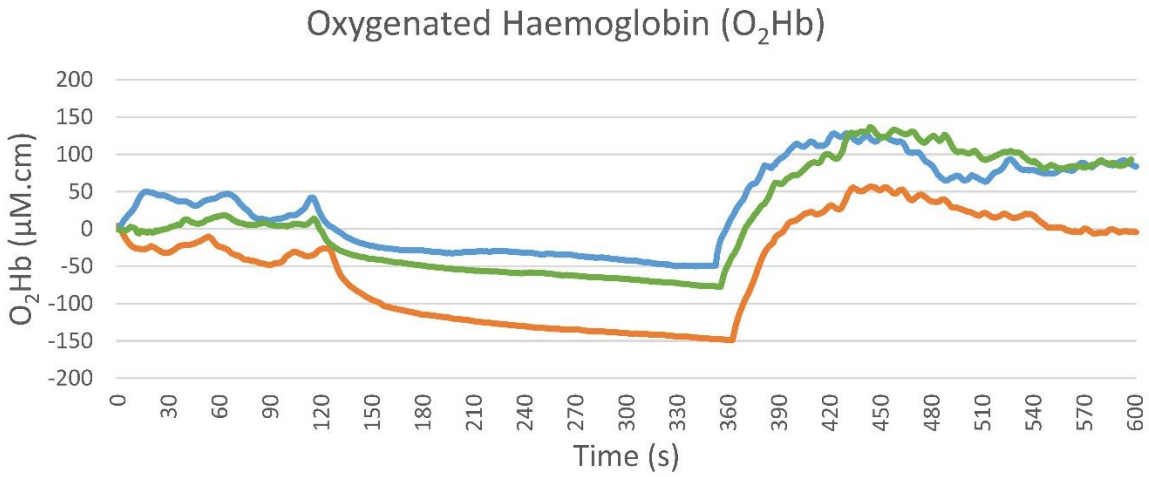

Appendix J: Blood oxygenation level dependent (BOLD) MRI case series

J.1: Rationale and aim

BOLD MRI protocols use T2* weighted sequences to demonstrate temporal changes of oxygenation levels in haemoglobin within tissues of interest, taking advantage of the diamagnetic properties of oxygenated haemoglobin (O_2Hb) and paramagnetic properties of deoxygenated haemoglobin (HHb). Assuming constant blood volume, a relative increase in HHb will decrease T2* signal due to the localised effect of HHb on the magnetic properties of Hydrogen atoms in the surrounding tissue [98]. BOLD protocols are commonly used to image oxygenation changes in the brain during functional MRI protocols. They have also been used to demonstrate oxygenation changes in muscle during arterial occlusion [103]. However, no precedence was identified for the use of BOLD imaging in bone tissue.

A BOLD non-contrast MRI protocol for imaging bone is of interest as it could potentially provide temporal scanning of a participants leg during arterial occlusion whilst in the MRI scanner, with signal changes representing changes in oxygenation status of bone tissue, thus potentially providing a direct comparison with the NIRS arterial occlusion protocol [97]. In principle BOLD protocols are ideal for validation of NIRS haemodynamic markers as they can similarly demonstrate oxygenation changes in real time with temporal imaging during an intervention such as an arterial occlusion protocol. BOLD protocols have been used to demonstrate strong correlations with cerebral NIRS measurements obtained during motor-task related activities [104, 105] and in skeletal muscle during exercise [106].

As part of the protocol development stage of this PhD project, a small feasibility study was performed with the aim of investigating whether T2* derived signal changes in bone marrow during arterial occlusion could be reliably recorded using a BOLD protocol, and if so, whether these changes were associated with recorded NIRS changes measured simultaneously with MRI compatible NIRS optodes. This feasibility work would determine if a BOLD protocol might be useful for validation of NIRS for measuring bone tissue haemodynamics in a more diversely sampled population.

J.2: Methods

Four participants undertook the imaging protocol, which was repeated twice at both the proximal tibia (TP) and tibial diaphysis (TD) sites, producing eight datasets in total. Ethical approval was not sought as participants all formed part of the immediate research team. Following MRI safety screening processes, the participant was positioned supine on the

scanner, with some propping of legs to allow placement of an occlusion cuff at the distal thigh, and to minimise movement during distal thigh cuff expansion. NIRS optodes were placed at either the TP or TD position using the positioning protocols previously described in Section 4.2. There was a 15 minute acclimatisation period before commencing MRI scanning. Two minutes of temporal imaging of the tissue of interest was then performed before initiating the distal thigh arterial occlusion to 200mmHg of pressure for up to four minutes, followed by up to four minutes of imaging post occlusion release. NIRS data were recorded simultaneously, with the NIRS based haemodynamic markers outlined in Section 4.4 used for data analysis.

During the occlusion protocol, BOLD MRI scans were acquired using a Phillips Intera 1.5T scanner and a dual element “sense flex” coil. Axial volumes were selected at the proximal tibia and tibial diaphysis (see Figure J.1). An echo-planar imaging (EPI) sequence with fat suppression was used with an echo time (TE) of 11ms and repetition time (TR) of 4 seconds. A single slice volume of 5mm thickness was obtained.

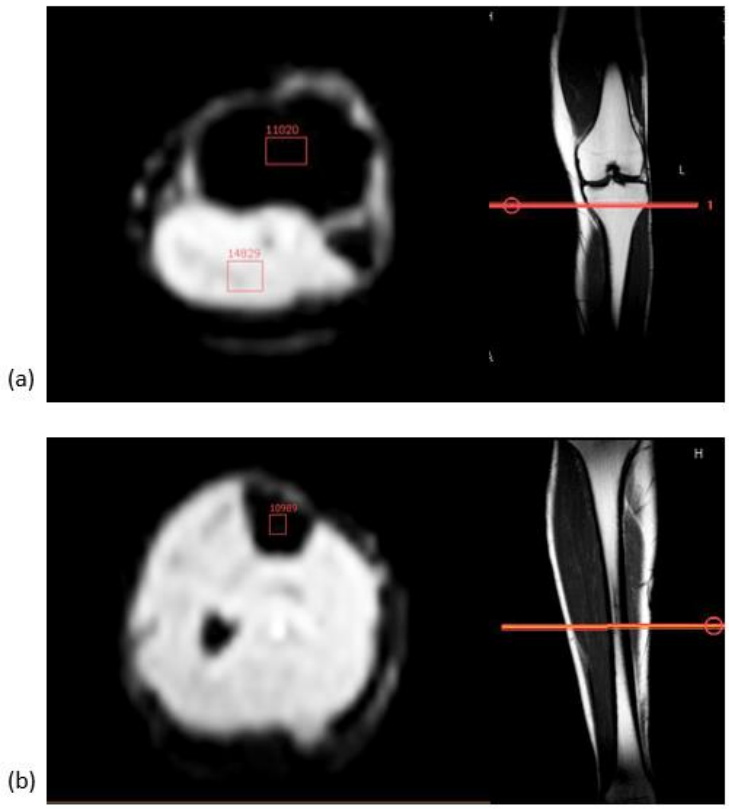

Figure J.1: Example ROI placement of (a) the proximal tibia and (b) the tibial diaphysis for time-signal analysis during the BOLD MRI arterial occlusion protocol.

NIRS readings of the lateral calf were unable to be taken, with only one set of MRI compatible optodes available. However BOLD measurements were also taken at the lateral

calf, as this anatomy was included within the scanned volume. Finger pulse and arterial saturation measurements were taken throughout the protocol to rule out confounding systematic physiological changes.

Following imaging, a region of interest (ROI) was placed over the marrow of the bone and over the lateral calf muscle. The signal in cortical bone was not measured as the volume of interest was deemed too small to measure changes in oxygenation accurately. The average signal intensity within the ROI for each scan was measured and graphed temporally to observe MRI signal changes (see Figure J.2 for examples).

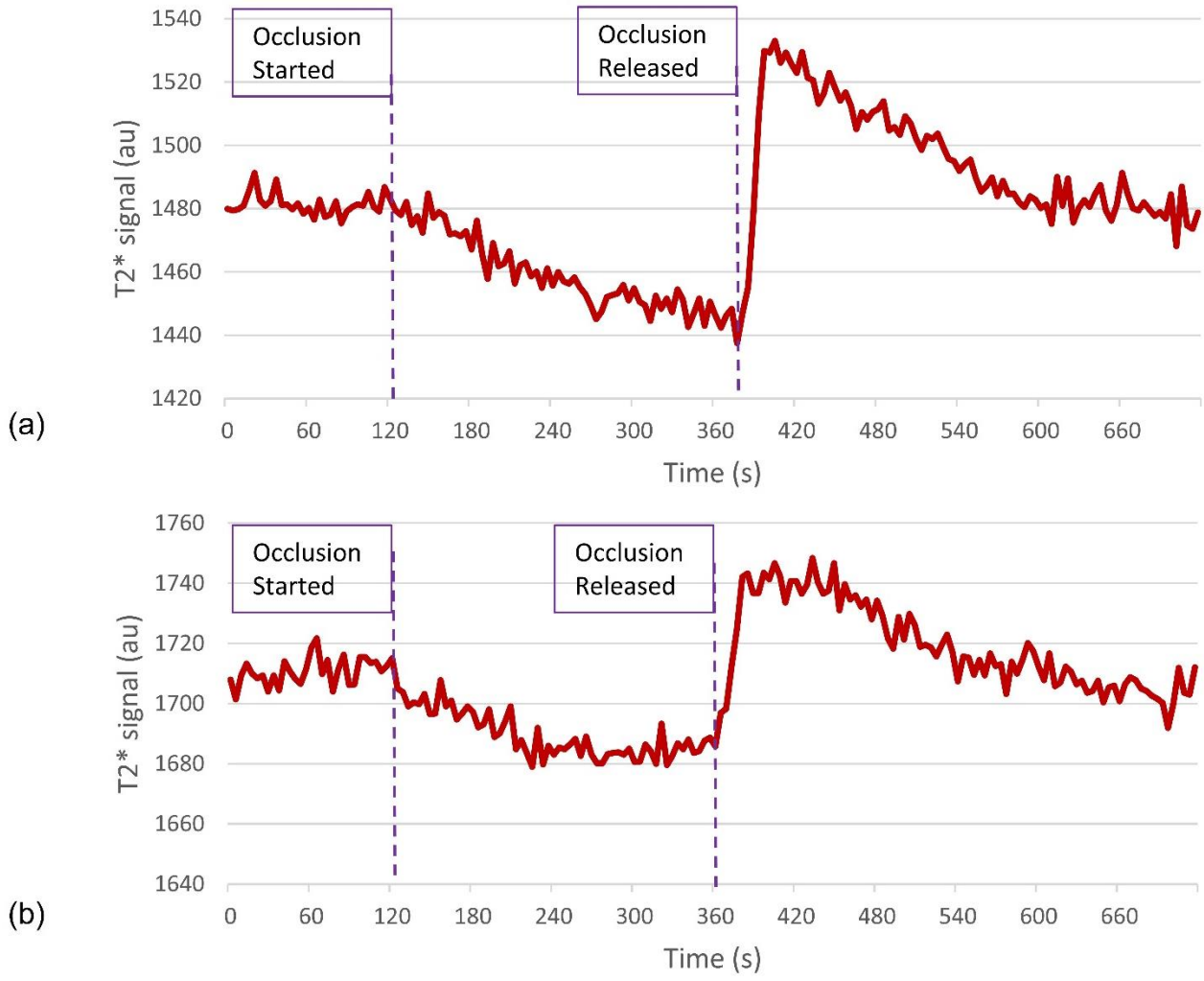

Figure J.2: Examples of MRI signal change at the lateral calf muscle. All eight occlusions showed a decrease in signal suggesting good arterial occlusion. However two patterns emerged: (a) a continuous decrease in signal, and more commonly (b) a sharp decrease and plateau of lower signal. All eight data sets demonstrated a post occlusive hyperaemic response (PORH) post occlusion release at the calf.

Pearson's correlation was used to assess for associations between haemodynamic markers obtained using NIRS and BOLD MRI. A p-value of 0.05 was deemed the threshold for

statistical significance. The strength of associations was assessed using the scale proposed by Evans 1996 with an r-value of <0.4 deemed “poor”, 0.4 to 0.6 deemed “moderate”, 0.6 to 0.8 deemed “strong”, and >0.8 deemed “very strong” [304].

J.3: Results

MRI signal changes at the lateral calf appeared reliable at registering signal change in line with oxygenation changes during and after arterial occlusion. On all eight data sets, signal intensity decreased with arterial occlusion and recorded a post occlusive hyperaemic response (PORH) at occlusion release (see Figure J.2 (a) for an example). Interestingly, signal decrease was typically not a regular continuous decrease as observed with NIRS, but rather showed a sharper initial decrease followed by a plateau of decreased signal during occlusion (see Figure J.2 (b)). Unfortunately, NIRS readings of the lateral calf were not taken simultaneously for comparison as only one set of MRI compatible NIRS probes were available. Despite this, MRI signal changes at the lateral calf gave confidence that arterial occlusions were effective at occluding arterial blood flow to the leg, and that the BOLD imaging sequence was sensitive to oxygenation changes.

MRI signal changes at the tibia were less consistent than at the lateral calf. Three of eight data sets showed a paradoxical increase in MRI signal, and so these data were removed from analysis. The remaining five data sets had high levels of noise in time-signal data, but did seem to show signal decreases corresponding with occlusion (see Figure J.3 for an individual example).

The high variability within time signal results was not surprising as signal at tibial sites was far lower than at the lateral calf, leaving these readings susceptible to low signal to noise. Results at tibial sites also often followed the pattern of signal change most commonly seen at the lateral calf, with an initial drop in signal and subsequent plateau until occlusion release. As such, in order to allow for low signal to noise and produce markers indicative of oxygenation change in response to occlusion, the differences in mean signal values were taken between a 60 second period at pre occlusion, during the last 60 seconds of occlusion, and from the point of peak recovery of signal post occlusion release. This approach is consistent with the data analysis of Towse et al 2016 [103].

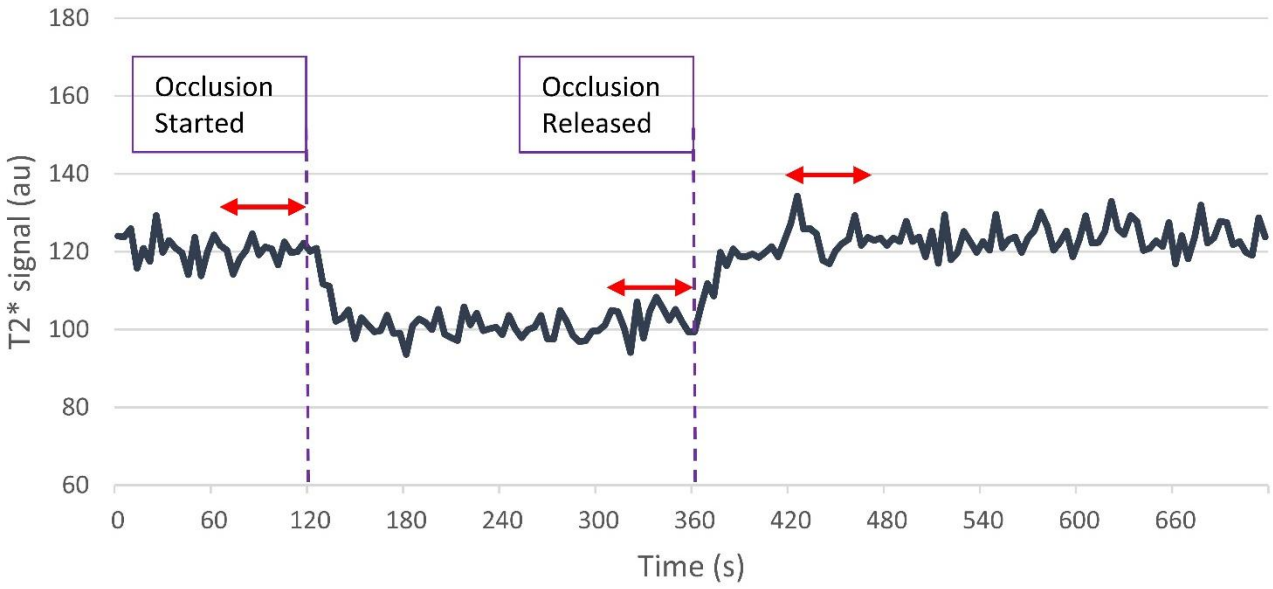

Figure J.3: An example of MRI signal change during arterial occlusion at the tibia. A decrease in signal is seen although it is not a continuous linear decrease as observed with NIRS. No discernible post occlusive hyperaemic response (PORH) is seen upon occlusion release as observed at the lateral calf (see Figure J.2). This is comparable with NIRS where PORH is generally not observed in TOI post occlusion markers at the tibia, but is observed at the calf. Red arrows indicate the measurement periods of mean MRI signal results taken over 60 seconds before arterial occlusion, during the last 60s of occlusion, and 60s following the peak post occlusion signal measurement observed.

NIRS measurements were successfully obtained from the tibia for all eight data sets with TOI decreases observed during occlusion, and mirrored changes in O_2Hb and HHb observed during and after occlusion, as expected. The NIRS markers previously discussed in Section 4.5 (and presented below in Figure J.4) are referred to in the following results.

A poor non-significant negative Pearson's correlation was found between resting tibial TOI values on NIRS and corresponding resting MRI signal (-0.123; p=0.77). This was anticipated to be a stronger positive correlation as the relative increase in O_2Hb associated with higher TOI should theoretically reflect in higher MRI signal. It is theorised this unexpected finding is explained by the fact that when using raw data from MRI signal, signal intensity is proportional to the absolute amount of O_2Hb and HHb present, which is dependent on blood volume. However, baseline TOI is a ratio value, and as such is independent of blood volume. This fundamental difference may be key to why these results do not correlate. Similarly, correlations between MRI signal changes and other relevant TOI NIRS markers during occlusion and post occlusion release (TOI_DO_60s and TOI_PO_absΔ) were weak and non-significant.

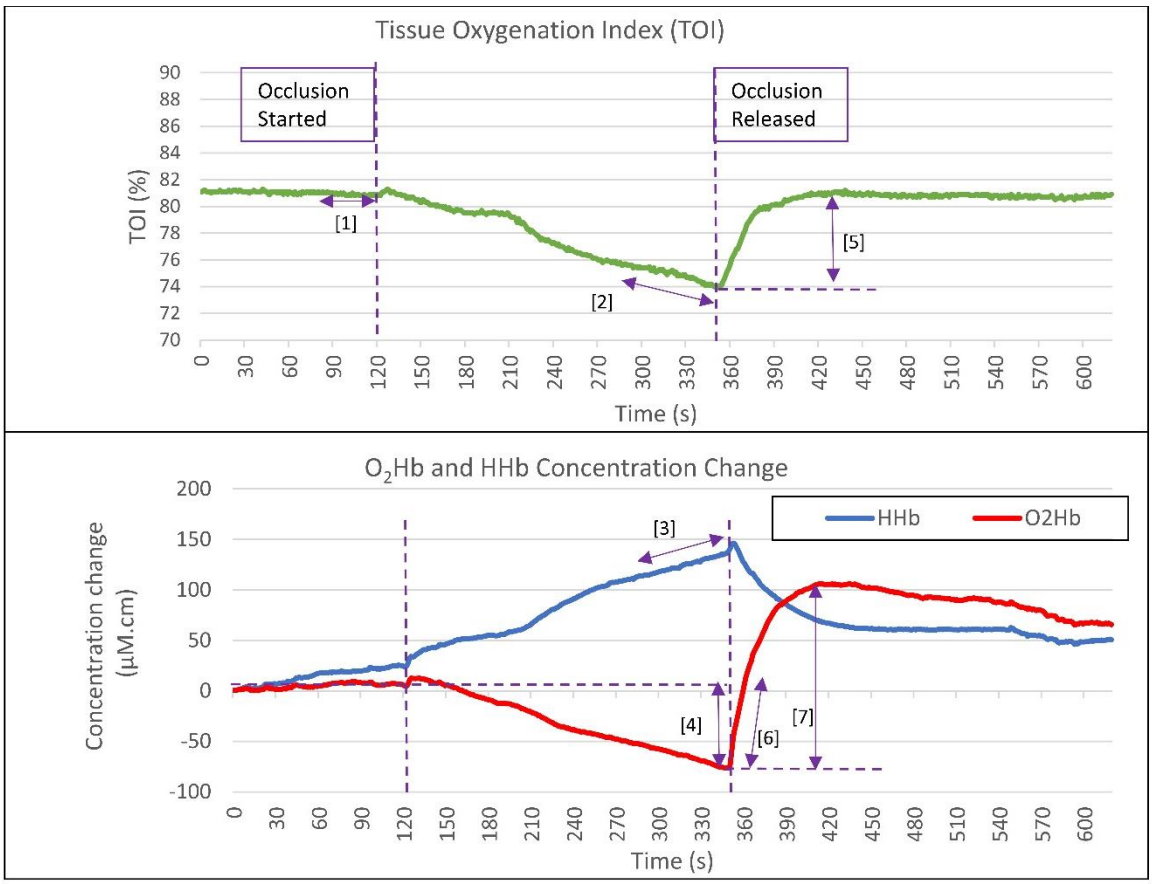

Figure J.4: Graphical display of the NIRS haemodynamic markers relevant to this appendix.
[1] Baseline TOI at rest prior to the occlusion (TOI_rest; (%))
[2] Rate of TOI decrease in the last 60s of occlusion (TOI_DO_ 60s (%/s))
[3] Rate of HHb increase in the last 60s of occlusion (HHb_DO_60s (µM.cm/s))
[4] Absolute change in O_2Hb during the occlusion (µM.cm; O_2Hb_DO_absΔ)
[5] Maximal absolute change in TOI post occlusion (TOI_PO_absΔ (%))
[6] Rate of O_2Hb increase in first 20s post occlusion release (O_2Hb_PO_20s (µM.cm/s))
[7] Maximal absolute change in O_2Hb post occlusion (O_2Hb_PO_absΔ (µM.cm))

Some correlations between MRI signal changes and modified Beer Lambert derived NIRS markers involving HHb and O_2Hb were stronger, as described below. This may be in part because these readings represent change in absolute haemoglobin concentration, rather than being a ratio value like TOI. A moderate positive correlation was found between HHb_DO_60s and MRI signal change during occlusion (r=0.54; p=0.35; see Figure J.5). This demonstrates an expected association, that a stronger drop in MRI signal during occlusion associated with more rapid accumulation of deoxygenated haemoglobin detected by NIRS. The correlation between MRI signal change during occlusion and O_2Hb_DO_absΔ was in the expected direction, with increased differences in MRI signal at occlusion correlating with increased drops in O_2Hb during occlusion, however the observed correlation was weak (r=0.25; p=0.68).

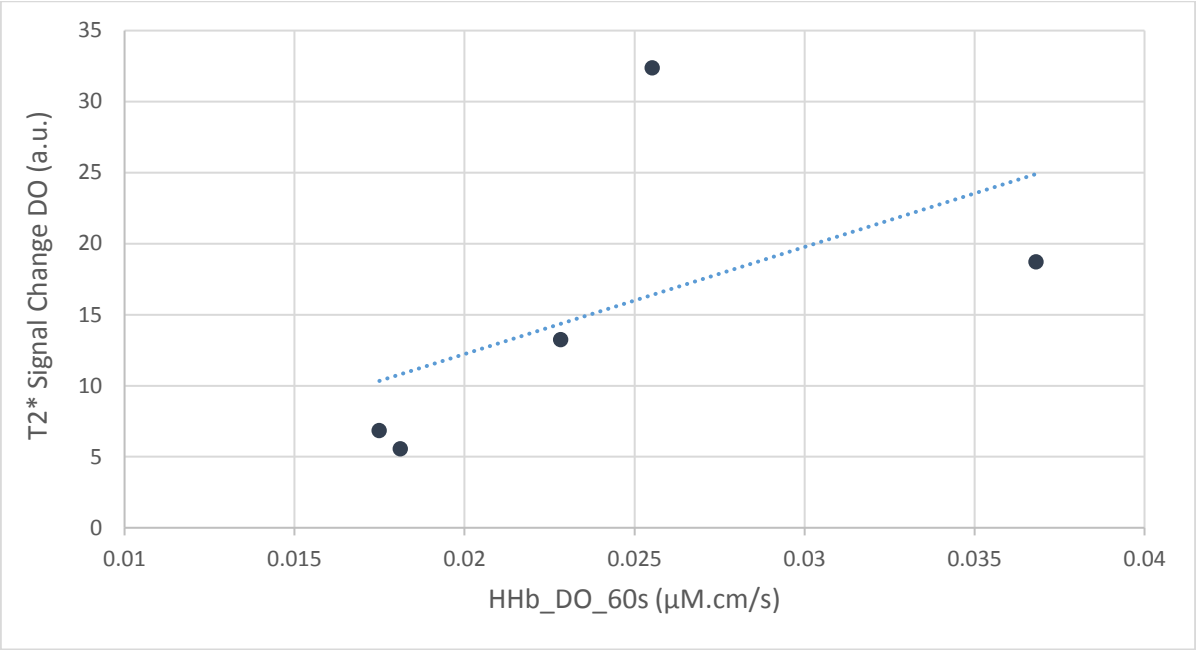

Figure J.5: A scatterplot of HHb_DO_60s NIRS results and MRI signal changes during occlusion at the tibia. The line of best fit demonstrates a positive correlation between rates of HHb accumulation during occlusion (measured with NIRS), and MRI signal change from BOLD MRI scans during occlusion (r=0.54; p=0.35).

Differences in MRI signal post occlusion release correlated strongly with rates of O_2Hb recovery (O_2Hb_PO_20s; r=0.85; p=0.07; see Figure J.6). This is also an expected association, as MRI signal change increases with increased oxygenation and arterial blood volume post occlusion release. The correlation between MRI signal change post occlusion release and O_2Hb_PO_absΔ was in the expected direction, with increased differences in MRI signal post occlusion release correlating with increased changes in O_2Hb concentration post occlusion release, however the observed correlation was weaker (r=0.54; p=0.35).

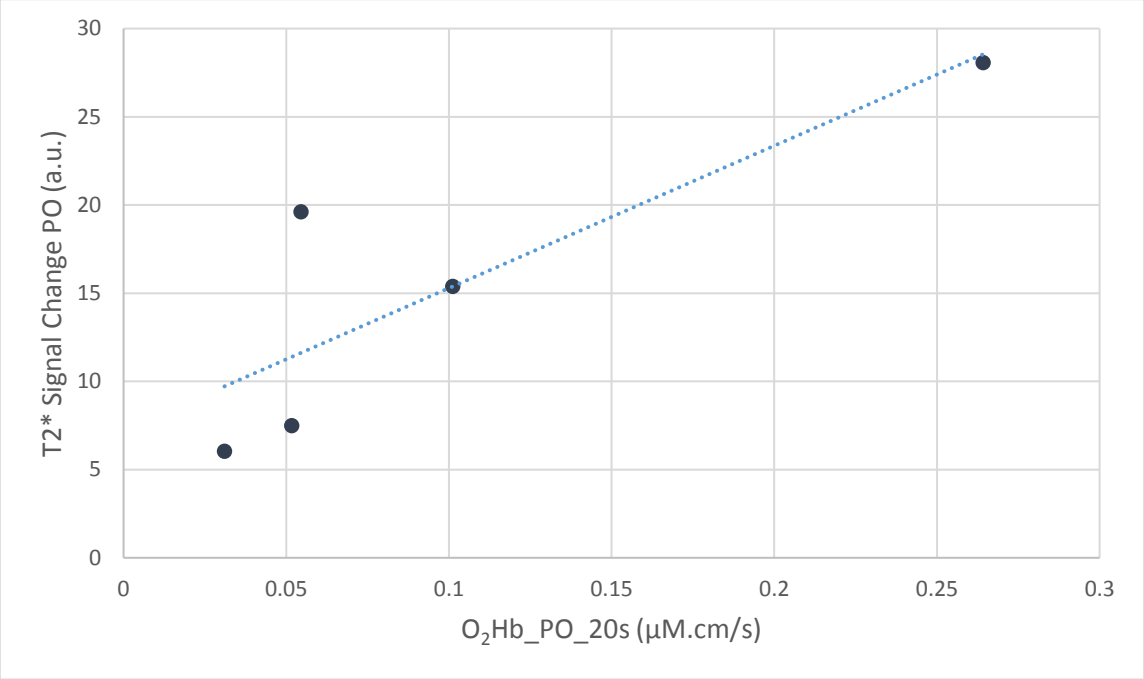

Figure J.6: A plot of O_2Hb_PO_20s NIRS results and MRI signal changes post occlusion (PO) release at the tibia. The line of best fit demonstrates a positive correlation between rates of O_2Hb accumulation post occlusion release measured with NIRS, and MRI signal change from BOLD MRI scans post occlusion release (r=0.85; p=0.07).

J.4: Conclusion

The results presented suggest MRI signal changes at the tibia during and after a mid-thigh arterial occlusion protocol showed some notable associations with NIRS-based haemodynamic markers taken simultaneously. This demonstrated some promise in the BOLD MRI protocol which was otherwise untested in the wider evidence base in bone tissue. The associations demonstrated also gave confidence in the approach to validate NIRS-based haemodynamic markers in bone with alternative tests of haemodynamics at the same anatomical site. However it was decided not to adopt this BOLD arterial occlusion protocol further as a validation comparator with NIRS. This was for a number of reasons explained in this section, also with reference to the advantages of the dynamic contrast enhanced MRI (DCE-MRI) protocol which was adopted instead.

Although participant numbers were low in this pilot testing, three of eight datasets were excluded from data analysis as they showed a physiologically unexpected rise in MRI signal during occlusion. This is likely to be an unacceptable rate of data loss, which may be expected to be worse in a wider volunteer population, given the potential stress to the participant of an arterial occlusion protocol, combined with the intimidating environment of the MRI scan room.

Anecdotally, the arterial occlusion protocol was also more susceptible to issues with the execution of the arterial occlusion in the MRI setting. A MRI compatible blood pressure inflation system was required that did not facilitate the rapid inflation used with the NIRS arterial occlusion protocol, as described in Section 4.4. The risk of a slow inflation is that unacceptable blood volume increases occur during cuff inflation (measured by the nTHI parameter), as partial venous occlusion is sustained for longer before full arterial occlusion.

It was expected that MRI signal in bone would be much lower than muscle due to its lower water content, resulting in lower Hydrogen density and mobility within bone. It is especially important to have high signal with BOLD protocols as signal changes due to changes in oxygenation status are typically small. BOLD protocols are also prone to susceptibility artefact potentially introduced by adjacent cortical bone, which may have potentially added error to signal measurements [(98)]. The tibial BOLD data sets that were included demonstrated unacceptably low signal to noise, as demonstrated in Figure J.3 above, with many following an unexpected non-linear change in MRI signal during occlusion.

That said, the reduced MRI signal observed at the calf during occlusion is in line with the decreases in MRI signal at the medial gastrocnemius muscle reported by Muller et al 2016 [(106)] during an exercise protocol involving plantar flexion of the foot. Likewise in this study the magnitude of MRI signal changes was positively associated with NIRS changes in oxygenation observed during the exercise protocol. Muller et al 2016 [(106)] also reports a pattern of increased initial signal reduction and subsequent plateau of reduced signal comparable to the pattern demonstrated in Figure J.2(b) and J.3. It may be that increased quantities of paramagnetic HHb accumulating in the imaged volume reach a threshold where the susceptibility effects that cause MRI signal change are saturated. The authors argue this pattern of signal change may be due to T2* signal changes representing “intravascular” signal changes within larger vessels, as opposed to “extravascular” T2* signal changes representative of the response to oxygenation changes from cellular demand immediately surrounding capillaries within tissue.

Towse et al 2016 [(103)] supports this and argues BOLD sequences at greater field strengths of 7 Tesla may provide signal change that is more representative of oxygen extraction from microcirculation in tissue. This study demonstrates more linear continuous T2* signal decreases at greater field strengths and proposes that this is because the greater field strength vastly reduces the relaxation time of “intravascular” MRI signal in whole blood, relative to relaxation times of haemoglobin in and around capillary flow supplying tissue, therefore better distinguishing the two more than can be achieved at lower field strengths.

A higher field strength of 7T may be a beneficial development as BOLD protocols would better represent the direct oxygen extraction of tissue. Towse et al 2016 [103] also demonstrated significantly greater signal to noise ratio and contrast to noise ratio of BOLD sequences of skeletal muscle involving arterial occlusion when increasing from a 3 Tesla field strength MRI to a 7 Tesla system (results presented in this appendix were acquired with a 1.5 Tesla field strength). However, these technological developments remain in the development stages, even in more established measurements sites such as the brain and skeletal muscle. More research is required as BOLD protocols are especially prone to susceptibility artefact especially when imaging heterogeneous tissues such as bone, and this risk of this artefact is increased with increasing field strength [98].

There also remains some uncertainty around what contributes (and may confound) BOLD signal changes, including factors such as changes in blood flow, blood volume, and systemic physiological changes (such as pulse rate and systemic blood pressure). This is further complicated by a lack of consensus in intervention protocols adopted (such as around the tissue of interest and duration of intervention). This has led to conflicting results reported in the evidence base around BOLD signal changes, for example when looking at skeletal muscle during exercise [106]. Arterial occlusion protocols are likely to produce more controlled conditions than exercise protocols, with blood volume and blood flow minimised by a well-executed arterial occlusion.

As a result of the feasibility work presented in this appendix, it was decided to opt for a DCE-MRI protocol, which is outlined in Section 6.2.4. This protocol has a more established evidence base for measurement of *in vivo* bone haemodynamics for comparison, with evidenced reproducibility [130-132]. DCE-MRI was also expected to be more tolerable than the BOLD protocol as participants were only required to remain still for the duration of the scan, without an arterial occlusion protocol. This was deemed to be more acceptable, even in consideration of the requirements of a Gadolinium injection, and the small risks associated (discussed in Section 6.2.4).

Appendix K: Bland-Altman plots

Bland-Altman plots were used to visualise the differences between test/retest measurements plotted against the mean of the two repeated measurements. This was performed in order to help to assess whether the differences between test/retest measurements follow a normal distribution, and whether there is any systematic bias in the differences between test/retest measurements. Bland-Altman plots can also demonstrate any changes in the variance of differences as the mean measurement value increases [305, 306]. Bland-Altman plots were produced for all the haemodynamic markers assessed in test/retest reliability work in Chapter 7. There were no obvious systematic differences or bias observed across markers for same day or different day test/retest analysis at either the lateral calf or proximal tibia.

This appendix presents the Bland-Altman plots for test/retest reproducibility data (i.e. test/retest data taken on different days) at the proximal tibia. Plots include the seven haemodynamic markers which were adopted in the analysis presented in Chapters 8, 9 and 10, presented in Figure 7.2 (page 202).

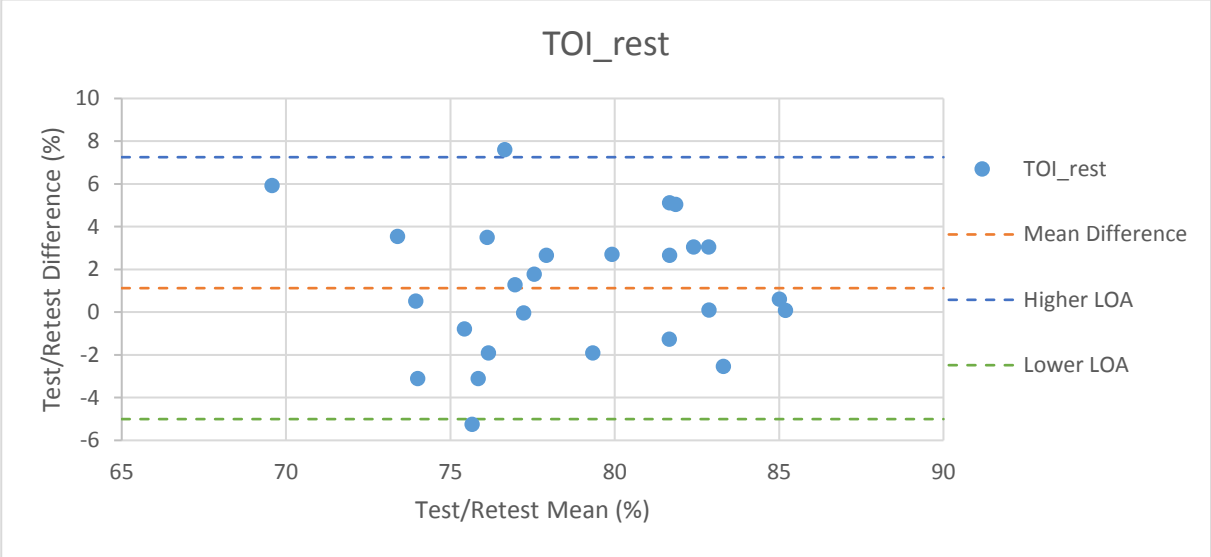

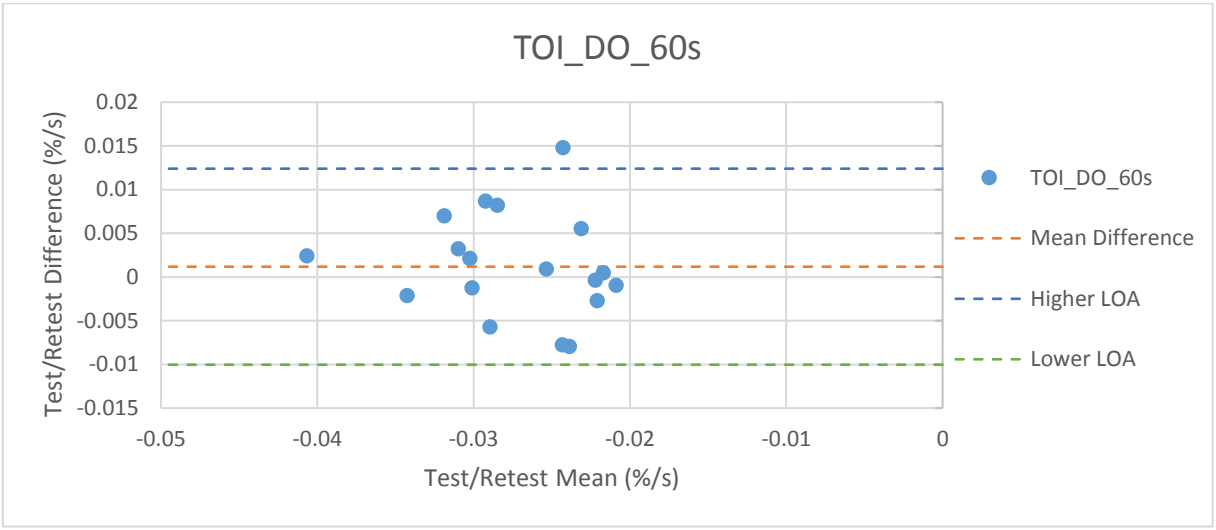
TOI_DO_60s
Test/Retest Difference (%/s)
0.02
0.015
0.01
0.005
0
-0.005
-0.01
-0.015
-0.05
-0.04
-0.03
-0.02
-0.01
0
Test/Retest Mean (%/s)
TOI_DO_60s
Mean Difference
Higher LOA
Lower LOA

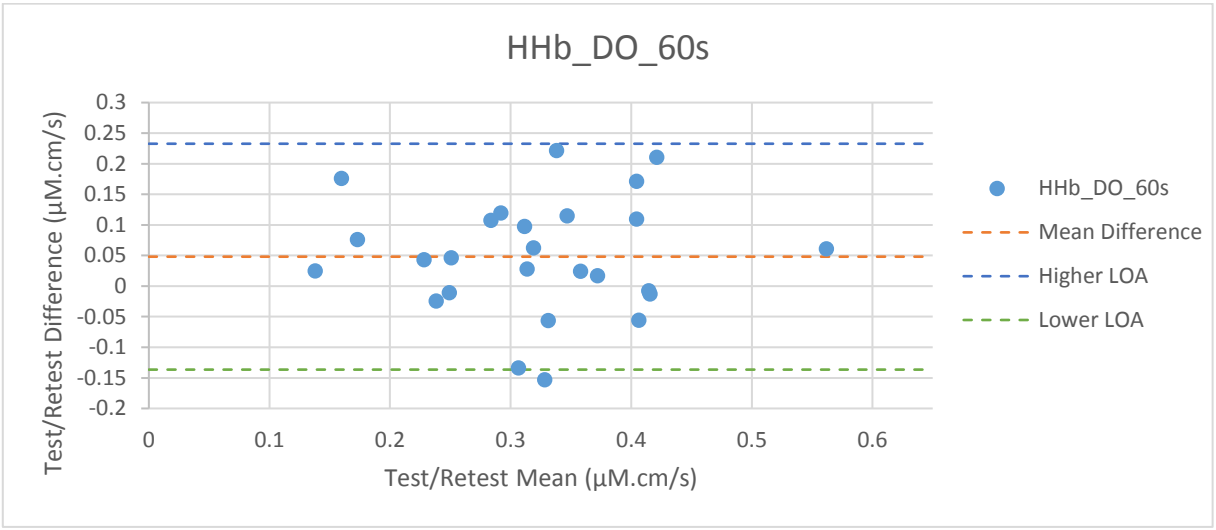
HHb_DO_60s
Test/Retest Difference (µM.cm/s)
0.3
0.25
0.2
0.15
0.1
0.05
0
-0.05
-0.1
-0.15
-0.2
0
0.1
0.2
0.3
0.4
0.5
0.6
Test/Retest Mean (µM.cm/s)
HHb_DO_60s
Mean Difference
Higher LOA
Lower LOA

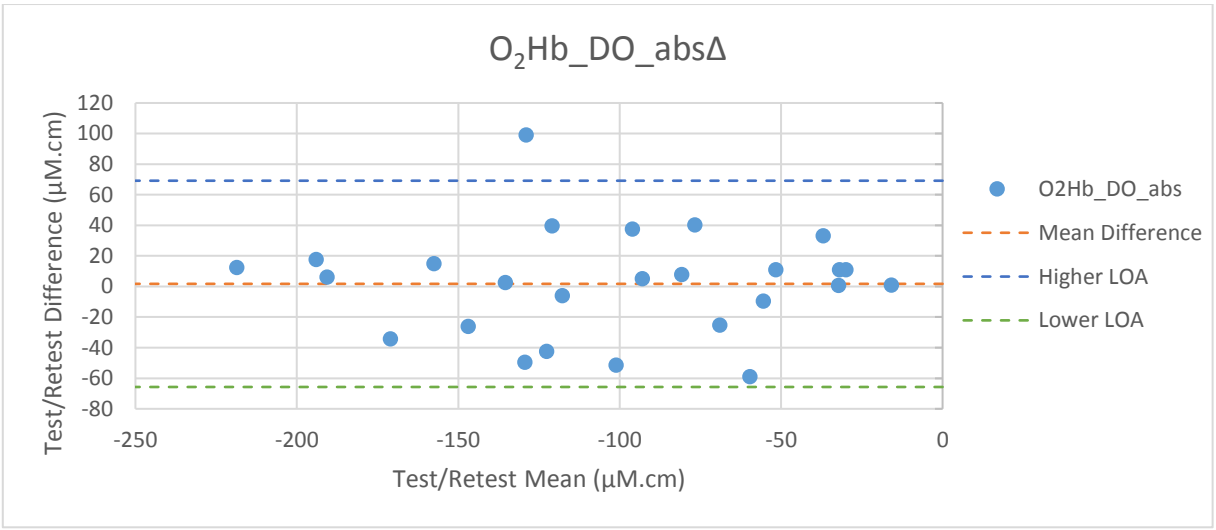
O2Hb_DO_absΔ
Test/Retest Difference (µM.cm)
120
100
80
60
40
20
0
-20
-40
-60
-80
-250
-200
-150
-100
-50
0
Test/Retest Mean (µM.cm)
O2Hb_DO_abs
Mean Difference
Higher LOA
Lower LOA

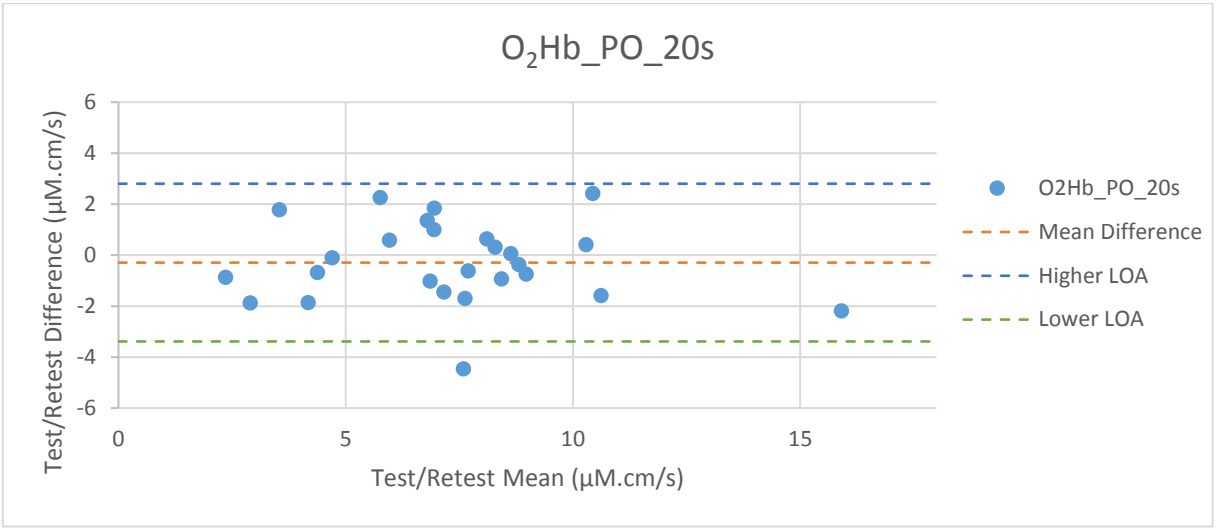
O2Hb_PO_20s
Test/Retest Difference (µM.cm/s)
Test/Retest Mean (µM.cm/s)
O2Hb_PO_20s
Mean Difference
Higher LOA
Lower LOA

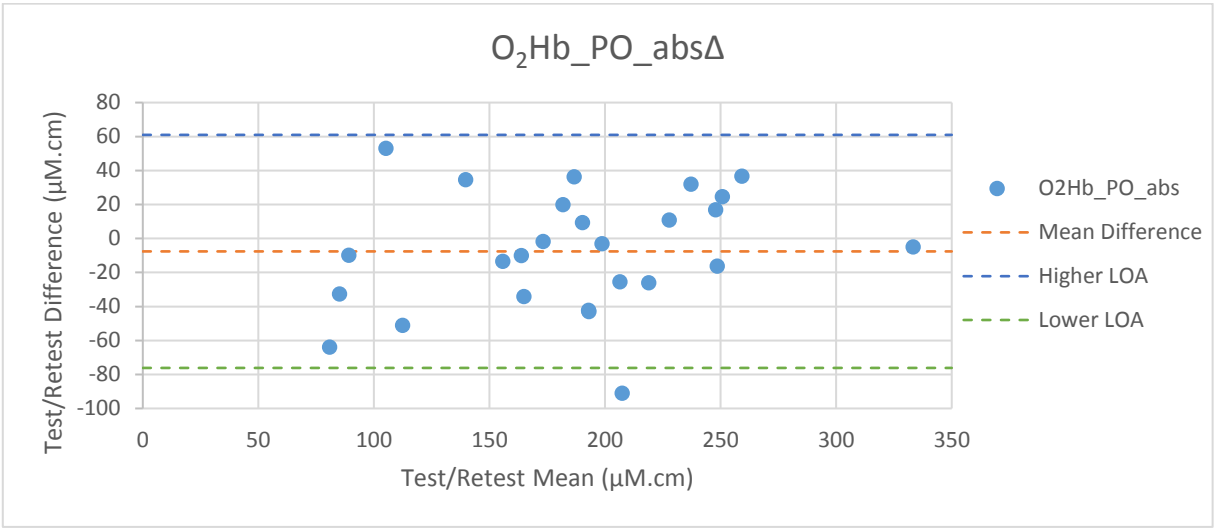
O2Hb_PO_absΔ
Test/Retest Difference (µM.cm)
Test/Retest Mean (µM.cm)
O2Hb_PO_abs
Mean Difference
Higher LOA
Lower LOA

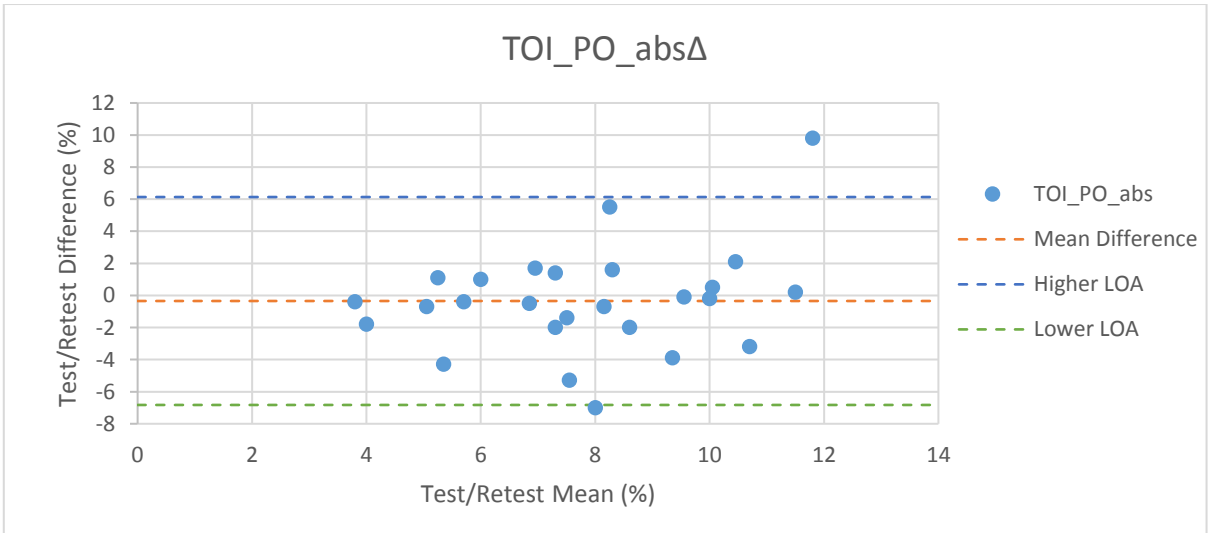
TOI_PO_absΔ
Test/Retest Difference (%)
Test/Retest Mean (%)
TOI_PO_abs
Mean Difference
Higher LOA
Lower LOA

Appendix L: Participant information sheet

National Institute of Health Research
Exeter Clinical Research Facility

Royal Devon and Exeter NHS
NHS Foundation Trust

Near Infrared Spectroscopy (NIRS) for the measurement of blood supply in bone tissue

A research project investigating if NIRS could be a useful new way to diagnose poor bone health by measuring the microvascular blood supply in bone tissue

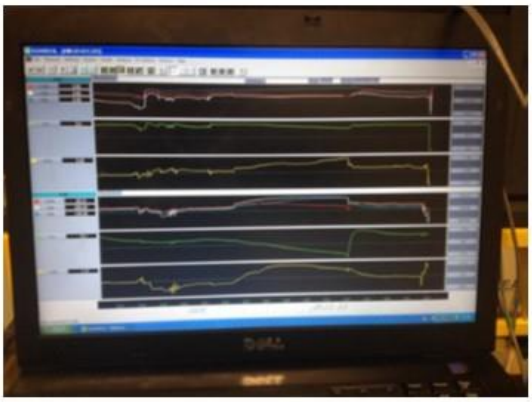

Could you spare some time to help researchers improve the testing of bone health, and so improve the bone health of the nation?

Principal Investigator: Robert Meertens

Why are we doing this research?

Measuring the blood supply in bone is difficult using existing techniques. This is because bone is dense and has a high mineral content. As such, researching the role of blood supply in certain bone diseases remains challenging. One example is in people with type 2 diabetes mellitus (T2DM), who are at risk of low impact fractures, often despite normal bone density. This could be because of the poor blood supply to bones associated with T2DM, resulting in poorer strength in bone, regardless of bone density.

NIRS may offer a potential method for investigating this type of disease process. NIRS uses technology similar to machines that take your pulse, and is safe and inexpensive. Unlike existing tests, it also provides information on oxygen levels in blood and measures blood supply in bone in real time. This allows easily repeated measurements or continuous monitoring. So NIRS could potentially investigate multiple diseases where altered blood supply in bone is a potential cause, including poor fracture healing and arthritis.

NIRS essentially involves placing two small probes on the skin as indicated in this picture.

Why have I been invited?

You may have been invited because you have already participated in the Exeter 10,000 (EXTEND) study, and now also meet the inclusion criteria for this new study.

Alternatively, you may have T2DM and have recently suffered a low impact fracture. One potential application of NIRS is predicting those with T2DM at a high risk of fracture and as such, we are interested in using your results in our study.

We are hoping to recruit 36 participants, 18 of whom have type 2 diabetes.

Do I have to take part in this study?

No, participation is entirely voluntary and please ask us any questions before deciding to join the study. If you agree to take part, we will ask you to sign a consent form including questions similar to those provided at the back of this leaflet. However, you are free to withdraw at any point without providing any reason. Participation in the study will not affect your treatment as an NHS patient.

What does participation involve?

Your participation will involve undergoing a series of different tests. You can choose whether you would like these tests done over 2 or 3 attendances. However, these tests must be carried out within a 4 week window. A flow chart of participation is provided overleaf. Testing includes:

- Blood samples and a urine test are to be taken early in the morning after an overnight fast.
- Basic physiological measurements (such as height, weight and blood pressure) will be taken as well as answering some questions on your medical history.
- NIRS testing of your lower leg will be performed. This involves applying two probes to different places on your lower leg. Testing can also involve use of a blood pressure cuff around your leg, inflated for up to four minutes.
- A MRI scan of your lower leg is required, which involves an injection of a gadolinium contrast agent (routinely used in clinical practice to demonstrate blood flow) (approximately 1.5 hours).
- A Dual Energy X-ray Absorptiometry (DXA) scan measuring your bone mineral density and bone strength. This test involves laying flat for no more than one hour.

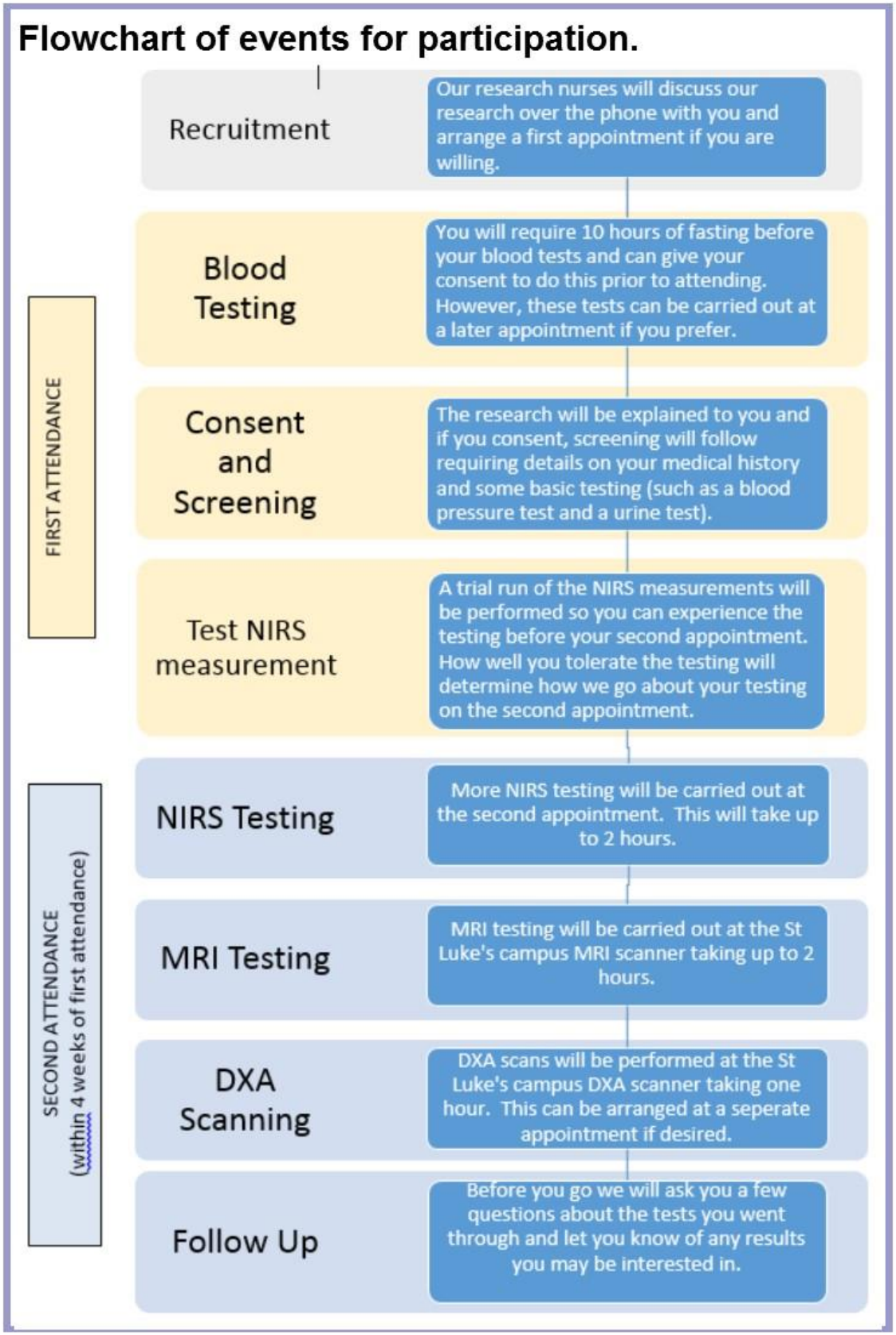
Flowchart of events for participation.
FIRST ATTENDANCE
SECOND ATTENDANCE (within 4 weeks of first attendance)
Recruitment
Our research nurses will discuss our research over the phone with you and arrange a first appointment if you are willing.
Blood Testing
You will require 10 hours of fasting before your blood tests and can give your consent to do this prior to attending. However, these tests can be carried out at a later appointment if you prefer.
Consent and Screening
The research will be explained to you and if you consent, screening will follow requiring details on your medical history and some basic testing (such as a blood pressure test and a urine test).
Test NIRS measurement
A trial run of the NIRS measurements will be performed so you can experience the testing before your second appointment. How well you tolerate the testing will determine how we go about your testing on the second appointment.
NIRS Testing
More NIRS testing will be carried out at the second appointment. This will take up to 2 hours.
MRI Testing
MRI testing will be carried out at the St Luke's campus MRI scanner taking up to 2 hours.
DXA Scanning
DXA scans will be performed at the St Luke's campus DXA scanner taking one hour. This can be arranged at a seperate appointment if desired.
Follow Up
Before you go we will ask you a few questions about the tests you went through and let you know of any results you may be interested in.

Are there any risks or benefits in taking part?

There are some risks to participation in this study, however these are considered low risks that are commonly encountered in clinical environments. All testing will be varied out by experienced clinical staff with emergency care facilities present.

During NIRS testing, small probes are placed on your leg. For some testing, blood supply to the leg is restricted using a blood pressure cuff for up to 4 minutes. This is common practice in vascular studies and is safe, but can be moderately uncomfortable. You will be offered a "test run" of this process, and are free to stop at any time if this is too uncomfortable for you. Any discomfort is quickly relieved when the blood pressure cuff is released.

Having a blood sample taken can be uncomfortable, and there is a small risk of a bruise at the injection site.

There are some contraindications for MRI (such as certain metal implants) and the contrast injection has a small risk of adverse events such as nausea and headaches (approx. 1 in 100) and less commonly, allergic reactions (approx. 1 in 1000).

As part of this study you will undergo a DXA scan of your whole body, spine, hips and knees. The DXA scanner uses a very small amount of ionising radiation, which is equivalent to no more than 4 days' worth of natural background radiation that everyone in the UK is exposed to. This equates to a risk of inducing cancer of smaller than one in one million.

The project is unlikely to benefit you directly, but will help us establish if NIRS is a test that could benefit diagnosis of bone diseases involving potential microvascular causes.

However, there is a chance we may uncover test results that are medically important to you. In this instance we will explain these test results to you and any follow up required. With your consent, we will contact your GP to inform them of your participation in the study and contact them if we unexpectedly identify anything that could impact on your clinical care.

What will happen to my samples and data?

All blood and urine samples and data will be stored anonymously under a unique study ID number for confidentiality. Samples will be analysed for test results relating to bone health, diabetes status and renal health. All samples will then be destroyed after analysis. Any unused samples will be destroyed at the end of the study.

Your participation in this study will be kept confidential within the research team. Any documentation containing your personal details will be destroyed or deleted at the end of the study. However, the anonymised results of your testing may be held for up to five years after the study finishes and may be used in future research, should you allow consent for this to occur.

Is there anything else I need to know?

All travel expenses will be paid. Food and refreshments will be provided.

The results of the study will be fed back to participants via their preferred contact method following completion of the study. It is anticipated that results will also be published in peer reviewed scientific journals and presented at medical conferences. This research is also contributing to a PhD thesis for Rob Meertens.

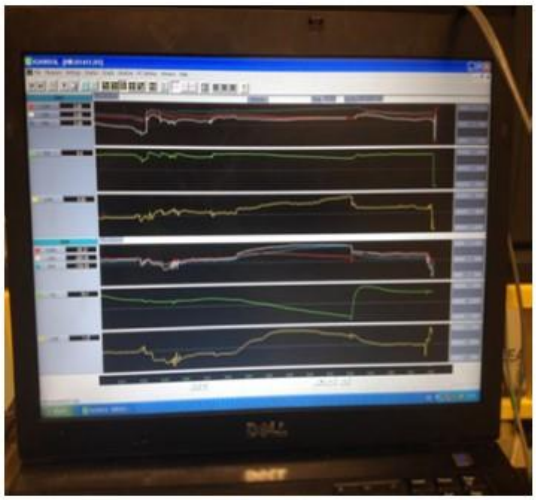

CONSENT STATEMENTS

If you wish to participate in this study, you will be asked **to sign a consent form in the presence of a member of the research team,** a copy of which you will be given to keep.

You may take as long as you need to consider consent and you may wish to discuss your participation with family, friends or your GP before consenting.

The consent form will include the following statements:

- I confirm that I have read this leaflet, I have had the opportunity to ask questions and have had these answered satisfactorily.
- I understand that my participation is voluntary and that I may withdraw at any time without my clinical care being affected.
- I agree to my General Practitioner being informed of my participation in the study and of any incidental findings that may result from my participation in this study.
- Likewise, I understand that I may request my data to be withdrawn from research use at any time. Should I lose the capacity to consent, my participation will be ceased in this study but my anonymised data will still be used in future analysis in this study and other research.
- I understand that relevant sections of my medical notes and data collected during the study may be looked at by individuals from the NHS Trust, where it is relevant to my taking part in this research. I give permission for these individuals to have access to my records.
- I understand that the information collected about me will be used to support other research in the future, and may be shared anonymously with other researchers.
- I understand that the information held and maintained by the Health and Social Care Information Centre and other central UK NHS bodies may be used to help contact me or provide information about my health status.
- I agree to take part in the study.

What if there is a problem?

If you were to experience any urgent medical complications during testing, there will be experienced research nurses and doctors present with emergency medical equipment on hand. Should you experience any medical complications outside of testing we would recommend calling an ambulance, attending an A&E or ringing your GP as appropriate. You can also contact Rob Meertens (Principal Investigator) on 01392 722511 or email r.m.meertens@exeter.ac.uk. The University of Exeter has insurance and processes in place to deal with any adverse incidents relating to participation in research.

The research team will be happy to discuss any problems you may have. However, if you have concerns or complaints arising from your experience of participating in this study which you do not wish to discuss with the research team directly, the RD&E Patient Engagement and Experience team (01392 402093) will provide independent advice.

Who is organising and funding this research?

The research will be managed through the NIHR Exeter Clinical Research Facility, which is funded by the National Institute of Health Research, a part of the NHS. Funding for the project is provided by the Society and College of Radiographers.

Where can I find out more?

For further information about the project, please contact Rob Meertens (Principal Investigator) on 01392 722511 or email r.m.meertens@exeter.ac.uk.

Who has reviewed this study?

This project has been reviewed by a local patient group and the National Research Ethics Committee South West-Exeter (IRAS ID:194070)

Thank You.

Thank you for reading this leaflet and for your interest in our study. This leaflet is yours to keep.

Appendix M: Pre consent form for fasting blood test

Royal Devon and Exeter NHS
NHS Foundation Trust

University of Exeter Medical School

Centre Number:

Study Number:

PRE-CONSENT FORM FOR FASTING BLOOD TEST

Title of Project: NIRS for the measurement of haemodynamic markers in bone tissue (NIRSBone).

Name of Researcher: Rob Meertens

	Please initial box
1. I confirm that I have read the information sheet dated..... (version.....) for the above study. I have had the opportunity to consider the information, ask questions and have had these answered satisfactorily.	
2. I understand that my participation in these blood tests is voluntary and that I am free to withdraw at any time without giving any reason, without my medical care or legal rights being affected.	
3. Likewise, I understand that I may request my data to be withdrawn from research use at any time. Should I lose the capacity to consent my participation will be ceased in this study, but any or all anonymised data already obtained up to this point of losing capacity to consent may still be used in future analysis relating to this study.	
5. I understand that the information collected about me will be used to support other research in the future, and may be shared anonymously with other researchers.	
6. I agree to being informed of any medically relevant incidental findings that may result from my participation in these blood tests.	
7. I agree to my General Practitioner being informed of my participation in the study and of any incidental findings that may result from my participation in this study.	
9. I give permission for staff outside the research team to access my results when doing so for the purpose of auditing and monitoring good practice in relation to the research being performed.	
10. I understand that blood and urine samples provided are being "gifted" and may be stored indefinitely for further research relating to this study, although these will be destroyed appropriately when no longer required at the conclusion of the study.	
11. I agree to take part in these fasting blood tests. I understand this involves not eating or drinking for 10 hours prior to testing.	

Name of Participant	Date	Signature
Name of Witness	Date	Signature

RMM_V1.0_20/09/2016

Appendix N: Consent form

Royal Devon and Exeter NHS
NHS Foundation Trust

University of Exeter Medical School

Centre Number:

IRAS ID: 194070

Participant Identification Number for this trial:

CONSENT FORM

Title of Project: NIRS for the measurement of haemodynamic markers in bone tissue (NIRSBone).

Name of Researcher: Rob Meertens

	Please initial box
1. I confirm that I have read the information sheet dated..... (version.....) for the above study. I have had the opportunity to consider the information, ask questions and have had these answered satisfactorily.	
2. I understand that my participation is voluntary and that I am free to withdraw at any time without giving any reason, without my medical care or legal rights being affected.	
3. Likewise, I understand that I may request my data to be withdrawn from research use at any time. Should I lose the capacity to consent my participation will be ceased in this study, but any or all anonymised data already obtained up to this point of losing capacity to consent may still be used in future analysis relating to this study.	
4. I understand that relevant sections of my medical notes and data collected during the study may be looked at by individuals from the NHS Trust, where it is relevant to my taking part in this research. I give permission for these individuals to have access to my records.	
5. I understand that the information collected about me will be used to support other research in the future, and may be shared anonymously with other researchers.	
6. I agree to being informed of any medically relevant incidental findings that may result from my participation in this study.	
7. I agree to my General Practitioner being informed of my participation in the study and of any incidental findings that may result from my participation in this study.	
8. I understand that the information held and maintained by the Health and Social Care Information Centre and other central UK NHS bodies may be used to help contact me or provide information about my health status.	
9. I give permission for staff outside the research team to access my results when doing so for the purpose of auditing and monitoring good practice in relation to the research being performed.	
10. I understand that blood and urine samples provided are being "gifted" and may be stored indefinitely for further research relating to this study, although these will be destroyed appropriately when no longer required at the conclusion of the study.	
11. I agree to take part in the above study.	
12. I would like to be informed of the results of this study. My preferred contact method is _____	

_____	_____	_____
Name of Participant	Date	Signature
_____	_____	_____
Name of Person taking consent	Date	Signature

RMM_V2.0_13/09/2016

A COPY OF THIS CONSENT FORM WILL BE GIVEN TO THE PARTICIPANT, A COPY WILL BE FILED IN PATIENT NOTES, AND AN ORIGINAL COPY WILL BE SAVED IN THE SITE FILE

PERSONAL DETAILS TO BE RECORDED AND KEPT CONFIDENTIALLY:

Participant Identification Number for this trial:

Name of Participant:

Date of Birth:

NHS Number:

Contact Address:

Contact Phone Number:

Contact email:

Preferred Method of Contact:

GP Details:

Appendix O: Participant questionnaire

The use of near infrared spectroscopy (NIRS) to measure haemodynamics in bone tissue

PARTICIPANT INFORMATION FORM

VERSION NUMBER 2.0 DATE: 13/09/2016

What is your age?: …….

What is your sex? …….

What is your ethnicity?: ……

Which is your dominate leg?: ……..

Are you or have you been a smoker? If yes, please provide details:

……

Do you have Type 2 Diabetes? If so, describe treatment for this and provide time since diagnosis:

……

……

How would you describe your general health?

Poor	Satisfactory	Good	Very Good	Other
☐	☐	☐	☐	☐

If not Good or Very Good, what is limiting your health?

……

Have you recently had a fracture? If so, please provide details of the fracture and if the treatment of your fracture:

……

Have you ever taken medications for your bone health (including medications, HRT or Calcium/Vitamin D supplementation)? If yes, please provide details:

……

……

Have you ever taken glucocorticoid steroids for an extended period? If yes, please provide details here:

……
……

Are you currently on any other medications? If so, please list here:

……
……..

Are you currently participating in any other research programmes? If so, please provide details:

……
……

Do you have any medical history of the following?

Type 1 Diabetes:	Y / N
Any form of Heart Disease or Cardiovascular disease:	Y / N
Osteoporosis:	Y / N
Any form of Arthritis:	Y / N
Serious Injury or disease to either leg:	Y / N
Any other form of disease affecting your bones:	Y / N
Any history of stroke or TIA:	Y / N
Any form of Heart Arrhythmias:	Y / N
Hypertension:	Y / N
Kidney disease or poor kidney function:	Y / N
Peripheral Artery Disease or leg pain after exercise (claudication):	Y / N
DVT:	Y / N
Claustrophobia:	Y / N
Needle Phobia:	Y / N

If you have answered Yes to any questions please add details as appropriate:

……..

……

IF FEMALE:

What is your menopausal status? If post-menopausal, for how many years?

……

Are you breastfeeding or pregnant (or trying)? ……..

Measurements to be taken by PI

Participant identifier …….

Date and Time …….

Leg of measurement …….

Height: …….

Weight: …….

BMI: …….

BP: …….

Pulse rate: …….

Baseline sO2 ……

Foot Temperature ……

O2C Foot Sats ……

O2C Baseline Foot Flow ……

O2C Foot Velocity ……

Leg Circumferences:

Knee …….

Calf …….

Ankle …….

Microfilament Score: …….

Vibration Sensitometry: …….

Any other notes:

……
……
……..

Appendix P: MRI screening questionnaire

Participant Safety Checklist

Name: **Date of Birth:**
Weight: **Name of Study/Volunteer Number:**

Please check the following list carefully, answering all appropriate questions.
Please do not hesitate to ask staff, if you have any queries regarding these questions.

1. Do you have a pacemaker, artificial heart valve or coronary stent? Yes/No

2. Have you ever had major surgery? Yes/No

If yes, please give brief details.

3. Do you have any aneurysm clips (clips put around blood vessels during surgery)? Yes/No

4. Do you have any implants in your body

Yes ☐ No ☐ Joint replacements, pins or wires
Yes ☐ No ☐ Implanted cardioverter defibrillator (ICD)
Yes ☐ No ☐ Electronic implant or device
Yes ☐ No ☐ Magnetically-activated implant or device
Yes ☐ No ☐ Neurostimulation system
Yes ☐ No ☐ Spinal cord stimulator
Yes ☐ No ☐ Insulin or infusion pump
Yes ☐ No ☐ Implanted drug infusion pump
Yes ☐ No ☐ Internal electrodes or wires
Yes ☐ No ☐ Bone growth/bone fusion stimulator
Yes ☐ No ☐ Any type of prosthesis
Yes ☐ No ☐ Heart valve prosthesis
Yes ☐ No ☐ Eyelid spring or wire
Yes ☐ No ☐ Metallic stent, filter or coil
Yes ☐ No ☐ Shunt (spinal or intraventricular)
Yes ☐ No ☐ Vascular access port and/or catheter
Yes ☐ No ☐ Wire mesh implant
Yes ☐ No ☐ Bone/joint pin, screw, nail, wire, plate etc.
Yes ☐ No ☐ Other Implant_____

5. Do you have an artificial limb, calliper or surgical corset? Yes/No

6. Do you have any shrapnel or metal fragments, for example from working in a machine tool shop? Yes/No

7. Do you have a cochlear implant? Yes/No

8. Do you wear dentures, plate or a hearing aid? Yes/No

9. Are you wearing a skin patch (e.g. anti-smoking medication), have any tattoos, body piercing, permanent makeup or coloured contact lenses? Yes/No

10. Are you aware of any metal objects present within or about your body, other than those described above? Yes/No

11. Are you susceptible to claustrophobia? Yes/No

12. Do you suffer from blackout, diabetes, epilepsy or fits? Yes/No

For women:

13. Are you pregnant or experiencing a late menstrual period? Yes/No

14. Do you have an intra-uterine contraceptive device fitted? Yes/No

15. Are you taking any type of fertility medication or having fertility treatment? Yes/No

Important Instructions

Remove all metallic objects before entering the scanner room including hearing aids, mobile phones, keys, glasses, hair pins, jewellery, watches, safety pins, paperclips, credit cards, magnetic strip cards, coins, pens, pocket knives, nail clippers, steel-toed boots/shoes and all tools. Loose metallic objects are especially prohibited within the MR environment.

I have understood the above questions and have marked the answers correctly.

Signature (Participant/Parent/Guardian) Date

MR Centre Staff Signature

Appendix Q: Post participation questionnaire

The use of near infrared spectroscopy (NIRS) to measure haemodynamics in bone tissue

POST PARTICIPATION QUESTIONNAIRE

VERSION NUMBER 1.0 DATE: 05/04/2016

To be answered after testing:

Did you experience any adverse reactions to any of the testing you undertook for this research study?:

……

……

How painful would you rate the occlusion from your blood pressure cuff at its worst point on a scale from zero to ten (ten being the worst pain imaginable)? ……

Would you be willing to go through this type of testing if it was a screening test that provided potential diagnostic information about your bone health?

……

……

Would you be willing to be contacted for further research similar to what you have just undertaken? If yes, the contact details provided on your consent will be used: …….

Did you have any other feedback or comments regarding the study?

……

……

……

……

Appendix R: Blood and urine testing methods

Serum/Urine Test	Assay/Method Used
Sodium (mmol/L)	ISE Indirect Na-K-Cl for Gen.2 test using Cobas 8000 DIRECT Ion Selective Electrode (ISE)
Pottasium (mmol/L)	ISE Indirect Na-K-Cl for Gen.2 test using Cobas 8000 DIRECT Ion Selective Electrode (ISE)
Creatinine (umol/L)	Creatinine Jaffe Gen.2 test using the Cobas 8000 702 Module
Alanine amino transferase (iu/L)	Aspartate aminotransferase acc. to IFCC without pyridoxal phosphate activation test using the Cobas 8000 702 Module
Total bilirubin (umol/L)	Bilirubin Total Gen.3 test using the Cobas 8000 702 Module
Alkaline Phosphatase (iu/L)	Alkaline phosphatase acc. to IFCC Gen.2 test using the Cobas 8000 702 Module
Albumin (g/L)	Albumin Gen.2 test using the Cobas 8000 702 Module
HbA1c (mmol/mol)	Ion exchange high performance liquid chromatography method
Vit D (nmol/L)	Elecsys Vitamin D total II test using the Cobas 8000 801 Module
Parathyroid Hormone (pmol/L)	Elecsys PTH assay using the Cobas 8000 801 Module
Cholesterol (mmol/L)	Cholesterol Gen.2 test using the Cobas 8000 702 Module
Triglycerides (mmol/L)	Triglycerides test using Cobas 8000 702 Module
HDL-Cholesterol (mmol/L)	HDL-Cholesterol plus 3rd Generation test using the Cobas 8000 702 Module
Urine Cr (mmol/L)	Creatinine Jaffe Gen.2 test using the Cobas 8000 702 Module
Urine Alb (mg/L)	Tina-quant Albumin Gen.2 test using the Cobas 8000 702 Module

Appendix S: DCE-MRI results versus DXA results

The primary aim of the approach to validation of NIRS for *in vivo* use in measuring tibial haemodynamics is to compare NIRS results with comparator tests also measuring bone haemodynamics (DCE-MRI), as well as other measures of bone health, primarily bone mineral density (BMD; measured with DXA). However, it is also of interest to investigate for associations between DCE-MRI and BMD results. If significant associations are present and in keeping with associations between NIRS and BMD, confidence can be gained in how these comparator tests were performed. This would also support the underpinning assumption of the validation approach; that vascular haemodynamics (as a marker of microvascular health) are associated with other markers of bone health, such as BMD.

Table S.1: Pearson correlation r-values between haemodynamic DCE-MRI markers taken at the proximal tibia and areal bone mineral density (BMD in g/cm^2) results at different measurement sites. Measurements of percentage tissue composition and cross-sectional area (in mm^2) are also presented. Asterisks indicate a statistically significant correlation with *p*-value <0.05. Associations that are colour coded were statistically significant and considered poor (<0.40; orange), moderate (0.4-0.6; yellow) and strong (>0.60; green), in line with the criteria set out in Evans 1996 [304].

	Gadolinium Enhancement Rate (au/s)	Gadolinium Enhancement Amplitude (au)
L1-L4 BMD	-0.39*	-0.33
Total Hip BMD	-0.24	-0.50*
Total Body % Bone	-0.62*	-0.43*
Total Body % Fat	0.48*	0.34
Total body BMD	-0.38*	-0.46*
Both legs BMD	-0.39*	-0.49*
Whole Tibia BMD (measured leg)	-0.32	-0.41*
Proximal Tibia BMD (measured leg)	-0.38*	-0.40*
Lower Leg % Fat Content	0.46*	0.43*
Total Bone Area (mm^2)	-0.19	-0.27
Cortical Bone Area (mm^2)	-0.29	-0.43*

Table S.1 shows associations involving the two DCE-MRI haemodynamic markers of interest: the initial linear rate of the first 60 seconds of Gadolinium enhancement, and the amplitude of maximum signal change following Gadolinium injection. Pearson's correlations were performed between these two markers and areal bone mineral density measured using DXA at various anatomical sites. Associations were generally statistically significant but of poor to moderate strength, based on Evans' scale of association strength [304]. The direction of the associations suggests that faster and greater Gadolinium signal enhancement at rest is associated with poorer bone mineral density.

There was also moderate statistically significant positive associations between the percentage fat content in the lower leg of the participant, and both DCE-MRI haemodynamic markers. The direction of these associations suggests that faster and greater Gadolinium signal enhancement at rest is associated with higher percentage fat content in the lower leg.

Figures S.1 and S.2 illustrate the associations of both DCE-MRI haemodynamic markers with BMD results of the legs, allowing the comparison with Figures 9.2 and 9.3 which demonstrates the strongest associations obtained between BMD results of the legs with O_2Hb_DO_absΔ ($r=-0.63$; $p<0.001$) and total body BMD with O_2Hb_PO_absΔ ($r=0.56$; $p<0.001$). Associations between DCE-MRI markers and BMD of the legs are slightly lower in strength but comparable with these NIRS associations.

Figure S.1 presents an outlying data point. Without the outlying data point the correlation is weaker but still statistically significant ($r=-0.41$; $p=0.03$). This outlying data point has not been excluded from analysis in this section as there has been no obvious error or confounding contributor to explain it, so has been assumed to be physiologically representative of the participant.

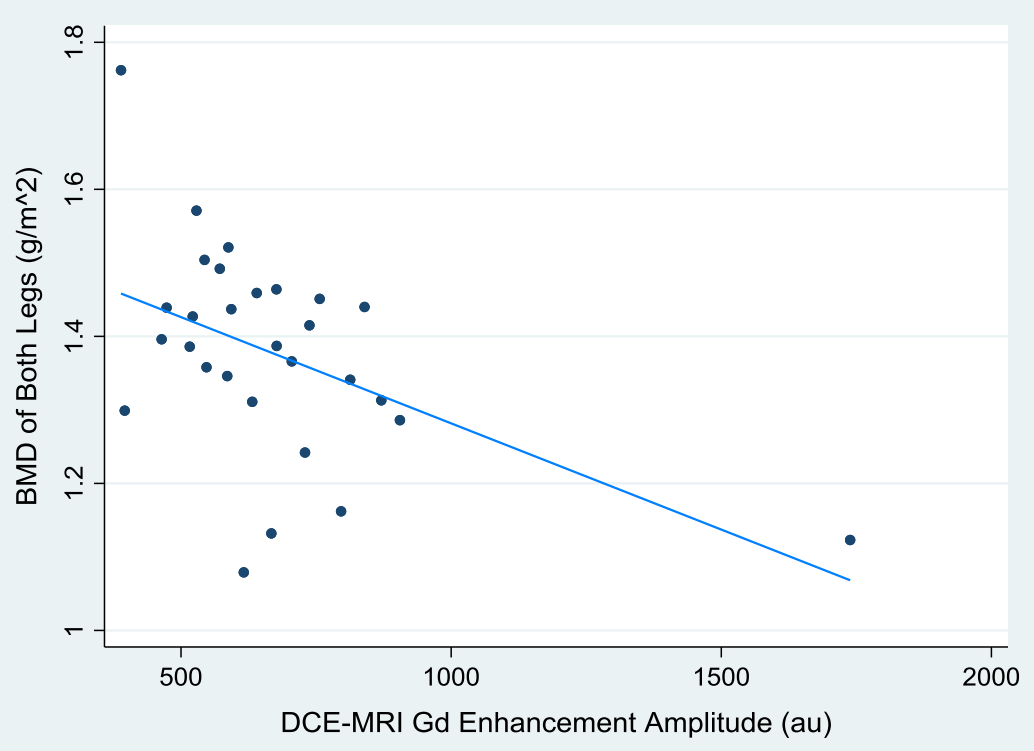

Figure S.1: Scatterplot with line of best fit demonstrating the association between BMD of both legs and DCE-MRI results for the amplitude of Gadolinium enhancement at the proximal tibia (r=-0.49; (p=0.006). Without the outlying data point the association is weaker (r=-0.41 p=0.03).

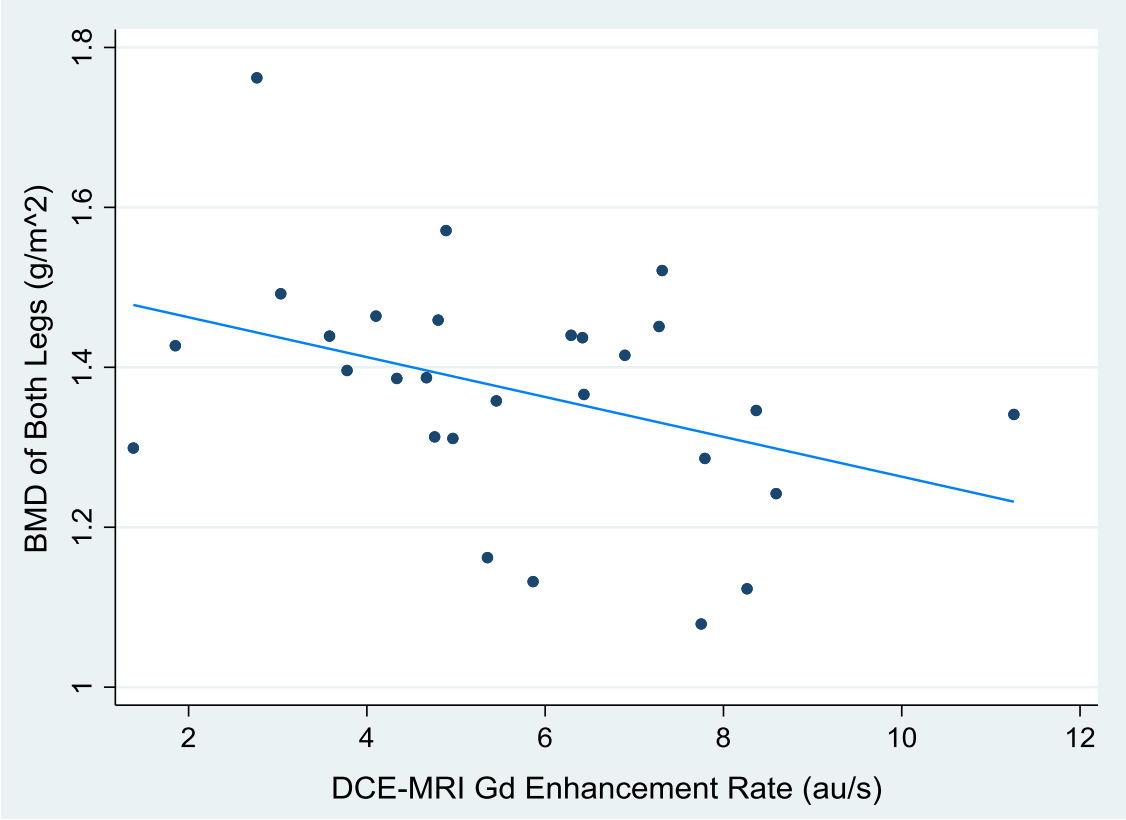

Figure S.2: Scatterplot with line of best fit demonstrating the association between BMD of both legs and DCE-MRI results for the initial rate of Gadolinium enhancement at the proximal tibia (r=-0.39; (p=0.04).

The associations between DCE-MRI and DXA measurements generally support, and are consistent with, the associations demonstrated between these data and with NIRS measurements. Associations are generally of comparable magnitude with those between NIRS markers and DCE-MRI presented in Chapter 9, and associations between NIRS and DXA measurements presented in Chapter 10. Associations presented in Section 10.2.1 generally demonstrated that stronger microvascular response to ischaemic stimuli, represented with NIRS markers, are associated with increased BMD. NIRS markers also generally inversely associated with DCE-MRI markers, showing stronger microvascular response associated with lower resting microvascular perfusion markers represented by DCE-MRI. As such, the results in this appendix are in keeping with the associations observed with NIRS, as BMD results were inversely correlated with DCE-MRI markers, suggesting lower resting perfusion markers (represented by DCE-MRI) may be associated with increased BMD.

Associations presented in Table S.1 demonstrate statistically significant positive associations between DCE-MRI markers and the percentage fat content in the lower leg and total body. The direction of these associations is expected as greater percentage fat content has also been negatively associated with BMD. Sex may also confound here, with the females in the sampled population having a statistically significant higher percentage fat content (mean 34.9% (SD 8.4) in females vs mean 19.1% (SD 3.9) in males; independent t-test $p<0.001$). Discussion on the relationships between sex and percentage fat content in the leg have been discussed in more depth in Section 9.4.2 regarding DCE-MRI, and Section 10.2.2.4 regarding BMD.

As discussed in Section 9.4, there is some indirect evidence to support the associations observed in this appendix. Whilst BMD measurements were not taken, Savvopoulou et al 2008 identified faster Gadolinium uptake in the lumbar spine of females over 50 years of age (with post-menopausal females expected to have lower BMD) compared with males in the same age bracket [93]. Libicher et al 2008 found increased vascularity with DCE-MRI in areas of increased bone turnover in those with Paget's disease [117], and the post-menopausal female cohort in this PhD project also have higher bone turnover and lower BMD than males (based on markers of bone metabolism presented in Section 10.5). Likewise Kristensen et al 2013 identified increased capillary density in areas of increased bone turnover using bone biopsies from the iliac crest [30]. As such, it may be expected that those participants with

anticipated higher bone turnover (i.e. post-menopausal women) had greater Gadolinium enhancement.

Conversely, there is more direct evidence that supports a relationship of reduced DCE-MRI markers at rest in participants with lower bone mineral density [34, 36, 37]. These studies investigate the spine and hip, arguing that reductions in bone mineral density are associated with increased fatty marrow with reduced vascularity. These studies contradict the associations observed in this appendix, however they differ in that they typically had larger cohorts of participants diagnosed with more severe osteoporosis and so may be highlighting a different pathophysiological relationship.

References

1. Jacques SL. Optical properties of biological tissues: a review. Phys Med Biol. 2013;58(11):R37-61.

2. Elwell CE. A Practical Users Guide to Near Infrared Spectroscopy. London: UCL Reprographics; 1995.

3. McAlinden C, Khadka J, Pesudovs K. Precision (repeatability and reproducibility) studies and sample-size calculation. Journal of Cataract & Refractive Surgery. 2015;41(12):2598-604.

4. Heale R, Twycross A. Validity and reliability in quantitative studies. Evidence Based Nursing. 2015;18(3):66-7.

5. Laroche M. Intraosseous circulation from physiology to disease. Joint Bone Spine. 2002;69(3):262-9.

6. Binzoni T, Spinelli L. Near-infrared photons: a non-invasive probe for studying bone blood flow regulation in humans. J Physiol Anthropol. 2015;34(1):1-6.

7. Sun C-W, Chuang C-C. Chapter 3: Hemodynamics Study Based on Near-Infrared Optical Assessment. In: Seda Artis A, editor. Hemodynamics - New Diagnostic and Therapeutic Approaches. Online: InTech; 2012.

8. Prisby RD. Mechanical, hormonal and metabolic influences on blood vessels, blood flow and bone. Journal of Endocrinology. 2017;235(3):R77-R100.

9. Pifferi A, Torricelli A, Taroni P, Bassi A, Chikoidze E, Giambattistelli E, et al. Optical biopsy of bone tissue: a step toward the diagnosis of bone pathologies. Journal of biomedical optics. 2004;9(3):474-80.

10. Binzoni T, Leung TS, Courvoisier C, Giust R, Tribillon G, Gharbi T, et al. Blood volume and haemoglobin oxygen content changes in human bone marrow during orthostatic stress. J Physiol Anthropol. 2006;25(1):1-6.

11. Dyke JP, Aaron RK. Noninvasive methods of measuring bone blood perfusion. Ann N Y Acad Sci. 2010;1192:95-102.

12. Humadi A, Alhadithi RH, Alkudiari SI. Validity of the DEXA diagnosis of involutional osteoporosis in patients with femoral neck fractures. Indian Journal of Orthopaedics. 2010;44(1):73-8.

13. Binzoni T, Van De Ville D. Noninvasive probing of the neurovascular system in human bone/bone marrow using near infrared light. Journal of Innovative Optical Health Sciences. 2011;04(02):183-9.

14. Meertens R, Casanova F, Knapp KM, Thorn C, Strain WD. Use of near-infrared systems for investigations of hemodynamics in human in vivo bone tissue: A systematic review. Journal of Orthopaedic Research. 2018;36(10):2595-603.

15. Farzam P, Zirak P, Binzoni T, Durduran T. Pulsatile and steady-state hemodynamics of the human patella bone by diffuse optical spectroscopy. Physiol Meas. 2013;34(8):839-57.

16. Aziz SM, Khambatta F, Vaithianathan T, Thomas JC, Clark JM, Marshall R. A near infrared instrument to monitor relative hemoglobin concentrations of human bone tissue in vitro and in vivo. Rev Sci Instrum. 2010;81(4):043111.

17. Clarke B. Normal bone anatomy and physiology. Clinical Journal of the American Society of Nephrology. 2008;3(Supplement 3):S131-S9.

18. Prisby RD. The clinical relevance of the bone vascular system: Age-related implications. Clinical Reviews in Bone and Mineral Metabolism. 2019;17(1):48-62.

19. Standring S. Gray's Anatomy : The Anatomical Basis of Clinical Practice. 40th ed. London, United Kingdom: Elsevier Health Sciences; 2008.

20. Bauer JS, Link TM. Advances in osteoporosis imaging. European Journal of Radiology. 2009;71(3):440-9.

21. Betts JG, Young KA, Wise JA, Johnson E, Poe B, Kruse DH, et al. Anatomy & Physiology: OpenStax; 2013 [15/10/2019]. Available from: https://openstax.org/books/anatomy-and-physiology/pages/6-3-bone-structure.

22. Karampinos DC, Ruschke S, Dieckmeyer M, Diefenbach M, Franz D, Gersing AS, et al. Quantitative MRI and spectroscopy of bone marrow. Journal of Magnetic Resonance Imaging. 2017.

23. McCarthy I. The physiology of bone blood flow: a review. J Bone Joint Surg Am. 2006;88 Suppl 3:4-9.

24. King DG. Bone Remodelling Illinois: Southern Illinois University; 2004 [cited 2020 31/01/2020]. Available from: http://www.siumed.edu/~dking2/ssb/remodel.htm.

25. Eastell R, Baumann M, Hoyle NR, Wieczorek. Bone Markers: Biochemical and Clinical Perspectives. London, United Kingdom: Martin Dunitz Ltd; 2001.

26. Oikawa A, Siragusa M, Quaini F, Mangialardi G, Katare RG, Caporali A, et al. Diabetes mellitus induces bone marrow microangiopathy. Arterioscler Thromb Vasc Biol. 2010;30(3):498-508.

27. Pittman RN, editor Regulation of tissue oxygenation. Colloquium series on integrated systems physiology: from molecule to function; 2011: Morgan & Claypool Life Sciences.

28. Clough GF, Kuliga KZ, Chipperfield AJ. Flow motion dynamics of microvascular blood flow and oxygenation: Evidence of adaptive changes in obesity and type 2 diabetes mellitus/insulin resistance. Microcirculation. 2017;24(2):e12331.

29. Sader MA, Celermajer DS. Endothelial function, vascular reactivity and gender differences in the cardiovascular system. Cardiovasc Res. 2002;53(3):597-604.

30. Kristensen HB, Andersen TL, Marcussen N, Rolighed L, Delaisse JM. Increased presence of capillaries next to remodeling sites in adult human cancellous bone. Journal of Bone and Mineral Research. 2013;28(3):574-85.

31. World Health Organisation. WHO Scientific group on the assessment of osteoporosis at primary health care level. 2004.

32. Meertens R, Strain WD, Knapp KM. A review of the mechanisms, diagnosis and preventative treatment options of osteoporotic fragility fractures in patients with type 2 diabetes mellitus. Journal of Endocrinology and Metabolism. 2015;5(1-2):157-162.

33. Laroche M, Pouilles J, Ribot C, Bendayan P, Bernard J, Boccalon H, et al. Comparison of the bone mineral content of the lower limbs in men with ischaemic atherosclerotic disease. Clinical Rheumatology. 1994;13(4):611-4.

34. Griffith JF, Yeung DK, Antonio GE, Lee FK, Hong AW, Wong SY, et al. Vertebral bone mineral density, marrow perfusion, and fat content in healthy men and men with osteoporosis: dynamic contrast-enhanced MR imaging and MR spectroscopy. Radiology. 2005;236(3):945-51.

35. Griffith JF, Yeung DK, Antonio GE, Wong SY, Kwok TC, Woo J, et al. Vertebral marrow fat content and diffusion and perfusion indexes in women with varying bone density: MR evaluation. Radiology. 2006;241(3):831-8.

36. Griffith JF, Yeung DK, Tsang PH, Choi KC, Kwok TC, Ahuja AT, et al. Compromised bone marrow perfusion in osteoporosis. Journal of Bone & Mineral Research. 2008;23(7):1068-75.

37. Griffith JF, Yeung DKW, Leung JCS, Kwok TCY, Leung PC. Prediction of bone loss in elderly female subjects by MR perfusion imaging and spectroscopy. European Radiology. 2011;21(6):1160-9.

38. Prisby R. Conversion of bone marrow blood vessels into bone leads to "microvascular dead space": A potential etiology for bone and bone marrow disease with advancing age. FASEB Journal. 2015;29 (1 Meeting Abstracts).

39. Bridgeman G, Brookes M. Blood supply to the human femoral diaphysis in youth and senescence. Journal of Anatomy. 1996;188(Pt 3):611.

40. Bousson V, Bergot C, Sutter B, Levitz P, Cortet B. Trabecular bone score (TBS): available knowledge, clinical relevance, and future prospects. Osteoporos Int. 2012;23(5):1489-501.

41. Dubey RK, Imthurn B, Barton M, Jackson EK. Vascular consequences of menopause and hormone therapy: Importance of timing of treatment and type of estrogen. Cardiovascular Research. 2005;66(2):295-306.

42. Prisby RD, Dominguez II JM, Muller-Delp J, Allen MR, Delp MD. Aging and estrogen status: a possible endothelium-dependent vascular coupling mechanism in bone remodeling. PloS one. 2012;7(11):e48564.

43. Wang YX, Griffith JF, Deng M, Yeung DK, Yuan J. Rapid Increase in Marrow Fat Content and Decrease in Marrow Perfusion in Lumbar Vertebra Following Bilateral Oophorectomy: An MR Imaging-Based Prospective Longitudinal Study. Korean J Radiol. 2015;16(1):154-9.

44. Roche B, Vanden-Bossche A, Malaval L, Normand M, Jannot M, Chaux R, et al. Parathyroid Hormone 1-84 Targets Bone Vascular Structure and Perfusion in Mice: Impacts of Its Administration Regimen and of Ovariectomy. Journal of Bone and Mineral Research. 2014;29(7):1608-18.

45. Zhou B, Lu Y, Hajifathalian K, Bentham J, Di Cesare M, Danaei G, et al. Worldwide trends in diabetes since 1980: a pooled analysis of 751 population-based studies with 4· 4 million participants. The Lancet. 2016;387(10027):1513-30.

46. Rathinavelu S, Guidry-Elizondo C, Banu J. Molecular Modulation of Osteoblasts and Osteoclasts in Type 2 Diabetes. Journal of diabetes research. 2018;2018.

47. Pritchard JM, Giangregorio LM, Atkinson SA, Beattie KA, Inglis D, Ioannidis G, et al. Association of larger holes in the trabecular bone at the distal radius in postmenopausal women with type 2 diabetes mellitus compared to controls. Arthritis care & research. 2012;64(1):83-91.

48. Leslie WD, Rubin MR, Schwartz AV, Kanis JA. Type 2 diabetes and bone. Journal of Bone & Mineral Research. 2012;27(11):2231-7.

49. Burghardt AJ, Issever AS, Schwartz AV, Davis KA, Masharani U, Majumdar S, et al. High-resolution peripheral quantitative computed tomographic imaging of cortical and trabecular bone microarchitecture in patients with type 2 diabetes mellitus. The Journal of Clinical Endocrinology & Metabolism. 2010;95(11):5045-55.

50. Ferrari SL, Abrahamsen B, Napoli N, Akesson K, Chandran M, Eastell R, et al. Diagnosis and management of bone fragility in diabetes: an emerging challenge. Osteoporosis International. 2018;29(12):2585-96.

51. An T, Hao J, Sun S, Li R, Yang M, Cheng G, et al. Efficacy of statins for osteoporosis: a systematic review and meta-analysis. Osteoporosis International. 2017;28(1):47-57.

52. Leutner M, Matzhold C, Bellach L, Deischinger C, Harreiter J, Thurner S, et al. Diagnosis of osteoporosis in statin-treated patients is dose-dependent. Annals of the rheumatic diseases. 2019;78(12):1706-11.

53. Lasschuit J, Center J, Greenfield J, Tonks K. Comparison of calcaneal quantitative ultrasound and bone densitometry parameters as fracture risk predictors in type 2 diabetes mellitus. Diabetic Medicine. 2019.

54. Netter FH. Atlas of human anatomy, Professional Edition E-Book: Elsevier Health Sciences; 2014.

55. Santolini E, Goumenos SD, Giannoudi M, Sanguineti F, Stella M, Giannoudis PV. Femoral and tibial blood supply: A trigger for non-union? Injury. 2014;45(11):1665-73.

56. Farzam P, Lindner C, Weigel UM, Suarez M, Urbano-Ispizua A, Durduran T. Noninvasive characterization of the healthy human manubrium using diffuse optical spectroscopies. Physiol Meas. 2014;35(7):1469-91.

57. Craig P, Dieppe P, Macintyre S, Michie S, Nazareth I, Petticrew M. Developing and evaluating complex interventions: the new Medical Research Council guidance. BMJ. 2008;337:a1655.

58. Ferrari M, Quaresima V. Near infrared brain and muscle oximetry: from the discovery to current applications. Journal of Near Infrared Spectroscopy. 2012;20(1):1-14.

59. Jobsis FF. Noninvasive, infrared monitoring of cerebral and myocardial oxygen sufficiency and circulatory parameters. Science. 1977;198(4323):1264-7.

60. Hamamatsu Photonics. Near Infrared Oxygenation Monitor NIRO-NX200 (Brochure). Hamamatsu Photonics; 2010.

61. Suzuki S, Takasaki S, Ozaki T, Kobayashi Y, editors. Tissue oxygenation monitor using NIR spatially resolved spectroscopy. BiOS '99 International Biomedical Optics Symposium, 1999; 1999.

62. Bakker A, Smith B, Ainslie P, Smith K. Near-infrared spectroscopy. Applied Aspects of Ultrasonography in Humans: IntechOpen; 2012.

63. Pereira MI, Gomes PS, Bhambhani YN. A brief review of the use of near infrared spectroscopy with particular interest in resistance exercise. Sports medicine. 2007;37(7):615-24.

64. Lange F, Dunne L, Hale L, Tachtsidis I. MAESTROS: a multiwavelength time-domain NIRS system to monitor changes in oxygenation and oxidation state of Cytochrome-C-Oxidase. IEEE Journal of Selected Topics in Quantum Electronics. 2018;25(1):1-12.

65. Thorn CE, Shore AC. The role of perfusion in the oxygen extraction capability of skin and skeletal muscle. American Journal of Physiology-Heart and Circulatory Physiology. 2016;15;310(10):H1277-84.

66. Mancini DM, Bolinger L, Li H, Kendrick K, Chance B, Wilson JR. Validation of near-infrared spectroscopy in humans. Journal of Applied Physiology. 1994;77(6):2740-7.

67. Wassenaar E, Van den Brand J. Reliability of near-infrared spectroscopy in people with dark skin pigmentation. Journal of clinical monitoring and computing. 2005;19(3):195-9.

68. Niwayama M. Voxel-based measurement sensitivity of spatially resolved near-infrared spectroscopy in layered tissues. J Biomed Opt. 2018;23(3):1-4.

69. Ferrari M, Mottola L, Quaresima V. Principles, techniques, and limitations of near infrared spectroscopy. Canadian Journal of Applied Physiology. 2004;29(4):463-87.

70. Sekar SKV, Farina A, Martinenghi E, Dalla Mora A, Taroni P, Pifferi A, et al., editors. Time-resolved diffused optical characterization of key tissue constituents of human bony prominence locations. European Conferences on Biomedical Optics; 2015.

71. Davies DJ, Clancy M, Lighter D, Balanos GM, Lucas SJE, Dehghani H, et al. Frequency-domain vs continuous-wave near-infrared spectroscopy devices: a comparison of clinically viable monitors in controlled hypoxia. Journal of clinical monitoring and computing. 2017;31(5):967-74.

72. Draghici AE, Potart D, Hollmann JL, Pera V, Fang Q, Dimarzio CA, et al. Near infrared spectroscopy for measuring changes in bone hemoglobin content after exercise in individuals with spinal cord injury. J Orthop Res. 2017.

73. Van Beekvelt MC, Colier WN, Wevers RA, Van Engelen BG. Performance of near-infrared spectroscopy in measuring local O(2) consumption and blood flow in skeletal muscle. Journal of Applied Physiology.90(2):511-9.

74. Shang Y, Li T, Yu G. Clinical applications of near-infrared diffuse correlation spectroscopy and tomography for tissue blood flow monitoring and imaging. Physiological measurement. 2017;38(4):R1.

75. Sekar SKV, Pagliazzi M, Negredo E, Martelli F, Farina A, Dalla Mora A, et al. In Vivo, Non-Invasive Characterization of Human Bone by Hybrid Broadband (600-1200 nm) Diffuse Optical and Correlation Spectroscopies. PLoS One. 2016;11(12):e0168426.

76. Vardi M, Nini A. Near-infrared spectroscopy for evaluation of peripheral vascular disease. A systematic review of literature. Eur J Vasc Endovasc Surg. 2008;35(1):68-74.

77. Mateus J, Hargens AR. Photoplethysmography for non-invasive in vivo measurement of bone hemodynamics. Physiol Meas. 2012;33(6):1027-42.

78. Siamwala JH, Lee PC, Macias BR, Hargens AR. Lower-body negative pressure restores leg bone microvascular flow to supine levels during head-down tilt. J Appl Physiol. 2015;119(2):101-9.

79. Rosenberry R, Munson M, Chung S, Samuel TJ, Patik J, Tucker WJ, et al. Age-related microvascular dysfunction: novel insight from near-infrared spectroscopy. Experimental physiology. 2018;103(2):190-200.

80. Bopp CM, Townsend DK, Warren S, Barstow TJ. Relationship between brachial artery blood flow and total [hemoglobin+ myoglobin] during post-occlusive reactive hyperemia. Microvascular research. 2014;91:37-43.

81. Roustit M, Cracowski JL. Non-invasive assessment of skin microvascular function in humans: an insight into methods. Microcirculation. 2012;19(1):47-64.

82. Allen J. Photoplethysmography and its application in clinical physiological measurement. Physiological measurement. 2007;28(3):R1.

83. Naslund J, Pettersson J, Lundeberg T, Linnarsson D, Lindberg LG. Non-invasive continuous estimation of blood flow changes in human patellar bone. Med Biol Eng Comput. 2006;44(6):501-9.

84. Binzoni T, Van De Ville D. Noninvasive probing of the neurovascular system in human bone/boone marrow using near infrared light. Journal of Innovative Optical Health Sciences. 2011;04(02):183-9.

85. Nicholls RL, Green D, Kuster MS. Patella intraosseous blood flow disturbance during a medial or lateral arthrotomy in total knee arthroplasty: A laser Doppler flowmetry study. Knee Surg Sports Traumatol Arthrosc. 2006;14(5):411-6.

86. Hasegawa M, Kawamura G, Wakabayashi H, Sudo A, Uchida A. Changes to patellar blood flow after minimally invasive total knee arthroplasty. Knee Surg Sports Traumatol Arthrosc. 2009;17(10):1195-8.

87. Kohl S, Evangelopoulos DS, Hartel M, Kohlhof H, Roeder C, Eggli S. Anterior knee pain after total knee arthroplasty: Does it correlate with patellar blood flow? Knee Surg Sports Traumatol Arthrosc. 2011;19(9):1453-9.

88. Fredriksson I, Fors C, Johansson J. Laser doppler flowmetry-a theoretical framework. Department of Biomedical Engineering, Linköping University. 2007:6-7.

89. Biffar A, Dietrich O, Sourbron S, Duerr HR, Reiser MF, Baur-Melnyk A. Diffusion and perfusion imaging of bone marrow. Eur J Radiol. 2010;76(3):323-8.

90. Shih TT-F, Liu H-C, Chang C-J, Wei S-Y, Shen L-C, Yang P-C. Correlation of MR Lumbar Spine Bone Marrow Perfusion with Bone Mineral Density in Female Subjects. Radiology. 2004;233(1):121-8.

91. Patsch JM, Li X, Baum T, Yap SP, Karampinos DC, Schwartz AV, et al. Bone marrow fat composition as a novel imaging biomarker in postmenopausal women with prevalent fragility fractures. Journal of Bone and Mineral Research. 2013;28(8):1721-8.

92. Ma HT, Lv H, Griffith JF, Yuan J, Leung PC. Bone marrow perfusion of proximal femur varied with BMD--a longitudinal study by DCE-MRI. Conf Proc IEEE Eng Med Biol Soc. 2013;2013:2607-10.

93. Savvopoulou V, Maris TG, Vlahos L, Moulopoulos LA. Differences in perfusion parameters between upper and lower lumbar vertebral segments with dynamic contrast-enhanced MRI (DCE MRI). Eur Radiol. 2008;18(9):1876-83.

94. Chen WT, Shih TT, Chen RC, Lo SY, Chou CT, Lee JM, et al. Vertebral bone marrow perfusion evaluated with dynamic contrast-enhanced MR imaging: significance of aging and sex. Radiology. 2001;220(1):213-8.

95. Biffar A, Schmidt GP, Sourbron S, D'Anastasi M, Dietrich O, Notohamiprodjo M, et al. Quantitative analysis of vertebral bone marrow perfusion using dynamic contrast-enhanced MRI: initial results in osteoporotic patients with acute vertebral fracture. J Magn Reson Imaging. 2011;33(3):676-83.

96. Griffith J, Yeung DKW, Leung JCS, Kwok TCY, Leung PC. Prediction of bone loss by MR perfusion imaging and spectroscopy. Bone. 2010;47:S373.

97. Martirosian P, Boss A, Schraml C, Schwenzer NF, Graf H, Claussen CD, et al. Magnetic resonance perfusion imaging without contrast media. Eur J Nucl Med Mol Imaging. 2010;37 Suppl 1:S52-64.

98. Chavhan GB, Babyn PS, Thomas B, Shroff MM, Haacke EM. Principles, techniques, and applications of T2*-based MR imaging and its special applications 1. Radiographics. 2009;29(5):1433-49.

99. Leach MO, Morgan B, Tofts PS, Buckley DL, Huang W, Horsfield MA, et al. Imaging vascular function for early stage clinical trials using dynamic contrast-enhanced magnetic resonance imaging. Eur Radiol. 2012;22(7):1451-64.

100. Mathew RC, Kramer CM. Recent advances in magnetic resonance imaging for peripheral artery disease. Vasc Med. 2018;23(2):143-52.

101. Tagliafico A, Bignotti B, Tagliafico G, Martinoli C. Peripheral nerve MRI: precision and reproducibility of T2*-derived measurements at 3.0-T. Skeletal radiology. 2015;44(5):679-86.

102. Grassedonio E, Meloni A, Positano V, De Marchi D, Toia P, Midiri M, et al. Quantitative T2* magnetic resonance imaging for renal iron overload assessment: normal values by age and sex. Abdominal imaging. 2015;40(6):1700-4.

103. Towse TF, Childs BT, Sabin SA, Bush EC, Elder CP, Damon BM. Comparison of muscle BOLD responses to arterial occlusion at 3 and 7 Tesla. Magnetic resonance in medicine. 2016;75(3):1333-40.

104. Mehagnoul-Schipper DJ, van der Kallen BF, Colier WN, van der Sluijs MC, van Erning LJTO, Thijssen HO, et al. Simultaneous measurements of cerebral oxygenation changes during brain activation by near-infrared spectroscopy and functional magnetic resonance imaging in healthy young and elderly subjects. Human brain mapping. 2002;16(1):14-23.

105. Huppert TJ, Hoge RD, Diamond SG, Franceschini MA, Boas DA. A temporal comparison of BOLD, ASL, and NIRS hemodynamic responses to motor stimuli in adult humans. Neuroimage. 2006;29(2):368-82.

106. Muller MD, Li Z, Sica CT, Luck JC, Gao Z, Blaha CA, et al. Muscle oxygenation during dynamic plantar flexion exercise: combining BOLD MRI with traditional physiological measurements. Physiological Reports. 2016;4(20).

107. Khalifa F, Soliman A, El-Baz A, El-Ghar MA, El-Diasty T, Gimel'farb G, et al. Models and methods for analyzing DCE-MRI: A review. Medical physics. 2014;41(12).

108. Dyke JP, Lazaro LE, Hettrich CM, Hentel KD, Helfet DL, Lorich DG. Regional analysis of femoral head perfusion following displaced fractures of the femoral neck. J Magn Reson Imaging. 2015;41(2):550-4.

109. Budzik JF, Lefebvre G, Forzy G, El Rafei M, Chechin D, Cotten A. Study of proximal femoral bone perfusion with 3D T1 dynamic contrast-enhanced MRI: a feasibility study. Eur Radiol. 2014;24(12):3217-23.

110. Store G, Smith HJ, Larheim TA. Dynamic MR imaging of mandibular osteoradionecrosis. Acta Radiol. 2000;41(1):31-7.

111. Rastogi A, Kubassova O, Krasnosselskaia LV, Lim AK, Satchithananda K, Boesen M, et al. Evaluating automated dynamic contrast enhanced wrist 3T MRI in healthy volunteers: one-year longitudinal observational study. Eur J Radiol. 2013;82(8):1286-91.

112. Muller GM, Mansson S, Muller MF, Ekberg O, Bjorkman A. Assessment of perfusion in normal carpal bones with dynamic gadolinium-enhanced MRI at 3 Tesla. J Magn Reson Imaging. 2013;38(1):168-72.

113. Seah S, Wheaton D, Li L, Dyke JP, Talmo C, Harvey WF, et al. The relationship of tibial bone perfusion to pain in knee osteoarthritis. Osteoarthritis Cartilage. 2012;20(12):1527-33.

114. Mattila KT, Komu ME, Dahlstrom S, Koskinen SK, Heikkila J. Medial tibial pain: a dynamic contrast-enhanced MRI study. Magn Reson Imaging. 1999;17(7):947-54.

115. Ehlinger M, Moser T, Adam P, Bierry G, Gangi A, de Mathelin M, et al. Early prediction of femoral head avascular necrosis following neck fracture. Orthop Traumatol Surg Res. 2011;97(1):79-88.

116. Libicher M, Kasperk C, Daniels-Wredenhagen M, Heye T, Kauczor HU, Nawroth P, et al. Dynamic contrast-enhanced MRI for monitoring bisphosphonate therapy in Paget's disease of bone. Skeletal Radiol. 2013;42(2):225-30.

117. Libicher M, Kasperk C, Daniels M, Hosch W, Kauczor HU, Delorme S. Dynamic contrast-enhanced MRI in Paget's disease of bone--correlation of regional microcirculation and bone turnover. Eur Radiol. 2008;18(5):1005-11.

118. Kwack KS, Cho JH, Lee JH, Cho JH, Oh KK, Kim SY. Septic arthritis versus transient synovitis of the hip: gadolinium-enhanced MRI finding of decreased perfusion at the femoral epiphysis. AJR Am J Roentgenol. 2007;189(2):437-45.

119. Merz M, Ritsch J, Kunz C, Wagner B, Sauer S, Hose D, et al. Dynamic contrast-enhanced magnetic resonance imaging for assessment of antiangiogenic treatment effects in multiple myeloma. Clin Cancer Res. 2015;21(1):106-12.

120. Barile A, Regis G, Masi R, Maggiori M, Gallo A, Faletti C, et al. Musculoskeletal tumours: preliminary experience with perfusion MRI. Radiol Med. 2007;112(4):550-61.

121. Howe BM, Johnson GB, Wenger DE. Current concepts in MRI of focal and diffuse malignancy of bone marrow. Seminars in musculoskeletal radiology. 2013;17(2):137-44.

122. Chu S, Karimi S, Peck KK, Yamada Y, Lis E, Lyo J, et al. Measurement of blood perfusion in spinal metastases with dynamic contrast-enhanced magnetic resonance imaging: evaluation of tumor response to radiation therapy. Spine. 2013;38(22):E1418-24.

123. Griffith JF. Functional imaging of the musculoskeletal system. Quantitative imaging in medicine and surgery. 2015;5(3):323.

124. Ma HT, Lv H, Griffith JF, Li AF, Yeung DK, Leung J, et al. Perfusion and bone mineral density as function of vertebral level at lumbar spine. Conf Proc IEEE Eng Med Biol Soc. 2012;2012:3488-91.

125. Yeung DK, Griffith JF, Antonio GE, Lee FK, Woo J, Leung PC. Osteoporosis is associated with increased marrow fat content and decreased marrow fat unsaturation: a proton MR spectroscopy study. Journal of Magnetic Resonance Imaging. 2005;22(2):279-85.

126. Chen WT, Shih TT. Correlation between the bone marrow blood perfusion and lipid water content on the lumbar spine in female subjects. J Magn Reson Imaging. 2006;24(1):176-81.

127. Bluemke DA, Petri M, Zerhouni EA. Femoral head perfusion and composition: MR imaging and spectroscopic evaluation of patients with systemic lupus erythematosus and at risk for avascular necrosis. Radiology. 1995;197(2):433-8.

128. Yeung DK, Lam SL, Griffith JF, Chan AB, Chen Z, Tsang PH, et al. Analysis of bone marrow fatty acid composition using high-resolution proton NMR spectroscopy. Chemistry & Physics of Lipids. 2008;151(2):103-9.

129. Li X, Shet K, Rodrguez JP, Pino AM, Kurhanewicz J, Schwartz A, et al. Unsaturation level decreased in bone marrow lipids of postmenopausal women with low bone density using high resolution hrmas nmr. Journal of Bone and Mineral Research. 2012;27.

130. Griffith JF, Yeung DKW, Chow SKK, Leung JCS, Ping CL. Reproducibility of MR perfusion and 1H spectroscopy of bone marrow. Journal of Magnetic Resonance Imaging. 2009;29(6):1438-42.

131. Padhani AR, Hayes C, Landau S, Leach MO. Reproducibility of quantitative dynamic MRI of normal human tissues. NMR in Biomedicine. 2002;15(2):143-53.

132. Yang C, Karczmar GS, Medved M, Oto A, Zamora M, Stadler WM. Reproducibility assessment of a multiple reference tissue method for quantitative dynamic contrast enhanced–MRI analysis. Magnetic resonance in medicine. 2009;61(4):851-9.

133. Machann J, Stefan N, Schick F. 1H MR spectroscopy of skeletal muscle, liver and bone marrow. European journal of radiology. 2008;67(2):275-84.

134. Ryan TE, Southern WM, Reynolds MA, McCully KK. A cross-validation of near-infrared spectroscopy measurements of skeletal muscle oxidative capacity with phosphorus magnetic resonance spectroscopy. Journal of Applied Physiology. 2013;115(12):1757-66.

135. Ohno N, Miyati T, Kasai H, Arai N, Kawano M, Shibamoto Y, et al. Evaluation of perfusion-related and true diffusion in vertebral bone marrow: a preliminary study. Radiol Phys Technol. 2015;8(1):135-40.

136. Biffar A, Sourbron S, Dietrich O, Schmidt G, Ingrisch M, Reiser MF, et al. Combined diffusion-weighted and dynamic contrast-enhanced imaging of patients with acute osteoporotic vertebral fractures. Eur J Radiol. 2010;76(3):298-303.

137. Yu G, Floyd TF, Durduran T, Zhou C, Wang J, Detre JA, et al. Validation of diffuse correlation spectroscopy for muscle blood flow with concurrent arterial spin labeled perfusion MRI. Opt Express. 2007;15(3):1064-75.

138. Wintermark P, Hansen A, Warfield SK, Dukhovny D, Soul JS. Near-Infrared Spectroscopy versus Magnetic Resonance Imaging To Study Brain Perfusion in Newborns with Hypoxic-Ischemic Encephalopathy Treated with Hypothermia. NeuroImage. 2014;85(0 1):287-93.

139. Du J, Bydder GM. Qualitative and quantitative ultrashort-TE MRI of cortical bone. NMR in Biomedicine. 2013;26(5):489-506.

140. Moore AE, Blake GM, Fogelman I. Quantitative measurements of bone remodeling using 99mTc-methylene diphosphonate bone scans and blood sampling. Journal of Nuclear Medicine. 2008;49(3):375-82.

141. Wong KK, Piert M. Dynamic Bone Imaging with 99mTc-Labeled Diphosphonates and 18F-NaF: Mechanisms and Applications. Journal of Nuclear Medicine. 2013;54(4):590-9.

142. Blake GM, Moore AE, Fogelman I, editors. Quantitative studies of bone using 99mTc-methylene diphosphonate skeletal plasma clearance. Seminars in nuclear medicine; 2009: Elsevier.

143. Wassberg C, Lubberink M, Sörensen J, Johansson S. Repeatability of quantitative parameters of 18F-fluoride PET/CT and biochemical tumour and specific bone remodelling markers in prostate cancer bone metastases. EJNMMI Research. 2017;7(1):42.

144. Siddique M, Frost ML, Blake GM, Moore AE, Al-Beyatti Y, Marsden PK, et al. The precision and sensitivity of 18F-fluoride PET for measuring regional bone metabolism: a comparison of quantification methods. Journal of Nuclear Medicine. 2011;52(11):1748-55.

145. Lafage-Proust M-H, Roche B, Langer M, Cleret D, Bossche AV, Olivier T, et al. Assessment of bone vascularization and its role in bone remodeling. BoneKEy reports. 2015;4.

146. Anetzberger H, Thein E, Becker M, Zwissler B, Messmer K. Microspheres accurately predict regional bone blood flow. Clin Orthop Relat Res. 2004(424):253-65.

147. Sugamoto K, Ochi T, Takahashi Y, Tamura T, Matsuoka T. Hemodynamic measurement in the femoral head using laser Doppler. Clin Orthop Relat Res. 1998(353):138-47.

148. Geis S, Prantl L, Mueller S, Gosau M, Lamby P, Jung EM. Quantitative Assessment of Bone Microvascularization After Osteocutaneous Flap Transplantation Using Contrast-Enhanced Ultrasound (CEUS). Ultraschall Med. 2013;34(03):272-9.

149. Müller S, Gosau M, Strobel D, Gehmert S, Moralis A, Reichert TE, et al. Assessment of bone microcirculation by contrast-enhanced ultrasound (CEUS) and [18F]-positron emission tomography/computed tomography in free osseous and osseocutaneus flaps for mandibular reconstruction: Preliminary results. Clinical Hemorheology and Microcirculation. 2011;49:115-28.

150. Krammer D, Schmidmaier G, Weber M-A, Doll J, Rehnitz C, Fischer C. Contrast-Enhanced Ultrasound Quantifies the Perfusion Within Tibial Non-Unions and Predicts the Outcome of Revision Surgery. Ultrasound in Medicine & Biology. 2018;44(8):1853-9.

151. Pozza S, De Marchi A, Albertin C, Albano D, Biino G, Aloj D, et al. Technical and clinical feasibility of contrast-enhanced ultrasound evaluation of long bone non-infected nonunion healing. La radiologia medica. 2018;123(9):703-9.

152. Kulak CAM, Dempster DW. Bone histomorphometry: a concise review for endocrinologists and clinicians. Arquivos Brasileiros de Endocrinologia & Metabologia. 2010;54(2):87-98.

153. Link TM. Osteoporosis imaging: State of the art and advanced imaging. Radiology. 2012;263(1):3-17.

154. Siris ES, Chen Y-T, Abbott TA, Barrett-Connor E, Miller PD, Wehren LE, et al. Bone mineral density thresholds for pharmacological intervention to prevent fractures. Archives of internal medicine. 2004;164(10):1108-12.

155. Hopkins SJ, Welsman JR, Knapp KM. Short-term precision error in dual energy x-ray absorptiometry, bone mineral density and trabecular bone score measurements; and effects of obesity on precision error. J Biomedical Graphics and Computing. 2014;4(2):8-14.

156. El Maghraoui A, Zounon ADS, Jroundi I, Nouijai A, Ghazi M, Achemlal L, et al. Reproducibility of bone mineral density measurements using dual X-ray absorptiometry in daily clinical practice. Osteoporosis international. 2005;16(12):1742-8.

157. Silva BC, Leslie WD, Resch H, Lamy O, Lesnyak O, Binkley N, et al. Trabecular bone score: a noninvasive analytical method based upon the DXA image. Journal of bone and mineral research : the official journal of the American Society for Bone and Mineral Research. 2014;29(3):518-30.

158. Leib E, Winzenrieth R, Aubry-Rozier B, Hans D. Vertebral microarchitecture and fragility fracture in men: A TBS study. Bone. 2014;62:51-5.

159. Bousson V, Bergot C, Sutter B, Levitz P, Cortet B, GRIO tSCot. Trabecular bone score (TBS): available knowledge, clinical relevance, and future prospects. Osteoporosis International. 2012;23(5):1489-501.

160. Hans D, Goertzen AL, Krieg MA, Leslie WD. Bone microarchitecture assessed by TBS predicts osteoporotic fractures independent of bone density: the Manitoba study. Journal of bone and mineral research : the official journal of the American Society for Bone and Mineral Research. 2011;26(11):2762-9.

161. Leslie WD, Aubry-Rozier B, Lamy O, Hans D, Program ftMBD. TBS (Trabecular Bone Score) and Diabetes-Related Fracture Risk. The Journal of Clinical Endocrinology & Metabolism. 2013;98(2):602-9.

162. McCloskey EV, Odén A, Harvey NC, Leslie WD, Hans D, Johansson H, et al. A Meta-Analysis of Trabecular Bone Score in Fracture Risk Prediction and Its Relationship to FRAX. Journal of Bone and Mineral Research. 2016;31(5):940-8.

163. Bandirali M, Poloni A, Sconfienza LM, Messina C, Papini GDE, Petrini M, et al. Short-term precision assessment of trabecular bone score and bone mineral density using dual-energy X-ray absorptiometry with different scan modes: an in vivo study. European Radiology. 2015;25(7):2194-8.

164. Kanis JA, Johnell O, Oden A, Johansson H, McCloskey E. FRAX™ and the assessment of fracture probability in men and women from the UK. Osteoporosis International. 2008;19(4):385-97.

165. Schwartz AV, Vittinghoff E, Bauer DC, Hillier TA, Strotmeyer ES, Ensrud KE, et al. Association of BMD and FRAX score with risk of fracture in older adults with type 2 diabetes. JAMA. 2011;305(21):2184-92.

166. Hippisley-Cox J, Coupland C. Derivation and validation of updated QFracture algorithm to predict risk of osteoporotic fracture in primary care in the United Kingdom: prospective open cohort study. BMJ. 2012;344:e3427.

167. National Institute for Health and Care Excellence. Osteoporosis: assessing the risk of fragility fracture. NICE; 2012.

168. Barco CMR, Arija SM, Pérez MR. Biochemical markers in osteoporosis: usefulness in clinical practice. Reumatología Clínica (English Edition). 2012;8(3):149-52.

169. Naylor K, Jacques R, Paggiosi M, Gossiel F, Peel N, McCloskey E, et al. Response of bone turnover markers to three oral bisphosphonate therapies in postmenopausal osteoporosis: the TRIO study. Osteoporosis International. 2016;27(1):21-31.

170. Szulc P, Naylor K, Hoyle N, Eastell R, Leary E. Use of CTX-I and PINP as bone turnover markers: National Bone Health Alliance recommendations to standardize sample handling and patient preparation to reduce pre-analytical variability. Osteoporosis International. 2017;28(9):2541-56.

171. Delmas P, Eastell R, Garnero P, Seibel M, Stepan J. The use of biochemical markers of bone turnover in osteoporosis. Osteoporosis international. 2000;11(18):S2-S17.

172. Hannon R, Eastell R. Preanalytical Variability of Biochemical Markers of Bone Turnover. Osteoporosis International. 2000;11(6):S30-S44.

173. Wu C, Kato TS, Pronschinske K, Qiu S, Naka Y, Takayama H, et al. Dynamics of bone turnover markers in patients with heart failure and following haemodynamic improvement through ventricular assist device implantation. European journal of heart failure. 2012;14(12):1356-65.

174. Meertens R, Knapp K, Strain WD, Casanova F. The use of near infrared spectroscopy for measuring haemodynamics of the microvascular blood supply in bone tissue: protocol for a systematic review. 2015 [cited 2015]. Available from: http://www.crd.york.ac.uk/PROSPERO/display_record.php?ID=CRD42015024463.

175. Moher D, Liberati A, Tetzlaff J, Altman DG. Preferred reporting items for systematic reviews and meta-analyses: the PRISMA statement. Annals of internal medicine. 2009;151(4):264-9.

176. Sordillo DC, Sordillo LA, Shi L, Budansky Y, Sordillo PP, Alfano RR. Novel, near-infrared spectroscopic, label-free, techniques to assess bone abnormalities such as Paget's disease, osteoporosis and bone fractures. SPIE BIOS 2015; San Francisco, California, 2015.

177. Reitsma J, Rutjes A, Whiting P, Vlassov V, Leeflang M, Deeks J. Chapter 9: Assessing methodological quality. In: Deeks J, Bossuyt P, Gatsonis C, editors. Cochrane Handbook for Systematic Reviews of Diagnostic Test Accuracy. Online: The Cochrane Collaboration; 2009.

178. National Heart Lung and Blood Institute. Study Quality Assessment Tools 2015. Available from: https://www.nhlbi.nih.gov/health-topics/study-quality-assessment-tools.

179. Higgins JP, Altman DG, Sterne JA, Cochrane Statistical Methods Group, Cochrane Bias Methods Group. Chapter 8: Assessing risk of bias in included studies 2015. Available from: https://handbook-5-1.cochrane.org/chapter_8/8_assessing_risk_of_bias_in_included_studies.htm.

180. Kim SY, Park JE, Lee YJ, Seo H-J, Sheen S-S, Hahn S, et al. Testing a tool for assessing the risk of bias for nonrandomized studies showed moderate reliability and promising validity. Journal of clinical epidemiology. 2013;66(4):408-14.

181. Sterne JA, Egger M, Moher D, Cochrane Bias Methods Group. Chapter 10: Addressing reporting biases. Cochrane Handbook for Systematic Reviews of Interventions, 2015.

182. Beaule PE, Campbell P, Shim P. Femoral head blood flow during hip resurfacing. Clin Orthop Relat Res. 2007(456):148-52.

183. Meertens R, Knapp K, Strain D, Casanova F. Near infrared spectroscopy: A potential tool for assessing haemodynamic markers of the microvascular blood supply within bone tissue. Osteoporos Int. 2016;27 (2 Supplement):S636-S7.

184. Minokawa S, Naito M, Yoshimura I, Kanazawa K, Hagio T. Effect of blood flow of the metatarsal head with hallux valgas after minimally invasive distal linear metatarsal osteotomy. J Orthop Res. 2016;34.

185. Klasing M, Zange J, editors. In vivo quantitative near-infrared spectroscopy in skeletal muscle and bone during rest and isometric exercise. European Conference on Biomedical Optics 2003; 2003: International Society for Optics and Photonics.

186. Alneami AI. Measuring blood perfusion in bone using NIRS (bone optical spectroscopy) [M.S.]: Northeastern University; 2015.

187. Al-Kassab BAM. Laser Doppler flowmetry in measuring microvascular responses in the oral mucosae and mandibular bone [Ph.D.]: The University of Manchester (United Kingdom); 1995.

188. Binzoni T, Blanchi S, Fasel JH, Bounameaux H, Hiltbrand E, Delpy D. Human tibia bone marrow blood perfusion by non-invasive near infrared spectroscopy: a new tool for studies on microgravity. J Gravit Physiol. 2002;9(1):P183-4.

189. Binzoni T, Leung T, Hollis V, Bianchi S, Fasel JH, Bounameaux H, et al. Human tibia bone marrow: defining a model for the study of haemodynamics as a function of age by near infrared spectroscopy. J Physiol Anthropol Appl Human Sci. 2003;22(5):211-8.

190. Cai Zg, Zhang J, Zhang Jg, Zhao Fy, Yu Gy, Li Y, et al. Evaluation of near infrared spectroscopy in monitoring postoperative regional tissue oxygen saturation for fibular flaps. Journal of Plastic, Reconstructive and Anaesthetic Surgery. 2008;61(3):289-96.

191. Hutchison IL, Cope M, Delpy DT, Richardson CE, Harris M. The investigation of osteoradionecrosis of the mandible by near infared spectroscopy. Br J Oral Maxillofac Surg. 1990;28(3):150-4.

192. Reher P, Chrcanovic BR, Springett R, Harris M. Near infrared spectroscopy: A diagnostic tool to evaluate effects of radiotherapy in the mandible? Spectroscopy. 2011;26(1):11-32.

193. Takami Y, Tajima K, Masumoto H. Near-infrared spectroscopy for noninvasive evaluation of chest wall ischemia immediately after left internal thoracic artery harvesting. Gen Thorac Cardiovasc Surg. 2008;56(6):281-7.

194. Binzoni T, Sanguinetti B, Van de Ville D, Zbinden H, Martelli F. Probability density function of the electric field in diffuse correlation spectroscopy of human bone in vivo. Applied optics. 2016;55(4):757-62.

195. Sekar SKV, Dalla Mora A, Bargigia I, Martinenghi E, Lindner C, Farzam P, et al. Broadband (600–1350 nm) Time-Resolved Diffuse Optical Spectrometer for Clinical Use. IEEE Journal of Selected Topics in Quantum Electronics. 2016;22(3):1-9.

196. Sørensen H, Thomsen J, Meyer AP, Terzic D, Hilsted L, Kjaergaard J, et al. Phenylephrine increases near-infrared spectroscopy determined muscle oxygenation in men. J Clin Monit Comput. 2017;31(6):1159-66.

197. Becker RL, Siamwala JH, Macias BR, Hargens AR. Tibia Bone Microvascular Flow Dynamics as Compared to Anterior Tibial Artery Flow During Body Tilt. Aerospace medicine and human performance. 2018;89(4):357-64.

198. Larsson A, Uusijärvi J, Näslund J, Lund I, Lindholm P. Bone and Soft Tissue Blood Flow during Normobaric and Hyperbaric Oxygen Breathing in Healthy Divers. Journal of Biomedical Science and Engineering. 2014;7:973-81.

199. Mateus J, Hargens AR. Bone hemodynamic responses to changes in external pressure. Bone. 2013;52(2):604-10.

200. Naslund E, Lindberg LG, Lund I, Naslund-Koch L, Larsson A, Frithiof R. Measuring arterial oxygen saturation from an intraosseous photoplethysmographic signal derived from the sternum. Journal of Clinical Monitoring and Computing. 2019.

201. Näslund J, Näslund S, Lundeberg E, Lindberg L, Lund I. Bone blood flow is influenced by muscle contractions. Journal of Biomedical Science and Engineering. 2011;4:490-6.

202. Naslund J, Walden M, Lindberg LG. Decreased pulsatile blood flow in the patella in patellofemoral pain syndrome. Am J Sports Med. 2007;35(10):1668-73.

203. Howden M, Siamwala JH, Hargens AR. Bone microvascular flow differs from skin microvascular flow in response to head-down tilt. J Appl Physiol. 2017;123(4):860.

204. Siamwala JH, Macias BR, Lee PC, Hargens AR. Gender differences in tibial microvascular flow responses to head down tilt and lower body negative pressure. Physiological Reports. 2017;5(4)(e13143).

205. Amarasekera HW, Costa ML, Foguet P, Krikler SJ, Prakash U, Griffin DR. The blood flow to the femoral head/neck junction during resurfacing arthroplasty: A comparison of two approaches using Laser Doppler flowmetry. Journal of Bone and Joint Surgery - Series B. 2008;90(4):442-5.

206. Bahn CH, Holloway GA, Jr. Effect of internal mammary artery mobilization on sternal blood flow. Chest. 1990;98(4):878-80.

207. Bassett GS, Barton KL, Skaggs DL. Laser Doppler flowmetry during open reduction for developmental dysplasia of the hip. Clin Orthop Relat Res. 1997(340):158-64.

208. Beaule PE, Campbell PA, Hoke R, Dorey F. Notching of the femoral neck during resurfacing arthroplasty of the hip. Journal of Bone and Joint Surgery - Series B. 2006;88(1):35-9.

209. Beck M, Siebenrock KA, Affolter B, Notzli H, Parvizi J, Ganz R. Increased intraarticular pressure reduces blood flow to the femoral head. Clin Orthop Relat Res. 2004(424):149-52.

210. Bogehoj M, Emmeluth C, Overgaard S. Blood flow and microdialysis in the human femoral head. Acta Orthop. 2007;78(1):56-62.

211. Degoute C-S, Preckel M-P, Dubreuil C, Banssillon V, Duclaux R. Sympathetic nerve regulation of cochlear blood flow during increases in blood pressure in humans. Eur J Appl Physiol Occup Physiol. 1997;75(4):326-32.

212. Drinias V, Granstrom G, Tjellstrom A. High age at the time of implant installation is correlated with increased loss of osseointegrated implants in the temporal bone. Clin Implant Dent Relat Res. 2007;9(2):94-9.

213. Duwelius PJ, Schmidt AH. Assessment of bone viability in patients with osteomyelitis: preliminary clinical experience with laser Doppler flowmetry. J Orthop Trauma. 1992;6(3):327-32.

214. ElMaraghy AW, Schemitsch EH, Waddell JP. Greater trochanteric blood flow during total hip arthroplasty using a posterior approach. Clin Orthop Relat Res. 1999(363):151-7.

215. ElMaraghy AW, Schemitsch EH, Waddell JP. Acetabular blood flow during total hip arthroplasty. Can J Surg. 2000;43(3):197-201.

216. Fukuoka S, Hotokebuchi T, Jingushi S, Fujii H, Sugioka Y, Iwamoto Y. Evaluation of blood flow within the subchondral bone of the femoral head: Use of the laser speckle method at surgery for osteonecrosis. J Orthop Res. 1999;17(1):80-7.

217. Green GE, Swistel DG, Castro J, Hillel Z, Thornton J. Sternal blood flow during mobilization of the internal thoracic arteries. Ann Thorac Surg. 1993;55(4):967-70.

218. Hempfing A, Dreimann M, Krebs S, Meier O, Notzli H, Metz-Stavenhagen P. Reduction of vertebral blood flow by segmental vessel occlusion: an intraoperative study using laser Doppler flowmetry. Spine. 2005;30(23):2701-5.

219. Hempfing A, Leunig M, Notzli HP, Beck M, Ganz R. Acetabular blood flow during Bernese periacetabular osteotomy: An intraoperative study using laser Doppler flowmetry. J Orthop Res. 2003;21(6):1145-50.

220. Hempfing A, Schoeniger R, Koch PP, Bischel O, Thomsen M. Patellar blood flow during knee arthroplasty surgical exposure: Intraoperative monitoring by laser Doppler flowmetry. J Orthop Res. 2007;25(10):1389-94.

221. Hertel R, Hempfing A, Stiehler M, Leunig M. Predictors of humeral head ischemia after intracapsular fracture of the proximal humerus. J Shoulder Elbow Surg. 2004;13(4):427-33.

222. Hughes SS, Cammarata A, Steinmann SP, Pellegrini Jr VD. Effect of standard total knee arthroplasty surgical dissection on human patellar blood flow in vivo: an investigation using laser Doppler flowmetry. J South Orthop Assoc. 1998;7(3):198-204.

223. Hupel TM, Schemitsch EH, Aksenov SA, Waddell JP. Blood flow changes to the proximal femur during total hip arthroplasty. Can J Surg. 2000;43(5):359-64.

224. Kamiya H, Akhyari P, Martens A, Karck M, Haverich A, Lichtenberg A. Sternal microcirculation after skeletonized versus pedicled harvesting of the internal thoracic artery: A randomized study. J Thorac Cardiovasc Surg. 2008;135(1):32-7.

225. Knobloch K, Lichtenberg A, Pichlmaier M, Mertsching H, Krug A, Klima U, et al. Microcirculation of the Sternum Following Harvesting of the Left Internal Mammary Artery. Thorac Cardiovasc Surg. 2003;51(5):255-9.

226. Kokovic V, Krsljak E, Andric M, Brkovic B, Milicic B, Jurisic M, et al. Correlation of Bone Vascularity in the Posterior Mandible and Subsequent Implant Stability: A Preliminary Study. Implant Dent. 2014;23(2):200-5.

227. Kretschmer WB, Baciut G, Baciut M, Zoder W, Wangerin K. Changes in bone blood flow in segmental LeFort I osteotomies. Oral Surgery, Oral Medicine, Oral Pathology, Oral Radiology, and Endodontology. 2009;108(2):178-83.

228. Kuhn MA, Lippert FG, 3rd, Phipps MJ, Williams C. Blood flow to the metatarsal head after chevron bunionectomy. Foot Ankle Int. 2005;26(7):526-9.

229. Lausten GS, Arnoldi CC. Blood perfusion uneven in femoral head osteonecrosis. Doppler flowmetry and intraosseous pressure in 12 cases. Acta Orthop Scand. 1993;64(5):533-6.

230. Lausten GS, Kiaer T, Dahl B. Laser Doppler flowmetry for estimation of bone blood flow: studies of reproducibility and correlation with microsphere technique. J Orthop Res. 1993;11(4):573-80.

231. Lorenzen ND, Stilling M, Ulrich-Vinther M, Trolle-Andersen N, Pryno T, Soballe K, et al. Increased post-operative ischemia in the femoral head found by microdialysis by the posterior surgical approach: A randomized clinical trial comparing surgical approaches in hip resurfacing arthroplasty. Arch Orthop Trauma Surg. 2013;133(12):1735-45.

232. Miller JM, Laurikainen EA, Grénman RA, Suonpää J, Bredberg G. Epinephrine-induced changes in human cochlear blood flow. Otol Neurotol. 1994;15(3):299-306.

233. Miller JM, Ren T-Y, Nuttall AL. Studies of inner ear blood flow in animals and human beings. Otolaryngology-Head and Neck Surgery. 1995;112(1):101-13.

234. Nakashima T, Hattori T, Sato E, Sone M, Tominaga M. Blood flow measurements in the ears of patients receiving cochlear implants. Ann Otol Rhinol Laryngol. 2002;111(11):998-1001.

235. Nakashima T, Hattori T, Sone M, Asahi K, Matsuda N, Teranishi M, et al. Cochlear blood flow and speech perception ability in cochlear implant users. Otol Neurotol. 2012;33(2):165-8.

236. Nakashima T, Sato E, Hattori T, Tominaga M, Sone M, Sugiura M. Blood flow in the ears of patients receiving cochlear implants. Ann Otol Rhinol Laryngol. 2004;113(6):426-30.

237. Nakashima T, Sone M, Fujii H, Teranishi M, Yamamoto H, Otake H, et al. Blood flow to the promontory in cochlear otosclerosis. Clin Otolaryngol. 2006;31(2):110-5.

238. Nishi H, Mitsuno M, Tanaka H, Ryomoto M, Fukui S, Miyamoto Y. Decreasing sternum microcirculation after harvesting the internal thoracic artery. Eur J Cardiothorac Surg. 2011;40(1):240-4.

239. Notzli HP, Siebenrock KA, Hempfing A, Ramseier LE, Ganz R. Perfusion of the femoral head during surgical dislocation of the hip. Journal of Bone and Joint Surgery - Series B. 2002;84(2):300-4.

240. Schoeniger R, Espinosa N, Sierra RJ, Leunig M, Ganz R. Role of the extraosseus blood supply in osteoarthritic femoral heads? Clin Orthop Relat Res. 2009;467(9):2235-40.

241. Schuurman AH, Bos KE, Van Nus YH. Laser Doppler bone probe in vascularized fibula transfers: a preliminary report. Microsurgery. 1987;8(4):186-9.

242. Selmani IP, H. Ishizaki, TI Marttila, Z. Cochlear Blood Flow Measurement in Patients with Me´ niere's Disease and Other Inner Ear Disorders. Acta Otolaryngol. 2001;121(545):10-3.

243. Sone M, Yoshida T, Otake H, Kato K, Teranishi M, Naganawa S, et al. Evaluation of vascular activity in otosclerosis by laser Doppler flowmetry: comparison with computed tomographic densitometry. Otol Neurotol. 2013;34(9):1559-63.

244. Stoffel KK, Flivik G, Yates PJ, Nicholls RL. Intraosseous blood flow of the everted or laterally-retracted patella during total knee arthroplasty. The Knee Journal. 2007;14(6):434-8.

245. Swiontkowski MF. Criteria for bone debridement in massive lower limb trauma. Clin Orthop Relat Res. 1989(243):41-7.

246. Swiontkowski MF, Ganz R, Schlegel U, Perren SM. Laser Doppler flowmetry for clinical evaluation of femoral head osteonecrosis. Preliminary experience. Clin Orthop Relat Res. 1987(218):181-5.

247. Swiontkowski MF, Hagan K, Shack RB. Adjunctive use of laser Doppler flowmetry for debridement of osteomyelitis. J Orthop Trauma. 1989;3(1):1-5.

248. Swiontkowski MF, Hanel DP, Vedder NB, Schwappach JR. A comparison of short- and long-term intravenous antibiotic therapy in the postoperative management of adult osteomyelitis. Journal of Bone & Joint Surgery, British Volume. 1999;81-B(6):1046-50.

249. Tono YU, Naoto Nagata, Atsushi Haruta, Shizuo Komune, Tetsuya. Effects of trimetaphan-induced deliberate hypotension on human cochlear blood flow. Acta Otolaryngol. 1998;118(539):40-3.

250. Verdonck HW, Meijer GJ, Kessler P, Nieman FH, de Baat C, Stoelinga PJ. Assessment of bone vascularity in the anterior mandible using laser Doppler flowmetry. Clin Oral Implants Res. 2009;20(2):140-4.

251. Wannfors K, Gazelius B. Blood flow in jaw bones affected by chronic osteomyelitis. Br J Oral Maxillofac Surg. 1991;29(3):147-53.

252. Wong K. Laser Doppler flowmetry for clinical detection of blood flow as a measure of vitality in sinus bone grafts. Implant Dent. 2000;9(2):133-42.

253. Ziebarth K, Leunig M, Slongo T, Kim YJ, Ganz R. Slipped capital femoral epiphysis: Relevant pathophysiological findings with open surgery hip. Clin Orthop Relat Res. 2013;471(7):2156-62.

254. Binzoni T, Tchernin D, Hyacinthe JN, Van De Ville D, Richiardi J. Pulsatile blood flow in human bone assessed by laser-Doppler flowmetry and the interpretation of photoplethysmographic signals. Physiol Meas. 2013;34(3):N25-N40.

255. Vasovic M, Todorovic VS, Krsljak E, Kanjevac T, Kokovic V. Assessment of bone vascularity in the posterior maxilla during dental implant insertion by laser doppler flowmetry. Biomedical Research. 2017;28(9):4228-32.

256. Halawi MJ, Brigati DP, Brooks PJ. Surgical hip dislocation through a modified direct lateral approach: real-time perfusion monitoring. Arthroplasty Today. 2019.

257. Notzli HP, Swiontkowski MF, Thaxter ST, Carpenter GK, 3rd, Wyatt R. Laser Doppler flowmetry for bone blood flow measurements: helium-neon laser light attenuation and depth of perfusion assessment. J Orthop Res. 1989;7(3):413-24.

258. Sakharia A, Muthusekar MR. A comparative assessment of maxillary perfusion between two different Le Fort I osteotomy techniques. International Journal of Oral & Maxillofacial Surgery. 2015;44(3):343-8.

259. Ghosh A, Elwell C, Smith M. Cerebral near-infrared spectroscopy in adults: a work in progress. Anesthesia & Analgesia. 2012;115(6):1373-83.

260. Gross PM, Heistad DD, Marcus ML. Neurohumoral regulation of blood flow to bones and marrow. American Journal of Physiology-Heart and Circulatory Physiology. 1979;237(4):H440-H8.

261. Yu G, Durduran T, Lech G, Zhou C, Chance B, Mohler ER, et al. Time-dependent blood flow and oxygenation in human skeletal muscles measured with noninvasive near-infrared diffuse optical spectroscopies. Journal of biomedical optics. 2005;10(2):024027-02402712.

262. Nüesch E, Trelle S, Reichenbach S, Rutjes AW, Tschannen B, Altman DG, et al. Small study effects in meta-analyses of osteoarthritis trials: meta-epidemiological study. BMJ. 2010;341:c3515.

263. Hyttel-Sorensen S, Sorensen LC, Riera J, Greisen G. Tissue oximetry: a comparison of mean values of regional tissue saturation, reproducibility and dynamic range of four NIRS-instruments on the human forearm. Biomedical Optics Express. 2011;2(11):3047-57.

264. Yang Y, Soyemi OO, Scott PJ, Landry MR, Lee SMC, Stroud L, et al. Quantitative measurement of muscle oxygen saturation without influence from skin and fat using continuous-wave near infrared spectroscopy. Optics Express. 2007;15(21):13715-30.

265. Pienaar P, Micklesfield L, Gill J, Shore A, Gooding K, Levitt N, et al. Ethnic differences in microvascular function in apparently healthy South African men and women. Experimental physiology. 2014;99(7):985-94.

266. Farzam P, Zirak P, Binzoni T, Durduran T, editors. Pulsatile and static hemodynamics of human patella during rest and cuff inflation. Digital Holography and Three-Dimensional Imaging; 2012: Optical Society of America.

267. Lemon M, Somayaji H, Khaleel A, Elliott D. Fragility fractures of the ankle: stabilisation with an expandable calcaneotalotibial nail. The Journal of bone and joint surgery 2005;87(6):809-13.

268. Popp A, Senn C, Franta O, Krieg M, Perrelet R, Lippuner K. Tibial or hip BMD predict clinical fracture risk equally well: results from a prospective study in 700 elderly Swiss women. Osteoporosis international. 2009;20(8):1393-9.

269. Pedersen BL, Baekgaard N, Quistorff B. A near infrared spectroscopy-based test of calf muscle function in patients with peripheral arterial disease. International Journal of Angiology. 2015;24(1):25-34.

270. Torricelli A, Quaresima V, Pifferi A, Biscotti G, Spinelli L, Taroni P, et al. Mapping of calf muscle oxygenation and haemoglobin content during dynamic plantar flexion exercise by multi-channel time-resolved near-infrared spectroscopy. Phys Med Biol. 2004;49(5):685-99.

271. Adingupu DD, Thorn CE, Casanova F, Elyas S, Gooding K, Gilchrist M, et al. Blood oxygen saturation after ischemia is altered with abnormal microvascular reperfusion. Microcirculation. 2015;22(4):294-305.

272. Gerovasili V, Dimopoulos S, Tzanis G, Anastasiou-Nana M, Nanas S. Utilizing the vascular occlusion technique with NIRS technology. International Journal of Industrial Ergonomics. 2010;40(2):218-22.

273. Kernick D, Tooke J, Shore A. The biological zero signal in laser Doppler fluximetry–origins and practical implications. Pflügers Archiv. 1999;437(4):624-31.

274. Kragelj R, Jarm T, Miklavčič D. Reproducibility of Parameters of Postocclusive Reactive Hyperemia Measured by Near Infrared Spectroscopy and Transcutaneous Oximetry. Annals of Biomedical Engineering. 2000;28(2):168-73.

275. Hassan IA, Spencer SA, Wickramasinghe YA, Palmer KS. Measurement of peripheral oxygen utilisation in neonates using near infrared spectroscopy: comparison between arterial and venous occlusion methods. Early Human Development.57(3):211-24.

276. Kragelj R, Jarm T, Erjavec T, Presern-Strukelj M, Miklavcic D. Parameters of postocclusive reactive hyperemia measured by near infrared spectroscopy in patients with peripheral vascular disease and in healthy volunteers. Ann Biomed Eng. 2001;29(4):311-20.

277. Buchheit M, Ufland P, Haydar B, Laursen PB, Ahmaidi S. Reproducibility and sensitivity of muscle reoxygenation and oxygen uptake recovery kinetics following running exercise in the field. Clinical Physiology and Functional Imaging. 2011;31(5):337-46.

278. McLay KM, Nederveen JP, Pogliaghi S, Paterson DH, Murias JM. Repeatability of vascular responsiveness measures derived from near-infrared spectroscopy. Physiological Reports. 2016;4(9).

279. Crenshaw AG, Elcadi GH, Hellstrom F, Mathiassen SE. Reliability of near-infrared spectroscopy for measuring forearm and shoulder oxygenation in healthy males and females. European Journal of Applied Physiology. 2012;112(7):2703-15.

280. McCully KK, Landsberg L, Suarez M, Hofmann M, Posner JD. Identification of peripheral vascular disease in elderly subjects using optical spectroscopy. J Gerontol A Biol Sci Med Sci. 1997;52(3):B159-65.

281. Willingham TB, Southern WM, McCully KK. Measuring reactive hyperemia in the lower limb using near-infrared spectroscopy. Journal of biomedical optics. 2016;21(9):091302-.

282. Lacroix S, Gayda M, Gremeaux V, Juneau M, Tardif J-C, Nigam A. Reproducibility of near-infrared spectroscopy parameters measured during brachial artery occlusion and reactive hyperemia in healthy men. Journal of Biomedical Optics. 2012;17(7):0770101-5.

283. Brizendine JT, Ryan TE, Larson RD, McCully KK. Skeletal muscle metabolism in endurance athletes with near-infrared spectroscopy. Med Sci Sports Exerc. 2013;45(5):869-75.

284. Nagasawa T, Hamaoka T, Sako T, Murakami M, Kime R, Homma T, et al. A practical indicator of muscle oxidative capacity determined by recovery of muscle O 2 consumption using NIR spectroscopy. European Journal of Sport Science. 2003;3(2):1-10.

285. Motulsky HJ. How to: Plateau followed by one phase association: GraphPad Curve Fitting Guide. Available from: https://www.graphpad.com/guides/prism/7/curve-fitting/index.htm?reg_exponential_plateau_then_association.htm.

286. Motulsky H. Prism 4 statistics guide—statistical analyses for laboratory and clinical researchers. GraphPad Software Inc, San Diego, CA. 2003:122-6.

287. Comerota AJ, Throm RC, Kelly P, Jaff M. Tissue (muscle) oxygen saturation (StO2): A new measure of symptomatic lower-extremity arterial disease. Journal of Vascular Surgery. 2003;38(4):724-9.

288. Meertens RM, Knapp KM, Casanova F, Strain WD. The effects of lumbar sympathectomy on bone and soft tissue haemodynamics of the leg recorded using near infrared spectroscopy: A case report. Journal of Biomedical Engineering and Informatics. 2016;3(1):28.

289. Nakajima T, Kurano M, Iida H, Takano H, Oonuma H, Morita T, et al. Use and safety of KAATSU training: results of a national survey. International Journal of KAATSU Training Research. 2006;2(1):5-13.

290. Koch S, Katsnelson M, Dong C, Perez-Pinzon M. Remote Ischemic Limb Preconditioning After Subarachnoid Hemorrhage. Stroke. 2011;42(5):1387-91.

291. Wagner BA, Venkataraman S, Buettner GR. The rate of oxygen utilization by cells. Free Radical Biology and Medicine. 2011;51(3):700-12.

292. Nielsen SL, Sejrsen P. Reactive hyperemia in subcutaneous adipose tissue in man. Acta Physiologica Scandinavica. 1972;85(1):71-7.

293. Waters RE, Rotevatn S, Li P, Annex BH, Yan Z. Voluntary running induces fiber type-specific angiogenesis in mouse skeletal muscle. American Journal of Physiology-Cell Physiology. 2004;287(5):C1342-C8.

294. Laughlin MH, Davis MJ, Secher NH, van Lieshout JJ, Arce-Esquivel AA, Simmons GH, et al. Peripheral circulation. Comprehensive Physiology. 2011;2(1):321-447.

295. Heinonen I, Kemppainen J, Kaskinoro K, Langberg H, Knuuti J, Boushel R, et al. Bone blood flow and metabolism in humans: effect of muscular exercise and other physiological perturbations. Journal of bone and mineral research. 2013;28(5):1068-74.

296. Bland JM, Altman DG. Multiple significance tests: the Bonferroni method. BMJ. 1995;310(6973):170.

297. Perneger TV. What's wrong with Bonferroni adjustments. BMJ. 1998;316(7139):1236-8.

298. Bartlett J, Frost C. Reliability, repeatability and reproducibility: analysis of measurement errors in continuous variables. Ultrasound in Obstetrics & Gynecology. 2008;31(4):466-75.

299. Hopkins WG. Measures of reliability in sports medicine and science. Sports medicine. 2000;30(1):1-15.

300. Knapp KM, Welsman JR, Hopkins SJ, Fogelman I, Blake GM. Obesity Increases Precision Errors in Dual-Energy X-Ray Absorptiometry Measurements. Journal of Clinical Densitometry. 2012;15(3):315-9.

301. Bland JM, Altman DG. Statistics notes: Measurement error. BMJ. 1996;312(7047):1654.

302. Bland M. How should I calculate a within-subject coefficient of variation? 2006 [updated 16/10/2006; cited 2019 13/02/2019]. Available from: https://www-users.york.ac.uk/~mb55/meas/cv.htm.

303. Shrout PE, Fleiss JL. Intraclass correlations: uses in assessing rater reliability. Psychological bulletin. 1979;86(2):420.

304. Evans JD. Straightforward statistics for the behavioral sciences. Belmont, CA, US: Thomson Brooks/Cole Publishing Co; 1996. xxii, 600-xxii, p.

305. Bland JM, Altman DG. Applying the right statistics: analyses of measurement studies. Ultrasound Obstet Gynecol. 2003;22(1):85-93.

306. Bland JM, Altman D. Statistical methods for assessing agreement between two methods of clinical measurement. The Lancet. 1986;327(8476):307-10.

307. Doros G, Lew R. Design based on intra-class correlation coefficients. American Journal of Biostatistics. 2010;1(1):1.

308. International Society of Clinical Densitometry. 2019 ISCD Official Positions – Adult: International Society of Clinical Densitometry; 2019 [04/04/2020]. Available from: https://www.iscd.org/official-positions/2019-iscd-official-positions-adult/.

309. Högler W, Blimkie C, Cowell C, Kemp A, Briody J, Wiebe P, et al. A comparison of bone geometry and cortical density at the mid-femur between prepuberty and young adulthood using magnetic resonance imaging. Bone. 2003;33(5):771-8.

310. Centers for Disease Control and Prevention. Dual Energy X-ray Absorptiometry (DXA) Procedures Manual. National Health and Nutrition Examination Survey. 2007.

311. Kanis JA, McCloskey EV. Bone turnover and biochemical markers in malignancy. Cancer. 1997;80(S8):1538-45.

312. Song L. Calcium and Bone Metabolism Indices. Adv Clin Chem. 2017;82:1-46.

313. Lorbergs AL, Noseworthy MD, Adachi JD, Stratford PW, MacIntyre NJ. Fat infiltration in the leg is associated with bone geometry and physical function in healthy older women. Calcified tissue international. 2015;97(4):353-63.

314. Pickering TG, Hall JE, Appel LJ, Falkner BE, Graves J, Hill MN, et al. Recommendations for blood pressure measurement in humans and experimental animals: part 1: blood pressure measurement in humans: a statement for professionals from the Subcommittee of Professional and Public Education of the American Heart Association Council on High Blood Pressure Research. Circulation. 2005;111(5):697-716.

315. Stabley JN, Prisby RD, Behnke BJ, Delp MD. Type 2 diabetes alters bone and marrow blood flow and vascular control mechanisms in the ZDF rat. Journal of Endocrinology. 2015;225(1):47-58.

316. Brandmaier AM, Wenger E, Bodammer NC, Kuhn S, Raz N, Lindenberger U. Assessing reliability in neuroimaging research through intra-class effect decomposition (ICED). Elife. 2018;7.

317. Harris RA, Padilla J, Rink LD, Wallace JP. Variability of flow-mediated dilation measurements with repetitive reactive hyperemia. Vascular Medicine. 2006;11(1):1-6.

318. Matcher S, Elwell C, Cooper C, Cope M, Delpy D. Performance comparison of several published tissue near-infrared spectroscopy algorithms. Analytical biochemistry. 1995;227(1):54-68.

319. Maggio D, McCloskey E, Camilli L, Cenci S, Cherubini A, Kanis J, et al. Short-term reproducibility of proximal femur bone mineral density in the elderly. Calcified tissue international. 1998;63(4):296-9.

320. Adami A, Cao R, Porszasz J, Casaburi R, Rossiter HB. Reproducibility of NIRS assessment of muscle oxidative capacity in smokers with and without COPD. Respiratory physiology & neurobiology. 2017;235:18-26.

321. Re R, Pirovano I, Contini D, Spinelli L, Torricelli A. Time Domain Near Infrared Spectroscopy Device for Monitoring Muscle Oxidative Metabolism: Custom Probe and In Vivo Applications. Sensors. 2018;18(1):264.

322. Ubbink DT, Koopman B. Near-infrared Spectroscopy in the Routine Diagnostic Work-up of Patients With Leg Ischaemia. European Journal of Vascular and Endovascular Surgery. 2006;31(4):394-400.

323. Fulford J, Liepa A, Barker AR, Meakin J. The reliability of 31P-MRS and NIRS measurements of spinal muscle function. International journal of sports medicine. 2014;35(13):1078-83.

324. Choo HC, Nosaka K, Peiffer JJ, Ihsan M, Yeo CC, Abbiss CR. Reliability of laser Doppler, near-infrared spectroscopy and Doppler ultrasound for peripheral blood flow measurements during and after exercise in the heat. Journal of sports sciences. 2017;35(17):1715-23.

325. Lucero AA, Addae G, Lawrence W, Neway B, Credeur DP, Faulkner J, et al. Reliability of muscle blood flow and oxygen consumption response from exercise using near-infrared spectroscopy. Experimental physiology. 2018;103(1):90-100.

326. Niemeijer VM, Spee RF, Jansen JP, Buskermolen AB, van Dijk T, Wijn PF, et al. Test–retest reliability of skeletal muscle oxygenation measurements during

submaximal cycling exercise in patients with chronic heart failure. Clinical physiology and functional imaging. 2017;37(1):68-78.

327. Vaz S, Falkmer T, Passmore AE, Parsons R, Andreou P. The Case for Using the Repeatability Coefficient When Calculating Test–Retest Reliability. PLoS ONE. 2013;8(9):e73990.

328. Florkowski C. HbA1c as a diagnostic test for diabetes mellitus–reviewing the evidence. The Clinical Biochemist Reviews. 2013;34(2):75.

329. Goodwin LD, Leech NL. Understanding correlation: Factors that affect the size of r. The Journal of Experimental Education. 2006;74(3):249-66.

330. Fillingim RB. Sex, gender, and pain: women and men really are different. Current Review of Pain. 2000;4(1):24-30.

331. Aubrun F, Salvi N, Coriat P, Riou B. Sex-and age-related differences in morphine requirements for postoperative pain relief. Anesthesiology: The Journal of the American Society of Anesthesiologists. 2005;103(1):156-60.

332. Heinonen I, Kemppainen J, Kaskinoro K, Langberg H, Knuuti J, Boushel R, et al. Bone blood flow and metabolism in humans: effect of muscular exercise and other physiological perturbations. Journal of bone and mineral research : the official journal of the American Society for Bone and Mineral Research. 2013;28(5):1068-74.

333. Jones S, D'Silva A, Bhuva A, Lloyd G, Manisty C, Moon JC, et al. Improved exercise-related skeletal muscle oxygen consumption following uptake of endurance training measured using near-infrared spectroscopy. Frontiers in physiology. 2017;8:1018.

334. Adelnia F, Cameron D, Bergeron CM, Fishbein KW, Spencer RG, Reiter DA, et al. The Role of Muscle Perfusion in the Age-Associated Decline of Mitochondrial Function in Healthy Individuals. Frontiers in Physiology. 2019;10(427).

335. Frikha-Benayed D, Basta-Pljakic J, Majeska RJ, Schaffler MB. Regional differences in oxidative metabolism and mitochondrial activity among cortical bone osteocytes. Bone. 2016;90:15-22.

336. Duteil S, Bourrilhon C, Raynaud J, Wary C, Richardson R, Leroy-Willig A, et al. Metabolic and vascular support for the role of myoglobin in humans: a multiparametric NMR study. American Journal of Physiology-Regulatory, Integrative and Comparative Physiology. 2004;287(6):R1441-R9.

337. Brodal P, Ingjer F, Hermansen L. Capillary supply of skeletal muscle fibers in untrained and endurance-trained men. American Journal of Physiology-Heart and Circulatory Physiology. 1977;232(6):H705-H12.

338. Stabley JN, Moningka NC, Behnke BJ, Delp MD. Exercise training augments regional bone and marrow blood flow during exercise. Medicine and science in sports and exercise. 2014;46(11):2107.

339. Mantooth WP, Mehta RK, Rhee J, Cavuoto LA. Task and sex differences in muscle oxygenation during handgrip fatigue development. Ergonomics. 2018;61(12):1646-56.

340. Paradis-Deschênes P, Joanisse DR, Billaut F. Sex-specific impact of ischemic preconditioning on tissue oxygenation and maximal concentric force. Frontiers in physiology. 2017;7:674.

341. Wascher, Bammer, Stollberger, Bahadori, Wallner, Toplak. Forearm composition contributes to differences in reactive hyperaemia between healthy men and women. European Journal of Clinical Investigation. 1998;28(3):243-8.

342. Kao W-L, Sun C-W. Gender-related effect in oxygenation dynamics by using far-infrared intervention with near-infrared spectroscopy measurement: a gender differences controlled trial. PloS one. 2015;10(11):e0135166.

343. Wells JCK. Sexual dimorphism of body composition. Best Practice & Research Clinical Endocrinology & Metabolism. 2007;21(3):415-30.

344. Bradbury KE, Guo W, Cairns BJ, Armstrong MEG, Key TJ. Association between physical activity and body fat percentage, with adjustment for BMI: a large cross-sectional analysis of UK Biobank. BMJ Open. 2017;7(3):e011843.

345. Gomes JLP, Fernandes T, Soci UPR, Silveira AC, Barretti DLM, Negrão CE, et al. Obesity downregulates microRNA-126 inducing capillary rarefaction in skeletal muscle: Effects of aerobic exercise training. Oxidative medicine and cellular longevity. 2017;2017.

346. Frayn K, Coppack S, Humphreys S, Whyte P. Metabolic characteristics of human adipose tissue in vivo. Clinical Science. 1989;76(5):509-16.

347. Kohri S, Hoshi Y, Tamura M, Kato C, Kuge Y, Tamaki N. Quantitative evaluation of the relative contribution ratio of cerebral tissue to near-infrared signals in the adult human head: a preliminary study. Physiological measurement. 2002;23(2):301.

348. Olive JL, DeVan AE, McCully KK. The effects of aging and activity on muscle blood flow. Dynamic Medicine. 2002;1(1):2.

349. Costes F, Denis C, Roche F, Prieur F, Enjolras F, Barthelemy J. Age-associated alteration of muscle oxygenation measured by near infrared spectroscopy during exercise. Archives of physiology and biochemistry. 1999;107(2):159-67.

350. Mohler ER, 3rd, Lech G, Supple GE, Wang H, Chance B. Impaired exercise-induced blood volume in type 2 diabetes with or without peripheral arterial disease measured by continuous-wave near-infrared spectroscopy. Diabetes Care. 2006;29(8):1856-9.

351. Bauer TA, Reusch JE, Levi M, Regensteiner JG. Skeletal muscle deoxygenation after the onset of moderate exercise suggests slowed microvascular blood flow kinetics in type 2 diabetes. Diabetes care. 2007;30(11):2880-5.

352. McClatchey PM, Bauer TA, Regensteiner JG, Schauer IE, Huebschmann AG, Reusch JE. Dissociation of local and global skeletal muscle oxygen transport metrics in type 2 diabetes. Journal of diabetes and its complications. 2017;31(8):1311-7.

353. VandeBerg BC, Malghem J, Lecouvet FE, Maldague B. Magnetic resonance imaging of the normal bone marrow. Skeletal radiology. 1998;27(9):471-83.

354. Biffar A, Sourbron S, Schmidt G, Ingrisch M, Dietrich O, Reiser MF, et al. Measurement of perfusion and permeability from dynamic contrast-enhanced MRI in normal and pathological vertebral bone marrow. Magn Reson Med. 2010;64(1):115-24.

355. Moorthi R, Fadel W, Eckert G, Ponsler-Sipes K, Moe S, Lin C. Bone marrow fat is increased in chronic kidney disease by magnetic resonance spectroscopy. Osteoporosis International. 2015;26(6):1801-7.

356. Jensen KE, Jensen M, Grundtvig P, Thomsen C, Karle H, Henriksen O. Localized in vivo proton spectroscopy of the bone marrow in patients with leukemia. Magnetic resonance imaging. 1990;8(6):779-89.

357. Wang L, Salibi N, Chang G, Vieira RL, Babb JS, Krasnokutsky S, et al. Assessment of subchondral bone marrow lipids in healthy controls and mild osteoarthritis patients at 3T. NMR in Biomedicine. 2012;25(4):545-55.

358. Prescot AP, Dzik-Jurasz AS, Leach MO, Sirohi B, Powles R, Collins DJ. Localized COSY and DQF-COSY 1H-MRS sequences for investigating human tibial bone marrow in vivo and initial application to patients with acute leukemia. Journal of Magnetic Resonance Imaging: An Official Journal of the International Society for Magnetic Resonance in Medicine. 2005;22(4):541-8.

359. Lidell M, Enerbäck S. Brown adipose tissue and bone. International journal of obesity supplements. 2015;5(1):S23-S7.

360. Grey A, Beckley V, Doyle A, Fenwick S, Horne A, Gamble G, et al. Pioglitazone increases bone marrow fat in type 2 diabetes: results from a randomized controlled trial. European Journal of Endocrinology. 2012;166(6):1087.

361. Sheu Y, Amati F, Schwartz AV, Danielson ME, Li X, Boudreau R, et al. Vertebral bone marrow fat, bone mineral density and diabetes: The Osteoporotic Fractures in Men (MrOS) study. Bone. 2017;97:299-305.

362. El Rafei M, Teixeira P, Norberciak L, Badr S, Cotten A, Budzik J-F. Dynamic contrast-enhanced MRI perfusion of normal muscle in adult hips: Variation of permeability and semi-quantitative parameters. European journal of radiology. 2018;108:92-8.

363. Tyml K, Mathieu-Costello O, Noble E. Microvascular response to ischemia, and endothelial ultrastructure, in disused skeletal muscle. Microvascular research. 1995;49(1):17-32.

364. Tyml K, Mathieu-Costello O. Structural and functional changes in the microvasculature of disused skeletal muscle. Front Biosci. 2001;6(6):D45-D52.

365. Jan Y-K, Liao F, Cheing GL, Pu F, Ren W, Choi HM. Differences in skin blood flow oscillations between the plantar and dorsal foot in people with diabetes mellitus and peripheral neuropathy. Microvascular research. 2019;122:45-51.

366. Tibiriçá E, Rodrigues E, Cobas R, Gomes MB. Increased functional and structural skin capillary density in type 1 diabetes patients with vascular complications. Diabetology & metabolic syndrome. 2009;1(1):24.

367. Hinsbergh VWMv. Endothelial Permeability for Macromolecules. Arteriosclerosis, Thrombosis, and Vascular Biology. 1997;17(6):1018-23.

368. Tostes R, Nigro D, Fortes Z, Carvalho M. Effects of estrogen on the vascular system. Brazilian Journal of Medical and Biological Research. 2003;36(9):1143-58.

369. Claesson-Welsh L. Vascular permeability—the essentials. Upsala journal of medical sciences. 2015;120(3):135-43.

370. Zheng J, Hasting MK, Zhang X, Coggan A, An H, Snozek D, et al. A pilot study of regional perfusion and oxygenation in calf muscles of individuals with diabetes with a noninvasive measure. Journal of vascular surgery. 2014;59(2):419-26.

371. Weber M-A, Krakowski-Roosen H, Delorme S, Renk H, Krix M, Millies J, et al. Relationship of skeletal muscle perfusion measured by contrast-enhanced ultrasonography to histologic microvascular density. Journal of ultrasound in medicine. 2006;25(5):583-91.

372. Ma HT, Griffith JF, Yeung DK, Leung P. Modified brix model analysis of bone perfusion in subjects of varying bone mineral density. Journal of Magnetic Resonance Imaging: An Official Journal of the International Society for Magnetic Resonance in Medicine. 2010;31(5):1169-75.

373. Banfi G, Lombardi G, Colombini A, Lippi G. Bone metabolism markers in sports medicine. Sports Medicine. 2010;40(8):697-714.

374. Takeuchi A, Araki R, Proskurin S, Takahashi Y, Yamada Y, Ishii J, et al. A new method of bone tissue measurement based upon light scattering. Journal of Bone and Mineral Research. 1997;12(2):261-6.

375. Corretti MC, Anderson TJ, Benjamin EJ, Celermajer D, Charbonneau F, Creager MA, et al. Guidelines for the ultrasound assessment of endothelial-dependent flow-mediated vasodilation of the brachial artery: a report of the International Brachial Artery Reactivity Task Force. Journal of the American College of Cardiology. 2002;39(2):257-65.

376. Kuliga KZ, McDonald EF, Gush R, Michel C, Chipperfield AJ, Clough GF. Dynamics of microvascular blood flow and oxygenation measured simultaneously in human skin. Microcirculation. 2014;21(6):562-73.

377. Moayeri A, Mohamadpour M, Mousavi SF, Shirzadpour E, Mohamadpour S, Amraei M. Fracture risk in patients with type 2 diabetes mellitus and possible risk factors: a systematic review and meta-analysis. Therapeutics and clinical risk management. 2017;13:455.

378. Majmudar N, Robson S, Ford G. Effects of the menopause, gender, and estrogen replacement therapy on vascular nitric oxide activity. The Journal of Clinical Endocrinology & Metabolism. 2000;85(4):1577-83.

379. Cvijetić S, Koršić M. Apparent bone mineral density estimated from DXA in healthy men and women. Osteoporosis International. 2004;15(4):295-300.

380. Silva BC, Leslie WD, Resch H, Lamy O, Lesnyak O, Binkley N, et al. Trabecular Bone Score: A Noninvasive Analytical Method Based Upon the DXA Image. Journal of Bone and Mineral Research. 2014;29(3):518-30.

381. Leslie WD, Aubry-Rozier B, Lamy O, Hans D. TBS (trabecular bone score) and diabetes-related fracture risk. The Journal of Clinical Endocrinology & Metabolism. 2013;98(2):602-9.

382. Dhaliwal R, Cibula D, Ghosh C, Weinstock RS, Moses AM. Bone quality assessment in type 2 diabetes mellitus. Osteoporosis International. 2014;25(7):1969-73.

383. Kim JH, Choi HJ, Ku EJ, Kim KM, Kim SW, Cho NH, et al. Trabecular Bone Score as an Indicator for Skeletal Deterioration in Diabetes. The Journal of Clinical Endocrinology & Metabolism. 2015;100(2):475-82.

384. Zhukouskaya VV, Ellen-Vainicher C, Gaudio A, Privitera F, Cairoli E, Ulivieri FM, et al. The utility of lumbar spine trabecular bone score and femoral neck bone mineral density for identifying asymptomatic vertebral fractures in well-compensated type 2 diabetic patients. Osteoporosis International. 2016;27(1):49-56.

385. Rosen CJ, Glowacki J, Craig W. Sex steroids, the insulin-like growth factor regulatory system, and aging: implications for the management of older postmenopausal women. The Journal of Nutrition, Health & Aging. 1998;2(1):39-44.

386. Wong S, Kwok T, Woo J, Lynn H, Griffith J, Leung J, et al. Bone mineral density and the risk of peripheral arterial disease in men and women: results from Mr. and Ms Os, Hong Kong. Osteoporosis International. 2005;16(12):1933-8.

387. Starup-Linde J. Diabetes, Biochemical Markers of Bone Turnover, Diabetes Control, and Bone. Frontiers in Endocrinology. 2013;4(21).

388. Burch J, Rice S, Yang H, Neilson A, Stirk L, Francis R, et al. Systematic review of the use of bone turnover markers for monitoring the response to osteoporosis treatment: the secondary prevention of fractures, and primary prevention of fractures in high-risk groups. In: Assessment HT, editor.: NIHR Journals Library; 2014.

389. Buckley E, Parthasarathy A, Grant PE, Yodh A, Franceschini MA. Diffuse correlation spectroscopy for measurement of cerebral blood flow: future prospects. Neurophotonics. 2014;1(1):011009.

390. Lee JH, Dyke JP, Ballon D, Ciombor DM, Tung G, Aaron RK. Assessment of bone perfusion with contrast-enhanced magnetic resonance imaging. Orthop Clin North Am. 2009;40(2):249-57.

391. Torricelli A, Pifferi A, Taroni P, Giambattistelli E, Cubeddu R. In vivo optical characterization of human tissues from 610 to 1010 nm by time-resolved reflectance spectroscopy. Phys Med Biol. 2001;46(8):2227-37.

392. Karjalainen J, Riekkinen O, Schousboe J, Kröger H. Sensitivity and specificity of osteoporosis diagnostics at primary healthcare with Bindex. WCO-IOF-ESCEO Malaga 20162016. p. 70.2-9.5.

393. Casciaro S, Conversano F, Pisani P, Peccarisi M, Greco A, Di Paola M, et al. Accuracy of the echographic measured "osteoporosis score" in estimating spine mineral density in patients aged over 65 years. Ultrasound Med Biol. 2015;41(1):281-300.

394. Sekar SKV, Pagliazzi M, Negredo E, Martelli F, Farina A, Dalla Mora A, et al. In Vivo, non-invasive characterization of human bone by hybrid broadband (600-1200 nm) diffuse optical and correlation spectroscopies. PLoS One. 2016;11 (12).

395. Ugryumova N, Matcher SJ, Attenburrow DP. Measurement of bone mineral density via light scattering. Phys Med Biol. 2004;49(3):469-83.

396. Firbank M, Hiraoka M, Essenpreis M, Delpy D. Measurement of the optical properties of the skull in the wavelength range 650-950 nm. Physics in Medicine & Biology. 1993;38(4):503.

397. Afara IO, Florea C, Olumegbon IA, Eneh CT, Malo MK, Korhonen RK, et al. Characterizing human subchondral bone properties using near-infrared (NIR) spectroscopy. Scientific reports. 2018;8(1):1-10.

398. Chung C, Chen YP, Leu TH, Sun CW. Near-infrared bone densitometry: A feasibility study on distal radius measurement. Journal of Biophotonics. 2018;11(7):e201700342.

399. Shanas Na, Querido W, Dumont A, Yonko E, Carter E, Ok J, et al. Clinical Application of Near Infrared Fiber Optic Spectroscopy for Non-Invasive Bone Assessment. Journal of Biophotonics. 2020.

400. Bale G, Mitra S, de Roever I, Sokolska M, Price D, Bainbridge A, et al. Oxygen dependency of mitochondrial metabolism indicates outcome of newborn brain injury. Journal of Cerebral Blood Flow & Metabolism. 2019;39(10):2035-47.

401. Piper SK, Krueger A, Koch SP, Mehnert J, Habermehl C, Steinbrink J, et al. A wearable multi-channel fNIRS system for brain imaging in freely moving subjects. NeuroImage. 2014;85:64-71.

402. Yao P, Guo W, Sheng X, Zhang D, Zhu X, editors. A portable multi-channel wireless NIRS device for muscle activity real-time monitoring. 2014 36th Annual International Conference of the IEEE Engineering in Medicine and Biology Society; 2014 26-30 Aug. 2014.

403. Goguin A, Lesage F, Leblond H, Pelegrini-Issac M, Rossignol S, Benali H. A Low-Cost Implantable Near-Infrared Imaging System of Spinal Cord Activity in the Cat. IEEE Transactions on Biomedical Circuits and Systems. 2010;4(5):329-35.

404. Krucker T, Sandanaraj BS. Optical imaging for the new grammar of drug discovery. Philosophical Transactions of the Royal Society A: Mathematical, Physical and Engineering Sciences. 2011;369(1955):4651-65.

405. Le LV, Chendke GS, Gamsey S, Wisniewski N, Desai TA. Near-Infrared Optical Nanosensors for Continuous Detection of Glucose. Journal of Diabetes Science and Technology.0(0):1932296819886928.

406. Hansrani V, Khanbhai M, Bhandari S, Pillai A, McCollum CN. The role of compression in the management of soft tissue ankle injuries: a systematic review. European Journal of Orthopaedic Surgery & Traumatology. 2015;25(6):987-95.

407. Winge R, Bayer L, Gottlieb H, Ryge C. Compression therapy after ankle fracture surgery: a systematic review. European Journal of Trauma and Emergency Surgery. 2017;43(4):451-9.

408. Park SH, Silva M. Intermittent pneumatic soft tissue compression: Changes in periosteal and medullary canal blood flow. J Orthop Res. 2008;26(4):570-7.

409. Çatma MF, Şeşen H, Aydın A, Ünlü S, Demirkale İ, Altay M. Remote ischemic preconditioning enhances fracture healing. Journal of orthopaedics. 2015;12(4):168-73.

410. Qiao J, Zhou M, Li Z, Ren J, Gao G, Cao G, et al. Comparison of remote ischemic preconditioning and intermittent hypoxia training in fracture healing. Molecular medicine reports. 2019;19(3):1867-74.